Prepared in cooperation with
U.S. Department of Transportation
Federal Highway Administration

Attribution of Monotonic Trends and Change Points in Peak Streamflow Across the Conterminous United States Using a Multiple Working Hypotheses Framework, 1941–2015 and 1966–2015

Professional Paper 1869

U.S. Department of the Interior
U.S. Geological Survey

Attribution of Monotonic Trends and Change Points in Peak Streamflow Across the Conterminous United States Using a Multiple Working Hypotheses Framework, 1941–2015 and 1966–2015

Karen R. Ryberg, editor

Prepared in cooperation with
U.S. Department of Transportation
Federal Highway Administration

Professional Paper 1869

U.S. Department of the Interior
U.S. Geological Survey

U.S. Geological Survey, Reston, Virginia: 2022

Suggested citation:
Ryberg, K.R., ed., 2022, Attribution of monotonic trends and change points in peak streamflow across the conterminous United States using a multiple working hypotheses framework, 1941–2015 and 1966–2015: U.S. Geological Survey Professional Paper 1869, 8 chapters (A–H), variously paged, https://doi.org/10.3133/pp1869.

Associated data for this publication:
Dudley, R.W., Archfield, S.A., Hodgkins, G.A., Renard, B., and Ryberg, K.R., 2018, Peak-streamflow trends and changepoints and basin characteristics for 2,683 U.S. Geological Survey streamgages in the conterminous U.S. (ver. 3.0, April 2019): U.S. Geological Survey data release, https://doi.org/10.5066/P9AEGXY0.

York, B.C., Ryberg, K.R., Asquith, W.H., Chase, K.J., Dickinson, J.E., Dudley, R.W., Harden, T.M., Hodgkins, G.A., Holtschlag, D.J., Humberson, D.G., Konrad, C.P., Levin, S.B., Restivo, D.E., Sando, R., Sando, S.K., Swain, E.D., Tillery, A.C., and Totten, A.R., 2022, Attributions for nonstationary peak streamflow records across the conterminous United States, 1941–2015 and 1966–2015: U.S. Geological Survey data release, https://doi.org/10.5066/P9FOUVWG.

ISSN 2330-7102 (online)

Acknowledgments

The Federal Highway Administration of the U.S. Department of Transportation funded the work described in this professional paper through Interagency Agreement DTFH6116X30020, “Flood Frequency Estimation for Hydraulic Design.” The authors thank Joseph Krolak and Kornel Kerenyi of the Federal Highway Administration for their support of this project.

The authors also thank Stacey Archfield and Julie Kiang of the U.S. Geological Survey, who originally planned this work and other phases of the project funded by the Federal Highway Administration.

Contents

[Letters designate the chapters]

Attribution of Monotonic Trends and Change Points in Peak Streamflow Across the Conterminous United States Using a Multiple Working Hypotheses Framework, 1941–2015 and 1966–2015

By Karen R. Ryberg[1]

Abstract

The U.S. Geological Survey has a long history of leading flood-frequency analysis studies. These studies play a critical role in the assessment of risk, protection of lives, and planning and design of flood protection infrastructure. Standard flood-frequency analysis is based on the assumption of stationarity—that is, that the distribution of floods at a given site varies around a particular mean within a particular envelope of variance (and skew) and that these parameters of the underlying statistical distribution representative of the floods do not vary over time. Gradual or abrupt changes in one or more of the distributional parameters are called nonstationarities and violate the underlying assumptions of current U.S. Federal Government guidelines for flood-frequency analysis. Uncertainty exists as to what degree of violations calls for the use of a modified method for flood-frequency analysis and what the modified method(s) should be.

When deciding whether to perform nonstationary flood-frequency analysis and choosing a method for such analysis, it is important to understand the causes of the nonstationarity. Gradual or abrupt changes in distributional properties of floods may be the result of numerous factors, such as regulation, diversion, land-use change, or climate change.

In the interest of developing a cohesive national approach for better understanding the causes of nonstationarities and incorporating potential or observed changes into flood-frequency estimates, subject-matter experts from the U.S. Geological Survey and cooperators worked together to develop a multiple working hypotheses framework for making attributions and a common vocabulary for making provisions of confidence. Seven regional teams of these experts used ancillary datasets and institutional knowledge to evaluate plausible causes for monotonic trends and change points in annual peak-streamflow data for the conterminous United States that had been identified in an earlier phase of the project.

The first chapter of this professional paper describes the development of a list of the potential attributions, presents a literature review of the potential attributions, describes the regional approach, summarizes insights obtained from the attribution process, and suggests future research. The other chapters provide the methods used for attribution in the seven regions—Pacific Northwest, Upper Plains, Midwest, Northeast, Southwest, South-Central, and Southeast—and summarize the regional patterns of nonstationarities.

[1]U.S. Geological Survey.

Introduction to Attribution of Monotonic Trends and Change Points in Peak Streamflow Across the Conterminous United States Using a Multiple Working Hypotheses Framework, 1941–2015 and 1966–2015

By Nancy A. Barth, Karen R. Ryberg, Angela Gregory, and Annalise G. Blum

Chapter A of

Attribution of Monotonic Trends and Change Points in Peak Streamflow Across the Conterminous United States Using a Multiple Working Hypotheses Framework, 1941–2015 and 1966–2015

Karen R. Ryberg, editor

Prepared in cooperation with
U.S. Department of Transportation
Federal Highway Administration

Professional Paper 1869

U.S. Department of the Interior
U.S. Geological Survey

U.S. Geological Survey, Reston, Virginia: 2022

For more information on the USGS—the Federal source for science about the Earth, its natural and living resources, natural hazards, and the environment—visit https://www.usgs.gov or call 1–888–ASK–USGS.

For an overview of USGS information products, including maps, imagery, and publications, visit https://store.usgs.gov.

Suggested citation:
Barth, N.A., Ryberg, K.R., Gregory, A., and Blum, A.G., 2022, Introduction to attribution of monotonic trends and change points in peak streamflow across the conterminous United States using a multiple working hypotheses framework, 1941–2015 and 1966–2015, chap. A *of* Ryberg, K.R., ed., Attribution of monotonic trends and change points in peak streamflow across the conterminous United States using a multiple working hypotheses framework, 1941–2015 and 1966–2015: U.S. Geological Survey Professional Paper 1869, p. A1–A29, https://doi.org/10.3133/pp1869.

Associated data for this publication:
Dudley, R.W., Archfield, S.A., Hodgkins, G.A., Renard, B., and Ryberg, K.R., 2018, Peak-streamflow trends and changepoints and basin characteristics for 2,683 U.S. Geological Survey streamgages in the conterminous U.S. (ver. 3.0, April 2019): U.S. Geological Survey data release, https://doi.org/10.5066/P9AEGXY0.

York, B.C., Ryberg, K.R., Asquith, W.H., Chase, K.J., Dickinson, J.E., Dudley, R.W., Harden, T.M., Hodgkins, G.A., Holtschlag, D.J., Humberson, D.G., Konrad, C.P., Levin, S.B., Restivo, D.E., Sando, R., Sando, S.K., Swain, E.D., Tillery, A.C., and Totten, A.R., 2022, Attributions for nonstationary peak streamflow records across the conterminous United States, 1941–2015 and 1966–2015: U.S. Geological Survey data release, https://doi.org/10.5066/P9FOUVWG.

ISSN 2330-7102 (online)

Acknowledgments

The work described in this professional paper was funded by the Federal Highway Administration of the U.S. Department of Transportation through Interagency Agreement DTFH6116X30020, “Flood Frequency Estimation for Hydraulic Design.” The authors would like to acknowledge Benjamin York of the U.S. Geological Survey (USGS) for the creation of figures A1 and A2 and for additional geographic information system (GIS) support throughout the project. Jacqueline C. Olson (USGS) updated figures A1 and A2, provided consistency among many figures in the eight chapters, and ensured that they adhered to USGS standards for illustrations. The authors thank Kathleen Macek-Rowland and Jory Hecht of the USGS for their thoughtful colleague reviews.

Contents

Figures

Tables

Conversion Factors

Multiply	By	To obtain
	Length	
inch (in.)	2.54	centimeter (cm)
inch (in.)	25.4	millimeter (mm)
mile (mi)	1.609	kilometer (km)
meter (m)	3.281	foot (ft)

Temperature in degrees Fahrenheit (°F) may be converted to degrees Celsius (°C) as follows:

$$°C = (°F - 32) / 1.8.$$

Datum

Horizontal coordinate information is referenced to the North American Datum of 1983 (NAD 83).

Supplemental Information

A “water year” is the 12-month period from October 1 through September 30 of the following year that is designated by the calendar year in which it ends.

The 75-year and 50-year study periods described in this report span water years 1941–2015 and 1966–2015, respectively.

Abbreviations

<	less than
AMO	Atlantic Multidecadal Oscillation
AO	Arctic Oscillation
AR	atmospheric river
CADDIS	Causal Analysis/Diagnosis Decision Information System
CONUS	conterminous United States
ENSO	El Niño-Southern Oscillation
EPA	U.S. Environmental Protection Agency
ETC	extratropical cyclone
FHWA	Federal Highway Administration
GAGES-II	Geospatial Attributes of Gages for Evaluating Streamflow, Version II
HCDN	Hydro-Climatic Data Network of Slack and Landwehr (1992)
HCDN-2009	Hydro-Climatic Data Network 2009
HUCs	hydrologic unit codes
IPCC	Intergovernmental Panel on Climate Change
MCS	mesoscale convective system
MWHs	multiple working hypotheses
NAM	North American Monsoon
NAO	North Atlantic Oscillation
NPI	North Pacific Index
NWIS	National Water Information System
PDO	Pacific Decadal Oscillation
PDSI	Palmer Drought Severity Index
PFF	peak-flow file
PNA	Pacific/North American teleconnection pattern
p-value	attained significance level
SOI	Southern Oscillation Index
TC	tropical cyclone
USGS	U.S. Geological Survey
WSCVD	winter-spring center of volume dates

Introduction to Attribution of Monotonic Trends and Change Points in Peak Streamflow Across the Conterminous United States Using a Multiple Working Hypotheses Framework, 1941–2015 and 1966–2015

By Nancy A. Barth,[1] Karen R. Ryberg,[1] Angela Gregory,[1] and Annalise G. Blum[2]

Abstract

Flood-frequency analysis plays a critical role in the assessment of risk, protection of lives, and planning and design of flood protection infrastructure. Traditional flood-frequency analysis is based on the assumption of stationarity—that is, that the distribution of floods at a given site varies around a particular mean within a particular envelope of variance (and skew) and that these parameters of the distribution do not vary over time. Uncertainty remains as to what degree of violations of the assumption of stationarity warrants the use of a modified method for flood-frequency analysis and what the modified method(s) should be. The current U.S. Federal Government guidelines for flood-frequency analysis, known as Bulletin 17C, do not provide methods to address nonstationarity (J.F. England, Jr., and others, 2018, U.S. Geological Survey Techniques and Methods, book 4, chap. B5).

Potential changes to flood distributions may be the result of numerous factors, some of which operate at the watershed scale, the regional scale, or the continental or global scale. To develop a cohesive national approach for incorporating potential or observed changes into flood-frequency estimates, national and regional experts from the U.S. Geological Survey and cooperators worked together to develop a multiple working hypotheses framework for making attributions and a common vocabulary for making provisions of confidence. Seven regional teams of subject-matter experts used datasets to evaluate plausible causes for statistically significant (*p*-value [attained significance level] <0.10) monotonic trends and change points in annual peak-streamflow data for the conterminous United States. These seven regions are the Pacific Northwest, Upper Plains, Midwest, Northeast, Southwest, South-Central, and Southeast. This first chapter describes the development of a list of factors to which monotonic trends and change points in annual peak-streamflow data may be attributed and presents a literature review. The subsequent chapters provide the methods used for causal attribution in the seven regions.

Overall, metrics of precipitation and the degree of regulation were the most common attributions used to account for monotonic trends and change points. Different regional teams focused more specifically on several types of precipitation they believed were dominant in their regions. The use of these different methodologies by the regional teams highlights the findings that changes in precipitation alone may not always affect annual peak streamflows directly and that the effects of precipitation vary across the country. Additional research may allow for better determination of which precipitation metrics affect particular hydrologic regions as well as whether there are temporal lags between a particular metric and a flood response. There are many definitions of flow regulation, and more research is also needed on what degree of regulation might induce a signal in the peak streamflow. A comparison of existing definitions followed by a comparison between the definitions and the regulation coding of the U.S. Geological Survey peak-flow file would be informative and could lead to a better definition of regulation that affects peak streamflow. As we continue to better understand natural and anthropogenic causes of changes in flood regimes, more and better ancillary data can help to inform causal attributions used to account for observed changes.

Introduction

Flood-frequency analysis plays a critical role in the assessment of risk, protection of lives, and planning and design of flood protection infrastructure. Analysis of the frequency of floods is commonly based on the assumption that the observed record is representative of long-term features of the flood distribution at a site. That is, traditional flood-frequency analysis assumes stationarity—that the distribution of floods at a given site varies around a particular mean within a particular envelope of variance (and skew) and that these

[1]U.S. Geological Survey.

[2]Johns Hopkins University.

parameters of the distribution do not vary over time. However, the hydrologic community acknowledges that there are many violations of the assumption of stationarity in the distribution of floods at a site and that the nonstationarities (gradual or abrupt) are caused by natural or human-induced changes to the environment (Milly and others, 2008; Olsen and others, 2010; Hirsch, 2011; Barros and others, 2014; Gül and others, 2014; Bayazit, 2015; Razavi and others, 2015; Kolars and others, 2016). In the most extreme cases of nonstationarity, it is critical to explore the nature of the relationship between flood frequency and magnitude by using the observed flood records, as well as the changing state of atmospheric, land-surface and land-cover, and channel characteristics that affect floods (Villarini and Slater, 2017).

Adjustment of flood-frequency analysis for nonstationarity remains an active area of research. Uncertainty remains as to what degree of violations of the assumption of stationarity should require the use of a modified method for flood-frequency analysis and what the modified method(s) should be (Koutsoyiannis, 2006; Kiang and others, 2011; Vogel and others, 2011; Westra and others, 2014; Read and Vogel, 2015, 2016; Obeysekera and Salas, 2016; Salas and others, 2018; Mondal and Daniel, 2019). The current U.S. Federal Government guidelines for flood-frequency analysis, known as Bulletin 17C, do not provide methods to address nonstationarity. In Bulletin 17C, England and others (2018, p. 37) stated:

> There is much concern about changes in flood risk associated with climate variability and long-term climate change. Time invariance was assumed in the development of these Guidelines. In those situations where there is sufficient scientific evidence to facilitate quantification of the impact of climate variability or change in flood risk, this knowledge should be incorporated in flood frequency analysis by employing time-varying parameters or other appropriate techniques. All such methods employed need to be thoroughly documented and justified.

Much has been done to describe and apply methodologies to detect and model nonstationarities. Bulletin 17C provides guidance in examining annual peak-streamflow time series for errors in the data, autocorrelation, trends, and shifts (England and others, 2018); the U.S. Army Corps of Engineers has created the Nonstationarity Detection Tool (Friedman and others, 2018); and there is a global body of research results reporting trends and change points in annual peak-streamflow data.

Potential changes to flood distributions may be the result of a number of factors, some of which operate at the watershed scale (such as changes to land drainage or urbanization), some of which operate at the regional scale (such as changes to snowpack), and some of which operate at the continental or global scale (such as changes to climate and large-scale weather patterns) (Leopold, 1968; Hollis, 1975; Wibben, 1976; Graf, 1977; Sauer and others, 1983; Changnon and Demissie, 1996; Dudley and others, 2001; Smith and others, 2002; Shuster and others, 2005; Moglen and Shivers, 2006; White and Greer, 2006; Hejazi and Markus, 2009; Sheng and Wilson, 2009; Ogden and others, 2011; Merz and others, 2012; Over and others, 2016; Zhang and others, 2018).

This current work builds upon a previous effort by the U.S. Geological Survey (USGS) and the Federal Highway Administration (FHWA) of the U.S. Department of Transportation to identify statistically significant monotonic trends (trends) and change points in annual peak streamflows (peaks) across the conterminous United States (Dudley and others, 2018; Hodgkins and others, 2019; Ryberg, Hodgkins, and Dudley, 2020). In an effort to develop a cohesive national approach for incorporating potential or observed changes into flood-frequency estimates when necessary, national and regional experts from the USGS and cooperators worked together to develop a multiple working hypotheses (MWHs) framework for attributions and a common vocabulary for making provisions of confidence.

Graphs of annual peak-streamflow data may show monotonic trends and change points. Monotonic trends are gradual changes in which annual peak streamflow is generally increasing or generally decreasing, but the change is not necessarily linear. Change points (also called step trends) are abrupt changes in the distribution parameters of annual peak streamflow.

Using the work of Dudley and others (2018), Hodgkins and others (2019), and Ryberg, Hodgkins, and Dudley (2020), regional subject-matter experts in the USGS examined statistically significant (p-value<0.10) monotonic trends and change points in the peak-streamflow data, along with ancillary datasets that might explain the changes, and made attributions when possible. These regional expert teams then independently developed and applied methods to quantify the relationship between changes in watershed conditions and changes in peak streamflows and made provisions of confidence in the attributions.

This professional paper reports the methods and findings of the effort made by the USGS scientists and cooperators for the conterminous United States (CONUS). In this first chapter, the development of a list of attributions for trends is discussed and presented with a literature review for the attributions. Also discussed is the development of a vocabulary for a provision of confidence in attribution. The subsequent chapters provide the methods used for causal attribution in the seven CONUS regions we examined, whereas this chapter highlights some of the challenges of making attributions across hydrologically heterogeneous regions of the United States. Differences in how each regional team approached the problem can inform future work on attributions.

Data and Development of Attribution Methodology

This section describes site selection, annual peak-streamflow data, analysis periods, and regional study boundaries. This section also describes the MWHs framework and potential causal mechanisms that explain trends and change points.

Site Selection, Regional Teams, and Regions

The sites used in this study are identical to those used in the first phase of work, which entailed the detection of monotonic trends and change points in annual peak-streamflow data from streamgages. This first phase, also funded by the FHWA, resulted in two papers publishing the trends results (Hodgkins and others, 2019; Ryberg, Hodgkins, and Dudley, 2020) and a data release providing some streamgage characteristics (Dudley and others, 2018). Site selection was described in those publications and is summarized here.

The streamgages used for the analyses across the United States were selected from version II of the Geospatial Attributes of Gages for Evaluating Streamflow (GAGES-II) database (Falcone, 2011), which contains the geospatial data available for each streamgage, including several hundred basin characteristics that could facilitate subsequent attribution efforts. Streamgages were assigned to four categories: (1) basins with minimal human alterations from the USGS Hydro-Climatic Data Network 2009 (HCDN-2009), which represents streamgages that are suitable for analyzing hydrologic variations and trends caused by climatic changes (Lins, 2012); (2) regulated basins (high regulation and low urbanization); (3) urban basins (greater than 10-percent developed and having low flow regulation); and (4) basins not in these categories (uncategorized). The 2,683 streamgages used with selected geospatial attributes, the categories to which they were assigned, and the definitions of the categories are available in the above-mentioned data release by Dudley and others (2018). The annual peak-streamflow data used in this study came from the dataset known as the “peak-flow file” (PFF) and are available as part of the USGS public web interface, the National Water Information System (NWIS), at https://nwis.waterdata.usgs.gov/usa/nwis/peak (U.S. Geological Survey, 2019a).

Three periods were selected for trend and change-point analysis: (1) a 100-year period, 1916–2015; (2) a 75-year period, 1941–2015; and (3) a 50-year period, 1966–2015. The years are water years; each represents the 12-month period from October 1 through September 30 of the following year and is designated by the calendar year in which it ends. Three trend periods provide a tradeoff between being able to make statements based on the longest streamgage records in the country and the better spatial resolution available with shorter periods of record. As with any trend analysis, the trends reported can be sensitive to the start and end dates of the trend period. Peak-streamflow records in each of these time periods were required to have 80-percent completeness for each decade; for example, 1930–39 was required to have 8 of 10 water years of record. For partial decades, 1916–19 was required to have 3 of 4 years; 1941–49, 7 of 9 years; 1966–69, 3 of 4 years; and 2010–15, 5 of 6 years. Because of sparse spatial coverage for period 1, periods 2 and 3 were the focus of this second phase of the project, attribution of monotonic trends and change points.

Seven regional teams of USGS staff and cooperators with subject-matter expertise in peak streamflows, regional hydrology, and data analysis were formed. Then the CONUS was divided into seven regions based on water-resources regions, which are geographic areas that either contain the entire drainage area of a major river, such as the Missouri water-resources region, or combine drainage areas of geographically proximate rivers, such as the Texas-Gulf region, which includes a number of rivers draining into the Gulf of Mexico. These regions are based on those identified by two-digit hydrologic unit codes described in Seaber and others (1987). Then minor modifications were made to some regions by adding or subtracting subregions, defined by four-digit hydrologic unit codes (Seaber and others, 1987), in the interest of geographic cohesiveness or hydrologic-setting similarity. Although some regions are shown on maps in this report as extending into Canada or Mexico because of the topography of stream drainage basins, the watersheds considered for attribution are within the CONUS.

The seven regions used in this study are as follows:

1. Pacific Northwest region: water-resources region 17 (Pacific Northwest), plus subregion 1801 (Klamath-Northern California Coastal) of water-resources region 18 (California)

2. Upper Plains region: water-resources regions 09 (Souris-Red-Rainy) and 10 (Missouri)

3. Midwest region: water-resources regions 04 (Great Lakes), minus subregions 0413 (Southwestern Lake Ontario), 0414 (Southeastern Lake Ontario), and 0415 (Northeastern Lake Ontario-Lake Ontario-St. Lawrence); 05 (Ohio); and 07 (Upper Mississippi)

4. Northeast region: water-resources regions 01 (New England) and 02 (Mid-Atlantic) plus subregions 0413 (Southwestern Lake Ontario), 0414 (Southeastern Lake Ontario), and 0415 (Northeastern Lake Ontario-Lake Ontario-St. Lawrence) of water-resources region 04 (Great Lakes)

5. Southwest region: water-resources regions 14 (Upper Colorado), 15 (Lower Colorado), 16 (Great Basin), and 18 (California), minus subregion 1801 (Klamath-Northern California Coastal)

6. South-Central region: water-resources regions 11 (Arkansas-White-Red), 12 (Texas-Gulf), and 13 (Rio Grande)
7. Southeast region: water-resources regions 03 (South Atlantic-Gulf), 06 (Tennessee), and 08 (Lower Mississippi)

The seven regions are depicted in figure A1 and are further described in the subsequent chapters of this professional paper. In figure A1, the colored areas within the regions, such as the Southeast, indicate the watersheds considered for attribution.

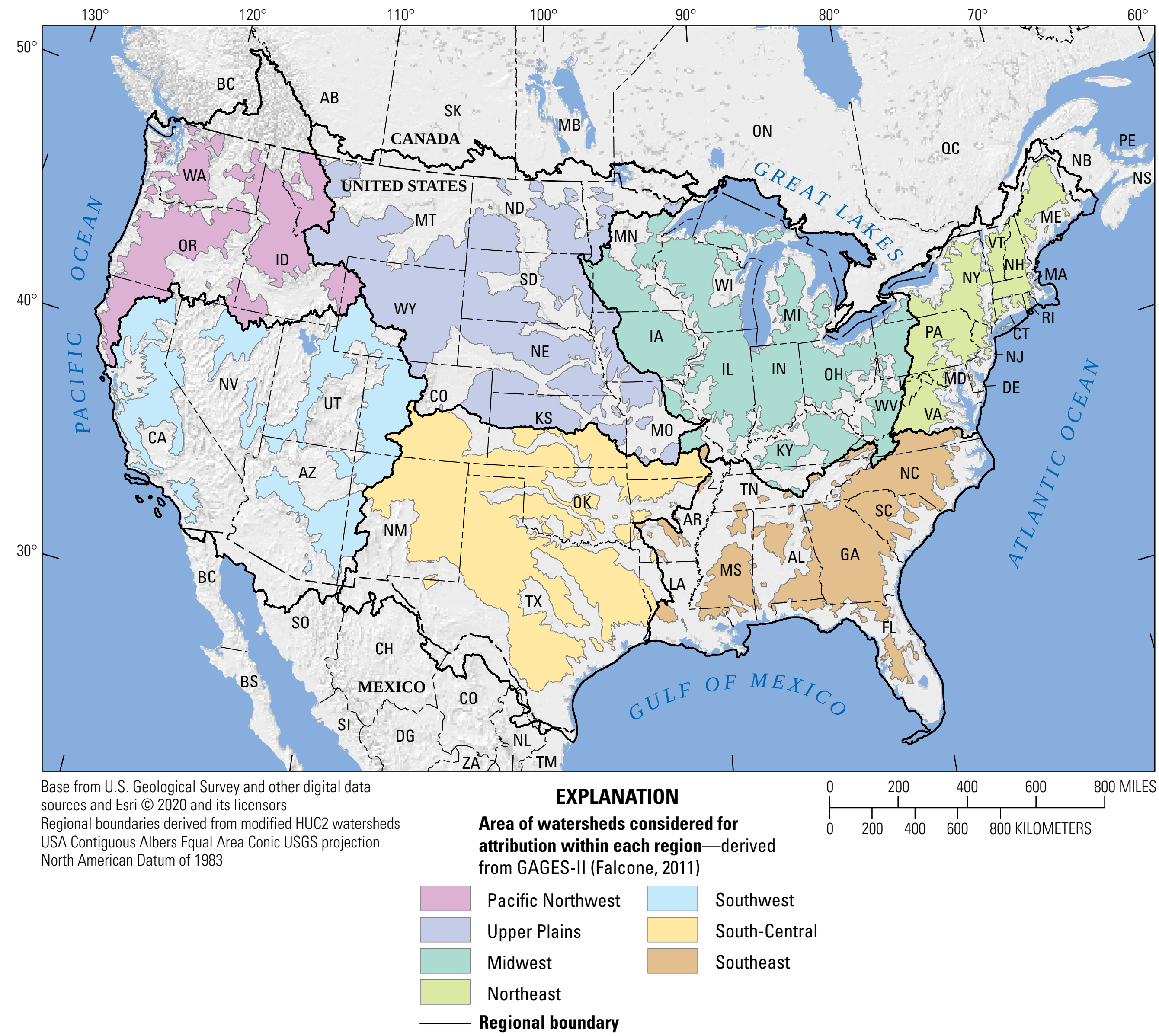

Figure A1. Map of the conterminous United States (CONUS) and adjacent areas in Canada and Mexico showing the seven regions in this study and the watersheds in the CONUS considered for attribution (colored areas). Although the study regions are shown as extending into Canada or Mexico because of the topography of stream drainage basins, the watersheds considered for attribution are within the CONUS. For this study, the regions were based on water-resources regions identified by two-digit hydrologic unit codes (HUC2s) described by Seaber and others (1987), and some regions were modified slightly by adding or subtracting subregions (HUC4s) to achieve geographic cohesiveness or hydrologic-setting similarity. GAGES-II, Geospatial Attributes of Gages for Evaluating Streamflow, Version II (Falcone, 2011).

Attribution Versus Statements of Causality

Terminology related to causal analysis is fraught. Many people with statistical training have repeatedly heard the adage, “correlation is not causation.” Many examples of spurious correlation exist as cautionary tales about blindly interpreting correlation as causation (Vigen, 2015).

Historically, there have been two extreme views for causal analysis: (1) it cannot be done, or (2) it can be done only with controlled laboratory experiments (Ward, 2009). The philosopher, logician, and mathematician Bertrand Russell exemplified the first extreme in his 1912 address to the Aristotelian Society in which he said (Russell, 1913, p. 1):

> I wish, first, to maintain that the word “cause” is so inextricably bound up with misleading associations as to make its complete extrusion from the philosophical vocabulary desirable. All philosophers, of every school, imagine that causation is one of the fundamental axioms or postulates of science, yet, oddly enough, in advanced sciences such as gravitational astronomy, the word “cause” never occurs.

These extremes were discussed by Ward (2009, p. 1) in an epidemiological context in which “one of the most important problems in the social and health sciences concerns making justified causal inferences using non-experimental, observational data.” This problem also exists for earth and environmental sciences. The complex interactions in the environment cannot all be controlled and observed in a laboratory, in part because of complexity, but also in part because of how different spatial and temporal scales affect the outcomes of interest. Yet, to make their work useful to resource managers and other decision makers, hydrologists make some statements about cause and effect.

The concept of causal analysis has been expanded beyond controlled laboratory experiments by Judea Pearl (2000), who described the possibility of doing causal analysis through a combination of graphical methods (acyclical directed graphs), structural equations, mathematically defined causal criteria, counterfactuals, and comparisons to predicted consequences. Such causal analysis is still daunting to many. Pearl has more recently espoused the concept of “causal thinking” to bring causal study to a broader audience (Pearl and MacKenzie, 2018). In Pearl and MacKenzie (2018, p. 89), Pearl documented how the rule of “correlation is not causation” actually delayed development of causal methods and acknowledged the inherent subjectivity in causal analysis:

> … [C]ausal analysis requires the user to make a subjective commitment. She must draw a causal diagram that reflects her qualitative belief—or, better yet, the consensus belief of researchers in her field of expertise—about the topology of the causal processes at work. She must abandon the centuries-old dogma of objectivity for objectivity’s sake. Where causation is concerned, a grain of wise subjectivity tells us more about the real world than any amount of objectivity.

Despite these new views on causality, the term remains burdened with many positive and negative connotations. The body of hydrologic literature used to inform this work is more apt to use the terms “attribute” and “attribution,” which have causal meanings, but without as much historical and philosophical baggage. As described in the section, “Establishing Potential Attributions of Trends and Change Points by Using a Multiple Working Hypotheses Framework,” the method of MWHs has been used recently in hydrology as a way to investigate potential causal factors for the phenomena being studied. Papers cited that influenced our development of MWHs used the words “attribute” or “attribution” in the title: “More Efforts and Scientific Rigour are Needed To Attribute Trends in Flood Time Series” (Merz and others, 2012) and “Attribution of Detected Changes in Streamflow Using Multiple Working Hypotheses” (Harrigan and others, 2014). These words are also commonly used in publications discussing the causes (often described as “drivers” because of the hesitancy of many to use the term “cause”) of changes in streamflow, flooding, and climate (see for example, Wang and others, 2009; Hegerl and Zwiers, 2011; Kay and others, 2011; Trenberth, 2011; Alter and others, 2018; Neri and others, 2019).

Informed by Pearl’s causal analysis and causal thinking philosophy, statistical methodology, and the literature on attribution hydrology and climatology, experts assigned to this project used a variety of methods to support attributions of monotonic trends and change points in peak-streamflow data. These methods included the development and group discussion of multiple working hypotheses for the causes of changes in peak streamflow, correlation analyses, numerous graphical analyses, the comparisons of trends in variables representative of causes and effects, citing the works of others, application of subject-matter expertise on earth and environmental processes and cause-and-effect relations (causal thinking), and the accumulation of multiple lines of evidence. Each regional team used a different set of methodologies for many reasons, including the fact that not all causal factors are the same across the CONUS (for example, some flood regimes are more influenced by atmospheric rivers than others), some potential explanatory datasets are not available nationwide (such as the Missouri River Basin Depletions Database [Bureau of Reclamation, 2012], which is available for that basin only), and some regional teams could rely on detailed studies by other hydrologists more than other teams.

Establishing Potential Attributions of Trends and Change Points by Using a Multiple Working Hypotheses Framework

T.C. Chamberlin suggested the “method of multiple working hypotheses” in 1890 as a way to promote thoroughness and an open mind about how potential causal factors interact, while highlighting deficiencies in our knowledge. The method involves listing the hypotheses that explain the phenomenon in question prior to study in the interest in of being open minded and thorough in thinking before analysis.

Chamberlin described the method as a means by which to avoid “the dangers of parental affection” for pre-existing theory (Chamberlin, 1890, 1897; Railsback, 2004). The MWHs method has been criticized as a chimera (Johnson, 1990), or an illusory goal, and it is still subject to the biases of analysts; however, the concept periodically resurfaces and is defended as a useful means of organizing research (Chamberlin, 1965; Railsback and others, 1990; Rau and Chamberlin, 1995; Railsback, 2004).

Recently, MWHs have resurfaced in hydrology. Clark and others (2011) advocated for the MWHs framework in hydrologic modeling. Merz and others (2012, p. 1379) argued that flood trend attribution is generally “based on qualitative reasoning or even speculation” and often is a listing of references to related works that support the authors’ conclusions. Harrigan and others (2014) cited the work of Merz and others (2012) and used Chamberlin’s (1890) method of MWHs for attribution of detected changes in streamflow by identifying a wider set of potential drivers of hydrological change in a basin. They described each hypothesized driver’s potential influence on the basin, made a judgment as to whether the driver affected the basin (or acknowledged lack of current information), and identified which drivers were appropriate for further statistical analysis (Harrigan and others, 2014). The USGS has been using MWHs to provide a framework for thinking about ways to better support attributional statements about trends (Ryberg, 2017; Ryberg and others, 2018; Ryberg, Stone, and Baker, 2020), and other examples can be found in Harrigan and others (2014) and Michalak and others (2013). This framework can acknowledge proximate and underlying causes of flood nonstationarity and factors that affect both moisture inputs and watershed response.

Using a MWHs framework, the seven regional teams first developed a list of potential mechanisms for nonstationarity in annual peak-streamflow records for their regions and investigated whether data were available to test these hypotheses. The MWHs were then combined, the wording was refined, and, in some cases, categories were combined. This process resulted in a list of the possible attributions (table A1) that each team then used to assess potential causal mechanisms in trends and change points and to make attributions. These potential attributions are discussed in the following literature review.

Some of the attribution hypotheses (table A1) are easier to test than others because of their larger effect (large artificial impoundments versus the aggregate effect of small artificial impoundments) or because of data availability. This variation in testability is a hallmark of the multiple working hypotheses framework. The fact that one identifies a factor as a potential mechanism does not mean that one can test it. However, one can still show that these factors were considered.

Provision of Confidence Level

Unique to this attribution effort for changes in peak streamflow was a provision of confidence level. In any attribution of a trend or change point, the degree of confidence may vary from a hunch to certainty based on the analyst’s understanding of hydrological processes at a site and the degree to which the change has been studied or modeled. In addition, the vocabulary of confidence and the comfort with ascribing an attribution can vary among analysts. In the interest of developing a common language of confidence levels, we surveyed such efforts made in other areas of environmental science.

The U.S. Environmental Protection Agency (EPA) developed a Causal Analysis/Diagnosis Decision Information System (CADDIS) to support causal assessments of aquatic ecosystems (U.S. Environmental Protection Agency, 2018a). Members of the EPA provided a vocabulary for describing the strength of evidence for candidate causes of impairments. Their words or phrases for strength of evidence include “refuted” (that is, the cause was refuted by indisputable evidence or diagnostic systems), “diagnosed,” “probable,” “probable with low confidence,” “unlikely,” “unlikely with low confidence,” and “additional information required” (U.S. Environmental Protection Agency, 2018b).

A guidance note for authors of the Intergovernmental Panel on Climate Change (IPCC) Fifth Assessment Report was developed to support a common approach and language for uncertainties (Mastrandrea and Mach, 2011; Mastrandrea and others, 2011). The evidence and agreement statements were combined into a matrix with nine cells; the *x*-axis provides levels of evidence—limited, medium, robust—and the *y*-axis provides levels of agreement—low, medium, high. In this matrix, the lower left cell represents limited evidence for a finding based on low agreement of multiple lines of evidence. The upper right cell represents robust evidence for a finding based on high agreement of multiple lines of evidence (Mastrandrea and others, 2011, fig. 2).

The “Climate Science Special Report,” which is volume I of the “Fourth National Climate Assessment” released by the U.S. Global Change Research Program (Wuebbles and others, 2017), uses two metrics: confidence and likelihood. The “Guide to the Report” in the front matter of volume I contains a section titled “Treatment of Uncertainties: Likelihoods, Confidence, and Risk Framing.” In figure 2 of that section, the terminology used in volume I is explained. The four confidence categories used were “low,” “medium,” “high,” and “very high,” whereas the nine likelihood categories ranged from “virtually certain” (99–100 percent) and “extremely likely” (95–100 percent), through “about as likely as not” (33–66 percent) to “extremely unlikely” (0–5 percent) and “exceptionally unlikely” (0–1 percent).

Table A1. List of attributions used in the multiple working hypotheses framework to assess potential causal mechanisms for monotonic trends and change points in peak-streamflow records from seven regions of the conterminous United States.

[Attributions were made in this study on the basis of peak-streamflow records and ancillary datasets. Attributions in this table are listed in the order in which they are described in the section of this chapter titled “Literature Review of Attributions”; that order was generally based on the likelihood of the attributions being made for the conterminous United States in the study time periods. --, indicates no additional description]

Attribution	General description
	Climate variability
Short-term precipitation	Short-term precipitation (event-related heavy and extreme precipitation) or increases in heavy precipitation.
Long-term precipitation	Long-term precipitation (monthly to multiyear precipitation representative of month-long storm systems, antecedent wetness or dryness, climatic persistence, or multi-decadal climate variability caused by oceanic or atmospheric patterns).
Multidecadal climate variability	In some cases, attribution was a combination of long-term precipitation and air temperature, and the primary cause could not be determined. In those cases, multi-decadal climate variability was the primary attribution.
Snowpack	Snowpack and ice development and melt (caused by seasonal air temperature and precipitation), or solid precipitation.
Air temperature	Air temperature other than snowpack related.
	Impoundments and diversions
Large artificial impoundments	Large artificial impoundments that are big enough to influence peak streamflows.
Small artificial impoundments	Small artificial impoundments, such as run-of-the-river dams, changes to outlets of natural lakes and ponds, stock dams, or other such features that in aggregate influence peak streamflows.
Surface-water withdrawals	Surface-water withdrawals, such as irrigation, municipal water supply, or other.
Groundwater withdrawals	Groundwater withdrawals, such as irrigation, municipal water supply, or other.
Artificial wastewater and water-supply discharges	--
Agricultural drainage activities	Agricultural drainage activities, including those that cause the loss of wetlands.
Interbasin water transfers	--
	Land-use and land-cover changes
Agricultural crop production	Agricultural crop production, such as conversion from perennial to annual vegetation, conversion from small grains to row crops, or multiple plantings of different crops within the same fields.
Rangeland grazing activities	--
Invasive woody species (riparian)	--
Deforestation and wildfire	--
Urban effects	Urban effects, such as how urban land covers affect precipitation patterns and storm runoff. Urban effects also include increases in impervious area and stormwater infrastructure, curbs and gutters, and loss of wetlands. Urban water use is a separate issue.
	Glaciation, geomorphological changes, volcanic activity, and sea-level rise—Potential attributions considered in this study but not identified as primary or secondary attributions
Glaciation	--
Geomorphological changes	Geomorphological changes, including changes induced by seismic activity.
Volcanic activity	--
Sea-level rise	--
	Unknown causes
Unknown causes	Unknown causes, including statistical analysis methods that may result in false positives for trends or change points; therefore, there may be no known mechanism for causing a trend or change point.

Members of the regional teams for the current study also observed variations in how team members interpreted statements of likelihood or confidence; they found that there is a great deal of variation in the interpretation of words associated with confidence or probability, as was previously discussed by Mauboussin and Mauboussin (2018). Given the ambiguity and variation in interpretation, simple statements about the level of evidence and confidence for attributions were desired for this study. Only positive attributions were made, in contrast to the EPA system, which included refutation of possible causal mechanisms (U.S. Environmental Protection Agency, 2018b). An option was included for regional teams to indicate that the attribution is to unknown causes, and additional information is required. Table A2 shows the vocabulary used to support attributional statements in this study.

Literature Review of Attributions

This section provides a literature review of potential attributions for monotonic trends and change points in peak-streamflow data examined by the regional subject-matter experts.

Inconsistent Quality in Annual Peak-Streamflow Data and Ancillary Data

Before attempting to attribute changes in annual floods to potentially correlate with variations in ancillary data, it is important to understand the extent to which inconsistencies in data quality may confound these associations. The primary data used in this study come from the dataset known as the “peak-flow file” (PFF) and are available as part of the USGS public web interface, NWIS, at https://nwis.waterdata.usgs.gov/usa/nwis/peak (U.S. Geological Survey, 2019a). This dataset is commonly used by organizations outside the USGS to design water and transportation infrastructure, delineate floodplain boundaries, and regulate development and utilization of lands throughout the United States, and it provides essential information for understanding the implications of climate change on flooding (Ryberg, 2008).

The methods to accurately estimate peak streamflow from stage-discharge relations, high-water marks, indirect measurements, or routing/modeling techniques have varied over time, and so has the documentation of these estimates (Ryberg and others, 2017). However, the extent of temporal changes in data quality is unknown. As with any other dataset, the PFF has been subject to a variety of human errors. Internal technical reviews, regional-flood studies, and user inquiries have identified many minor and some major problems in the PFF; therefore, a years-long effort to improve the quality and consistency of the dataset was undertaken in 2008 and summarized in 2017 (Ryberg, 2008; Ryberg and others, 2017; Williams-Sether and others, 2017). Because of this effort to improve the quality and consistency of annual peak-streamflow data, the data were assumed to be correct and consistent for this study. In addition to the peak-streamflow data, various other data sources were used to make attributional statements. These ancillary data also likely vary temporally in quality; however, an investigation of such issues in ancillary data is beyond the scope of this study.

Climate Variability—Short-Term and Long-Term Precipitation, Snowpack, and Air Temperature

This section describes temporal and spatial changes in climate characteristics that can be attributed to observed trends in annual peak-streamflow data. Hodgkins and others (2019) examined, among other basin types across the CONUS, minimally altered basins from the HCDN-2009 (USGS Hydro-Climatic Data Network 2009, which represents streamgages that are suitable for analyzing hydrologic variations and trends caused by climatic changes; Lins, 2012) for historical trends that would be forced primarily by climatic changes.

Table A2. Vocabulary used to support attributional statements used in this study.

Vocabulary	Further description
Robust evidence	One or more of the following: strong and consistent results, multiple sources (datasets, studies, analyses), well-documented data, and attribution that is consistent with causal mechanisms.
Medium evidence	One or more of the following: moderate consistency, emerging results, or weight of evidence points in the direction of attribution but there may be some divergent findings.
Limited evidence	Limited sources or inconsistent findings.
Unknown attribution, additional information required	Insufficient evidence to make an attribution.

In general, they found a low percentage of basins with significant increases or decreases (5–14 percent and 5–10 percent, respectively) during the 50-, 75-, and 100-year periods. However, for 50-year records, they found large decreases in the peak-flow trend magnitude in the central United States (from the Dakotas to Texas) and large increases in the Midwest. Often, precipitation and temperature are the first attributions explored for observed trends in annual peak streamflows. Yet in recent studies (Small and others, 2006; Ivancic and Shaw, 2015; Neri and others, 2019), more attention has focused on evaluating the combination of extreme precipitation events and periods with extreme floods with the additional contributions from antecedent soil moisture. Burn and others (2016), Burn and Whitfield (2018), and Vano and others (2019) found changes in the flood-generating mechanisms from snowmelt dominated to a mixture of rainfall and snowmelt dominated. As described in Hirschboeck (2009), in the subfield of hydroclimatology, there is a need to evaluate hydroclimatic changes and hydrologic extremes in the temporal and spatial domains across a variety of scales such as from watershed or basin scales (Archfield and others, 2016) to regional scales. For additional reviews on attributions related to climate variability and flooding, see Villarini and Slater (2017) and Villarini and others (2018).

Short-Term Precipitation

In recent years, much attention has been given to investigating changes in short-term (event-related) heavy and extreme precipitation. Short-term precipitation events include those related to atmospheric rivers (ARs; long and narrow corridors transporting large amounts of moisture from the tropics to the extratropics [Zhu and Newell, 1998]), mesoscale convective systems (MCSs; organized clusters of storms), tropical cyclones (TCs) and their remnant precipitation, and the North American Monsoon (NAM) (Kunkel and others, 2012; Barth and others, 2018). On the basis of nine designated regions in the CONUS, Kunkel and others (2012) found upward trends in the following: the frontal category (extratropical cyclone near a front) in five of the nine regions; extratropical cyclones near the center of a low (ETCs) in the Northeast and the eastern north-central region; NAMs in the west; and TCs in the central region. Easterling and others (2017) found that MCSs, the main mechanisms for the warm-season precipitation in the central United States, have increased in occurrence and precipitation amounts since 1979. Meanwhile, Collins and others (2014) found little evidence of changes in the proportion of storm tracks, such as those generated from Great Lakes-sourced storms and Nor'easters that affect lower and higher magnitude annual peak floods in the Northeast, between the pre- and post-1970s periods in longer term annual peak streamflow records from 1949 to 2006.

As recently summarized in Volume 1 of the "Fourth National Climate Assessment" (Easterling and others, 2017) and in Kunkel and others (2012), heavy precipitation (defined as the 1-percent heaviest of all daily events) increased in most of the United States in both intensity and frequency from 1958 to 2012. The greatest observed changes are found in the Northeast, Midwest, Southeast, and Great Plains. Groisman and others (2004) and the Soil and Water Conservation Society (2003) found increases in heavy and very heavy (daily rain events between 2 to 4 inches) precipitation over the CONUS primarily occurring since 1970. Groisman and others (2012) found that, over the past 30 years, there had been significant increases in the frequency of very heavy and extreme precipitation events (defined as daily and multiday rain events with totals above 6 inches) as well as a 40-percent increase in the frequency of daily and multiday events in the central United States. Similarly, Mallakpour and Villarini (2015) found a stronger signal in the changes in the frequency of heavy precipitation across the CONUS rather than in magnitude. They found an increasing trend in the frequency of heavy precipitation events over most of the CONUS with the notable exception of the Northwest and northern California. Most recently, during the spring of 2019, these increases in the frequency of multiday events of very heavy precipitation led to devastating floods and resulting losses in Iowa ($1.6 billion per Hardy and Cannon, 2019) and Nebraska ($1.3 billion per Schwartz, 2019).

In addition to the significant changes in intensity and frequency of heavy precipitation events, Villarini and others (2011) found evidence of change points in the mean and variance in annual maximum daily rainfall likely linked to changes in the rainfall regime. Similarly, Huang and others (2017) found significant increases in extreme precipitation since 1901 in the northeastern United States best characterized by an abrupt shift (change point) in 1996. They attributed this increase to significant increases in precipitation in the fall and spring; increases in the fall have been attributed to increased heavy precipitation associated with tropical cyclones (Kunkel and others, 2010; Agel and others, 2015; Huang and others, 2017).

Long-Term Precipitation

Long-term precipitation represents monthly to multiyear precipitation from entrainments of month-long persistent storm tracks, antecedent wetness or dryness, climatic persistence, and (or) multidecadal climate variability caused by oceanic and atmospheric patterns such as the Pacific Decadal Oscillation (PDO) and the North Atlantic Oscillation (NAO). In Volume I of the "Fourth National Climate Assessment," Easterling and others (2017) attributed observed trends in long-term precipitation to changes in recurring patterns in large-scale atmospheric circulation (such as the NAO) and the oceanic and atmospheric patterns (such as El Niño-Southern Oscillation, ENSO). In the Pacific Northwest, shifts in the interdecadal climatic oscillations, such as the PDO and ENSO, have been associated with shifts in the amount and location of precipitation in the region (Cayan and Peterson, 1989; Latif and Barnett, 1994; Trenberth and Hurrell, 1994; Minobe, 1997; McCabe and Dettinger, 1999; Nigam and others, 1999;

Bond and Harrison, 2000). In addition, a notable climate shift occurred around 1976 to 1988, which "advected warmer and moister air along the west coast of North America ... [and caused] a southward shift in the storm tracks" (Trenberth and Hurrell, 1994, p. 303).

Recently Dickinson and others (2019) found distinct regional clusters with relations between precipitation and climate indices in the western United States. They also found the most significant correlations between annual peak streamflow and ENSO (via the Multivariate El Niño Southern Oscillation [ENSO] Index [MEI]), the PDO, and the Pacific/North American teleconnection pattern (PNA) in the northwest, southern, and central United States. Their study highlights regional cohesive variations in flood magnitudes across multiple watershed boundaries with various climate indices.

For the north-central United States, extensive research (for example, Vecchia, 2008; Hirsch and Ryberg, 2012; Ryberg and others, 2014, 2016; Ryberg, 2015; Kolars and others, 2016) has identified distinct hydroclimatic persistence characterized by alternating wet and dry periods dating back to the early 1700s. Although some of the researchers have investigated relative contributions from natural and anthropogenic effects on hydroclimatic variability (Wang and Hejazi, 2011; Hirsch and Ryberg, 2012), it is difficult to conclusively separate the effects. Villarini and others (2011) found changes in the clustering of heavy rainfall events, as the NAO, Atlantic Multidecadal Oscillation (AMO), Southern Oscillation Index (SOI), and PDO represented significant predictors for the observed clustering. Similarly, Mallakpour and Villarini (2016) found that the strongest connections between the frequency (not magnitude) of heavy rainfall events (defined as the 95th percentile of the precipitation distribution) and a climate mode were with the PDO, SOI, and PNA.

In addition to the researchers who have examined changes in extreme precipitation and their meteorological causes, many other researchers have focused on the relationship between observed changes in heavy precipitation and changes in streamflow. Their investigations largely stem from studies in which researchers have found nonstationarities in streamflow records via temporal changes as indicated by linear and monotonic trends (Villarini and others, 2009; Peterson and others, 2013), change points such as step changes (McCabe and Wolock, 2002; Villarini and others, 2009), the frequency of floods (Archfield and others, 2016; Neri and others, 2019), and flood inundation (Slater and Villarini, 2016). Commonly, researchers have investigated the relationships between precipitation and flooding by using spatial relationships and direct correlation techniques (see Villarini and Slater, 2017, for a thorough review). For example, McCabe and Wolock (2002) found a shift in mean discharge around 1970 and related the increases in annual streamflow statistics to an increase in precipitation around the same year in the eastern United States (Karl and Knight, 1998). In the north-central United States, changes in precipitation and potential evapotranspiration can be used to explain most of the multidecadal variability in runoff and flood magnitudes, and precipitation has been the dominant driver (Ryberg and others, 2014). On the basis of hydrologic modeling, Frans and others (2013) found that climate change, rather than land-use and land-cover changes, was the dominant driver for the observed increases in runoff from 1918 to 2007 in the Upper Mississippi River Basin.

Berghuijs and others (2016) found that precipitation alone does a poor job of describing the interannual variability of peak streamflows. They found that soil moisture, basin wetness, and rain-on-snow events are much better predictors for flood responses. Similarly, Slater and Villarini (2017) and Neri and others (2019) found that while streamflows have notably increased in the Midwest, of the five predictors used to model the streamflow rates in the Midwest (precipitation, antecedent moisture, air temperature, agriculture, and population density), precipitation is key for modeling high flows, while antecedent moisture is an important secondary driver for low and medium flows. Ivancic and Shaw (2015) found that models which included both soil moisture and heavy precipitation events (top 1 percent) result in better correlations with the top 1-percent annual discharge in the CONUS. From a longer term perspective, Munoz and others (2018) found that extremes in flooding events in the Lower Mississippi River Basin over the past 500 years are associated with the combined effects from ENSO, where El Niño conditions can increase antecedent soil moisture, and the AMO, which controls the flux of moisture from the Gulf of Mexico inland.

In terms of the frequency of heavy precipitation events and flooding, Mallakpour and Villarini (2016) found that the observed changes in the central United States can be largely attributed to variability in climate systems—with the PNA playing a dominant role. Furthermore, Mallakpour and others (2017) found that the Arctic Oscillation (AO) and PNA are both important predictors in explaining the clustering of flood and heavy precipitation events in the central United States. With respect to major floods (defined as floods with a 25- to 100-year return period), Hodgkins and others (2017) found that temporal changes in major floods were dominated by multidecadal variability, such as the AMO, rather than long-term trends. Armstrong and others (2014) and Collins (2019) also found statistical relationships between lagged NAO and flood data as well as a hydroclimatic step increase after 1970 for the Northeast. Wise and others (2018) found that the interactions of both the Pacific and Atlantic Oceans account for the diverse hydroclimatology in the Missouri River Basin. They found that precipitation and resulting flows in the Upper Missouri River Basin are predominantly controlled by zonal patterns from the Pacific Ocean in the winter (the PNA and North Pacific Index [NPI]). In contrast, in the Lower Missouri River Basin, precipitation and flows are controlled by late spring and early summer precipitation from Gulf of Mexico moisture associated with the NAO.

As more attention has been given to investigating the changes in heavy precipitation and the connection to observed changes in streamflow through attribution studies, there is also an emerging body of literature highlighting the need for caution when assessing the potential flood impacts of changes in heavy precipitation. Small and others (2006) and Ivancic and Shaw (2015) examined why trends in heavy precipitation do not always produce trends in streamflow (including high flows). Small and others (2006) found that increases in precipitation in the eastern United States did not augment annual floods because much of the increase took place during the fall, when soil moisture is often depleted and, consequently, flows are generally lower. Other studies (such as one by Slater and Villarini, 2016) have found increasing trends in the low and median flows but not among the high flows. These apparent inconsistencies highlight the need to also examine the timing of increases in flows and heavy precipitation. Sharma and others (2018) added that other basin characteristics may contribute to the seeming paradox that "if precipitation extremes are increasing, [then] why aren't floods?" They suggested that additional attributes such as decreases in soil moisture, storm extent, and snowmelt, for example, should also be investigated.

Snowpack

Mechanisms that have changed seasonal snowpack mass and energy balance include the following: (1) global surface-temperature increases (Hansen and others, 2010); (2) recent precipitation increases in the Dakotas (Wang and others, 2009); (3) pine beetle infestation resulting in tree mortality that reduces canopy cover and increases ground litter, thus ultimately increasing incoming shortwave radiation and decreasing albedo relative to pre-infestation conditions (Winkler and others, 2010, 2014), and (4) alteration of the snowpack energy balance immediately following severe wildfires (Gleason and others, 2013; Harpold and others, 2013). Mote and others (2005, 2018) found a nearly consistent decrease in snowpack in the western United States for the period of 1955–2016. Thirty-three percent of the 699 SNOTEL stations included in the Mote and others (2018) study were found to have experienced statistically significant decreases in peak snow water equivalent measurements taken on April 1 of each year. These observed changes in snowmelt runoff could have an effect on peak streamflows.

In an analysis of snowmelt runoff at 84 sites in the western United States from the original HCDN of Slack and Landwehr (1992), mean April–July runoff during 1950–2003 accounted for 52–87 percent of total annual streamflow on average (McCabe and Clark, 2005). The volume of snowmelt runoff is related to maximum snow water equivalent, the timing of snowmelt, the amount of precipitation falling as snow, watershed characteristics (such as soil type or vegetation cover), and location-specific hydroclimatic conditions.

Increases in air temperatures across the CONUS have led to earlier dates of peak streamflows (Ryberg and others, 2016) or earlier winter-spring center of volume dates (WSCVDs) in many basins (Dudley and others, 2017). The WSCVD values are determined by identifying the time at which 50 percent of streamflow volume has passed a streamgage during some identified period that is usually chosen to limit having to account for the influence of individual rain events (Court, 1962). Because few studies are available on the alteration of peak streamflows resulting from changes in snowpack conditions, the WSCVD is used as a proxy to describe how peak streamflows have changed. Increased temperatures have been widely identified as the most significant contributing factor to earlier WSCVDs (Mote and others, 2005; Regonda and others, 2005; Stewart and others, 2005; Hodgkins and Dudley, 2006; Dudley and others, 2017).

Changes in the quantity and phase of falling precipitation have been only partially implicated in changes in the WSCVD relative to temperature effects. Moreover, in other studies that have focused on trends in solid-phase precipitation, the researchers have come to mixed conclusions. Analyses of snow cover extent, snow water equivalent, and snow depth have also yielded mixed results. April snow cover extent in the western United States for the period of 1967–2015 has generally decreased while April snow cover extent in the central United States has increased (Kunkel and others, 2016). Dudley and others (2017) found that the WSCVD was related to both temperature and precipitation for high-elevation basins in the West. They also found that the WSCVD relation with temperature was much stronger and more common than the relation with precipitation in the East and in low-elevation sites primarily in the Northwest.

Air Temperature

As described in the "Fourth National Climate Assessment" (Vose and others, 2017), the annual average air temperature over the CONUS has increased by 1.2 °F from the period 1901–1960 to the period 1986–2016. In addition to affecting snowpack, temperature changes affect streamflow in several ways, such as by reducing runoff efficiency, increasing the severity of droughts, modifying the seasonality of annual floods, and changing evaporative demand.

Because of the recent onslaught of long-term historic droughts in the western United States, researchers have conducted several studies to examine the contribution of air temperature changes to changes in streamflow by affecting runoff efficiency (Woodhouse and others, 2016). Nowak and others (2012) found that the low-frequency hydroclimatic variability in runoff efficiency in the Upper Colorado River Basin is related to temperature changes while decadal variability is strongly tied to the delivery of precipitation. Peterson and others (2013) described how a watershed's soil-moisture "memory" over many years can add to the complexity of extreme dry periods that are enhanced by temperature changes. Periods with extreme wetness or dryness can have an influence on runoff.

Recent studies have demonstrated the concurrence of abnormally warm periods with severe droughts in numerous CONUS regions. Woodhouse and others (2016) found that recent droughts in the Upper Colorado River Basin were amplified by warmer temperatures with modest precipitation deficits. Similarly, Diffenbaugh and others (2015) and Shukla and others (2015) found that precipitation deficits in California were more than twice as likely to yield droughts if they occurred when conditions were warm and that the 2014 drought year was exacerbated by warm temperatures. Diffenbaugh and others (2015) also found increasing probabilities that precipitation deficits occurred during warmer conditions and that precipitation deficits caused droughts. McCabe and others (2004) found a 22-percent increase in the variance of drought frequency to be related to increasing North American temperatures outside of the more likely contributions from the PDO and AMO.

In watersheds affected by snow, climatological changes in storm temperatures can be as important to water management as storm precipitation totals (Vano and others, 2019). As recently illustrated with the Oroville Dam in northern California, the combination of storm precipitation totals during the 2016 winter season and temperatures prior to and during the storms played a critical role in determining the runoff-contributing area of the watersheds (Vano and others, 2019). The cumulative precipitation during the 2016 winter season not only negated the historic 2012–2015 statewide droughts in California but added to the failure risk of the Oroville Dam (Vano and others, 2019).

Air temperature can also play a role in changing evaporative demand. Griffin and Friedman (2017) evaluated changes in precipitation, temperature, and streamflow in the Little Missouri River in the northern Great Plains. They found substantial increases in the minimum and maximum temperatures in January through April and in June even though their analysis showed only small changes in annual and growing season precipitation over these periods. They found an increased winter atmospheric evaporative demand in 1976–2012, compared to the demand in 1939–1975, as well as an increased summer evaporation. Likely both contributed to decreased runoff. Griffin and Friedman (2017) found a 41-percent decrease in annual peak streamflows for the 1976–2012 period compared to streamflows in 1939–1975, which they attributed to changes in temperature.

Impoundments and Diversions

Dams with large impoundments, built with the intention of storing inflows for later use or flood control, can be found in all regions of the CONUS. While much focus has been placed on the flow-altering effects of large dams (Graf, 2006), relatively little attention has been given to the cumulative effects of small dams from 2 to 12 meters tall with limited storage capacity (U.S. Army Corps of Engineers, 2013). In addition to impoundments, other features such as artificial diversions, wastewater and water-supply discharge, agricultural drainage activities, and interbasin water transfers may all alter streamflow characteristics.

Large Artificial Impoundments

Flood waves downstream of large impoundments are often attenuated and delayed, and hydrographs may show modified rising and receding limbs (Poff and others, 1997). FitzHugh and Vogel (2011) found that dams in the CONUS reduce median annual floods by 55 percent for large rivers, 25 percent for medium rivers, and 10 percent for small rivers. Similarly, in an analysis of historical peak-streamflow trends in regulated basins (large reservoir storage) with minimal urbanization, peak flows decreased significantly during the 75-year period of 1941–2015, with the largest decreases in peak flows generally occurring in the largest basins (Hodgkins and others, 2019).

In addition, dams indirectly affect peak streamflows by cutting off upstream sediment supplies. This supply reduction can lead to riverbed armoring immediately downstream of the dam and the deposition of these eroded sediments further downstream (Kondolf, 1997). Downstream deposition can lead to an increased risk of flooding from reduced channel capacity (Stover and Montgomery, 2001).

Small Artificial Impoundments

Types of small artificial impoundments include run-of-the-river dams, outlet-controlled natural lakes and ponds, stock dams, and detention ponds. Their cumulative effect on peak streamflows is frequently ignored in flood-frequency analysis, as data on their storage and release capabilities are often difficult to acquire. Yet, an existing body of literature, which shows that inclusions of small impoundments in some basins have altered peaks and have had a negligible effect in other basins, indicates the need for further research. For instance, in the Valley Creek watershed of Pennsylvania, Emerson and others (2005) found that volume-based storm management implementation or detention pond outlet modification to a series of 100 detention basins could slightly decrease peak streamflow. The 100 basins, if left as is, could either slightly increase or decrease peak flow depending on where precipitation fell and the timing of peak streamflows. In another study, Ayalew and others (2017) evaluated how small dams in sub-watersheds and the main stem of the Soap Creek watershed in Iowa cumulatively impacted peaks and found that percentage decreases in peak streamflow resulting from the presence of small dams increased as watershed size decreased.

Artificial Withdrawals, Discharges, and Transfers

This section describes changes in artificial diversions that have the potential to affect a range of peak streamflows over time; the diversions include surface-water and groundwater withdrawals (such as for irrigation or municipal water supply); artificial wastewater and water-supply discharge; agricultural drainage activities (including those that cause the loss of wetlands); and interbasin water transfers. These fluxes of direct withdrawals and return flows lower and raise, respectively, peak streamflows and often have a greater effect on lower flows. For example, irrigation has been associated with a reduction in streamflow, while the disposal of wastewater and other water-supply discharges influence the receiving water body. Allaire and others (2015) found elevated flows during the late-summer low-flow season depending on sources of water that included water use for an urbanizing basin in Massachusetts. Interbasin transfers are water withdrawals in which water is transferred from one basin to another and can deplete streamflow in donor basins while augmenting them in recipient basins (Zhuang, 2016). In the western United States, regional or rural water systems that move water across political boundaries or make interbasin transfers are quite common (National Research Council, 1992, p. 257–259). Additionally, water transfers between key streamgages can cause accounting problems with withdrawals.

According to the 2015 USGS report on the estimated water use in the United States (Dieter and others, 2018), water-use categories with the highest water use and withdrawals include thermoelectric power (41 percent), irrigation (37 percent), and public supply (12 percent) whereas industrial usage is 5 percent and, collectively, aquaculture, domestic use, and livestock account for 4 percent. Programs to collect water-use data are variable in purpose and funding among States. Commonly, water-use estimates are made from coefficients that relate water use to another characteristic (such as population or urban development; Reilly and others, 2008). However, in the Upper Plains region, a detailed and in-depth report from the Bureau of Reclamation (2012) describes depletions in the Missouri River Basin related to irrigated agriculture, surface-water public supply, and historical depletions on streamflows.

Groundwater withdrawals across the CONUS more than doubled between 1950 and 1975 but have subsequently remained fairly steady (Reilly and others, 2008). Hutson and others (2004) found that irrigation accounted for nearly two-thirds of the total groundwater withdrawals in the United States. In the central United States, changes in surface-water and groundwater levels have been caused by substantial irrigation with groundwater from the High Plains aquifer since predevelopment generally before 1950 (McGuire, 2014). Zeng and Cai (2014) found significant decreases in streamflow in the Republican River Basin since the 1950s due to groundwater-fed irrigation, which changed the interaction between surface water and groundwater. Painter and others (2017) found that more than 75 percent (10 out of 13) of the USGS streamgages primarily located in western Kansas had statistically significant decreasing monotonic trends in annual peak streamflows. They attributed these decreasing trends primarily to groundwater withdrawals. Similarly, Mallakpour and Villarini (2015) found that during the summer months, the largest fraction of decreasing floods in the central United States was concentrated in Kansas and Nebraska.

Land-Use and Land-Cover Changes

Changes in land use and land cover may alter streamflow characteristics. Such changes include those related to agricultural crop production, rangeland grazing activities, invasive woody species, deforestation and wildfire, and urbanization. Figure A2 is a map of the CONUS showing the land-cover classification based on Falcone (2015). Some land-cover classes on the map relate to the topics in this section as follows: crop production relates to agricultural crop production and rangeland grazing activities; perennial land cover relates to invasive woody species and deforestation and wildfire; and developed land and semi-developed land relate to urbanization.

Agricultural Crop Production and Rangeland Grazing Activities

The extent to which agricultural crop production affects streamflow varies depending on the characteristics of the natural land cover, the agricultural crop land cover (including multiple plantings of different crops within the same fields), and tillage, planting, and harvesting practices. Zhang and Schilling (2006) attributed increased Mississippi River flow to increased baseflow because of land-use change, including the conversion of perennial vegetation to row crops. Villarini and others (2009) found change points clustered in the 1940s data from gages in the Mississippi River Basin and related them to “profound” land-use and land-cover changes; they cited Zhang and Schilling (2006) and Schilling and others (2008). Schilling and others (2008) found that increased corn production in the Raccoon River watershed of Iowa could decrease annual evapotranspiration and increase streamflow (water yield). In a study of data from one streamgage at Keokuk, Iowa, Schilling and others (2010) found that increased soybean acreage corresponded to an increase in the slope of the graphed discharge-precipitation relation and concluded that increased row crop production would result in increased water yield.

According to Park and others (2017), changes in grazing management practices on rangelands can have substantial hydrologic effects by altering land cover and soil properties. Simulated grazing management changes from heavy continuous grazing to adaptive multipaddock grazing in north-central Texas had the simulated hydrologic effects of decreased surface runoff, increased infiltration, decreased streamflow, and decreased peak streamflows (Park and others, 2017). However, data at the watershed scale on grazing management practices and changes in those practices are generally not available, especially for the 50- and 75-year periods used for the study described in this report. Therefore, the hydrologic effects associated with agricultural grazing activities are not well quantified and are difficult to incorporate into regional-scale investigations.

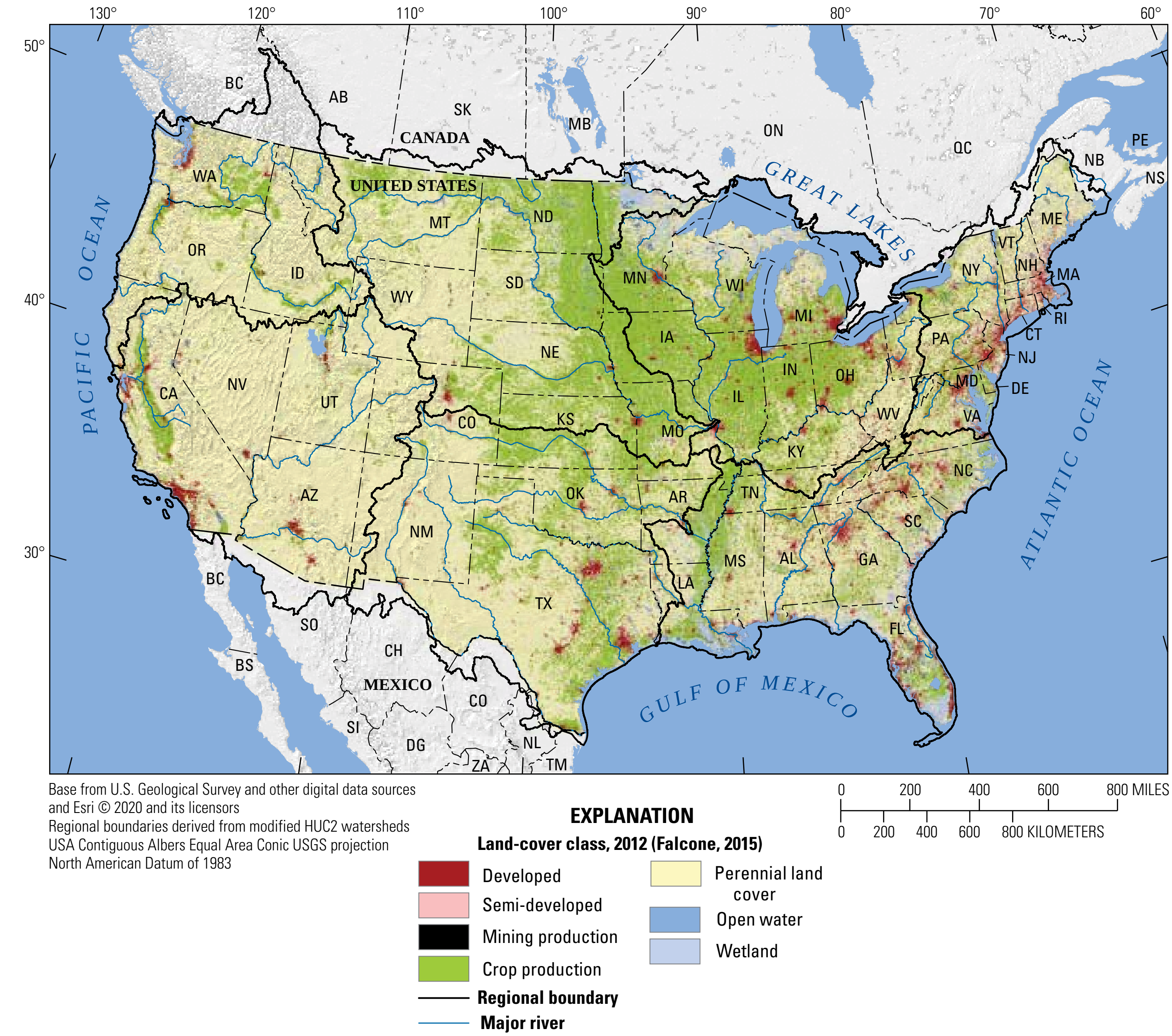

Figure A2. Map of the conterminous United States (CONUS) showing the seven regions in this study and broad land-cover classes in 2012 from Falcone (2015).

For agricultural watersheds, the degree to which climate interactions with land-use and land-cover change affect streamflow can be difficult to parse, and the relative contributions of their effects may differ across the country. Tomer and Schilling (2009) used an ecohydrology approach in four agricultural watersheds to show that climate change has increased discharge in U.S. Midwest watersheds. Ryberg and others (2014) used a nonlinear water-balance model to show that precipitation was the primary driver of variability in runoff and 7-day high runoff in the north-central United States, with some of the unexplained variability being attributed to land use. Gupta and others (2015) used regression methods to show that increased streamflow in the upper midwestern United States is caused mainly by precipitation, as opposed to land-use and land-cover changes. Slater and Villarini (2017) used statistical time-series models to show that, when using five predictors in the Midwest (precipitation, antecedent wetness, temperature, agriculture, and population density), precipitation variability was the most important for modeling high streamflows. Also, in agricultural basins, harvested acreage was important for changing streamflow with a seasonally variable influence. Neri and others (2019) found that, of these same five predictors of seasonal flood events in the U.S. Midwest, precipitation and antecedent wetness conditions were the strongest predictors, temperature was an important predictor in the northern Great Plains because of snowmelt, and population density and agriculture were less important than the climate predictors.

Invasive Woody Species

When invasive woody plant species in riparian corridors substantially alter vegetation communities, streamflows can theoretically be impacted because of increased or decreased transpiration. Despite concern about *Tamarix* spp. (commonly called salt cedar) along rivers in the southwestern United States (Shafroth and Briggs, 2008), McDonald and others (2015) found that transpiration from salt cedar had a negligible effect on flows in a 3-kilometer reach of the Pecos River near Mentone, Texas. In numerous other studies of different water use by native and non-native plant species, researchers have found that differences between the two plant classes are insignificant (Shafroth and others, 2010).

Another potential mechanism for change of peak streamflows by invasive woody plant species is the physical attenuation of floods caused by increased channel and floodplain resistance. During periods of overbank flows, the submersion of riparian vegetation is theorized to increase the hydraulic roughness of streams and cause decreased velocities along with backwater pooling (Thomas and Nisbet, 2007). For vegetation to influence peak streamflows that would result in identification of a change point or trend, the riparian vegetation would need to be disturbed by events such as erosion, channel realignment, or drought mortality that would decrease bank roughness. Thomas and Nisbet (2007) found that the planting of woody plant species has the potential to decrease flood magnitude by increasing the degree of flood attenuation and may be suitable for mitigating flood effects by increasing the amount of flood wave attenuation.

Deforestation and Wildfire

Because forested land makes up large parts of many watersheds, large-scale changes in forest cover can affect peak streamflows. Two of the most investigated mechanisms for alteration of streamflow related to changes in forests are wildfires and forest treatments, either through deforestation by logging or afforestation.

Recent increases in the size and frequency of wildfires and the number of locations affected (Dennison and others, 2014), particularly in the western United States, have led to more focus on wildfires as they pertain to peak streamflow generation, mass wasting, debris flows, and water-quality effects. In the Sierra Nevada and Cascade Mountains in California and Nevada, high-severity wildfires are larger and occur more frequently than those that occurred between 1908 and 1940, when national fire suppression policies began implementation (Miller and others, 2009). The severity of a wildfire is an indicator of the ecological conditions above and below ground and of the soil's potential hydrological response (Neary and others, 2005). Measurable increases in peak streamflows, relative to those in an unburned watershed, can result from increased water velocities caused by a reduction in vegetative ground cover and decreased infiltration caused by changes in the soil profile that result in hydrophobic soils, air entrapment, and soil pore sealing (Moody and others, 2013). The response of a burned watershed is further dependent on the soil characteristics, precipitation intensity and duration, and basin morphology (Moody and Martin, 2009). These factors and several others may be associated with increased peak streamflows, although the extent to which peaks will increase is uncertain. However, there is the potential for missing the attribution of a fire-related flood if the flood produced fits within the existing distribution of annual peak streamflows. The identification of a statistically significant increase in peak streamflow is challenging because of the eventual regrowth of vegetation that can return peaks to their previous distribution within 5 years (Larsen and others, 2009). Additionally, a lack of streamflow measurement stations; the misalignment of rainstorms with burned watersheds; the heterogeneity of fire location, size, and severity; and the likely reduced ability to gather meteorological data at the scale of the wildfire make it more challenging to complete large studies of attribution in hydrologic regions.

Peak streamflows observed after wildfires have been compared with peaks modeled before wildfires by many researchers such as Tiedemann and others (1979), Helvey (1980), and Wine and others (2018). For example, in the year following the Cerro Grande fire in New Mexico in 2000, streamflows near Los Alamos National Laboratory were 3.7 times larger than pre-fire streamflows but quickly decreased in the following years (Gallagher and Koch, 2004). Similarly, dry season water yields following the 2003 Old fire in southern California increased to 1.3 times the yields during pre-wildfire conditions in Devil Canyon and 2.4 times those in City Creek, returning to the previous streamflow regime within 10 years (Kinoshita and Hogue, 2015). Wine and Cadol (2016) found that wildfires have the potential to increase peak streamflows and overall water supply, offsetting decreases in streamflow resulting from climate warming, if a sufficiently sized wildfire has occurred in a large basin. Increases in water yield would be expected for several years after the occurrence of wildfire.

Numerous investigations on the effects of forest alteration on peak streamflows have been conducted through paired watershed studies and comparisons of watersheds before and after forest treatments. Paired watershed studies evaluate the differences between a control watershed and an experimental watershed. Hibbert (1967) and Bosch and Hewlett (1982) completed a review of 39 and 94 studies, respectively, about water yield following forest removal. Most studies have found that measurable increases in streamflow resulted from tree removal only after stand density decreased by at least 20 percent (McMinn and Hewlett, 1975). The response of streamflow to tree removal is variable and dependent on hydroclimatic factors, tree type, soils, beginning forest density, and the decrease in forest density (Bosch and Hewlett, 1982). The increases in streamflow are attributed to decreased evapotranspiration and soil disturbance (Tollan, 2002). Many of the studies focused on tree removal have not focused explicitly on peaks (Alila and others, 2009). For instance, Bowling and others (2000) evaluated annual minimum streamflow, mean annual flow, instantaneous peaks-over-threshold, daily peaks-over-threshold, and maximum annual streamflow trends in 23 basins that had experienced varying degrees of logging in western Washington, and the only trend they were able to detect was a positive trend in annual minimum streamflow.

Urban Effects

Over the last half century, many studies have linked the effects of urbanization to increased flood frequency and magnitude (Leopold, 1968; Hollis, 1975; Graf, 1977; Shuster and others, 2005; Sheng and Wilson, 2009; Villarini and Slater, 2017). Leopold (1968) described how urbanization increases peak streamflows as water runs off faster from paved surfaces (such as streets and roofs) than from vegetated surfaces, decreasing lag times and increasing runoff. In addition, Graf (1977) and Smith and others (2002) found that the efficiency of urban drainage networks also plays a critical role in increasing peak streamflows through decreases in flow travel time. Effects of urbanization vary according to flood return periods. Hollis (1975) and White and Greer (2006) found that effects of urbanization decline with increasing flood recurrence intervals as soils can become fully saturated and less pervious during the largest storms. Beyond changes in flood response, urbanization can also affect flooding by altering the distribution of heavy rainfall (Yang and others, 2014) or by increasing a storm's total rainfall, as illustrated by Zhang and others (2018) for Houston, Texas, and Niyogi and others (2017) for the eastern United States. For a meta-analysis of how urbanization modifies rainfall, refer to Liu and Niyogi (2019).

Various simulation and data-based approaches have been used to assess how urbanization affects flooding for basins in the United States. For a small urbanized basin near Baltimore, Maryland, Ogden and others (2011) used a gridded surface/subsurface model to compare simulated flood magnitudes based on actual imperviousness to the simulated magnitudes based on the assumption of no imperviousness. Hejazi and Markus (2009) applied the Hydrologic Engineering Center for Hydrologic Modeling System (HEC-HMS) model to 12 small urbanizing watersheds in northeastern Illinois and concluded that average increases in urbanization from 11 to 62 percent caused, on average, a 34-percent larger increase in peak streamflows than the increase attributed to climate variability. They found that changes in imperviousness had a significant effect on peak streamflows for the most extreme storms, except the very largest events, for which impervious basin cover was less important. Changnon and Demissie (1996) used a paired catchment approach and found two urban basins in Illinois to be more responsive to shifts in precipitation than rural basins. In this approach, rural basins similar to each urban basin were used to represent a counterfactual for expected changes in the urban basin, had urbanization not occurred. In a study of 20 basins in the Los Angeles metropolitan region, Sheng and Wilson (2009) found that the increase in flood discharge varied on the basis of the distribution of the imperviousness within the basin and the use of flood mitigation practices. Hodgkins and others (2019) evaluated historical trends for urbanized basins with low reservoir storage across the CONUS, and most qualifying basins were in the Midwest and Northeast. Overall, they found high percentages of significant increases and, more notably, that the magnitude of peak trends does not generally rise with increased urbanization until the amount of the developed area reaches 25 percent.

Although most studies have found that urbanization resulted in larger or more frequent floods, a few studies have found no effects or insignificant effects associated with increases in impervious cover. Dudley and others (2001) found no effect related to increases of 1.3–3.5 percent in impervious cover in a basin in southern Maine. For 14 basins in Tennessee with impervious cover fractions of 3–36 percent, Wibben (1976) found no effect of increased urbanization, which he attributed to the low permeability of soil in the region.

In a few USGS reports, researchers have proposed equations that adjust for urbanization when they are used for estimating flood frequency. Sauer and others (1983) developed regression models to adjust USGS flood-frequency equations across a range of return periods for rural areas to urban settings. The basin development factor was found to be an important covariate, along with impervious cover, drainage area, slope, rainfall intensity, lake and reservoir storage, and basin lag time. Moglen and Shivers (2006) adapted these equations so that field measurements of watershed characteristics were not needed, and they incorporated a scaled imperviousness function. They found that the best performing models included covariates representing peak streamflow discharge at comparable rural streams, impervious cover or population density, and changes in the impervious cover or population density. Focusing on small basins in northeastern Illinois, Over and others (2016) developed temporal longitudinal methods to update flood frequency estimates by adjusting the historical record to reflect recent urbanization.

Glaciation, Geomorphological Changes, Volcanic Activity, and Sea-Level Rise

As part of the initial multiple working hypotheses framework, the regional teams identified potential attributions for the observed changes in annual peak streamflows. This section lists attributions uniquely found in different regions in the CONUS that may not be prevalent among all the other regions like the other above-mentioned attributes. They include glaciation, geomorphological changes (including changes induced by seismic activities related to active tectonic environments in the western United States), volcanic activity, and sea-level rise. Slater and others (2015) evaluated trends in flood hazards related to geomorphological changes in channel capacity and streamflow. They found that, while changes in flood hazard due to channel capacity were smaller than changes in streamflow, they were more numerous and could have unforeseen consequences for flood management. Melillo and others (2014) found that sea-level rise and storm surge may result in more frequent and severe flooding. However, because all USGS streamgages considered in this study are riverine gages with no tidal influence, no team used changes in sea-level rise as an attribution for changes in peak streamflows. Upon further in-depth analysis by the regional teams, none of these attributions were identified as the primary or secondary attributions for observed trends or change points. Perhaps in future studies, these regional attributions could still be considered.

Unknown Causes

The change-point results used in this study were part of a project that also compared change-point detection methods (Ryberg, Hodgkins, and Dudley, 2020). As part of that comparison, random data were generated by using the lmomco R package (Asquith, 2021) and the log-Pearson Type III distribution parameters (mean, standard deviation, and skew) of peak streamflow at a series of six streamgages selected for their different hydrologic settings, drainage basin sizes, and record lengths. The researchers then used these random datasets to compare the false positive rates of change-point methods. The method used to detect the change points in this study, the Pettitt test (Pettitt, 1979), had the lowest false positive rate, but we acknowledge that some of the change points may be artifacts of the data and not caused by a physical process. In addition, there may be change points or trends that are caused by physical processes that are yet unknown because data are insufficient or because the variability in the peak-flow or ancillary data is such that a causal pattern is not clear. Therefore, some trends and change points were attributed to unknown causes.

Methods for Causal Attributions

The seven regional teams were tasked with making attributions for the monotonic trends and change points in peak-streamflow data that were statistically significant at a significance level of 0.10 (that is, all results with a p-value<0.10 were candidates for attribution). The teams used a variety of methodologies and investigative techniques to ascribe primary and secondary attributions to trends and change points in annual peak-streamflow records and to assign a provision of confidence level. All the teams used the same list of candidate attributions (table A1) and vocabulary of confidence level (table A2), but they used different techniques because different regions of the country have different causal mechanisms for flooding. The team for the Pacific Northwest, for example, investigated atmospheric rivers. As another example, different teams looked at different metrics of precipitation because differences in snowmelt dominance mean that accumulation is more important in some regions than others.

The attributions and additional data were published in a USGS data release (York and others, 2022). The methods and results are described in chapters B–H of this professional paper.

Insights From Attribution Work

As evidenced by the large body of literature evaluating changes in the magnitude, frequency, and inundation depth of annual peak streamflows and their relation to changes in annual precipitation or other atmospheric and oceanic teleconnections, for example, there is not a consistent “story” of a direct relation between these drivers and changes in peaks. In most of these studies, researchers evaluated changes in the potential drivers used for consideration in the MWHs framework (table A1) at the CONUS, regional, or basin scale. For the current study, researchers leveraged the expert knowledge from the regional teams to determine (when possible) the candidate attributions for the detected trends and (or) change points for each individual USGS peak-streamflow record. The methodologies used by each regional team (chap. B–H) to ascribe attributions for the observed trends were not amenable to one-size-fits-all approaches. Overall, precipitation and the degree of regulation were the most common attributions used to account for these monotonic trends and change points in peak-streamflow data. However, the regional teams noted that limited data sources and time also added to some challenges in ascribing attributions.

Using MWHs, researchers separated precipitation data into two categories: short term and long term (table A1). The short-term data were event related, such as increases in heavy precipitation. The long-term data were acquired for conditions such as monthly to multiyear precipitation representative of month-long storm systems, antecedent wetness or dryness, climatic persistence, and multidecadal climate variability caused by oceanic and atmospheric patterns. Different regional teams focused on specific indicators of short- and long-term precipitation that they believed were dominant in their regions. For instance, the teams for the Northeast and Midwest focused on short-term precipitation, the team for the Upper Plains focused on total annual and seasonal precipitation (important for storage of solid precipitation), the team for the South-Central region used the Palmer Drought Severity Index (PDSI), and the team for the Pacific Northwest looked at integrated water vapor (a proxy for atmospheric rivers). The team for the Southwest looked at both short- and long-term precipitation. The use of these different methodologies by the regional teams highlights the finding that precipitation alone may not have a direct effect on peak streamflow and its effect is not the same across the country.

Peak streamflows that are affected to some unknown or known degree by regulation have USGS NWIS qualification codes 5 or 6, respectively. Definitions and a discussion of these codes can be found in Ryberg and others (2017). These definitions are vague and, therefore, have been applied in an inconsistent temporal and spatial manner in the United States. In the trend detection phase, a definition was developed to identify regulated sites (see the section on “Site Selection, Regional Teams, and Regions”) as a potential way for grouping sites and for supporting attributions. Once analysis was begun at the regional level, it was quickly discovered that some sites that were considered regulated by subject-matter experts were not labeled as such. Teams used station descriptions available in NWIS (U.S. Geological Survey, 2019b) to find statements about the degree of regulation, diversion, and other artificial conveyance, and they used resources from other agencies, such as the “National Inventory of Dams” (U.S. Army Corps of Engineers, 2013), to explore regulation.

Some excellent data sources for attribution work are not available on a national level. For example, the team for the Upper Plains region used the “Missouri River Basin Depletions Database” published by the Bureau of Reclamation (2012). This valuable database on surface-water and groundwater withdrawals is available only for the Missouri River Basin (hydrologic unit 10).

Future Research Directions

Future research may allow for better determination of which precipitation metrics (for example, seasonal precipitation, annual precipitation, multiyear precipitation, increases in heavy and extreme precipitation) affect particular hydrologic regions, as well as whether there are temporal lags between a particular metric and a flood response. There are many definitions of flow regulation, and more research is also needed on what degree of regulation might induce a signal in peak streamflows. Additional complexities related to storage capacity, release capacity, and the ability to draw down reservoirs prior to large events could also induce changes in peak streamflows. A comparison of existing definitions followed by a comparison between the definitions and the regulation coding of the USGS PFF would be informative and could lead to a better definition of regulation that affects peak streamflow.

In addition, there are many potential causal factors (such as tile drainage and agricultural practices) for which there are no adequate, long-term datasets. As we continue to better understand natural and anthropogenic causes of changes in flood regimes, more and better ancillary data can help to inform causal attributions used to account for observed changes; examples include the “Missouri River Basin Depletions Database” (Bureau of Reclamation, 2012) and other local or regional datasets.

Summary

Flood-frequency analysis plays a critical role in the assessment of risk, protection of lives, and planning and design of flood protection infrastructure. Traditional flood-frequency analysis is based on the assumption of stationarity—that is, that the distribution of floods at a given site varies around a particular mean within a particular envelope of variance (and skew) and that these parameters of the distribution do not vary over time. Uncertainty remains as to what degree of violations of the assumption of stationarity warrants the use of a modified method of flood-frequency analysis and what the modified method(s) should be. The current U.S. Federal Government guidelines for flood-frequency analysis, known as Bulletin 17C (England and others, 2018), do not provide methods to address nonstationarity.

Potential changes to flood distributions may be the result of numerous factors, some of which operate at the watershed scale (such as changes to land drainage or urbanization), some of which operate at the regional scale (such as changes to snowpack), and some of which operate at the continental or global scale (such as changes to climate and large-scale weather patterns). In an effort to develop a cohesive national approach to incorporating potential or observed changes into flood-frequency estimates when necessary, national and regional experts from the U.S. Geological Survey and cooperators worked together to develop a multiple working hypotheses framework for attributions and a common vocabulary for making provisions of confidence. Regional subject-matter experts examined statistically significant (p-value<0.10) monotonic trends and change points in peak-streamflow data, along with ancillary datasets that might explain the changes, and made attributions, when possible, along with a provision of confidence in each attribution. This first chapter describes the development of the list of attributions and presents a literature review for the potential attributions.

The sites used in this study were those used in the first phase of work, which was also funded by the Federal Highway Administration of the U.S. Department of Transportation; the first phase entailed the detection of monotonic trends and change points in annual peak-streamflow data from streamgages. The data on annual peak streamflows used in this study came from the dataset known as the “peak-flow file” and are available as part of the U.S. Geological Survey National Water Information System. Two trend-analysis periods were used for attribution: a 75-year period (water years 1941–2015) and a 50-year period (1966–2015). Seven regional teams were formed to use subject-matter expertise to make attributions for changes in annual peak streamflows in their regions of the conterminous United States. The seven regions are described as Pacific Northwest, Upper Plains, Midwest, Northeast, Southwest, South-Central, and Southeast. Using a multiple working hypotheses framework, the regional teams first developed a list of potential mechanisms for nonstationarity in annual peak-streamflow records for their regions and investigated whether data were available to test these hypotheses. The multiple working hypotheses were then combined into broad categories, which are discussed in the literature review in this chapter.

The seven regional teams were tasked with making attributions for the monotonic trends and change points that were statistically significant at a significance level of 0.10. The teams used a variety of methodologies and investigative techniques to ascribe primary and secondary attributions to monotonic trends and change points in annual peak-streamflow records and to assign a provision of confidence level. All the teams used the same list of candidate attributions and vocabulary of confidence level, but they used different techniques because different regions of the country have different causal mechanisms for flooding. The attributions and additional data were published in a USGS data release (York and others, 2022). The methods and results are described in chapters B–H of this professional paper.

Overall, precipitation and the degree of regulation were the most common attributions used to account for these trends and change points. Different regional teams focused more specifically on several types of precipitation they believed were dominant in their regions. The use of these different methodologies by the regional teams highlights the findings that changes in precipitation alone may not always affect annual peak streamflows directly and that the effects of precipitation vary across the country.

Additional research may allow for better determination of which metrics of precipitation affect particular hydrologic regions as well as whether there are temporal lags between a particular metric and a flood response. There are many definitions of flow regulation, and more research is also needed on what degree of regulation might induce a signal in the peak streamflow. A comparison of existing definitions followed by a comparison between the definitions and the regulation coding of the USGS peak-flow file would be informative and could lead to a better definition of regulation that affects peak streamflow. In addition, there are many potential causal factors (such as tile drainage and agricultural practices) for which there are no adequate long-term datasets. As we continue to better understand natural and anthropogenic causes of changes in flood regimes, more and better ancillary data can help to inform causal attributions used to account for observed changes; examples include the "Missouri River Basin Depletions Database" (Bureau of Reclamation, 2012) and other local or regional datasets.

References Cited

Agel, L., Barlow, M., Qian, J.-H., Colby, F., Douglas, E., and Eichler, T., 2015, Climatology of daily precipitation and extreme precipitation events in the northeast United States: Journal of Hydrometeorology, v. 16, no. 6, p. 2537–2557.

Alila, Y., Kuraś, P.K., Schnorbus, M., and Hudson, R., 2009, Forests and floods—A new paradigm sheds light on age-old controversies: Water Resources Research, v. 45, no. 8, article W08416, 24 p., accessed August 23, 2021, at https://doi.org/10.1029/2008WR007207.

Allaire, M.C., Vogel, R.M., and Kroll, C.N., 2015, The hydromorphology of an urbanizing watershed using multivariate elasticity: Advances in Water Resources, v. 86, pt. A, p. 147–154.

Alter, R.E., Douglas, H.C., Winter, J.M., and Eltahir, E.A.B., 2018, Twentieth century regional climate change during the summer in the central United States attributed to agricultural intensification: Geophysical Research Letters, v. 45, no. 3, p. 1586–1594.

Archfield, S.A., Hirsch, R.M., Viglione, A., and Blöschl, G., 2016, Fragmented patterns of flood change across the United States: Geophysical Research Letters, v. 43, no. 19, p. 10232–10239.

Armstrong, W.H., Collins, M.J., and Snyder, N.P., 2014, Hydroclimatic flood trends in the northeastern United States and linkages with large-scale atmospheric circulation patterns: Hydrological Sciences Journal, v. 59, no. 9, p. 1636–1655.

Asquith, W.H., 2021, lmomco—L-moments, censored L-moments, trimmed L-moments, L-comoments, and many distributions: R package version 2.3.7 (dated August 4, 2021), accessed August 23, 2021, at https://cran.r-project.org/package=lmomco.

Ayalew, T.B., Krajewski, W.F., Mantilla, R., Wright, D.B., and Small, S.J., 2017, Effect of spatially distributed small dams on flood frequency—Insights from the Soap Creek watershed: Journal of Hydrologic Engineering, v. 22, no. 7, article 04017011, 11 p., accessed August 24, 2021, at https://ascelibrary.org/doi/10.1061/%28ASCE%29HE.1943-5584.0001513.

Barros, A.P., Duan, Y., Brun, J., and Medina, M.A., Jr., 2014, Flood nonstationarity in the southeast and mid-Atlantic regions of the United States: Journal of Hydrologic Engineering, v. 19, no. 10, article 05014014, 11 p., accessed March 15, 2021, at https://ascelibrary.org/doi/10.1061/(ASCE)HE.1943-5584.0000955.

Barth, N.A., Villarini, G., and White, K., 2018, Contribution of eastern North Pacific tropical cyclones and their remnants on flooding in the western United States: International Journal of Climatology, v. 38, no. 14, p. 5441–5446.

Bayazit, M., 2015, Nonstationarity of hydrological records and recent trends in trend analysis—A state-of-the-art review: Environmental Processes, v. 2, no. 3, p. 527–542.

Berghuijs, W.R., Woods, R.A., Hutton, C.J., and Sivapalan, M., 2016, Dominant flood generating mechanisms across the United States: Geophysical Research Letters, v. 43, no. 9, p. 4382–4390.

Bond, N.A., and Harrison, D.E., 2000, The Pacific decadal oscillation, air-sea interaction and central north Pacific winter atmospheric regimes: Geophysical Research Letters, v. 27, no. 5, p. 731–734.

Bosch, J.M., and Hewlett, J.D., 1982, A review of catchment experiments to determine the effect of vegetation changes on water yield and evapotranspiration: Journal of Hydrology, v. 55, nos. 1–4, p. 3–23.

Bowling, L.C., Storck, P., and Lettenmaier, D.P., 2000, Hydrologic effects of logging in western Washington, United States: Water Resources Research, v. 36, no. 11, p. 3223–3240.

Bureau of Reclamation, 2012, Missouri River Basin depletions database—Great Plains region: Bureau of Reclamation, [97] p., accessed November 29, 2018, at https://www.usbr.gov/gp/dkao/naws/FSEIS/missouri_river_basin_depletions_database.pdf.

Burn, D.H., and Whitfield, P.H., 2018, Changes in flood events inferred from centennial length streamflow data records: Advances in Water Resources, v. 121, p. 333–349.

Burn, D.H., Whitfield, P.H., and Sharif, M., 2016, Identification of changes in floods and flood regimes in Canada using a peaks over threshold approach: Hydrological Processes, v. 30, no. 18, p. 3303–3314.

Cayan, D.R., and Peterson, D.H., 1989, The influence of north Pacific atmospheric circulation on streamflow in the West, *in* Peterson, D.H., ed., Aspects of climate variability in the Pacific and the western Americas: American Geophysical Union Geophysical Monograph Series, v. 55, p. 375–397.

Chamberlin, T.C., 1890, The method of multiple working hypotheses: Science, v. 15, p. 92–96.

Chamberlin, T.C., 1897, The method of multiple working hypotheses: Journal of Geology, v. 5, p. 837–848.

Chamberlin, T.C., 1965, The method of multiple working hypotheses (reprint): Science, v. 148, no. 3671, p. 754–759.

Changnon, S.A., and Demissie, M., 1996, Detection of changes in streamflow and floods resulting from climate fluctuations and land use-drainage changes: Climatic Change, v. 32, no. 4, p. 411–421.

Clark, M.P., Kavetski, D., and Fenicia, F., 2011, Pursuing the method of multiple working hypotheses for hydrological modeling: Water Resources Research, v. 47, no. 9, article W09301, 16 p., accessed August 24, 2021, at https://doi.org/10.1029/2010WR009827.

Collins, M.J., 2019, River flood seasonality in the Northeast United States—Characterization and trends: Hydrological Processes, v. 33, no. 5, p. 687–698.

Collins, M.J., Kirk, J.P., Pettit, J., DeGaetano, A.T., McCown, M.S., Peterson, T.C., Means, T.N., and Zhang, X., 2014, Annual floods in New England (USA) and Atlantic Canada—Synoptic climatology and generating mechanisms: Physical Geography, v. 35, no. 3, p. 195–219.

Court, A., 1962, Measures of streamflow timing: Journal of Geophysical Research, v. 67, no. 11, p. 4335–4339.

Dennison, P.E., Brewer, S.C., Arnold, J.D., and Moritz, M.A., 2014, Large wildfire trends in the western United States, 1984–2011: Geophysical Research Letters, v. 41, no. 8, p. 2928–2933.

Dickinson, J.E., Harden, T.M., and McCabe, G.J., 2019, Seasonality of climatic drivers of flood variability in the conterminous United States: Scientific Reports, v. 9, no. 1, article 15321, 10 p., accessed March 18, 2021, at https://doi.org/10.1038/s41598-019-51722-8.

Dieter, C.A., Maupin, M.A., Caldwell, R.R., Harris, M.A., Ivahnenko, T.I., Lovelace, J.K., Barber, N.L., and Linsey, K.S., 2018, Estimated use of water in the United States in 2015: U.S. Geological Survey Circular 1441, 65 p., accessed March 18, 2021, at https://pubs.er.usgs.gov/publication/cir1441.

Diffenbaugh, N.S., Swain, D.L., and Touma, D., 2015, Anthropogenic warming has increased drought risk in California: Proceedings of the National Academy of Sciences, v. 112, no. 13, p. 3931–3936.

Dudley, R.W., Archfield, S.A., Hodgkins, G.A., Renard, B., and Ryberg, K.R., 2018, Peak-streamflow trends and change-points and basin characteristics for 2,683 U.S. Geological Survey streamgages in the conterminous U.S. (ver. 3.0, April 2019): U.S. Geological Survey data release, accessed June 6, 2019, at https://doi.org/10.5066/P9AEGXY0.

Dudley, R.W., Hodgkins, G.A., Mann, A., and Chisolm, J., 2001, Evaluation of the effects of development on peak-flow hydrographs for Collyer Brook, Maine: U.S. Geological Survey Water-Resources Investigations Report 2001–4156, 11 p., 2 pls., accessed March 18, 2021, at https://pubs.er.usgs.gov/publication/wri20014156.

Dudley, R.W., Hodgkins, G.A., McHale, M.R., Kolian, M.J., and Renard, B., 2017, Trends in snowmelt-related streamflow timing in the conterminous United States: Journal of Hydrology, v. 547, p. 208–221.

Easterling, D.R., Kunkel, K.E., Arnold, J.R., Knutson, T., LeGrande, A.N., Leung, L.R., Vose, R.S., Waliser, D.E., and Wehner, M.F., 2017, Precipitation change in the United States, chap. 7 *of* Wuebbles, D.J., Fahey, D.W., Hibbard, K.A., Dokken, D.J., Stewart, B.C., and Maycock, T.K., eds., Climate science special report, v. I *of* Fourth national climate assessment: Washington, D.C., U.S. Global Change Research Program, p. 207–230.

Emerson, C.H., Welty, C., and Traver, R.G., 2005, Watershed-scale evaluation of a system of storm water detention basins: Journal of Hydrologic Engineering, v. 10, no. 3, p. 237–242.

England, J.F., Jr., Cohn, T.A., Faber, B.A., Stedinger, J.R., Thomas, W.O., Jr., Veilleux, A.G., Kiang, J.E., and Mason, R.R., Jr., 2018, Guidelines for determining flood flow frequency—Bulletin 17C (ver. 1.1, May 2019): U.S. Geological Survey Techniques and Methods, book 4, chap. B5, 148 p., accessed March 18, 2020, at https://doi.org/10.3133/tm4B5.

Falcone, J.A., 2011, GAGES–II—Geospatial attributes of gages for evaluating streamflow: U.S. Geological Survey dataset, accessed July 15, 2015, at http://pubs.er.usgs.gov/publication/70046617.

Falcone, J.A., 2015, U.S. conterminous wall-to-wall anthropogenic land use trends (NWALT), 1974–2012: U.S. Geological Survey Data Series 948, 33 p. plus appendixes 3–6 as separate files, accessed March 18, 2021, at https://doi.org/10.3133/ds948.

FitzHugh, T.W., and Vogel, R.M., 2011, The impact of dams on flood flows in the United States: River Research and Applications, v. 27, no. 10, p. 1192–1215.

Frans, C., Istanbulluoglu, E., Mishra, V., Munoz-Arriola, F., and Lettenmaier, D.P., 2013, Are climatic or land cover changes the dominant cause of runoff trends in the Upper Mississippi River Basin?: Geophysical Research Letters, v. 40, no. 6, p. 1104–1110.

Friedman, D., Schechter, J., Sant-Miller, A.M., Mueller, C., Villarini, G., White, K.D., and Baker, B., 2018, US Army Corps of Engineers Nonstationarity Detection Tool user guide: U.S. Army Corps of Engineers, accessed August 24, 2021, at http://corpsmapu.usace.army.mil/rccinfo/nsd/docs/Nonstationarity_Detection_Tool_User_Guide.pdf.

Gallagher, B.M., and Koch, R.J., 2004, Cerro Grande fire impacts to water quality and stream flow near Los Alamos National Laboratory—Results of four years of monitoring: Los Alamos National Laboratory Report LA–14177, 195 p., accessed May 14, 2019, at https://permalink.lanl.gov/object/tr?what=info:lanl-repo/lareport/LA-14177.

Gleason, K.E., Nolin, A.W., and Roth, T.R., 2013, Charred forests increase snowmelt—Effects of burned woody debris and incoming solar radiation on snow ablation: Geophysical Research Letters, v. 40, no. 17, p. 4654–4661.

Graf, W.L., 1977, Network characteristics in suburbanizing streams: Water Resources Research, v. 13, no. 2, p. 459–463.

Graf, W.L., 2006, Downstream hydrologic and geomorphic effects of large dams on American rivers: Geomorphology, v. 79, nos. 3–4, p. 336–360.

Griffin, E.R., and Friedman, J.M., 2017, Decreased runoff response to precipitation, Little Missouri River Basin, northern Great Plains, USA: JAWRA, Journal of the American Water Resources Association, v. 53, no. 3, p. 576–592.

Groisman, P.Y., Knight, R.W., and Karl, T.R., 2012, Changes in intense precipitation over the central United States: Journal of Hydrometeorology, v. 13, no. 1, p. 47–66.

Groisman, P.Y., Knight, R.W., Karl, T.R., Easterling, D.R., Sun, B., and Lawrimore, J.H., 2004, Contemporary changes of the hydrological cycle over the contiguous United States—Trends derived from in situ observations: Journal of Hydrometeorology, v. 5, no. 1, p. 64–85.

Gül, G.O., Aşıkoğlu, Ö.L., Gül, A., Gülçem Yaşoğlu, F., and Benzeden, E., 2014, Nonstationarity in flood time series: Journal of Hydrologic Engineering, v. 19, no. 7, p. 1349–1360, accessed March 18, 2021, at https://ascelibrary.org/doi/full/10.1061/%28ASCE%29HE.1943-5584.0000923.

Gupta, S.C., Kessler, A.C., Brown, M.K., and Zvomuya, F., 2015, Climate and agricultural land use change impacts on streamflow in the upper midwestern United States: Water Resources Research, v. 51, no. 7, p. 5301–5317.

Hansen, J., Ruedy, R., Sato, M., and Lo, K., 2010, Global surface temperature change: Reviews of Geophysics, v. 48, no. 4, article RG4004, 29 p., accessed May 14, 2019, at https://doi.org/10.1029/2010RG000345.

Hardy, K., and Cannon, A., 2019, Iowa flooding—Damage from floodwaters reaches $1.6B, Gov. Kim Reynolds estimates: Des Moines [Iowa] Register, March 22, 2019, accessed June 6, 2019, at https://www.desmoinesregister.com/story/news/2019/03/22/iowa-flooding-damage-estimate-governor-kim-reynolds-federal-flood-relief-trump-nebraska-missouri/3232934002/.

Harpold, A.A., Biederman, J.A., Condon, K., Merino, M., Korgaonkar, Y., Nan, T., Sloat, L.L., Ross, M., and Brooks, P.D., 2013, Changes in snow accumulation and ablation following the Las Conchas Forest Fire, New Mexico, USA: Ecohydrology, v. 7, no. 2, p. 440–452.

Harrigan, S., Murphy, C., Hall, J., Wilby, R.L., and Sweeney, J., 2014, Attribution of detected changes in streamflow using multiple working hypotheses: Hydrology and Earth System Sciences, v. 18, no. 5, p. 1935–1952.

Hegerl, G., and Zwiers, F., 2011, Use of models in detection and attribution of climate change: WIREs (Wiley Interdisciplinary Reviews) Climate Change, v. 2, no. 4, p. 570–591.

Hejazi, M.I., and Markus, M., 2009, Impacts of urbanization and climate variability on floods in northeastern Illinois: Journal of Hydrologic Engineering, v. 14, no. 6, p. 606–616.

Helvey, J.D., 1980, Effects of a north central Washington wildfire on runoff and sediment production: American Water Resources Association Water Resources Bulletin, v. 16, no. 4, p. 627–634.

Hibbert, A.R., 1967, Forest treatment effects on water yield, *in* Sopper, W.E., and Lull, H.W., eds., Forest hydrology: New York, Pergamon, p. 527–543.

Hirsch, R.M., 2011, A perspective on nonstationarity and water management: JAWRA, Journal of the American Water Resources Association, v. 47, no. 3, p. 436–446.

Hirsch, R.M., and Ryberg, K.R., 2012, Has the magnitude of floods across the USA changed with global CO_2 levels?: Hydrological Sciences Journal, v. 57, no. 1, p. 1–9.

Hirschboeck, K.K., 2009, Future hydroclimatology and the research challenges of a post-stationary world: Journal of Contemporary Water Research & Education, v. 142, no. 1, p. 4–9.

Hodgkins, G.A., and Dudley, R.W., 2006, Changes in the timing of winter–spring streamflows in eastern North America, 1913–2002: Geophysical Research Letters, v. 33, no. 6, article L06402, 5 p., accessed August 24, 2021, at https://doi.org/10.1029/2005GL025593.

Hodgkins, G.A., Dudley, R.W., Archfield, S.A., and Renard, B., 2019, Effects of climate, regulation, and urbanization on historical flood trends in the United States: Journal of Hydrology, v. 573, p. 697–709.

Hodgkins, G.A., Whitfield, P.H., Burn, D.H., Hannaford, J., Renard, B., Stahl, K., Fleig, A.K., Madsen, H., Mediero, L., Korhonen, J., Murphy, C., and Wilson, D., 2017, Climate-driven variability in the occurrence of major floods across North America and Europe: Journal of Hydrology, v. 552, p. 704–717.

Hollis, G.E., 1975, The effect of urbanization on floods of different recurrence interval: Water Resources Research, v. 11, no. 3, p. 431–435.

Huang, H., Winter, J.M., Osterberg, E.C., Horton, R.M., and Beckage, B., 2017, Total and extreme precipitation changes over the northeastern United States: Journal of Hydrometeorology, v. 18, no. 6, p. 1783–1798.

Hutson, S.S., Barber, N.L., Kenny, J.F., Linsey, K.S., Lumia, D.S., and Maupin, M.A., 2004, Estimated use of water in the United States in 2000 (revised February 2005): U.S. Geological Survey Circular 1268, 46 p., accessed August 9, 2019, at https://doi.org/10.3133/cir1268.

Ivancic, T.J., and Shaw, S.B., 2015, Examining why trends in very heavy precipitation should not be mistaken for trends in very high river discharge: Climatic Change, v. 133, no. 4, p. 681–693.

Johnson, J.G., 1990, Method of multiple working hypotheses—A chimera: Geology, v. 18, no. 1, p. 44–45.

Karl, T.R., and Knight, R.W., 1998, Secular trends of precipitation amount, frequency, and intensity in the United States: Bulletin of the American Meteorological Society, v. 79, no. 2, p. 231–241.

Kay, A.L., Crooks, S.M., Pall, P., and Stone, D.A., 2011, Attribution of autumn/winter 2000 flood risk in England to anthropogenic climate change—A catchment-based study: Journal of Hydrology, v. 406, nos. 1–2, p. 97–112.

Kiang, J.E., Olsen, J.R., and Waskom, R.M., 2011, Introduction to the featured collection on “Nonstationarity, Hydrologic Frequency Analysis, and Water Management”: JAWRA, Journal of the American Water Resources Association, v. 47, no. 3, p. 433–435.

Kinoshita, A.M., and Hogue, T.S., 2015, Increased dry season water yield in burned watersheds in southern California: Environmental Research Letters, v. 10, no. 1, article 014003, 9 p., accessed August 24, 2021, at https://iopscience.iop.org/article/10.1088/1748-9326/10/1/014003/pdf.

Kolars, K.A., Vecchia, A.V., and Ryberg, K.R., 2016, Stochastic model for simulating Souris River Basin precipitation, evapotranspiration, and natural streamflow: U.S. Geological Survey Scientific Investigations Report 2015–5185, 55 p., accessed April 20, 2016, at http://dx.doi.org/10.3133/sir20155185.

Kondolf, G.M., 1997, Profile—Hungry water—Effects of dams and gravel mining on river channels: Environmental Management, v. 21, no. 4, p. 533–551.

Koutsoyiannis, D., 2006, Nonstationarity versus scaling in hydrology: Journal of Hydrology, v. 324, nos. 1–4, p. 239–254.

Kunkel, K.E., Easterling, D.R., Kristovich, D.A.R., Gleason, B., Stoecker, L., and Smith, R., 2010, Recent increases in U.S. heavy precipitation associated with tropical cyclones: Geophysical Research Letters, v. 37, no. 24, article L24706, 4 p., accessed May 23, 2019, at https://agupubs.onlinelibrary.wiley.com/doi/pdf/10.1029/2010GL045164.

Kunkel, K.E., Easterling, D.R., Kristovich, D.A.R., Gleason, B., Stoecker, L., and Smith, R., 2012, Meteorological causes of the secular variations in observed extreme precipitation events for the conterminous United States: Journal of Hydrometeorology, v. 13, no. 3, p. 1131–1141.

Kunkel, K.E., Robinson, D.A., Champion, S., Yin, X., Estilow, T., and Frankson, R.M., 2016, Trends and extremes in Northern Hemisphere snow characteristics: Current Climate Change Reports, v. 2, no. 2, p. 65–73.

Larsen, I.J., MacDonald, L.H., Brown, E., Rough, D., Welsh, M.J., Pietraszek, J.H., Libohova, Z., de Dios Benavides-Solorio, J., and Schaffrath, K., 2009, Causes of post-fire runoff and erosion—Water repellency, cover, or soil sealing?: Soil Science Society of America Journal, v. 73, no. 4, p. 1393–1407.

Latif, M., and Barnett, T.P., 1994, Causes of decadal climate variability over the north Pacific and North America: Science, v. 266, no. 5185, p. 634–637.

Leopold, L.B., 1968, Hydrology for urban land planning—A guidebook on the hydrologic effects of urban land use: U.S. Geological Survey Circular 554, 18 p.

Lins, H.F., 2012, USGS Hydro-Climatic Data Network 2009 (HCDN–2009): U.S. Geological Survey Fact Sheet 2012–3047, 4 p., accessed March 23, 2018, at https://pubs.usgs.gov/fs/2012/3047/.

Liu, J., and Niyogi, D., 2019, Meta-analysis of urbanization impact on rainfall modification: Scientific Reports, v. 9, no. 1, article 7301, 14 p., accessed March 18, 2021, at https://www.nature.com/articles/s41598-019-42494-2.

Mallakpour, I., and Villarini, G., 2015, The changing nature of flooding across the central United States: Nature Climate Change, v. 5, no. 3, p. 250–254.

Mallakpour, I., and Villarini, G., 2016, Investigating the relationship between the frequency of flooding over the central United States and large-scale climate: Advances in Water Resources, v. 92, p. 159–171.

Mallakpour, I., Villarini, G., Jones, M.P., and Smith, J.A., 2017, On the use of Cox regression to examine the temporal clustering of flooding and heavy precipitation across the central United States: Global and Planetary Change, v. 155, p. 98–108.

Mastrandrea, M.D., and Mach, K.J., 2011, Treatment of uncertainties in IPCC assessment reports—Past approaches and considerations for the Fifth Assessment Report: Climatic Change, v. 108, no. 4, p. 659–673.

Mastrandrea, M.D., Mach, K.J., Plattner, G.-K., Edenhofer, O., Stocker, T.F., Field, C.B., Ebi, K.L., and Matschoss, P.R., 2011, The IPCC AR5 guidance note on consistent treatment of uncertainties—A common approach across the working groups: Climatic Change, v. 108, no. 4, p. 675–691.

Mauboussin, A., and Mauboussin, M.J., 2018, If you say something is “likely,” how likely do people think it is?: Harvard Business Review web page, accessed March 14, 2019, at https://hbr.org/2018/07/if-you-say-something-is-likely-how-likely-do-people-think-it-is.

McCabe, G.J., and Clark, M.P., 2005, Trends and variability in snowmelt runoff in the western United States: Journal of Hydrometeorology, v. 6, no. 4, p. 476–482.

McCabe, G.J., and Dettinger, M.D., 1999, Decadal variations in the strength of ENSO teleconnections with precipitation in the western United States: International Journal of Climatology, v. 19, no. 13, p. 1399–1410.

McCabe, G.J., and Wolock, D.M., 2002, A step increase in streamflow in the conterminous United States: Geophysical Research Letters, v. 29, no. 24, p. 2185–2189.

McCabe, G.J., Palecki, M.A., and Betancourt, J.L., 2004, Pacific and Atlantic Ocean influences on multidecadal drought frequency in the United States: Proceedings of the National Academy of Sciences, v. 101, no. 12, p. 4136–4141.

McDonald, A.K., Wilcox, B.P., Moore, G.W., Hart, C.R., Sheng, Z., and Owens, M.K., 2015, *Tamarix* transpiration along a semiarid river has negligible impact on water resources: Water Resources Research, v. 51, no. 7, p. 5117–5127.

McGuire, V.L., 2014, Water-level changes and change in water in storage in the High Plains aquifer, predevelopment to 2013 and 2011–13: U.S. Geological Survey Scientific Investigations Report 2014–5218, 14 p., accessed August 9, 2019, at https://pubs.er.usgs.gov/publication/sir20145218.

McMinn, J.W., and Hewlett, J.D., 1975, First-year water yield increase after forest cutting—An alternative model: Journal of Forestry, v. 73, no. 10, p. 654–655.

Melillo, J.M., Richmond, T.C., and Yohe, G.W., eds., 2014, Climate change impacts in the United States—The third national climate assessment: Washington, D.C., U.S. Global Change Research Program, 841 p.

Merz, B., Vorogushyn, S., Uhlemann, S., Delgado, J., and Hundecha, Y., 2012, HESS Opinions: “More efforts and scientific rigour are needed to attribute trends in flood time series”: Hydrology and Earth System Sciences, v. 16, no. 5, p. 1379–1387.

Michalak, A.M., Anderson, E.J., Beletsky, D., Boland, S., Bosch, N.S., Bridgeman, T.B., Chaffin, J.D., Cho, K., Confesor, R., Daloğlu, I., DePinto, J.V., Evans, M.A., Fahnenstiel, G.L., He, L., Ho, J.C., Jenkins, L., Johengen, T.H., Kuo, K.C., LaPorte, E., Liu, X., McWilliams, M.R., Moore, M.R., Posselt, D.J., Richards, R.P., Scavia, D., Steiner, A.L., Verhamme, E., Wright, D.M., and Zagorski, M.A., 2013, Record-setting algal bloom in Lake Erie caused by agricultural and meteorological trends consistent with expected future conditions: Proceedings of the National Academy of Sciences, v. 110, no. 16, p. 6448–6452.

Miller, J.D., Safford, H.D., Crimmins, M., and Thode, A.E., 2009, Quantitative evidence for increasing forest fire severity in the Sierra Nevada and Southern Cascade Mountains, California and Nevada, USA: Ecosystems, v. 12, no. 1, p. 16–32.

Milly, P.C.D., Betancourt, J., Falkenmark, M., Hirsch, R.M., Kundzewicz, Z.W., Lettenmaier, D.P., and Stouffer, R.J., 2008, Stationarity is dead—Whither water management?: Science, v. 319, no. 5863, p. 573–574.

Minobe, S., 1997, A 50–70 year climatic oscillation over the North Pacific and North America: Geophysical Research Letters, v. 24, no. 6, p. 683–686.

Moglen, G.E., and Shivers, D.E., 2006, Methods for adjusting U.S. Geological Survey rural regression peak discharges in an urban setting: U.S. Geological Survey Scientific Investigations Report 2006–5270, 55 p., accessed March 18, 2021, at https://pubs.er.usgs.gov/publication/sir20065270.

Mondal, A., and Daniel, D., 2019, Return levels under nonstationarity—The need to update infrastructure design strategies: Journal of Hydrologic Engineering, v. 24, no. 1, article 04018060, 11 p., accessed August 24, 2021, at https://ascelibrary.org/doi/full/10.1061/%28ASCE%29HE.1943-5584.0001738.

Moody, J.A., and Martin, D.A., 2009, Synthesis of sediment yields after wildland fire in different rainfall regimes in the western United States: International Journal of Wildland Fire, v. 18, no. 1, p. 96–115.

Moody, J.A., Shakesby, R.A., Robichaud, P.R., Cannon, S.H., and Martin, D.A., 2013, Current research issues related to post-wildfire runoff and erosion processes: Earth-Science Reviews, v. 122, p. 10–37.

Mote, P.W., Hamlet, A.F., Clark, M.P., and Lettenmaier, D.P., 2005, Declining mountain snowpack in western North America: Bulletin of the American Meteorological Society, v. 86, no. 1, p. 39–50.

Mote, P.W., Li, S., Lettenmaier, D.P., Xiao, M., and Engel, R., 2018, Dramatic declines in snowpack in the western US: npj Climate and Atmospheric Science, v. 1, article 2, 6 p., accessed August 24, 2021, at https://www.nature.com/articles/s41612-018-0012-1.

Munoz, S.E., Giosan, L., Therrell, M.D., Remo, J.W.F., Shen, Z., Sullivan, R.M., Wiman, C., O’Donnell, M., and Donnelly, J.P., 2018, Climatic control of Mississippi River flood hazard amplified by river engineering: Nature, v. 556, no. 7699, p. 95–98.

National Research Council, 1992, Water transfers in the West—Efficiency, equity, and the environment: Washington, D.C., National Academies Press, 320 p.

Neary, D.G., Ryan, K.C., and DeBano, L.F., eds., 2005, Wildland fire in ecosystems—Effects of fire on soils and water (2008 ed.): U.S. Department of Agriculture, Forest Service, Rocky Mountain Research Station, General Technical Report RMRS–GTR–42–volume 4, 250 p.

Neri, A., Villarini, G., Slater, L.J., and Napolitano, F., 2019, On the statistical attribution of the frequency of flood events across the U.S. Midwest: Advances in Water Resources, v. 127, p. 225–236.

Nigam, S., Barlow, M., and Berbery, E.H., 1999, Analysis links Pacific decadal variability to drought and streamflow in United States: Eos, Transactions, American Geophysical Union, v. 80, no. 51, p. 621–625.

Niyogi, D., Lei, M., Kishtawal, C., Schmid, P., and Shepherd, M., 2017, Urbanization impacts on the summer heavy rainfall climatology over the eastern United States: Earth Interactions, v. 21, no. 5, p. 1–17.

Nowak, K., Hoerling, M., Rajagopalan, B., and Zagona, E., 2012, Colorado River Basin hydroclimatic variability: Journal of Climate, v. 25, no. 12, p. 4389–4403.

Obeysekera, J., and Salas, J.D., 2016, Frequency of recurrent extremes under nonstationarity: Journal of Hydrologic Engineering, v. 21, no. 5, article 04016005, 9 p., accessed May 5, 2016, at https://doi.org/10.1061/(ASCE)HE.1943-5584.0001339.

Ogden, F.L., Pradhan, N.R., Downer, C.W., and Zahner, J.A., 2011, Relative importance of impervious area, drainage density, width function, and subsurface storm drainage on flood runoff from an urbanized catchment: Water Resources Research, v. 47, no. 12, p. 1–12.

Olsen, J.R., Kiang, J.E., and Waskom, R., eds., 2010, Workshop on nonstationarity, hydrologic frequency analysis, and water management: Colorado Water Institute Information Series 109, 304 p., accessed February 1, 2017, at http://www.cwi.colostate.edu/publications/is/109.pdf.

Over, T.M., Saito, R.J., and Soong, D.T., 2016, Adjusting annual maximum peak discharges at selected stations in northeastern Illinois for changes in land-use conditions: U.S. Geological Survey Scientific Investigations Report 2016–5049, 33 p., 4 tables as separate online files, accessed March 18, 2021, at http://pubs.er.usgs.gov/publication/sir20165049.

Painter, C.C., Heimann, D.C., and Lanning-Rush, J.L., 2017, Methods for estimating annual exceedance-probability streamflows for streams in Kansas based on data through water year 2015 (ver. 1.1, September 2017): U.S. Geological Survey Scientific Investigations Report 2017–5063, 22 p., 4 tables as separate online files, accessed March 18, 2021, at https://doi.org/10.3133/sir20175063.

Park, J.Y., Ale, S., Teague, W.R., and Dowhower, S.L., 2017, Simulating hydrologic responses to alternate grazing management practices at the ranch and watershed scales: Journal of Soil and Water Conservation, v. 72, no. 2, p. 102–121.

Pearl, J., 2000, Causality—Models, reasoning, and inference (1st ed.): New York, Cambridge University Press, 400 p.

Pearl, J., and MacKenzie, D., 2018, The book of why—The new science of cause and effect: New York, Basic Books, 418 p.

Peterson, T.C., Heim, R.R., Jr., Hirsch, R., Kaiser, D.P., Brooks, H., Diffenbaugh, N.S., Dole, R.M., Giovannettone, J.P., Guirguis, K., Karl, T.R., Katz, R.W., Kunkel, K., Lettenmaier, D., McCabe, G.J., Paciorek, C.J., Ryberg, K.R., Schubert, S., Silva, V.B.S., Stewart, B.C., Vecchia, A.V., Villarini, G., Vose, R.S., Walsh, J., Wehner, M., Wolock, D., Wolter, K., Woodhouse, C.A., and Wuebbles, D., 2013, Monitoring and understanding changes in heat waves, cold waves, floods, and droughts in the United States—State of knowledge: Bulletin of the American Meteorological Society, v. 94, no. 6, p. 821–834.

Pettitt, A.N., 1979, A non-parametric approach to the change-point problem: Journal of the Royal Statistical Society, Series C (Applied Statistics), v. 28, no. 2, p. 126–135.

Poff, N.L., Allan, J.D., Bain, M.B., Karr, J.R., Prestegaard, K.L., Richter, B.D., Sparks, R.E., and Stromberg, J.C., 1997, The natural flow regime—A paradigm for river conservation and restoration: BioScience, v. 47, no. 11, p. 769–784.

Railsback, L.B., 2004, T. C. Chamberlin's "Method of Multiple Working Hypotheses"—An encapsulation for modern students: Houston Geological Society Bulletin, v. 47, no. 2, p. 68–69.

Railsback, L.B., Locke, W.W., and Johnson, J.G., 1990, Comments and reply on "Method of Multiple Working Hypotheses: A chimera," by J.G. Johnson: Geology, v. 18, no. 9, p. 917–918.

Raup, D.C., and Chamberlin, T.C., 1995, The method of multiple working hypotheses: Journal of Geology, v. 103, no. 3, p. 349–354.

Razavi, S., Elshorbagy, A., Wheater, H., and Sauchyn, D., 2015, Toward understanding nonstationarity in climate and hydrology through tree ring proxy records: Water Resources Research, v. 51, no. 3, p. 1813–1830.

Read, L.K., and Vogel, R.M., 2015, Reliability, return periods, and risk under nonstationarity: Water Resources Research, v. 51, no. 8, p. 6381–6398.

Read, L.K., and Vogel, R.M., 2016, Hazard function analysis for flood planning under nonstationarity: Water Resources Research, v. 52, no. 5, p. 4116–4131.

Regonda, S.K., Rajagopalan, B., Clark, M., and Pitlick, J., 2005, Seasonal cycle shifts in hydroclimatology over the western United States: Journal of Climate, v. 18, no. 2, p. 372–384.

Reilly, T.E., Dennehy, K.F., Alley, W.M., and Cunningham, W.L., 2008, Ground-water availability in the United States: U.S. Geological Survey Circular 1323, 70 p., accessed March 18, 2021, at https://pubs.usgs.gov/circ/1323/pdf/Circular1323_book_508.pdf.

Russell, B., 1913, I.—On the notion of cause: Proceedings of the Aristotelian Society, v. 13, no. 1, p. 1–26.

Ryberg, K.R., 2008, PFReports—A program for systematic checking of annual peaks in NWISWeb: U.S. Geological Survey Open-File Report 2008–1284, 18 p., accessed March 18, 2021, at http://pubs.er.usgs.gov/publication/ofr20081284.

Ryberg, K.R., 2015, The impact of climate variability on streamflow and water quality in the North Central United States: Fargo, N. Dak., North Dakota State University, Ph.D. dissertation, 277 p.

Ryberg, K.R., 2017, Structural equation model of total phosphorus loads in the Red River of the North Basin, USA and Canada: Journal of Environmental Quality, v. 46, no. 5, p. 1072–1080.

Ryberg, K.R., Blomquist, J.D., Sprague, L.A., Sekellick, A.J., and Keisman, J., 2018, Modeling drivers of phosphorus loads in Chesapeake Bay tributaries and inferences about long-term change: Science of The Total Environment, v. 616–617, p. 1423–1430.

Ryberg, K.R., Goree, B.B., Williams-Sether, T., and Mason, R.R., Jr., 2017, The U.S. Geological Survey peak-flow file data verification project, 2008–16: U.S. Geological Survey Scientific Investigations Report 2017–5119, 63 p., 2 app., accessed March 18, 2021, at https://pubs.er.usgs.gov/publication/sir20175119.

Ryberg, K.R., Hodgkins, G.A., and Dudley, R.W., 2020, Change points in annual peak streamflows—Method comparisons and historical change points in the United States: Journal of Hydrology, v. 583, article 124307, accessed March 18, 2021, at https://doi.org/10.1016/j.jhydrol.2019.124307.

Ryberg, K.R., Lin, W., and Vecchia, A.V., 2014, Impact of climate variability on runoff in the north-central United States: Journal of Hydrologic Engineering, v. 19, no. 1, p. 148–158.

Ryberg, K.R., Stone, W.W., and Baker, N.T., 2020, Causal factors for pesticide trends in streams of the United States—Atrazine and deethylatrazine: Journal of Environmental Quality, v. 49, no. 1, p. 152–162, accessed August 24, 2021, at https://doi.org/10.1002/jeq2.20045.

Ryberg, K.R., Vecchia, A.V., Akyüz, F.A., and Lin, W., 2016, Tree-ring-based estimates of long-term seasonal precipitation in the Souris River region of Saskatchewan, North Dakota and Manitoba: Canadian Water Resources Journal/Revue canadienne des ressources hydriques, v. 41, no. 3, p. 412–428.

Salas, J.D., Obeysekera, J., and Vogel, R.M., 2018, Techniques for assessing water infrastructure for nonstationary extreme events—A review: Hydrological Sciences Journal, v. 63, no. 3, p. 325–352.

Sauer, V.B., Thomas, W.O., Jr., Stricker, V.A., and Wilson, K.V., 1983, Flood characteristics of urban watersheds in the United States: U.S. Geological Survey Water-Supply Paper 2207, 63 p.

Schilling, K.E., Chan, K.-S., Liu, H., and Zhang, Y.-K., 2010, Quantifying the effect of land use land cover change on increasing discharge in the Upper Mississippi River: Journal of Hydrology, v. 387, nos. 3–4, p. 343–345.

Schilling, K.E., Jha, M.K., Zhang, Y.-K., Gassman, P.W., and Wolter, C.F., 2008, Impact of land use and land cover change on the water balance of a large agricultural watershed—Historical effects and future directions: Water Resources Research, v. 44, no. 7, article W00A09, 12 p., accessed August 24, 2021, at https://doi.org/10.1029/2007WR006644.

Schwartz, M.S., 2019, Nebraska faces over $1.3 billion in flood losses: NPR, March 21, 2019, accessed June 6, 2019, at https://www.npr.org/2019/03/21/705408364/nebraska-faces-over-1-3-billion-in-flood-losses.

Seaber, P.R., Kapinos, F.P., and Knapp, G.L., 1987, Hydrologic unit maps: U.S. Geological Survey Water-Supply Paper 2294, 63 p., 1 pl., accessed March 9, 2021, at https://pubs.usgs.gov/wsp/wsp2294/.

Shafroth, P.B., and Briggs, M.K., 2008, Restoration ecology and invasive riparian plants—An introduction to the special section on *Tamarix* spp. in western North America: Restoration Ecology, v. 16, no. 1, p. 94–96.

Shafroth, P.B., Wilcox, A.C., Lytle, D.A., Hickey, J.T., Andersen, D.C., Beauchamp, V.B., Hautzinger, A., McMullen, L.E., and Warner, A., 2010, Ecosystem effects of environmental flows—Modelling and experimental floods in a dryland river: Freshwater Biology, v. 55, no. 1, p. 68–85.

Sharma, A., Wasko, C., and Lettenmaier, D.P., 2018, If precipitation extremes are increasing, why aren't floods?: Water Resources Research, v. 54, no. 11, p. 8545–8551.

Sheng, J., and Wilson, J.P., 2009, Watershed urbanization and changing flood behavior across the Los Angeles metropolitan region: Natural Hazards, v. 48, no. 1, p. 41–57.

Shukla, S., Safeeq, M., AghaKouchak, A., Guan, K., and Funk, C., 2015, Temperature impacts on the water year 2014 drought in California: Geophysical Research Letters, v. 42, no. 11, p. 4384–4393.

Shuster, W.D., Bonta, J., Thurston, H., Warnemuende, E., and Smith, D.R., 2005, Impacts of impervious surface on watershed hydrology—A review: Urban Water Journal, v. 2, no. 4, p. 263–275.

Slack, J.R., and Landwehr, J.M., 1992, Hydro-Climatic Data Network (HCDN)—A U.S. Geological Survey streamflow data set for the United States for the study of climate variations, 1874–1988: U.S. Geological Survey Open-File Report 92–129, 193 p., accessed March 18, 2021, at https://pubs.er.usgs.gov/publication/ofr92129.

Slater, L.J., and Villarini, G., 2016, Recent trends in U.S. flood risk: Geophysical Research Letters, v. 43, no. 24, p. 12428–12436.

Slater, L.J., and Villarini, G., 2017, Evaluating the drivers of seasonal streamflow in the U.S. Midwest: Water, v. 9, no. 9, article 695, 22 p., accessed August 24, 2021, at https://doi.org/10.3390/w9090695.

Slater, L.J., Singer, M.B., and Kirchner, J.W., 2015, Hydrologic versus geomorphic drivers of trends in flood hazard: Geophysical Research Letters, v. 42, no. 2, p. 370–376.

Small, D., Islam, S., and Vogel, R.M., 2006, Trends in precipitation and streamflow in the eastern U.S.—Paradox or perception?: Geophysical Research Letters, v. 33, no. 3, article L03403, 4 p., accessed May 23, 2019, at https://doi.org/10.1029/2005GL024995.

Smith, J.A., Baeck, M.L., Morrison, J.E., Sturdevant-Rees, P., Turner-Gillespie, D.F., and Bates, P.D., 2002, The regional hydrology of extreme floods in an urbanizing drainage basin: Journal of Hydrometeorology, v. 3, no. 3, p. 267–282.

Soil and Water Conservation Society, 2003, Conservation implications of climate change—Soil erosion and runoff from cropland: Ankeny, Iowa, Soil and Water Conservation Society, 24 p., accessed March 18, 2021, at https://www.swcs.org/static/media/cms/Climate_changefinal_112904154622.pdf.

Stewart, I.T., Cayan, D.R., and Dettinger, M.D., 2005, Changes toward earlier streamflow timing across western North America: Journal of Climate, v. 18, no. 8, p. 1136–1155.

Stover, S.C., and Montgomery, D.R., 2001, Channel change and flooding, Skokomish River, Washington: Journal of Hydrology, v. 243, nos. 3–4, p. 272–286.

Thomas, H., and Nisbet, T.R., 2007, An assessment of the impact of floodplain woodland on flood flows: Water and Environment Journal, v. 21, no. 2, p. 114–126.

Tiedemann, A.R., Conrad, C.E., Dieterich, J.H., Hornbeck, J.W., Megahan, W.F., Viereck, L.A., and Wade, D.D., 1979, Effects of fire on water—A state-of-knowledge review: U.S. Department of Agriculture Forest Service General Technical Report WO–10, 28 p.

Tollan, A., 2002, Land-use change and floods—What do we need most, research or management?: Water Science and Technology, v. 45, no. 8, p. 183–190.

Tomer, M.D., and Schilling, K.E., 2009, A simple approach to distinguish land-use and climate-change effects on watershed hydrology: Journal of Hydrology, v. 376, nos. 1–2, p. 24–33.

Trenberth, K.E., 2011, Attribution of climate variations and trends to human influences and natural variability: Wiley Interdisciplinary Reviews (WIREs) Climate Change, v. 2, no. 6, p. 925–930.

Trenberth, K.E., and Hurrell, J.W., 1994, Decadal atmosphere-ocean variations in the Pacific: Climate Dynamics, v. 9, no. 6, p. 303–319.

U.S. Army Corps of Engineers, 2018, National inventory of dams: U.S. Army Corps of Engineers database, accessed August 9, 2019, at https://nid.sec.usace.army.mil/ords/f?p=105:1.

U.S. Environmental Protection Agency, 2018a, Basic information about CADDIS [Causal Analysis/Diagnosis Decision Information System]: U.S. Environmental Protection Agency website, accessed March 14, 2019, at https://www.epa.gov/causal-analysisdiagnosis-decision-information-system-caddis/caddis-basic-information.

U.S. Environmental Protection Agency, 2018b, Step 5. Identify probable causes—Weigh the evidence for each cause, *in* CADDIS [Causal Analysis/Diagnosis Decision Information System] Volume 1, Stressor identification: U.S. Environmental Protection Agency web page, accessed March 14, 2019, at https://www.epa.gov/caddis-vol1/caddis-volume-1-stressor-identification-evaluating-multiple-types-of-evidence-consistency-of-evidence.

U.S. Geological Survey, 2019a, Peak streamflow for the Nation: U.S. Geological Survey National Water Information System, [peak-flow file], accessed March 12, 2019, at https://nwis.waterdata.usgs.gov/usa/nwis/peak.

U.S. Geological Survey, 2019b, USGS water data for the Nation: U.S. Geological Survey National Water Information System database, accessed March 18, 2021, at https://doi.org/10.5066/F7P55KJN.

Vano, J.A., Dettinger, M.D., Cifelli, R., Curtis, D., Dufour, A., Miller, K., Olsen, J.R., and Wilson, A.M., 2019, Hydroclimatic extremes as challenges for the water management community—Lessons from Oroville Dam and Hurricane Harvey: Bulletin of the American Meteorological Society, v. 100, no. 1, supplement, p. S9–S14, accessed March 18, 2021, at http://www.ametsoc.net/eee/2017a/ch3_EEEof2017_Vano.pdf.

Vecchia, A.V., 2008, Climate simulation and flood risk analysis for 2008–40 for Devils Lake, North Dakota: U.S. Geological Survey Scientific Investigations Report 2008–5011, 28 p., accessed March 18, 2021, at https://pubs.er.usgs.gov/publication/sir20085011.

Vigen, T., 2015, Spurious correlations: New York, Hachette Books, 208 p.

Villarini, G., and Slater, L.J., 2017, Climatology of flooding in the United States, *in* Cutter, S.L., ed., Oxford research encyclopedia of natural hazard science: Oxford, England, Oxford University Press, accessed March 18, 2021, at https://dspace.lboro.ac.uk/2134/24451.

Villarini, G., Serinaldi, F., Smith, J.A., and Krajewski, W.F., 2009, On the stationarity of annual flood peaks in the continental United States during the 20th century: Water Resources Research, v. 45, no. 8, article W08417, 17 p., accessed May 23, 2019, at https://doi.org/10.1029/2008WR007645.

Villarini, G., Smith, J.A., Baeck, M.L., Vitolo, R., Stephenson, D.B., and Krajewski, W.F., 2011, On the frequency of heavy rainfall for the Midwest of the United States: Journal of Hydrology, v. 400, nos. 1–2, p. 103–120.

Villarini, G., Taylor, S., Wobus, C., Vogel, R.M., Hecht, J., White, K., Baker, B., Gilroy, K., Olsen, J.R., and Raff, D., 2018, Floods and nonstationarity—A review: U.S. Army Corps of Engineers Civil Works Technical Series CWTS 2018–01, 83 p., accessed March 1, 2019, at https://usace.contentdm.oclc.org/digital/collection/p266001coll1/id/6036/.

Vogel, R.M., Yaindl, C., and Walter, M., 2011, Nonstationarity—Flood magnification and recurrence reduction factors in the United States: JAWRA, Journal of the American Water Resources Association, v. 47, no. 3, p. 464–474.

Vose, R.S., Easterling, D.R., Kunkel, K.E., LeGrande, A.N., and Wehner, M.F., 2017, Temperature changes in the United States, chap. 6 *of* Wuebbles, D.J., Fahey, D.W., Hibbard, K.A., Dokken, D.J., Stewart, B.C., and Maycock, T.K., eds., Climate science special report, v. I *of* Fourth national climate assessment: Washington, D.C., U.S. Global Change Research Program, p. 185–206.

Wang, D., and Hejazi, M., 2011, Quantifying the relative contribution of the climate and direct human impacts on mean annual streamflow in the contiguous United States: Water Resources Research, v. 47, no. 10, article W00J12, 16 p., accessed November 7, 2019, at https://doi.org/10.1029/2010WR010283.

Wang, H., Schubert, S., Suarez, M., Chen, J., Hoerling, M., Kumar, A., and Pegion, P., 2009, Attribution of the seasonality and regionality in climate trends over the United States during 1950–2000: Journal of Climate, v. 22, no. 10, p. 2571–2590.

Ward, A.C., 2009, The role of causal criteria in causal inferences—Bradford Hill's "aspects of association": Epidemiologic Perspectives & Innovations, v. 6, article 2, 22 p., accessed August 24, 2021, at https://pubmed.ncbi.nlm.nih.gov/19534788/.

Westra, S., Thyer, M., Leonard, M., Kavetski, D., and Lambert, M., 2014, A strategy for diagnosing and interpreting hydrological model nonstationarity: Water Resources Research, v. 50, no. 6, p. 5090–5113.

White, M.D., and Greer, K.A., 2006, The effects of watershed urbanization on the stream hydrology and riparian vegetation of Los Peñasquitos Creek, California: Landscape and Urban Planning, v. 74, no. 2, p. 125–138.

Wibben, H.C., 1976, Effects of urbanization on flood characteristics in Nashville-Davidson County, Tennessee: U.S. Geological Survey Water-Resources Investigations Report 76–121, 33 p., accessed March 18, 2021, at https://pubs.usgs.gov/wri/wri76-121/pdf/wrir_76-121_a.pdf.

Williams-Sether, T., Ryberg, K.R., and Goree, B.B., 2017, Data documenting the U.S. Geological Survey peak-flow file data verification project, 2008–16: U.S. Geological Survey data release, accessed March 12, 2019, at https://doi.org/10.5066/F7GH9G3P.

Wine, M.L., and Cadol, D., 2016, Hydrologic effects of large southwestern USA wildfires significantly increase regional water supply—Fact or fiction?: Environmental Research Letters, v. 11, no. 8, article 085006, 13 p., accessed March 15, 2021, at https://iopscience.iop.org/article/10.1088/1748-9326/11/8/085006.

Wine, M.L., Cadol, D., and Makhnin, O., 2018, In ecoregions across western USA streamflow increases during post-wildfire recovery: Environmental Research Letters, v. 13, no. 1, article 014010, 14 p., accessed March 15, 2021, at https://iopscience.iop.org/article/10.1088/1748-9326/aa9c5a.

Winkler, R., Boon, S., Zimonick, B., and Baleshta, K., 2010, Assessing the effects of post-pine beetle forest litter on snow albedo: Hydrological Processes, v. 24, no. 6, p. 803–812.

Winkler, R., Boon, S., Zimonick, B., and Spittlehouse, D., 2014, Snow accumulation and ablation response to changes in forest structure and snow surface albedo after attack by mountain pine beetle: Hydrological Processes, v. 28, no. 2, p. 197–209.

Wise, E.K., Woodhouse, C.A., McCabe, G.J., Pederson, G.T., and St-Jacques, J.-M., 2018, Hydroclimatology of the Missouri River Basin: Journal of Hydrometeorology, v. 19, no. 1, p. 161–182.

Woodhouse, C.A., Pederson, G.T., Morino, K., McAfee, S.A., and McCabe, G.J., 2016, Increasing influence of air temperature on upper Colorado River streamflow: Geophysical Research Letters, v. 43, no. 5, p. 2174–2181.

Wuebbles, D.J., Fahey, D.W., Hibbard, K.A., Dokken, D.J., Stewart, B.C., and Maycock, T.K., eds., 2017, Climate science special report, v. I *of* Fourth national climate assessment: U.S. Global Change Research Program, 470 p., accessed October 29, 2018, at https://science2017.globalchange.gov/.

Yang, L., Smith, J.A., Baeck, M.L., Bou-Zeid, E., Jessup, S.M., Tian, F., and Hu, H., 2014, Impact of urbanization on heavy convective precipitation under strong large-scale forcing—A case study over the Milwaukee–Lake Michigan region: Journal of Hydrometeorology, v. 15, no. 1, p. 261–278.

York, B.C., Ryberg, K.R., Asquith, W.H., Chase, K.J., Dickinson, J.E., Dudley, R.W., Harden, T.M., Hodgkins, G.A., Holtschlag, D.J., Humberson, D.G., Konrad, C.P., Levin, S.B., Restivo, D.E., Sando, R., Sando, S.K., Swain, E.D., Tillery, A.C., and Totten, A.R., 2022, Attributions for nonstationary peak streamflow records across the conterminous United States, 1941–2015 and 1966–2015: U.S. Geological Survey data release, https://doi.org/10.5066/P9FOUVWG.

Zeng, R., and Cai, X., 2014, Analyzing streamflow changes—Irrigation-enhanced interaction between aquifer and streamflow in the Republican River Basin: Hydrology and Earth System Sciences, v. 18, p. 493–502, accessed March 12, 2021, at https://doi.org/10.5194/hess-18-493-2014.

Zhang, W., Villarini, G., Vecchi, G.A., and Smith, J.A., 2018, Urbanization exacerbated the rainfall and flooding caused by Hurricane Harvey in Houston: Nature, v. 563, no. 7731, p. 384–388.

Zhang, Y.-K., and Schilling, K.E., 2006, Increasing streamflow and baseflow in Mississippi River since the 1940s—Effect of land use change: Journal of Hydrology, v. 324, nos. 1–4, p. 412–422.

Zhu, Y., and Newell, R.E., 1998, A proposed algorithm for moisture fluxes from atmospheric rivers: Monthly Weather Review, v. 126, no. 3, p. 725–735.

Zhuang, W., 2016, Eco-environmental impact of inter-basin water transfer projects—A review: Environmental Science and Pollution Research, v. 23, no. 13, p. 12867–12879.

Attribution of Monotonic Trends and Change Points in Peak Streamflow in the Pacific Northwest Region of the United States, 1941–2015 and 1966–2015

By Christopher P. Konrad and Daniel E. Restivo

Chapter B of

Attribution of Monotonic Trends and Change Points in Peak Streamflow Across the Conterminous United States Using a Multiple Working Hypotheses Framework, 1941–2015 and 1966–2015

Karen R. Ryberg, editor

Prepared in cooperation with
U.S. Department of Transportation
Federal Highway Administration

Professional Paper 1869

U.S. Department of the Interior
U.S. Geological Survey

U.S. Geological Survey, Reston, Virginia: 2022

Suggested citation:
Konrad, C.P., and Restivo, D.E., 2022, Attribution of monotonic trends and change points in peak streamflow in the Pacific Northwest region of the United States, 1941–2015 and 1966–2015, chap. B *of* Ryberg, K.R., ed., Attribution of monotonic trends and change points in peak streamflow across the conterminous United States using a multiple working hypotheses framework, 1941–2015 and 1966–2015: U.S. Geological Survey Professional Paper 1869, p. B1–B31, https://doi.org/10.3133/pp1869.

Associated data for this publication:
Dudley, R.W., Archfield, S.A., Hodgkins, G.A., Renard, B., and Ryberg, K.R., 2018, Peak-streamflow trends and change-points and basin characteristics for 2,683 U.S. Geological Survey streamgages in the conterminous U.S. (ver. 3.0, April 2019): U.S. Geological Survey data release, https://doi.org/10.5066/P9AEGXY0.

York, B.C., Ryberg, K.R., Asquith, W.H., Chase, K.J., Dickinson, J.E., Dudley, R.W., Harden, T.M., Hodgkins, G.A., Holtschlag, D.J., Humberson, D.G., Konrad, C.P., Levin, S.B., Restivo, D.E., Sando, R., Sando, S.K., Swain, E.D., Tillery, A.C., and Totten, A.R., 2022, Attributions for nonstationary peak streamflow records across the conterminous United States, 1941–2015 and 1966–2015: U.S. Geological Survey data release, https://doi.org/10.5066/P9FOUVWG.

ISSN 2330-7102 (online)

Acknowledgments

The work described in this professional paper was funded by the Federal Highway Administration of the U.S. Department of Transportation through Interagency Agreement DTFH6116X30020, "Flood Frequency Estimation for Hydraulic Design."

Contents

Figures

Tables

Conversion Factors

Multiply	By	To obtain
	Length	
millimeter (mm)	0.03937	inch (in.)
meter (m)	3.281	foot (ft)
kilometer (km)	0.6214	mile (mi)
	Flow rate	
cubic foot per second (ft^3/s)	0.02832	cubic meter per second (m^3/s)
	Mass	
kilogram (kg)	2.205	pound, avoirdupois (lb)
	Mass transport rate	
kilogram per meter per second (kg/m/s)	0.6720	pound per foot per second (lb/ft/s)

Datum

Vertical coordinate information is referenced to the North American Vertical Datum of 1988 (NAVD 88).

Horizontal coordinate information is referenced to the North American Datum of 1983 (NAD 83).

Altitude, as used in this report, refers to distance above the vertical datum.

Supplemental Information

A “water year” is the 12-month period from October 1 through September 30 of the following year that is designated by the calendar year in which it ends.

The 75-year and 50-year study periods described in this report span water years 1941–2015 and 1966–2015, respectively.

Abbreviations

>	greater than
<	less than
ENSO	El Niño-Southern Oscillation
GAGES-II	Geospatial Attributes of Gages for Evaluating Streamflow, Version II
HCDN	Hydro-Climatic Data Network 2009
HUC4	four-digit hydrologic unit code
IVT	vertically integrated water vapor transport
NAD 83	North American Datum of 1983
NAVD 88	North American Vertical Datum of 1988
NAWQA	National Water-Quality Assessment Program
NLCD 2011	2011 National Land Cover Database
NWALT	NAWQA Wall-to-Wall Anthropogenic Land Use Trends
NWIS	National Water Information System
PDO	Pacific Decadal Oscillation
p-value	probability used to reject the null hypothesis in a statistical test
USGS	U.S. Geological Survey

Attribution of Monotonic Trends and Change Points in Peak Streamflow in the Pacific Northwest Region of the United States, 1941–2015 and 1966–2015

By Christopher P. Konrad[1] and Daniel E. Restivo[1]

Abstract

Nonstationarity of annual peak streamflow was evaluated at 264 U.S. Geological Survey (USGS) streamgages in the Pacific Northwest region of the United States. This study is part of the second phase of an investigation by the U.S. Geological Survey (USGS), in collaboration with the Federal Highway Administration of the U.S. Department of Transportation, that identified statistically significant changes (*p*-value<0.10, where the *p*-value is the probability used to reject the null hypothesis in a statistical test) in the magnitude of annual peak streamflows across the conterminous United States. Monotonic trends and change points (herein referred to as “trends”) in the median annual peak-streamflow data for two time periods (1941–2015 and 1966–2015) were attributed to factors related to climate, water management, or land use by applying a nationally consistent multiple working hypotheses framework. The attribution of a trend and the strength of the attribution was determined with a qualitative weight-of-evidence approach.

Of the 71 streamgages in the Pacific Northwest region that were part of the USGS Hydro-Climatic Data Network 2009 (HCDN), 22 had significant trends in annual peak streamflow, most of which were attributed to changes in short-term precipitation. Eleven of these HCDN streamgages had positive trends, 10 of which were attributed to short-term precipitation with medium to robust evidence because of more frequent and intense landfalling atmospheric rivers, particularly from the late 1990s through 2010 in western Washington. Positive trends at these 10 HCDN streamgages attributed to short-term precipitation may instead be the result of multidecadal climate variability, but the limited period of record at these streamgages does not provide evidence about the historical magnitude and frequency of annual peaks. Three of the 71 HCDN streamgages had negative trends that reflect recent dry years in northern California when annual peaks were low. Trends were attributed to short-term precipitation at two of the HCDN streamgages without long streamflow records and to multidecadal climate variability at one HCDN streamgage with records extending back to the 1930s (which indicates historical periods of comparably low annual peak streamflow).

Of the 193 non-HCDN streamgages in the Pacific Northwest region, 84 streamgages had significant trends. Thirty-nine of these non-HCDN streamgages had negative trends attributed to large artificial impoundments. Short-term precipitation and multidecadal climate variability are also likely to have produced trends at 28 of the non-HCDN streamgages where the timing and direction of those trends are consistent with trends at nearby HCDN streamgages.

Attributions of trends in annual peak streamflow have medium evidence at most streamgages in the Pacific Northwest in part because attributions are not mutually exclusive. For example, trends were attributed to multidecadal climate variability rather than short-term precipitation only in cases where the peak streamflow record demonstrated more than one period when peaks were abnormally low or high. Likewise, the distinction between an attribution of a trend to snowpack and air temperature is inexact in the Pacific Northwest because the accumulation of low-altitude snowpack—which affects the magnitude of spring/summer snowmelt peaks and autumn/winter rain-on-snow peaks—is sensitive to both precipitation and air temperature.

Introduction

The magnitude and frequency of annual peak streamflows are important for flood risk management, water supply, land-use planning, and the ecological integrity of rivers and streams. Flood-frequency analyses typically require an assumption that annual peak streamflow at a streamgage has a stationary mean and variance over time, but this presumption should be tested as an initial step in determining the frequency of annual peak streamflow at a streamgage (England and others, 2018). Where the magnitude of annual peak streamflow has a trend over time, further examination of potential factors contributing to the trend can inform how the trend should be treated in the frequency analysis.

[1]U.S. Geological Survey.

Purpose and Scope

This current work builds upon a previous effort by the U.S. Geological Survey (USGS), in collaboration with the Federal Highway Administration of the U.S. Department of Transportation, to identify statistically significant monotonic trends and change points in annual peak-streamflow data across the conterminous United States. This chapter describes changes over time in the magnitude of annual peak streamflow at 264 USGS streamgages in the Pacific Northwest region of the United States; these changes were attributed to factors related to climate, land use, or water management. Dudley and others (2018) identified these changes as statistically significant monotonic trends or change points in annual peak streamflow for two time periods: water years 1941 to 2015 (a 75-year time period) and 1966 to 2015 (a 50-year time period). The 75-year period indicates more persistent changes in annual peak streamflow while the 50-year period expands the number of streamgages that could be tested for trends. Although data from the period of record were analyzed at each streamgage, attributions for monotonic trends and change points apply only to the 75- and 50-year periods. This region includes 71 streamgages in the USGS Hydro-Climatic Data Network 2009 (HCDN), which includes streamgages for which streamflow primarily reflects meteorological conditions and excludes streamgages where streamflow is affected by human activities (Lins, 2012).

A monotonic trend (also referred to as a rank trend) is a time series of annual peak streamflow when values are generally increasing or decreasing over time (Dudley and others, 2018). A monotonic trend is indicated by a significant Mann-Kendall test (Mann, 1945). A change point is a year when the median value of annual peak streamflow before the year is different than the median value after the year, which represents a step trend (Dudley and others, 2018). A change point is indicated by a significant Pettitt test (Pettitt, 1979), and the change point associated with the largest change in annual streamflow is used here to identify when the step in annual peak streamflow occurred. For this chapter, the standalone term “trends” is used to refer to a change in annual peak-streamflow data that could either be a monotonic trend or a change point because the two are not necessarily mutually exclusive.

The Pacific Northwest region is defined here as water-resources region 17 (Pacific Northwest) plus subregion 1801 (Klamath-Northern California Coastal) of water-resources region 18 (California) from Seaber and others (1987). The Pacific Northwest region includes Washington, most of Idaho and Oregon, and parts of California, Montana, Nevada, Utah, and Wyoming (fig. B1). Although the northern part of the Pacific Northwest region extends into Canada because of the topography of stream drainage basins, the watersheds considered for trend attributions are within the conterminous United States.

Attributions were selected from a nationally consistent typology (Barth and others, this volume, chap. A, table A1) that represents climate, water management, land use, and other factors based on readily available, spatially comprehensive information for the attribution. The definitions for the attributions considered for this investigation are not mutually exclusive. In cases where all but one attribution cannot be excluded, the primary attribution had medium evidence. For example, trends were attributed to multidecadal climate variability rather than short-term precipitation only in cases where the peak streamflow record demonstrated more than one period when peaks were abnormally low or high. Likewise, the distinction between an attribution of a trend to snowpack and air temperature is inexact in the Pacific Northwest because the accumulation of low-altitude snowpack—which affects the magnitude of spring/summer snowmelt peaks and autumn/winter rain-on-snow peaks—is sensitive to both precipitation and air temperature. In cases where there was limited evidence for a specific attribution, the results have high uncertainty and may require additional information or refined definitions of possible attributions that clarifies their distinctions.

Hydroclimatic Setting

The Pacific Northwest region has diverse landforms and climate conditions that affect the production, timing, and magnitudes of annual peak streamflow (table B1; Berghuijs and others, 2016). Most precipitation is delivered to the region via storms between October and April (Cayan and others, 1998). The frequencies and tracks of storms are related to large-scale atmospheric and ocean-temperature forcing, including the Pacific Decadal Oscillation (PDO) and the El Niño-Southern Oscillation (ENSO) (Cayan and Peterson, 1989; Hamlet and Lettenmaier, 1999; McCabe and Dettinger, 1999; Bond and Harrison, 2000; Mantua and Hare, 2002; Wang and Liu, 2015). The PDO is characterized by sea-surface temperature anomalies in the northern Pacific Ocean; it also affects atmospheric ridging and troughing and storm tracks (Mantua and others, 1997; Bond and Harrison, 2000). ENSO is characterized by sea-surface temperature anomalies in the eastern tropical Pacific Ocean.

Figure B1 (facing page). Map of the Pacific Northwest region showing elevation, hydrologic subregions as defined by Seaber and others (1987), hydroclimatic subregions as defined in this chapter, and the 264 U.S. Geological Survey streamgages from Falcone (2011) that were included in the attributional analysis. Although the northern part of the Pacific Northwest region extends into Canada because of the topography of stream drainage basins, the watersheds considered for monotonic trend and change point attributions are within the conterminous United States. For this study, the hydrologic regions were based on watersheds identified by two-digit hydrologic unit codes (HUC2s) described by Seaber and others (1987) and were modified slightly by adding or subtracting subregions (HUC4s) to achieve geographic cohesiveness or hydrologic-setting similarity. Term: GAGES-II, Geospatial Attributes of Gages for Evaluating Streamflow, Version II (Falcone, 2011).

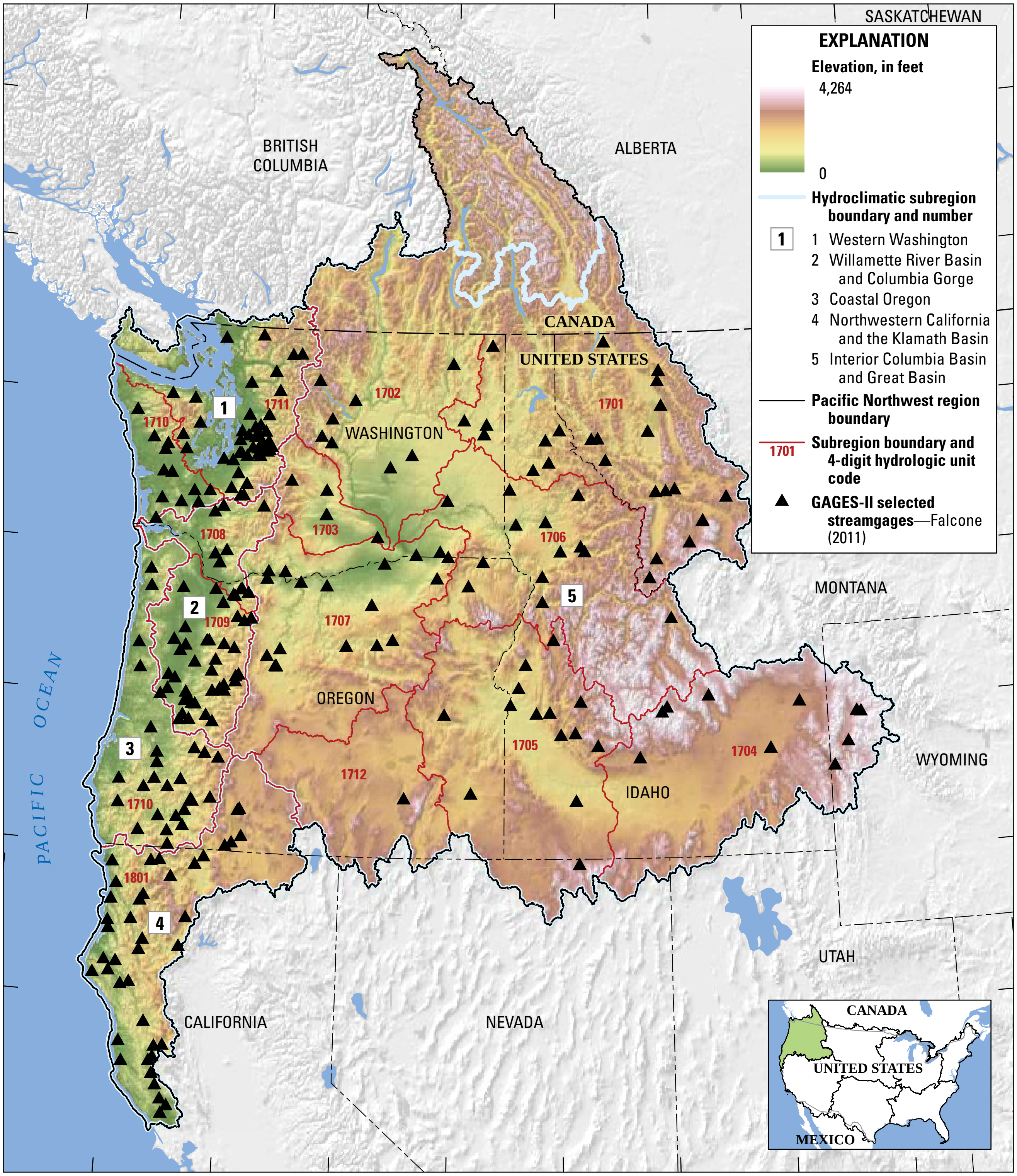

Base from U.S. Geological Survey and other digital data sources and Esri © 2020 and its licensors
North America elevation 1-kilometer-resolution GRID (USGS, 2007)
Regional boundaries derived from modified HUC2 watersheds
USA Contiguous Albers Equal Area Conic USGS projection
North American Datum of 1983

Table B1. Hydroclimatic subregions of the Pacific Northwest region as defined for this study as well as their corresponding landforms, primary hydroclimatological factors influencing annual peak streamflow, and hydrologic unit codes.

[The entries in column three are modified from Konrad and Dettinger (2017). Hydrologic unit codes (HUCs) are from Seaber and others (1987)]

Hydroclimatic subregion	Landforms	Primary hydroclimatological factors influencing annual peak streamflow	HUCs (fig. B1)
Interior Columbia Basin and Great Basin	Columbia Plateau, east slope Cascade Range, Snake River Plain, northern Rocky Mountains, Great Basin	Spring and early summer snowpack, atmospheric rivers in winter, convective rainstorms in summer (smaller basins)	1701–1707, 1712
Willamette River Basin and Columbia Gorge	West slope Cascade Range, east slope Coast Range, Willamette Valley, Columbia Gorge	Atmospheric rivers in autumn and winter, spring snowpack	1708, 1709
Coastal Oregon	West slope Coast Range	Atmospheric rivers in autumn and winter	1710
Western Washington	Coast Range, Olympic Mountains, west slope Cascade Range, Puget Lowland	Atmospheric rivers in autumn and winter	1710, 1711
Northwestern California and the Klamath Basin	Coast Range, Siskiyou Mountains	Atmospheric rivers in winter	1801

The large-scale atmospheric and ocean-temperature cycles of the PDO and ENSO play an important role in annual peak streamflow variability in the Pacific Northwest region, but their phases are not synchronized and their effects on winter storms and snowpack for a given year do not necessarily extend uniformly across the entire region. According to Mantua and Hare (2002), the warm phase PDO is associated with above-average air temperatures for November–April and below-average springtime snowpack and annual peak streamflow whereas the cold phase PDO is associated with colder winters and increased precipitation for the Pacific Northwest. Winters in the El Niño phase of ENSO are characterized by dry and warm conditions whereas winters during the La Niña phase of ENSO are characterized by wet and cold conditions in the Pacific Northwest (Cayan and others, 1999). In contrast, winters in northern California are generally wetter during El Niño and drier during La Niña (Cayan and others, 1999; McCabe and Wolock, 2014). The effects of PDO and ENSO on air temperature and precipitation in the Pacific Northwest are interdependent: when PDO and ENSO are in phase (such that the warm phase PDO coincides with El Niño or the cool phase PDO coincides with La Niña), the climate signal is stronger and more consistent; however, when the PDO and ENSO are out of phase, the climate signal is weaker (Rasmusson and Wallace, 1983; Dettinger and others, 1998; Gershunov and Barnett, 1998; McCabe and Dettinger, 1999; Abatzoglou and others, 2014).

The Cascade Range, Coast Range, and Olympic Mountains are barriers to the prevailing westerly atmospheric flow that transports water vapor from the Pacific Ocean over the region. Precipitation is enhanced by orographic lift over the mountains that forces water vapor out of the atmosphere. As a result, the western slopes of the Cascade Range and Sierra Nevada are wetter than the eastern slopes and the interior Columbia River Basin. Precipitation during winter often falls as snow in the interior Columbia River Basin, in the Great Basin, on the northern Rocky Mountains, and on areas of higher altitudes (>2000 meters [m]) in the Olympic Mountains and Cascade Range. Many areas, particularly at altitudes of about 1,000 m, can receive either rain or snow depending on the temperature of a particular storm.

Rivers draining the Coast Range, Olympic Mountains, west slopes of the Cascade Range and Sierra Nevada, and lowland areas west of the Cascade Range and Sierra Nevada crests have annual peak streamflows during fall and winter that are almost exclusively a result of landfalling atmospheric rivers (Neiman and others, 2011; Konrad and Dettinger, 2017), although annual peaks can also be a result of rain and snowpack at higher altitudes in the Cascade Range and Olympic Mountains during the spring and early summer (Jefferson, 2011). Atmospheric rivers are narrow corridors of vertically integrated water vapor transport (IVT) exceeding 250 kilograms per meters per second (kg/m/s) in the troposphere (Newell and Zhu, 1994; Zhu and Newell, 1998; American Meteorological Society, 2019). The dominant latitude of landfalling atmospheric rivers shifts south across the region from autumn to winter (Neiman and others, 2008). As a result, western Washington rivers typically have annual peaks in late autumn and early winter whereas northern California and Klamath Basin rivers have annual peaks primarily in winter. Eldardiry and others (2019) found that the most extreme annual precipitation events are associated with atmospheric rivers during January and February. Although the magnitude of runoff from atmospheric rivers is related to their IVT, it is also influenced by the combined orographic effect of basin aspect and wind direction, air temperature, antecedent soil moisture, and snowmelt from higher altitude areas (McCabe and others, 2007; Neiman and others, 2008, 2011; Ralph and others, 2013; Konrad and Dettinger, 2017).

East of the Cascade Range crest in the interior Columbia River Basin and Great Basin, annual peak streamflow commonly results from spring and early summer snowmelt.

Strong winter atmospheric rivers can reach the interior Pacific Northwest region, particularly where lower or less continuous topography facilitates inland penetration (Rutz and others, 2014). Convective storms during summer can also produce annual peaks, particularly in smaller streams. Lower altitude areas in the interior Pacific Northwest are generally arid, so the annual variation of peak streamflow is high and peaks in some years do not represent major floods (Konrad and Dettinger, 2017).

Summary of Reported Trends in Annual Peak Streamflow

Many studies have investigated the timing, direction, and causes of long-term streamflow variability and trends in the Pacific Northwest region, including national studies that have regionalized results (for example, Lins and Slack, 1999; McCabe and Wolock, 2014; Archfield and others, 2016). Although the focus of many of the studies has been climate-related trends (Lins and Slack, 1999; Kalra and others, 2008; Luce and others, 2013), research has been done on the effects of land use and reservoir operation (Konrad and Booth, 2002; Hatcher and Jones, 2013).

Lins and Slack (1999) analyzed trends in annual maximum daily mean streamflow at 52 HCDN streamgages for 30-, 40-, 50-, 60-, 70-, and 80-year periods ending in 1993. Lins and Slack (1999) found negative trends (decreasing flood magnitude) in the Pacific Northwest region for the 50-year period (mainly in northwest California and east of the Cascade Range) and noted that trends displayed interdecadal variability. Lins and Slack (2005) updated the analysis for the 60-year period of 1940 to 1999 and found positive trends (increasing flood magnitude) at 4 of the HCDN streamgages in the Pacific Northwest region and negative trends at none of the HCDN streamgages. McCabe and Wolock (2014) analyzed annual departures from the mean seasonal maximum daily streamflow for a cluster of minimally altered streamgages in the Pacific Northwest that had similar temporal variability. They found cyclical changes in seasonal maximum daily streamflow with a general wet period in the 1950s, the early 1980s, and the late 1990s, as well as a general dry period in the late 1970s and early 2000s.

Archfield and others (2016) found regionally consistent increases in the frequency and magnitude of daily peak streamflow for northwestern Washington for the period from 1940 to 2013. Hodgkins and others (2019) analyzed long-term trends (periods of 50 years or longer, ending in 2015) in frequent peaks (those that typically occur multiple times in a year) and found increases in western Washington and decreases in western Oregon and northern California; these results are consistent with the findings of Archfield and others (2016). Mastin and others (2016) analyzed long-term trends in the frequency of independent peaks above a threshold at unregulated, non-urbanized streamgages in Washington and found that all 16 positive trends were confined to the western side of the Cascade Range and that 3 of the 5 negative trends were confined to the eastern side. Looking at trends in annual peak streamflow lasting at least 10 years and persisting through 2015, Mastin and others (2016) found that positive trends were common for periods beginning in the 1940s or after 1965 and that negative trends were common for periods beginning around 1945 or after 1972. When examining 10-year trends in annual peak streamflow, Mastin and others (2016) found positive trends for decades centered around 1945, 1956, 1970, 1992, and 2004, and negative trends for decades centered around 1936, 1990, 2000, and 2010. These patterns indicate that regional climate variation can have a systematic influence on trend tests when the starting or ending of a period coincides with a wetter or drier period.

Annual peak streamflow in the Pacific Northwest region has cyclic variability at decadal scales due to the PDO and ENSO, the two dominant cycles in sea-surface temperature that affect precipitation and snowpack in the Pacific Northwest (Cayan and Peterson, 1989; Dettinger and others, 1998; McCabe and Wolock, 2014; Mastin and others, 2016). Both precipitation and air temperature influence peak streamflow in the region and are both affected by cyclic climate variability. As a result, the timing of regional climate cycles (relative to the period of analysis used for trend tests) is essential context for interpreting trends in annual peak streamflow.

Kalra and others (2008) found decreasing annual and seasonal streamflows from before and after 1977 in the Pacific Northwest region (mostly west of the Cascade Range). This change point is consistent with the rapid climatic shift accompanying the transition in prevailing PDO regimes from cool to warm during this year (Mantua and others, 1997; Mantua and Hare, 2002). Prior to 1977, the PDO had been in a cool phase since the late 1940s, with only brief (<5 year) departures into warm phases (Mantua and others, 1997). There is limited evidence of recent increases in the intensity of precipitation for the Pacific Northwest region (Mass and others, 2011; Easterling and others, 2017), but projections from climate models indicate a strong likelihood of more frequent and intense atmospheric rivers and more dry years where annual peak streamflow may be relatively small, particularly for California (Warner and others, 2015; Gershunov and others, 2019).

Not all climate effects on annual peak streamflows can be attributed to the PDO or ENSO, particularly for peaks of snowmelt-dominant and transitional systems. Hatcher and Jones (2013) found that the timing of annual snowmelt-runoff peaks in five of seven headwater basins of the Columbia River Basin shifted to be a few days earlier in the year over the period of 1950 to 2010, which is consistent with the earlier timing of overall runoff (Knowles and others, 2006). Luce and others (2013) suggested that observed decreases in snowpack in the Cascade Range and northern Rocky Mountains of the Pacific Northwest region may be linked to decreases in lower tropospheric westerly wind speeds and reduced orographic enhancement of precipitation.

Regional trends highlighted in the above cited literature are useful for understanding the mechanisms driving tends in annual peak streamflows in the Pacific Northwest region. However, Archfield and others (2016) concluded that the complex, geographically fragmented patterns of trends and the relatively low explanatory power of regional and global explanatory variables suggest that trend attributions are most confidently made on a catchment scale. It is possible, for example, that changes in regional climate are not represented in the data for all streamgages because of the high variability of annual peaks and, as a result, low statistical power to detect trends (Konrad and Restivo, 2020).

Reservoirs, land-cover changes, and engineered drainage systems affect annual peak streamflow for many rivers in the region, and the historical timing of these human activities is likely to determine when trends are observed at affected streamgages (Konrad and Booth, 2002; Gendaszek and others, 2012). Water management with reservoirs has been integral to the development of agriculture, industries, and cities beginning in the late 19th century and continuing through the 20th century. Reservoirs are operated for hydropower, water supply, and flood control and are expected to reduce peak streamflow because runoff from large storms and periods of snowmelt is stored (Graf, 2006). Land-cover changes associated with timber harvesting, agriculture, and urban development are pervasive in the Pacific Northwest region, but their consequences for annual peak streamflow may be limited except where changes have a relatively large spatial extent (Bowling and others, 2000; Jones, 2000; Konrad and others, 2005).

Approach and Methods

Nonstationarity in the distribution of annual peak streamflow was examined at 264 USGS streamgages in the Pacific Northwest region (fig. B1). Annual peak-streamflow data at these streamgages were previously identified by Dudley and others (2018) as having statistically significant (p-value<0.10, where the p-value is the probability used to reject the null hypothesis in a statistical test) trends for the periods of 1941–2015 or 1966–2015. Trends at these streamgages were attributed to nationally consistent factors (Barth and others, this volume, chap. A, table A1) related to climate, water management, or land use by applying a nationally consistent multiple working hypotheses framework; the strength of each attribution was evaluated using a weight-of-evidence approach as opposed to a definitive test based on a single criterion. Key principles for this application of a weight-of-evidence approach are (1) attributions of trends to climatic or meteorological factors must be related to the dominant mechanisms producing floods in particular rivers, which vary by subregion, and should be evident in each subregion in rivers unaffected by large artificial impoundments or land use; (2) attributions related to land use and large artificial impoundments (reservoirs) must be consistent with known and, thus, predictable effects on floods; and (3) different attributions are not necessarily mutually exclusive and may depend on different types of evidence, so the primary attribution may reflect the availability of evidence. The weight-of-evidence approach was implemented by identifying the possible attributions for a trend at each streamgage and then selecting the primary attribution with the most supporting evidence and a secondary attribution when the primary attribution had limited evidence.

Streamgages were assigned to one of five hydroclimatic subregions, which are based on hydrologic subregions defined by four-digit hydrologic unit codes (HUC4s; Seaber and others, 1987) (fig. B1; tables B1, B2). For the weight-of-evidence approach, the attribution at each streamgage with a trend was generally based on the dominant climatological and meteorological mechanisms that generated floods in its

Table B2. Summary of the numbers and types of U.S. Geological Survey streamgages where monotonic trends and change points were analyzed for the five hydroclimatic subregions in the Pacific Northwest region.

[Regulated streamgages (column four) have upstream reservoir storage volume that is equivalent to a depth of more than 30 millimeters over the streamgage basin (Falcone, 2017). Streamgage data are from Dudley and others (2018). HCDN, Hydro-Climatic Data Network 2009]

Hydroclimatic subregion	Number of streamgages	Streamgages in the HCDN	Regulated streamgages	Urban streamgages	Non-HCDN streamgages with 75 or more years of record	HCDN streamgages with 75 or more years of record
Interior Columbia Basin and Great Basin	95	21	23	0	57	10
Willamette River Basin and Columbia Gorge	49	13	29	1	31	7
Coastal Oregon	26	6	11	0	16	4
Western Washington	54	21	19	1	27	12
Northwestern California and the Klamath Basin	40	10	19	0	19	2
Total	**264**	**71**	**101**	**2**	**150**	**35**

subregion (table B1; Berghuijs and others, 2016) and streamflow responses to recent regional climatology (DeFlorio and others, 2013; Mastin and others, 2016). Annual peak streamflow in western Washington, coastal Oregon, the Willamette River Basin, the Columbia Gorge, and northwestern California is generally a result of short-term precipitation delivered by atmospheric rivers, which typically last from 10 to 100 hours over a location (Konrad and Dettinger, 2017). Snowmelt commonly yields annual peak streamflow in high-altitude basins, the interior Columbia River Basin, and the Great Basin. Convective storms during the summer can also produce annual peak streamflow (particularly in the interior parts of the Pacific Northwest region), but this is not a dominant mechanism for any hydroclimatic subregion.

Within each hydroclimatic subregion, we determined whether trends were present at HCDN streamgages and identified the periods when those trends manifested. Because HCDN streamgages are presumed to be unaffected by land use or water management, climate-related attributions were made for trends at HCDN streamgages. If a trend at a non-HCDN streamgage was consistent with the direction (positive or negative) and timing of a trend at HCDN streamgage(s) in the same hydroclimatic subregion, then the climate-related attribution for the HCDN streamgage was also attributed to the trend at the non-HCDN streamgage. In cases where the record length at a streamgage with a trend did not span a period of climate variability indicated at nearby HCDN streamgages, the trend was attributed to a proximate factor (either short-term precipitation, snowpack, or air temperature). If a non-HCDN streamgage had a trend with a different direction or distinct timing from a HCDN streamgage in the same subregion, then factors related to land use and water management were evaluated as alternatives to climatic or meteorological factors for attribution.

Climate-Related Trends

Climate-related attributions for annual peak-streamflow trends in the Pacific Northwest region were short-term precipitation, snowpack, and air temperature as proximate factors and multidecadal climate variability as a longer term factor that can encompass the proximate factors. The location of a drainage basin relative to the coast, its mean altitude, and the median day of the year for annual peak streamflow were used to determine whether rainfall, snowmelt, or both were the dominant mechanisms that produced floods at each streamgage. Trends were generally not attributed to long-term precipitation. Rivers in the Pacific Northwest region, except for the Columbia and Snake Rivers, are short (<500 kilometers [km] long) and steep, so runoff and routing of high flows is relatively rapid. Antecedent conditions (such as depression storage and soil moisture) can influence the flood magnitude but generally reflect storms from the previous few days rather than long-term seasonal precipitation because of the steep, well-drained terrain and short storm durations. Given the combination of short, steep rivers and the short duration of atmospheric rivers, long-term precipitation (over time scales greater than 30 days) generally does not generate annual peak streamflow in the region other than for higher altitude basins where snow is the dominant form of precipitation (Konrad and Dettinger, 2017). In such cases, trends were attributed to snowpack.

Timing of Trends

The timing of trends in annual peak streamflow was examined at each streamgage that had a significant trend for the 50- or 75-year periods for evidence that the trend was persistent rather than an artifact of years with extremely low or high values near the start or end of the series (Wahl, 1998). To identify persistent trends, the Mann-Kendall test for rank trends (Mann, 1945) was applied repeatedly for all possible starting and ending year pairs that were separated by at least 10 water years for the period of record at each streamgage, which may have started prior to 1941 (York and others, 2022). The results of these tests are depicted on flag plots as Mann-Kendall rank correlation coefficients. We used a higher level of significance (p-value<0.05) for these tests than for the 50-year and 75-year tests for trends because of the large number of tests at each streamgage and to improve the resolution of trend timing. The rank correlation coefficients between annual peak streamflow and year determined from the Mann-Kendall test were plotted as colors (blue indicating a strong positive rank correlation, red indicating a strong negative rank correlation) for each pair of starting years (x-axis values) and ending years (y-axis values) (McCabe and Wolock, 2002) that had a significant Mann-Kendall test result. The flag plots were inspected visually to determine the timing of trends. The earliest ending year and the latest starting year of the long-term trend was noted, as well as if the trend persisted for later starting years. If the trend did not persist, the earliest starting year after which there are no trends was noted; the lack of a persistent trend indicates a change point.

We presumed that streamgages in close proximity to each other would have consistent starting and ending years for trends attributed to climatic factors. Differences between monotonic trends and change points can be discerned in some cases, as can multiple steps and short-term cyclic trends that may not be significant over a longer period of record. If the timing of a trend at a non-HCDN streamgage was consistent with the timing of a trend at a HCDN streamgage within the same hydroclimatic subregion, the trend at the non-HCDN streamgage was attributed to the same causal factor as the trend at the HCDN streamgage.

Given that the cool phases of the PDO and ENSO were dominant from the late 1940s through the mid-1970s, monotonic trends for the 50-year period at streamgages without monotonic trends for the 75-year period were attributed to multidecadal climate variability (Bond and Harrison, 2000; Mehta, 2017). For streamgages in California with longer periods of record, attribution of trends to multidecadal climate variability was also evidenced by a period with low annual peak streamflow in the 1920s and 1930s, given the prolonged drought during this period (Jones, 2020). Flag plots of trends for all possible starting and ending years separated by at least 10 years were created and examined to determine if trends at a streamgage with a short record were synchronized with trends at streamgages with longer records. In most cases, however, multidecadal climate variability was not used as the attribution for trends at streamgages with short records because of limited evidence; instead, an attribution with more evidence (for example, short-term precipitation) was used.

Differentiating Short-Term Precipitation From Multidecadal Climate Variability

The intensity of atmospheric rivers was used as evidence supporting the attribution of trends to short-term precipitation. The intensity of atmospheric rivers was indexed by daily IVT for cells measuring 2.5° × 2.5° in the latitudinal and longitudinal directions (Rutz and others, 2014). The IVT data were available starting in water year 1948. The grid cells used to calculate IVT are larger than river basins and, since IVT varies spatially within a cell depending on storm tracks and runoff depends on antecedent conditions, high rates of IVT are likely to produce large annual peak streamflows in some rivers in a cell (Konrad and Dettinger, 2017). As such, an attribution of a trend to short-term precipitation was supported by a correlation (p-value<0.05) between the rank of annual peak streamflow and the rank of mean IVT on the day of the peak or the day before the peak, whichever was greater. The correlation of annual peak streamflow with IVT on the days of the peaks, however, does not exclude the possibility that multidecadal climate variability had an effect on trends.

The Mann-Kendall test (p-value<0.05) was applied repeatedly for all possible starting and ending year pairs from 1948 to 2015 to both the annual maximum daily IVT and the number of days when daily IVT exceeded 500 kg/m/s in each cell to identify atmospheric rivers likely to cause flooding (Konrad and Dettinger, 2017). The results were used to determine the timing of multidecadal trends in the intensity and frequency of atmospheric rivers. During wet years (>90th percentile for annual precipitation), atmospheric rivers are more frequent and result in heavier precipitation and more snow accumulation than during dry years (<10th percentile for annual precipitation) (Eldardiry and others, 2019). The timing of monotonic trends in annual peak streamflow at an individual streamgage was compared to the timing of monotonic trends in annual maximum daily IVT and monotonic trends in of the number of days when IVT>500 kg/m/s for the corresponding grid cell. Similar timing of trends in peak streamflow and IVT (annual maximum daily or number of days) was used as evidence for attributing a trend in annual peak streamflow to multidecadal climate variability.

Atmospheric river intensity (annual maximum daily IVT) and duration (number of days when IVT>500 kg/m/s) have similar trends for a cell in the Western Washington hydroclimatic subregion (fig. B2*A*, *B*) and for a cell in the Northwestern California and the Klamath Basin hydroclimatic subregion (fig. B2*C*, *D*) even as the timing of trends in atmospheric river intensity and duration vary between the cells. Overall, from 1948 to 2015, atmospheric river intensity was increasing for the Western Washington hydroclimatic subregion, with higher intensity atmospheric rivers indicated for 1965–1975 and 1987–2002 and less intense atmospheric rivers indicated for 1950–1964 and 1977–1986. Atmospheric river intensity did not follow consistent trends in the Northwestern California and the Klamath Basin hydroclimatic subregion for 1950–2015, but higher intensity atmospheric rivers were indicated for 1980–1990 and 1996–2001 and less intense atmospheric rivers were indicated for 1968–1980, 1990–1995, and 2002–2015.

Quantile Trends

Trends in the 10th, 50th, and 90th annual peak-streamflow quantiles were analyzed by quantile regression of annual peak streamflow on water year for the period of record at the streamgage. Significant trends in a quantile were identified when the probability that a quantile had a slope of zero (no trend) was p-value<0.10 (Konrad and Restivo, 2020). The presence of significant trends in each quantile was noted for each streamgage and was used to assess whether trends were present over the frequency spectrum of annual peaks and to provide additional characteristics of trends that can be used to make attributions (Konrad and others, 2005; Konrad and others, 2012). For example, trends in the 10th or 50th percentile could indicate land-cover changes or trends in antecedent conditions that affect smaller, more frequent floods; trends in the 90th percentile could indicate changes in short-term precipitation that could have substantial effects on the spatial extent and severity of larger, less frequent floods.

Day-of-Peak Streamflow

Trends in the day of the water year for each annual peak streamflow (or "day-of-peak," where day 1 is defined here as October 1st) were used as an indicator for changes in the dominant process or processes that produce annual peaks at each streamgage. Shifts in day-of-peak to earlier in the year can indicate large storms occurring earlier in the autumn or winter, an increased proportion of autumn and winter rainfall relative to snow at higher altitudes (including rain-on-snow events), and (or) warmer air temperatures and earlier snowmelt. The day-of-peak was identified at each streamgage for its period of record through water year 2015 (U.S. Geological Survey, 2019). Quantile regression was applied to determine if the median day-of-peak had a significant trend over time

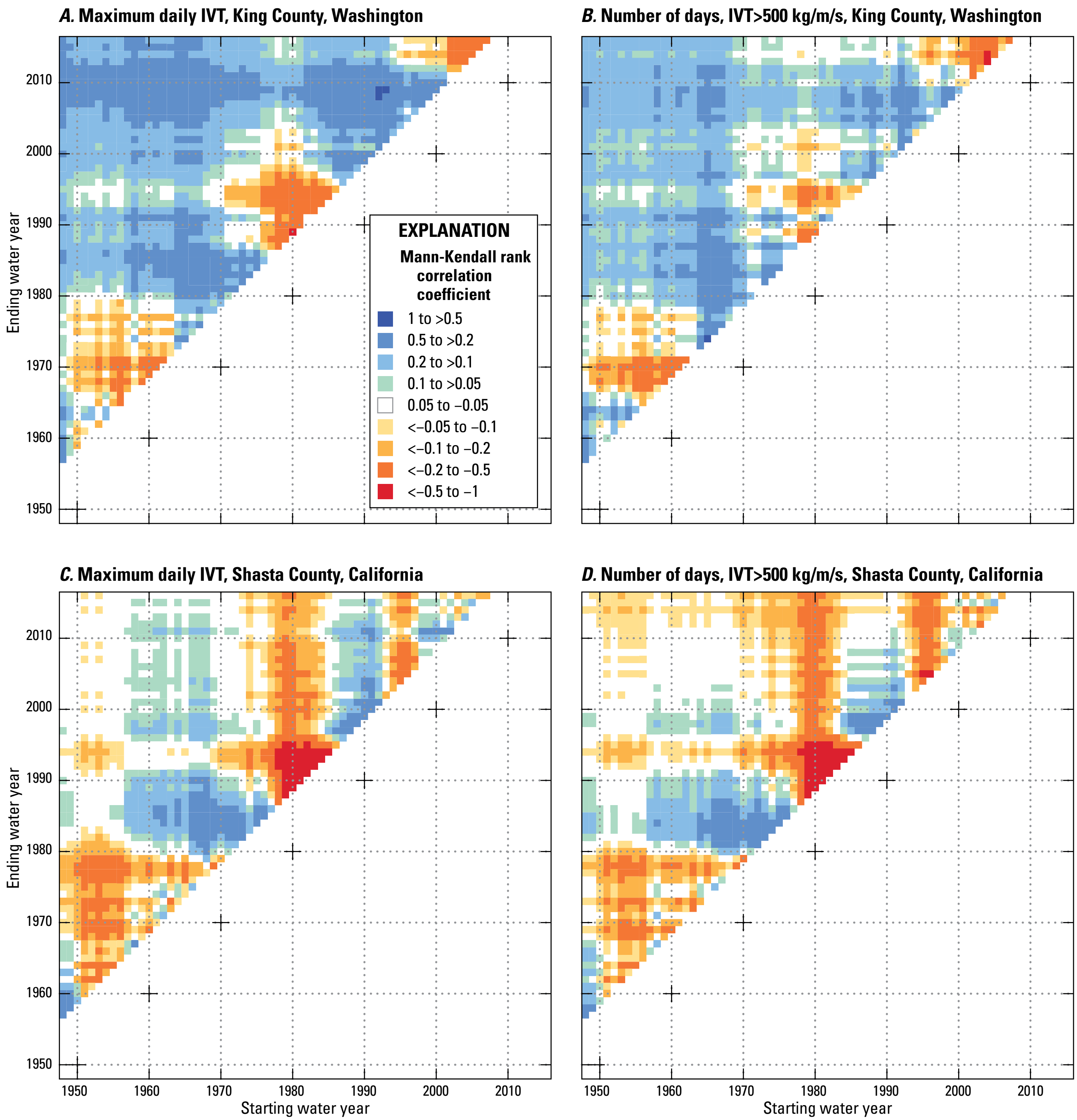

Figure B2. Flag plots of Mann-Kendall rank correlation coefficients by water year in (*A*, *C*) maximum daily vertically integrated water vapor transport (IVT) and (*B*, *D*) the number of days when IVT exceeded 500 kilograms per meter per second (kg/m/s). Plots of *A* and *B* are centered around lat 47.5° N., long 122.5° W. (King County, Washington), and *C* and *D* are centered around lat 40° N., long 122.5° W. (Shasta County, California). These plots show a daily time series of IVT data for each 2.5° × 2.5° grid cell from Rutz and others (2014). The IVT data were available starting in water year 1948, and only periods when the starting and ending years were separated by 10 years or more were tested for monotonic trends.

(probability that the median quantile had a slope of zero [no trend] was *p*-value<0.05). The day-of-peak generally occurs during late autumn or winter across the Pacific Northwest region (fig. B3), indicating the dominance of rainfall or mid-winter snowmelt for the production of peaks in streamflow. The Interior Columbia Basin and Great Basin hydroclimatic subregion has a wider variety of river types, including those where annual peaks are common in the spring and summer because of higher altitude snowpack.

The warming climate over the last century has led to less snowfall, lower snowpack, earlier snowmelt, and earlier peak streamflow across most of the western United States (Dettinger and Cayan, 1995; Cayan, 1996; Hamlet and others, 2005; McCabe and Clark, 2005; Mote and others, 2005; Stewart and others, 2005; Knowles and others, 2006; Mote and others, 2018). The effects of increasing air temperature can be particularly strong in mid-altitude basins at the transitional zone between snow and rain (Das and others, 2009;

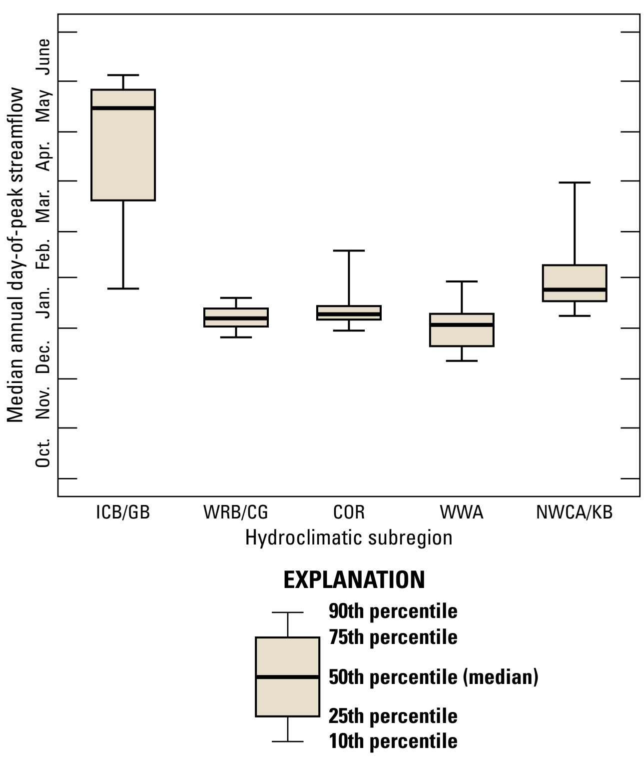

Figure B3. Boxplots showing the temporal distributions of median annual day-of-peak streamflow for each hydroclimatic subregion in the Pacific Northwest region. Months with no annual day-of-peak streamflow are omitted. Terms for hydroclimatic subregions: ICB/GB, Interior Columbia Basin and Great Basin; WRB/CG, Willamette River Basin and Columbia Gorge; COR, Coastal Oregon; WWA, Western Washington; NWCA/KB, Northwestern California and the Klamath Basin.

Dudley and others, 2017), which is typically between 1,000 and 2,000 m of elevation in the Pacific Northwest region (Klos and others, 2014). Increasing air temperatures can affect the timing and magnitude of annual peak streamflow in three distinct ways:

1. Precipitation in winter as rain rather than snow can increase winter peaks and advance the timing of peaks from spring to winter
2. Less spring snowpack can decrease peaks in spring and summer from snowmelt
3. More rapid snowmelt can advance the timing and increase the magnitude of peaks in spring and summer from snowmelt.

The decision to attribute a trend to air temperature or snowpack for basins in the transitional zone was based on the direction and timing of the trend in day-of-peak and the direction of the trend in annual peak streamflow. Snowpack-related trends were indicated by a significant trend to earlier day-of-peak for April–July and a negative trend in annual peak streamflow (Jefferson, 2011; Hatcher and Jones, 2013; Mote and others, 2018). Temperature-related trends were indicated by a significant trend to earlier day-of-peak and a positive trend in annual peak streamflow (Dettinger and Cayan, 1995; Déry and others, 2009).

Basin-Specific Anthropogenic Attributions Other Than Climate

Anthropogenic attributions (other than those related to climate) for trends were evaluated by examining the changes in water management and land use in the basin of each non-HCDN streamgage in relation to the direction and timing of trends. Attributions related to water management (large artificial impoundments, small artificial impoundments, surface-water withdrawals, groundwater withdrawals, artificial wastewater and water-supply discharges, agricultural drainage activities, and interbasin water transfers) were considered if they appeared in the streamgage description in the National Water Information System (NWIS; U.S. Geological Survey, 2019) database, if there was reservoir storage upstream of the streamgage (Falcone, 2011), or if there were agricultural or urban areas upstream of the streamgage (Falcone, 2011). Large artificial impoundments were considered likely in cases where there was a negative change point, the change point was not present for periods when reservoir storage was stable, and where the change point was distinct (in direction or timing) from trends at HCDN streamgages within the same hydroclimatic subregion. Neither surface-water withdrawals nor interbasin water transfers would likely reduce annual peak streamflows at any streamgage unless there was a large artificial impoundment that stored water. Groundwater withdrawals were considered a likely attribution only where there were negative trends and the area upstream of the streamgage has substantial, documented declines in groundwater level over time (Vaccaro and others, 2015).

Attributions related to land-cover change (agricultural crop production, rangeland grazing activities, invasive woody species, deforestation and wildfire, and urban effects) were evaluated using the 2011 National Land Cover Database (NLCD 2011) aggregated by drainage area for each streamgage and the National Water-Quality Assessment Program (NAWQA) Wall-to-Wall Anthropogenic Land Use Trends (NWALT) database, which provides a consistent time series of land use in 1974, 1982, 1992, 2002, and 2012 (Falcone, 2015, 2017). Urban effects were a possible attribution where a high percentage (>5 percent) of land in the drainage basin was classified as “Developed High Intensity” in the NLCD 2011; this attribution was further supported by an increasing percentage of developed land over time. The deforestation and wildfire attribution was considered for streamgages where a relatively high change (>1.5 percent) in maximum annual percentage of land in the drainage basin was classified as timberland (Falcone, 2017) during the analysis period. This attribution was also considered at streamgages with positive trends in basins that are primarily forested (Falcone, 2017) and had major wildfires between 1984 and 2017 based on the “Monitoring Trends in Burn Severity” program and geodatabase (U.S. Department of Agriculture Forest Service, 2021). As with attributions related to water management, attributions related to land-cover change were considered possible if the timing of land-cover change coincided with the timing of the trend.

Trends in Annual Peak Streamflow

Primary attributions were made for statistically significant monotonic trends and change points at the 22 HCDN streamgages (table B3) and the 84 non-HCDN streamgages (table B4) in the Pacific Northwest region for the two time periods (York and others, 2022). Generally, streamgages with a monotonic trend also had a change point (56 of 60 streamgages with monotonic trends from 1941 to 2015 and 42 of 61 streamgages with monotonic trends from 1966 to 2015) and streamgages with a change point had a monotonic trend (56 of 63 streamgages with a change point from 1941 to 2015 and 42 of 49 streamgages with a change point from 1966 to 2015). Although attributions were made only for significant monotonic trends or change points for the two periods, the

Table B3. The number of HCDN streamgages with primary attributions for statistically significant monotonic trends or change points in annual peak streamflow in each hydroclimatic subregion of the Pacific Northwest region.

[The terms “positive” and “negative” indicate that the streamgage has at least one significant positive or significant negative monotonic trend or change point in annual peak streamflow for the period of 1941–2015 or 1966–2015. Abbreviations: HCDN, Hydro-Climatic Data Network 2009; ICB/GB, Interior Columbia Basin and Great Basin; WRB/CG, Willamette River Basin and Columbia Gorge; COR, Coastal Oregon; WWA, Western Washington; NWCA/KB, Northwestern California and the Klamath Basin]

Primary attributions of trends and types of streamgages	ICB/GB	WRB/CG	COR	WWA	NWCA/KB	Total
Numbers of HCDN streamgages with each kind of primary attribution						
Multidecadal climate variability:						
Positive	0	1	0	1	0	2
Negative	1	1	0	0	1	3
Short-term precipitation:						
Positive	1	0	0	10	0	11
Negative	0	0	1	0	2	3
Snowpack (negative)	2	0	0	0	0	2
Air temperature (positive)	1	0	0	0	0	1
Numbers of HCDN streamgages						
Number of HCDN streamgages with monotonic trends or change points	5	2	1	11	3	22
Number of HCDN streamgages without monotonic trends or change points	16	11	5	10	7	49
Total HCDN streamgages	**21**	**13**	**6**	**21**	**10**	**71**

Table B4. The number of non-HCDN streamgages with primary attributions for statistically significant monotonic trends or change points in annual peak streamflow in each hydroclimatic subregion of the Pacific Northwest region.

[The terms "positive" and "negative" indicate that the streamgage has at least one significant positive or significant negative monotonic trend or change point in annual peak streamflow for the period of 1941–2015 or 1966–2015. The term "inconsistent" indicates that a streamgage has a significant positive monotonic trend or change point in annual peak streamflow for one of the periods (1941–2015 or 1966–2015) and a significant negative monotonic trend or change point for the other period. Abbreviations: HCDN, Hydro-Climatic Data Network 2009; ICB/GB, Interior Columbia Basin and Great Basin; WRB/CG, Willamette River Basin and Columbia Gorge; COR, Coastal Oregon; WWA, Western Washington; NWCA/KB, Northwestern California and the Klamath Basin]

Primary attributions of trends and types of streamgages	ICB/GB	WRB/CG	COR	WWA	NWCA/KB	Total
Numbers of non-HCDN streamgages with each kind of primary attribution						
Forest cover/composition (negative)	1	0	0	0	0	1
Groundwater withdrawals (negative)	2	0	0	0	0	2
Large artificial impoundments:						
Positive	0	0	0	1	0	1
Negative	7	19	10	5	3	44
Inconsistent	0	0	0	0	2	2
Multidecadal climate variability:						
Positive	1	1	0	0	0	2
Negative	7	1	0	0	4	12
Short-term precipitation:						
Positive	0	1	0	5	0	6
Negative	1	0	0	0	7	8
Snowpack (negative)	2	0	0	0	0	2
Surface-water withdrawals (negative)	0	0	1	0	0	1
Air temperature (positive)	1	0	0	0	0	1
Urban effects (positive)	0	0	0	2	0	2
Numbers of non-HCDN streamgages						
Number of non-HCDN streamgages with monotonic trends or change points	22	22	11	13	16	84
Number of non-HCDN streamgages without monotonic trends or change points	52	14	9	20	14	109
Total non-HCDN streamgages	**74**	**36**	**20**	**33**	**30**	**193**

fraction of streamgages in the Pacific Northwest region with significant monotonic trends was found to vary based on the starting and ending years for the Mann-Kendall test (fig. B4); positive monotonic trends were common for periods starting before 1940 and ending after 1950, while negative monotonic trends were common for periods starting before 1970 and ending after 1980. Hydroclimatic subregions within the Pacific Northwest have different timing and direction in annual peak-streamflow trends, so these periods overlap.

The timing of annual peak streamflow has been stationary at most streamgages in the Pacific Northwest region: only 38 of 264 streamgages had statistically significant changes in the annual day-of-peak and 10 of the streamgages with trends in day-of-peak were regulated (table B5). Spring snowmelt generates annual peak streamflow at most of the streamgages with a change in annual day-of-peak and these streamgages generally had negative trends. Peak streamflow that is both earlier in the spring and lower in magnitude indicates years with less spring snowpack; however, negative trends at streamgages where median annual day-of-peak is earlier in the spring (table B5) could be attributed to either snowpack or air temperature.

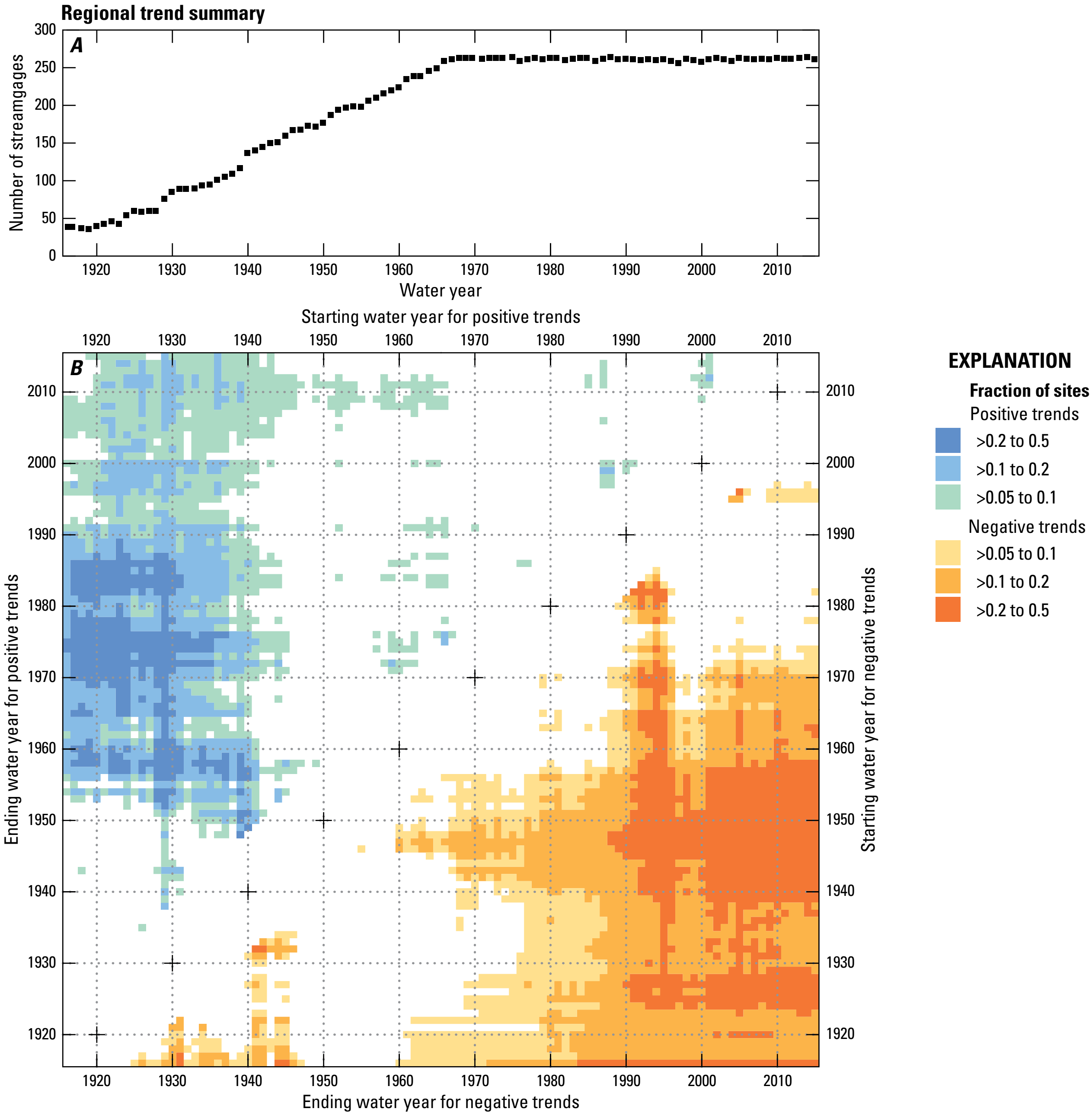

Figure B4. Two plots of data for streamgages in the Pacific Northwest region showing (*A*) the number of streamgages per water year and (*B*) the fraction of streamgages with significant Mann-Kendall rank correlation coefficients between annual peak streamflow and water years for all possible starting and ending year pairs separated by at least 10 years. Monotonic trends at a streamgage are statistically significant if the probability that the Mann-Kendall correlation coefficient is zero is *p*-value<0.05.

Table B5. U.S. Geological Survey streamgages in the Pacific Northwest region that have significant trends in the annual day-of-peak streamflow.

[For the change in median annual day-of-peak streamflow (in units of days per year; column three), negative values indicate earlier occurrence in the year and positive values indicate later occurrence in the year. Terms for hydroclimatic subregions: ICB/GB, Interior Columbia Basin and Great Basin; WRB/CG, Willamette River Basin and Columbia Gorge; COR, Coastal Oregon; WWA, Western Washington; NWCA/KB, Northwestern California and the Klamath Basin. Other terms: USGS, U.S. Geological Survey; HCDN, Hydro-Climatic Data Network 2009 streamgage; NS, no significant monotonic trend or change point for water years 1941–2015 or 1966–2015; --, indicates a non-HCDN streamgage without an upstream large artificial impoundment]

USGS streamgage number	Median annual day-of-peak streamflow	Change in median annual day-of-peak streamflow (days per year)	Hydroclimatic subregion	Streamgage type	Direction of significant monotonic trends or change points
10396000	4-Apr	0.47	ICB/GB	HCDN	NS
12329500	5-Jun	0.16	ICB/GB	Regulated	Negative
12362500	17-May	−0.35	ICB/GB	Regulated	Negative
12389500	18-May	−0.18	ICB/GB	Regulated	NS
12413000	9-Apr	−0.58	ICB/GB	HCDN	NS
12414500	4-May	−0.13	ICB/GB	HCDN	NS
12422500	1-May	−0.29	ICB/GB	Regulated	Negative
12433000	27-Apr	−0.35	ICB/GB	Regulated	Negative
12449950	26-May	−0.31	ICB/GB	--	NS
12451000	24-May	−0.13	ICB/GB	HCDN	NS
12459000	21-May	−0.15	ICB/GB	--	NS
12462500	19-May	−0.96	ICB/GB	--	NS
12484500	9-May	−0.32	ICB/GB	Regulated	NS
12488500	19-May	−0.2	ICB/GB	HCDN	Negative
12510500	23-Mar	−0.61	ICB/GB	Regulated	NS
13011500	31-May	−0.23	ICB/GB	HCDN	Positive
13049500	29-May	−0.16	ICB/GB	Regulated	Positive
13141500	8-Apr	−0.1	ICB/GB	Regulated	Negative
13217500	2-May	0.45	ICB/GB	Regulated	NS
13266000	2-Mar	0.46	ICB/GB	--	NS
13302500	7-Jun	−0.14	ICB/GB	--	NS
13316500	30-May	−0.31	ICB/GB	--	NS
13331500	29-May	−0.31	ICB/GB	HCDN	NS
14034500	5-Apr	0.75	ICB/GB	Regulated	NS
14087400	23-Mar	1.39	ICB/GB	Regulated	NS
14103000	2-Feb	−0.25	ICB/GB	Regulated	NS
14181500	3-Jan	0.6	WRB/CG	Regulated	Negative
14309000	18-Jan	−0.33	COR	Regulated	Negative
14338000	7-Jan	−0.35	COR	--	Negative
14357500	7-Feb	−0.5	COR	Regulated	NS
14377100	9-Jan	−0.47	COR	--	NS
12026150	8-Jan	0.46	WWA	Regulated	NS
12048000	22-Dec	−0.42	WWA	HCDN	Positive
12059500	20-Dec	−0.8	WWA	Regulated	Positive
12143700	27-May	2.37	WWA	--	NS
11509500	18-Mar	−0.42	NWCA/KB	Regulated	Negative
11516530	1-Mar	1.43	NWCA/KB	Regulated	Negative
11525500	29-Mar	0.92	NWCA/KB	Regulated	Negative

Interior Columbia Basin and Great Basin Hydroclimatic Subregion

Trends in annual peak streamflow were not pervasive in the Interior Columbia Basin and Great Basin hydroclimatic subregion, as only 5 of the 21 HCDN streamgages had significant trends (table B3). These trends were observed at streamgages with clusters of wet and dry years at the start and end of the period of analysis (1966–2015) because the climate was oscillating between wet and dry periods and not because of a persistent change. Of the 5 HCDN streamgages with significant trends, 2 had significant positive trends for 1966–2015 and 3 had significant negative trends for 1966–2015. There were no HCDN streamgages that had significant trends for 1941–2015. Six HCDN streamgages had significant negative trends in day-of-peak (which indicated earlier snowmelt and possible attributions of either snowpack or air temperature), and one had a significant positive trend in day-of-peak (table B5).

Annual peak streamflow for USGS streamgage 12411000 (at the North Fork Cour d'Alene River above Shoshone Creek, Idaho) had a significant negative monotonic trend for the period of 1966–2015 which was attributed to short-term precipitation. Annual peak streamflow for USGS streamgage 12488500 (at the American River near Nile, Washington) had significant negative trends for 1966–2015 which were attributed to multidecadal climate variability; however, this streamgage did not have significant trends for 1941–2015, which may also be a result of elevated peaks from 1974 to 1981 (fig. B5). Likewise, the negative trend for data at USGS streamgage 13023000 (at the Greys River near Alpine, Wyoming), which was attributed to snowpack, was only significant for 1966–2015 (more generally, the Mann-Kendall tests were significant at p-value<0.05 for all starting years between 1960 and 1970 and all ending years between 2000 and 2010). The significant positive trend for data at USGS streamgage 13011500 (at Pacific Creek at Moran, Wyo.), which was attributed to air temperature, could be a result of warming since 1980 or cyclic variation in precipitation. Annual peak streamflow for USGS streamgage 13161500 (at the Bruneau River at Rowland, Nevada) had a significant negative change point for 1966–2015 that was attributed to snowpack, but not a corresponding monotonic trend. A large artificial impoundment is located upstream of this streamgage, which could have a minor effect on peak streamflow.

The annual day-of-peak occurred earlier in the spring at six HCDN streamgages in this hydroclimatic subregion (table B5), but only two of these streamgages had significant trends for 1941–2015 or 1966–2015. All of the HCDN streamgages with earlier day-of-peak have annual peak streamflow generated by snowmelt (median annual day-of-peak after April 1st), which suggests that earlier or reduced snowmelt has advanced the timing of peaks to earlier in the year. Two of the HCDN streamgages had significant trends for 1966–2015, but the trends had different directions and attributions. Annual peak streamflow for USGS streamgage 12488500 (at the American River near Nile, Wash.) had a negative trend attributed to snowpack; annual peak streamflow for USGS streamgage 13011500 (at Pacific Creek at Moran, Wyo.) had a positive trend attributed to air temperature.

Of the 74 non-HCDN streamgages in the Interior Columbia River and Great Basin hydroclimatic subregion, 22 had significant trends, most of which were negative (table B4). Negative trends were common for both the 1941–2015 and the 1966–2015 time periods. Trends at non-HCDN streamgages were primarily attributed to multidecadal climate variability (8 streamgages) and large artificial impoundments (7 streamgages), but there was generally limited or medium levels of evidence for these primary attributions. Snowpack was primarily attributed to trends at 2 streamgages but was a common secondary attribution (for 12 streamgages) where it may have affected annual peak streamflow. A period of higher peaks from 1950 to 1960 and lower peaks from 1985 to 1995 underlie the significant trends at many of the streamgages in hydrologic subregion 1701. Otherwise, streamgage data have relatively distinct trends in terms of timing and quantiles affected. Fourteen non-HCDN streamgages had significant negative trends in the timing of the day-of-peak while five non-HCDN streamgages had significant positive trends in the timing of the day-of-peak (table B5).

Willamette River Basin and Columbia Gorge Hydroclimatic Subregion

Of the 13 HCDN streamgages in the Willamette River Basin and Columbia Gorge hydroclimatic subregion, 2 had significant but opposing trends in annual peak streamflow (table B3), both of which were attributed to multidecadal climate variability with limited evidence. One of these two streamgages (USGS streamgage 14141500 at the Little Sandy River near Bull Run, Oregon) had significant negative trends in annual peak streamflow for the 75-year period but not the 50-year period; trends were mainly for starting years in the mid-1940s to early 1970s and ending years after 1984 (fig. B6). At the other HCDN streamgage (USGS streamgage 14158790 at the Smith River above Smith River Reservoir near Belknap Springs, Oreg.), significant positive trends in annual peak streamflow appear mainly for starting years in the middle-to-late 1960s and ending years after 1985 (fig. B7). The record of annual peak streamflow for the Smith River streamgage starts in water year 1961, so trends prior to water year 1961 are unknown. None of the 13 HCDN streamgages in the Willamette River and Columbia Gorge hydroclimatic subregion had significant trends in the timing of the day-of-peak. Annual peaks were significantly correlated with IVT for the day-of-peak at 12 of the 13 HCDN streamgages.

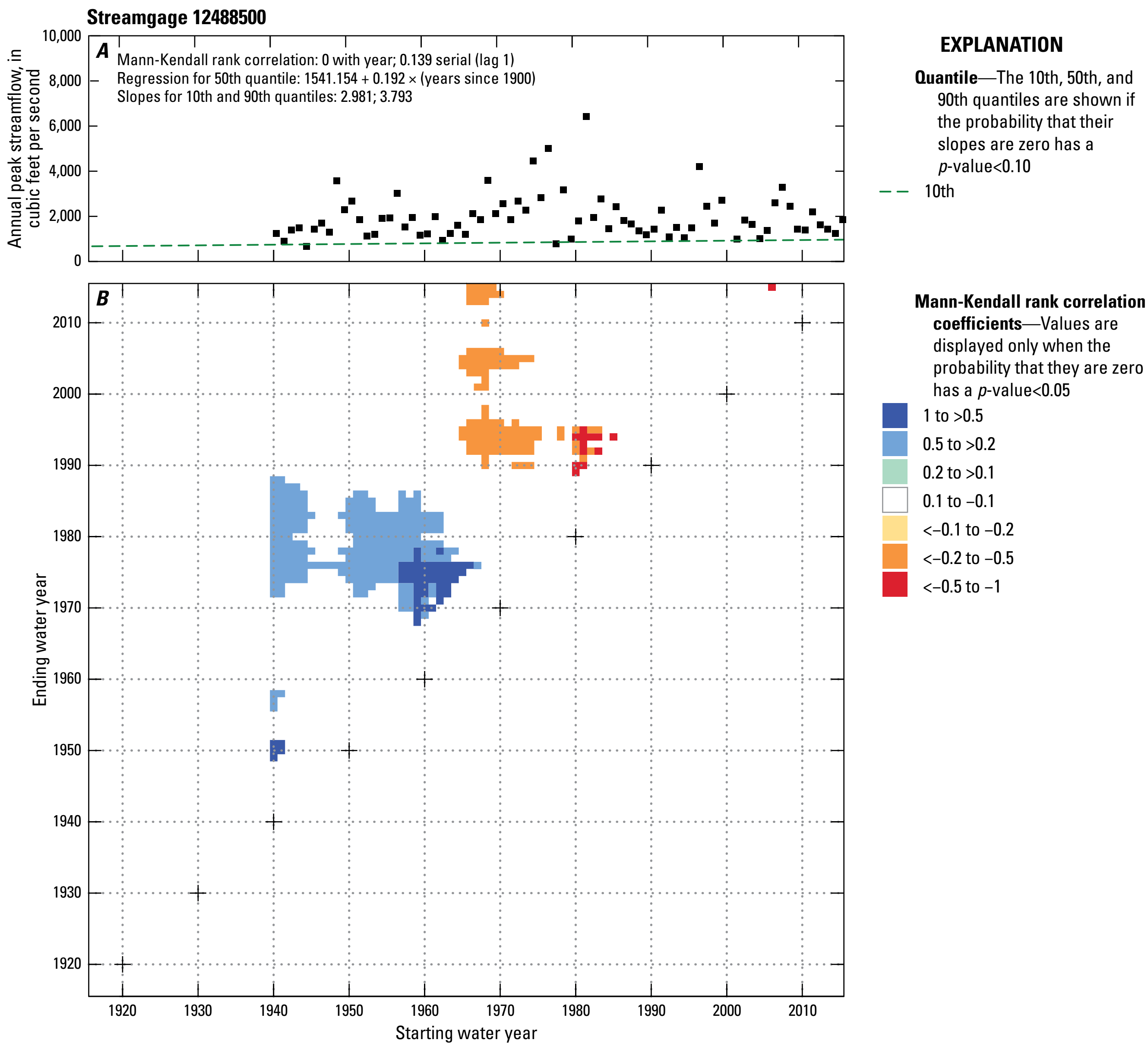

Figure B5. Annual peak streamflow time series and its rank correlation coefficients with water year for U.S. Geological Survey streamgage 12488500 at the American River near Nile, Washington. *A*, Time series of annual peak streamflow for the period of record. *B*, Flag plot of Mann-Kendall rank correlation coefficients for annual peak streamflow and water year calculated for every pair of starting and ending water years that were separated by at least 10 years. The significant negative monotonic trend or change point from 1966 to 2015 was attributed to multidecadal climate variability.

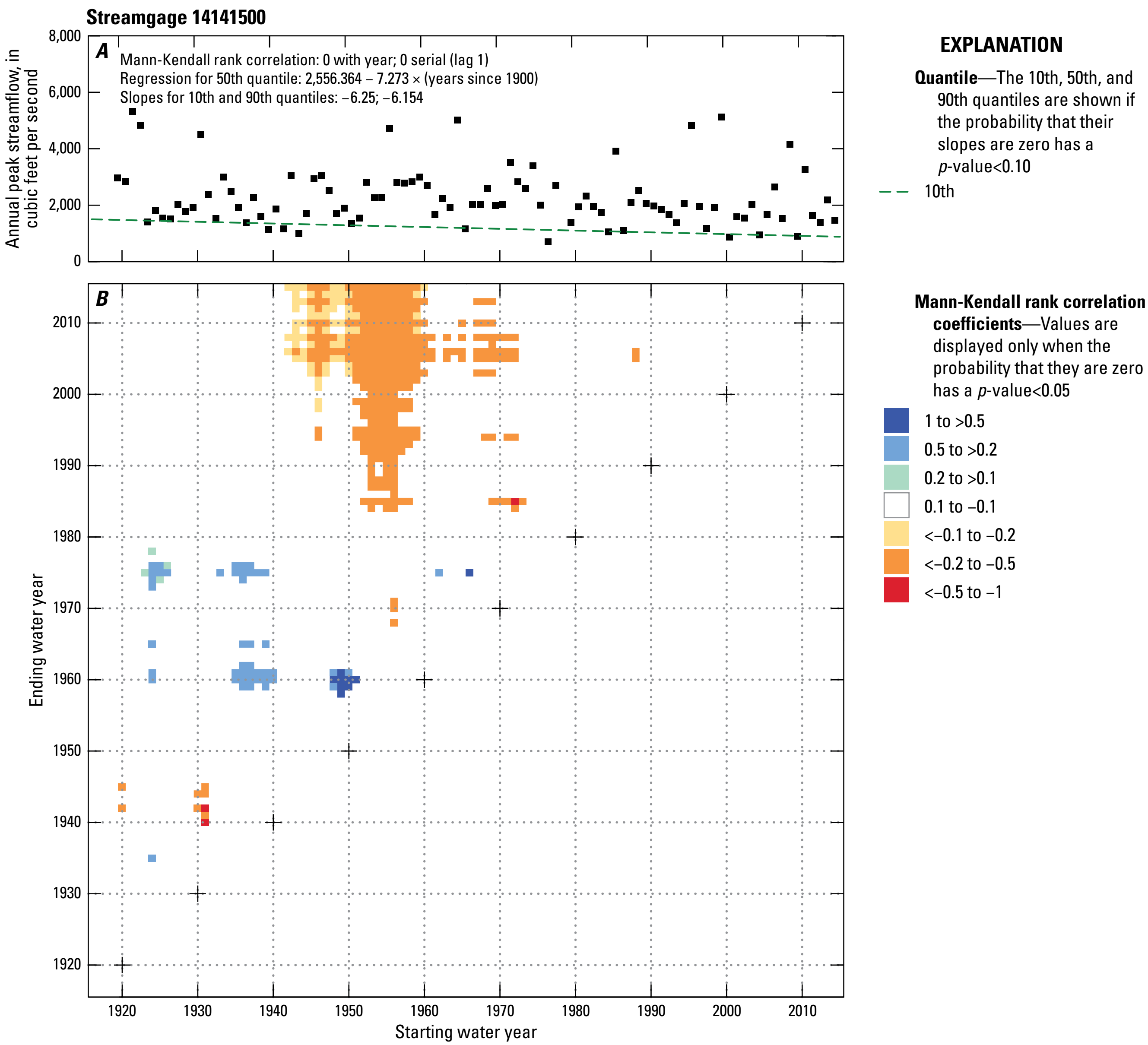

Figure B6. Annual peak streamflow time series and its rank correlation coefficients with water year for U.S. Geological Survey streamgage 14141500 at the Little Sandy River near Bull Run, Oregon. *A*, Time series of annual peak streamflow for the period of record. *B*, Flag plot of Mann-Kendall rank correlation coefficients for annual peak streamflow and water year calculated for every pair of starting and ending water years that were separated by at least 10 years. The significant negative monotonic trend or change point from 1941 to 2015 was attributed to multidecadal climate variability.

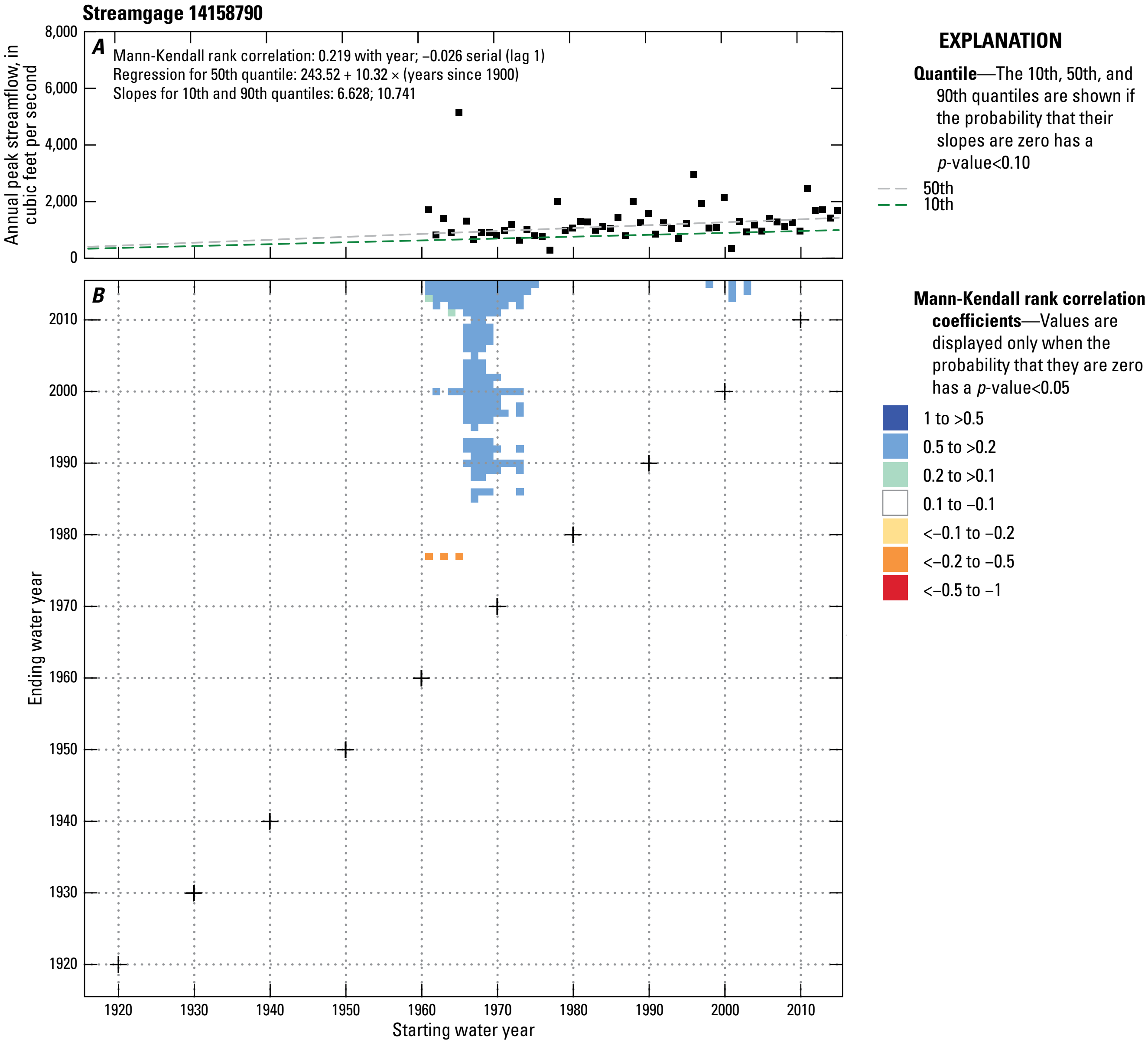

Figure B7. Annual peak streamflow time series and its rank correlation coefficients with water year for U.S. Geological Survey streamgage 14158790 at the Smith River above Smith River Reservoir near Belknap Springs, Oregon. *A*, Time series of annual peak streamflow for the period of record. *B*, Flag plot of Mann-Kendall rank correlation coefficients for annual peak streamflow and water year calculated for every pair of starting and ending water years that were separated by at least 10 years. The significant positive monotonic trend or change point from 1966 to 2015 was attributed to multidecadal climate variability.

Of the 36 non-HCDN streamgages in this hydroclimatic subregion, 2 had significant positive trends and 20 had significant negative trends in annual peak streamflow (table B4). Of these, 19 were primarily attributed to large artificial impoundments, 2 to multidecadal climate variability, and 1 to short-term precipitation. Change points generally coincided closely with changes in regulation that occurred in the 1950s and 1960s, such as at USGS streamgage 14145500 (at the Middle Fork Willamette River above Salt Creek near Oakridge, Oreg.) (fig. B8), which has been regulated since 1961 and also had a change point at 1961. One non-HCDN streamgage had a significant positive trend in the timing of the day-of-peak, which indicated that peaks occurred later in the winter (table B5). Attributions for trends in this hydroclimatic subregion were generally made with medium evidence and robust evidence.

Coastal Oregon Hydroclimatic Subregion

There were 6 HCDN streamgages in the Coastal Oregon hydroclimatic subregion and only 1 of them had a significant trend (table B3). This significant negative trend was at USGS streamgage 14306500 (at the Alsea River near Tidewater, Oreg.) (fig. B9) and was primarily attributed to short-term precipitation. Eleven of the 20 non-HCDN streamgages had significant negative trends, 10 of which were attributed to large artificial impoundments and 1 of which was attributed to surface-water withdrawals (table B4). USGS streamgage 143090000 (at Cow Creek near Azalea, Oreg.) recorded a large decrease in annual peak streamflow beginning in 1995 (fig. B10). Four non-HCDN streamgages had significant negative trends in the timing of the day-of-peak, but only two of these (USGS streamgages 14309000 and 14338000) also had significant trends (table B5), both of which were negative. Attributions for trends in this hydroclimatic subregion were generally made with medium evidence and robust evidence.

Western Washington Hydroclimatic Subregion

Significant trends in annual peak streamflow were present at 11 of the 21 HCDN streamgages that were analyzed in the Western Washington hydroclimatic subregion (table B3). All 11 of these trends were positive, 10 of which were attributed to short-term precipitation and 1 of which was attributed to multidecadal climate variability. The significance of changes in annual peak streamflow at HCDN streamgages was sensitive to clusters of relatively small or large annual peaks around either the starting year or ending year of a trend test, such as for USGS streamgage 12035000 (at the Satsop River near Satsop, Wash.) (fig. B11).

Significant positive trends in annual peak streamflow were present at 8 of the 33 non-HCDN streamgages that were analyzed in the Western Washington hydroclimatic subregion (table B4). Five of these non-HCDN streamgages with positive trends had trend periods consistent with HCDN streamgages and were therefore primarily attributed to short-term precipitation. The trends at two non-HCDN streamgages (USGS streamgage 12120000 [at Mercer Creek near Bellevue, Wash.] and USGS streamgage 12091200 [at Leach Creek near Fircrest, Wash.]) were primarily attributed to urban effects. The streamgage at the Cedar River at Cedar Falls, Wash. (USGS streamgage 12116500), which is downstream of a large artificial impoundment, only had a significant positive monotonic trend for the 75-year period, which was primarily attributed to a large artificial impoundment; this attribution is consistent with the findings of Gendaszek and others (2012). All 8 non-HCDN streamgages with positive trends for 1941–2015 or 1966–2015 also had significant positive rank correlation of annual peak-streamflow magnitude with IVT on the day-of-peaks (table B5). The positive trends at these non-HCDN sites were attributed to short-term precipitation. Negative trends were present at 5 of the 33 non-HCDN streamgages, all of which were attributed to large artificial impoundments (table B4). Attributions for trends in this hydroclimatic subregion were generally made with medium evidence and robust evidence.

Northwestern California and the Klamath Basin Hydroclimatic Subregion

The Northwestern California and the Klamath Basin hydroclimatic subregion had three HCDN streamgages with significant negative trends in annual peak streamflow (table B3): USGS streamgages 11469000 (at the Mattole River near Petrolia, California), 11473900 (at the Middle Fork Eel River near Dos Rios, Calif.), and 11482500 (at Redwood Creek at Orick, Calif.). The trends for these streamgages were only significant for the period of 1966–2015 and only the Mattole River streamgage had a significant change point. The flag plots for these streamgages indicate that the trends are generally limited to periods beginning between 1950 to 1970 and ending after 1990. The negative trends for annual peaks at the streamgages at Mattole River and Middle Fork Eel River were attributed to short-term precipitation because (1) atmospheric rivers are the dominant mechanism that produce floods in this hydroclimatic subregion (Konrad and Dettinger, 2017) and (2) the negative trends are primarily a result of large peaks prior to 1970 (fig. B12). The negative trend for the streamgage at Redwood Creek was attributed to multidecadal climate variability because of frequent high peaks prior to 1980 (fig. B13). Trends were not significant at the other seven HCDN streamgages in the subregion.

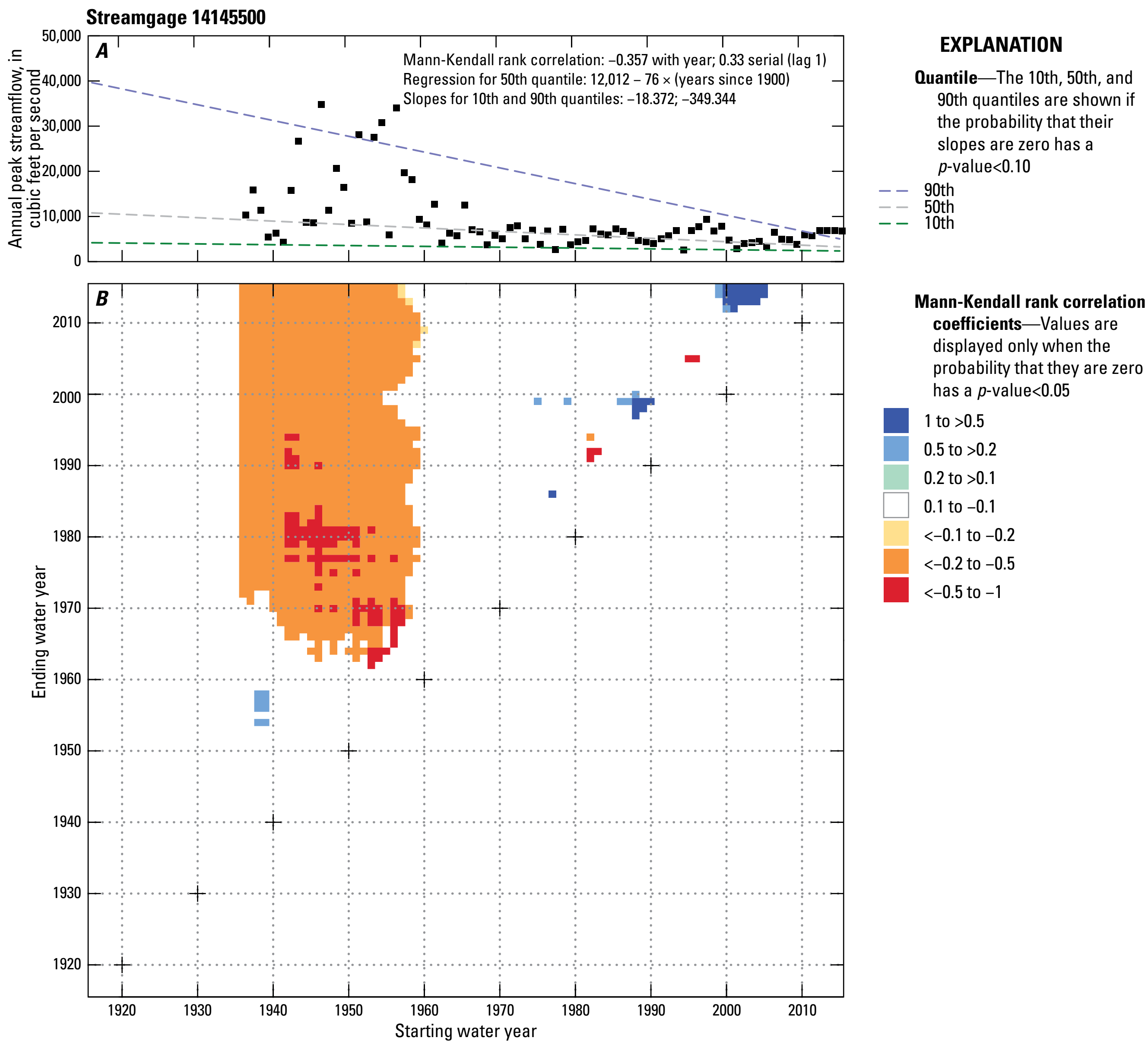

Figure B8. Annual peak streamflow time series and its rank correlation coefficients with water year for U.S. Geological Survey streamgage 14145500 at the Middle Fork Willamette River near Oakridge, Oregon. *A*, Time series of annual peak streamflow for the period of record. *B*, Flag plot of Mann-Kendall rank correlation coefficients for annual peak streamflow and water year calculated for every pair of starting and ending water years that were separated by at least 10 years. The significant negative monotonic trend or change point from 1941 to 2015 was attributed to a large artificial impoundment.

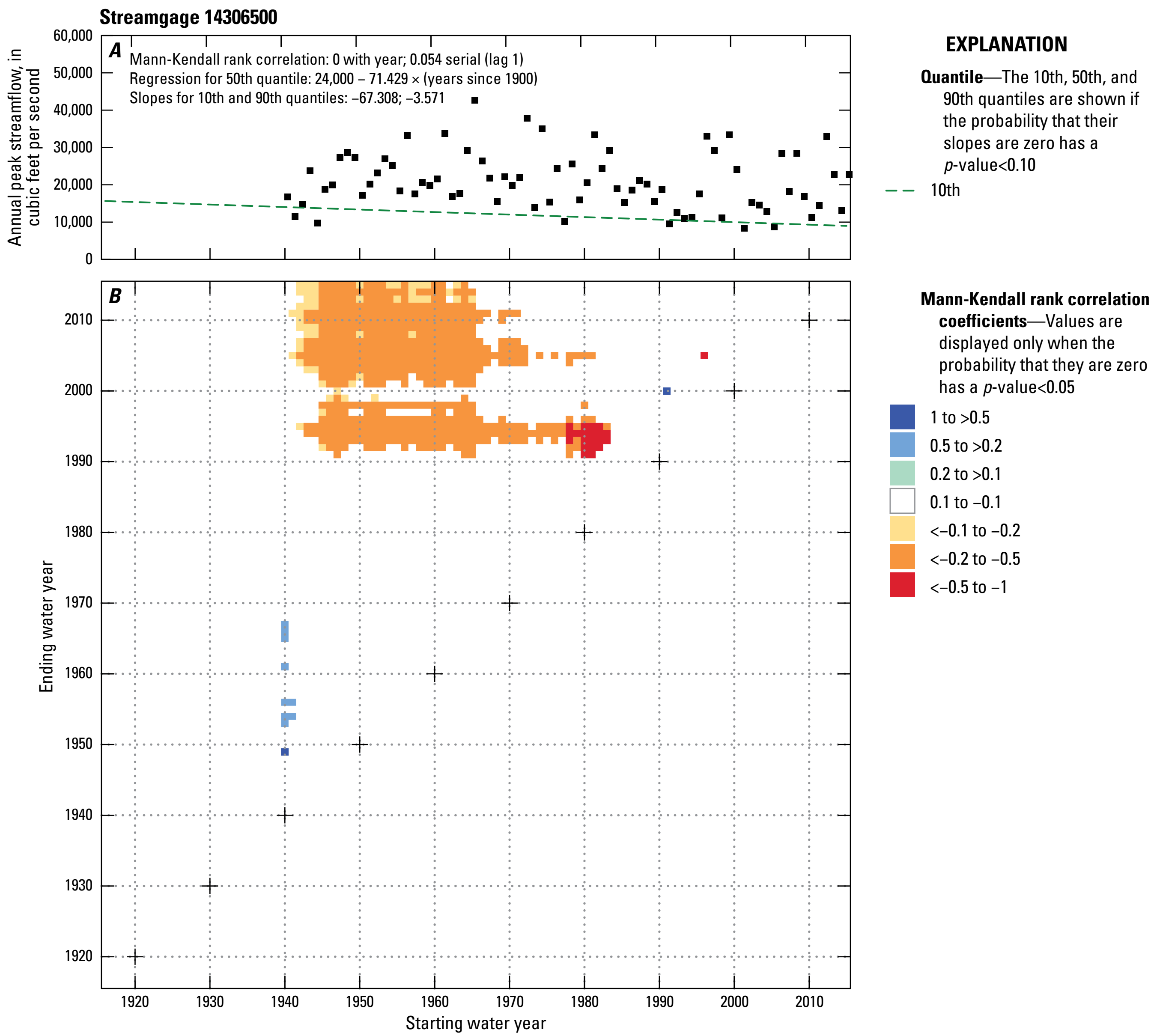

Figure B9. Annual peak streamflow time series and its rank correlation coefficients with water year for U.S. Geological Survey streamgage 14306500 at the Alsea River near Tidewater, Oregon. *A*, Time series of annual peak streamflow for the period of record. *B*, Flag plot of Mann-Kendall rank correlation coefficients for annual peak streamflow and water year calculated for every pair of starting and ending water years that were separated by at least 10 years. The significant negative monotonic trend or change point from 1941 to 2015 was attributed to short-term precipitation.

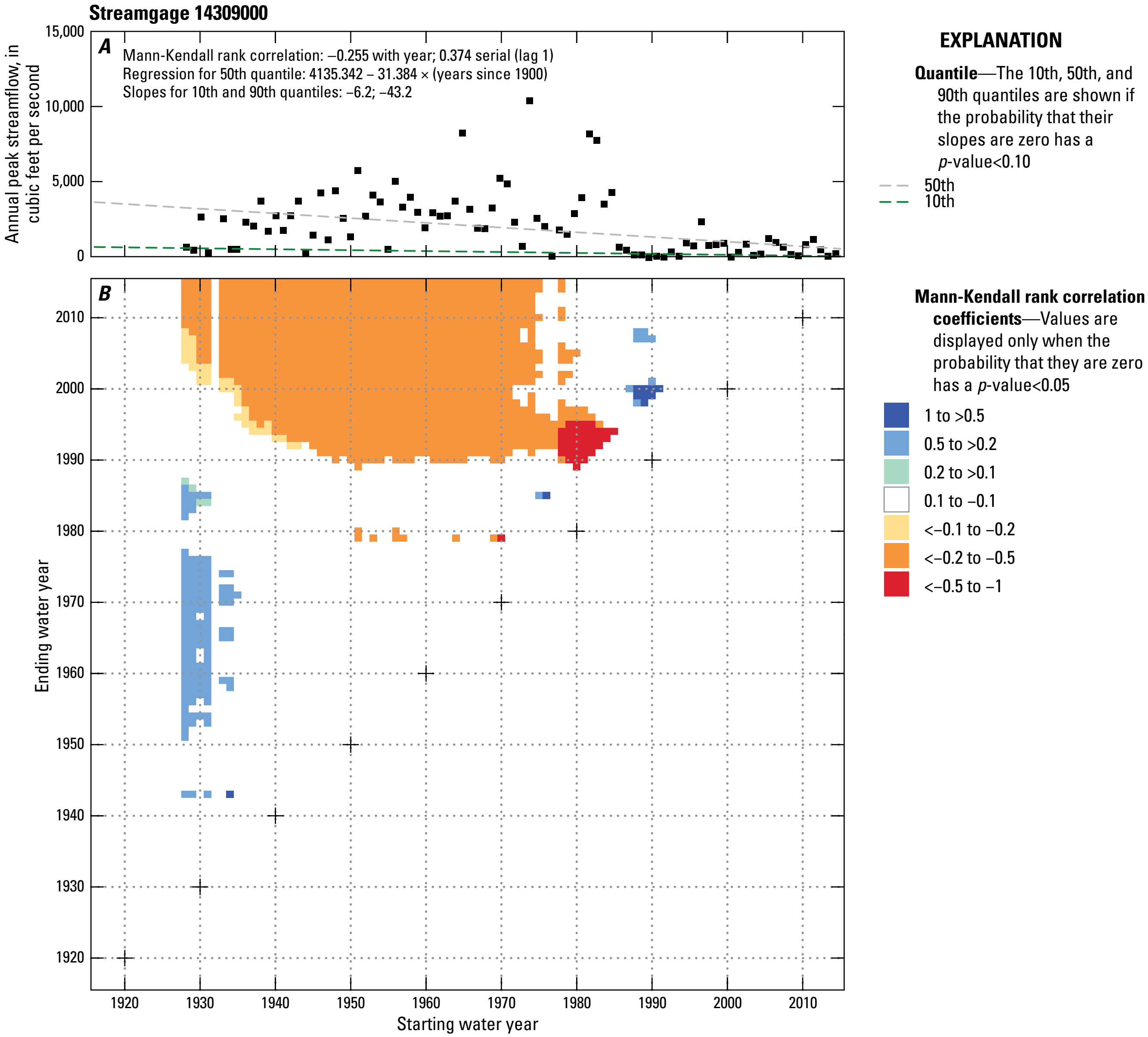

Figure B10. Annual peak streamflow time series and its rank correlation coefficients with water year for U.S. Geological Survey streamgage 14309000 at Cow Creek near Azalea, Oregon. *A*, Time series of annual peak streamflow for the period of record. *B*, Flag plot of Mann-Kendall rank correlation coefficients for annual peak streamflow and water year calculated for every pair of starting and ending water years that were separated by at least 10 years. The significant negative monotonic trends or change points from 1941 to 2015 and 1966 to 2015 were attributed to a large artificial impoundment.

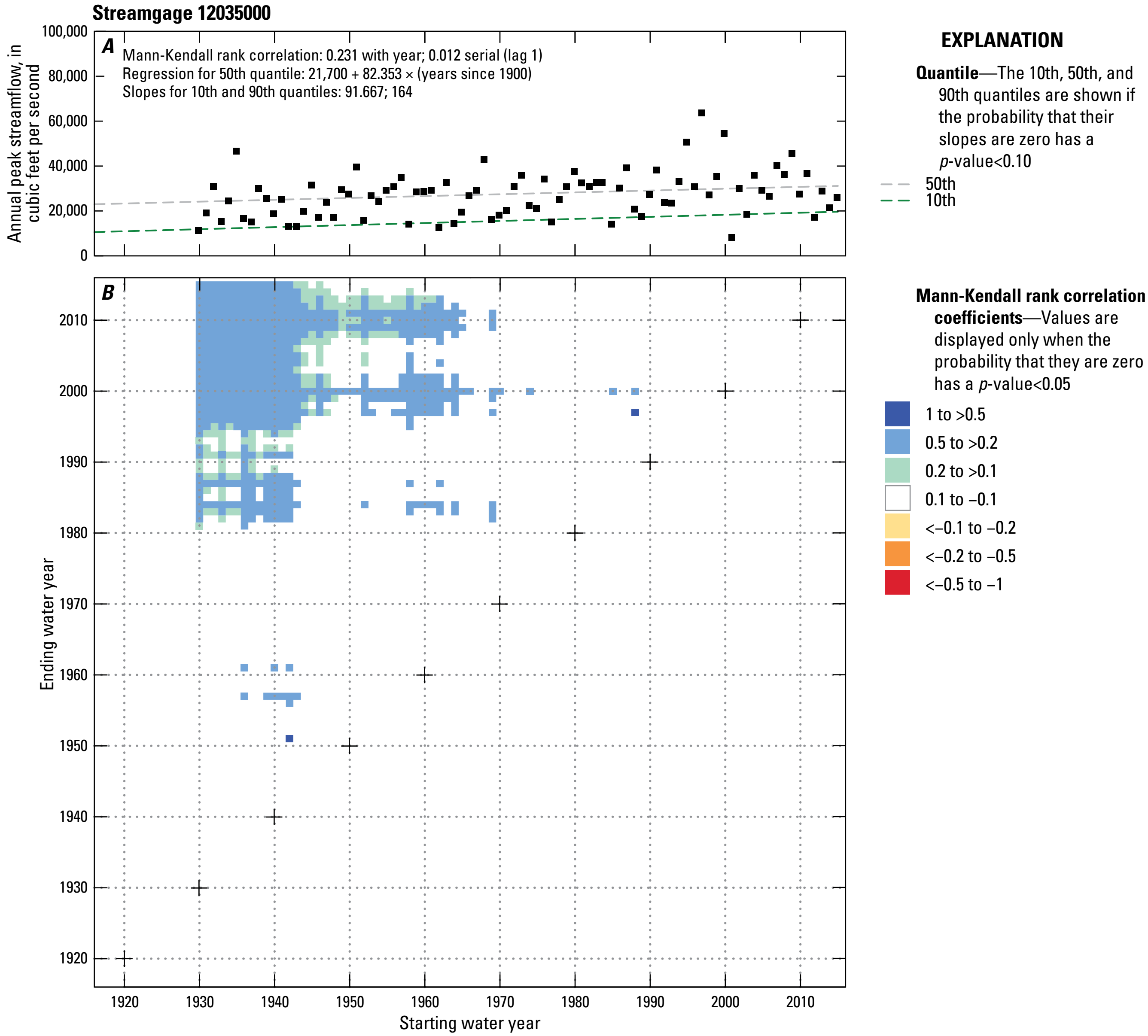

Figure B11. Annual peak streamflow time series and its rank correlation coefficients with water year for U.S. Geological Survey streamgage 12035000 at the Satsop River near Satsop, Washington. *A*, Time series of annual peak streamflow for the period of record. *B*, Flag plot of Mann-Kendall rank correlation coefficients for annual peak streamflow and water year calculated for every pair of starting and ending water years that were separated by at least 10 years. The significant positive monotonic trend or change point from 1941 to 2015 was attributed to short-term precipitation.

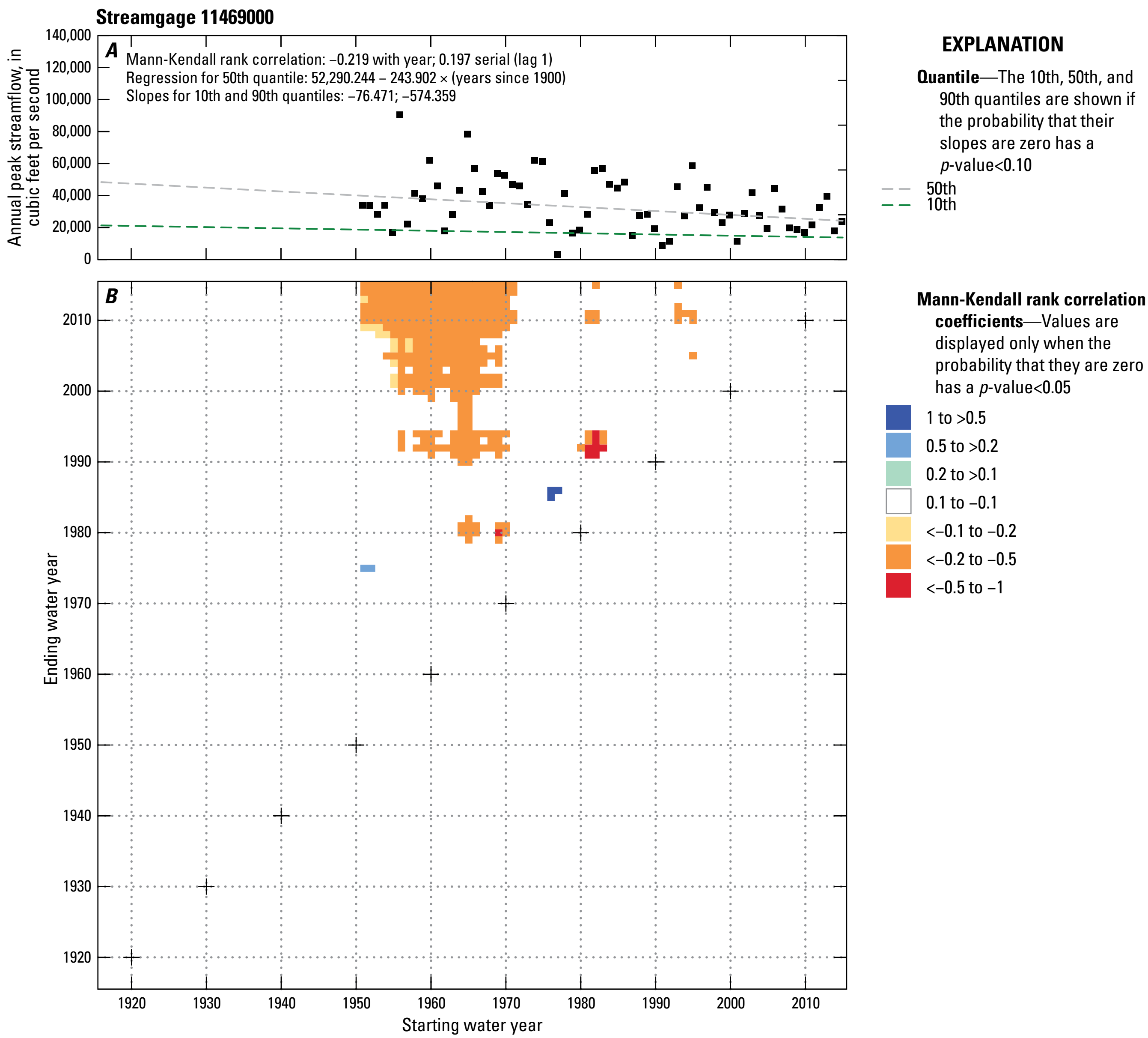

Figure B12. Annual peak streamflow time series and its rank correlation coefficients with water year for U.S. Geological Survey streamgage 11469000 at the Mattole River near Petrolia, California. *A*, Time series of annual peak streamflow for the period of record. *B*, Flag plot of Mann-Kendall rank correlation coefficients for annual peak streamflow and water year calculated for every pair of starting and ending water years that were separated by at least 10 years. The significant negative monotonic trend or change point from 1966 to 2015 was attributed to short-term precipitation.

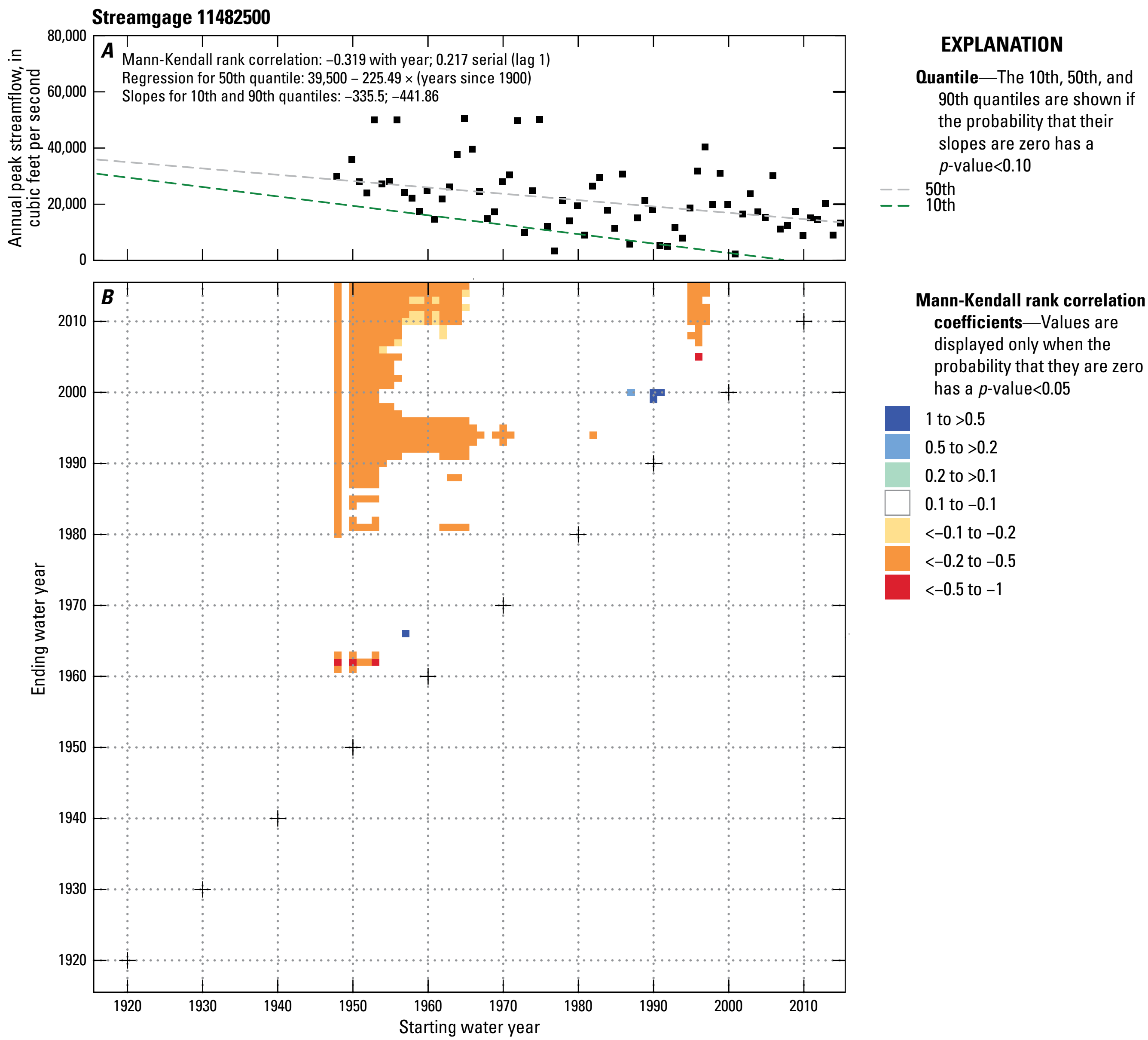

Figure B13. Annual peak streamflow time series and its rank correlation coefficients with water year for U.S. Geological Survey streamgage 11482500 at Redwood Creek at Orick, California. *A*, Time series of annual peak streamflow for the period of record. *B*, Flag plot of Mann-Kendall rank correlation coefficients for annual peak streamflow and water year calculated for every pair of starting and ending water years that were separated by at least 10 years. The significant negative monotonic trend or change point from 1966 to 2015 was attributed to multidecadal climate variability.

The Northwestern California and the Klamath Basin hydroclimatic subregion was relatively dry during the 1920s and early 1930s (Jones, 2020), as indicated by low annual peak streamflow for USGS streamgage 11477000 (at the Eel River near Scotia, Calif.) (fig. B14). As a result, negative monotonic trends generally were significant only for periods starting between the mid-1940s and mid-1960s and ending after water year 2009. The monotonic trend at USGS streamgage 11477000 for 1966–2015 was attributed to short-term precipitation with medium evidence. Multidecadal climate variability is a possible attribution for trends in peak streamflows throughout this hydroclimatic subregion; however, there is limited evidence for this attribution because peak-streamflow records at most streamgages began after the 1930s.

There were 16 non-HCDN streamgages with significant trends in annual peak streamflow in this hydroclimatic subregion, 14 of which were negative (table B4). USGS streamgage 11525500 (at the Trinity River at Lewiston, Calif.) had negative trends from 1941 to 2015 and positive trends from 1966 to 2015 as a result of changes in the operation of a trans-basin diversion (Konrad and others, 2011). USGS streamgage 11516530 (at the Klamath River below Iron Gate Dam, Calif.) had a negative monotonic trend from 1966 to 2015 but a positive change point for the same period; this positive change point was presumed to be due to changes in regulation. Trends at non-HCDN streamgages were primarily attributed to short-term precipitation at 7 streamgages, large-artificial impoundments at 5 streamgages, and multidecadal climate variability associated with consistently low peaks since 2008 at 4 streamgages.

Discussion of Regional Heterogeneity in Attributions

For many streamgages in the Pacific Northwest region with trends, partitioning the contributions from short-term precipitation volume, the phase transition of precipitation (snow to rain), and snowpack remains an important question. The attribution decisions between short-term precipitation and multidecadal climate variability as well as between air temperature and snowpack have uncertainty, in part, because these attributions often overlap. In these cases of climate-related factors, the distinctions may be mostly reflecting nuances of conceptual definitions rather than indicating different physical processes.

Multidecadal climate variability in the region affects the results of both the 75-year (1941–2015) and 50-year (1966–2015) trend tests. The period from 1966 to 2015 begins during a positive phase (a colder phase) PDO and ends in a more neutral or negative phase (a warmer phase) in the Pacific Northwest region. Longer periods of record are needed to discern whether trends are an expression of multidecadal climate variability. For example, the Northwestern California and the Klamath Basin hydroclimatic subregion had a dry period that spanned the 1920s to the 1930s (during which annual peak streamflow was comparable to annual peak streamflow since 2008), so negative trends may indicate multidecadal climate variability. Generally, multidecadal climate variability is indicated in the Northwestern California and the Klamath Basin hydroclimatic subregion by no trend in annual peak streamflow for periods starting before 1950, but negative trends for periods starting after 1950 and ending after 1980. In contrast, multidecadal climate variability is indicated in the Western Washington hydroclimatic subregion by positive trends for periods starting before 1960 and ending after 1980. The broad spatial patterns of positive, but limited trends in the northern part of the Pacific Northwest region and negative, but limited trends in the southern part of the region are consistent with geographic trends in extreme precipitation identified by Mass and others (2011).

Recent trends in precipitation for the Pacific Northwest region are increasing, but only moderately when compared to trends in the eastern, north-central, and south-central United States (Easterling and others, 2017). As a result of increasing precipitation, annual peak streamflow has increased substantially in some rivers (particularly in the Western Washington hydroclimatic subregion), but not pervasively across the region. A shift in precipitation from snow to rain and earlier snowpack (Aguado and others, 1992; Dettinger and Cayan, 1995; McCabe and others, 2007) likely contributes to changes in annual peak streamflow in the region, particularly for the Interior Columbia Basin and Great Basin hydroclimatic subregion where many streamgages had systemic decreases in the timing of the day-of-peak. The shift from snow to rain may also contribute to increased annual peak streamflow for streamgages in the Western Washington hydroclimatic subregion, but spatially explicit information about snow levels at the time of annual peak streamflow would be required to test this hypothesis.

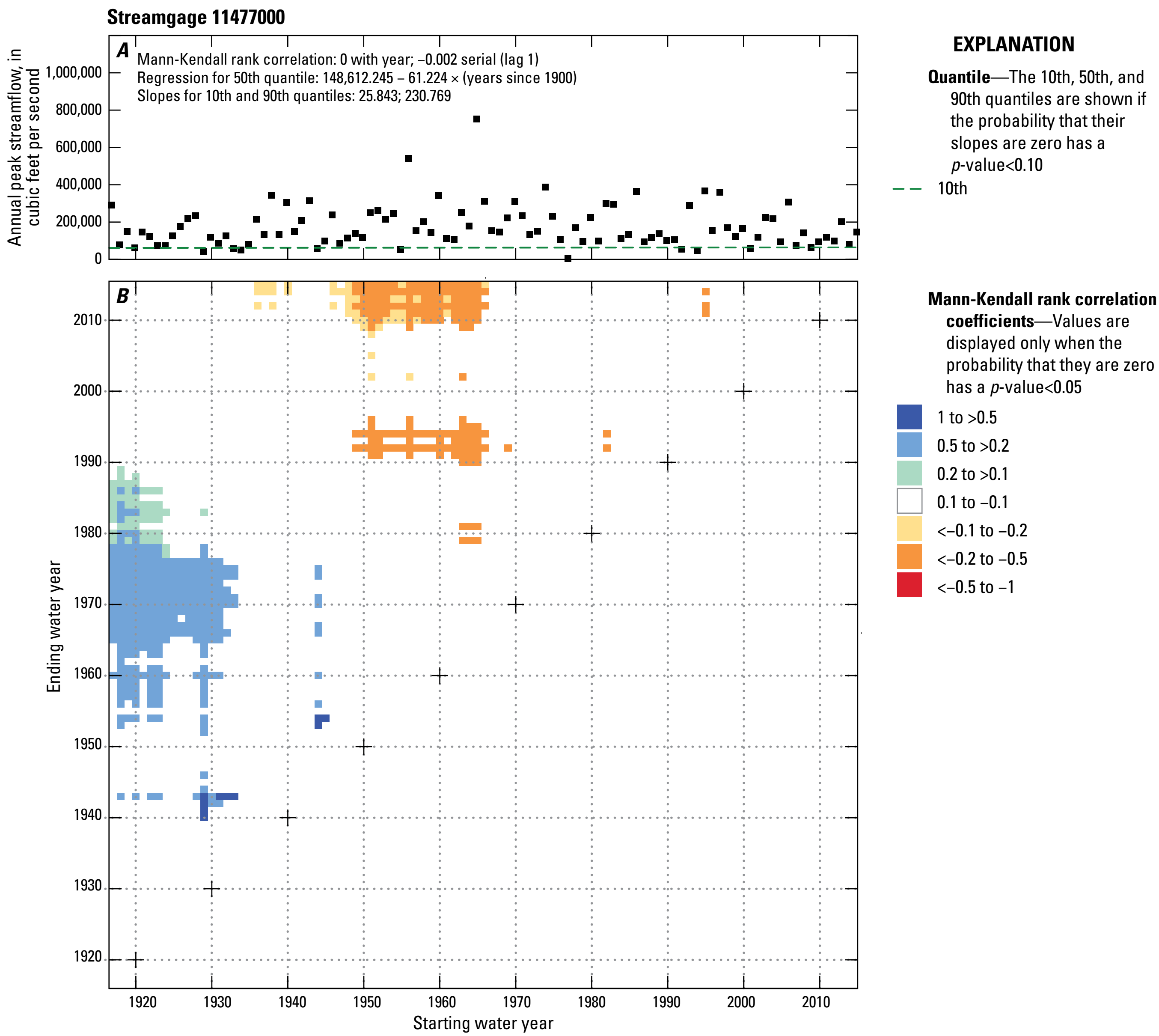

Figure B14. Annual peak streamflow time series and its rank correlation coefficients with water year for U.S. Geological Survey streamgage 11477000 at the Eel River near Scotia, California. *A*, Time series of annual peak streamflow for the period of record. *B*, Flag plot of Mann-Kendall rank correlation coefficients for annual peak streamflow and water year calculated for every pair of starting and ending water years that were separated by at least 10 years. The significant negative monotonic trends or change points from 1941 to 2015 and 1966 to 2015 were attributed to short-term precipitation.

Summary

Most streamgages in the Pacific Northwest region of the United States did not have statistically significant (*p*-value<0.10, where the *p*-value is the probability used to reject the null hypothesis in a statistical test) monotonic trends or change points (herein referred to as "trends") in annual peak-streamflow data for the periods of 1941–2015 or 1966–2015. Positive trends were identified at 14 U.S. Geological Survey (USGS) Hydro-Climatic Data Network 2009 (HCDN) streamgages in the Interior Columbia Basin and Great Basin, the Willamette River Basin and Columbia Gorge, and the Western Washington hydroclimatic subregions; these trends were attributed to short-term precipitation, air temperature, or multidecadal climate variability. Negative trends were identified at 8 HCDN streamgages in the Interior Columbia Basin and Great Basin, the Willamette River Basin and Columbia Gorge, the Coastal Oregon, and the Northwestern California and the Klamath Basin hydroclimatic subregions; these trends were attributed to short-term precipitation, snowpack, or multidecadal climate variability. Trends at non-HCDN streamgages were mostly attributed to large artificial impoundments (47 streamgages) or climate-related factors (31 streamgages).

References Cited

Abatzoglou, J.T., Rupp, D.E., and Mote, P.W., 2014, Seasonal climate variability and change in the Pacific Northwest of the United States: Journal of Climate, v. 27, no. 5, p. 2125–2142, accessed November 19, 2021, at https://doi.org/10.1175/JCLI-D-13-00218.1.

Aguado, E., Cayan, D., Riddle, L., and Roos, M., 1992, Climatic fluctuations and the timing of West Coast streamflow: Journal of Climate, v. 5, no. 12, p. 1468–1483.

American Meteorological Society, 2019, Atmospheric river: Meteorology Glossary, accessed November 19, 2021, at http://glossary.ametsoc.org/wiki/Atmospheric_river.

Archfield, S.A., Hirsch, R.M., Viglione, A., and Blöschl, G., 2016, Fragmented patterns of flood change across the United States: Geophysical Research Letters, v. 43, no. 19, p. 10232–10239.

Berghuijs, W.R., Woods, R.A., Hutton, C.J., and Sivapalan, M., 2016, Dominant flood generating mechanisms across the United States: Geophysical Research Letters, v. 43, no. 9, p. 4382–4390.

Bond, N.A., and Harrison, D.E., 2000, The Pacific Decadal Oscillation, air-sea interaction and central north Pacific winter atmospheric regimes: Geophysical Research Letters, v. 27, no. 5, p. 731–734.

Bowling, L.C., Storck, P., and Lettenmaier, D.P., 2000, Hydrologic effects of logging in western Washington, United States: Water Resources Research, v. 36, no. 11, p. 3223–3240, accessed November 19, 2021, at https://doi.org/10.1029/2000WR900138.

Cayan, D.R., 1996, Interannual climate variability and snowpack in the western United States: Journal of Climate, v. 9, no. 5, p. 928–948.

Cayan, D.R., Dettinger, M.D., Diaz, H.F., and Graham, N.E., 1998, Decadal variability of precipitation over western North America: Journal of Climate, v. 11, no. 12, p. 3148–3166.

Cayan, D.R., and Peterson, D.H., 1989, The influence of north Pacific atmospheric circulation on streamflow in the West, *in* Peterson, D.H., ed., Aspects of climate variability in the Pacific and the western Americas: American Geophysical Union Geophysical Monograph Series, v. 55, p. 375–397.

Cayan, D.R., Redmond, K.T., and Riddle, L.G., 1999, ENSO and hydrologic extremes in the western United States: Journal of Climate, v. 12, no. 9, p. 2881–2893.

Das, T., Hidalgo, H.G., Pierce, D.W., Barnett, T.P., Dettinger, M.D., Cayan, D.R., Bonfils, C., Bala, G., and Mirin, A., 2009, Structure and detectability of trends in hydrological measures over the western United States: Journal of Hydrometeorology, v. 10, no. 4, p. 871–892, accessed November 19, 2021, at https://doi.org/10.1175/2009JHM1095.1.

DeFlorio, M.J., Pierce, D.W., Cayan, D.R., and Miller, A.J., 2013, Western U.S. extreme precipitation events and their relation to ENSO and PDO in CCSM4: Journal of Climate, v. 26, no. 12, p. 4231–4243.

Déry, S.J., Stahl, K., Moore, R.D., Whitfield, P.H., Menounos, B., and Burford, J.E., 2009, Detection of runoff timing changes in pluvial, nival, and glacial rivers of western Canada: Water Resources Research, v. 45, no. 4, article W04426, 11 p.

Dettinger, M.D., and Cayan, D.R., 1995, Large-scale atmospheric forcing of recent trends toward early snowmelt runoff in California: Journal of Climate, v. 8, no. 3, p. 606–623.

Dettinger, M.D., Cayan, D.R., Diaz, H.F., and Meko, D.M., 1998, North-south precipitation patterns in western North America on interannual-to-decadal timescales: Journal of Climate, v. 11, no. 12, p. 3095–3111, accessed November 19, 2021, at https://doi.org/10.1175/1520-0442(1998)011<3095:NSPPIW>2.0.CO;2.

Dudley, R.W., Archfield, S.A., Hodgkins, G.A., Renard, B., and Ryberg, K.R., 2018, Peak-streamflow trends and change-points and basin characteristics for 2,683 U.S. Geological Survey streamgages in the conterminous U.S. (ver. 3.0, April 2019): U.S. Geological Survey data release. [Also available at https://doi.org/10.5066/P9AEGXY0.]

Dudley, R.W., Hodgkins, G.A., McHale, M.R., Kolian, M.J., and Renard, B., 2017, Trends in snowmelt-related streamflow timing in the conterminous United States: Journal of Hydrology, v. 547, p. 208–221.

Easterling, D.R., Kunkel, K.E., Arnold, J.R., Knutson, T., LeGrande, A.N., Leung, L.R., Vose, R.S., Waliser, D.E., and Wehner, M.F., 2017, Precipitation change in the United States, chap. 7 *of* Wuebbles, D.J., Fahey, D.W., Hibbard, K.A., Dokken, D.J., Stewart, B.C., and Maycock, T.K., eds., Climate science special report, v. I *of* Fourth national climate assessment: Washington, D.C., U.S. Global Change Research Program, p. 207–230.

Eldardiry, H., Mahmood, A., Chen, X., Hossain, F., Nijssen, B., and Lettenmaier, D.P., 2019, Atmospheric river-induced precipitation and snowpack during the western United States cold season: Journal of Hydrometeorology, v. 20, no. 4, p. 613–630.

England, J.F., Jr., Cohn, T.A., Faber, B.A., Stedinger, J.R., Thomas, W.O., Jr., Veilleux, A.G., Kiang, J.E., and Mason, R.R., Jr., 2018, Guidelines for determining flood flow frequency—Bulletin 17C (ver. 1.1, May 2019): U.S. Geological Survey Techniques and Methods, book 4, chap. B5, 148 p., accessed November 19, 2021, at https://doi.org/10.3133/tm4B5.

Falcone, J.A., 2011, GAGES-II—Geospatial attributes of gages for evaluating streamflow: U.S. Geological Survey dataset, accessed November 19, 2021, at http://pubs.er.usgs.gov/publication/70046617.

Falcone, J.A., 2015, U.S. conterminous wall-to-wall anthropogenic land use trends (NWALT), 1974–2012: U.S. Geological Survey Data Series 948, 33 p. plus appendixes 3–6 as separate files, accessed November 19, 2021, at https://doi.org/10.3133/ds948.

Falcone, J.A., 2017, U.S. Geological Survey GAGES-II time series data from consistent sources of land use, water use, agriculture, timber activities, dam removals, and other historical anthropogenic influences: U.S. Geological Survey data release, accessed November 19, 2021, at https://doi.org/10.5066/F7HQ3XS4.

Gendaszek, A.S., Magirl, C.S., and Czuba, C.R., 2012, Geomorphic response to flow regulation and channel and floodplain alteration in the gravel-bedded Cedar River, Washington, USA: Geomorphology, v. 179, p. 258–268.

Gershunov, A., and Barnett, T.P., 1998, Interdecadal modulation of ENSO teleconnections: Bulletin of the American Meteorological Society, v. 79, no. 12, p. 2715–2726.

Gershunov, A., Shulgina, T., Clemesha, R.E.S., Guirguis, K., Pierce, D.W., Dettinger, M.D., Lavers, D.A., Cayan, D.R., Polade, S.D., Kalansky, J., and Ralph, F.M., 2019, Precipitation regime change in western North America—The role of atmospheric rivers: Scientific Reports, v. 9, article 9944, 11 p., accessed May 7, 2020, at https://doi.org/10.1038/s41598-019-46169-w.

Graf, W.L., 2006, Downstream hydrologic and geomorphic effects of large dams on American rivers: Geomorphology, v. 79, nos. 3–4, p. 336–360.

Hamlet, A.F., and Lettenmaier, D.P., 1999, Effects of climate change on hydrology and water resources in the Columbia River Basin: Journal of the American Water Resources Association, v. 35, no. 6, p. 1597–1623.

Hamlet, A.F., Mote, P.W., Clark, M.P., and Lettenmaier, D.P., 2005, Effects of temperature and precipitation variability on snowpack trends in the western United States: Journal of Climate, v. 18, no. 21, p. 4545–4561.

Hatcher, K.L., and Jones, J.A., 2013, Climate and streamflow trends in the Columbia River Basin—Evidence for ecological and engineering resilience to climate change: Atmosphere-Ocean, v. 51, no. 4, p. 436–455.

Hodgkins, G.A., Dudley, R.W., Archfield, S.A., and Renard, B., 2019, Effects of climate, regulation, and urbanization on historical flood trends in the United States: Journal of Hydrology, v. 573, p. 697–709.

Jefferson, A.J., 2011, Seasonal versus transient snow and the elevation dependence of climate sensitivity in maritime mountainous regions: Geophysical Research Letters, v. 38, no. 16, article L16402, 7 p.

Jones, J., 2020, California's most significant droughts—Comparing historical and recent conditions: California Department of Water Resources, accessed March 19, 2021, at https://water.ca.gov/-/media/DWR-Website/Web-Pages/What-We-Do/Drought-Mitigation/Files/Publications-And-Reports/CalSigDroughts19_v9_ay11.pdf.

Jones, J.A., 2000, Hydrologic processes and peak discharge response to forest removal, regrowth, and roads in 10 small experimental basins, Western Cascades, Oregon: Water Resources Research, v. 36, no. 9, p. 2621–2642, accessed November 19, 2021, at https://doi.org/10.1029/2000WR900105.

Kalra, A., Piechota, T.C., Davies, R., and Tootle, G.A., 2008, Changes in the U.S. streamflow and western U.S. snowpack: Journal of Hydrologic Engineering, v. 13, no. 3, p. 156–163.

Klos, P.Z., Link, T.E., and Abatzoglou, J.T., 2014, Extent of the rain-snow transition zone in the western U.S. under historic and projected climate: Geophysical Research Letters, v. 41, no. 13, p. 4560–4568.

Knowles, N., Dettinger, M.D., and Cayan, D.R., 2006, Trends in snowfall versus rainfall in the western United States: Journal of Climate, v. 19, no. 18, p. 4545–4559.

Konrad, C.P., and Booth, D.B., 2002, Hydrologic trends associated with urban development for selected streams in the Puget Sound basin, western Washington: U.S. Geological Survey Water-Resources Investigation Report 2002–4040, 40 p.

Konrad, C.P., Booth, D.B., and Burges, S.J., 2005, Effects of urban development in the Puget Lowland, Washington, on interannual streamflow patterns—Consequences for channel form and streambed disturbance: Water Resources Research, v. 41, no. 7, article W07009, 15 p.

Konrad, C.P., and Dettinger, M.D., 2017, Flood runoff in relation to water vapor transport by atmospheric rivers over the western United States, 1949–2015: Geophysical Research Letters, v. 44, no. 22, p. 11456–11462.

Konrad, C.P., Olden, J.D., Lytle, D.A., Melis, T.S., Schmidt, J.C., Bray, E.N., Freeman, M.C., Gido, K.B., Hemphill, N.P., Kennard, M.J., McMullen, L.E., Mims, M.C., Pyron, M., Robinson, C.T., Williams, J.G., 2011, Large-scale flow experiments for managing river systems: Bioscience, v. 61, no. 12, p. 948–959, accessed November 19, 2021, at https://doi.org/10.1525/bio.2011.61.12.5.

Konrad, C.P., and Restivo, D.E., 2020, Trends in annual peak streamflow quantiles for 2,683 U.S. Geological Survey streamgages in the conterminous United States: U.S. Geological Survey data release, accessed November 19, 2021, at https://doi.org/10.5066/P95DRY7D.

Konrad, C.P., Warner, A.W., and Higgins, J.V., 2012, Evaluating dam re-operation for freshwater conservation in the sustainable rivers project: River Research and Applications, v. 28, no. 6, p. 777–792.

Lins, H.F., 2012, USGS Hydro-Climatic Data Network 2009 (HCDN–2009): U.S. Geological Survey Fact Sheet 2012–3047, 4 p., accessed November 19, 2021, at https://pubs.usgs.gov/fs/2012/3047/.

Lins, H.F., and Slack, J.R., 1999, Streamflow trends in the United States: Geophysical Research Letters, v. 26, no. 2, p. 227–230.

Lins, H.F., and Slack, J.R., 2005, Seasonal and regional characteristics of U.S. streamflow trends in the United States from 1940 to 1999: Physical Geography, v. 26, no. 6, p. 489–501.

Luce, C.H., Abatzoglou, J.T., and Holden. Z.A., 2013, The missing mountain water—Slower westerlies decrease orographic enhancement in the Pacific Northwest USA: Science, v. 342, no. 6164, p. 1360–1364, accessed November 19, 2021, at https://doi.org/10.1126/science.1242335.

Mann, H.B., 1945, Non-parametric tests against trend: Econometrica, v. 13, no. 3, p. 245–259.

Mantua, N.J., and Hare, S.R., 2002, The Pacific Decadal Oscillation: Journal of Oceanography, v. 58, p. 35–44.

Mantua, N.J., Hare, S.R., Zhang, Y., Wallace, J.M., and Francis, R.C., 1997, A Pacific interdecadal climate oscillation with impacts on salmon production: Bulletin of the American Meteorological Society, v. 78, no. 6, p. 1069–1079.

Mass, C., Skalenakis, A., and Warner, M., 2011, Extreme precipitation over the west coast of North America—Is there a trend?: Journal of Hydrometeorology, v. 12, no. 2, p. 310–318, accessed November 19, 2021, at https://doi.org/10.1175/2010JHM1341.1.

Mastin, M.C., Konrad, C.P., Veilleux, A.G., and Tecca, A.E., 2016, Magnitude, frequency, and trends of floods at gaged and ungaged stations in Washington, based on data through water year 2014 (ver. 1.2, November 2017): U.S. Geological Survey Scientific Investigations Report 2016–5118, 70 p., accessed November 19, 2021, at https://doi.org/10.3133/sir20165118.

McCabe, G.J., and Clark, M.P., 2005, Trends and variability in snowmelt runoff in the western United States: Journal of Hydrometeorology, v. 6, no. 4, p. 476–482, accessed November 19, 2021, at https://doi.org/10.1175/JHM428.1.

McCabe, G.J., Clark, M.P., and Hay, L.E., 2007, Rain-on-snow events in the western United States: Bulletin of the American Meteorological Society, v. 88, no. 3, p. 319–328.

McCabe, G.J., and Dettinger, M.D., 1999, Decadal variations in the strength of ENSO teleconnections with precipitation in the western United States: International Journal of Climatology, v. 19, no. 13, p. 1399–1410.

McCabe, G.J., and Wolock, D.M., 2002, A step increase in streamflow in the conterminous United States: Geophysical Research Letters, v. 29, no. 24, p. 2185–2189.

McCabe, G.J., and Wolock, D.M., 2014, Spatial and temporal patterns in conterminous United States streamflow characteristics: Geophysical Research Letters, v. 41, no. 19, p. 6889–6897.

Mehta, V.M., 2017, Natural decadal climate variability—Societal impacts: Boca Raton, Fla., CRC Press, 332 p.

Mote, P.W., Hamlet, A.F., Clark, M.P., and Lettenmaier, D.P., 2005, Declining mountain snowpack in western North America: Bulletin of the American Meteorological Society, v. 86, no. 1, p. 39–50.

Mote, P.W., Li, S., Lettenmaier, D.P., Xiao, M., and Engel, R., 2018, Dramatic declines in snowpack in the western US: Climate and Atmospheric Science, v. 1, article 2, 6 p.

Neiman, P.J., Ralph, F.M., Wick, G.A., Lundquist, J.D., and Dettinger, M.D., 2008, Meteorological characteristics and overland precipitation impacts of atmospheric rivers affecting the west coast of North America based on eight years of SSM/I satellite observations: Journal of Hydrometeorology, v. 9, no. 1, p. 22–47.

Neiman, P.J., Schick, L.J., Ralph, F.M., Hughes, M., and Wick, G.A., 2011, Flooding in western Washington—The connection to atmospheric rivers: Journal of Hydrometeorology, v. 12, no. 6, p. 1337–1358.

Newell, R.E., and Zhu, Y., 1994, Tropospheric rivers—A one-year record and a possible application to ice core data: Geophysical Research Letters, v. 21, no. 2, p. 113–116.

Pettitt, A.N., 1979, A non-parametric approach to the change-point problem: Journal of the Royal Statistical Society, Series C (Applied Statistics), v. 28, no. 2, p. 126–135.

Ralph, F.M., Coleman, T., Neiman, P.J., Zamora, R.J., and Dettinger, M.D., 2013, Observed impacts of duration and seasonality of atmospheric-river landfalls on soil moisture and runoff in coastal northern California: Journal of Hydrometeorology, v. 14, no. 2, p. 443–459.

Rasmusson, E.M., and Wallace, J.M., 1983, Meteorological aspects of the El Niño/Southern Oscillation: Science, v. 222, no. 4629, p. 1195–1202.

Rutz, J.J., Steenburgh, W.J., and Ralph, F.M., 2014, Climatological characteristics of atmospheric rivers and their inland penetration over the western United States: Monthly Weather Review, v. 142, no. 2, p. 905–921.

Seaber, P.R., Kapinos, F.P., and Knapp, G.L., 1987, Hydrologic unit maps: U.S. Geological Survey Water-Supply Paper 2294, 63 p., 1 pl., accessed November 19, 2021, at https://pubs.usgs.gov/wsp/wsp2294/.

Stewart, I.T., Cayan, D.R., and Dettinger, M.D., 2005, Changes toward earlier streamflow timing across western North America: Journal of Climate, v. 18, no. 8, p. 1136–1155, accessed November 19, 2021, at https://doi.org/10.1175/JCLI3321.1.

U.S. Department of Agriculture [USDA] Forest Service, 2021, MTBS [Monitoring Trends in Burn Severity] burn area boundary [dataset]; S_USA.MTBS_BURN_AREA_BOUNDARY: USDA Forest Service, FSGeodata Clearinghouse website, accessed March 12, 2021, at https://data.fs.usda.gov/geodata/edw/datasets.php?xmlKeyword=MTBS.

U.S. Geological Survey, 2007, North American elevation 1-kilometer resolution GRID [dataset]: U.S. Geological Survey ScienceBase Catalog website, accessed May 1, 2019, at https://www.sciencebase.gov/catalog/item/4fb5495ee4b04cb937751d6d.

U.S. Geological Survey, 2019, USGS water data for the Nation: U.S. Geological Survey National Water Information System database, accessed March 12, 2019, at https://doi.org/10.5066/F7P55KJN.

Vaccaro, J.J., Kahle, S.C., Ely, D.M., Burns, E.R., Snyder, D.T., Haynes, J.V., Olsen, T.D., Welch, W.B., and Morgan, D.S., 2015, Groundwater availability of the Columbia Plateau Regional Aquifer System, Washington, Oregon, and Idaho: U.S. Geological Survey Professional Paper 1817, 87 p., accessed November 19, 2021, at http://doi.org/10.3133/pp1817.

Wahl, K.L., 1998, Sensitivity of non-parametric trend analyses to multi-year extremes, *in* Proceedings of the Western Snow Conference, April 20–23, 1998: Snowbird, Utah, Western Snow Conference, p. 157–160.

Wang, X., and Liu, H., 2015, PDO modulation of ENSO effect on tropical cyclone rapid intensification in the western North Pacific: Climate Dynamics, v. 46, p. 15–28, accessed April 5, 2019, at https://doi.org/10.1007/s00382-015-2563-8.

Warner, M.D., Mass, C.F., and Salathé, E.P., Jr., 2015, Changes in winter atmospheric rivers along the North American west coast in CMIP5 climate models: Journal of Hydrometeorology, v. 16, no. 1, p. 118–128.

York, B.C., Ryberg, K.R., Asquith, W.H., Chase, K.J., Dickinson, J.E., Dudley, R.W., Harden, T.M., Hodgkins, G.A., Holtschlag, D.J., Humberson, D.G., Konrad, C.P., Levin, S.B., Restivo, D.E., Sando, R., Sando, S.K., Swain, E.D., Tillery, A.C., and Totten, A.R., 2022, Attributions for nonstationary peak streamflow records across the conterminous United States, 1941–2015 and 1966–2015: U.S. Geological Survey data release, https://doi.org/10.5066/P9FOUVWG.

Zhu, Y., and Newell, R.E., 1998, A proposed algorithm for moisture fluxes from atmospheric rivers: Monthly Weather Review, v. 126, no. 3, p. 725–735.

Attribution of Monotonic Trends and Change Points in Peak Streamflow in the Upper Plains Region of the United States, 1941–2015 and 1966–2015

By Roy Sando, Steven K. Sando, Karen R. Ryberg, and Katherine J. Chase

Chapter C of
Attribution of Monotonic Trends and Change Points in Peak Streamflow Across the Conterminous United States Using a Multiple Working Hypotheses Framework, 1941–2015 and 1966–2015
Karen R. Ryberg, editor

Prepared in cooperation with
U.S. Department of Transportation
Federal Highway Administration

Professional Paper 1869

U.S. Department of the Interior
U.S. Geological Survey

U.S. Geological Survey, Reston, Virginia: 2022

For more information on the USGS—the Federal source for science about the Earth, its natural and living resources, natural hazards, and the environment—visit https://www.usgs.gov or call 1–888–ASK–USGS.

For an overview of USGS information products, including maps, imagery, and publications, visit https://store.usgs.gov.

Suggested citation:
Sando, R., Sando, S.K., Ryberg, K.R., and Chase, K.J., 2022, Attribution of monotonic trends and change points in peak streamflow in the Upper Plains region of the United States, 1941–2015 and 1966–2015, chap. C *of* Ryberg, K.R., ed., Attribution of monotonic trends and change points in peak streamflow across the conterminous United States using a multiple working hypotheses framework, 1941–2015 and 1966–2015: U.S. Geological Survey Professional Paper 1869, p. C1–C36, https://doi.org/10.3133/pp1869.

Associated data for this publication:
Dudley, R.W., Archfield, S.A., Hodgkins, G.A., Renard, B., and Ryberg, K.R., 2018, Peak-streamflow trends and change-points and basin characteristics for 2,683 U.S. Geological Survey streamgages in the conterminous U.S. (ver. 3.0, April 2019): U.S. Geological Survey data release, https://doi.org/10.5066/P9AEGXY0.

York, B.C., Ryberg, K.R., Asquith, W.H., Chase, K.J., Dickinson, J.E., Dudley, R.W., Harden, T.M., Hodgkins, G.A., Holtschlag, D.J., Humberson, D.G., Konrad, C.P., Levin, S.B., Restivo, D.E., Sando, R., Sando, S.K., Swain, E.D., Tillery, A.C., and Totten, A.R., 2022, Attributions for nonstationary peak streamflow records across the conterminous United States, 1941–2015 and 1966–2015: U.S. Geological Survey data release, https://doi.org/10.5066/P9FOUVWG.

ISSN 2330-7102 (online)

Acknowledgments

The work described in this professional paper was funded by the Federal Highway Administration of the U.S. Department of Transportation through Interagency Agreement DTFH6116X30020, “Flood Frequency Estimation for Hydraulic Design.”

Thank you to U.S. Geological Survey colleagues Gregg Wiche and Benjamin Dietsch for their reviews of this report.

Contents

Figures

Tables

[Tables C1–C13 follow the References Cited for chapter C]

Conversion Factors

Multiply	By	To obtain
	Length	
inch (in.)	2.54	centimeter (cm)
inch (in.)	25.4	millimeter (mm)
foot (ft)	0.3048	meter (m)
mile (mi)	1.609	kilometer (km)
kilometer (km)	0.6214	mile (mi)
	Area	
acre	4,047	square meter (m^2)
acre	0.004047	square kilometer (km^2)
square mile (mi^2)	2.590	square kilometer (km^2)
	Volume	
gallon (gal)	3.785	liter (L)
cubic foot (ft^3)	0.02832	cubic meter (m^3)
acre-foot (acre-ft)	1,233	cubic meter (m^3)
	Volume per square unit of area	
megaliter per square kilometer (ML/km^2)	2.099	acre-foot per square mile ($acre\text{-}ft/mi^2$)
	Flow rate	
cubic foot per second (ft^3/s)	0.02832	cubic meter per second (m^3/s)

Datum

Horizontal coordinate information is referenced to the North American Datum of 1983 (NAD 83).

Supplemental Information

A “water year” is the 12-month period from October 1 through September 30 of the following year that is designated by the calendar year in which it ends.

The 75-year and 50-year study periods described in this report span water years 1941–2015 and 1966–2015, respectively.

Abbreviations

>	greater than
≥	greater than or equal to
<	less than
BGSS	between-group sum of squares
GAGES-II	Geospatial Attributes of Gages for Evaluating Streamflow, Version II
HCDN-2009	Hydro-Climatic Data Network 2009
MWHs	multiple working hypotheses
NAD 83	North American Datum of 1983
NID	National Inventory of Dams
NWIS	National Water Information System
PFTZ	peak-flow trend zone
p-value	attained significance level
USGS	U.S. Geological Survey
VRC	variance ratio criterion
WGSS	within-group sum of squares

Attribution of Monotonic Trends and Change Points in Peak Streamflow in the Upper Plains Region of the United States, 1941–2015 and 1966–2015

By Roy Sando,[1] Steven K. Sando,[1] Karen R. Ryberg,[1] and Katherine J. Chase[1]

Abstract

In 2016, the U.S. Geological Survey (USGS), in cooperation with the Federal Highway Administration of the U.S. Department of Transportation, began a national three-phase study to research methods for detecting and addressing potential nonstationarities in annual peak-streamflow records associated with changes in climate, land use, land cover, and other potential drivers of nonstationarity in the conterminous United States. The work described in this professional paper represents the second phase of the project, which focused on making attributions for significant nonstationarities in annual peak streamflows that were detected in the first phase of the project. Two time periods were selected for the study: a 50-year period (water years 1966–2015) and a 75-year period (water years 1941–2015).

The purpose of this chapter is to describe attributions made for monotonic trends and change points in annual peak-streamflow data that were detected in the Upper Plains region of the United States. This chapter also quantifies spatial patterns in the sign and timing of these nonstationarities. Of the 269 streamgages suitable for 50-year analyses in this region, 68 streamgages had significant monotonic trends (48 negative and 20 positive) and 61 streamgages had significant change points (40 negative and 21 positive) in annual peak-streamflow data. Of the 109 streamgages suitable for 75-year analyses, 52 streamgages had significant monotonic trends (34 negative and 18 positive) and 46 had significant change points (30 negative and 16 positive) in annual peak-streamflow data.

Because of heterogeneity in hydroclimatic conditions and causal factors potentially contributing to trends in annual peak streamflows in the Upper Plains region, the region was divided into eight zones (two of which were subdivided) called peak-flow trend zones. The relations between the attributions described in chapter A of this professional paper and annual peak-streamflow trends were investigated for streamgages in the Upper Plains region by using multiple quantitative and qualitative methods. The most common attributions for monotonic trends and change points in this region were long-term precipitation, groundwater withdrawals, and multidecadal climate variability, but large artificial impoundments, air temperature, groundwater and (or) surface-water withdrawals, and urban effects were additional relevant attributions. Attributions for some monotonic trends and change points could not be confidently made. The most common attribution that was associated with positive monotonic trends and (or) change points was long-term precipitation. The most common attributions associated with negative monotonic trends and (or) change points were groundwater withdrawals as well as groundwater and (or) surface-water withdrawals.

Introduction

The estimation of the frequency of floods is essential in many water-resources management applications, including critical infrastructure design and floodplain mapping. Given the many natural and anthropogenic factors that can affect flooding in the United States, it is important to understand the processes that contribute to changes in flood characteristics and the reliability of assumptions used by flood-frequency analysts. One of the fundamental assumptions is that the mean and variance of the series of annual peak streamflows is stationary through time (England and others, 2018), meaning that annual peak streamflows vary around a constant mean within a particular range of variance. Historical observations of changes to factors like climate, land cover, and agricultural and land-drainage practices (all of which are related to annual peak streamflow) suggest that assumptions of stationarity in flood magnitudes are likely not valid for many streams. Assuming stationarity where it does not apply could result in inaccuracies in the predictions of flood magnitudes used by planning and coordination agencies.

In 2016, the U.S. Geological Survey (USGS), in cooperation with the Federal Highway Administration of the U.S. Department of Transportation, began a national study to research methods for detecting and addressing potential nonstationarities (violations of the assumption of constant mean and variance, primarily indicated by monotonic trends and change points) in annual peak-streamflow records associated

[1]U.S. Geological Survey.

with changes in climate, land use, land cover, and other hypothesized drivers of hydrologic change. The objectives of the national study are as follows: (1) identify monotonic trends (gradual changes in which annual peak streamflow is increasing or decreasing over time, but the change is not necessarily linear; Helsel and others [2020]) and change points (abrupt temporal changes in the statistical distribution parameters of annual peak-streamflow data); (2) investigate and make attributions for hypothesized drivers of significant monotonic trends and change points where they are found; and (3) determine methods for modifying standard peak-streamflow frequency analyses to account for significant monotonic trends and change points. The work described in this professional paper addresses the second objective. Two time periods were selected for this study: a 50-year period (water years 1966–2015) and a 75-year period (water years 1941–2015).

For the national study, annual peak-streamflow records were analyzed for 2,683 USGS streamgages that were included in the Geospatial Attributes of Gages for Evaluating Streamflow, Version II (GAGES-II) database (Falcone, 2011). The GAGES-II database includes several hundred basin characteristics intended to facilitate hydrologic investigations but does not include streamgages associated with drainage basins that extend into Canada because of data limitations associated with some of the basin characteristic datasets. Subsequently, streamgages associated with drainage basins that extend into Canada were excluded from this analysis. More information on the streamgages and the annual peak-streamflow data used in the monotonic trend and change-point analysis are available in two data releases (Dudley and others, 2018; York and others, 2022).

Across the United States, annual peak-streamflow characteristics can be associated with or affected by different hydroclimatic, anthropogenic, and physiographic factors. Further, changes in annual peak streamflows might be associated with changes in the mechanisms that can affect the magnitude and timing of peak streamflows. To better understand these relations, it can be helpful to study them within regions of relatively similar hydroclimatic conditions (Saharia and others, 2017).

The focus of this chapter is the Upper Plains region, which is comprised of the United States part of the Missouri River and the Souris-Red-Rainy water-resources regions (regions 10 and 09, respectively) as defined by Seaber and others (1987). This region includes all of Nebraska and parts of Colorado, Iowa, Kansas, Minnesota, Missouri, Montana, North Dakota, South Dakota, and Wyoming (fig. C1). Of the 2,683 streamgages included in the national study, 269 of these were in the Upper Plains region.

The Upper Plains region experiences the continental climate extremes of winter storms, extreme heat and cold, severe thunderstorms, drought, and heavy rain-induced flooding (Shafer and others, 2014). Annual peak streamflows in much of the region are driven by spring snowmelt, which can combine with liquid precipitation to induce rain-on-snow flooding; however, much of the region, particularly west of the 100th meridian, is semi-arid and prone to severe droughts. Because of these large fluctuations in annual runoff, reservoirs have been constructed to store snowmelt runoff during wet years and provide water during dry periods.

Trends in annual peak streamflow and other annual streamflow characteristics have been identified and investigated in many previous studies of the hydrology of the Upper Plains region (McCabe and Wolock, 2002; Hirsch and Ryberg, 2012; Peterson and others, 2013; Norton and others, 2014; Sando and others, 2016). Several studies have also investigated the relations between changing climatic conditions and streamflow characteristics. Ryberg (2015) showed that the north-central United States—much of which is coincident with the Upper Plains region as defined in this chapter—is prone to climatic persistence that can cause spatially and temporally clustered large floods and serially correlated periods of low streamflow. Additionally, the region can shift, in an unpredictable manner, from comparatively wet conditions to comparatively dry conditions (Vecchia, 2008; Ryberg and others, 2014; Kolars and others, 2016). Such a shift from wet to dry has been well documented in North Dakota (Williams-Sether, 1999) and has been noted in Minnesota (Runkle and others, 2017). The effect of shifting climatic persistence has also been studied extensively in the region (Hansen and Miller, 1992; Vecchia, 2008; Ryberg and others, 2014; Ryberg, 2015; Kolars and others, 2016; Nustad and others, 2016; Ryberg and others, 2016). Southwestern North Dakota and contributing drainage areas in nearby States appear to be subject to a change toward less runoff in the precipitation-runoff relation starting sometime in the 1970s; this change has been attributed to increased air temperature and, to a lesser degree, surface-water withdrawals (Griffin and Friedman, 2017). Annual peak streamflow in southwestern North Dakota was also sensitive to a drought that lasted from the late 1980s to the early 1990s (Williams-Sether and others, 1994).

Previous investigators have also studied the effect of groundwater and surface-water withdrawals on annual peak-streamflow trends. In the southern part of the Upper Plains region, negative monotonic trends in annual peak streamflows have been shown to be likely associated with groundwater withdrawals and the construction of ponds and terraces (Mallakpour and Villarini, 2015). Similarly, another study showed that a declining water table was likely a contributing factor for negative monotonic trends on selected rivers in Kansas (Rasmussen and Perry, 2001).

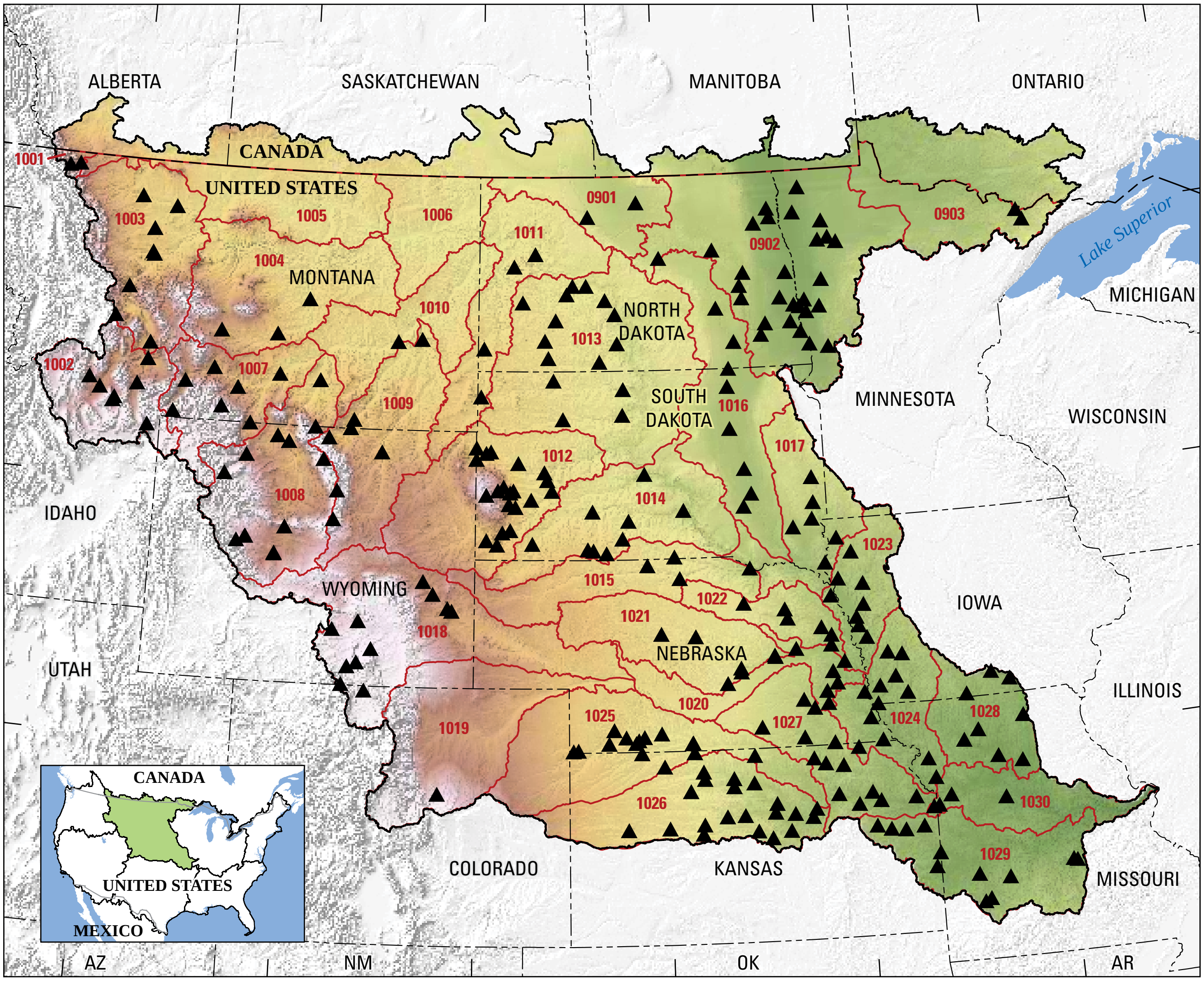

Base from U.S. Geological Survey and other digital data sources and Esri © 2020 and its licensors
North America elevation 1-kilometer-resolution GRID (USGS, 2007)
Regional boundaries derived from modified HUC2 watersheds
USA Contiguous Albers Equal Area Conic USGS projection
North American Datum of 1983

0 100 200 300 MILES
0 100 200 300 KILOMETERS

EXPLANATION

Elevation, in feet
1,891
1

Upper Plains region boundary

1019 **Subregion boundary and 4-digit hydrologic unit code**

GAGES-II selected streamgages —Falcone (2011)

Figure C1. Map of the Upper Plains region of the United States showing hydrologic unit codes as defined by Seaber and others (1987) and the locations of streamgages that were used in this study. Although the northern part of the Upper Plains region extends into Canada because of the topography of stream drainage basins, the watersheds considered for monotonic trend and change-point attributions are within the conterminous United States. For this study, the regions were based on watersheds identified by two-digit hydrologic unit codes (HUC2s) described by Seaber and others (1987) and were modified slightly by adding or subtracting subregions (HUC4s) to achieve geographic cohesiveness or hydrologic-setting similarity. Term: GAGES-II, Geospatial Attributes of Gages for Evaluating Streamflow, Version II (Falcone, 2011).

Purpose and Scope

The purpose of this study is to identify and make attributions for statistically significant monotonic trends and change points in annual peak-streamflow data at selected streamgages in the Upper Plains region of the United States for a 50-year period (water years 1966–2015) and a 75-year period (water years 1941–2015). The results are not intended to be an exhaustive explanation of the causes of all changes in annual peak-streamflow data. Instead, this study is intended to provide a general basis for understanding the major attributions for positive or negative monotonic trends and change points in annual peak streamflow at the selected streamgages to inform potential adjustments to flood-frequency analysis methods to account for nonstationarity. There are streamgages in the study area that have significant monotonic trends or change points in the peak-streamflow data, but an attribution could not be confidently made.

Methods

Methods used to detect monotonic trends and change points in annual peak-streamflow data as part of the first phase of the national study are summarized in chapter A of this professional paper and are described in more detail by Hodgkins and others (2019) and Ryberg and others (2020). Consequently, only methodological information relevant to the second phase (this study) is described in the sections below.

Annual peak-streamflow data from 2,683 streamgages in the conterminous United States were analyzed for (1) monotonic trends (Hodgkins and others, 2019) by using the Mann-Kendall trend test (Kendall, 1938; Mann, 1945) and (2) change points in the median annual peak streamflow (Ryberg and others, 2020) by using the Pettitt test (Pettitt, 1979). The streamgage selection is further summarized in chapter A of this professional paper.

Only the monotonic trend and change-point results for the periods of water years 1941–2015 and water years 1966–2015 that had *p*-values<0.10 were considered for attribution here, where the *p*-value is the attained significance level. The monotonic trends and change points with *p*-values<0.10 were considered statistically significant whereas the monotonic trends and change points with *p*-values≥0.10 were considered nonsignificant. All monotonic trends and change points discussed in this chapter are statistically significant unless otherwise specified.

Some streamgages with 50 years of record or more within the Upper Plains region were not included in the analysis because the national trend studies upon which this work is based only used data from streamgages that were in the GAGES-II database (Falcone, 2011). Because the GAGES-II database only includes streamgages with associated drainage basins that lie entirely within the United States, it is possible that the inclusion of additional streamgages whose drainage basins extend outside of the United States could influence the attributions that were made in this study.

Peak-Flow Trend Zone Delineation

The results of the analyses done by Hodgkins and others (2019) and Ryberg and others (2020) demonstrated both spatial and temporal patterns in monotonic trends and change points in annual peak-streamflow data recorded at streamgages across the Upper Plains region. The presence of spatial and temporal patterns might indicate important differences in the causal factors driving hydrologic nonstationarity in the region. Based on these patterns, the Upper Plains region was divided into subregions called peak-flow trend zones (PFTZs) to identify and describe the most common and most important attributions of monotonic trends and change points. The following steps were integrated together to define PFTZ boundaries.

As a first step to delineate PFTZ boundaries, spatial groups of streamgages were identified via cluster analysis using the Grouping Analysis tool in ArcGIS (Esri, 2017). The tool uses the Caliński-Harabasz variance ratio criterion (*VRC*; Caliński and Harabasz, 1974), which uses the ratio of between-group dispersion to within-group dispersion to identify the optimal number of groups. The *VRC* is calculated for the number of groups (k; 2 to 15 for this study) using the following equation:

$$VRC = \frac{BGSS}{k-1} / \frac{WGSS}{n-k} \tag{C1}$$

where

- $BGSS$ is the between-group sum of squares,
- $WGSS$ is the within-group sum of squares,
- k is the number of groups (2 to 15), and
- n is the number of streamgages.

The optimal number of groups is identified as the k value that maximizes the *VRC*. To ensure spatial representation of the geometric mean of the basin areas represented by peak-streamflow trend values used in the cluster analysis, basin centroids were used for the location of each streamgage. The variable used to calculate the *BGSS* and *WGSS* was the 50-year monotonic trend percentage change, which was selected because it allowed for inclusion of the greatest number of streamgages in the analysis.

The PFTZ boundaries were delineated to be consistent with the drainage basin boundaries for streamgages included in the GAGES-II dataset. This was done to avoid introducing false assumptions about areas of the Upper Plains region that are ungaged, and thus potentially not well represented in the annual peak-streamflow dataset. For example, a large part of northeastern Montana did not have any streamgages that met the requirements for inclusion in the analysis (fig. C2) and was therefore not included. Rather than extend the surrounding PFTZ boundaries to incorporate the ungaged part of northeastern Montana, the boundaries were constrained to the area associated with drainage basins for streamgages that were included in the analysis.

The general PFTZ boundaries and results from 50- and 75-year monotonic trend and change-point attribution analyses are shown in figure C2. These boundaries indicate the general area; because it was sometimes difficult to delineate distinct boundaries for different PFTZs, there are some PFTZs that overlap slightly with, or contain small pockets of, other PFTZs. The scale and complexity of the maps in figure C2 do not support showing these pockets. Readers that want more detail on the sites in specific PFTZs and sub-PFTZs should consult the associated data release (York and others, 2022).

Initially, the number of groups with the highest *VRC* value was 15; however, in some cases, clusters of streamgages were merged because of similar statistical characteristics of trends, proximity, and similar magnitudes. For example, if two clusters had positive monotonic trends (indicative of general increases in annual peak-streamflow magnitudes) and were located near each other, they would likely be merged into a single PFTZ. After this step, eight PFTZs remained (fig. C2). Streamflow data for streamgages within a given PFTZ are assumed to be statistically similar and spatially grouped, allowing for an organization scheme to better describe the patterns in attributions in the Upper Plains region.

Following the identification and delineation of the PFTZs using the 50-year monotonic trend analysis results with the cluster analysis, two PFTZs (1 and 2) were further subdivided into sub-PFTZs, which are denoted by the addition of an “A,” “B,” or “C” to the PFTZ number. It was deemed necessary to further segregate clusters of streamgages in PFTZs 1 and 2 because, while all streamgages within each of these PFTZs showed the same general patterns (positive or negative) in the monotonic trends and (or) change points, each had differences that are important to describe. Specifically, in the case of PFTZ 1, different attributions for monotonic trends and change points warranted distinguishing sub-PFTZs. In the case of PFTZ 2, differences in the magnitudes of the monotonic trends and change points and the spatial clustering of the streamgages warranted distinguishing sub-PFTZs.

Attribution Methodology

Attributions for monotonic trends and change points in annual peak-streamflow data for streamgages in the Upper Plains region were made using a multiple working hypotheses (MWHs) framework. The method involves listing of all physically reasonable hypotheses that may explain an observed phenomenon of interest prior to analysis to avoid inadvertently favoring a false theoretical explanation (Chamberlin, 1890, 1897; Railsback, 2004). Further explanation of the MWHs approach and a list of attributions used in the MWHs framework are presented in chapter A of this professional paper.

Hypothesized attributions important to the Upper Plains region, as defined in table A1 (Barth and others, this volume, chap. A), included climatic factors (long-term precipitation, air temperature, and multidecadal climate variability), large artificial impoundments, urban effects, groundwater withdrawals, and groundwater and (or) surface-water withdrawals. The multidecadal climate variability attribution is defined here as a combination of long-term precipitation and air temperature and was used when the two were not clearly separable. The groundwater and (or) surface-water withdrawals attribution is defined here as a combination of groundwater withdrawals and surface-water withdrawals and was used when the two were not clearly separable.

When appropriate and possible, primary and secondary hypothesized attributions were made for statistically significant monotonic trends and change points in annual peak-streamflow data for the 50- and 75-year periods. Levels of evidence were also designated for each attribution. The levels of evidence used for this study were termed “robust evidence,” “medium evidence,” “limited evidence,” and “additional information required.” Table A2 provides descriptions of each level of evidence (Barth and others, this volume, chap. A).

Many previous studies have investigated nonstationarity (in the form of monotonic trends and [or] change points) in annual peak-streamflow data and other streamflow characteristics in the Upper Plains region. Based on these studies, common causal factors were identified as potential attributions for significant monotonic trends and (or) change points for this study of the Upper Plains region. These causal factors include multidecadal climate variability, long-term variability in precipitation (Williams-Sether, 1999; Ryberg and others, 2016; Runkle and others, 2017), air temperature (Williams-Sether and others, 1994; Griffin and Friedman, 2017), large artificial impoundments (Costigan and Daniels, 2012), groundwater withdrawals (Bureau of Reclamation, 2012), and surface-water withdrawals (Bureau of Reclamation, 2012; Griffin and Friedman, 2017). While other factors might affect annual peak streamflow at a given streamgage in the Upper Plains region, it was outside the scope of this work to conduct an exhaustive investigation of each one.

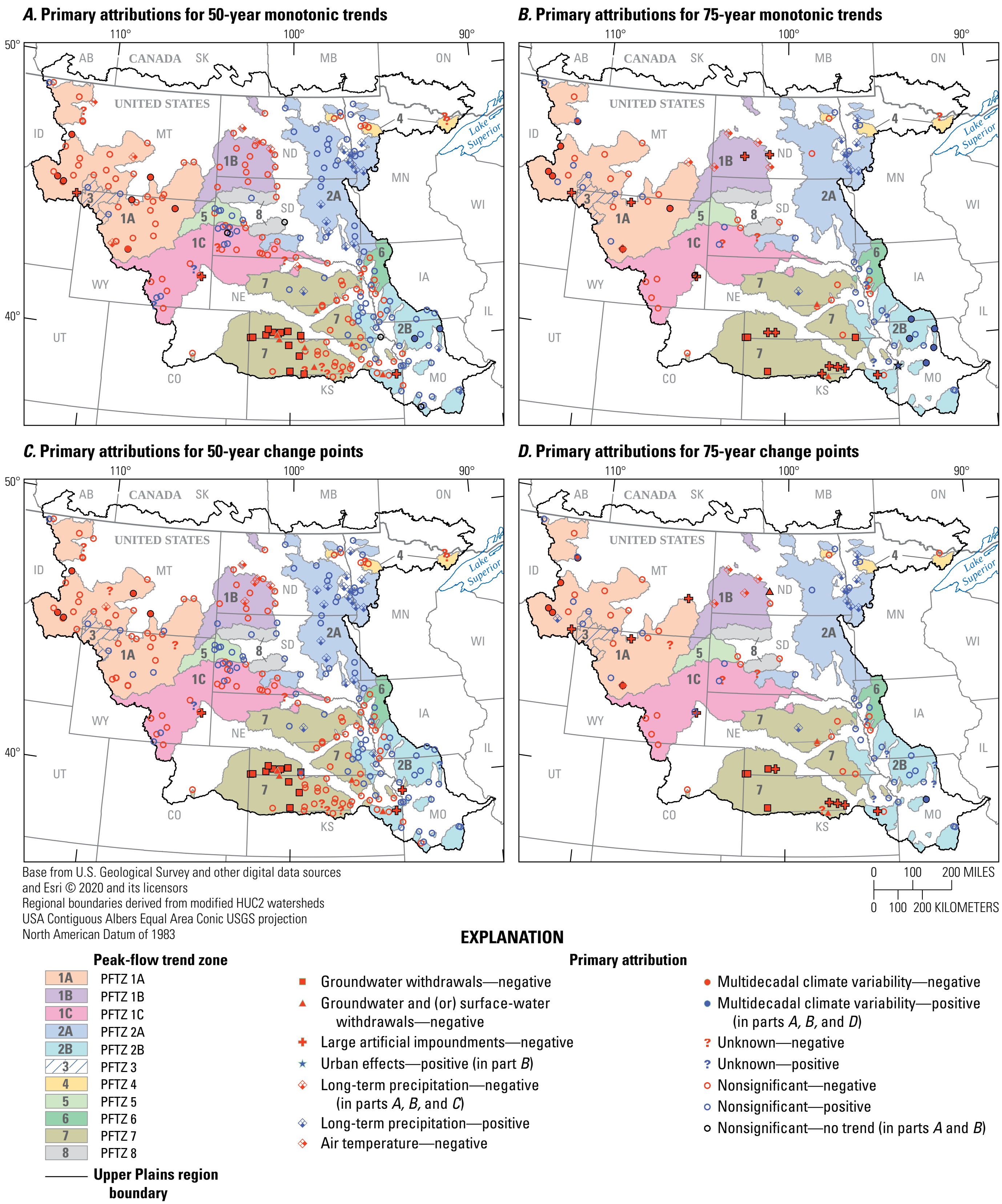
A. Primary attributions for 50-year monotonic trends
B. Primary attributions for 75-year monotonic trends
C. Primary attributions for 50-year change points
D. Primary attributions for 75-year change points
110°
100°
90°
50°
40°
AB
CANADA
SK
MB
ON
UNITED STATES
ID
MT
ND
MN
WI
SD
WY
NE
IA
IL
UT
CO
KS
MO
Lake Superior
1A
1B
1C
2A
2B
3
4
5
6
7
8
Base from U.S. Geological Survey and other digital data sources
and Esri © 2020 and its licensors
Regional boundaries derived from modified HUC2 watersheds
USA Contiguous Albers Equal Area Conic USGS projection
North American Datum of 1983
0 100 200 MILES
0 100 200 KILOMETERS
EXPLANATION
Peak-flow trend zone
PFTZ 1A
PFTZ 1B
PFTZ 1C
PFTZ 2A
PFTZ 2B
PFTZ 3
PFTZ 4
PFTZ 5
PFTZ 6
PFTZ 7
PFTZ 8
Upper Plains region boundary
Primary attribution
Groundwater withdrawals—negative
Groundwater and (or) surface-water withdrawals—negative
Large artificial impoundments—negative
Urban effects—positive (in part B)
Long-term precipitation—negative (in parts A, B, and C)
Long-term precipitation—positive
Air temperature—negative
Multidecadal climate variability—negative
Multidecadal climate variability—positive (in parts A, B, and D)
Unknown—negative
Unknown—positive
Nonsignificant—negative
Nonsignificant—positive
Nonsignificant—no trend (in parts A and B)

Multidecadal Climate Variability, Long-Term Precipitation, and Air Temperature

Multiple steps were used to gather evidence for attributing climatic factors relevant to the Upper Plains region. These steps included (1) comparing non-normalized and rank-normalized annual peak-streamflow data to annual characteristics of precipitation (PRISM Climate Group, 2019) and air temperature (for example, fig. C3; Livneh and others, 2015; Chase and others, 2022; York and others, 2022) and (2) analyzing double-mass plots of rainfall-runoff relations (for example, fig. C4).

Rank-normalized and non-normalized annual peak streamflows at each streamgage were compared with corresponding annual precipitation and air temperature characteristics in the drainage basin upstream from the streamgage. For this study, rank normalization consisted of ranking each annual peak streamflow for a streamgage and dividing each ranked annual peak streamflow by the total number of years of record for that streamgage. Scatterplot smooth functions (fig. C3) of rank-normalized annual peak streamflows, rank-normalized annual total precipitation, and rank-normalized annual mean maximum air temperature were analyzed for abrupt and synchronous changes in slope to identify potential associations. Similarly, double-mass plots of cumulative annual runoff and precipitation (fig. C4) were analyzed for changes in slope that could indicate changes in rainfall runoff mass balance.

Monthly precipitation data (PRISM Climate Group, 2019) were used to calculate annual precipitation variables from water years 1941 to 2015, including the annual total, two seasonal totals (winter [from November to March] and spring/early summer [from April to July]), and a two-year moving total. Monthly minimum and maximum air temperature data (Livneh and others, 2015) were used to calculate annual monthly minimum and maximum air temperature variables that were averaged to derive values for the drainage basins upstream from each streamgage. Annual air temperature variables included annual mean monthly minimum and maximum, mean monthly minimum and maximum for November–March, and mean monthly minimum and maximum for April–July.

Correlation and trend analyses were used to investigate the effects of each annual precipitation and air temperature variable on annual peak streamflow at streamgages where significant 50- and 75-year monotonic trends were detected. For all statistical analyses, only climate data for years with corresponding annual peak-streamflow data were used. Relations between climate variables and annual peak streamflow observed at each streamgage were quantified using simple correlation analysis and significance testing (Pearson's *r*; Helsel and others, 2020). The quantities were calculated using the "cor" and "cor.test" base functions in R (R Core Team, 2018). The Mann-Kendall trend test (Pohlert, 2018) was used to identify temporal trends in climate variable data for periods overlapping with significant monotonic trends in annual peak streamflows. Finally, partial Mann-Kendall trend tests (Libiseller and Grimvall, 2002) were used to test for significant monotonic trends in annual peak streamflow while accounting for each climatic variable. The Mann-Kendall and partial Mann-Kendal trend tests were done using the "trend" package (Pohlert, 2018) in R.

For significant 50- and 75-year change points, comparisons were made for precipitation, runoff relations, and air temperature variables between the 20-year periods before and after the indicated change point at each streamgage. The intent of these comparisons was to identify potential associations between the presence of significant change points and corresponding changes in precipitation, runoff relations, and air temperature for the same time periods.

To distinguish between different climatic attributions for monotonic trends and change points observed in peak streamflow data at streamgages, it is important to define variables that represent unique climatic characteristics. Multidecadal climate variability was attributed when evidence of association between monotonic trends or change points in annual peak-streamflow data and both air temperature and long-term precipitation was present and made sense hydrologically with the sign (positive or negative) of the monotonic trend or change point. For example, a positive 50-year monotonic trend in annual peak-streamflow data for a streamgage that also had a positive monotonic trend in 50-year annual precipitation data and a negative monotonic trend in 50-year annual air temperature data would likely have been primarily attributed to multidecadal climate variability. However, when annual peak-streamflow data at a streamgage showed evidence of an association between monotonic trends or change points and either precipitation or air temperature, only the associated variable was primarily attributed.

Figure C2 (facing page). Maps of the Upper Plains region showing the peak-flow trend zone (PFTZ) boundaries and the primary attributions for statistically significant and nonsignificant monotonic trends and change points in annual peak-streamflow data for streamgages in the 50- and 75-year study periods: *A*, Primary attributions for monotonic trends for water years 1966–2015; *B*, Primary attributions for monotonic trends for water years 1941–2015; *C*, Primary attributions for change points for water years 1966–2015; and *D*, Primary attributions for change points for water years 1941–2015. Positive, negative, and no trend (neither positive nor negative) indicate the sign of the monotonic trend or change point for the associated attribution. The boundaries for the PFTZs indicate the general areas for each, but the scale and complexity of the map do not support showing small pockets of some PFTZs that might overlap with other PFTZs.

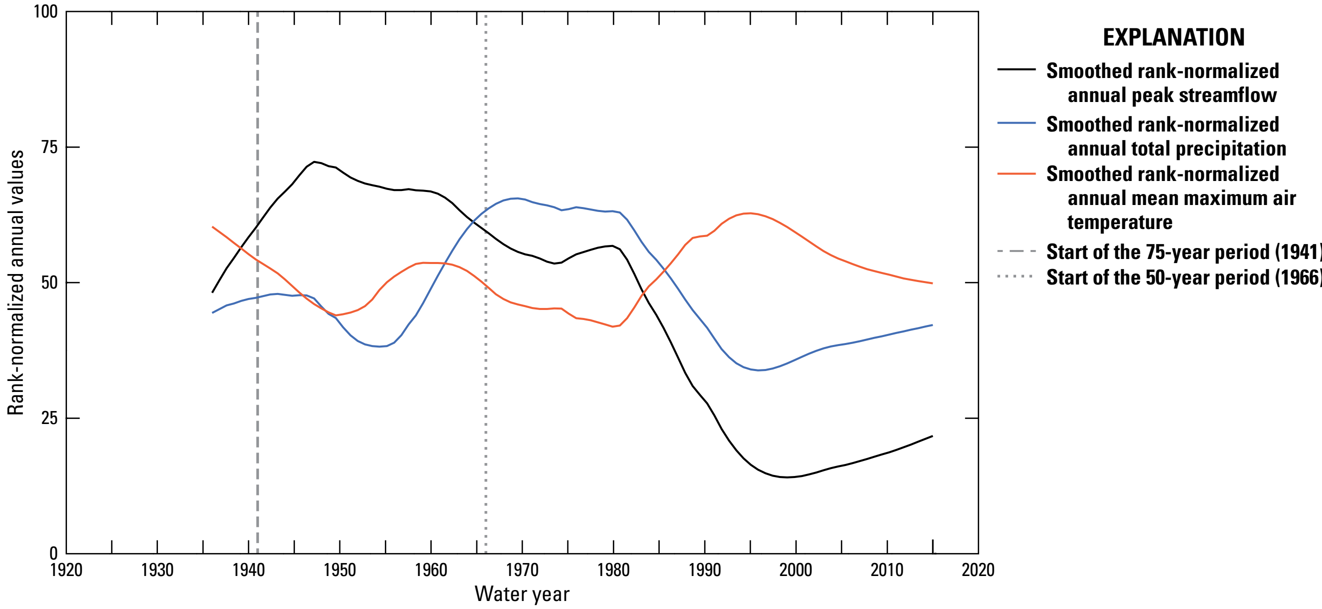

Figure C3. Example plot of smoothed rank-normalized annual peak-streamflow data, rank-normalized annual total precipitation data, and rank-normalized annual mean maximum air temperature data for the drainage basin that is monitored by U.S. Geological Survey streamgage 06018500 on Beaverhead River near Twin Bridges, Montana. Rank-normalized data were smoothed using the locally weighted scatterplot smoothing (LOWESS) procedure (Cleveland and McGill, 1984; Cleveland, 1985; Helsel and others, 2020). Rank-normalized values are based on basin averages. Although attributions were made for the periods of 1966–2015 and 1941–2015, data prior to 1941 were also included in this plot.

Large Artificial Impoundments

Quantitative and qualitative methods were used for the primary or secondary attribution of monotonic trends and change points in annual peak streamflow to large artificial impoundments. These methods included (1) analyzing hydrologic overview plots (for example, fig. C5) for indications of changes in daily hydrologic frequency characteristics before and after change points and (or) the development of large artificial impoundments; (2) consideration of annual peak-streamflow qualification codes and streamgage description files (U.S. Geological Survey, 2018) to identify annual peak streamflows that were potentially affected by regulation; and (3) quantification of the number of dams and total storage in the drainage basin using available data (for example, fig. C6). Streamgage description files were obtained from the National Water Information System (NWIS; U.S. Geological Survey, 2018) database and were used to identify streamgages that had large artificial impoundments upstream from the streamgage. In some cases, these descriptions also included the construction date of the impoundment. The GAGES-II database (Falcone, 2011) was also used to identify streamgages where the corresponding drainage basins were recorded as having streamflows affected by the addition or removal of a dam. Locations of dams and associated storage capacities were obtained from the National Inventory of Dams (NID; U.S. Army Corps of Engineers, 2018). For some dams, additional information on regulation was available and was used to supplement the NID data (for example, U.S. Army Corps of Engineers, 1993).

Withdrawals

To investigate whether monotonic trends or change points in annual peak streamflow data at streamgages in the Upper Plains region should be attributed to a category of withdrawals, agricultural depletions (for example, fig. C7; Bureau of Reclamation, 2012) were considered along with changes in groundwater levels in the High Plains aquifer (McGuire, 2017a, b), which underlies part of the study area. Monotonic trends or change points were primarily attributed to groundwater withdrawals if they were positively correlated with changes in groundwater levels and negatively correlated with groundwater depletions.

If the changes in groundwater levels were either not correlated with monotonic trends and (or) change points or were not available for a streamgage's drainage basin but changes in groundwater depletions were negatively correlated with monotonic trends and (or) change points, groundwater and (or) surface-water withdrawals were primarily attributed with limited evidence. Large artificial impoundments were assumed to not affect annual peak streamflows observed at streamgages where the groundwater and (or) surface-water withdrawals attribution was made.

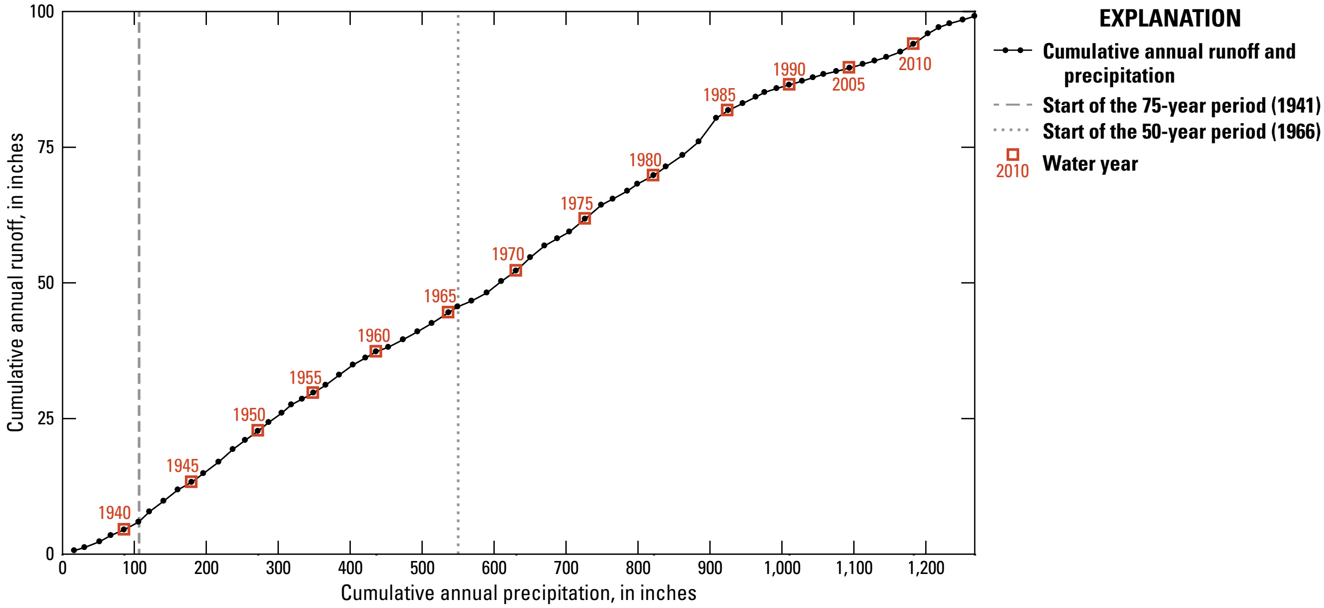

Figure C4. Example of a double-mass plot of cumulative annual runoff and precipitation for the drainage basin that is monitored by U.S. Geological Survey streamgage 06018500 on Beaverhead River near Twin Bridges, Montana. The time period for the data shown in this example plot is 1935–2015; however, no data were available for 1992–2001. Although attributions were made for the periods of 1966–2015 and 1941–2015, data prior to 1941 were also included in this plot. For more information on the double-mass plot method, see Kohler (1949).

Unknown Causes

In some cases, despite the analyses described above, an attribution could not be made for some significant monotonic trends and change points in annual peak-streamflow data; these were attributed to unknown causes. These monotonic trends and change points could be statistical anomalies rather than evidence of changes in physical process (Ryberg and others, 2020). In addition, the monotonic trends and change points could be the result of a complex combination or temporal accumulation of multiple different factors, including those considered here or other factors that were not included in our stated hypotheses. Chapter A of this professional paper has additional discussion of the “unknown causes” attribution.

Results

The following results include a general summary of the attributional analysis for the Upper Plains region as well as a summary of the attribution results for each of the PFTZs. The primary and secondary attributions for each monotonic trend and change point are provided in a USGS data release (York and others, 2022) associated with this professional paper. All attributions referred to in this chapter are primary attributions unless otherwise noted.

General Results

In the Upper Plains region, 269 streamgages were suitable for 50-year monotonic trend and change-point analyses and 109 streamgages were suitable for 75-year monotonic trend and change-point analyses in the peak-streamflow records (tables C1, C2; tables C1–C13 follow the References Cited). Of the 269 streamgages suitable for 50-year analyses, 68 streamgages had significant monotonic trends (48 negative and 20 positive) and 61 streamgages had significant change points (40 negative and 21 positive) in annual peak-streamflow data. Of the 109 streamgages suitable for 75-year analyses, 52 streamgages had significant monotonic trends (34 negative and 18 positive) and 46 had significant change points (30 negative and 16 positive) in annual peak-streamflow data.

The results of monotonic trend and change-point analyses showed spatial and temporal patterns in the PFTZs. Broadly, PFTZs in the western half of the study area commonly had negative monotonic trends in annual peak-streamflow data while PFTZs in the eastern half of the study area commonly had positive monotonic trends (fig. C2). Exceptions to this generalization include an area around the Black Hills of South Dakota (PFTZ 5) as well as eastern parts of Kansas and Nebraska in the south-central part of the study area (PFTZ 7).

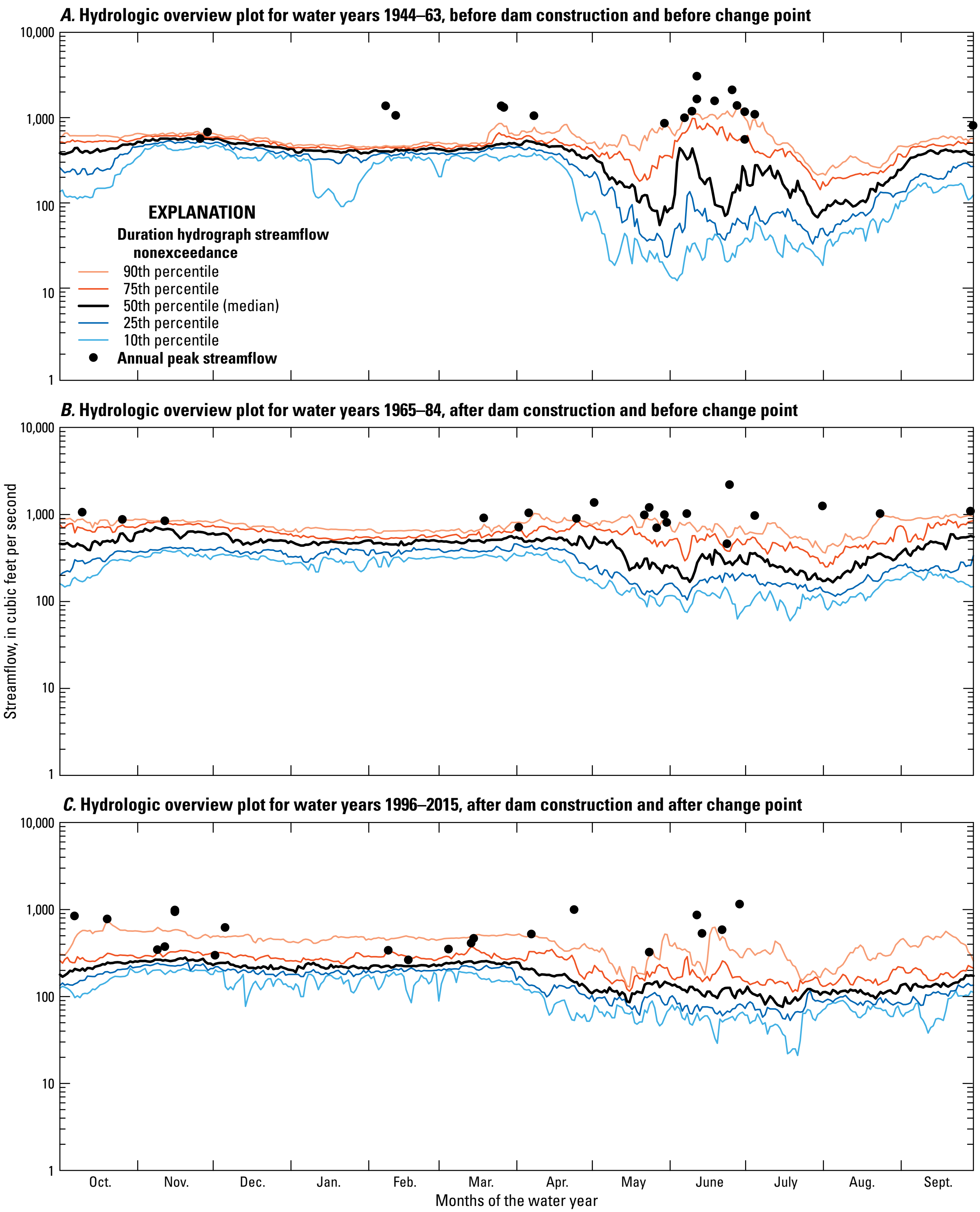
A. Hydrologic overview plot for water years 1944–63, before dam construction and before change point
EXPLANATION
Duration hydrograph streamflow nonexceedance
90th percentile
75th percentile
50th percentile (median)
25th percentile
10th percentile
Annual peak streamflow
B. Hydrologic overview plot for water years 1965–84, after dam construction and before change point
C. Hydrologic overview plot for water years 1996–2015, after dam construction and after change point
Streamflow, in cubic feet per second
10,000
1,000
100
10
1
Oct.
Nov.
Dec.
Jan.
Feb.
Mar.
Apr.
May
June
July
Aug.
Sept.
Months of the water year

Temporal patterns in change-point years varied among PFTZs. For example, results from change-point analyses for annual peak-streamflow data in sub-PFTZ 2A showed a consistent significant change point associated with a positive change for most streamgages around 1991 (fig. C8). Conversely, in PFTZ 7, the years identified as change points in annual peak streamflows, while consistently negative, appear to be gradual over time (fig. C8). Boundaries for PFTZs 3, 4, 5, 6, and 8 and sub-PFTZ 2B were generally poorly defined because the spatial and statistical characteristics associated with data at streamgages in these PFTZs lacked clear patterns. Boundaries for PFTZ 7 and sub-PFTZs 1A, 1B, 1C, and 2A were generally well defined.

Eight primary attributions were identified as causally associated with significant monotonic trends and (or) change points in data from streamgages in the Upper Plains region (fig. C9; tables C3 through C13). The most common attribution associated with positive monotonic trends and (or) change points was long-term precipitation. The most common attributions associated with negative monotonic trends and (or) change points were groundwater withdrawals as well as groundwater and (or) surface-water withdrawals.

Results for Each Peak-Flow Trend Zone

Peak-Flow Trend Zone 1

As described in the "Peak-Flow Trend Zone Delineation" section, streamgages within PFTZ 1 showed the same general patterns in the monotonic trends and (or) change points. Most significant monotonic trends and change points in annual peak-streamflow data recorded at streamgages in PFTZ 1 were negative. The most common attributions for significant monotonic trends and change points were air temperature, long-term precipitation, and multidecadal climate variability. Three sub-PFTZs were distinguished within PFTZ 1 because the attributions of monotonic trends and change points varied across the area.

Sub-Peak-Flow Trend Zone 1A

Sub-peak-flow trend zone 1A is located in Montana and Wyoming (fig. C2) and mainly consists of a mountain and plains setting. In sub-PFTZ 1A, there are 42 streamgages with significant and nonsignificant monotonic trends and change points (tables C1, C2). All significant monotonic trends and change points are negative (fig. C2; Dudley and others, 2018). Most streamgages with significant monotonic trends in annual peak-streamflow data have predominantly negative monotonic trends in annual precipitation and positive monotonic trends in annual air temperature (Chase and others, 2022). The similarity of monotonic trends (in terms of sign and magnitude) across sub-PFTZ 1A suggests that causal factors that influenced those monotonic trends may also be causal factors for monotonic trends on the scale of the entire Upper Plains region.

Regional characteristics of precipitation and air temperature might contribute to negative monotonic trends in sub-PFTZ 1A. A small number of streamgages had nonsignificant change points identified around 1999, which might indicate that a general change in annual peak-streamflow characteristics happened around this time in this area; however, many other streamgages with significant change points had change-point years from 1976 to 1984 (table C2; fig. C8).

In sub-PFTZ 1A, multidecadal climate variability was the most common attribution for monotonic trends in annual peak-streamflow data (table C3; fig. C9). For the 9 streamgages with significant negative 75-year monotonic trends in sub-PFTZ 1A, 6 were attributed to multidecadal climate variability, 1 was attributed to long-term precipitation, 1 was attributed to air temperature, and 1 was attributed to a large artificial impoundment. For the 11 significant negative 50-year monotonic trends in sub-PFTZ 1A, 7 were attributed to multidecadal climate variability, 1 was attributed to long-term precipitation, 2 were attributed to air temperature, and 1 was attributed to unknown causes. For the 10 significant negative 75-year change points, 5 were attributed to multidecadal climate variability, 1 was attributed to long-term precipitation, and 1 was attributed to air temperature. The attributions for the three remaining significant 75-year change points were large artificial impoundments and unknown causes. For the 9 significant negative 50-year change-points, 5 were attributed to multidecadal climate variability, 1 was attributed to long-term precipitation, and 3 were attributed to unknown causes.

Figure C5 (facing page). Examples of hydrologic overview plots of data from U.S. Geological Survey (USGS) streamgage 06018500 on Beaverhead River near Twin Bridges, Montana, for specific time periods: *A*, Water years 1944–63, a 20-year period before the construction of Clark Canyon Dam and before the change-point year; *B*, Water years 1965–84, a 20-year period after the construction of Clark Canyon Dam and before the change-point year; and, *C*, Water years 1996–2015, a 20-year period after the construction of Clark Canyon Dam and after the change-point year. Clark Canyon Dam was completed in 1964 and the 50-year and 75-year change point for USGS streamgage 06018500 was in water year 1985. Duration hydrograph streamflow nonexceedance values were calculated using daily streamflow data obtained from the U.S. Geological Survey National Water Information System (NWIS; U.S. Geological Survey, 2018). Duration hydrograph streamflow nonexceedance values represent, for each day, the streamflow values associated with the n^{th} percentile for all daily streamflows recorded on that day of the year. All annual peak streamflows are presented and plotted at the calendar day of occurrence. In these examples, there was no peak-streamflow value available for 1945 (for part *A*) and two peak-streamflow values (for part *C*) occurred on the same day, November 16.

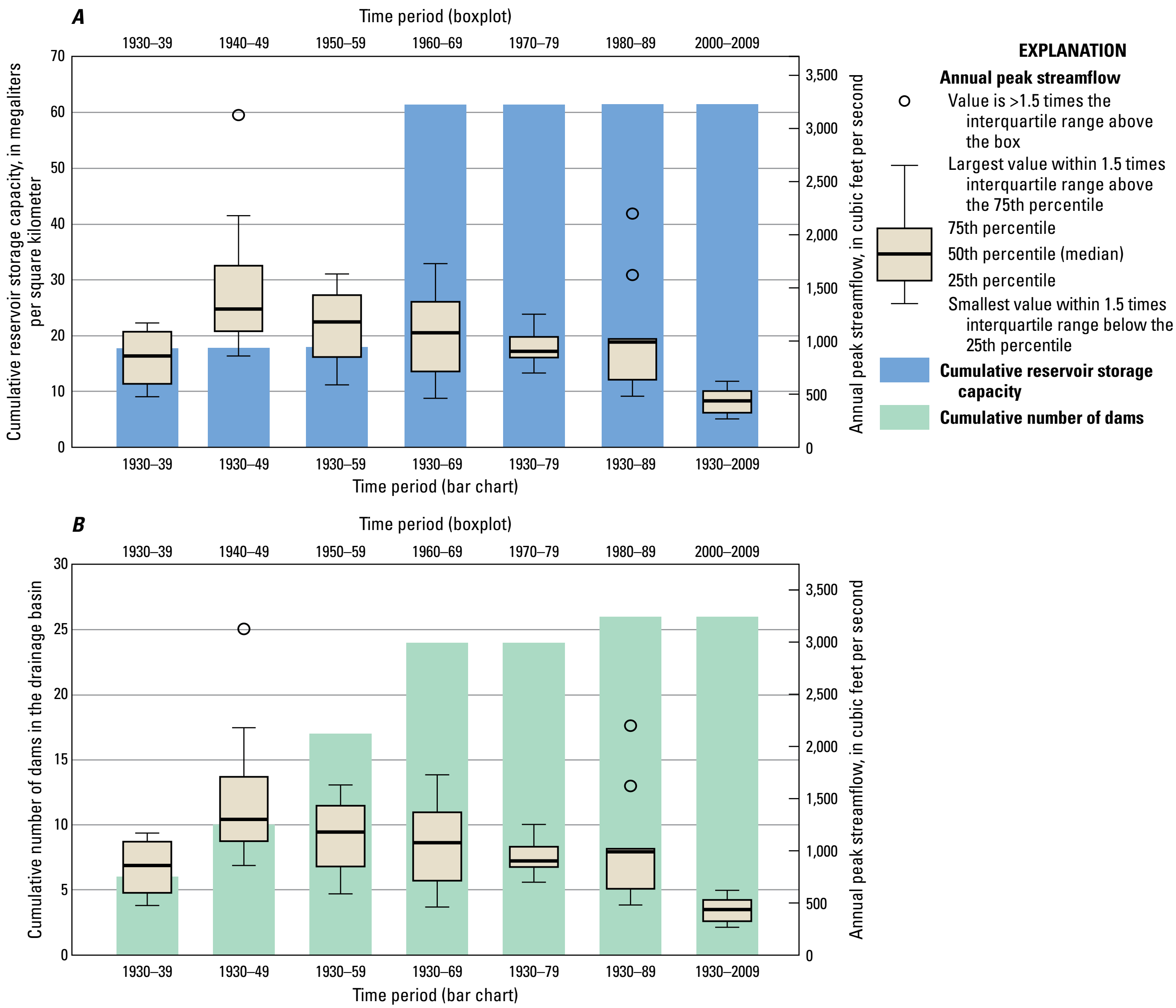

Figure C6. Examples of graphs showing statistics of annual peak-streamflow data for decadal periods as well as (*A*) cumulative reservoir storage capacity and (*B*) the cumulative number of dams in the drainage basin that is monitored by U.S. Geological Survey streamgage 06018500 on Beaverhead River near Twin Bridges, Montana. Bar plots of cumulative reservoir storage capacity and the cumulative number of dams correspond to time periods on the bottom axes; boxplots of annual peak streamflow correspond to time periods on the top axes. The time period for storage capacity and number of dams is from 1930 to 2009. No data on reservoir storage capacity or the number of dams were available from 1990 to 1999. The construction of some dams did not notably contribute to reservoir storage capacity.

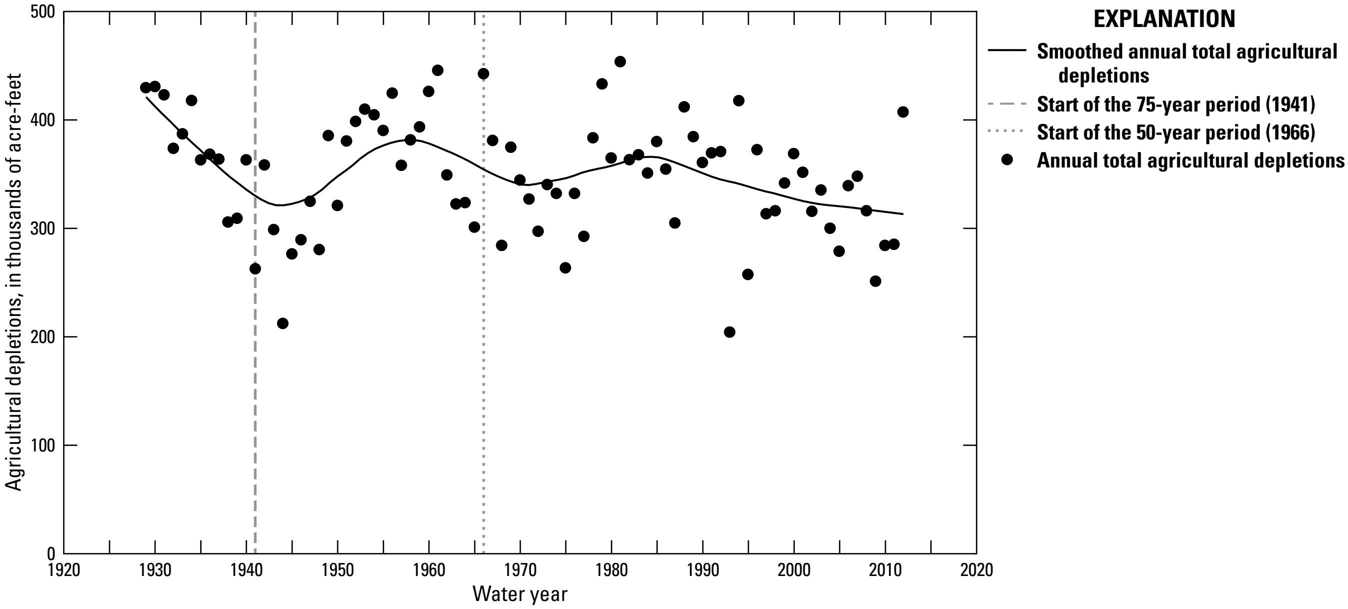

Figure C7. Example scatterplot and smoothed line of annual total agricultural depletions for the drainage basin that is monitored by U.S. Geological Survey streamgage 06018500 on Beaverhead River near Twin Bridges, Montana. The smoothed trend line was created using the locally weighted scatterplot smoothing (LOWESS) procedure (Cleveland and McGill, 1984; Cleveland, 1985; Helsel and others, 2020). Although attributions were made for the periods of 1966–2015 and 1941–2015, data prior to 1941 were also included in this plot. Annual agricultural depletions data were sourced from the Bureau of Reclamation (2012).

Sub-Peak-Flow Trend Zone 1B

Sub-peak-flow trend zone 1B is located in North Dakota and South Dakota (fig. C2) and mainly consists of a plains setting. In sub-PFTZ 1B, there are 18 streamgages with significant and nonsignificant monotonic trends and change points (tables C1, C2). Most streamgages in the area have negative monotonic trends and the median change-point year is more recent (1987; fig. C2; Dudley and others, 2018). Most of the streamgages with significant monotonic trends or change points had nonsignificant positive monotonic trends in annual precipitation and significant positive monotonic trends in annual air temperature. Like sub-PFTZ 1A, most streamgages in sub-PFTZ 1B had change points from 1972 to 1987 (table C2; fig. C8). Most of the change points occurred in the 1970s for the 75-year period and in the 1980s for the 50-year period.

The most common attribution for significant monotonic trends and change points in sub-PFTZ 1B was air temperature (table C4; fig. C9). Some of the streamgages in this area are in the USGS Hydro-Climatic Data Network 2009 (HCDN-2009), which only includes streamgages that monitor drainage basins with minimal human alterations that are suitable for analyzing hydrologic nonstationarity caused by climatic changes (Lins, 2012). The inclusion of some of the streamgages in the HCDN-2009 provides additional support that the regional change-point pattern may be caused by climatic changes.

Air temperature as an attribution for monotonic trends and change points in sub-PFTZ 1B is also supported by other studies. In the Little Missouri River Basin (within sub-PFTZ 1B), Griffin and Friedman (2017) found an increased winter and summer atmospheric evaporative demand in 1976–2012 when compared to 1939–1975. Because atmospheric evaporative demand is a metric used to assess the amount of water that is potentially transferred from the land surface to the atmosphere, it is likely that increases in winter and summer atmospheric evaporative demand contributed to decreased runoff. Griffin and Friedman (2017) determined that air temperature was the dominant cause of reduced runoff from rainfall. Griffin and Friedman (2017) also determined that surface-water withdrawals had a noticeable effect on the hydrology in the area, although they only accounted for less than 12 percent of the reduction in average annual streamflow volume. Griffin and Friedman (2017) found no evidence of substantial streamflow reduction caused by groundwater pumping. These results generally agree with the attributions for sub-PFTZ 1B. While data from the depletions database (Bureau of Reclamation, 2012) does show an increase in depletions, only one change point (for the 75-year period) was attributed to groundwater and (or) surface-water withdrawals in sub-PFTZ 1B (table C4; fig. C9).

For the three streamgages with significant change points identified for the 50-year period that were attributed to long-term precipitation in sub-PFTZ 1B, a drought is the most likely reason. The mean year of change point for these three streamgages is 1987 (table C4), which coincides with a severe drought that North Dakota experienced from 1988 to 1992.

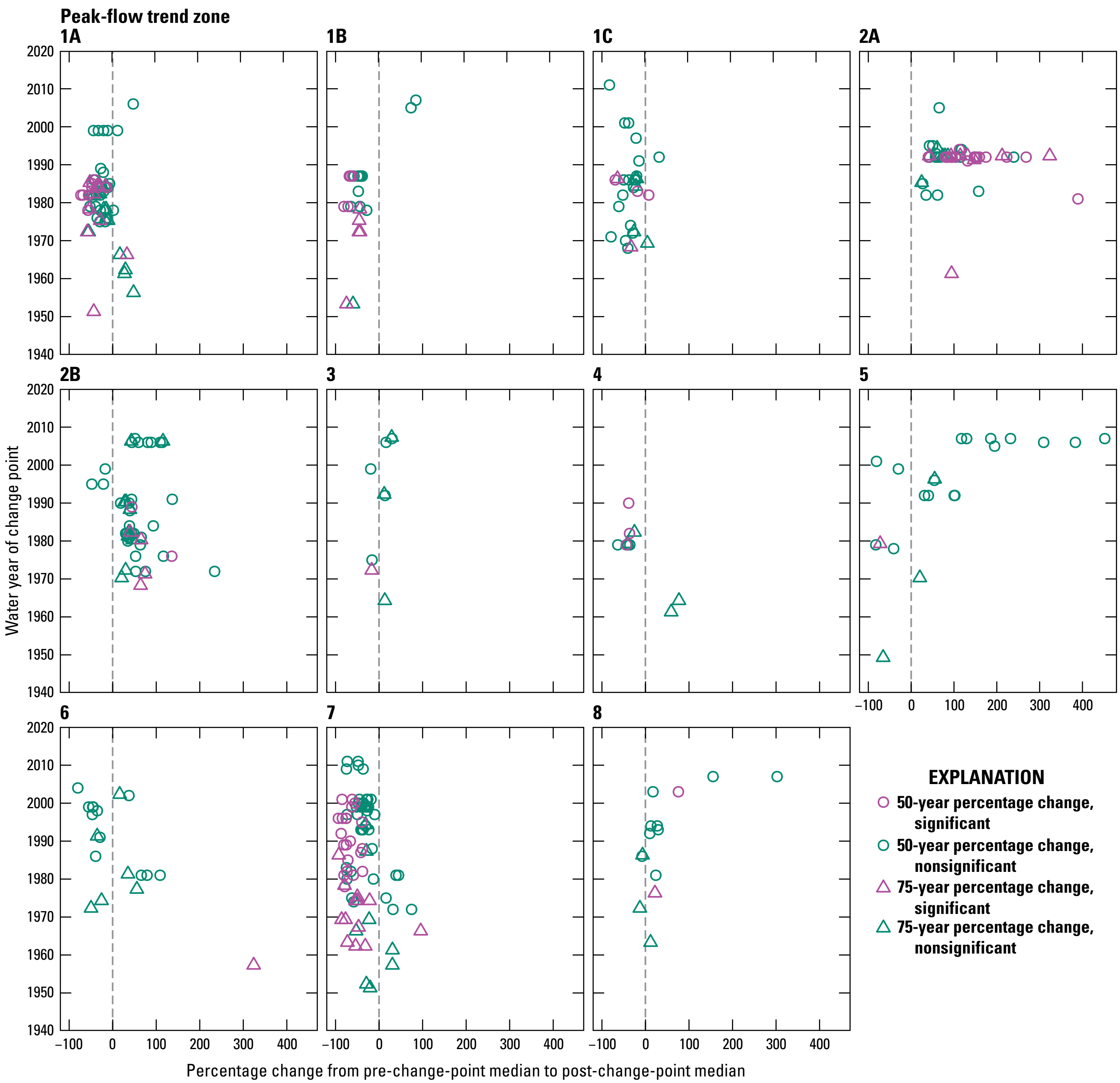

Figure C8. Scatterplots showing the water year and the percentage change from pre- to post-change-point median annual peak streamflow for significant and nonsignificant 50- and 75-year change points at streamgages in each peak-flow trend zone. The Pettitt test (Pettitt, 1979) was used to determine if a change point was significant (*p*-value<0.10) or nonsignificant (*p*-value≥0.10), where the *p*-value is the attained significance level.

Figure 2 of Williams-Sether and others (1994) shows the departure from normal monthly precipitation during the period of 1988–1992 for each climatic division in North Dakota and shows a dramatic decline in precipitation starting in 1987 in some areas.

Finally, two significant 75-year monotonic trends were attributed to large artificial impoundments (table C4; fig. C9). Causal factors in sub-PFTZ 1B are more varied than in sub-PFTZ 1A and sub-PFTZ 1B did not have a single attribution that clearly accounted for most of the significant monotonic trends and change points. Unlike sub-PFTZ 1A, no trends in sub-PFTZ 1B were attributed to multidecadal climate variability.

Sub-Peak-Flow Trend Zone 1C

Sub-peak-flow trend zone 1C is located in Colorado, Nebraska, South Dakota, and Wyoming (fig. C2) and mainly consists of a mountains and plains setting. In sub-PFTZ 1C, there are 22 streamgages with significant and nonsignificant monotonic trends and change points in annual peak-streamflow data (tables C1, C2). Most streamgages in sub-PFTZ 1C have negative monotonic trends and change points in peak-streamflow data. Also, four streamgages with significant monotonic trends have predominantly positive monotonic trends in precipitation and annual air temperature. There are some streamgages in sub-PFTZ 1C (within drainage basins associated with the Black Hills in west-central South Dakota) that have nonsignificant positive monotonic trends. Temporally, most of the change points in sub-PFTZ 1C occurred from 1970 to 1990 (table C2; fig. C8).

Most significant monotonic trends and change points in annual peak streamflow in sub-PFTZ 1C were attributed to unknown causes (table C5; fig. C9). The attributions for the two significant negative 75-year monotonic trends were large artificial impoundments and unknown causes. For the 5 significant negative 50-year monotonic trends, 1 was attributed to air temperature, 1 was attributed to a large artificial impoundment, and 3 were attributed to unknown causes. The attributions for the two significant negative 75-year change points were large artificial impoundments and unknown causes. The attributions for the three significant negative 50-year change points were large artificial impoundments and unknown causes.

Temporal and spatial patterns of monotonic trends and change points in sub-PFTZ 1C are less clearly defined, so making attributions was more difficult for this sub-PFTZ when compared to others with more distinct patterns. Because of this, defining a clear, representative boundary for sub-PFTZ 1C was difficult.

Peak-Flow Trend Zone 2

As described in the "Peak-Flow Trend Zone Delineation" section, streamgages within PFTZ 2 showed the same general patterns in the signs of monotonic trends and (or) timing of change points; however, the patterns notably differed in ways that are important to describe. Specifically, differences in the magnitudes of the monotonic trends and change points as well as the spatial clustering of the streamgages warranted distinguishing sub-PFTZs. Most monotonic trends and change points in annual peak-streamflow data recorded at streamgages in PFTZ 2 were positive. The most common attributions for monotonic trends and change points were long-term precipitation and multidecadal climate variability.

Sub-Peak-Flow Trend Zone 2A

Sub-peak-flow trend zone 2A is located in Minnesota, North Dakota, and South Dakota (fig. C2) and mainly consists of a glaciated prairie setting. In sub-PFTZ 2A, there are 39 streamgages with significant and nonsignificant monotonic trends and change points (tables C1, C2), most of which are positive. A substantial number of streamgages with significant monotonic trends and change points have predominantly positive monotonic trends in annual precipitation and variable (positive and negative) monotonic trends in annual air temperature.

Annual peak streamflow in sub-PFTZ 2A has been shown to be increasing in the last 30 years in national studies (Hirsch and Ryberg, 2012; Peterson and others, 2013). This area has been extensively studied because of large, costly floods on Devils Lake, the Red River of the North, and the Souris River (for example, Vecchia, 2008; Ryberg and others, 2014; Kolars and others, 2016; Nustad and others, 2016; Ryberg and others, 2016). Because of the supporting studies and the monotonic trends in precipitation that were identified in this chapter, increasing long-term precipitation was attributed to nearly all significant monotonic trends and change points in sub-PFTZ 2A (table C6; fig. C9). Change-point years in sub-PFTZ 2A in both study periods are clustered around 1992 and have remarkably little variation around that year (table C2; fig. C8). The 1992 change point for this zone is also consistent with the findings of Williams-Sether (1999), who documented a sudden switch from drought to wet conditions in North Dakota around 1992–1993.

Sub-Peak-Flow Trend Zone 2B

Sub-peak-flow trend zone 2B is located in Iowa, Kansas, Missouri, and Nebraska (fig. C2). In sub-PFTZ 2B, there are 32 streamgages with significant and nonsignificant monotonic trends and change points (tables C1, C2). The streamgages in sub-PFTZ 2B have predominantly positive monotonic trends in annual peak-streamflow data (table C1); also, a moderate number of streamgages with significant monotonic trends and change points have predominantly positive monotonic trends in annual precipitation and negative monotonic trends in annual air temperature. The general consistency in monotonic trend and change-point characteristics in this relatively large zone suggests that the factors affecting peak streamflow may also have regional patterns. Regional characteristics of precipitation and air temperature might contribute to the

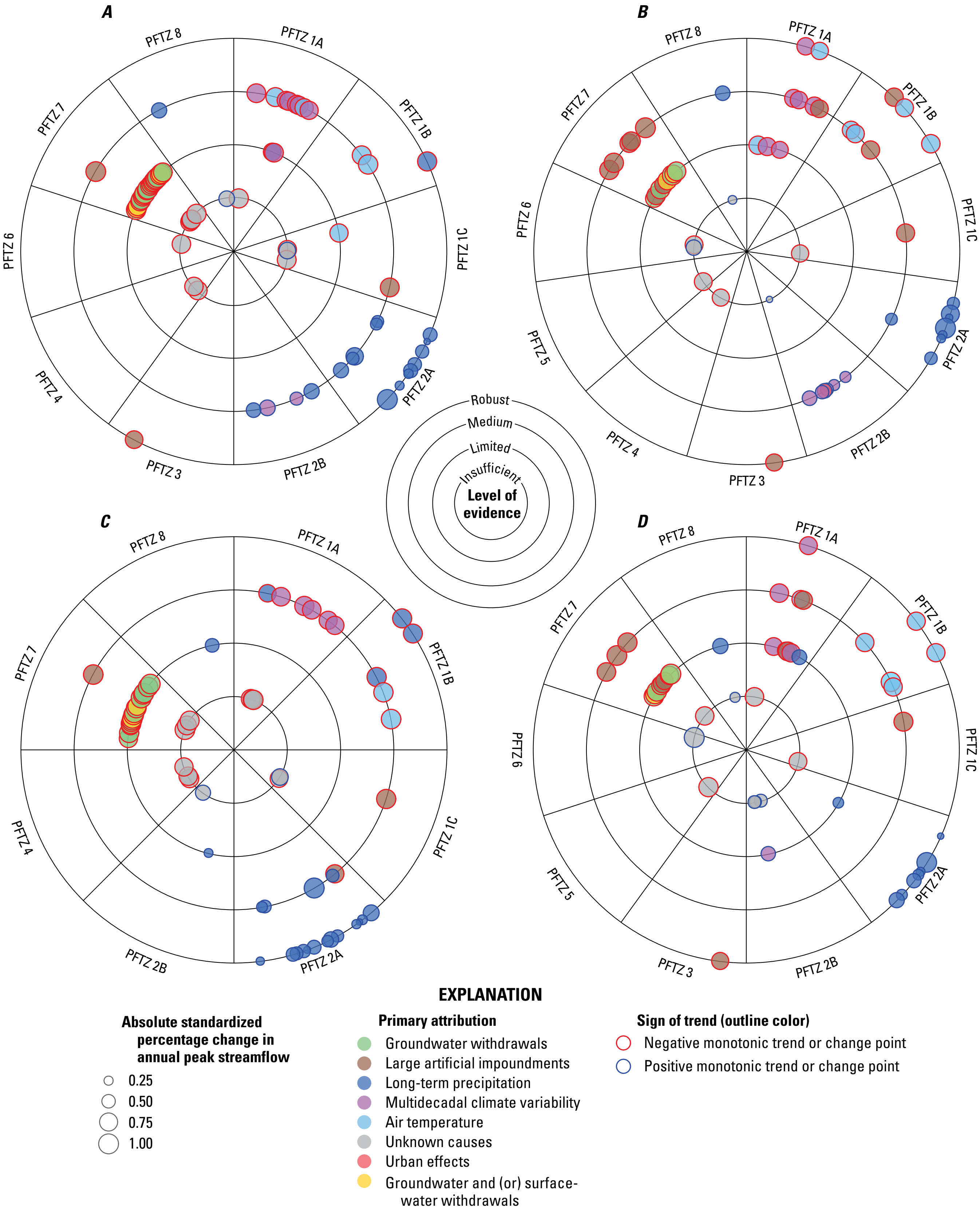
A
B
C
D
PFTZ 8
PFTZ 1A
PFTZ 1B
PFTZ 1C
PFTZ 2A
PFTZ 2B
PFTZ 3
PFTZ 4
PFTZ 5
PFTZ 6
PFTZ 7
Robust
Medium
Limited
Insufficient
Level of evidence
EXPLANATION
Absolute standardized percentage change in annual peak streamflow
0.25
0.50
0.75
1.00
Primary attribution
Groundwater withdrawals
Large artificial impoundments
Long-term precipitation
Multidecadal climate variability
Air temperature
Unknown causes
Urban effects
Groundwater and (or) surface-water withdrawals
Sign of trend (outline color)
Negative monotonic trend or change point
Positive monotonic trend or change point

positive monotonic trends and change points in sub-PFTZ 2B. There is a cluster of nine streamgages in sub-PFTZ 2B that have nonsignificant change points in annual peak-streamflow data around 2006; however, most streamgages have significant change points from 1974 to 1989 (table C2; fig. C8), which suggests a different attribution for change points as compared to sub-PFTZ 2A.

The most common attributions for significant monotonic trends and change points in sub-PFTZ 2B were long-term precipitation and multidecadal climate variability (table C7; fig. C9). For the 7 significant positive 75-year monotonic trends, 5 were attributed to multidecadal climate variability, 1 was attributed to urban effects, and 1 was attributed to unknown causes. For the 4 significant positive 50-year monotonic trends, 2 were attributed to multidecadal climate variability, and the other 2 were attributed to long-term precipitation.

For the 4 significant positive 75-year change points, 1 was attributed to long-term precipitation and 3 were attributed to unknown causes. For the 2 significant positive 50-year change points, 1 was attributed to long-term precipitation and 1 was attributed to unknown causes.

Peak-Flow Trend Zone 3

Peak-flow trend zone 3 is located in Idaho, Montana, and Wyoming (fig. C2) and mainly consists of mountainous high-altitude areas in Yellowstone National Park and downstream areas. In PFTZ 3, there are four streamgages with significant and nonsignificant monotonic trends and change points in annual peak-streamflow data (tables C1, C2) in Montana. The streamgages in PFTZ 3 have predominantly nonsignificant positive monotonic trends and change points in peak-streamflow data. There was only one significant monotonic trend, which we attributed to a large artificial impoundment (table C8; fig. C9).

Data from streamgages that were included in PFTZ 3 represent annual peak-streamflow conditions that were somewhat anomalous compared with data from streamgages in the surrounding PFTZs. Although surrounding PFTZs generally have negative monotonic trends in annual peak-streamflow data, PFTZ 3 generally has positive monotonic trends. Because all streamgages in this PFTZ record streamflow from drainage within or near Yellowstone National Park, we suspect that the unique interactions between groundwater and surface water in and around Yellowstone National Park contribute to these locally different monotonic trends.

Figure C9 (facing page). Charts showing primary attributions, levels of evidence for each attribution, the sign of trend (positive or negative), and the absolute standardized percentage change in annual peak-streamflow data for streamgages in each peak-flow trend zone (PFTZ) for the 50- and 75-year monotonic trends and change points: *A*, Monotonic trends for 1966–2015; *B*, Monotonic trends for 1941–2015; *C*, Change points for 1966–2015; and D, Change points for 1941–2015. Concentric circles represent levels of evidence for each attribution. Points positioned on the innermost concentric circle (labeled “Insufficient”) are those for which additional information is required to make an attribution (other than “unknown causes”). A wedge for a PFTZ is only shown if attributions were made in that zone. The absolute standardized percentage change in annual peak-streamflow values were generated by scaling all negative trend percentages from zero to negative one, converting them to positive (zero to one for visualization), and combining the values with scaled (zero to one) positive trend percentages. See tables C3 through C13 for the attribution data included in these charts.

Peak-Flow Trend Zone 4

Peak-flow trend zone 4 is located in North Dakota and Minnesota (fig. C2) and mainly consists of glaciated prairies and forest settings. In PFTZ 4, there are seven streamgages with significant and nonsignificant monotonic trends and change points (tables C1, C2). The streamgages in PFTZ 4 have predominantly negative monotonic trends in annual peak-streamflow data. There are 2 streamgages with significant negative monotonic trends for the 50-year period, 1 with a significant negative monotonic trend for the 75-year period, 3 with significant change points for the 50-year period, and 0 with significant change points for the 75-year period (table C9; fig. C9). The streamgages with significant monotonic trends and change points in annual peak-streamflow data have predominantly negative monotonic trends in annual precipitation and variable (positive and negative) monotonic trends in annual air temperature.

Dorigo and others (2012) also identified a slight negative monotonic trend in soil moisture in the far northeastern corner of the Upper Plains region, which potentially affects two streamgages (USGS streamgages 05127500 and 05124480) that are included in PFTZ 4. The evidence, however, is not strong enough to make an attribution for negative monotonic trends or change points in data from these or other streamgages in PFTZ 4. Thus, the attribution for all significant monotonic trends and change points in PFTZ 4 was unknown causes (table C9; fig. C9).

Peak-Flow Trend Zone 5

Peak-flow trend zone 5 is located in and near the Black Hills of South Dakota (fig. C2), which consists of a plains setting. In PFTZ 5, there are 17 significant and nonsignificant monotonic trends and change points (tables C1, C2). The streamgages in PFTZ 5 have predominantly nonsignificant monotonic trends and change points in annual peak-streamflow data that are both positive and negative; there is only one streamgage with a significant monotonic trend or change point, which is associated with the 75-year period. The large variability in the results and the near absence of significant peak-streamflow trends complicates the definition of temporal patterns in annual peak streamflow in PFTZ 5. The attribution for the only significant trend in PFTZ 5 was unknown causes (table C10; fig. C9).

A defining characteristic of PFTZ 5 is that it does not conform to the general patterns of attributions for monotonic trends and change points in the PFTZs to the west. It is possible that the Black Hills serve as a climatic buffer (due to their high altitude) and reduce the potential for negative monotonic trends and change points in annual peak streamflows for streams connected to them. However, this hypothesis requires further research to be adequately tested.

Peak-Flow Trend Zone 6

Peak-flow trend zone 6 is located in Iowa and Nebraska (fig. C2) and mainly consists of an agricultural plains setting. In this PFTZ, there are 12 streamgages with significant and nonsignificant monotonic trends and change points in annual peak-streamflow data, only 4 of which are significant (tables C1, C2). There is 1 streamgage with a significant negative monotonic trend for the 50-year period, and 2 streamgages with significant negative monotonic trends for the 75-year period. There are 0 streamgages with significant change points for the 50-year period, and 1 streamgage with a significant change point for the 75-year period.

Most streamgages in PFTZ 6 have predominantly negative monotonic trends and change points (tables C1, C2). Some streamgages that have positive monotonic trends and (or) change points are close in proximity to streamgages with negative monotonic trends and (or) change points, which highlights the hydrologic complexity of PFTZ 6. Additionally, PFTZ 6 is located between sub-PFTZ 2A and sub-PFTZ 2B, both of which have predominantly positive monotonic trends and change points in their respective peak-streamflow data. Inconsistencies in monotonic trends and change points between PFTZ 6 and the adjacent sub-PFTZs complicate the attributions in PFTZ 6. The attribution for all significant monotonic trends and change points in PFTZ 6 was unknown causes (table C11; fig. C9).

Peak-Flow Trend Zone 7

Peak-flow trend zone 7 is located in Colorado, Kansas, and Nebraska (fig. C2) and mainly consists of plains and rolling hills. Precipitation generally decreases from east to west in PFTZ 7, and groundwater withdrawals for irrigation are common and have been reported to decrease the magnitude and frequency of annual peak streamflows (Rasmussen and Perry, 2001; Painter and others, 2017). Water table levels in the High Plains aquifer underlying most of PFTZ 7 have generally declined over the past 65 years (McGuire, 2017a, b). Negative monotonic trends in annual peak streamflow have been attributed to groundwater withdrawals in other studies of the area (Zeng and Cai, 2014; Mallakpour and Villarini, 2015).

In PFTZ 7, there are 57 significant and nonsignificant monotonic trends and change points (tables C1, C2). In PFTZ 7, all monotonic trends in annual peak-streamflow data were negative. There are 26 streamgages with significant negative monotonic trends for the 50-year period, and 13 streamgages with significant negative monotonic trends for the 75-year period. There are 20 streamgages with significant change points for the 50-year period, and 12 streamgages with significant change points for the 75-year period. A substantial number of streamgages with significant monotonic trends in peak-streamflow data have predominantly positive monotonic trends in annual precipitation and variable (positive and negative) trends in annual air temperature; these trends indicate that declines in precipitation and (or) increases in air temperature are unlikely causes of peak streamflow declines. Thus, the most common attributions for significant monotonic trends and change points in PFTZ 7 were groundwater withdrawals as well as groundwater and (or) surface-water withdrawals (table C12; fig. C9).

There is a wide range of significant change-point years in PFTZ 7. This considerable variability in change-point years (fig. C8) combined with the consistent patterns of negative monotonic trends in PFTZ 7 suggests a regional spatial pattern in the attribution of nonstationarity. Additionally, the lack of temporal clustering in the change-point years suggests that the factors affecting change points in PFTZ 7 have been influencing streamflow over much of the study period.

Peak-Flow Trend Zone 8

Peak-flow trend zone 8 is mainly located in South Dakota (fig. C2) and consists of various types of landscape settings. In PFTZ 8, there are 19 streamgages with significant and nonsignificant monotonic trends and change points (tables C1, C2). Two streamgages had significant positive monotonic trends for the 50-year and 75-year periods. One streamgage had a significant change point for the 50-year period, and two streamgages had significant change points for the 75-year period. The data for streamgages in PFTZ 8 did not generally adhere to the statistical or spatial patterns of the other PFTZs and sub-PFTZs. Thus, the defining characteristic of streamgages included in PFTZ 8 is that there is large uncertainty regarding any underlying attribution for the monotonic trends and change points.

The streamgages in PFTZ 8 have predominantly nonsignificant variable monotonic trends and change points in annual peak-streamflow data, but there are some with significant monotonic trends and change points. The streamgages in PFTZ 8 commonly have monotonic trends and change points that are inconsistent with nearby streamgages in better defined PFTZs, such as 1B, 1C, and 2A (fig. C2). The considerable variability in the years associated with change points and the near absence of significant monotonic trends and change points complicates the definition of temporal patterns in peak streamflows in PFTZ 8. Consequently, the monotonic trends and change points in PFTZ 8 were attributed to long-term precipitation or unknown causes (table C13; fig. C9).

Summary

The U.S. Geological Survey (USGS) investigated and attributed potential causes of monotonic trends and change points in annual peak-streamflow data from USGS streamgages in the conterminous United States. Only monotonic trends and change points for the periods of 1966–2015 (a 50-year period) and 1941–2015 (a 75-year period) that had *p*-values<0.10 were considered for attribution, where the *p*-value is the attained significance level. Because of complexities specific to hydroclimatic regions across the United States, multiple study areas with distinct hydroclimatic conditions were delineated. This chapter summarizes the methods and results of analyses for the Upper Plains region.

In the Upper Plains region, 269 streamgages were suitable for 50-year monotonic trend and change-point analyses and 109 streamgages were suitable for 75-year monotonic trend and change-point analyses in the peak-streamflow records. For the 50-year period, 68 streamgages were found to have significant monotonic trends (48 negative and 20 positive) and 61 streamgages were found to have significant change points (40 negative and 21 positive) in annual peak-streamflow data. For the 75-year period, 52 streamgages were found to have significant monotonic trends (34 negative and 18 positive) and 46 were found to have significant change points (30 negative and 16 positive).

The Upper Plains region was divided into regions termed peak-flow trend zones (PFTZs) which broadly represent the heterogeneity in hydroclimatic conditions as well as in the potential physical and hydrologic drivers of monotonic trends and change points across the region. Peak-flow trend zones were delineated using a cluster analysis of the 50-year monotonic trend percentage change. A total of eight PFTZs were defined in the Upper Plains region. Two PFTZs (1 and 2) were further subdivided into sub-PFTZs because of important distinctions within these zones.

Spatial and temporal patterns were present in the monotonic trends and change points of the Upper Plains region. Streamgages in the western half of the study area more commonly had negative monotonic trends and change points in annual peak-streamflow data, while streamgages in the eastern half of the study area more commonly had positive monotonic trends and change points. Some notable exceptions to this pattern included an area around the Black Hills of South Dakota (in PFTZ 5) and parts of Kansas and Nebraska in the south-central part of the study area (in PFTZ 7). Temporally, patterns in change points varied among PFTZs. For example, results from change-point analyses at most streamgages in sub-PFTZ 2A showed a consistent increase in annual peak streamflows around 1991. Conversely, in PFTZ 7, the years identified as change points in peak flows, while consistently negative, appear to be gradual over time.

Within each PFTZ, evidence for various attributions of monotonic trends and change points was collected using multiple quantitative and qualitative methods. When appropriate and possible, primary and secondary attributions were made for monotonic trends and change points in each time period. Attributions that were made in the Upper Plains region included climatic factors (multidecadal climate variability, long-term precipitation, and air temperature), large artificial impoundments, urban effects, groundwater withdrawals, groundwater and (or) surface-water withdrawals, and unknown causes. A level of evidence was designated for each attribution; these levels were defined as “robust evidence,” “medium evidence,” “limited evidence,” or “additional information required” (see chapter A for further descriptions of the levels of evidence).

Streamgages with significant nonstationarity in PFTZ 1, including sub-PFTZs 1A, 1B, and 1C, have predominantly negative monotonic trends and change points. The most common attributions in these sub-PFTZs were long-term precipitation, air temperature, and multidecadal climate variability.

Streamgages with significant nonstationarity in PFTZ 2, including sub-PFTZs 2A and 2B, have predominantly positive monotonic trends and change points. The most common attributions in these sub-PFTZs were long-term precipitation and multidecadal climate variability.

Peak-flow trend zone 3 is a small, poorly defined area in the western part of the Upper Plains region. All monotonic trends and change points in this PFTZ were at one streamgage and were all attributed to a large artificial impoundment.

Peak-flow trend zone 4 is a small, poorly defined area in the northeastern part of the Upper Plains region. All significant monotonic trends and change points in PFTZ 4 were attributed to unknown causes.

Peak-flow trend zone 5 is a small area in the central part of the Upper Plains region. A defining characteristic of PFTZ 5 is that it does not conform to the general patterns of attributions for significant monotonic trends and change points in PFTZs that border it to the west.

Peak-flow trend zone 6 is a small area in the southeast part of the Upper Plains region. All significant monotonic trends and change points in PFTZ 6 were attributed to unknown causes.

Peak-flow trend zone 7 is a moderately large area in the south-central part of the Upper Plains region. The most common attributions for significant monotonic trends and change points in PFTZ 7 were groundwater withdrawals, groundwater and (or) surface-water withdrawals, and large artificial impoundments.

Peak-flow trend zone 8 is a poorly defined area interspersed throughout the Upper Plains region in various types of settings. Peak-streamflow trend characteristics for streamgages in this PFTZ were inconsistent with those at nearby streamgages and there was large uncertainty in assigning a PFTZ. All significant monotonic trends and change points in PFTZ 8 were attributed to long-term precipitation or unknown causes.

References Cited

Bureau of Reclamation, 2012, Missouri River Basin depletions database—Great Plains region: Bureau of Reclamation, [97] p., accessed June 2019 at https://www.usbr.gov/gp/dkao/naws/FSEIS/missouri_river_basin_depletions_database.pdf.

Caliński, T., and Harabasz, J., 1974, A dendrite method for cluster analysis: Communications in Statistics, v. 3, no. 1, p. 1–27.

Chamberlin, T.C., 1890, The method of multiple working hypotheses: Science, v. 15, p. 92–96.

Chamberlin, T.C., 1897, The method of multiple working hypotheses: Journal of Geology, v. 5, p. 837–848.

Chase, K.J., Sando, S.K., Sando, R., Ryberg, K.R., and York, B.C., 2022, Upper Plains region ancillary supporting attribution data, *in* York, B.C., Ryberg, K.R., Asquith, W.H., Chase, K.J., Dickinson, J.E., Dudley, R.W., Harden, T.M., Hodgkins, G.A., Holtschlag, D.J., Humberson, D.G., Konrad, C.P., Levin, S.B., Restivo, D.E., Sando, R., Sando, S.K., Swain, E.D., Tillery, A.C., and Totten, A.R., Attributions for nonstationary peak streamflow records across the conterminous United States, 1941–2015 and 1966–2015: U.S. Geological Survey data release, https://doi.org/10.5066/P9FOUVWG. [Data directly accessible at https://www.sciencebase.gov/catalog/item/5d8a312ee4b0c4f70d0ae563.]

Cleveland, W.S., 1985, The elements of graphing data: Monterey, Calif., Wadsworth Publishing Company, 323 p.

Cleveland, W.S., and McGill, R., 1984, The many faces of a scatterplot: Journal of the American Statistical Association, v. 79, no. 388, p. 807–822.

Costigan, K.H., and Daniels, M.D., 2012, Damming the prairie—Human alteration of Great Plains river regimes: Journal of Hydrology, v. 444–445, p. 90–99, accessed February 8, 2021, at https://doi.org/10.1016/j.jhydrol.2012.04.008.

Dorigo, W., de Jeu, R., Chung, D., Parinussa, R., Liu, Y., Wagner, W., and Fernández-Prieto, D., 2012, Evaluating global trends (1988–2010) in harmonized multi-satellite surface soil moisture: Geophysical Research Letters, v. 39, no. 18, article L18405, 7 p., accessed October 2019 at https://doi.org/10.1029/2012GL052988.

Dudley, R.W., Archfield, S.A., Hodgkins, G.A., Renard, B., and Ryberg, K.R., 2018, Peak-streamflow trends and change-points and basin characteristics for 2,683 U.S. Geological Survey streamgages in the conterminous U.S. (ver. 3.0, April 2019): U.S. Geological Survey data release, accessed June 6, 2019, at https://doi.org/10.5066/P9AEGXY0.

England, J.F., Jr., Cohn, T.A., Faber, B.A., Stedinger, J.R., Thomas, W.O., Jr., Veilleux, A.G., Kiang, J.E., and Mason, R.R., Jr., 2018, Guidelines for determining flood flow frequency—Bulletin 17C (ver. 1.1, May 2019): U.S. Geological Survey Techniques and Methods, book 4, chap. B5, 148 p., accessed June 20, 2019, at https://doi.org/10.3133/tm4B5.

Esri, 2017, ArcGIS Desktop, release 10.5.1: Redlands, Calif., Environmental Systems Research Institute.

Falcone, J., 2011, GAGES-II—Geospatial attributes of gages for evaluating streamflow: U.S. Geological Survey dataset, accessed November 2018 at http://pubs.er.usgs.gov/publication/70046617.

Griffin, E.R., and Friedman, J.M., 2017, Decreased runoff response to precipitation, Little Missouri River Basin, northern Great Plains, USA: JAWRA, Journal of the American Water Resources Association, v. 53, no. 3, p. 576–592, accessed August 2020 at https://doi.org/10.1111/1752-1688.12517.

Hansen, D.S., and Miller, W.A., 1992, Climatological and hydrological factors affecting the Lake Thompson Chain of Lakes in Eastern South Dakota, *in* Subitzky, S., ed., Selected papers in the hydrologic sciences 1988–92: U.S. Geological Survey Water-Supply Paper 2340, p. 21–38, accessed August 2020 at http://pubs.usgs.gov/wsp/wsp2340/.

Helsel, D.R., Hirsch, R.M., Ryberg, K.R., Archfield, S.A., and Gilroy, E.J., 2020, Statistical methods in water resources: U.S. Geological Survey Techniques and Methods, book 4, chap. A3, 458 p., accessed December 2020 at https://doi.org/10.3133/tm4a3. [Supersedes USGS Techniques of Water-Resources Investigations, book 4, chap. A3, version 1.1.]

Hirsch, R.M., and Ryberg, K.R., 2012, Has the magnitude of floods across the USA changed with global CO_2 levels?: Hydrological Sciences Journal, v. 57, no. 1, p. 1–9.

Hodgkins, G.A., Dudley, R.W., Archfield, S.A., and Renard, B., 2019, Effects of climate, regulation, and urbanization on historical flood trends in the United States: Journal of Hydrology, v. 573, p. 697–709.

Kendall, M.G., 1938, A new measure of rank correlation: Biometrika, v. 30, nos. 1–2, p. 81–93.

Kohler, M.A., 1949, On the use of double-mass analysis for testing the consistency of meteorological records and for making required adjustments: Bulletin of the American Meteorological Society, v. 30, no. 5, p. 188–195.

Kolars, K.A., Vecchia, A.V., and Ryberg, K.R., 2016, Stochastic model for simulating Souris River Basin precipitation, evapotranspiration, and natural streamflow: U.S. Geological Survey Scientific Investigations Report 2015–5185, 55 p., accessed August 2019 at http://dx.doi.org/10.3133/sir20155185.

Libiseller, C., and Grimvall, A., 2002, Performance of partial Mann-Kendall tests for trend detection in the presence of covariates: Environmetrics, v. 13, no. 1, p. 71–84, accessed June 2019 at https://doi.org/10.1002/env.507.

Lins, H.F., 2012, USGS Hydro-Climatic Data Network 2009 (HCDN–2009): U.S. Geological Survey Fact Sheet 2012–3047, 4 p., accessed March 23, 2018, at https://pubs.usgs.gov/fs/2012/3047/.

Livneh, B., Bohn, T.J., Pierce, D.W., Munoz-Arriola, F., Nijssen, B., Vose, R., Cayan, D.R., and Brekke, L., 2015, A spatially comprehensive, hydrometeorological data set for Mexico, the U.S., and Southern Canada 1950–2013: Scientific Data, v. 2, article 150042, 12 p., accessed December 2018 at https://doi.org/10.1038/sdata.2015.42.

Mallakpour, I., and Villarini, G., 2015, The changing nature of flooding across the central United States: Nature Climate Change, v. 5, p. 250–254, accessed June 2019 at https://doi.org/10.1038/NCLIMATE2516.

Mann, H.B., 1945, Nonparametric tests against trend: Econometrica, v. 13, no. 3, p. 245–259.

McCabe, G.J., and Wolock, D.M., 2002, A step increase in streamflow in the conterminous United States: Geophysical Research Letters, v. 29, no. 24, p. 38–1 to 38–4.

McGuire, V.L., 2017a, Data used to map water-level changes in the High Plains aquifer, predevelopment (about 1950) to 2015 and 2013 to 2015: U.S. Geological Survey data release, accessed June 2019 at https://doi.org/10.5066/F7SB43WM.

McGuire, V.L., 2017b, Water-level and recoverable water in storage changes, High Plains aquifer, predevelopment to 2015 and 2013–15: U.S. Geological Survey Scientific Investigations Report 2017–5040, 14 p., accessed June 2019 at https://doi.org/10.3133/sir20175040.

Norton, P.A., Anderson, M.T., and Stamm, J.F., 2014, Trends in annual, seasonal, and monthly streamflow characteristics at 227 streamgages in the Missouri River watershed, water years 1960–2011: U.S. Geological Survey Scientific Investigations Report 2014–5053, 128 p., accessed June 2019 at http://dx.doi.org/10.3133/sir20145053.

Nustad, R.A., Kolars, K.A., Vecchia, A.V., and Ryberg, K.R., 2016, 2011 Souris River flood—Will it happen again?: U.S. Geological Survey Fact Sheet 2016–3073, 4 p., accessed August 2020 at https://doi.org/10.3133/fs20163073.

Painter, C.C., Heimann, D.C., and Lanning-Rush, J.L., 2017, Methods for estimating annual exceedance-probability streamflows for streams in Kansas based on data through water year 2015 (ver. 1.1, September 2017): U.S. Geological Survey Scientific Investigations Report 2017–5063, 20 p., accessed November 2018 at https://doi.org/10.3133/sir20175063.

Peterson, T.C., Heim, R.R., Jr., Hirsch, R., Kaiser, D.P., Brooks, H., Diffenbaugh, N.S., Dole, R.M., Giovannettone, J.P., Guirguis, K., Karl, T.R., Katz, R.W., Kunkel, K., Lettenmaier, D., McCabe, G.J., Paciorek, C.J., Ryberg, K.R., Schubert, S., Silva, V.B.S., Stewart, B.C., Vecchia, A.V., Villarini, G., Vose, R.S., Walsh, J., Wehner, M., Wolock, D., Wolter, K., Woodhouse, C.A., and Wuebbles, D., 2013, Monitoring and understanding changes in heat waves, cold waves, floods, and droughts in the United States—State of knowledge: Bulletin of the American Meteorological Society, v. 94, no. 6, p. 821–834.

Pettitt, A.N., 1979, A non-parametric approach to the change-point problem: Journal of the Royal Statistical Society, Series C (Applied Statistics), v. 28, no. 2, p. 126–135.

Pohlert, T., 2018, Trend—Non-parametric trend tests and change-point detection (R package, version 1.1.1): R Foundation for Statistical Computing software release, accessed June 2019 at https://CRAN.R-project.org/package=trend.

PRISM Climate Group, 2019, PRISM [Parameter-elevation Regressions on Independent Slopes Model] climate data: Oregon State University database, accessed June 2019 at http://prism.oregonstate.edu.

Railsback, L.B., 2004, T.C. Chamberlin's "Method of Multiple Working Hypotheses"—An encapsulation for modern students: Houston Geological Society Bulletin, v. 47, no. 2, p. 68–69.

Rasmussen, T.J., and Perry, C.A., 2001, Trends in peak flows of selected streams in Kansas: U.S. Geological Survey Water-Resources Investigations Report 01–4203, 62 p.

R Core Team, 2018, R—A language and environment for statistical computing: R Foundation for Statistical Computing, accessed July 2018 at https://www.R-project.org/.

Runkle, J., Kunkel, K.E., Frankson, R., Easterling, D., and Champion, S., 2017, Minnesota State climate summary: NOAA (National Oceanic and Atmospheric Administration) Technical Report NESDIS (National Environmental Satellite, Data, and Information Service) 149–MN, 4 p., accessed June 2019 at https://statesummaries.ncics.org/mn.

Ryberg, K.R., 2015, The impact of climate variability on streamflow and water quality in the North Central United States: Fargo, North Dakota, North Dakota State University, Ph.D. dissertation, 226 p., 4 apps.

Ryberg, K.R., Hodgkins, G.A., and Dudley, R.W., 2020, Change points in annual peak streamflows—Method comparisons and historical change points in the United States: Journal of Hydrology, v. 583, article 124307, accessed July 2020 at https://doi.org/10.1016/j.jhydrol.2019.124307.

Ryberg, K.R., Lin, W., and Vecchia, A.V., 2014, Impact of climate variability on runoff in the north-central United States: Journal of Hydrologic Engineering, v. 19, no. 1, p. 148–158, accessed June 2019 at https://doi.org/10.1061/(ASCE)HE.1943-5584.0000775.

Ryberg, K.R., Vecchia, A.V., Akyüz, F.A., and Lin, W., 2016, Tree-ring-based estimates of long-term seasonal precipitation in the Souris River region of Saskatchewan, North Dakota and Manitoba: Canadian Water Resources Journal / Revue canadienne des ressources hydriques, v. 41, no. 3, p. 412–428, accessed August 2020 at https://doi.org/10.1080/07011784.2016.1164627.

Saharia, M., Kirstetter, P., Vergara, H., Gourley, J.J., and Hong, Y., 2017, Characterization of floods in the United States: Journal of Hydrology, v. 548, p. 524–535, accessed February 8, 2021, at https://doi.org/10.1016/j.jhydrol.2017.03.010.

Sando, S.K., McCarthy, P.M., Sando, R., and Dutton, D.M., 2016, Temporal trends and stationarity in annual peak flow and peak-flow timing for selected long-term streamflow-gaging stations in or near Montana through Water Year 2011: U.S. Geological Survey Scientific Investigations Report 2015–5019–B, 48 p.

Seaber, P.R., Kapinos, F.P., and Knapp, G.L., 1987, Hydrologic unit maps: U.S. Geological Survey Water-Supply Paper 2294, 63 p.

Shafer, M., Ojima, D., Antle, J.M., Kluck, D., McPherson, R.A., Petersen, S., Scanlon, B., and Sherman, K., 2014, Great Plains, chap. 19 *of* Melillo, J.M., Richmond, T.C., and Yohe, G.W., eds., Climate change impacts in the United States—The Third National Climate Assessment: Washington, D.C., U.S. Global Change Research Program, p. 441–461.

U.S. Army Corps of Engineers, [1993], Orwell Lake—Fergus Falls, Minnesota: [St. Paul, Minn.], U.S. Army Corps of Engineers brochure, accessed June 2019 at https://www.mvp.usace.army.mil/Portals/57/docs/Public%20Affairs/Brochure/Recreation/orwell_brochure.pdf?ver=2013-01-06-153532-813.

U.S. Army Corps of Engineers, 2018, National inventory of dams: U.S. Army Corps of Engineers database, accessed June 2019 at https://nid.usace.army.mil.

U.S. Geological Survey, 2007, North America elevation 1-kilometer-resolution GRID [dataset]: U.S. Geological Survey ScienceBase Catalog website, accessed May 1, 2019, at https://www.sciencebase.gov/catalog/item/4fb5495ee4b04cb937751d6d.

U.S. Geological Survey, 2018, USGS water data for the Nation: U.S. Geological Survey National Water Information System database, accessed November 28, 2018, at https://doi.org/10.5066/F7P55KJN.

Vecchia, A.V., 2008, Climate simulation and flood risk analysis for 2008–40 for Devils Lake, North Dakota: U.S. Geological Survey Scientific Investigations Report 2008–5011, 28 p., accessed June 2019 at http://pubs.usgs.gov/sir/2008/5011/.

Williams-Sether, T., 1999, From dry to wet, 1988–97, North Dakota: U.S. Geological Survey Fact Sheet 075–99, 4 p., accessed June 2019 at https://doi.org/10.3133/fs07599.

Williams-Sether, T., Macek-Rowland, K.M., and Emerson, D.G., 1994, Climatic and hydrologic aspects of the 1988–92 drought and the effect on people and resources of North Dakota: North Dakota State Water Commission, Water Resources Investigations [report] 29, accessed June 2019 at https://www.swc.nd.gov/info_edu/reports_and_publications/pdfs/wr_investigations/wr29_report.pdf.

York, B.C., Ryberg, K.R., Asquith, W.H., Chase, K.J., Dickinson, J.E., Dudley, R.W., Harden, T.M., Hodgkins, G.A., Holtschlag, D.J., Humberson, D.G., Konrad, C.P., Levin, S.B., Restivo, D.E., Sando, R., Sando, S.K., Swain, E.D., Tillery, A.C., and Totten, A.R., 2022, Attributions for nonstationary peak streamflow records across the conterminous United States, 1941–2015 and 1966–2015: U.S. Geological Survey data release, https://doi.org/10.5066/P9FOUVWG.

Zeng, R., and Cai, X., 2014, Analyzing streamflow changes—Irrigation-enhanced interaction between aquifer and streamflow in the Republican River basin: Hydrology and Earth System Sciences, v. 18, p. 493–502, accessed June 2019 at https://doi.org/10.5194/hess-18-493-2014.

Tables C1–C13

Table C1. Summary of monotonic trend analyses and the number of streamgages in the Upper Plains region that have statistically significant and nonsignificant monotonic trends in annual peak-streamflow data for each peak-flow trend zone (PFTZ) or all PFTZs (“All zones”) in the 50- and 75-year study periods.

[Monotonic trend percentages represent the percentage change per year and were estimated using Sen’s slope estimator (see Hodgkins and others, 2019). Monotonic trends are significant if *p*-value<0.10, where the *p*-value is the attained significance level. Interquartile ranges represent the difference between the 25th and 75th percentiles. Data for streamgages with significant monotonic trends or change points are available from Chase and others (2022). Term: --, not applicable]

		Monotonic trend analyses							
		Summary of 50-year monotonic trend analyses				Summary of 75-year monotonic trend analyses			
		All streamgages		Streamgages with significant monotonic trends		All streamgages		Streamgages with significant monotonic trends	
Peak-flow trend zone (PFTZ)	Number of streamgages in the PFTZ	Number of streamgages included in 50-year monotonic trend analyses	Median 50-year monotonic trend percentage (interquartile range)	Number of streamgages with significant 50-year monotonic trends	Median significant 50-year monotonic trend percentage (interquartile range)	Number of streamgages included in 75-year monotonic trend analyses	Median 75-year monotonic trend percentage (interquartile range)	Number of streamgages with significant 75-year monotonic trends	Median significant 75-year monotonic trend percentage (interquartile range)
1A	42	42	−22 (−35 to −12)	11	−42 (−58 to −38)	24	−21 (−36 to −8)	9	−44 (−55 to −36)
1B	18	18	−38 (−49 to −27)	3	−75 (−79 to −69)	6	−57 (−62 to −54)	6	−57 (−62 to −54)
1C	22	22	−21 (−32 to −9)	5	−43 (−62 to −41)	7	−29 (−34 to −10)	2	−45 (−51 to −39)
2A	39	39	70 (35 to 100)	13	125 (102 to 171)	13	80 (31 to 128)	8	122 (102 to 194)
2B	32	32	34 (18 to 45)	4	60 (48 to 77)	14	33 (22 to 65)	7	68 (44 to 135)
3	4	4	0 (−7 to 3)	1	−21 (−21 to −21)	4	10 (0 to 13)	1	−29 (−29 to −29)
4	7	7	−34 (−47 to −11)	2	−52 (−54 to −51)	4	−5 (−23 to 17)	1	−29 (−29 to −29)
5	17	17	11 (0 to 25)	0	--	4	7 (−25 to 31)	1	−47 (−47 to −47)
6	12	12	−15 (−34 to 12)	1	−51 (−51 to −51)	7	5 (−34 to 30)	2	88 (20 to 156)
7	57	57	−45 (−70 to −19)	26	−72 (−86 to −61)	18	−66 (−83 to −29)	13	−71 (−89 to −64)
8	19	19	6 (−4 to 25)	2	47 (44 to 50)	8	3 (−5 to 22)	2	79 (55 to 103)
All zones	269	269	−10 (−35 to 23)	68	−50 (−68 to 44)	109	−9 (−37 to 24)	52	−38 (−62 to 69)

Table C2. Summary of change-point analyses and the number of streamgages in the Upper Plains region that have statistically significant and nonsignificant change points in annual peak-streamflow data for each peak-flow trend zone (PFTZ) or all PFTZs (“All zones”) in the 50- and 75-year study periods.

[Change-point percentages represent the change in median annual peak streamflow from the period of record before the change-point year to the period of record after the change-point year. Change points are significant if *p*-value<0.10, where the *p*-value is the attained significance level. Interquartile ranges represent the difference between the 25th and 75th percentiles. Data for streamgages with significant monotonic trends or change points are available from Chase and others (2022). Term: --, not applicable]

Peak-flow trend zone (PFTZ)	Number of streamgages in the PFTZ	Change-point analyses											
		Summary of 50-year change-point analyses						Summary of 75-year change-point analyses					
		All streamgages			Streamgages with significant change points			All streamgages			Streamgages with significant change points		
		Number of streamgages included in 50-year change-point analyses	Median 50-year change-point percentage (interquartile range)	Median 50-year change point (interquartile range)	Number of streamgages with significant 50-year change points	Median significant 50-year change-point percentage (interquartile range)	Median significant 50-year change point (interquartile range)	Number of streamgages included in 75-year change-point analyses	Median 75-year change-point percentage (interquartile range)	Median 75-year change point (interquartile range)	Number of streamgages with significant 75-year change points	Median significant 75-year change-point percentage (interquartile range)	Median significant 75-year change point (interquartile range)
1A	42	42	−29 (−43 to −17)	1984 (1982 to 1985)	9	−48 (−57 to −40)	1984 (1982 to 1984)	24	−25 (−43 to −12)	1976 (1970 to 1982)	10	−40 (−51 to −30)	1980 (1972 to 1984)
1B	18	18	−47 (−64 to −40)	1987 (1980 to 1987)	5	−69 (−72 to −66)	1987 (1979 to 1987)	6	−46 (−57 to −45)	1972 (1957 to 1974)	5	−46 (−47 to −44)	1972 (1972 to 1975)
1C	22	22	−36 (−50 to −22)	1986 (1979 to 1990)	3	−19 (−44 to −6)	1983 (1982 to 1984)	7	−22 (−30 to −21)	1984 (1970 to 1986)	2	−49 (−57 to −41)	1977 (1972 to 1981)
2A	39	39	91 (56 to 143)	1992 (1992 to 1992)	17	128 (91 to 155)	1992 (1992 to 1992)	13	90 (71 to 128)	1992 (1992 to 1992)	8	119 (91 to 159)	1992 (1991 to 1992)
2B	32	32	50 (38 to 82)	1983 (1980 to 1993)	3	44 (3 to 90)	1982 (1979 to 1985)	14	39 (32 to 59)	1981 (1974 to 1989)	4	64 (58 to 67)	1975 (1970 to 1980)
3	4	4	−2 (−17 to 17)	1995 (1987 to 2001)	0	--	--	4	12 (4 to 17)	1982 (1970 to 1995)	1	−17 (−17 to −17)	1972 (1972 to 1972)
4	7	7	−41 (−44 to −38)	1979 (1979 to 1980)	3	−39 (−42 to −38)	1982 (1980 to 1986)	4	17 (−30 to 63)	1971 (1963 to 1979)	0	--	--
5	17	17	99 (29 to 190)	2001 (1992 to 2007)	0	--	--	4	−24 (−68 to 26)	1974 (1964 to 1983)	1	−73 (−73 to −73)	1979 (1979 to 1979)
6	12	12	−37 (−46 to 44)	1997 (1984 to 1999)	0	--	--	7	16 (−31 to 45)	1977 (1973 to 1986)	1	324 (324 to 324)	1957 (1957 to 1957)
7	57	57	−48 (−74 to −31)	1996 (1987 to 1999)	20	−74 (−81 to −61)	1989 (1984 to 1996)	18	−49 (−68 to −30)	1971 (1964 to 1977)	12	−54 (−78 to −49)	1971 (1966 to 1974)
8	19	19	17 (−26 to 35)	1994 (1983 to 2005)	1	76 (76 to 76)	2003 (2003 to 2003)	8	2 (−17 to 24)	1966 (1961 to 1973)	2	59 (40 to 77)	1971 (1968 to 1973)
All zones	269	269	−21 (−45 to 49)	1991 (1982 to 1998)	61	−42 (−69 to 82)	1975 (1968 to 1984)	109	−15 (−42 to 37)	1977 (1969 to 1986)	46	−34 (−53 to 58)	1975 (1968 to 1984)

Table C3. Summary of the number of primary attributions, associated levels of evidence, and mean percentage changes for the statistically significant 50- and 75-year monotonic trends and change points in annual peak-streamflow data for streamgages in sub-peak-flow trend zone 1A of the Upper Plains region.

[A description of levels of evidence can be found in table A2 (Barth and others, this volume, chap. A). Mean percentage change values represent the percentage change per year and were estimated using Sen's slope estimator (see Hodgkins and others, 2019). Data are available from Chase and others (2022). Terms: *n*, number of streamgages; --, not applicable]

Sub-peak-flow trend zone 1A	Monotonic trend analyses									
	50-year period					75-year period				
Primary attribution	Additional information required *n* (mean percentage change)	Limited evidence *n* (mean percentage change)	Medium evidence *n* (mean percentage change)	Robust evidence *n* (mean percentage change)	Total *n* (mean percentage change)	Additional information required *n* (mean percentage change)	Limited evidence *n* (mean percentage change)	Medium evidence *n* (mean percentage change)	Robust evidence *n* (mean percentage change)	Total *n* (mean percentage change)
Air temperature	--	--	2 (−55.9)	--	2 (−55.9)	--	1 (−64.0)	--	--	1 (−64.0)
Groundwater and (or) surface-water withdrawals	--	--	--	--	--	--	--	--	--	--
Groundwater withdrawals	--	--	--	--	--	--	--	--	--	--
Large artificial impoundments	--	--	--	--	--	--	--	1 (−43.4)	--	1 (−43.4)
Long-term precipitation	--	1 (−23.6)	--	--	1 (−23.6)	--	--	--	1 (−33.4)	1 (−33.4)
Multidecadal climate variability	--	1 (−55.3)	6 (−41.4)	--	7 (−43.3)	--	2 (−37.9)	3 (−52.2)	1 (−36.0)	6 (−44.7)
Unknown causes	1 (−73.9)	--	--	--	1 (−73.9)	--	--	--	--	--
Urban effects	--	--	--	--	--	--	--	--	--	--

	Change-point analyses									
	50-year period					75-year period				
Primary attribution	Additional information required *n* (mean percentage change; mean year of change point)	Limited evidence *n* (mean percentage change; mean year of change point)	Medium evidence *n* (mean percentage change; mean year of change point)	Robust evidence *n* (mean percentage change; mean year of change point)	Total *n* (mean percentage change; mean year of change point)	Additional information required *n* (mean percentage change; mean year of change point)	Limited evidence *n* (mean percentage change; mean year of change point)	Medium evidence *n* (mean percentage change; mean year of change point)	Robust evidence *n* (mean percentage change; mean year of change point)	Total *n* (mean percentage change; mean year of change point)
Air temperature	--	--	--	--	--	--	--	1 (−28.5; 1975)	--	1 (−28.5; 1975)
Groundwater and (or) surface-water withdrawals	--	--	--	--	--	--	--	--	--	--
Groundwater withdrawals	--	--	--	--	--	--	--	--	--	--
Large artificial impoundments	--	--	--	--	--	--	1 (−58.4; 1972)	1 (−43.4; 1951)	--	2 (−50.9; 1962)
Long-term precipitation	--	--	1 (−14.2; 1984)	--	1 (−14.2; 1984)	--	1 (32.9; 1966)	--	--	1 (32.9; 1966)
Multidecadal climate variability	--	--	5 (−47.5; 1984)	--	5 (−47.5; 1984)	--	3 (−31.2; 1983)	1 (−52.5; 1985)	1 (−35.9; 1984)	5 (−36.4; 1984)
Unknown causes	3 (−61.8; 1981)	--	--	--	3 (−61.8; 1981)	1 (−52.8; 1978)	--	--	--	1 (−52.8; 1978)
Urban effects	--	--	--	--	--	--	--	--	--	--

Table C4. Summary of the number of primary attributions, associated levels of evidence, and mean percentage changes for the statistically significant 50- and 75-year monotonic trends and change points in annual peak-streamflow data for streamgages in sub-peak-flow trend zone 1B of the Upper Plains region.

[A description of levels of evidence can be found in table A2 (Barth and others, this volume, chap. A). Mean percentage change values represent the percentage change per year and were estimated using Sen's slope estimator (see Hodgkins and others, 2019). Data are available from Chase and others (2022). Terms: *n*, number of streamgages; --, not applicable]

Sub-peak-flow trend zone 1B	Monotonic trend analyses									
	50-year period					75-year period				
Primary attribution	Additional information required *n* (mean percentage change)	Limited evidence *n* (mean percentage change)	Medium evidence *n* (mean percentage change)	Robust evidence *n* (mean percentage change)	Total *n* (mean percentage change)	Additional information required *n* (mean percentage change)	Limited evidence *n* (mean percentage change)	Medium evidence *n* (mean percentage change)	Robust evidence *n* (mean percentage change)	Total *n* (mean percentage change)
Air temperature	--	--	2 (−73.3)	--	2 (−73.3)	--	--	2 (−49.2)	2 (−59.3)	4 (−54.3)
Groundwater and (or) surface-water withdrawals	--	--	--	--	--	--	--	--	--	--
Groundwater withdrawals	--	--	--	--	--	--	--	--	--	--
Large artificial impoundments	--	--	--	--	--	--	--	1 (−58.4)	1 (−62.1)	2 (−60.3)
Long-term precipitation	--	--	--	1 (−74.1)	1 (−74.1)	--	--	--	--	--
Multidecadal climate variability	--	--	--	--	--	--	--	--	--	--
Unknown causes	--	--	--	--	--	--	--	--	--	--
Urban effects	--	--	--	--	--	--	--	--	--	--

	Change-point analyses									
	50-year period					75-year period				
Primary attribution	Additional information required *n* (mean percentage change; mean year of change point)	Limited evidence *n* (mean percentage change; mean year of change point)	Medium evidence *n* (mean percentage change; mean year of change point)	Robust evidence *n* (mean percentage change; mean year of change point)	Total *n* (mean percentage change; mean year of change point)	Additional information required *n* (mean percentage change; mean year of change point)	Limited evidence *n* (mean percentage change; mean year of change point)	Medium evidence *n* (mean percentage change; mean year of change point)	Robust evidence *n* (mean percentage change; mean year of change point)	Total *n* (mean percentage change; mean year of change point)
Air temperature	--	--	2 (−75.9; 1979)	--	2 (−75.9; 1979)	--	--	2 (−45.9; 1974)	2 (−43.8, 1975)	4 (−44.5; 1974)
Groundwater and (or) surface-water withdrawals	--	--	--	--	--	--	--	1 (−74.9; 1953)	--	1 (−74.9; 1953)
Groundwater withdrawals	--	--	--	--	--	--	--	--	--	--
Large artificial impoundments	--	--	--	--	--	--	--	--	--	--
Long-term precipitation	--	--	1 (−68.3; 1987)	2 (−63.0; 1987)	3 (−64.7; 1987)	--	--	--	--	--
Multidecadal climate variability	--	--	--	--	--	--	--	--	--	--
Unknown causes	--	--	--	--	--	--	--	--	--	--
Urban effects	--	--	--	--	--	--	--	--	--	--

Table C5. Summary of the number of primary attributions, associated levels of evidence, and mean percentage changes for the statistically significant 50- and 75-year monotonic trends and change points in annual peak-streamflow data for streamgages in sub-peak-flow trend zone 1C of the Upper Plains region.

[A description of levels of evidence can be found in table A2 (Barth and others, this volume, chap. A). Mean percentage change values represent the percentage change per year and were estimated using Sen's slope estimator (see Hodgkins and others, 2019). Data are available from Chase and others (2022). Terms: *n*, number of streamgages; --, not applicable]

Sub-peak-flow trend zone 1C	Monotonic trend analyses									
	50-year period					75-year period				
Primary attribution	Additional information required *n* (mean percentage change)	Limited evidence *n* (mean percentage change)	Medium evidence *n* (mean percentage change)	Robust evidence *n* (mean percentage change)	Total *n* (mean percentage change)	Additional information required *n* (mean percentage change)	Limited evidence *n* (mean percentage change)	Medium evidence *n* (mean percentage change)	Robust evidence *n* (mean percentage change)	Total *n* (mean percentage change)
Air temperature	--	1 (−41.0)	--	--	1 (−41.0)	--	--	--	--	--
Groundwater and (or) surface-water withdrawals	--	--	--	--	--	--	--	--	--	--
Groundwater withdrawals	--	--	--	--	--	--	--	--	--	--
Large artificial impoundments	--	--	1 (−62.6)	--	1 (−62.6)	--	--	1 (−56.1)	--	1 (−56.1)
Long-term precipitation	--	--	--	--	--	--	--	--	--	--
Multidecadal climate variability	--	--	--	--	--	--	--	--	--	--
Unknown causes	3 (−30.1)	--	--	--	3 (−30.1)	1 (−32.0)	--	--	--	1 (−32.0)
Urban effects	--	--	--	--	--	--	--	--	--	--

	Change-point analyses									
	50-year period					75-year period				
Primary attribution	Additional information required *n* (mean percentage change; mean year of change point)	Limited evidence *n* (mean percentage change; mean year of change point)	Medium evidence *n* (mean percentage change; mean year of change point)	Robust evidence *n* (mean percentage change; mean year of change point)	Total *n* (mean percentage change; mean year of change point)	Additional information required *n* (mean percentage change; mean year of change point)	Limited evidence *n* (mean percentage change; mean year of change point)	Medium evidence *n* (mean percentage change; mean year of change point)	Robust evidence *n* (mean percentage change; mean year of change point)	Total *n* (mean percentage change; mean year of change point)
Air temperature	--	--	--	--	--	--	--	--	--	--
Groundwater and (or) surface-water withdrawals	--	--	--	--	--	--	--	--	--	--
Groundwater withdrawals	--	--	--	--	--	--	--	--	--	--
Large artificial impoundments	--	--	1 (−69.4; 1986)	--	1 (−69.4; 1986)	--	--	1 (−64.2; 1986)	--	1 (−64.2; 1986)
Long-term precipitation	--	--	--	--	--	--	--	--	--	--
Multidecadal climate variability	--	--	--	--	--	--	--	--	--	--
Unknown causes	2 (−5.30; 1983)	--	--	--	2 (−5.30; 1983)	1 (−32.9; 1986)	--	--	--	1 (−32.9; 1986)
Urban effects	--	--	--	--	--	--	--	--	--	--

Table C6. Summary of the number of primary attributions, associated levels of evidence, and mean percentage changes for the statistically significant 50- and 75-year monotonic trends and change points in annual peak-streamflow data for streamgages in sub-peak-flow trend zone 2A of the Upper Plains region.

[A description of levels of evidence can be found in table A2 (Barth and others, this volume, chap. A). Mean percentage change values represent the percentage change per year and were estimated using Sen's slope estimator (see Hodgkins and others, 2019). Data are available from Chase and others (2022). Terms: *n*, number of streamgages; --, not applicable]

Sub-peak-flow trend zone 2A	Monotonic trend analyses									
	50-year period					75-year period				
Primary attribution	Additional information required *n* (mean percentage change)	Limited evidence *n* (mean percentage change)	Medium evidence *n* (mean percentage change)	Robust evidence *n* (mean percentage change)	Total *n* (mean percentage change)	Additional information required *n* (mean percentage change)	Limited evidence *n* (mean percentage change)	Medium evidence *n* (mean percentage change)	Robust evidence *n* (mean percentage change)	Total *n* (mean percentage change)
Air temperature	--	--	--	--	--	--	--	--	--	--
Groundwater and (or) surface-water withdrawals	--	--	--	--	--	--	--	--	--	--
Groundwater withdrawals	--	--	--	--	--	--	--	--	--	--
Large artificial impoundments	--	--	--	--	--	--	--	--	--	--
Long-term precipitation	--	--	5 (204)	8 (163)	13 (179)	--	--	1 (80.9)	7 (175)	8 (164)
Multidecadal climate variability	--	--	--	--	--	--	--	--	--	--
Unknown causes	--	--	--	--	--	--	--	--	--	--
Urban effects	--	--	--	--	--	--	--	--	--	--

	Change-point analyses									
	50-year period					75-year period				
Primary attribution	Additional information required *n* (mean percentage change; mean year of change point)	Limited evidence *n* (mean percentage change; mean year of change point)	Medium evidence *n* (mean percentage change; mean year of change point)	Robust evidence *n* (mean percentage change; mean year of change point)	Total *n* (mean percentage change; mean year of change point)	Additional information required *n* (mean percentage change; mean year of change point)	Limited evidence *n* (mean percentage change; mean year of change point)	Medium evidence *n* (mean percentage change; mean year of change point)	Robust evidence *n* (mean percentage change; mean year of change point)	Total *n* (mean percentage change; mean year of change point)
Air temperature	--	--	--	--	--	--	--	--	--	--
Groundwater and (or) surface-water withdrawals	--	--	--	--	--	--	--	--	--	--
Groundwater withdrawals	--	--	--	--	--	--	--	--	--	--
Large artificial impoundments	--	--	1 (−37.8; 1982)	--	1 (−37.8; 1982)	--	--	--	--	--
Long-term precipitation	--	--	4 (184; 1989)	13 (131; 1992)	17 (143; 1991)	--	1 (91.4; 1961)	--	7 (148; 1992)	8 (141; 1988)
Multidecadal climate variability	--	--	--	--	--	--	--	--	--	--
Unknown causes	--	--	--	--	--	--	--	--	--	--
Urban effects	--	--	--	--	--	--	--	--	--	--

Table C7. Summary of the number of primary attributions, associated levels of evidence, and mean percentage changes for the statistically significant 50- and 75-year monotonic trends and change points in annual peak-streamflow data for streamgages in sub-peak-flow trend zone 2B of the Upper Plains region.

[A description of levels of evidence can be found in table A2 (Barth and others, this volume, chap. A). Mean percentage change values represent the percentage change per year and were estimated using Sen's slope estimator (see Hodgkins and others, 2019). Data are available from Chase and others (2022). Terms: *n*, number of streamgages; --, not applicable]

Sub-peak-flow trend zone 2B	Monotonic trend analyses									
	50-year period					75-year period				
Primary attribution	Additional information required *n* (mean percentage change)	Limited evidence *n* (mean percentage change)	Medium evidence *n* (mean percentage change)	Robust evidence *n* (mean percentage change)	Total *n* (mean percentage change)	Additional information required *n* (mean percentage change)	Limited evidence *n* (mean percentage change)	Medium evidence *n* (mean percentage change)	Robust evidence *n* (mean percentage change)	Total *n* (mean percentage change)
Air temperature	--	--	--	--	--	--	--	--	--	--
Groundwater and (or) surface-water withdrawals	--	--	--	--	--	--	--	--	--	--
Groundwater withdrawals	--	--	--	--	--	--	--	--	--	--
Large artificial impoundments	--	--	--	--	--	--	--	--	--	--
Long-term precipitation	--	--	2 (60.1)	--	2 (60.1)	--	--	--	--	--
Multidecadal climate variability	--	--	2 (71.2)	--	2 (71.2)	--	--	5 (90.6)	--	5 (90.6)
Unknown causes	--	--	--	--	--	1 (121)	--	--	--	1 (121)
Urban effects	--	--	--	--	--	--	--	1 (32.2)	--	1 (32.2)

	Change-point analyses									
	50-year period					75-year period				
Primary attribution	Additional information required *n* (mean percentage change; mean year of change point)	Limited evidence *n* (mean percentage change; mean year of change point)	Medium evidence *n* (mean percentage change; mean year of change point)	Robust evidence *n* (mean percentage change; mean year of change point)	Total *n* (mean percentage change; mean year of change point)	Additional information required *n* (mean percentage change; mean year of change point)	Limited evidence *n* (mean percentage change; mean year of change point)	Medium evidence *n* (mean percentage change; mean year of change point)	Robust evidence *n* (mean percentage change; mean year of change point)	Total *n* (mean percentage change; mean year of change point)
Air temperature	--	--	--	--	--	--	--	--	--	--
Groundwater and (or) surface-water withdrawals	--	--	--	--	--	--	--	--	--	--
Groundwater withdrawals	--	--	--	--	--	--	--	--	--	--
Large artificial impoundments	--	--	--	--	--	--	--	--	--	--
Long-term precipitation	--	1 (136; 1976)	--	--	1 (136; 1976)	--	--	--	--	--
Multidecadal climate variability	--	--	--	--	--	--	1 (40.0; 1982)	--	--	1 (40.0; 1982)
Unknown causes	1 (44.1; 1989)	--	--	--	1 (44.1; 1989)	3 (68.1; 1973)	--	--	--	3 (68.1; 1973)
Urban effects	--	--	--	--	--	--	--	--	--	--

Table C8. Summary of the number of primary attributions, associated levels of evidence, and mean percentage changes for the statistically significant 50- and 75-year monotonic trends and change points in annual peak-streamflow data for streamgages in peak-flow trend zone 3 of the Upper Plains region.

[A description of levels of evidence can be found in table A2 (Barth and others, this volume, chap. A). Mean percentage change values represent the percentage change per year and were estimated using Sen's slope estimator (see Hodgkins and others, 2019). Data are available from Chase and others (2022). Terms: *n*, number of streamgages; --, not applicable]

Peak-flow trend zone 3	Monotonic trend analyses									
	50-year period					75-year period				
Primary attribution	Additional information required *n* (mean percentage change)	Limited evidence *n* (mean percentage change)	Medium evidence *n* (mean percentage change)	Robust evidence *n* (mean percentage change)	Total *n* (mean percentage change)	Additional information required *n* (mean percentage change)	Limited evidence *n* (mean percentage change)	Medium evidence *n* (mean percentage change)	Robust evidence *n* (mean percentage change)	Total *n* (mean percentage change)
Air temperature	--	--	--	--	--	--	--	--	--	--
Groundwater and (or) surface-water withdrawals	--	--	--	--	--	--	--	--	--	--
Groundwater withdrawals	--	--	--	--	--	--	--	--	--	--
Large artificial impoundments	--	--	--	1 (−20.7)	1 (−20.7)	--	--	--	1 (−28.1)	1 (−28.1)
Long-term precipitation	--	--	--	--	--	--	--	--	--	--
Multidecadal climate variability	--	--	--	--	--	--	--	--	--	--
Unknown causes	--	--	--	--	--	--	--	--	--	--
Urban effects	--	--	--	--	--	--	--	--	--	--

	Change-point analyses									
	50-year period					75-year period				
Primary attribution	Additional information required *n* (mean percentage change; mean year of change point)	Limited evidence *n* (mean percentage change; mean year of change point)	Medium evidence *n* (mean percentage change; mean year of change point)	Robust evidence *n* (mean percentage change; mean year of change point)	Total *n* (mean percentage change; mean year of change point)	Additional information required *n* (mean percentage change; mean year of change point)	Limited evidence *n* (mean percentage change; mean year of change point)	Medium evidence *n* (mean percentage change; mean year of change point)	Robust evidence *n* (mean percentage change; mean year of change point)	Total *n* (mean percentage change; mean year of change point)
Air temperature	--	--	--	--	--	--	--	--	--	--
Groundwater and (or) surface-water withdrawals	--	--	--	--	--	--	--	--	--	--
Groundwater withdrawals	--	--	--	--	--	--	--	--	--	--
Large artificial impoundments	--	--	--	--	--	--	--	--	1 (−16.9; 1972)	1 (−16.9; 1972)
Long-term precipitation	--	--	--	--	--	--	--	--	--	--
Multidecadal climate variability	--	--	--	--	--	--	--	--	--	--
Unknown causes	--	--	--	--	--	--	--	--	--	--
Urban effects	--	--	--	--	--	--	--	--	--	--

Table C9. Summary of the number of primary attributions, associated levels of evidence, and mean percentage changes for the statistically significant 50- and 75-year monotonic trends and change points in annual peak-streamflow data for streamgages in peak-flow trend zone 4 of the Upper Plains region.

[A description of levels of evidence can be found in table A2 (Barth and others, this volume, chap. A). Mean percentage change values represent the percentage change per year and were estimated using Sen's slope estimator (see Hodgkins and others, 2019). Data are available from Chase and others (2022). Terms: *n*, number of streamgages; --, not applicable]

Peak-flow trend zone 4	Monotonic trend analyses									
	50-year period					75-year period				
Primary attribution	Additional information required *n* (mean percentage change)	Limited evidence *n* (mean percentage change)	Medium evidence *n* (mean percentage change)	Robust evidence *n* (mean percentage change)	Total *n* (mean percentage change)	Additional information required *n* (mean percentage change)	Limited evidence *n* (mean percentage change)	Medium evidence *n* (mean percentage change)	Robust evidence *n* (mean percentage change)	Total *n* (mean percentage change)
Air temperature	--	--	--	--	--	--	--	--	--	--
Groundwater and (or) surface-water withdrawals	--	--	--	--	--	--	--	--	--	--
Groundwater withdrawals	--	--	--	--	--	--	--	--	--	--
Large artificial impoundments	--	--	--	--	--	--	--	--	--	--
Long-term precipitation	--	--	--	--	--	--	--	--	--	--
Multidecadal climate variability	--	--	--	--	--	--	--	--	--	--
Unknown causes	2 (−52.0)	--	--	--	2 (−52.0)	1 (−28.2)	--	--	--	1 (−28.2)
Urban effects	--	--	--	--	--	--	--	--	--	--

	Change-point analyses									
	50-year period					75-year period				
Primary attribution	Additional information required *n* (mean percentage change; mean year of change point)	Limited evidence *n* (mean percentage change; mean year of change point)	Medium evidence *n* (mean percentage change; mean year of change point)	Robust evidence *n* (mean percentage change; mean year of change point)	Total *n* (mean percentage change; mean year of change point)	Additional information required *n* (mean percentage change; mean year of change point)	Limited evidence *n* (mean percentage change; mean year of change point)	Medium evidence *n* (mean percentage change; mean year of change point)	Robust evidence *n* (mean percentage change; mean year of change point)	Total *n* (mean percentage change; mean year of change point)
Air temperature	--	--	--	--	--	--	--	--	--	--
Groundwater and (or) surface-water withdrawals	--	--	--	--	--	--	--	--	--	--
Groundwater withdrawals	--	--	--	--	--	--	--	--	--	--
Large artificial impoundments	--	--	--	--	--	--	--	--	--	--
Long-term precipitation	--	--	--	--	--	--	--	--	--	--
Multidecadal climate variability	--	--	--	--	--	--	--	--	--	--
Unknown causes	3 (−39.5; 1984)	--	--	--	3 (−39.5; 1984)	--	--	--	--	--
Urban effects	--	--	--	--	--	--	--	--	--	--

Table C10. Summary of the number of primary attributions, associated levels of evidence, and mean percentage changes for the statistically significant 50- and 75-year monotonic trends and change points in annual peak-streamflow data for streamgages in peak-flow trend zone 5 of the Upper Plains region.

[A description of levels of evidence can be found in table A2 (Barth and others, this volume, chap. A). Mean percentage change values represent the percentage change per year and were estimated using Sen's slope estimator (see Hodgkins and others, 2019). Data are available from Chase and others (2022). Terms: *n*, number of streamgages; --, not applicable]

Peak-flow trend zone 5	Monotonic trend analyses									
	50-year period					75-year period				
Primary attribution	Additional information required *n* (mean percentage change)	Limited evidence *n* (mean percentage change)	Medium evidence *n* (mean percentage change)	Robust evidence *n* (mean percentage change)	Total *n* (mean percentage change)	Additional information required *n* (mean percentage change)	Limited evidence *n* (mean percentage change)	Medium evidence *n* (mean percentage change)	Robust evidence *n* (mean percentage change)	Total *n* (mean percentage change)
Air temperature	--	--	--	--	--	--	--	--	--	--
Groundwater and (or) surface-water withdrawals	--	--	--	--	--	--	--	--	--	--
Groundwater withdrawals	--	--	--	--	--	--	--	--	--	--
Large artificial impoundments	--	--	--	--	--	--	--	--	--	--
Long-term precipitation	--	--	--	--	--	--	--	--	--	--
Multidecadal climate variability	--	--	--	--	--	--	--	--	--	--
Unknown causes	--	--	--	--	--	1 (−47.0)	--	--	--	1 (−47.0)
Urban effects	--	--	--	--	--	--	--	--	--	--

	Change-point analyses									
	50-year period					75-year period				
Primary attribution	Additional information required *n* (mean percentage change; mean year of change point)	Limited evidence *n* (mean percentage change; mean year of change point)	Medium evidence *n* (mean percentage change; mean year of change point)	Robust evidence *n* (mean percentage change; mean year of change point)	Total *n* (mean percentage change; mean year of change point)	Additional information required *n* (mean percentage change; mean year of change point)	Limited evidence *n* (mean percentage change; mean year of change point)	Medium evidence *n* (mean percentage change; mean year of change point)	Robust evidence *n* (mean percentage change; mean year of change point)	Total *n* (mean percentage change; mean year of change point)
Air temperature	--	--	--	--	--	--	--	--	--	--
Groundwater and (or) surface-water withdrawals	--	--	--	--	--	--	--	--	--	--
Groundwater withdrawals	--	--	--	--	--	--	--	--	--	--
Large artificial impoundments	--	--	--	--	--	--	--	--	--	--
Long-term precipitation	--	--	--	--	--	--	--	--	--	--
Multidecadal climate variability	--	--	--	--	--	--	--	--	--	--
Unknown causes	--	--	--	--	--	1 (−72.7; 1979)	--	--	--	1 (−72.7; 1979)
Urban effects	--	--	--	--	--	--	--	--	--	--

Table C11. Summary of the number of primary attributions, associated levels of evidence, and mean percentage changes for the statistically significant 50- and 75-year monotonic trends and change points in annual peak-streamflow data for streamgages in peak-flow trend zone 6 of the Upper Plains region.

[A description of levels of evidence can be found in table A2 (Barth and others, this volume, chap. A). Mean percentage change values represent the percentage change per year and were estimated using Sen's slope estimator (see Hodgkins and others, 2019). Data are available from Chase and others (2022). Terms: *n*, number of streamgages; --, not applicable]

Peak-flow trend zone 6	Monotonic trend analyses									
	50-year period					75-year period				
Primary attribution	Additional information required *n* (mean percentage change)	Limited evidence *n* (mean percentage change)	Medium evidence *n* (mean percentage change)	Robust evidence *n* (mean percentage change)	Total *n* (mean percentage change)	Additional information required *n* (mean percentage change)	Limited evidence *n* (mean percentage change)	Medium evidence *n* (mean percentage change)	Robust evidence *n* (mean percentage change)	Total *n* (mean percentage change)
Air temperature	--	--	--	--	--	--	--	--	--	--
Groundwater and (or) surface-water withdrawals	--	--	--	--	--	--	--	--	--	--
Groundwater withdrawals	--	--	--	--	--	--	--	--	--	--
Large artificial impoundments	--	--	--	--	--	--	--	--	--	--
Long-term precipitation	--	--	--	--	--	--	--	--	--	--
Multidecadal climate variability	--	--	--	--	--	--	--	--	--	--
Unknown causes	1 (−50.7)	--	--	--	1 (−50.7)	2 (88.7)	--	--	--	2 (88.7)
Urban effects	--	--	--	--	--	--	--	--	--	--

	Change-point analyses									
	50-year period					75-year period				
Primary attribution	Additional information required *n* (mean percentage change; mean year of change point)	Limited evidence *n* (mean percentage change; mean year of change point)	Medium evidence *n* (mean percentage change; mean year of change point)	Robust evidence *n* (mean percentage change; mean year of change point)	Total *n* (mean percentage change; mean year of change point)	Additional information required *n* (mean percentage change; mean year of change point)	Limited evidence *n* (mean percentage change; mean year of change point)	Medium evidence *n* (mean percentage change; mean year of change point)	Robust evidence *n* (mean percentage change; mean year of change point)	Total *n* (mean percentage change; mean year of change point)
Air temperature	--	--	--	--	--	--	--	--	--	--
Groundwater and (or) surface-water withdrawals	--	--	--	--	--	--	--	--	--	--
Groundwater withdrawals	--	--	--	--	--	--	--	--	--	--
Large artificial impoundments	--	--	--	--	--	--	--	--	--	--
Long-term precipitation	--	--	--	--	--	--	--	--	--	--
Multidecadal climate variability	--	--	--	--	--	--	--	--	--	--
Unknown causes	--	--	--	--	--	1 (325; 1957)	--	--	--	1 (325; 1957)
Urban effects	--	--	--	--	--	--	--	--	--	--

Table C12. Summary of the number of primary attributions, associated levels of evidence, and mean percentage changes for the statistically significant 50- and 75-year monotonic trends and change points in annual peak-streamflow data for streamgages in peak-flow trend zone 7 of the Upper Plains region.

[A description of levels of evidence can be found in table A2 (Barth and others, this volume, chap. A). Mean percentage change values represent the percentage change per year and were estimated using Sen's slope estimator (see Hodgkins and others, 2019). Data are available from Chase and others (2022). Terms: *n*, number of streamgages; --, not applicable]

Peak-flow trend zone 7	Monotonic trend analyses									
	50-year period					75-year period				
Primary attribution	Additional information required *n* (mean percentage change)	Limited evidence *n* (mean percentage change)	Medium evidence *n* (mean percentage change)	Robust evidence *n* (mean percentage change)	Total *n* (mean percentage change)	Additional information required *n* (mean percentage change)	Limited evidence *n* (mean percentage change)	Medium evidence *n* (mean percentage change)	Robust evidence *n* (mean percentage change)	Total *n* (mean percentage change)
Air temperature	--	--	--	--	--	--	--	--	--	--
Groundwater and (or) surface-water withdrawals	--	7 (−65.9)	--	--	7 (−65.9)	--	2 (−55.4)	--	--	2 (−55.4)
Groundwater withdrawals	--	14 (−78.3)	--	--	14 (−78.3)	--	4 (−77.6)	--	--	4 (−77.6)
Large artificial impoundments	--	--	1 (−97.9)	--	1 (−97.9)	--	2 (−56.3)	5 (−85.3)	--	7 (−77.0)
Long-term precipitation	--	--	--	--	--	--	--	--	--	--
Multidecadal climate variability	--	--	--	--	--	--	--	--	--	--
Unknown causes	4 (−64.0)	--	--	--	4 (−64.0)	--	--	--	--	--
Urban effects	--	--	--	--	--	--	--	--	--	--

	Change-point analyses									
	50-year period					75-year period				
Primary attribution	Additional information required *n* (mean percentage change; mean year of change point)	Limited evidence *n* (mean percentage change; mean year of change point)	Medium evidence *n* (mean percentage change; mean year of change point)	Robust evidence *n* (mean percentage change; mean year of change point)	Total *n* (mean percentage change; mean year of change point)	Additional information required *n* (mean percentage change; mean year of change point)	Limited evidence *n* (mean percentage change; mean year of change point)	Medium evidence *n* (mean percentage change; mean year of change point)	Robust evidence *n* (mean percentage change; mean year of change point)	Total *n* (mean percentage change; mean year of change point)
Air temperature	--	--	--	--	--	--	--	--	--	--
Groundwater and (or) surface-water withdrawals	--	4 (−60.0; 1992)	--	--	4 (−60.0; 1992)	--	2 (−48.1; 1971)	--	--	2 (−48.1; 1971)
Groundwater withdrawals	--	12 (−71.6; 1988)	--	--	12 (−71.6; 1988)	--	4 (−75.5; 1977)	--	--	4 (−75.5; 1977)
Large artificial impoundments	--	--	1 (−80.3; 1981)	--	1 (−80.3; 1981)	--	2 (−26.5; 1968)	3 (−70.7; 1965)	--	5 (−53.0; 1966)
Long-term precipitation	--	--	--	--	--	--	--	--	--	--
Multidecadal climate variability	--	--	--	--	--	--	--	--	--	--
Unknown causes	3 (−67.2; 2001)	--	--	--	3 (−67.2; 2001)	1 (−49.7; 1975)	--	--	--	1 (−49.7; 1975)
Urban effects	--	--	--	--	--	--	--	--	--	--

Table C13. Summary of the number of primary attributions, associated levels of evidence, and mean percentage changes for the statistically significant 50- and 75-year monotonic trends and change points in annual peak-streamflow data for streamgages in peak-flow trend zone 8 of the Upper Plains region.

[A description of levels of evidence can be found in table A2 (Barth and others, this volume, chap. A). Mean percentage change values represent the percentage change per year and were estimated using Sen's slope estimator (see Hodgkins and others, 2019). Data are available from Chase and others (2022). Terms: *n*, number of streamgages; --, not applicable]

Peak-flow trend zone 8	Monotonic trend analyses									
	50-year period					75-year period				
Primary attribution	Additional information required *n* (mean percentage change)	Limited evidence *n* (mean percentage change)	Medium evidence *n* (mean percentage change)	Robust evidence *n* (mean percentage change)	Total *n* (mean percentage change)	Additional information required *n* (mean percentage change)	Limited evidence *n* (mean percentage change)	Medium evidence *n* (mean percentage change)	Robust evidence *n* (mean percentage change)	Total *n* (mean percentage change)
Air temperature	--	--	--	--	--	--	--	--	--	--
Groundwater and (or) surface-water withdrawals	--	--	--	--	--	--	--	--	--	--
Groundwater withdrawals	--	--	--	--	--	--	--	--	--	--
Large artificial impoundments	--	--	--	--	--	--	--	--	--	--
Long-term precipitation	--	--	1 (53.6)	--	1 (53.6)	--	--	1 (31.3)	--	1 (31.3)
Multidecadal climate variability	--	--	--	--	--	--	--	--	--	--
Unknown causes	1 (41.2)	--	--	--	1 (41.2)	1 (128)	--	--	--	1 (128)
Urban effects	--	--	--	--	--	--	--	--	--	--

	Change-point analyses									
	50-year period					75-year period				
Primary attribution	Additional information required *n* (mean percentage change; mean year of change point)	Limited evidence *n* (mean percentage change; mean year of change point)	Medium evidence *n* (mean percentage change; mean year of change point)	Robust evidence *n* (mean percentage change; mean year of change point)	Total *n* (mean percentage change; mean year of change point)	Additional information required *n* (mean percentage change; mean year of change point)	Limited evidence *n* (mean percentage change; mean year of change point)	Medium evidence *n* (mean percentage change; mean year of change point)	Robust evidence *n* (mean percentage change; mean year of change point)	Total *n* (mean percentage change; mean year of change point)
Air temperature	--	--	--	--	--	--	--	--	--	--
Groundwater and (or) surface-water withdrawals	--	--	--	--	--	--	--	--	--	--
Groundwater withdrawals	--	--	--	--	--	--	--	--	--	--
Large artificial impoundments	--	--	--	--	--	--	--	--	--	--
Long-term precipitation	--	1 (76.1; 2003)	--	--	1 (76.1; 2003)	--	1 (22.1; 1976)	--	--	1 (22.1; 1976)
Multidecadal climate variability	--	--	--	--	--	--	--	--	--	--
Unknown causes	--	--	--	--	--	1 (96.1; 1966)	--	--	--	1 (96.1; 1966)
Urban effects	--	--	--	--	--	--	--	--	--	--

Attribution of Monotonic Trends and Change Points in Peak Streamflow in the Midwest Region of the United States, 1941–2015 and 1966–2015

By Sara B. Levin and David J. Holtschlag

Chapter D of
Attribution of Monotonic Trends and Change Points in Peak Streamflow Across the Conterminous United States Using a Multiple Working Hypotheses Framework, 1941–2015 and 1966–2015
Karen R. Ryberg, editor

Prepared in cooperation with
U.S. Department of Transportation
Federal Highway Administration

Professional Paper 1869

U.S. Department of the Interior
U.S. Geological Survey

U.S. Geological Survey, Reston, Virginia: 2022

For more information on the USGS—the Federal source for science about the Earth, its natural and living resources, natural hazards, and the environment—visit https://www.usgs.gov or call 1–888–ASK–USGS.

For an overview of USGS information products, including maps, imagery, and publications, visit https://store.usgs.gov.

Suggested citation:
Levin, S.B., and Holtschlag, D.J., 2022, Attribution of monotonic trends and change points in peak streamflow in the Midwest region of the United States, 1941–2015 and 1966–2015, chap. D *of* Ryberg, K.R., ed., Attribution of monotonic trends and change points in peak streamflow across the conterminous United States using a multiple working hypotheses framework, 1941–2015 and 1966–2015: U.S. Geological Survey Professional Paper 1869, p. D1–D22, https://doi.org/10.3133/pp1869.

Associated data for this publication:
Dudley, R.W., Archfield, S.A., Hodgkins, G.A., Renard, B., and Ryberg, K.R., 2018, Peak-streamflow trends and change-points and basin characteristics for 2,683 U.S. Geological Survey streamgages in the conterminous U.S. (ver. 3.0, April 2019): U.S. Geological Survey data release, https://doi.org/10.5066/P9AEGXY0.

York, B.C., Ryberg, K.R., Asquith, W.H., Chase, K.J., Dickinson, J.E., Dudley, R.W., Harden, T.M., Hodgkins, G.A., Holtschlag, D.J., Humberson, D.G., Konrad, C.P., Levin, S.B., Restivo, D.E., Sando, R., Sando, S.K., Swain, E.D., Tillery, A.C., and Totten, A.R., 2022, Attributions for nonstationary peak streamflow records across the conterminous United States, 1941–2015 and 1966–2015: U.S. Geological Survey data release, https://doi.org/10.5066/P9FOUVWG.

ISSN 2330-7102 (online)

Acknowledgments

The work described in this professional paper was funded by the Federal Highway Administration of the U.S. Department of Transportation through Interagency Agreement DTFH6116X30020, “Flood Frequency Estimation for Hydraulic Design.” The authors thank Alex Totten of the U.S. Geological Survey for his assistance in compiling data and providing code to automate data analysis, as well as Chris Sanocki, Jason Griffin, and Katherine Dooley of the U.S. Geological Survey for their helpful reviews of the manuscript.

Contents

Figures

Tables

Conversion Factors

U.S. customary units to International System of Units

Multiply	By	To obtain
	Length	
foot (ft)	0.3048	meter (m)
mile (mi)	1.609	kilometer (km)
	Area	
square foot (ft^2)	0.09290	square meter (m^2)
square mile (mi^2)	2.590	square kilometer (km^2)
	Flow rate	
cubic foot per second (ft^3/s)	0.02832	cubic meter per second (m^3/s)

International System of Units to U.S. customary units

Multiply	By	To obtain
	Length	
meter (m)	3.281	foot (ft)
kilometer (km)	0.6214	mile (mi)

Datum

Horizontal coordinate information is referenced to the North American Datum of 1983 (NAD 83).

Supplemental Information

A “water year” is the 12-month period from October 1 through September 30 of the following year that is designated by the calendar year in which it ends.

The 75-year and 50-year study periods described in this report span water years 1941–2015 and 1966–2015, respectively.

Abbreviations

>	greater than
<	less than
GAGES-II	Geospatial Attributes of Gages for Evaluating Streamflow, Version II
HUC2	two-digit hydrologic unit code
NAD 83	North American Datum of 1983
NOAA	National Oceanic and Atmospheric Administration
NWALT	National Water-Quality Assessment Program (NAWQA) Wall-to-Wall Anthropogenic Land Use Trends (dataset for the conterminous United States)
p-value	attained significance level
USGS	U.S. Geological Survey

Attribution of Monotonic Trends and Change Points in Peak Streamflow in the Midwest Region of the United States, 1941–2015 and 1966–2015

By Sara B. Levin[1] and David J. Holtschlag[1]

Abstract

Conventional methods of flood-frequency analysis require streamflow records with a constant long-term mean. There are many instances in which this assumption of stationarity of annual peak streamflows may not be met and for which traditional flood-frequency estimates may be unreliable. Causal attributions of significant monotonic trends and change points in annual peak streamflow were identified for 261 U.S. Geological Survey streamgages in the Midwest region of the United States for the 75-year period spanning water years 1941–2015 and the 50-year period spanning water years 1966–2015. The list of potential attributions considered for each site included urban effects (land-use change), the presence of large artificial impoundments, and short-term cumulative precipitation. Decision rules for each attribution were applied to assess the plausibility of each attribution at each streamgage site, and the most plausible attribution was listed as the primary attribution for change. In some cases, a secondary attribution was also listed. Attributions were assigned a level of evidence (robust evidence, medium evidence, or limited evidence) to designate the strength and confidence of the supporting evidence.

There were a total of 122 streamgages with significant monotonic trends (also referred to as "trends") and 105 streamgages with significant change points in the 75-year analysis period. Large artificial impoundments were associated with a decrease in annual peak streamflows and were attributed to 47 trends and 44 change points located primarily in Wisconsin and along the eastern part of the Midwest region. Changes from impoundments occurred primarily in the early part of the analysis period, with few impoundments put in place after 1980. Short-term precipitation was attributed to 38 trends and 17 change points and were mostly associated with increasing peak streamflows. There were 36 trends and 43 change points with unknown attributions. Urban effects were listed as the primary attribution for 1 trend and 1 change point.

There were 180 streamgages with significant trends and 114 streamgages with significant change points in the 50-year analysis period. Short-term precipitation was the most common attribution in the 50-year period. Many areas of the Midwest region experienced changes in precipitation starting in the 1980s. In many cases, significant trends and change points in cumulative 3-day or 10-day precipitation were observed for the shorter 50-year period, but not for the 75-year period. Short-term precipitation accounted for 97 trends and 38 change points in the 50-year period and were clustered primarily in the central part of the Midwest region, centered in Indiana. Large artificial impoundments accounted for 16 trends and 12 change points, and urban effects accounted for 9 trends and 2 change points in the 50-year period. There were 58 trends and 62 change points with unknown attributions. Many streamgage watersheds saw increases in urban area that were concurrent with upward trends in short-term, cumulative precipitation. Because of methodological limitations in this study, it is not possible to determine which of these attributions was truly dominant in their effects on streamflow without additional site-specific information. In these cases, short-term precipitation was listed as the primary attribution and urban effects were listed as a secondary attribution as a matter of convention; however, both attributions are considered equally important.

In all the analyses, there were a large number of streamgages for which no attribution could be made. Due to a lack of available data and limitations in the scope of the study, there were many attributions that could not be fully investigated, such as effects from agricultural tile drainage or irrigation, surface-water or groundwater withdrawals, wastewater return flows, or snowpack-related changes. Some streamgages had data that indicated an attribution, but the evidence was not strong enough to meet the criteria for an attribution.

[1]U.S. Geological Survey.

Introduction

Reliable peak-streamflow estimates are critical for the design of infrastructure such as roads and bridges and for land-use planning. Conventional methods of flood-frequency analysis require peak-streamflow records with a constant long-term mean. There are many instances in which this assumption of stationarity of peak streamflows may not be met and for which traditional flood-frequency estimates may be unreliable. For example, changing land-use patterns, changes in precipitation, the construction of dams, or water diversions into or out of a basin can cause gradual trends or sudden changes in peak-streamflow records.

This chapter of the professional paper is part of a larger U.S. Geological Survey effort to identify and characterize changes in peak streamflows across the conterminous United States and to develop methods for flood-frequency estimation under nonstationary conditions (Barth and others, this volume, chap. A). This larger U.S. Geological Survey (USGS) effort builds upon a previous study by the USGS and the Federal Highway Administration of the U.S. Department of Transportation to identify statistically significant monotonic trends (gradual changes) and change points (sudden changes) in annual peak streamflows across the conterminous United States (Dudley and others, 2018; Hodgkins and others, 2019; Ryberg and others, 2019). As part of this larger USGS study, streamgages across the conterminous United States are geographically located within seven water-resources regions that are defined by two-digit hydrologic-unit codes (HUCs) in Seaber and others (1987), and a common analysis framework was developed to examine potential causal mechanisms for nonstationarity in annual peak streamflows in each of the seven water-resources regions (Barth and others, this volume, chap. A, fig. A1). Some minor modifications were made to the seven regions by moving subregions (defined by four-digit HUCs; Seaber and others, 1987) in the interest of geographic cohesiveness or hydrologic-setting similarity.

This chapter describes the potential causal factors associated with changing peak streamflows in the Midwest region. Water-resources regions and their associated HUCs within the Midwest region of the United States are shown on figure D1 and include:

- 04 (Great Lakes), minus subregions 0413 (Southwestern Lake Ontario), 0414 (Southeastern Lake Ontario), and 0415 (Northeastern Lake Ontario-Lake Ontario-St. Lawrence);
- 05 (Ohio); and
- 07 (Upper Mississippi).

The Midwest region includes approximately 500,000 square miles; it is bounded to the north by the Great Lakes, and it extends southward to include parts of Tennessee, Kentucky, and Virginia (fig. D1). The central part of the region is flat with some low hills. Land use within the central part of the region is primarily agricultural and includes several major metropolitan areas including Chicago, Ill., Detroit, Mich., and many other smaller cities (fig. D2). The northern areas of Michigan, Minnesota, and Wisconsin, along with the eastern edge of the region, are characterized by slightly more relief with primarily forested land cover.

Changes in the magnitude and timing of streamflow in the Midwest region over the past century have been documented in many studies, although the results of the studies can vary widely depending on the data, period of record, and statistical methodology used. Villarini and others (2011a) detected many change points in annual peak streamflows across the Midwest but identified fewer statistically significant changes in monotonic trends (hereinafter also referred to as just "trends"). Mallakpour and Villarini (2015) found no widespread evidence of trends in the magnitude of annual peak streamflows but did find significant trends in the frequency of floods. Both upward trends (Olsen and others, 1999) and downward trends (Gebert and Krug, 1996; Kochendorfer and Hubbart, 2010) have been found in peak streamflows in unregulated parts of the Upper Mississippi River Basin. More recently, Rice and others (2016) and Hodgkins and others (2019) have found both upward and downward trends throughout the Midwest region, which includes basins that are urbanized or regulated.

Changing peak streamflows can be caused by a combination of drivers, including both climatic influences and anthropogenic causes, such as land-use change or streamflow regulation. Climate-driven floods in the Midwest region are often caused by snowmelt and large convective systems and can be affected by large-scale ocean and atmospheric oscillations (Rogers and Coleman, 2003; Tootle and others, 2005; Villarini and others, 2011a; Andresen and others, 2012). The Midwest region has experienced increases in annual precipitation since the 1930s, with the largest changes occurring in the later part of the 20th century (Andresen and others, 2012; Pathak and others 2017). Changes in both the frequency and magnitude of heavy rainfall events have been observed in the Midwest region, with primarily upward trends in Indiana, Michigan, and Ohio, and a mix of upward and downward trends in other States in the Midwest region (Angel and Huff, 1997; Kunkel, 2003). In addition to trends, change points have been identified in precipitation in the Midwest region, with most change points occurring in the later half of the 20th century (Villarini and others, 2011b; Pathak and others, 2017).

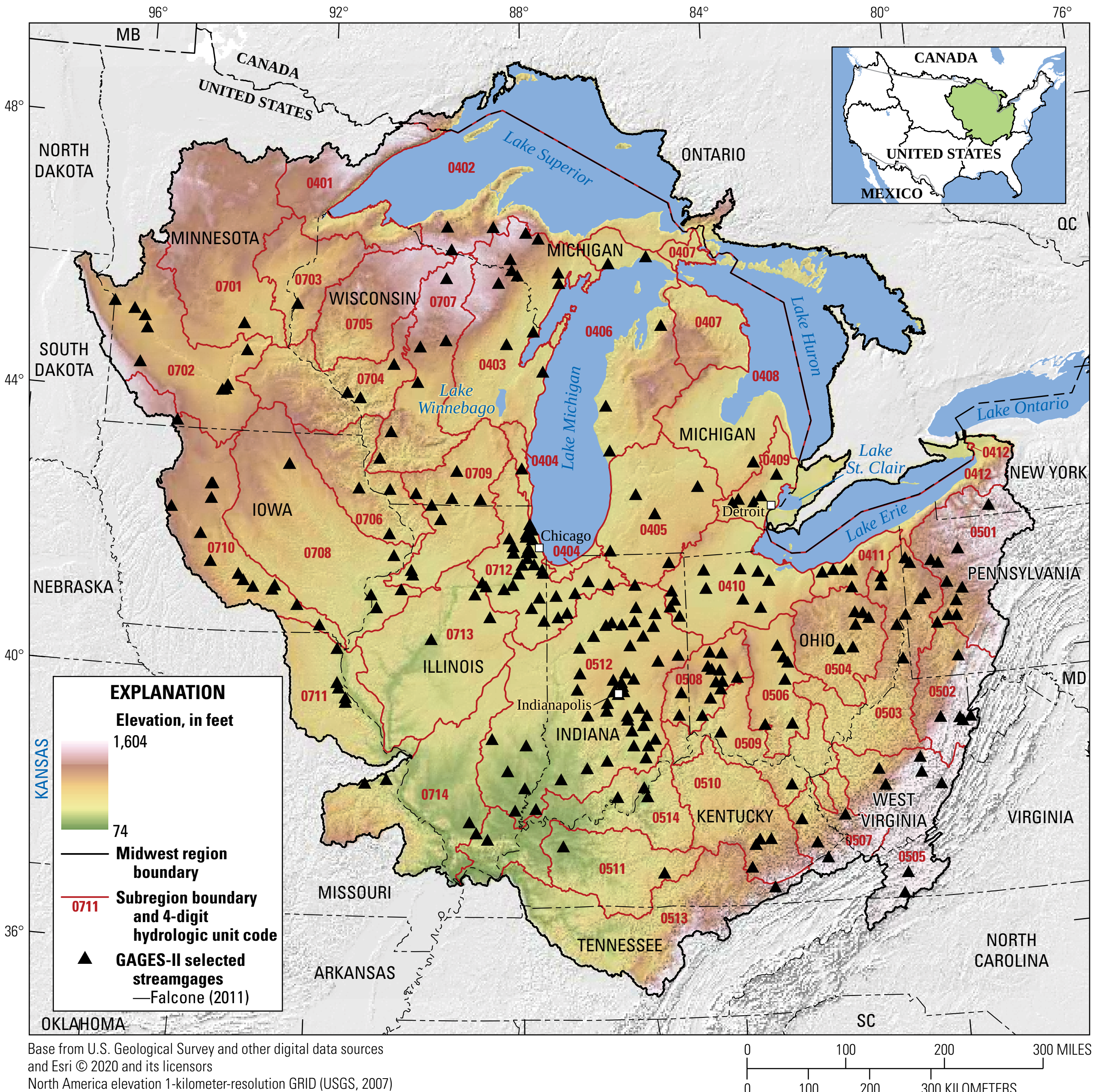

Base from U.S. Geological Survey and other digital data sources
and Esri © 2020 and its licensors
North America elevation 1-kilometer-resolution GRID (USGS, 2007)
Regional boundaries derived from modified HUC2 watersheds
USA Contiguous Albers Equal Area Conic USGS projection
North American Datum of 1983

Figure D1. Map showing the 261 U.S. Geological Survey streamgages selected for the attribution of monotonic trends and change points in annual peak streamflow within the Midwest region. For this study, the regions were based on watersheds identified by two-digit hydrologic unit codes (HUC2s) described by Seaber and others (1987), and some regions were modified slightly by adding or subtracting subregions (HUC4s) to achieve geographic cohesiveness or hydrologic-setting similarity. Note that although the northern part of the Midwest region extends into Canada because of the topography of stream drainage basins, the watersheds considered for the attributions of monotonic trends and change points are within the conterminous United States. Streamgage locations are from the National Water Information System (U.S. Geological Survey, 2020). GAGES-II, Geospatial Attributes of Gages for Evaluating Streamflow, Version II.

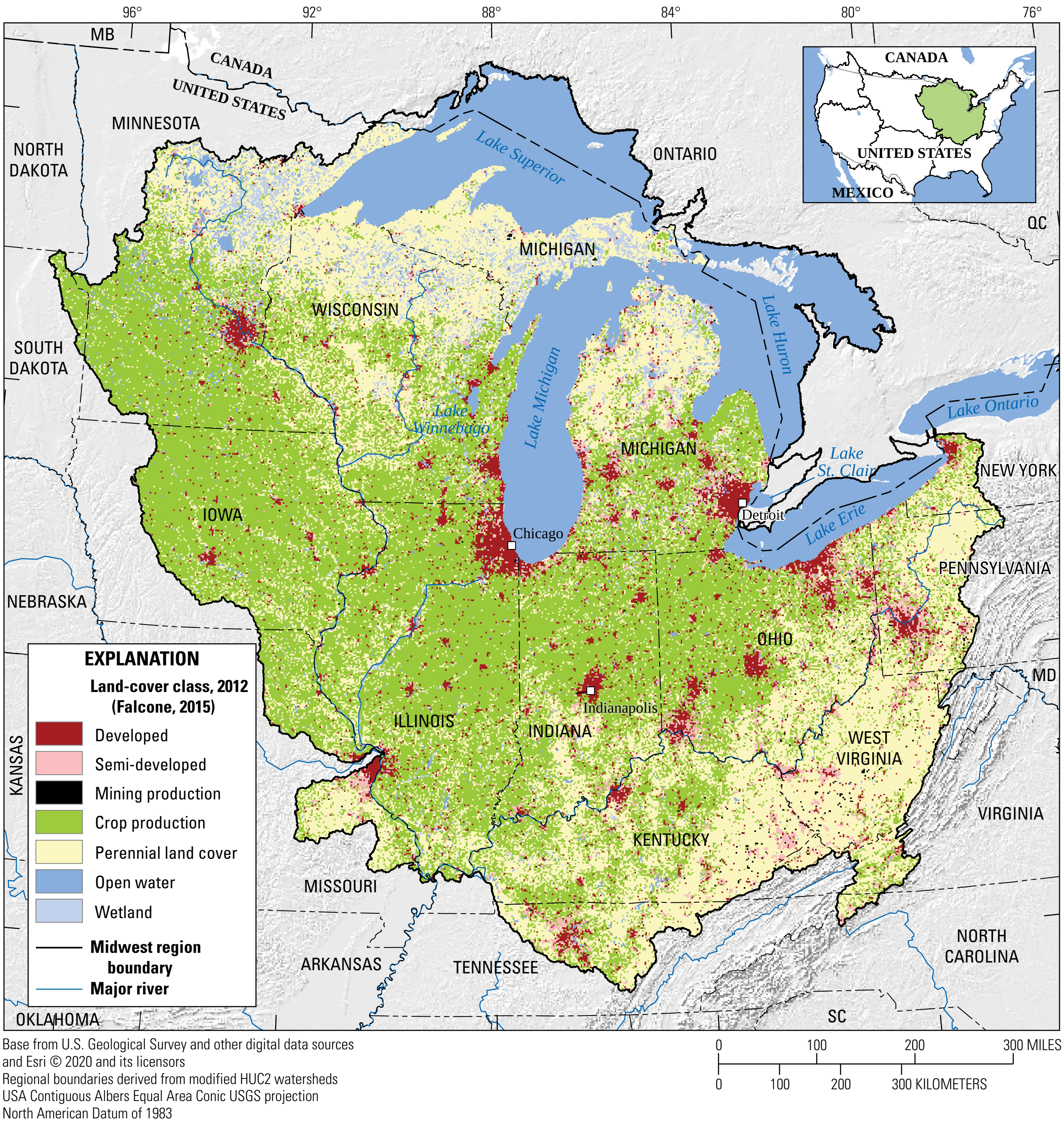

Figure D2. Map showing primary anthropogenic land-cover classes within the Midwest region in 2012. Land-cover classes are from Falcone (2015). Land-cover classes are also referred to as land-use classes in the report discussion.

There are many potential anthropogenic drivers of streamflow change, including changes in land use and land cover (fig. D2), the construction of dams, human water use, or other alterations of natural stream channels. Large-scale changes in land use in the Midwest region began in the mid-1800s with the conversion of forest and grasslands to agriculture (Steyaert and Knox, 2008). The conversion to agriculture was accompanied by drainage of wetland areas and the installation of tile drainage and agricultural ditching across the Midwest (Pavelis, 1987). Land-use change in the later part of the 20th century was predominantly urbanization, with developed land replacing agricultural land primarily in the southern part of the Midwest region and forested areas in the northern part of the Midwest region (Steyaert and Knox, 2008). Urbanization is associated with increased magnitude and frequency of floods because impervious surfaces reduce infiltration capacity of the watershed and accelerate runoff into nearby streams (Konrad and Booth, 2005).

The middle part of the 20th century experienced a large increase in the construction of dams, most of which were built between 1950 and 1970, with few dams constructed after 1980 (Graf, 1999). The majority of dams in the Midwest region are small- to medium-size dams, with storage capacity less than the annual runoff of the basin (Graf, 1999). Dams have a profound effect on streamflow downstream from the dam, affecting the magnitude, timing, and duration of streamflows, which then affect channel geomorphology, and ecological communities (Poff and others, 1997). Changes in magnitude, duration, and frequency of streamflows are often highly site specific and are related to regional hydroclimate, the size (storage capacity) of the dam, and specific dam operating rules (Magilligan and Nislow, 2005; FitzHugh and Vogel, 2011). McManamay (2014) found that dams used for a combination of flood control and water supply, and those used for hydropower, had the largest overall effect on streamflows. However, unlike all other classes of dams studied, hydropower dams occasionally caused an increase in annual peak streamflows.

This chapter attempts to attribute specific causes to monotonic trends and change points in annual peak streamflow across the Midwest region and builds upon the work of Hodgkins and others (2019), which identified statistically significant trends and change points in annual peak streamflow across the United States. At streamgages where changes in annual peak streamflow were identified, an attempt was made to assign primary attributions, and when necessary, secondary attributions to the streamflow changes. Prior to analysis, a list of all potential attributions of hydrologic change were compiled (Barth and others, this volume, chap. A). For each streamgage, available data and statistical tests (where possible) were used to evaluate evidence for causal relationships between streamflow trends and each of the potential attributions. The potential attributions with the strongest support were chosen as the primary and sometimes secondary attributions. Differences in the spatial and temporal precision of the available data sources, and limitations in the statistical methodology, complicated efforts to directly compare different potential attributions. In some cases, attributions were made with only limited evidence. Therefore, this study should be considered a first attempt at trend and change point attribution with the intent to aid future research in trend and change point analysis, and not as a definitive classification of attributions. Note that although the northern part of the Midwest region extends into Canada because of the topography of stream drainage basins, the watersheds considered for the attributions of trends and change points are within the conterminous United States.

Data and Methods

Hodgkins and others (2019) identified U.S. Geological Survey streamgages with statistically significant monotonic trends or change points for both a 50-year period for water years 1966–2015 and a 75-year period for water years 1941–2015. Trends are typically associated with gradual changes in the basin, such as land use or climate influences, while change points indicate a more abrupt change often caused by streamflow regulation. Trends were analyzed at each site using a Mann-Kendall test (Hodgkins and others, 2019). Change points were assessed using a Pettitt test (Pettitt, 1979). Within the Midwest region, a total of 261 sites that were identified by Hodgkins and others (2019) as having statistically significant trends or change points, were selected for further analysis in this study (fig. D1). Selected streamgages had drainage areas between 5.75 and 26,000 square miles, with a median of 450 square miles, and included both minimally altered and regulated basins across a variety of land-cover classes.

For streamgages in this study, an attempt was made to assign causal attributions to each trend or change point. Prior to beginning the analyses, a list of potential causal mechanisms of changing peak-streamflow patterns was developed for all the regions and is described in more detail in Barth and others (this volume, chap. A). Not all of the potential attributions identified in Barth and others (this volume, chap. A) could be analyzed in the Midwest region because of limitations in available data. The potential causal attributions that were considered for this study are described below and include urban effects (land-use change), the presence of large artificial impoundments, and short-term cumulative precipitation.

A set of decision rules was developed to determine whether each potential attribution was a likely driver of hydrologic change in the peak-streamflow time-series data (table D1). Attributions were given a level of evidence, which corresponds to the strength and confidence in the available data. Attributions were determined to have levels of robust evidence, medium evidence, or limited evidence based on the specific set of decision criteria for each attribution. In general, a level of robust evidence required support from multiple well-documented data sources, strong consistent results (statistical significance or correlational evidence), and the attribution was consistent with causal mechanisms; a level of medium evidence required moderately consistent results (marginal statistical significance or correlational evidence); and a level of limited evidence indicated inconsistent results or limited sources (see Barth and others, this volume, chap. A, table A2, for more details on evidence levels). "Additional information required" is denoted in cases where there was insufficient evidence to make an attribution (see Levin and others, 2022). In cases where more than one causal factor could be attributed to the peak-streamflow change point or trend, the attribution with the highest level of evidence was typically listed as the primary attribution followed by the secondary attribution. In some cases, if there were two plausible attributions, it was not possible to determine which should be listed as primary. For example, if both urban effects and short-term precipitation have robust evidence for attribution, the methods in this study could not be used to determine which of the two has greater influence on the peak streamflow without acquiring additional site-specific information. In these cases, short-term precipitation was listed as the primary attribution for consistency; however, both attributions are considered equally important.

Table D1. Decision criteria used to determine primary attributions of monotonic trends and change points at 261 U.S. Geological Survey streamgages located within the Midwest region.

[The ***p***-values were obtained from a Pettitt test for change points or Mann-Kendall test for monotonic trends (Mann, 1945; Pettitt, 1979). A ***p***-value is the probability that the observed peak streamflows would occur under stationary (no monotonic trend or change point) conditions. Data are from Levin and others (2022), which is part of the data release by York and others (2022)]

Attribution	Decision criteria	Level of evidence	Threshold for level of evidence
Urban effects	Increase in the proportion of developed land within the basin, concurrent with an upward monotonic trend in peak streamflow	Robust evidence	Increase greater than 25 percent of developed land in the watershed
		Medium evidence	Increase greater than 15 percent, but less than 25 percent, of developed land in the watershed
		Limited evidence	Increase greater than 5 percent, but less than 15 percent, of developed land in the watershed; or other reasons specified in the attribution table (Levin and others, 2022)
Large artificial impoundments	Increasing basin storage, concurrent with a decreasing change point in peak streamflow	Robust evidence	Increase in cumulative storage from impoundments within the same decade as a decreasing change point in streamflow, with corroborating information in streamgage annual reports
		Medium evidence	Increase in cumulative storage from impoundments within the same decade as a decreasing change point in streamflow, without corroborating information in streamgage annual reports
		Limited evidence	Decreasing change point in streamflow and regulation by dams indicated in annual reports, but with no change in cumulative storage or incomplete data regarding cumulative storage; or other reasons specified in the attribution table (Levin and others, 2022)
Short-term precipitation	Monotonic trend or change point in 3- or 10-day cumulative precipitation, concurrent with a monotonic trend or change point in peak streamflow in the same direction (both upward/increasing or both downward/decreasing)	Robust evidence	Statistically significant, cumulative, precipitation trend (p-value<0.05) and nonsignificant conditional trend test on streamflow (p-value>0.10); or statistically significant change point in cumulative precipitation (p-value<0.05) within 1 year of the change point in streamflow
		Medium evidence	Statistically significant, cumulative, precipitation trend (p-value between 0.05 and 0.10) and nonsignificant conditional trend test on streamflow (p-value>0.10); or statistically significant change point in cumulative precipitation (p-value<0.05) within 3 years of the change point in streamflow
		Limited evidence	Statistically significant, cumulative, precipitation trend (p-value<0.10) and statistically significant conditional trend test on streamflow (p-value<0.10); or statistically significant change point in cumulative precipitation (p-value<0.10) within 3 years of the change point in streamflow; or other reasons specified in the attribution table (Levin and others, 2022)

In some cases, exceptions to the decision criteria were made because of data irregularities or ambiguous statistical results. In these cases, the justification for the change was documented in the attribution table files (Levin and others, 2022) in the “Attribution notes and citations” column in each of the files. One source of ambiguity in the data was present in cases where statistical tests indicated that a streamgage had both a trend and a change point. In some cases, statistically significant results for both tests could indicate the presence of both a gradual change and an abrupt change that were caused by different mechanisms over time. In other cases, however, the gradual or abrupt nature of the change in streamflow may be difficult to determine from the two independent statistical tests, and the results of the statistical tests may not be reliable. Villarini and others (2009) show that performing a trend analysis in the presence of a step change can lead to the false conclusion that there is a monotonic trend and they recommend performing change-point tests first and performing trend tests on either side of the change point, if a change point is found. Rougé and others (2013) caution that there is no way for independent statistical tests to differentiate between gradual trends and abrupt step changes without visual confirmation by the analyst.

Figure D3 shows an example of a case where the statistical tests for trends and change points produce unreliable results requiring further examination and explanation. Figure D3*A* shows the peak-streamflow data at U.S. Geological Survey streamgage 03327500 located at the Wabash River in Peru, Indiana. The Mann-Kendall test for a monotonic trend over the 75-year period (water years 1941–2015) indicates a downward trend in annual peak streamflows at this site (fig. D3*A*). Note that peak-streamflow data for the years 1941 and 1942 were not available at this site. Despite a significant statistical result, the trend line is a poor fit for these data and does not adequately describe the nature of the change at this site. In figure D3*B*, a large decreasing change point was identified in water year 1966, which likely was caused by the construction of two large upstream flood control dams (Mississinewa Lake Dam in 1962 and Salaomonie Lake Dam in 1966) and trend tests were performed on either side of the change point. Performing trend tests on either side of the step change produced much different results; for example, trends were not observed prior to the change point, between water years 1941 and 1965, but there was an upward trend in annual peak streamflows after the change point, from water years 1967–2015, which coincides with a statistically significant upward trend in precipitation. In this case, if the statistical tests are performed independently, the upward trend observed after 1966 is not detected. For each site in this study, data were plotted and visually assessed to confirm that the results of the trend or change point tests were reasonable. In order to maintain consistency with the statistical methods in other chapters of this study, the trend tests were applied across the entire time period. However, descriptive notes were added to the attribution table (Levin and others, 2022) in cases where an exception to the attribution decision criteria was made because of mischaracterization by the statistical trend or change-point tests.

Land-Use Attributions

The National Water-Quality Assessment Program (NAWQA) Wall-to-Wall Anthropogenic Land Use Trends (NWALT) dataset was used to investigate effects of land-use change (Falcone, 2015). The NWALT dataset maps the anthropogenic land use for years 1974, 1982, 1992, 2002, and 2012. The NWALT 60-meter gridded dataset contains 6 broad classes and 19 subclasses of anthropogenic land use. For this analysis, the NWALT low use and very low use, conservation classes were combined into one class. The NWALT production class, which contains mining, timber, crops, pasture/hay, and grazing potential subclasses, was divided into two classes: agriculture and mining/timber. NWALT classes for water, developed, and semi-developed land use were also used. Gridded spatial data for each land-use class were spatially aggregated for each streamgage watershed to compute the percentage of land within the watershed in each land-use class (developed, semi-developed, mining/timber, agriculture, low use/conservation, and water/wetlands).

Land-use changes in the Midwest region were largely related to increased urbanization concurrent with a decrease in either agricultural land or forested land. Urbanization is associated with monotonic increases in streamflow caused by gradually increasing impervious surface area and sewering, which reduces the infiltration capacity of the basin and shortens runoff times after a precipitation event (Konrad and Booth, 2005). Urban effects were attributed to streamgages with upward monotonic trends concurrent with an increase of at least 5 percent of developed land in the watershed between 1974 to 2012. Sites with greater increases in developed land were assigned a higher level of evidence. Table D1 shows the decision criteria for each level of evidence for the attribution of urban effects.

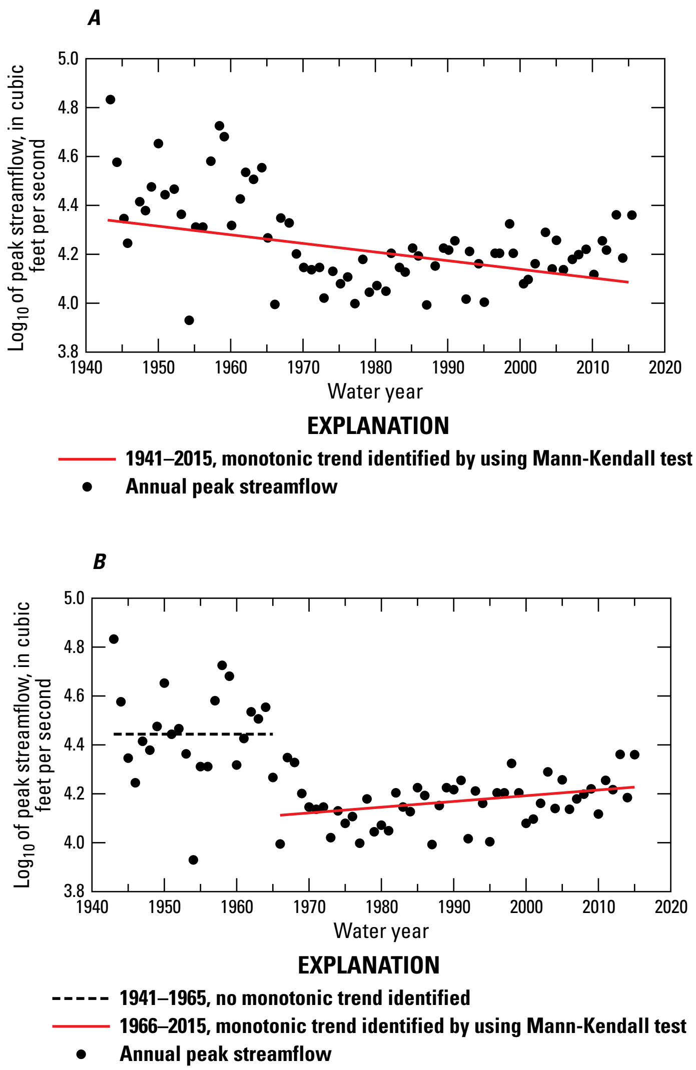

Figure D3. Graphs showing annual peak streamflows (black dots) at U.S. Geological Survey streamgage 03327500 located at the Wabash River in Peru, Indiana. *A*, The Mann-Kendall test for a monotonic trend during the 75-year period (water years 1941–2015, see red line) indicates a downward monotonic trend in annual peak streamflows at the site and does not accurately characterize the change in peak streamflow (shown in *B*); *B*, A large decreasing change point in annual peak streamflow (identified in water year 1966) is followed by a statistically significant upward monotonic trend identified using the Mann-Kendall test (see red line, p-value<0.01); the dashed black line in *B* shows no monotonic trend was identified between water years 1941 and 1965, prior to the 1966 change point. Peak streamflow data are from the National Water Information System (U.S. Geological Survey, 2020). No data are available for water years 1941 and 1942.

Short-Term Precipitation

Daily precipitation data from the National Centers for Environmental Information’s Global Historical Climatology Network (National Oceanic and Atmospheric Administration, 2019) were used to examine the relation between changes in cumulative precipitation and peak-streamflow trends. Average daily precipitation was calculated using all of the precipitation gages within the streamgage watershed boundary. If there were fewer than seven precipitation gages within the watershed, the next nearest precipitation gages to the streamgage were used until a minimum of seven stations were found. Because of differences in basin size and drainage properties, the optimal duration of cumulative precipitation to use for the relation with peak streamflows may vary. The cumulative 3-day and 10-day basin precipitation was calculated as the sum of the daily mean precipitation for the watershed prior to and including the day of each peak streamflow. In most cases, the 10-day cumulative precipitation had the strongest statistical trends, but at some streamgages, the 3-day precipitation was used if it yielded a more robust statistical relation. When 3-day cumulative precipitation was used, it was noted in the “Attribution notes and citations” column in the attribution table (Levin and others, 2022).

The Mann-Kendall test (Mann, 1945) was used to determine if a monotonic trend in cumulative 3- or 10-day precipitation was present. If a trend was detected in the cumulative precipitation, a partial Mann-Kendall test was used to evaluate the statistical significance of the peak-streamflow trend conditioned on the trend in precipitation (Libiseller and Grimvall, 2002). If the partial Mann-Kendall test was not statistically significant (*p*-value>0.10), then there is insufficient evidence that a trend exists in the peak streamflow after removing the effect of precipitation. A nonsignificant, partial Mann-Kendall test was considered evidence that the trend in peak streamflow is explained by the trend in precipitation. Short-term precipitation was listed as a primary attribution if the precipitation trend was statistically significant and the slope had the same sign (positive or negative) as the peak-streamflow trend. Table D1 lists the decision criteria for each level of evidence for a short-term precipitation attribution.

Although changes in precipitation are typically considered gradual changes, there have been change points identified in precipitation patterns in the Midwest region (Villarini and others, 2011b; Rahmani and others, 2015). For peak streamflow sites with change points, a Pettitt test (Pettitt, 1979) was performed on the cumulative precipitation time series. If the Pettitt test result was statistically significant (*p*-value<0.10), in the same direction (increasing or decreasing) as the change in peak streamflows, and the date of the change point in precipitation was within 3 years of the change point in peak streamflows, short-term precipitation was listed as an attribution. Table D1 lists the decision criteria for the level of evidence for a short-term precipitation attribution for significant change points in peak streamflow.

Impoundments

The cumulative storage of impoundments within each streamgage watershed is available in the Geospatial Attributes of Gages for Evaluating Streamflow, Version II (GAGES-II) dataset (Falcone, 2011). Storage information is available for 7 years (1940, 1950, 1960, 1970, 1980, 1990, and 2009). This information was used in conjunction with the remarks in the streamgage water-year summary (U.S. Geological Survey, 2020) to identify where dams may be causing changes in peak streamflow. Information in the water-year summaries may be inconsistent between streamgages as there is no requirement to identify upstream impoundments, diversions, or other effects to streamflow at a streamgage, and the level of detail included in the water-year summaries can vary widely. Therefore, this information was primarily used to corroborate the data in the GAGES-II dataset and provide additional confidence in the attribution. Although chapter A of this report (Barth and others, this volume) identifies large artificial impoundments and small artificial impoundments as two separate attributions for consideration in the analysis framework, there often was not enough information available to adequately distinguish the type of impoundments present in a streamgage watershed. Therefore, for the Midwest region, all impoundments were classified as large artificial impoundments in order to maintain a consistent terminology as defined in chapter A.

Impoundments are associated with decreasing change points in peak streamflows and a decrease in variability. In order to be considered a potential attribution for a change point, the construction of the dam had to be built concurrent with the observed, decreasing change point in streamflow. In some cases, specific dam names and dates of construction were listed in the water-year summary for the streamgage (U.S. Geological Survey, 2020). However, in most cases, the date of the dam construction was not available, and the decadal increase in cumulative storage was used to identify the decade in which a dam was constructed. Table D1 shows the decision criteria for each level of evidence for large artificial impoundments attribution.

Attributions of Monotonic Trends and Change Points in Annual Peak Streamflow

Causal attributions of statistically significant monotonic trends and change points in annual peak streamflows in the Midwest region for 261 USGS streamgages for the 75-year period (water years 1941–2015) and the 50-year period (water years 1966–2015) are documented in the attribution tables (Levin and others, 2022). The results of the analyses are described here and summarized in tables D2 and D3. There was a mix of both upward and downward trends and change points in annual peak streamflow across the Midwest region. Downward trends and decreasing change points were found primarily in Wisconsin, the upper peninsula of Michigan, and the southeastern part of the Midwest region in Kentucky, Ohio, and Pennsylvania, while upward trends and increasing change points were located primarily along the western edge and around the central part of the Midwest region (fig. D4).

Table D2. Primary and secondary attributions of monotonic trends and change points in annual peak streamflow at 261 U.S. Geological Survey streamgages for the 75-year period (water years 1941–2015) and the 50-year period (water years 1966–2015).

Primary attribution	Secondary attribution	Number of streamgages			
		Monotonic trend, 1941–2015	Monotonic trend, 1966–2015	Change point, 1941–2015	Change point, 1966–2015
Urban effects	Large artificial impoundments	0	1	1	2
	None listed	1	8	0	0
	Total	1	9	1	2
Large artificial impoundments	Short-term precipitation	0	2	1	0
	None listed	47	14	43	12
	Total	47	16	44	12
Short-term precipitation	Large artificial impoundments	0	0	4	1
	Urban effects	8	28	3	1
	None listed	30	69	10	36
	Total	38	97	17	38
Unknown		36	58	43	62
	Grand total	122	180	105	114

Table D3. Magnitude of change in annual peak streamflow at 261 U.S. Geological Survey streamgages with statistically significant monotonic trends and change points for the 75-year period (water years 1941–2015) and the 50-year period (water years 1966–2015).

Primary attribution	Median percentage change in peak streamflows, based on Sen's slope (Sen, 1968)		Median percentage change in peak streamflows, before and after change point	
	Monotonic trend, 1941–2015	Monotonic trend, 1966–2015	Change point, 1941–2015	Change point, 1966–2015
Urban effects	45.6	41.3	36.6	29.7
Large artificial impoundments	−39.2	−44.2	−34.3	−46.4
Short-term precipitation	56.0	55.7	38.7	51.9
Unknown	44.1	61.0	40.0	30.6

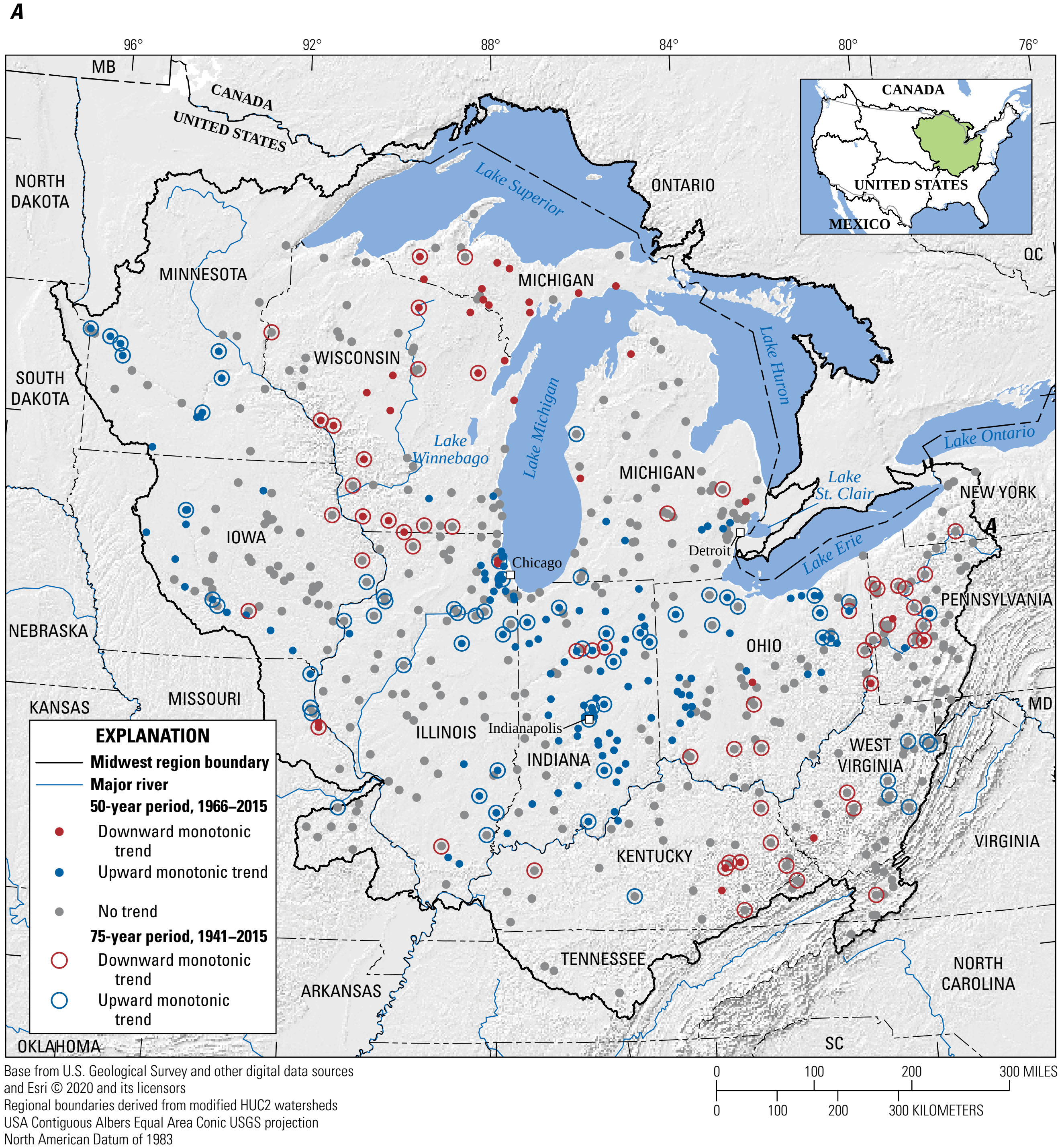

Figure D4. Maps showing the locations of 261 U.S. Geological Survey streamgages in the Midwest region with statistically significant monotonic trends and change points in annual peak streamflow during the 50-year period, water years 1966–2015, and the 75-year period, water years 1941–2015. *A*, Monotonic trends during the 50- and 75-year periods. *B*, Change points during the 50- and 75-year periods. The GAGES-II selected streamgages are from Falcone (2011). Peak streamflow data are from the National Water Information System (U.S. Geological Survey, 2020). GAGES-II, Geospatial Attributes of Gages for Evaluating Streamflow, Version II.

B

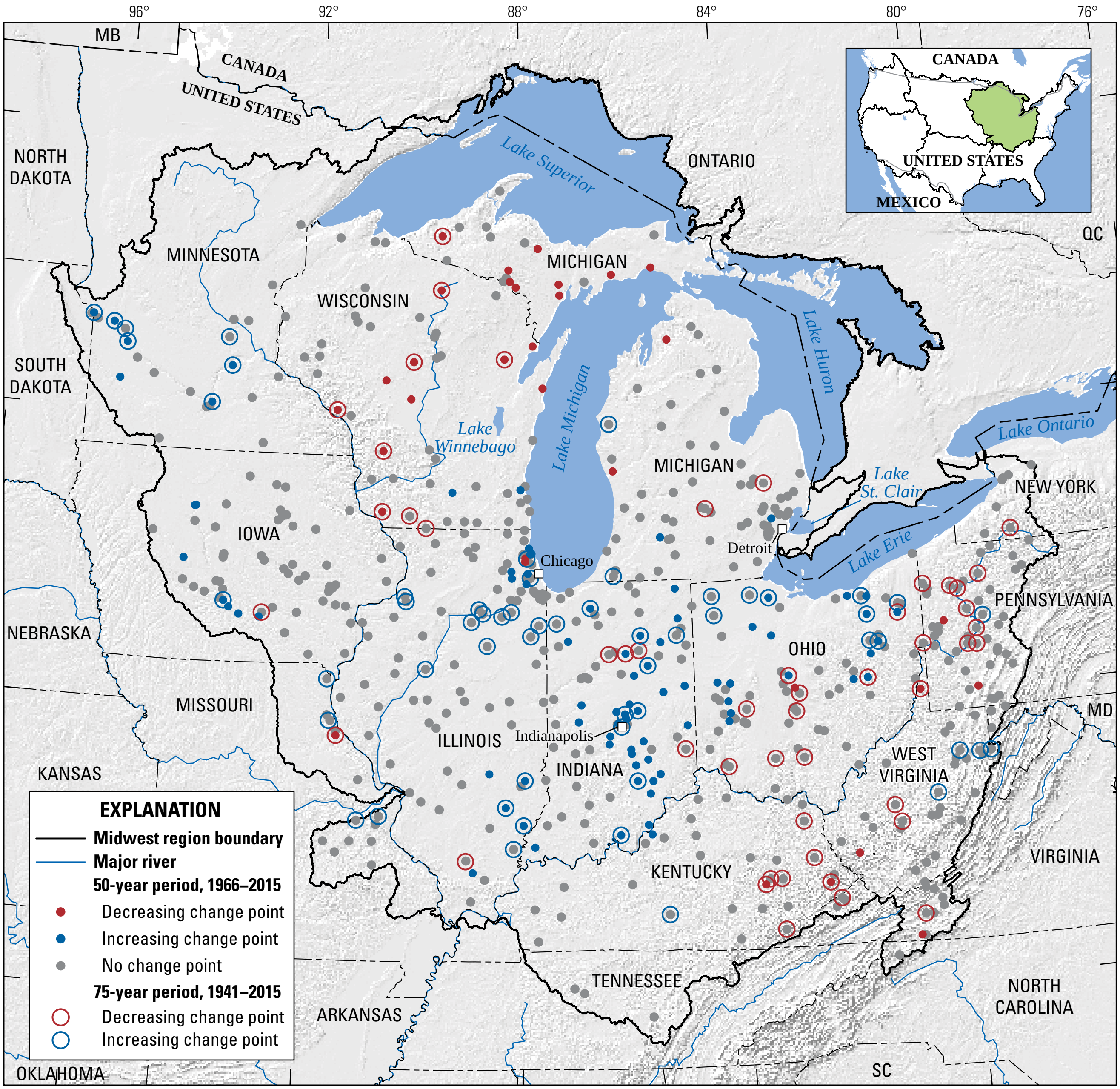

Base from U.S. Geological Survey and other digital data sources
and Esri © 2020 and its licensors
Regional boundaries derived from modified HUC2 watersheds
USA Contiguous Albers Equal Area Conic USGS projection
North American Datum of 1983

Figure D4. —Continued

Attributions of Monotonic Trends and Change Points in Annual Peak Streamflow for the 75-Year Analysis Period, Water Years 1941–2015

There were 122 streamgages with significant trends for the 75-year analysis period (table D2). Trends at 47 streamgages were attributed to large artificial impoundments, making it the most common attribution for this analysis period. Of the 47 impoundment attributions, 41 had a robust or medium level of evidence and 6 had a limited level of evidence. Impoundments are typically associated with change points rather than trends. At most streamgages where trends were attributed to impoundments, a significant change point in the peak streamflow was also identified and attributed to impoundments. In these cases, the test for a trend was influenced by the presence of the change point and it mischaracterized the type of change that was occurring, as in the example in figure D3. In most cases, there was not a significant trend either prior to or after the change point. There were four downward trends attributed to impoundments that did not have a corresponding change point. At these four streamgages, the notes in the water-year summaries (U.S. Geological Survey, 2020) indicated that many smaller dams were located upstream and there are corresponding increases in basin storage. In these cases, the presence of several smaller dams is likely decreasing the peak streamflows; however, because the dams were put in place at different times and were small in magnitude, the overall effect on streamflow is a downward trend. Short-term precipitation was attributed to trends at 38 streamgages (table D2), 21 with a robust or medium level of evidence and 17 with a limited level of evidence. Eight of the trends attributed with a short-term precipitation had urban effects as a secondary attribution. For these streamgages, the attribution primarily responsible for the upward trends in peak streamflows could not be determined, and both primary and secondary attributions are considered equally important. Urban effects were attributed to trends at one streamgage with a limited level of evidence. Trends at the remaining 36 streamgages have unknown primary or secondary attributions.

There were 105 streamgages with statistically significant change points for the 75-year analysis period (table D2). Large artificial impoundments was the primary attribution for change points at 44 streamgages, 41 with a robust or medium level of evidence, and 3 with a limited level of evidence. Short-term precipitation was the primary attribution for change points at 17 streamgages, 9 with a robust or medium level of evidence, and 8 with a limited level of evidence. There was one change point listed with urban effects as a primary attribution. Urban effects are typically considered an attribution for a monotonic trend; however, in this case there was a large artificial impoundment put in place concurrent with the change point and a substantial increase in developed land. Urbanization of this watershed likely is responsible for the overall higher peak streamflows; however, the dam likely mitigates those peak streamflows, preventing an upward trend. This site had a limited level of evidence. Finally, there were 43 streamgages with an unknown primary attribution.

Attributions of Monotonic Trends and Change Points in Annual Peak Streamflow for the 50-Year Analysis Period, Water Years 1966–2015

There were 180 streamgages with significant trends for the 50-year analysis period (table D2). Large artificial impoundments accounted for 16 primary attributions: 12 with a robust or medium level of evidence and 4 with a limited level of evidence. As with the 75-year trend analysis, streamgages at which trends were attributed to impoundments also had change points that were attributed to impoundments that likely confounded the results of the statistical test used to detect a trend. Short-term precipitation was attributed to 97 trends, which was the most common primary attribution for the 50-year analysis period. Short-term precipitation had a robust or medium level of evidence at 59 streamgages and a limited level of evidence at 38 streamgages. Of the trends with a short-term precipitation attribution, 28 had urban effects as a secondary attribution. At these 28 streamgages, the attribution with the larger effect on peak streamflow could not be determined and both are considered equally important without additional data. Urban effects was listed as a primary attribution for 9 trends, with robust or medium level of evidence at 6 streamgages and limited level of evidence at 3 streamgages. There were 58 trends with unknown primary or secondary attributions.

There were 114 streamgages with change points in the 50-year analysis period (table D2). Large artificial impoundments were listed as primary attributions for 12 change points, 6 with a robust or medium level of evidence, and 6 with a limited level of evidence. Short-term precipitation was attributed to 38 change points, 34 with a robust or medium level of evidence, and 4 with a limited level of evidence. Urban effects were listed as primary attributions for two increasing change points. In these cases, as with the change-point analysis for the 75-year period, large artificial impoundments were listed as a secondary attribution with a concurrent increase in developed land. It is likely, in these cases, that the urban increases were primarily the cause of the increase in peak streamflow; however, the concurrent construction of the dam prevented a significant trend from developing further. Finally, there were 62 streamgages that had unknown primary or secondary attributions.

In all four analyses, there were many streamgages for which primary attributions could not be determined. There are many potential attributions, which were not considered because of a lack of available data, including surface-water and groundwater withdrawals, wastewater return flows, interbasin water transfers, and snowpack-related changes (Barth and others, this volume, chap. A, table A1). Changes in agricultural practices also could not be adequately examined because of a lack of available data; however, other studies have indicated that the prevalence of tile drainage systems in the Midwest region can increase streamflow or amplify changes in streamflow caused by precipitation changes (Kelly and others, 2017).

Many trends and change points with an unknown primary attribution had evidence that indicated an attribution but did not meet the minimum criteria in table D1. For example, in the 50-year period, there were 62 change points with an unknown attribution. Of these, 24 had either trends in precipitation that were concurrent with the change point in peak streamflows, or a change point in precipitation that was greater than 3 years apart from the peak-streamflow change point. These cases do indicate that short-term precipitation may have some role in the increase in annual peak streamflows; however, the evidence did not meet the minimum decision criteria in table D1. The precise mechanism causing a change point in peak streamflow without a concurrent change point in precipitation is unclear and would need additional investigation. Similar evidence was present for urban effects and large artificial impoundments but would need additional data or investigation in order to determine an attribution. Detailed notes regarding streamflow trends, precipitation, land use, and known streamflow regulation are listed in the column labeled as “Attribution notes and citations” for each site in the attribution tables (Levin and others, 2022).

Maps in figure D5*A*–*D* show the geographic distribution of primary and secondary attributions. Streamgages with urban effects listed as a primary or secondary attribution were primarily located around some of the largest metropolitan areas in the region, for example, Chicago, Detroit, and Indianapolis. Streamgages with short-term precipitation attributions were located throughout the Midwest region but had the highest concentration in Indiana, Minnesota, and the eastern parts of Illinois. Large artificial impoundments attributions were located along the eastern edge of the Midwest region from western Pennsylvania south through Ohio, West Virginia, and eastern Kentucky. There is also a smaller cluster of large artificial impoundment attributions located in southern Wisconsin.

The magnitude of change in trends and change points in peak streamflow across the United States was calculated by Dudley and others (2018) and the data are summarized in table D3 and figure D6 for sites in the Midwest region. For change points, the change is calculated as the change in the median annual peak streamflow before and after the change point expressed as a percentage. For monotonic trends, the slope of the trend line was estimated using Sen’s slope (Sen, 1968), and the change in the magnitude of peak streamflow across the two time periods was calculated using the slope and expressed as a percentage (Dudley and others, 2018). All changes associated with large artificial impoundments were decreases in peak-streamflow magnitude, with the median change ranging from −46.4 to −34.3 percent across the four analyses (table D3, fig. D6). Trends and change points with urban effects as the primary attribution had increasing annual peak streamflow, with the median change ranging from 29.7 to 45.6 percent across analyses. Changes in annual peak streamflow associated with short-term precipitation were mostly increasing, although there were several streamgages with downward trends or decreasing change points that were attributed to short-term precipitation, including 3 streamgages in the 75-year trend analysis, 2 streamgages in the 50-year trend analysis, and 1 streamgage in the 50-year change-point analysis (Levin and others, 2022). Trends and change points with unknown attributions had a mix of increasing and decreasing annual peak streamflows.

A

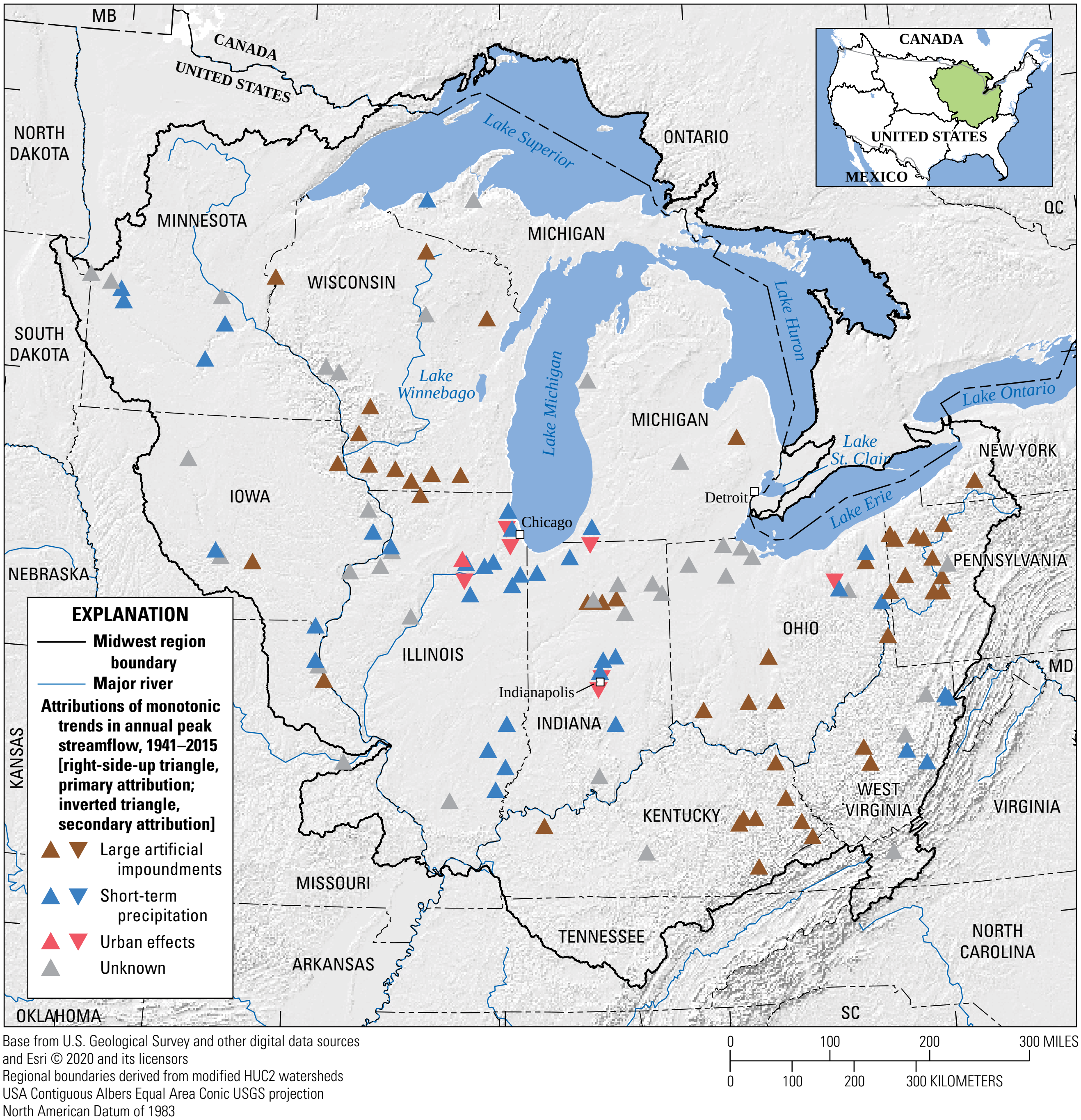

Figure D5. Maps of the Midwest region showing the primary and secondary attributions of monotonic trends and change points in annual peak streamflow at 261 U.S. Geological Survey streamgages for the 75- and 50-year periods. *A*, Primary and secondary attributions of monotonic trends in annual peak streamflow for the 75-year period (water years 1941–2015). *B*, Primary and secondary attributions of monotonic trends in annual peak streamflow for the 50-year period (water years 1966–2015). *C*, Primary and secondary attributions of change points in annual peak streamflow for the 75-year period (water years 1941–2015). *D*, Primary and secondary attributions of change points in annual peak streamflow for the 50-year period (water years 1966–2015). The GAGES-II selected streamgages are from Falcone (2011). Peak-streamflow data were obtained from the National Water Information System (U.S. Geological Survey, 2020). GAGES-II, Geospatial Attributes of Gages for Evaluating Streamflow, Version II.

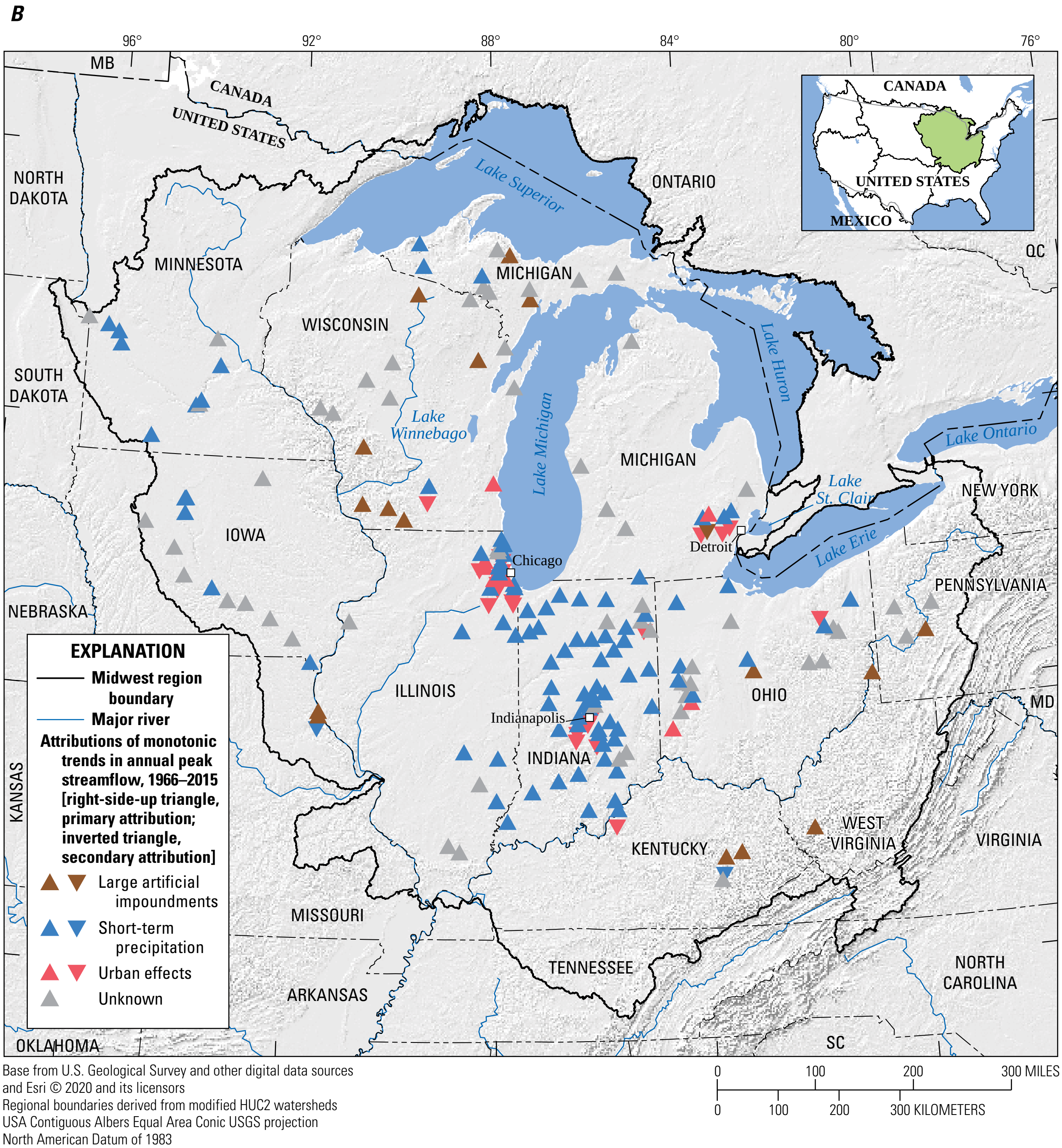

Figure D5. —Continued

C

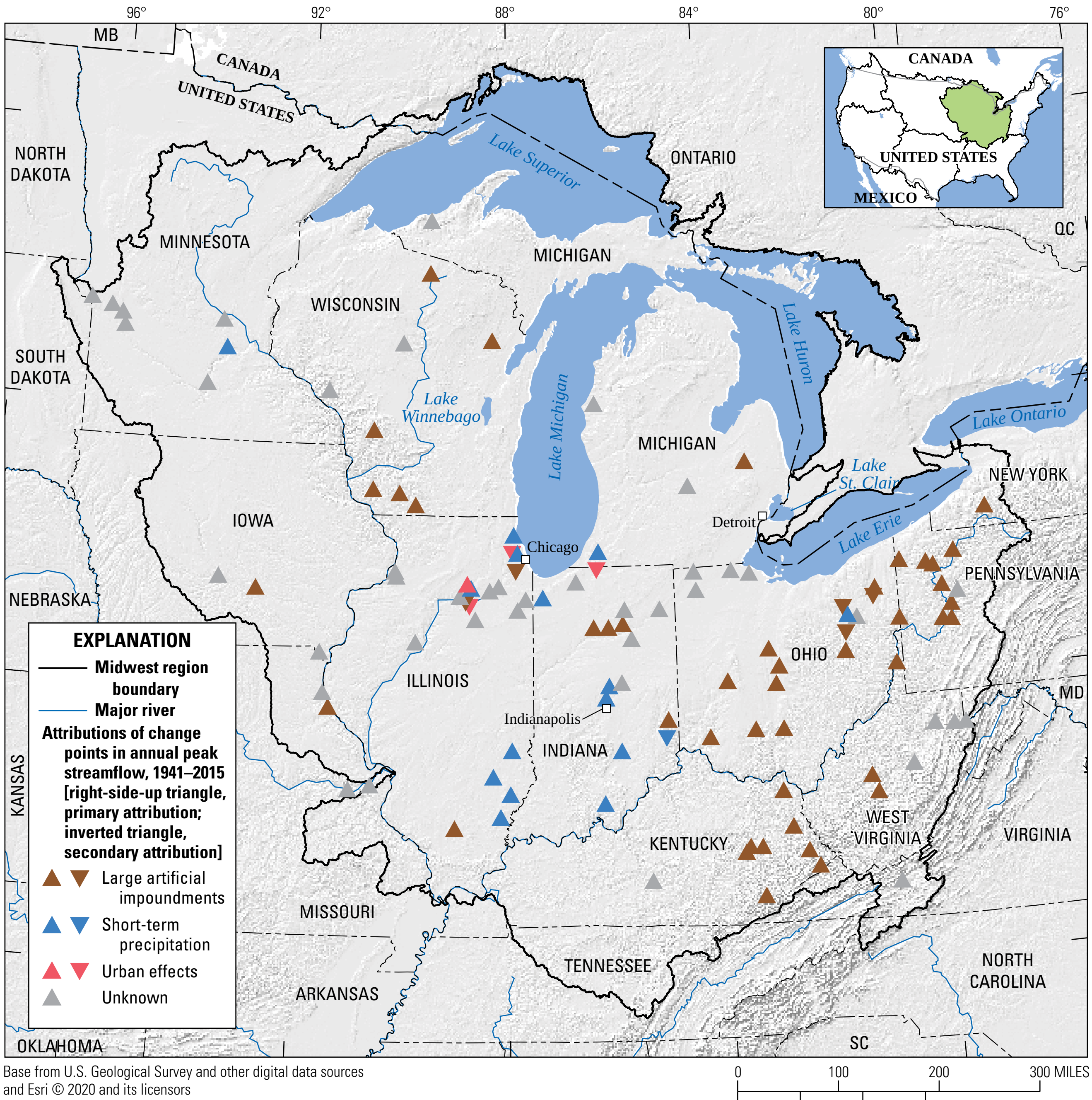

Base from U.S. Geological Survey and other digital data sources
and Esri © 2020 and its licensors
Regional boundaries derived from modified HUC2 watersheds
USA Contiguous Albers Equal Area Conic USGS projection
North American Datum of 1983

Figure D5. —Continued

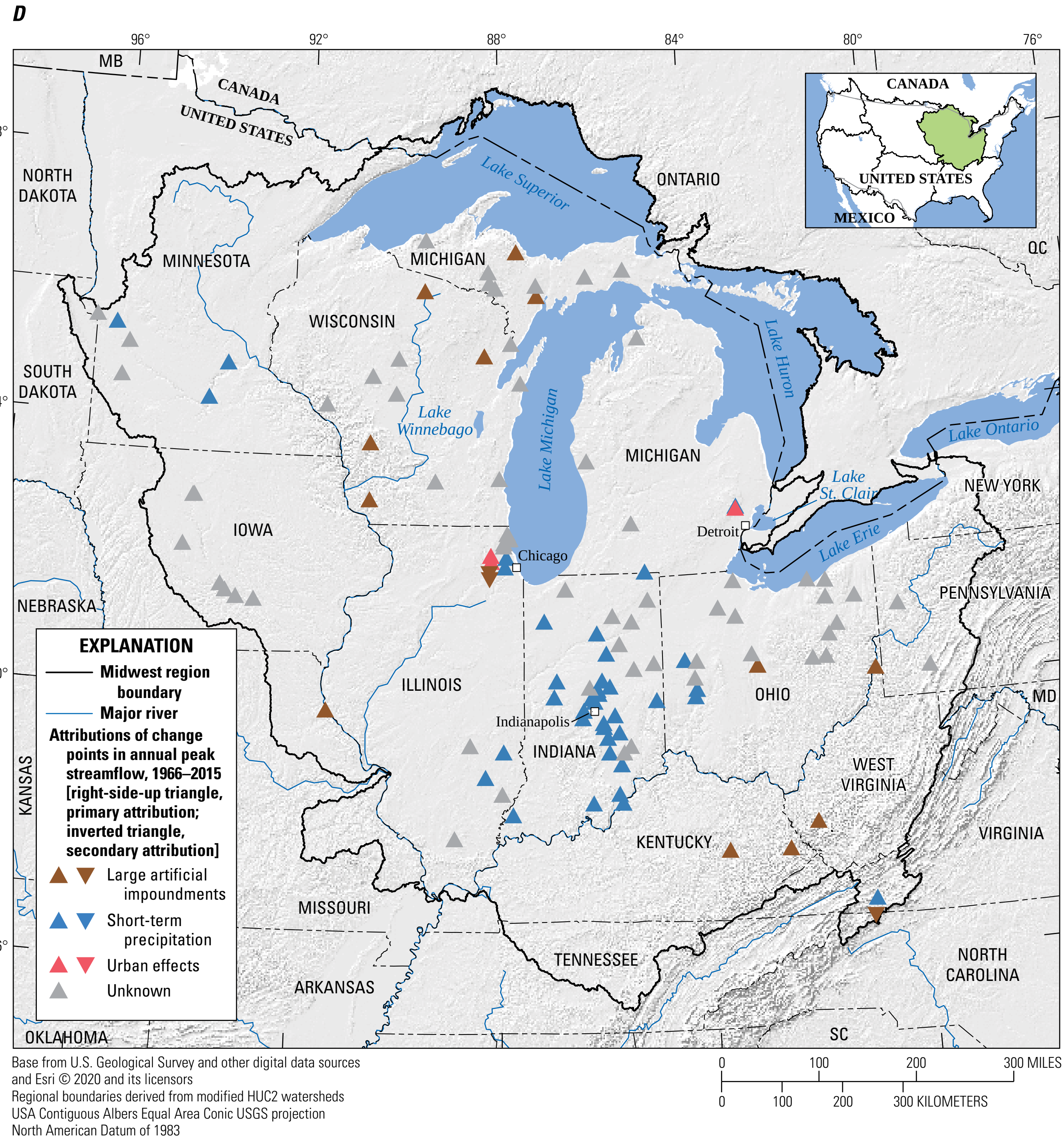

Figure D5. —Continued

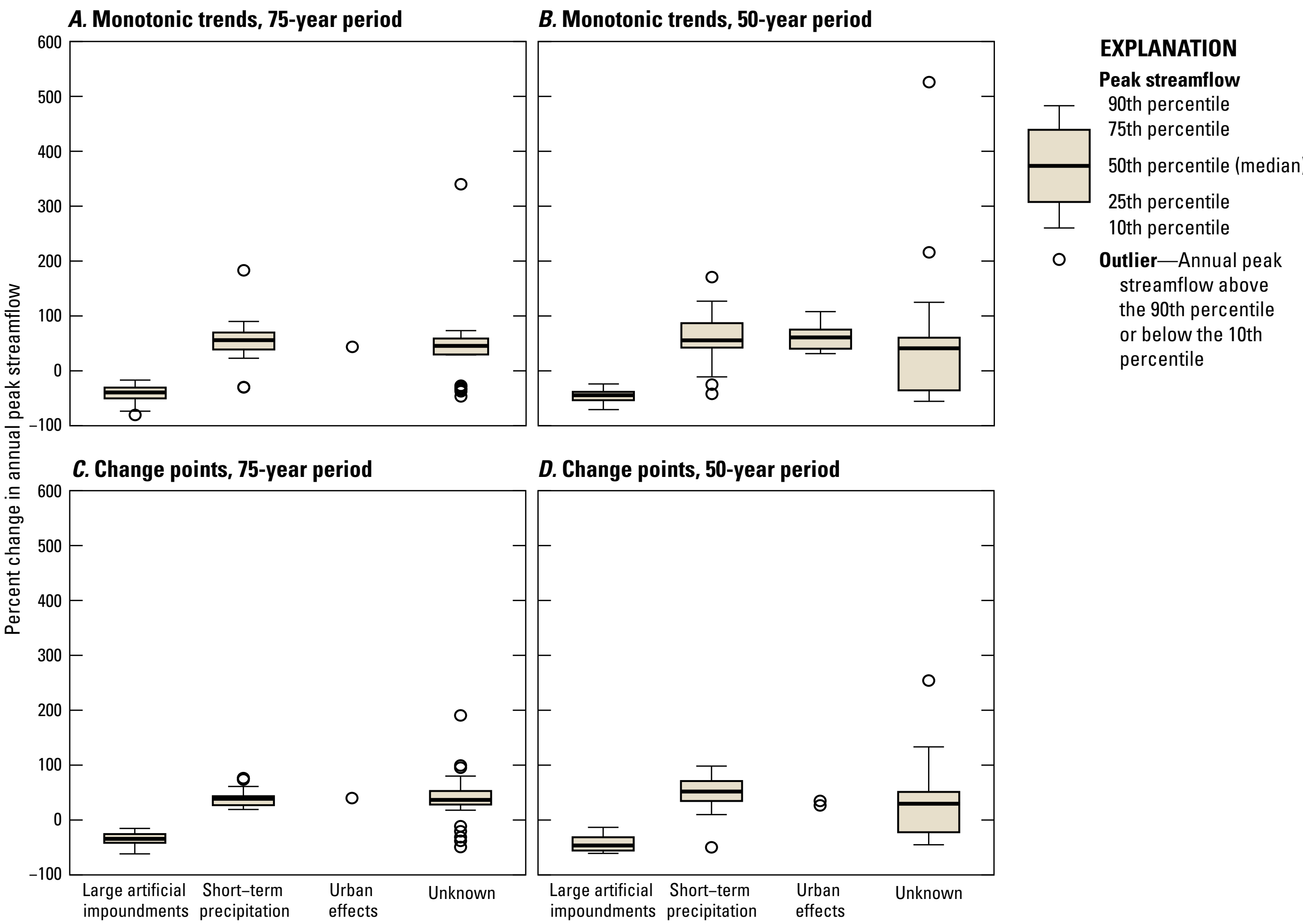

Figure D6. Boxplots showing the percentage change in annual peak streamflow by primary attribution for 261 U.S. Geological Survey streamgages with statistically significant monotonic trends and change points for the 75- and 50-year periods. *A*, Primary attributions of monotonic trends for the 75-year period (water years 1941–2015). *B*, Primary attributions of monotonic trends for the 50-year period (water years 1966–2015). *C*, Primary attributions of change points for the 75-year period (water years 1941–2015). *D*, Primary attributions of change points for the 50-year period (water years 1966–2015). Parts *A*, *C*, and *D* show no boxplots for urban effects because sample size was too small (not enough streamgages affected by urban effects). Peak-streamflow data were obtained from the National Water Information System (U.S. Geological Survey, 2020).

Summary

This study is one part of a larger U.S. Geological Survey effort to identify and characterize changes in annual peak streamflow across the conterminous United States in order to develop methods of estimating flood-frequency under non-stationary conditions. Streamgages with significant trends or change points were identified previously by Hodgkins and others (2019) for the 75-year period for water years 1941–2015 and for the 50-year period for water years 1966–2015. This report evaluated streamgages in the Midwest region to determine the primary factors causing the observed monotonic trends or change points identified by Hodgkins and others (2019). A list of potential attributions for change points in peak streamflows was compiled by Barth and others (this volume, chap. A). Attributions that were considered in the Midwest region included urban effects, large artificial impoundments, and changes in short-term precipitation (table D2).

There were a total of 122 streamgages with significant trends and 105 streamgages with significant change points in the 75-year analysis period. Primary attributions of trends in this analysis period consisted of large artificial impoundments at 47 streamgages, short-term precipitation at 38 streamgages, urban effects at 1 streamgage, and unknown attributions at 36 streamgages. Primary attributions for change points in the 75-year analysis period consisted of large artificial impoundments at 44 streamgages, short-term precipitation at 17 streamgages, urban effects at 1 streamgage, and unknown attributions at 43 streamgages.

There were a total of 180 streamgages with significant trends and 114 streamgages with significant change points in the 50-year analysis period. Primary attributions of monotonic trends in this analysis period consisted of large artificial impoundments at 16 streamgages, short-term precipitation at 97 streamgages, urban effects at 9 streamgages, and unknown attributions at 58 streamgages. Primary attributions of change points in the 50-year analysis period consisted of large artificial impoundments at 12 streamgages, short-term precipitation at 38 streamgages, urban effects at 2 streamgages, and unknown attributions at 62 streamgages.

There were both increasing and decreasing changes in annual peak streamflow in all four analyses within the two periods. Large artificial impoundments accounted for most of the downward trends and decreasing change points, with the median change in annual peak streamflow ranging from −46.4 to −34.3 percent across the four different analyses. Trends and change points associated with large artificial impoundments were located primarily in Wisconsin and the upper peninsula of Michigan, and along the southeastern edge of the Midwest region. Short-term precipitation was primarily responsible for upward trends and increasing change points that were particularly prevalent in the State of Indiana and Illinois. The median change in annual peak streamflow from short-term precipitation ranged from 38.7 to 56.0 percent. Trends and change points attributed to urban effects were located around the major metropolitan cities in the region, mainly in Chicago, Detroit, and Indianapolis; changes attributed to urban effects had a median change ranging from 29.7 to 45.6 percent.

Causes of changes in annual peak streamflow may be highly site-specific and may arise as a combination of interactions between many different changes within the basin, which underscores the difficulty in undertaking a large regional or national-scale attribution study. Documentation of anthropogenic hydrologic changes within a basin such as water use, dam operational rules, diversions, or other structural changes to the stream channel are often not widely available. There were a large number of trends and change points for which no primary attribution could be made with the methods and data available for this study. In addition, there were many trends for which short-term precipitation and urban effects were both potential causes. In these cases, the relative importance of one attribution over the other could not be determined without more in-depth, site-specific analyses. Despite the limitations encountered in this study, the current work may help inform future efforts to develop flood-frequency estimation methods by identifying the regional geographic and temporal patterns in trend and change point attributions in the Midwest region.

References Cited

Andresen, J., Hilberg, S., and Kunkel, K., 2012, Historical climate and climate trends in the midwestern USA, *in* Winkler, J., Andresen, J., Hatfield, J., Bidwell, D., and Brown, D., coords., U.S. National Climate Assessment Midwest Technical Input Report: Great Lakes Integrated Sciences and Assessments Center, 18 p., accessed July 9, 2020, at http://glisa.umich.edu/media/files/NCA/MTIT_Historical.pdf.

Angel, J.R., and Huff, F.A., 1997, Changes in heavy rainfall in midwestern United States: Journal of Water Resources Planning and Management, v. 123, no. 4, p. 246–249, accessed July 9, 2020, at https://doi.org/10.1061/(ASCE)0733-9496(1997)123:4(246).

Dudley, R.W., Archfield, S.A., Hodgkins, G.A., Renard, B., and Ryberg, K.R., 2018, Peak-streamflow trends and change-points and basin characteristics for 2,683 U.S. Geological Survey streamgages in the conterminous U.S. (ver. 3.0, April 2019): U.S. Geological Survey data release, accessed January 4, 2020, at https://doi.org/10.5066/P9AEGXY0.

Falcone, J.A., 2011, GAGES-II—Geospatial attributes of gages for evaluating streamflow: U.S. Geological Survey dataset, accessed July 9, 2020, at https://doi.org/10.3133/70046617.

Falcone, J.A., 2015, U.S. conterminous wall-to-wall anthropogenic land use trends (NWALT), 1974–2012: U.S. Geological Survey Data Series 948, 33 p. plus appendixes 3–6 as separate files, accessed July 9, 2020, at https://doi.org/10.3133/ds948.

FitzHugh, T.W., and Vogel, R.M., 2011, The impact of dams on flood flows in the United States: River Research and Applications, v. 27, no. 10, p. 1192–1215, accessed July 9, 2020, at https://doi.org/10.1002/rra.1417.

Gebert, W.A., and Krug, W.R., 1996, Streamflow trends in Wisconsin's driftless area: Journal of the American Water Resources Association, v. 32, no. 4, p. 733–744, accessed July 9, 2020, at https://doi.org/10.1111/j.1752-1688.1996.tb03470.x.

Graf, W.L., 1999, Dam nation—A geographic census of American dams and their large-scale hydrologic impacts: Water Resources Research, v. 35, no. 4, p. 1305–1311, accessed July 9, 2020, at https://doi.org/10.1029/1999WR900016.

Helsel, D.R., Hirsch, R.M., Ryberg, K.R., Archfield, S.A., and Gilroy, E.J., 2020, Statistical methods in water resources: U.S. Geological Survey Techniques and Methods 4–A3, 458 p., accessed April 7, 2021, at https://doi.org/10.3133/tm4a3.

Hodgkins, G.A., Dudley, R.W., Archfield, S.A., and Renard, B., 2019, Effects of climate, regulation, and urbanization on historical flood trends in the United States: Journal of Hydrology, v. 573, p. 697–709, accessed July 9, 2020, at https://doi.org/10.1016/j.jhydrol.2019.03.102.

Kelly, S.A., Takbiri, Z., Belmont, P., and Foufoula-Georgiou, E., 2017, Human amplified changes in precipitation-runoff patterns in large river basins of the Midwestern United States: Hydrology and Earth System Sciences, v. 21, no. 10, p. 5065–5088, accessed July 9, 2020, at https://doi.org/10.5194/hess-21-5065-2017.

Kochendorfer, J.P., and Hubbart, J.A., 2010, The roles of precipitation increases and rural land-use changes in streamflow trends in the Upper Mississippi River Basin: Earth Interactions, v. 14, no. 20, p. 1–12, accessed July 9, 2020, at https://doi.org/10.1175/2010EI316.1.

Konrad, C.P., and Booth, D.B., 2005, Hydrologic changes in urban streams and their ecological significance: American Fisheries Society Symposium, v. 47, p. 157–177, accessed July 9, 2020, at http://faculty.washington.edu/dbooth/Konrad%20and%20Booth%20AFS.pdf.

Kunkel, K.E., 2003, North American trends in extreme precipitation: Natural Hazards, v. 29, no. 2, p. 291–305, accessed July 9, 2020, at https://doi.org/10.1023/A:1023694115864.

Levin, S.B., Totten, A.R., Holtschlag, D.J., and York, B.C., 2022, Attributions for nonstationary peak streamflow records in the Midwest region, 1941–2015 and 1966–2015, and supporting information, *in* York, B.C., Ryberg, K.R., Asquith, W.H., Chase, K.J., Dickinson, J.E., Dudley, R.W., Harden, T.M., Hodgkins, G.A., Holtschlag, D.J., Humberson, D.G., Konrad, C.P., Levin, S.B., Restivo, D.E., Sando, R., Sando, S.K., Swain, E.D., Tillery, A.C., and Totten, A.R., Attributions for nonstationary peak streamflow records across the conterminous United States, 1941–2015 and 1966–2015: U.S. Geological Survey data release, https://doi.org/10.5066/P9FOUVWG. [Data directly accessible at https://www.sciencebase.gov/catalog/item/5cd5be2ce4b0e8a309e46229.]

Libiseller, C., and Grimvall, A., 2002, Performance of partial Mann-Kendall tests for trend detection in the presence of covariates: Environmetrics, v. 13, no. 1, p. 71–84, accessed July 9, 2020, at https://doi.org/10.1002/env.507.

Magilligan, F.J., and Nislow, K.H., 2005, Changes in hydrologic regime by dams: Geomorphology, v. 71, nos. 1–2, p. 61–78, accessed July 9, 2020, at https://doi.org/10.1016/j.geomorph.2004.08.017.

Mallakpour, I., and Villarini, G., 2015, The changing nature of flooding across the central United States: Nature Climate Change, v. 5, p. 250–254, accessed July 9, 2020, at https://doi.org/10.1038/nclimate2516.

Mann, H.B., 1945, Nonparametric test against trend: Econometrica, v. 13, no. 3, p. 245–259, accessed July 9, 2020, at https://www.jstor.org/stable/pdf/1907187.pdf.

McManamay, R.A., 2014, Quantifying and generalizing hydrologic responses to dam regulation using a statistical modeling approach: Journal of Hydrology, v. 519, pt. A, p. 1278–1296, accessed July 9, 2020, at https://doi.org/10.1016/j.jhydrol.2014.08.053.

National Oceanic and Atmospheric Administration, 2019, National Oceanic and Atmospheric Administration, National Centers for Environmental Information web page: Global Historical Climate Network daily summaries—Precipitation: accessed May 15, 2019, at https://www1.ncdc.noaa.gov/pub/data/ghcn/daily/.

Olsen, J.R., Stedinger, J.R., Matalas, N.C., and Stakhiv, E.Z., 1999, Climate variability and flood frequency estimation for the upper Mississippi and lower Missouri Rivers: Journal of the American Water Resources Association, v. 35, no. 6, p. 1509–1523, accessed July 9, 2020, at https://doi.org/10.1111/j.1752-1688.1999.tb04234.x.

Pathak, P., Kalra, A., and Ahmad, S., 2017, Temperature and precipitation changes in the midwestern United States—Implications for water management: International Journal of Water Resources Development, v. 33, no. 6, p. 1003–1019, accessed July 9, 2020, at https://doi.org/10.1080/07900627.2016.1238343.

Pavelis, G.A., ed., 1987, Farm drainage in the United States—History, status and prospects: Department of Agriculture, Economic Research Service, Miscellaneous Publication Number 1455, 186 p., accessed July 9, 2020, at https://eric.ed.gov/?id=ED295043.

Pettitt, A.N., 1979, A non-parametric approach to the change-point problem: Journal of the Royal Statistical Society, Series C (Applied Statistics), v. 28, no. 2, p. 126–135, accessed July 9, 2020, at https://doi.org/10.2307/2346729.

Poff, N.L., Allan, J.D., Bain, M.B., Karr, J.R., Prestegaard, K.L., Richter, B.D., Sparks, R.E., and Stromberg, J.C., 1997, The natural flow regime—A paradigm for river conservation and restoration: BioScience, v. 47, no. 11, p. 769–784, accessed July 9, 2020, at https://www.fs.fed.us/stream/Poffetal_1997.pdf.

Rahmani, V., Hutchinson, S.L., Harrington, J.A., Jr., Hutchinson, J.M.S, and Anandhi, A., 2015, Analysis of temporal and spatial distribution and change points for annual precipitation in Kansas, USA: International Journal of Climatology, v. 35, no. 13, p. 3879–3887, accessed July 9, 2020, at https://doi.org/10.1002/joc.4252.

Rice, J.S., Emanuel, R.E., and Vose, J.M., 2016, The influence of watershed characteristics on spatial patterns of trends in annual scale streamflow variability in the continental U.S.: Journal of Hydrology, v. 540, p. 850–860, accessed July 9, 2020, at https://doi.org/10.1016/j.jhydrol.2016.07.006.

Rogers, J.C., and Coleman, J.S.M., 2003, Interactions between the Atlantic Multidecadal Oscillation, El Niño/La Niña, and the PNA in winter Mississippi Valley streamflow: Geophysical Research Letters, v. 30, no. 10, 4 p., accessed July 9, 2020, at https://doi.org/10.1029/2003GL017216.

Rougé, C., Ge, Y., and Cai, X., 2013, Detecting gradual and abrupt changes in hydrological records: Advances in Water Resources, v. 53, p. 33–44, accessed July 9, 2020, at https://doi.org/10.1016/j.advwatres.2012.09.008.

Ryberg, K.R., Hodgkins, G.A., and Dudley, R.W., 2019, Change points in annual peak streamflows—Method comparisons and historical change points in the United States: Journal of Hydrology, v. 583, article 124307, 13 p., accessed December 30, 2020, at https://doi.org/10.1016/j.jhydrol.2019.124307.

Seaber, P.R., Kapinos, F.P., and Knapp, G.L., 1987, Hydrologic unit maps: U.S. Geological Survey Water-Supply Paper 2294, 63 p., accessed July 15, 2020, at https://doi.org/10.3133/wsp2294.

Sen, P.K., 1968, Estimates of the regression coefficient based on Kendall's tau: Journal of the American Statistical Association, v. 63, no. 324, p. 1379–1389, accessed July 9, 2020, at https://doi.org/10.1080/01621459.1968.10480934.

Steyaert, L.T., and Knox, R.G., 2008, Reconstructed historical land cover and biophysical parameters for studies of land-atmosphere interactions within the Eastern United States: Journal of Geophysical Research, v. 113, no. D2, 27 p., accessed July 9, 2020, at https://doi.org/10.1029/2006JD008277.

Tootle, G.A., Piechota, T.C., and Singh, A., 2005, Coupled oceanic-atmospheric variability and U.S. streamflow: Water Resources Research, v. 41, no. 12, 11 p., accessed July 9, 2020, at https://doi.org/10.1029/2005WR004381.

U.S. Geological Survey, 2007, North America elevation 1-kilometer-resolution GRID [dataset]: U.S. Geological Survey ScienceBase Catalog website, accessed May 1, 2019, at https://www.sciencebase.gov/catalog/item/4fb5495ee4b04cb937751d6d.

U.S. Geological Survey, 2020, National Water Information System—Peak Streamflow for the Nation and Water-Year Summaries, 1941–2016: U.S. Geological Survey National Water Information System database, accessed July 9, 2020, at https://doi.org/10.5066/F7P55KJN [Peak streamflow data accessible at https://nwis.waterdata.usgs.gov/nwis/peak/?site_no=05078000&agency_cd=USGS& and water-year summaries available at https://nwis.waterdata.usgs.gov/nwis/wys_rpt/?site_no=05078000&agency_cd=USGS.]

Villarini, G., Serinaldi, F., Smith, J.A., and Krajewski, W.F., 2009, On the stationarity of annual flood peaks in the continental United States during the 20th century: Water Resources Research, v. 45, no. 8, 17 p., accessed July 9, 2020, at https://doi.org/10.1029/2008WR007645.

Villarini, G., Smith, J.A., Baeck, M.L., and Krajewski, W.F., 2011a, Examining flood frequency distributions in the Midwest U.S.: Journal of the American Water Resources Association, v. 47, no. 3, p. 447–463, accessed July 9, 2020, at https://doi.org/10.1111/j.1752-1688.2011.00540.x.

Villarini, G., Smith, J.A., Baeck, M.L., Vitolo, R., Stephenson, D.B., and Krajewski, V.F., 2011b, On the frequency of heavy rainfall for the Midwest of the United States: Journal of Hydrology, v. 400, nos. 1–2, p. 103–120, accessed July 9, 2020, at https://doi.org/10.1016/j.jhydrol.2011.01.027.

York, B.C., Ryberg, K.R., Asquith, W.H., Chase, K.J., Dickinson, J.E., Dudley, R.W., Harden, T.M., Hodgkins, G.A., Holtschlag, D.J., Humberson, D.G., Konrad, C.P., Levin, S.B., Restivo, D.E., Sando, R., Sando, S.K., Swain, E.D., Tillery, A.C., and Totten, A.R., 2022, Attributions for nonstationary peak streamflow records across the conterminous United States, 1941–2015 and 1966–2015: U.S. Geological Survey data release, https://doi.org/10.5066/P9FOUVWG.

Attribution of Monotonic Trends and Change Points in Peak Streamflow in the Northeast Region of the United States, 1941–2015 and 1966–2015

By Glenn A. Hodgkins and Robert W. Dudley

Chapter E of
Attribution of Monotonic Trends and Change Points in Peak Streamflow Across the Conterminous United States Using a Multiple Working Hypotheses Framework, 1941–2015 and 1966–2015
Karen R. Ryberg, editor

Prepared in cooperation with
U.S. Department of Transportation
Federal Highway Administration

Professional Paper 1869

U.S. Department of the Interior
U.S. Geological Survey

U.S. Geological Survey, Reston, Virginia: 2022

For more information on the USGS—the Federal source for science about the Earth, its natural and living resources, natural hazards, and the environment—visit https://www.usgs.gov or call 1–888–ASK–USGS.

For an overview of USGS information products, including maps, imagery, and publications, visit https://store.usgs.gov.

Suggested citation:
Hodgkins, G.A., and Dudley, R.W., 2022, Attribution of monotonic trends and change points in peak streamflow in the Northeast region of the United States, 1941–2015 and 1966–2015, chap. E *of* Ryberg, K.R., ed., Attribution of monotonic trends and change points in peak streamflow across the conterminous United States using a multiple working hypotheses framework, 1941–2015 and 1966–2015: U.S. Geological Survey Professional Paper 1869, p. E1–E17, https://doi.org/10.3133/pp1869.

Associated data for this publication:
Dudley, R.W., Archfield, S.A., Hodgkins, G.A., Renard, B., and Ryberg, K.R., 2018, Peak-streamflow trends and change-points and basin characteristics for 2,683 U.S. Geological Survey streamgages in the conterminous U.S. (ver. 3.0, April 2019): U.S. Geological Survey data release, https://doi.org/10.5066/P9AEGXY0.

York, B.C., Ryberg, K.R., Asquith, W.H., Chase, K.J., Dickinson, J.E., Dudley, R.W., Harden, T.M., Hodgkins, G.A., Holtschlag, D.J., Humberson, D.G., Konrad, C.P., Levin, S.B., Restivo, D.E., Sando, R., Sando, S.K., Swain, E.D., Tillery, A.C., and Totten, A.R., 2022, Attributions for nonstationary peak streamflow records across the conterminous United States, 1941–2015 and 1966–2015: U.S. Geological Survey data release, https://doi.org/10.5066/P9FOUVWG.

ISSN 2330-7102 (online)

Acknowledgments

The work described in this professional paper was funded by the Federal Highway Administration of the U.S. Department of Transportation through Interagency Agreement DTFH6116X30020, "Flood Frequency Estimation for Hydraulic Design." We thank the following U.S. Geological Survey colleagues: David Holtschlag for the overall attribution framework that we used in this chapter, Jesse Dickinson for providing Daymet data, and Pamela Lombard and Amy Russell for helpful technical reviews.

Contents

Figures

Table

Conversion Factors

Multiply	By	To obtain
	Length	
inch (in.)	2.54	centimeter (cm)
inch (in.)	25.4	millimeter (mm)
foot (ft)	0.3048	meter (m)
kilometer (km)	0.6214	mile (mi)

Temperature in degrees Celsius (°C) may be converted to degrees Fahrenheit (°F) as follows:

$$°F = (1.8 \times °C) + 32.$$

Temperature in degrees Fahrenheit (°F) may be converted to degrees Celsius (°C) as follows:

$$°C = (°F - 32) / 1.8.$$

Datum

Horizontal coordinate information is referenced to the North American Datum of 1983 (NAD 83).

Supplemental Information

A “water year” represents the 12-month period from October 1 through September 30 of the following year that is designated by the calendar year in which it ends.

The 75-year and 50-year study periods described in this report span water years 1941–2015 and 1966–2015, respectively.

Abbreviations

>	greater than
<	less than
≤	less than or equal to
GAGES-II	Geospatial Attributes of Gages for Evaluating Streamflow, Version II
GHCN	Global Historical Climatology Network
HUC	hydrologic unit code
NAWQA	National Water-Quality Assessment Program (U.S. Geological Survey)
NWALT	NAWQA Wall-to-Wall Anthropogenic Land Use Trends
PDSI	Palmer Drought Severity Index
p-value	attained significance level
USGS	U.S. Geological Survey

Attribution of Monotonic Trends and Change Points in Peak Streamflow in the Northeast Region of the United States, 1941–2015 and 1966–2015

By Glenn A. Hodgkins[1] and Robert W. Dudley[1]

Abstract

Significant monotonic trends and change points (abrupt shifts) in peak streamflows for the Northeast region of the United States during 75-year and 50-year periods were statistically attributed to several causes. The attributions considered were short-term precipitation (storm-event precipitation related to individual peak streamflows), long-term precipitation (estimated by using the Palmer Drought Severity Index, a measure of antecedent basin moisture), large artificial impoundments, and urban effects. To attribute peak-streamflow trends and change points to short-term or long-term precipitation, we required that significant interannual correlations exist between peak streamflows and precipitation and that values for these variables have significant trends in the same direction as peak-flow trends. We also used trend and change-point magnitudes along with basin-specific information to infer whether peak-flow changes over time were caused by large impoundments or urban effects.

There were significant monotonic trends in peak flows at 125 U.S. Geological Survey streamgages for the 75-year period (water years 1941–2015). The primary attributions for a majority of these trends were short-term precipitation (43 gages) or long-term precipitation (29 gages). For the remaining gages, 23 trends were attributed to urban effects, 16 trends were attributed to large artificial impoundments, and 14 trends were attributed to unknown causes. The number of 75-year change points with a primary attribution of short-term precipitation was substantially less than the number of monotonic trends attributed to short-term precipitation. This difference indicates that more gradual than abrupt changes over time in short-term precipitation have led to annual peak-streamflow changes in the Northeast. Most of the change points for the 75-year period that were attributed to long-term or short-term precipitation occurred within the period from the late 1960s to the early 1970s. Most of the change points attributed to urban effects occurred in the late 1960s. The highest concentration of change points attributed to large artificial impoundments was in the early 1960s.

There were significant monotonic trends in peak flows at 61 U.S. Geological Survey streamgages for the 50-year period (water years 1966–2015). The largest attribution category for trends at these streamgages was large artificial impoundments (18), followed by short-term precipitation (14), unknown attribution (13), long-term precipitation (9), and urban effects (7). The much higher number of 75-year monotonic trends (125) than 50-year trends (61) may be a result of the 50-year period (water years 1966–2015) beginning mostly after change points in the 1960s and early 1970s had already occurred. All 75-year trends and change points in peak streamflows that were attributed to short-term and long-term precipitation increased in magnitude over time; all 50-year peak-flow trends and change points attributed to precipitation increased except for one. The attribution of historical trends and change points is very important for understanding future changes in peak streamflows.

Introduction

Potential changes to flood distributions may result from multiple factors. To develop a national approach for incorporating potential or observed changes into flood-frequency estimates, experts from the U.S. Geological Survey and cooperators designed a multiple working hypotheses framework for making attributions. Chapter A of this professional paper describes the approach. The work was done by the U.S. Geological Survey in cooperation with the Federal Highway Administration of the U.S. Department of Transportation.

As stated in chapter A of this volume (N.A. Barth and others, p. A1), "Seven regional teams of subject-matter experts used datasets to evaluate plausible causes for statistically significant (*p*-value [attained significance level] <0.10) monotonic trends and change points in annual peak-streamflow data for the conterminous United States." Results for the regions are summarized in chapters B–H of this professional paper.

The focus of this chapter E is the statistical attribution of significant monotonic trends (flood trends) and change points (abrupt shifts) in peak-streamflow data for the Northeast region of the United States. The Northeast comprises all or part of 13 States and the District of Columbia from Virginia in the south to Maine in the north (fig. E1).

[1]U.S. Geological Survey.

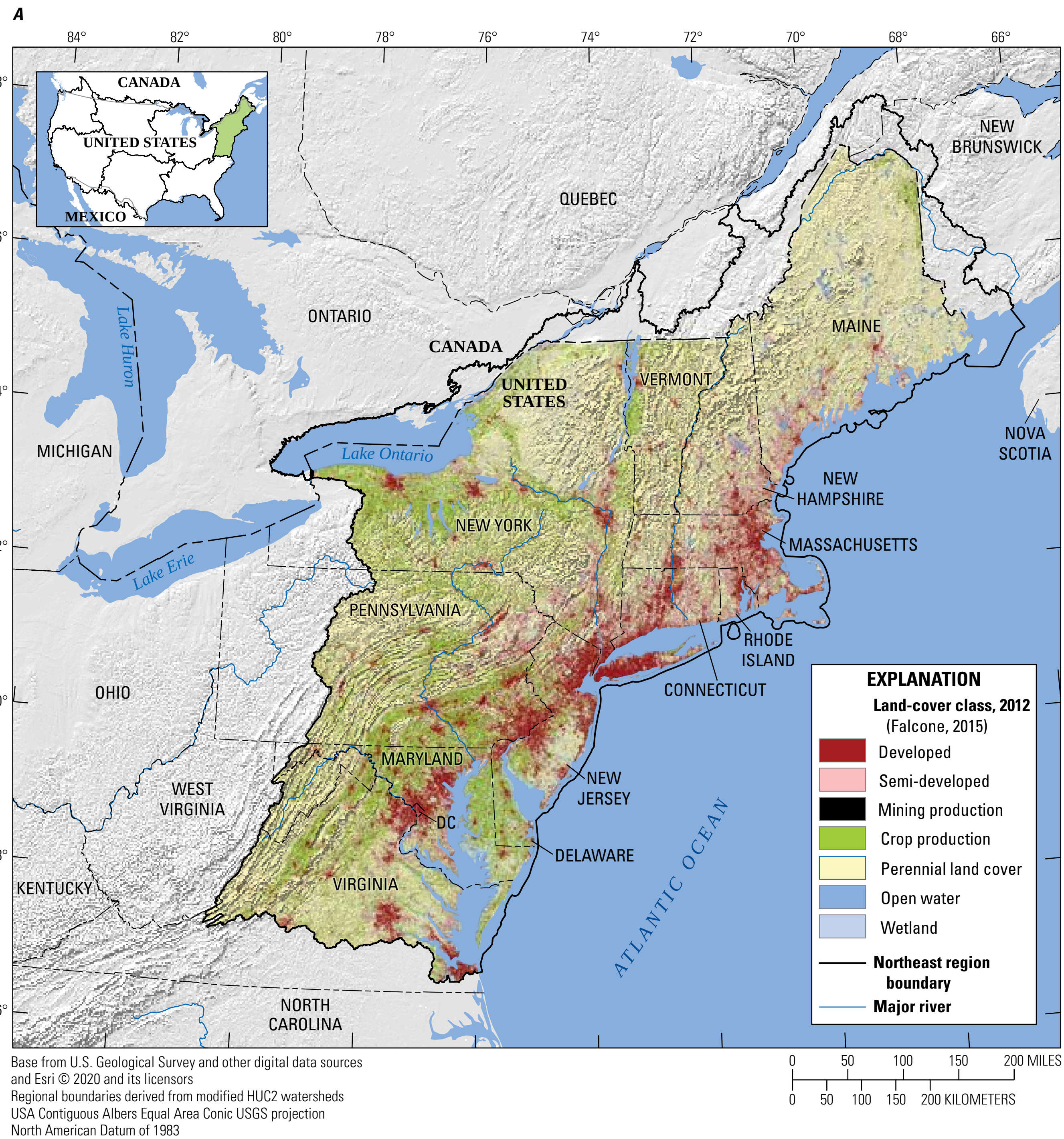

Figure E1. Maps of the Northeast region of the United States showing (*A*) land cover and (*B*) terrain and locations of the 191 streamgages for which data had significant monotonic trends and (or) change points (abrupt shifts) in peak streamflows for the 75- and (or) 50-year periods spanning water years 1941–2015 and 1966–2015, respectively. Although the study region is shown as extending into Canada because of the topography of stream drainage basins, the watersheds considered for attribution are within the United States. Land-cover classes for 2012 that are shown in figure E1*A* are from Falcone (2015). Because of the map scale, the mining production and wetland classes may be easier to see if the view is zoomed in. Streamgage locations shown in figure E1*B* are from the Geospatial Attributes of Gages for Evaluating Streamflow, Version II (GAGES-II) from Falcone (2011). USGS, U.S. Geological Survey.

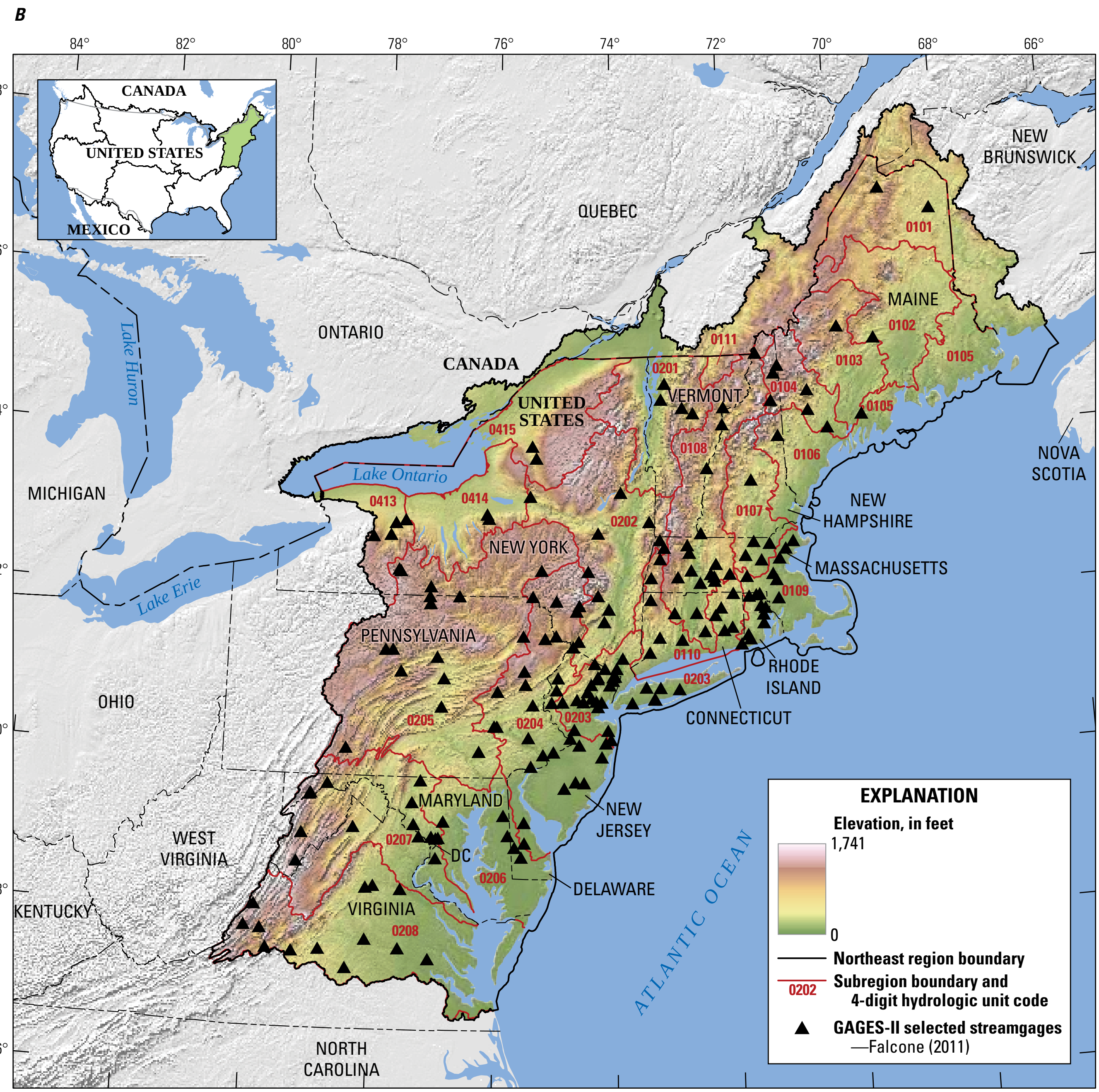

Base from U.S. Geological Survey and other digital data sources and Esri © 2020 and its licensors
North America elevation 1-kilometer-resolution GRID (USGS, 2007)
Regional boundaries derived from modified HUC2 watersheds
USA Contiguous Albers Equal Area Conic USGS projection
North American Datum of 1983

Figure E1. —Continued

The study regions were based on water-resources regions identified by two-digit hydrologic unit codes (HUC2s) described by Seaber and others (1987), which were modified slightly by adding or subtracting subregions (HUC4s) to achieve geographic cohesiveness or hydrologic-setting similarity. The Northeast study region consists of water-resources regions 01 (New England) and 02 (Mid-Atlantic) plus subregions 0413 (Southwestern Lake Ontario), 0414 (Southeastern Lake Ontario), and 0415 (Northeastern Lake Ontario-Lake Ontario-St. Lawrence) of water-resources region 04 (Great Lakes).

Landscape and Climate

The Northeast has a diverse landscape; it is both the most heavily forested and the most densely populated region in the country (Dupigny-Giroux and others, 2018). Developed areas are concentrated in coastal areas of the Northeast (fig. E1*A*). Landforms range from the Atlantic Coastal Plain to the Appalachian Mountains (fig. E1*B*).

The Northeast has a highly diverse climate with large spatial variations and strong seasonality (Kunkel and others, 2013). Mean annual temperatures generally decrease with increasing latitude and elevation. Mean annual precipitation ranges from less than 35 inches (in.) in parts of New York to more than 50 in. along the New England coast; orographic effects at inland locations, however, can produce localized mean annual precipitation of more than 60 in. (Kunkel and others, 2013). Northern and mountainous parts of the Northeast receive substantial amounts of snowfall in the winter.

Inland peak streamflows (flood flows) in the Northeast can result from multiple processes, including frontal systems, thunderstorms, nor'easters (coastal cyclones), snowmelt, and tropical storms (Kunkel and others, 2013; Collins and others, 2014; Berghuijs and others, 2016). Weather systems causing floods in the Northeast often pass through the Great Lakes or Ohio Valley regions or come up the east coast (Collins and others, 2014). Snowmelt can combine with rain to cause flooding in northern and mountainous parts of the Northeast. Antecedent soil moisture is an important factor for flooding throughout the region. Frozen soils also can be a factor in flooding for parts of the Northeast in the winter and spring.

In several studies, researchers have examined historical flood changes in the Northeast, and some national studies included results specific to the Northeast (Hodgkins and Dudley, 2005; Lins and Slack, 2005; Collins, 2009; Hirsch and Ryberg, 2012; Armstrong and others, 2014; Rice and others, 2015; Hodgkins and others, 2019; Ryberg and others, 2020). A large majority of basins had peak-streamflow increases from 1941 to 2015, which may be due to gradual (monotonic) trends (Hodgkins and others, 2019) or change points (abrupt shifts), with many of them occurring around 1970 (Dudley and others, 2018; Ryberg and others, 2020). Most basins in the Northeast with minimal human alteration had peak-flow increases from 1966 to 2015 (Hodgkins and others, 2019). Human alterations of basins have affected historical flood trends in the Northeast, particularly through urbanization and large impoundments. Some urbanized basins in the Northeast had large peak-flow increases while some basins with large artificial impoundments had peak-flow decreases.

Purpose and Scope

This chapter describes the statistical attribution of all significant monotonic trends and change points for peak streamflows from U.S. Geological Survey (USGS) streamgages in the Northeast for a 75-year period (water years 1941–2015) and a 50-year period (water years 1966–2015). Barth and others, in chapter A of this professional paper, describe attribution categories that were created for peak-streamflow (flood) trend and change-point attribution in the Northeast and six other regions in the United States. For the Northeast, analyses were focused on the most likely attribution categories that were feasible to study: short-term precipitation (storm-event precipitation related to individual peak streamflows), long-term precipitation (using a measure of antecedent moisture), large artificial impoundments, and urban effects.

Data and Methods

Attributions of significant historical monotonic trends and change points for peak streamflows from streamgages in basins in the Northeast are based on statistical tests and basin information. Basins include minimally altered ones as well as those with substantial human changes such as urbanization and reservoir storage. The following section describes the data used for this chapter, including peak-streamflow trends and change points, Palmer Drought Severity Index, precipitation, air temperature, basin reservoir storage (large artificial impoundments), and urban effects.

Data

Dudley and others (2018) provided monotonic trends and change points for USGS streamgages in the United States. The trends and change points were based on annual instantaneous peak flows at gages. Trend and change-point magnitude and significance values used for attribution in this chapter were from 191 streamgages in the Northeast (fig. E1*B*) that had significant (p-value<0.10) monotonic trends or change points for 50-year (1966–2015) or 75-year (1941–2015) periods. The monotonic trends and change points for streamgages in the Northeast are also contained in York and others (2022) along with attribution data.

Precipitation data were obtained from the Global Historical Climatology Network (GHCN; Menne and others, 2012); data in this network were evaluated on the basis of record length, completeness, and historical stability. Daily data from the five GHCN stations that were closest to the centroid of each study basin (within 75 kilometers [km]) and that had at least 40 years of record from 1941 through 2015 were downloaded using the rnoaa package (Chamberlain, 2019) for the statistical computing language and environment R (R Core Team, 2018); data downloading was done by using the rnoaa:ncdc function with datasetid = "GHCND." Data from selected stations from each basin were averaged by linear weighting of the distance from each station to the basin centroid. Year-to-year basin precipitation may be based on a variable number of stations, either due to fewer than five GHCN stations being within 75 km of a given basin centroid or due to incomplete meteorological records among stations that were within 75 km of basin centroids. We allowed the use of a variable number of stations in the calculation of mean basin precipitation to maximize the number of basins and years with associated precipitation data. Storm-event precipitation was summed for every peak-streamflow event for all basins for the day of the peak plus 3 days prior to the peak.

The Palmer Drought Severity Index (PDSI) is used in this chapter as a measure of relative basin moisture prior to peak streamflows. The PDSI is a standardized measure of cumulative moisture departure based on a simple water-balance model. The model uses precipitation, temperature, and water-holding capacity of the soil as inputs to compute moisture supply (precipitation), moisture demand (evapotranspiration), soil-moisture storage, and runoff (Palmer, 1965; Alley, 1984; Dai and others, 2004). The PDSI in the Northeast is related to long-term precipitation (see the "Monotonic Trend and Change-Point Attributions" section), and the term "long-term precipitation" is used later in the chapter in place of "PDSI." The PDSI for the climate division containing each basin centroid was downloaded from National Oceanic and Atmospheric Administration (2018). We used the monthly PDSI value for the month prior to each peak flow.

To better understand the reasons for significant relations between peak streamflows and PDSI, precipitation and air temperature data were used. Monthly climate-division air temperature and precipitation data were aggregated from Daymet data (Thornton and others, 2014) from 1980 to the end of our study period in 2015, for the same month as the PDSI (for each basin and year) and for prior months. Mean air temperature was computed by averaging the minimum and maximum daily air temperatures before computing monthly values. With these data, the interannual variability of the PDSI was compared with the interannual variability of precipitation and temperature.

To determine whether basins had large artificial impoundments, we used basin information from the Geospatial Attributes of Gages for Evaluating Streamflow, Version II (GAGES-II) dataset (Falcone and others, 2010; Falcone, 2011). Specifically, we used the fields for pre-1940 storage through pre-1990 storage, and remarks from USGS Annual Water Data Reports, which contain site-specific information derived by local USGS offices. We also used GAGES-II reservoir storage information from 2009 converted to flow-normalized reservoir storage (Dudley and others, 2018; Hodgkins and others, 2019).

To determine urban effects in basins, we used the percentages of developed land (DEVNLCD06, the sum of land-cover classes 21, 22, 23, and 24) in the GAGES-II database, which are from the National Land Cover Database 2006 (Fry and others, 2011). We also used developed-area data from the USGS National Water-Quality Assessment (NAWQA) Wall-to-Wall Anthropogenic Land Use Trends (NWALT) dataset (Falcone, 2015). The developed-area data are available for 1974, 1982, 1992, 2002, and 2012 and were used to look for changes in urban land use over time.

Methods for Statistical Attribution

Trends and Correlations

For our statistical attribution of the causes of significant (p-value<0.10, assuming time-series independence) peak-streamflow changes over time in the Northeast, we required that potential causal variables have significant trends (p-value<0.10) in the same direction as peak-flow trends. Causal variables tested were short-term storm-event precipitation (sum of precipitation for the day of each annual peak and 3 days prior) and antecedent basin moisture (PDSI in the month prior to the peak flow). The significance of all monotonic trends was computed with the Mann-Kendall test (Mann, 1945) by assuming independence of the time-series data; the magnitude was computed with the Sen slope (Theil, 1950; Sen, 1968; Helsel and Hirsch, 1992). The significance of change points was computed with the Pettitt test (Pettitt, 1979), and the magnitude was computed as the change in median values before and after a change point.

In addition to peak-flow and causal-variable trends being in the same direction, we required significant interannual correlation (p-value<0.10) between peak flows and causal variables. Correlations were computed with Kendall's tau (Sen, 1968; Helsel and Hirsch, 1992) by using the most recent 50 years (1966–2015) for all correlations. All correlations between causal variables and peaks were positive or near zero, as expected, for the variables tested. Interannual correlations between the PDSI and precipitation and temperature also were computed with Kendall's tau.

Decision Tree

We followed a decision tree to decide on peak-streamflow attributions and the confidence that we had in the attributions. Our first criterion was that the causal variable be significantly correlated (p-value<0.10) with the peak flows. If there were no significant correlations, then we did not attribute peak-flow changes to that causal variable, even if trends over time in the peak flows and causal variable were significant and in a consistent direction. This decision helped to avoid the attribution of peak-flow changes that may have been due to coincidental changes.

If a causal variable was significantly correlated (*p*-value<0.10) with peak streamflows and had a significant change in the same direction as the peak change (*p*-value<0.10), that variable was used for attribution with medium evidence (table E1). Additionally, for change points, the change-point year of the peaks and the causal variable were required to be ≤5 years apart. If both potential causal variables had significant correlations with peaks, and changes in the same direction as peaks, the variable with the lower trend *p*-value was considered the primary attribution, and the other variable was considered the secondary attribution. If causal-variable correlation significance with peaks was <0.05 and causal-variable change over time was significant at this same level, the variable was considered to have robust evidence for peak-flow attribution. If the significance of the causal-variable change over time was between 0.10 and 0.20, the variable was attributed with limited evidence (table E1). If the above conditions were not met at a streamgage that had a significant trend or change point, an attribution of "unknown" was assigned.

We also analyzed basin-specific information to infer whether peak-streamflow changes over time were caused by human alterations of basins. For each basin with reservoir storage, we looked at the direction of peak-flow changes over time. Because reservoir storage is expected to reduce peak streamflows (Williams and Wolman, 1984; Magilligan and Nislow, 2005; Graf, 2006; FitzHugh and Vogel, 2011), we considered attribution to reservoir storage only if peak flows had significant decreases over time. Reservoirs could moderate increases in peak flows over time, but for this study, they were not considered to be the cause of peak-flow increases.

For basins with large artificial impoundments, if storm-event precipitation changes over time were consistent with peak-streamflow changes (same direction and similar magnitude), precipitation was considered the primary attribution (if it met previously described criteria) with no attribution to large impoundments. If peaks decreased over time, and precipitation increased or did not change substantially, large impoundments were considered the primary attribution with robust evidence while medium evidence was used if precipitation decreased but substantially less than peaks decreased (>20 percentage point difference). To have robust evidence specifically with peak-flow change points, the year of the change point needed to be consistent with the timing of major storage additions; if it was not, the attribution was considered to have limited evidence. If the change-point timing was consistent with the timing of major storage additions, but peaks and precipitation decreased by similar amounts, attribution to regulation was also considered to have limited evidence.

Current urban land use is indicative of basin changes that can affect floods, such as added impervious area and faster flood conveyance (Leopold, 1968; Hollis, 1975; Sauer and others, 1983). Hodgkins and others (2019) found that urban development did not noticeably affect peak-flow trends if development affected <25 percent of the land area of a basin.

For basins with significant peak-streamflow increases and urban development greater than about 20 percent, we judged whether the changes should be attributed to urban development. If storm-event precipitation changes over time were consistent with peak-flow trends, precipitation was considered the primary attribution and there was no attribution to urbanization. If peak flows increased and urban development was high (>25 percent), but precipitation was decreasing or had little change, urban effects were considered the primary attribution with robust evidence. If precipitation was increasing but less than peak flows (by >20 percentage points), or if the amount of urban development was not high, the evidence was considered medium, or it was considered limited if there was a combination of factors. For change-point attributions, the respective attributions were classified as medium and limited, as specific information was not available to indicate that urban development caused change points.

Table E1. Attribution-evidence confidence categories for various combinations of correlation significance and significance of monotonic trends or change points in peak streamflow.

[Correlation significance, significance of the interannual correlation between peak streamflows and causal variables. The attained significance level is represented by the *p*-value, which is shortened to just "*p*" in the table. >, greater than; <, less than; ≤, less than or equal to]

Correlation significance	Causal variable trend or change-point significance[1]			
	p>0.20	0.20>*p*>0.10	0.10>*p*>0.05	*p*<0.05
p>0.10	Unknown	Unknown	Unknown	Unknown
0.10>*p*>0.05	Unknown	Limited evidence	Medium evidence	Medium evidence
p<0.05	Unknown	Limited evidence	Medium evidence	Robust evidence

[1]Additionally, for change points, the change-point year of the peak streamflows and the causal variable were required to be ≤5 years apart.

Monotonic Trend and Change-Point Attributions

The statistical attribution of significant monotonic trends and change points (abrupt shifts) for peak streamflows from USGS streamgages in the Northeast was completed for the periods 1941–2015 (75 years) and 1966–2015 (50 years) (fig. E2*A*–E2*D*). We focused our analyses on the most likely causes of floods in the Northeast that were feasible to study, including short-term precipitation (storm-event precipitation related to individual peak flows), long-term precipitation (using the PDSI, a measure of relative antecedent basin moisture), large artificial impoundments, and urban effects.

Since the PDSI is affected by both precipitation and air temperature, we tested the interannual correlation of the PDSI and these two variables in the Northeast. We hypothesized that precipitation would be more important to the PDSI. To verify this hypothesis, we correlated the PDSI values for the month prior to each annual peak flow with cumulative precipitation and temperature data for that month plus 5 previous months, for the 29 streamgages with primary PDSI attributions for 75-year trends. Twenty-two gages had a significant interannual correlation between the PDSI and precipitation (p-value<0.05) while one gage had significant correlations with both precipitation and air temperature. At that site, the correlation with precipitation was much more significant. Given the significant interannual correlation with the PDSI, we use the term "long-term precipitation" for the rest of this chapter rather than "PDSI."

Attributions for 75-Year Monotonic Trends and Change Points

There were 125 significant 75-year monotonic trends to attribute (York and others, 2022), and the primary attribution for a majority of them was short-term precipitation (43 streamgages) or long-term precipitation (29 streamgages) (fig. E2*A*). For the remaining gages, 23 trends were attributed to urban effects, 16 were attributed to large artificial impoundments, and 14 have an unknown attribution. For the 111 significant trends with known primary attributions, 101 were attributed with robust or medium evidence and 10 were attributed with limited evidence (York and others, 2022). For about half of the gages (46 percent) where the primary attribution was short-term or long-term precipitation, the secondary attribution was precipitation of the other time scale (York and others, 2022). For the gages for which trends had a primary attribution of urban effects, there was a single gage with a secondary attribution (long-term precipitation); for gages with a primary attribution of large impoundments, there were no gages with a secondary attribution.

There were 121 significant 75-year change points to attribute (York and others, 2022) compared to 125 significant monotonic trends for the same time period. There were 142 streamgages that had significant trends or change points in peak streamflows, and 104 of them (73.2 percent) had both significant trends and significant change points. The largest attribution category for significant 75-year change points contains 41 unknown attributions (fig. E2*B*). The second largest category contains 29 attributions to long-term precipitation. The three remaining attribution categories contain similar numbers of gages (16–18). The number of change points with a primary attribution of short-term precipitation was substantially less than the number of trends attributed to short-term precipitation. This difference indicates that more gradual than abrupt changes over time in the short-term precipitation changes led to annual peak-flow changes in the Northeast. The number of change points with a primary attribution of long-term precipitation was the same as the number of trends attributed to long-term precipitation; however, some of the 29 change points were for different streamgages than the 29 trends.

Most of the change points for the 75-year period that were attributed to long-term precipitation or short-term precipitation occurred within the period from the late 1960s to the early 1970s (fig. E3). Most of the change points attributed to urban effects occurred in the late 1960s. The range of change-point years for large artificial impoundments was larger than the ranges for other attributions, reflecting a variety of years when large impoundments were built; the highest concentration of change points was in the early 1960s (fig. E3).

Attributions for 50-Year Monotonic Trends and Change Points

The largest attribution category for the 61 streamgages with significant 50-year trends (fig. E2*C*) was large artificial impoundments (18), followed by short-term precipitation (14), unknown attribution (13), long-term precipitation (9), and urban effects (7). The 56 gages that have significant 50-year peak-flow change points (fig. E2*D*) were in the following attribution categories: unknown (30), large impoundments (13), urban effects (6), short-term precipitation (5), and long-term precipitation (2).

There were 110 streamgages that had significant 75-year peak-flow trends but lacked significant 50-year trends. The primary attribution for these 110 streamgages included all of the attribution categories: short-term precipitation (40 gages), long-term precipitation (23), urban effects (21), large impoundments (13), and unknown (13). There were only 13 gages that had significant 50-year peak-flow trends but lacked 75-year trends (where there was data for both periods), and 6 of them had a primary attribution of large impoundments (York and others, 2022). The much higher number of 75-year trends compared to 50-year trends may be a result of the 50-year period (1966–2015) beginning mostly after change points in the 1960s and early 1970s had already occurred (fig. E3).

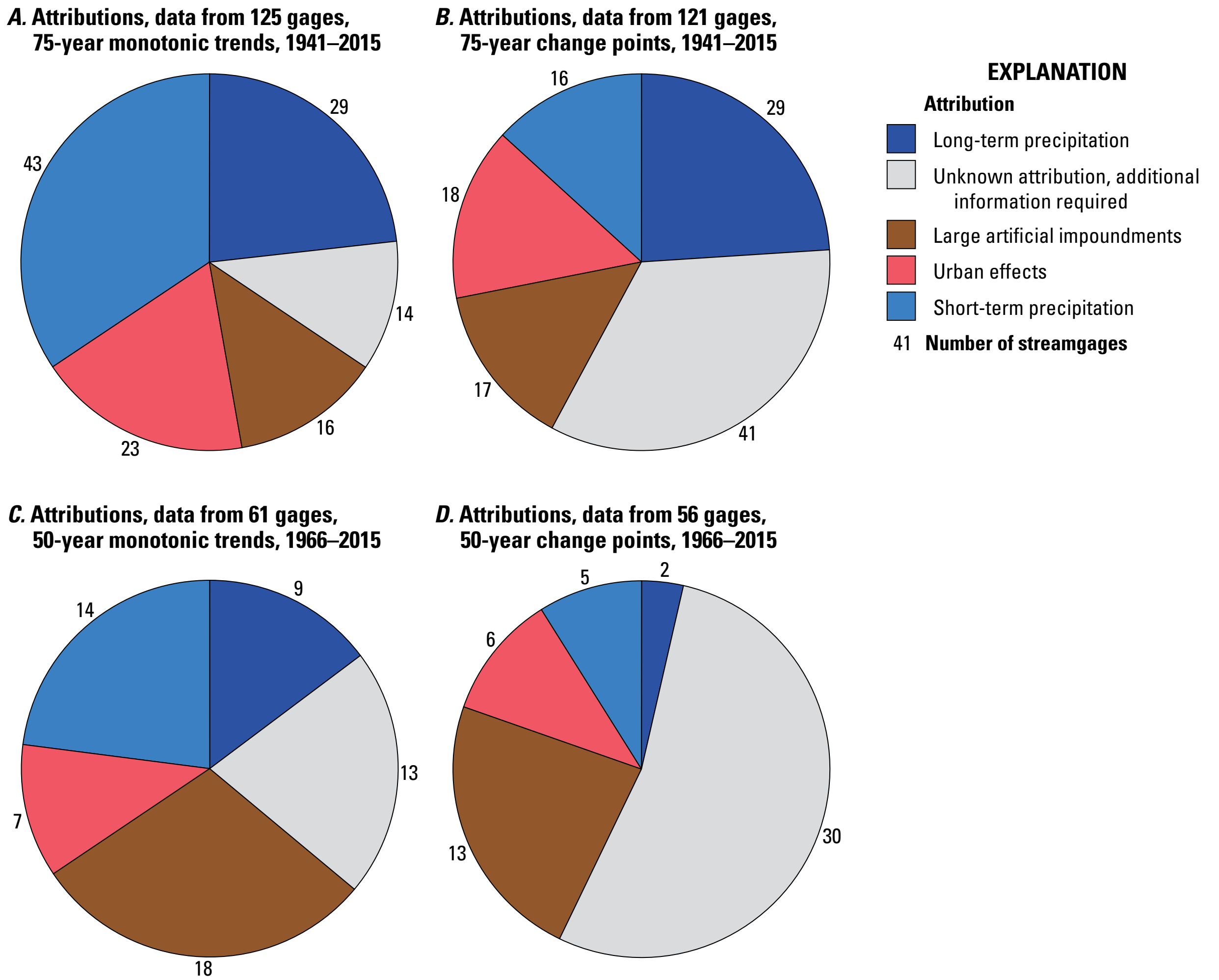

Figure E2. Pie charts showing the number of streamgages in each primary attribution category for peak flows in the Northeast region for (*A*) 75-year monotonic trends, (*B*) 75-year change points, (*C*) 50-year monotonic trends, and (*D*) 50-year change points.

Magnitude of Changes by Attribution Category

Both the magnitudes of 75-year monotonic trends and the magnitudes of 75-year change points for peak streamflows show similar patterns for each attribution category (fig. E4*A* and E4*B*). Trend magnitudes were computed with the Sen slope, and change-point magnitudes were computed as the median peak-flow magnitude after the change point minus the median peak-flow magnitude before the change point. Increases in peak flows at streamgages with the primary attribution of short-term precipitation were somewhat larger, in general, than those attributed to long-term precipitation. The urban-effects attribution category contains gages with much larger changes over time than those in the short- or long-term precipitation attribution categories. Streamgages in the large-impoundment attribution category had large decreases over time. A similar pattern of peak-flow-change magnitude between attribution categories is evident for 50-year trends and change points (fig. E4*C* and E4*D*); however, there are considerably fewer gages in each 50-year category. All 75-year peak-flow trends and change points attributed to short-term and long-term precipitation increased over time; all 50-year peak-flow trends and change points increased except for one (York and others, 2022).

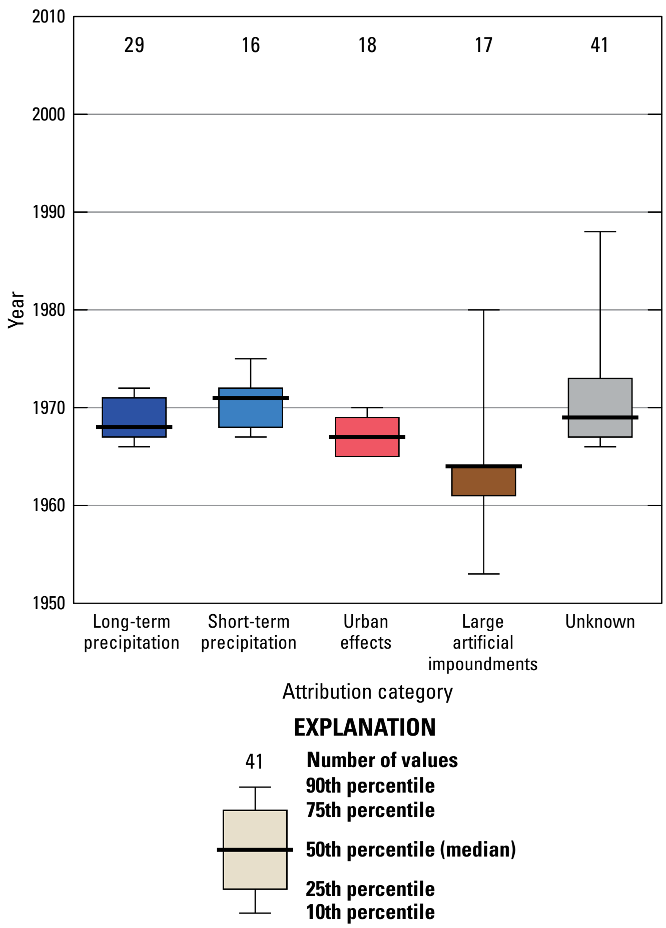

Figure E3. Boxplots showing the distribution of change-point years for peak streamflows in each primary attribution category for the 75-year change points in the Northeast region during 1941–2015. The years graphed extend from 1950 to 2010 because no 10th to 90th percentile change points occurred during 1941–1950 and 2010–2015. Unknown, unknown attribution, additional information required.

Geographic Distribution of Primary Attribution Categories

Streamgages that had monotonic trends and change points with a primary attribution of short-term or long-term precipitation for the 75-year period are located throughout the Northeast (figs. E5, E6). There is a high concentration of gages with short-term precipitation attributions for 75-year trends (fig. E5) in southern New England (Massachusetts, Connecticut, and Rhode Island). Gages where trends and change points are attributed to urban effects are concentrated in New Jersey and areas near Washington, D.C. Most of the gages where 75-year trends and change points were attributed to large impoundments are in western New York and northeastern Pennsylvania.

There are considerably fewer monotonic trends and change points to attribute for the 50-year period (figs. E7, E8) than for the 75-year period. Most of the streamgages where 50-year trends for peak streamflows are attributed to short-term or long-term precipitation changes are located from northern New Hampshire to northern New Jersey and northeastern Pennsylvania. The small number of gages with 50-year change points that are attributed to precipitation changes are mostly in New England. Most of the small number of gages where 50-year trends and change points are attributed to urban effects are near Washington, D.C., or New York City. Gages where trends and change points are attributed to large impoundments are located mostly in western New York, central Pennsylvania, and Virginia.

Comparison with Previous Studies

Ivancic and Shaw (2015) demonstrated that annual peak streamflows in the United States are not caused solely by short-term event precipitation; they found that the 99th percentile precipitation results in the 99th percentile streamflow only 36 percent of the time. However, during periods of high soil moisture, the occurrence of this result increases to 62 percent of the time. Slater and Villarini (2016) found that both short-term event precipitation and long-term (annual) precipitation were important to minor flood events for about 2,000 streamgages in the United States from 1985 to 2015. These studies agree with our finding of many peak-streamflow trends and change points being attributed to short-term event precipitation and (or) long-term precipitation in the Northeast. High soil moisture promotes greater peak flows for a given amount of event precipitation.

Hodgkins and others (2019) found that basin urbanization was an important factor in annual peak-streamflow trends in the United States during the last 50 years. For urbanized basins (which were mostly in the Northeast and Midwest), trend magnitude was significantly correlated with the amount of developed area in basins. That finding is consistent with this study where urban effects were the primary attribution for peak-flow changes in some highly developed areas of the Northeast.

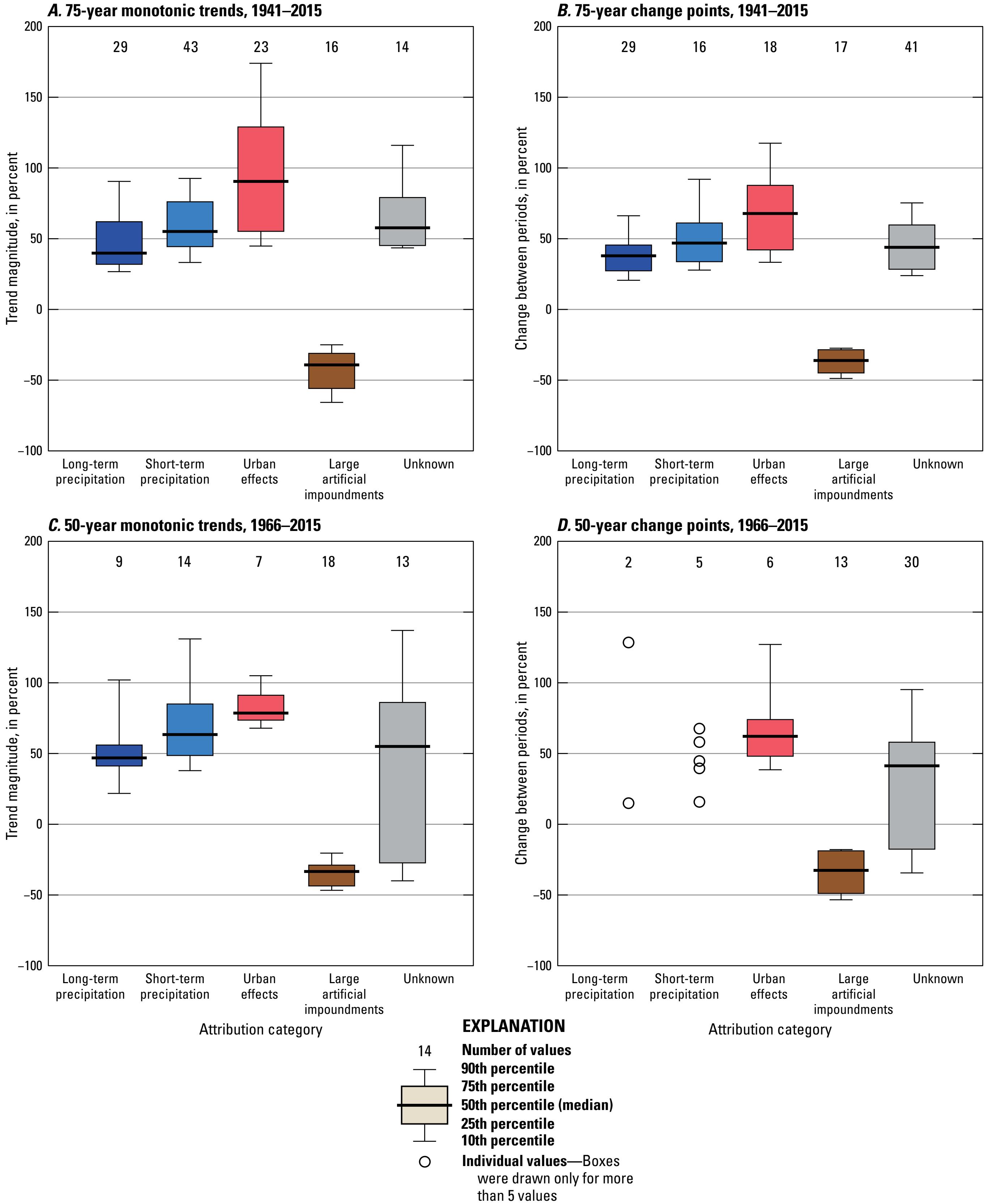

Figure E4. Boxplots showing the distribution of change magnitude in the Northeast region for various attribution categories for (*A*) 75-year monotonic trends, (*B*) 75-year change points, (*C*) 50-year monotonic trends, and (*D*) 50-year change points. Change-point magnitude is computed as the median peak-flow magnitude after the change point minus the median peak-flow magnitude before the change point. Unknown, unknown attribution, additional information required.

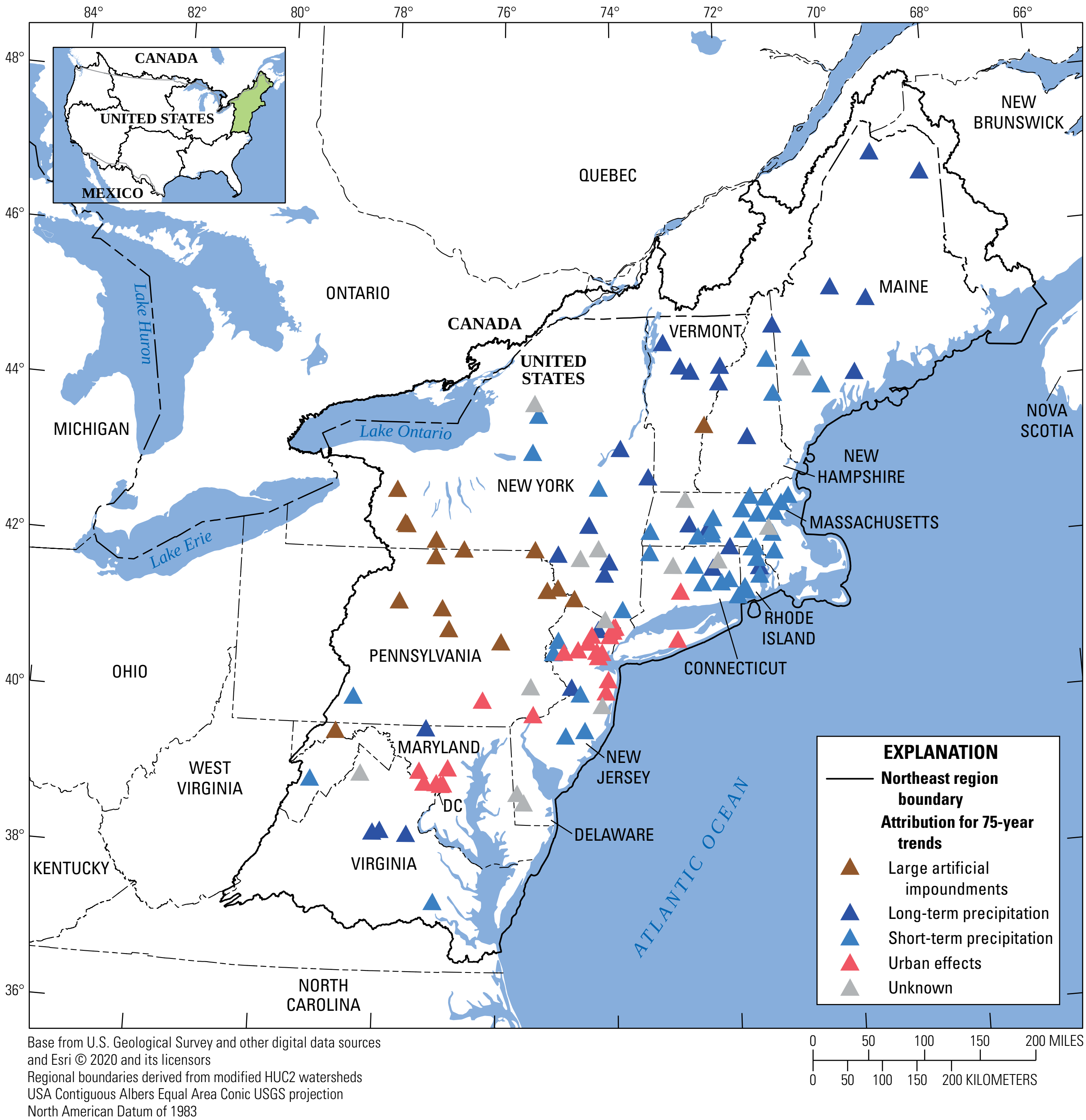

Figure E5. Map of the Northeast region showing the geographic distribution of streamgages that have peak-streamflow attributions in various categories for 75-year monotonic trends (1941–2015).

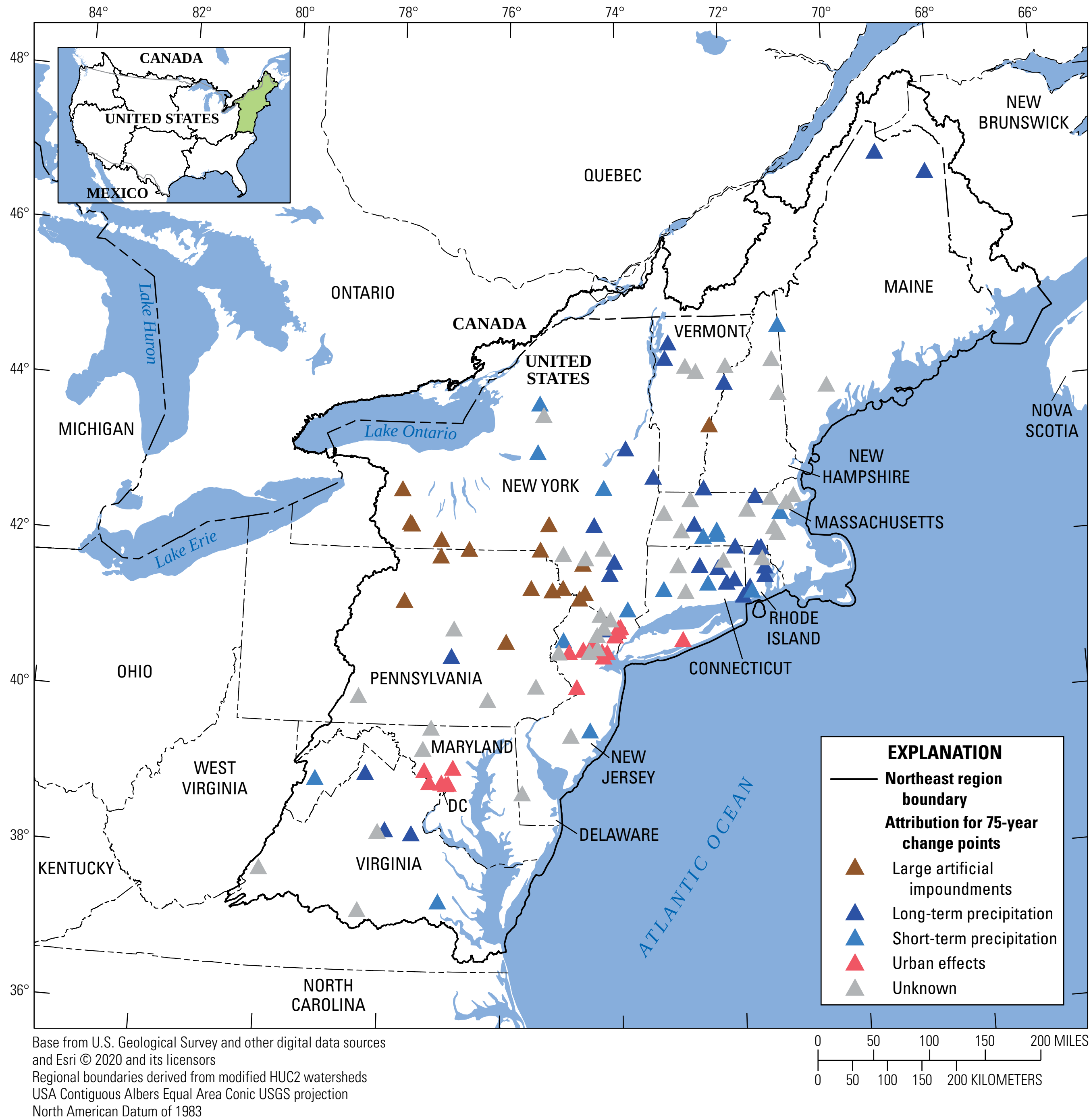

Figure E6. Map of the Northeast region showing the geographic distribution of streamgages that have peak-streamflow attributions in various categories for 75-year change points (1941–2015).

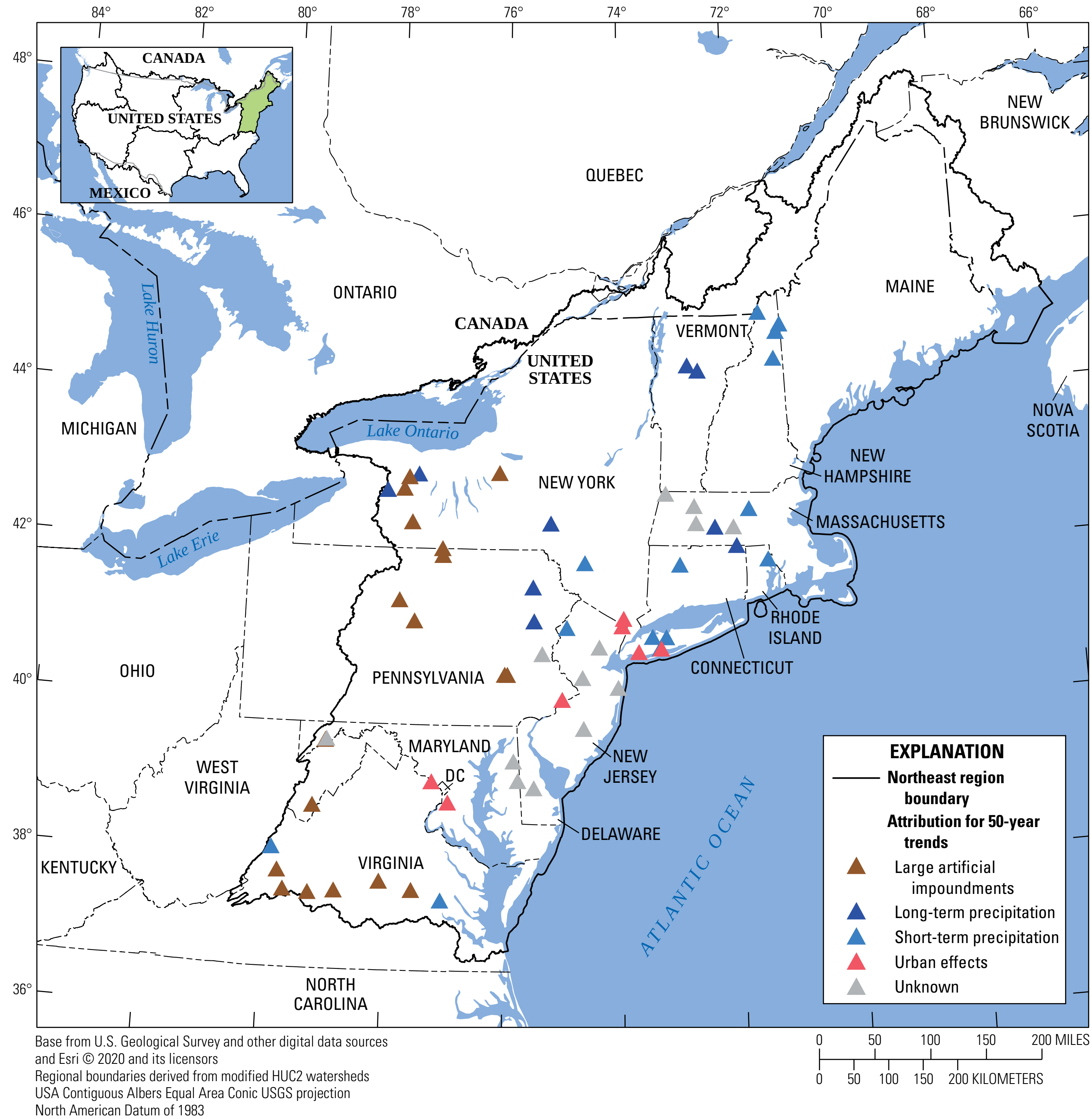

Figure E7. Map of the Northeast region showing the geographic distribution of streamgages that have peak-streamflow attributions in various categories for 50-year monotonic trends (1966–2015).

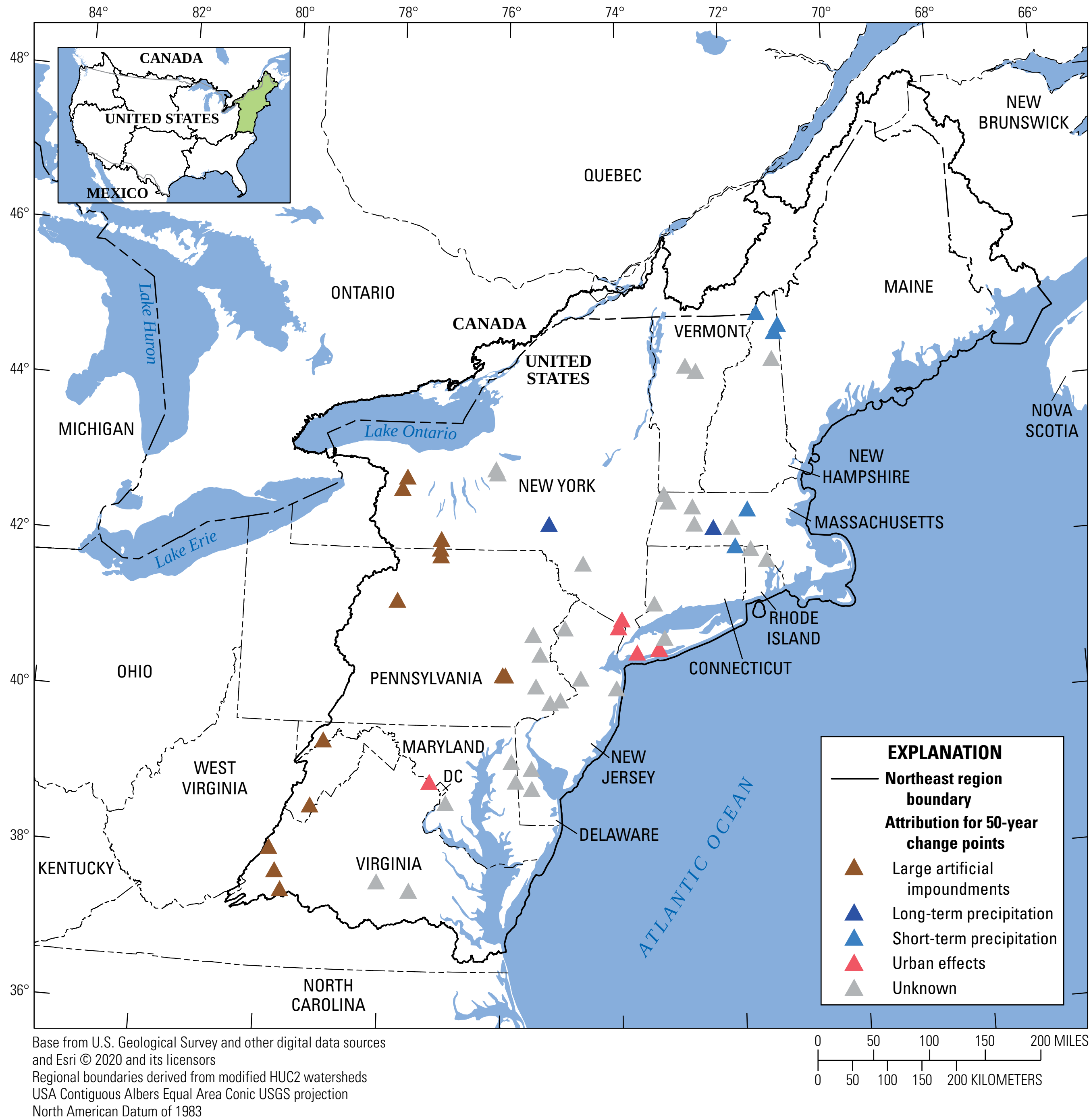

Figure E8. Map of the Northeast region showing the geographic distribution of streamgages that have peak-streamflow attributions in various categories for 50-year change points (1966–2015).

Summary

The statistical attribution of significant monotonic trends and change points (abrupt shifts) in peak streamflows for U.S. Geological Survey (USGS) streamgages in the Northeast region of the United States was completed for two time periods: 1941–2015 (75 water years) and 1966–2015 (50 water years). Analyses were focused on the most likely causal variables that were feasible to study: short-term precipitation (storm-event precipitation related to individual peak flows), long-term precipitation (using a measure of antecedent moisture), large artificial impoundments, and urban effects.

To attribute peak-streamflow trends and change points to short-term or long-term precipitation, we required that significant interannual correlations exist between peak streamflows and precipitation and that values for these variables have significant trends in the same direction as peak-flow trends. We also analyzed basin-specific information to infer whether peak-flow changes over time were caused by human alterations of basins. Since large impoundments are expected to reduce peak flows, we considered this attribution only if basins contained large impoundments and peak flows had significant decreases over time. For attributions to urban effects, basins needed to be at least about 20-percent developed and have peak flows that increased substantially more than storm-event precipitation.

There were 125 significant 75-year monotonic trends in peak flows to attribute, and the primary attribution for a majority of them was short-term precipitation (43 streamgages) or long-term precipitation (29 gages). For the remaining gages, 23 trends were attributed to urban effects, 16 were attributed to large artificial impoundments, and 14 have an unknown attribution. For about half of gages (46 percent) where the primary attribution was short-term or long-term precipitation, the secondary attribution was precipitation of the other time scale. The number of change points with a primary attribution of short-term precipitation was substantially less than the number of trends attributed to short-term precipitation. This difference indicates that more gradual than abrupt changes over time in the short-term precipitation changes led to annual peak-streamflow changes in the Northeast. The number of change points with a primary attribution of long-term precipitation was the same as the number of trends attributed to long-term precipitation.

Most of the change points for the 75-year period that were attributed to long-term precipitation or short-term precipitation occurred from the late 1960s to the early 1970s. Most of the change points attributed to urban effects occurred in the late 1960s. The range of change-point years for large artificial impoundments was larger than the ranges for other attributions, reflecting a variety of years when large impoundments were built; the highest concentration of change points was in the early 1960s.

There were 61 50-year trends in peak streamflows in the Northeast to attribute. The much higher number of 75-year trends compared to 50-year trends may be a result of the 50-year period (1966–2015) beginning mostly after change points in the 1960s and early 1970s had already occurred for basins in the Northeast.

Both 75-year monotonic trends and change points for peak streamflows show similar patterns in peak-flow change magnitude between attribution categories. Increases in peak flows at streamgages with the primary attribution of short-term precipitation were somewhat larger, in general, than those attributed to long-term precipitation. The urban-effects attribution category contains gages with much larger changes over time than those in the short- or long-term precipitation attribution categories. Gages in the large-impoundment attribution category had large decreases over time. A similar pattern of peak-flow-change magnitude between attribution categories is evident for 50-year trends and change points; however, there are considerably fewer gages in each 50-year category.

Gages that have peak-streamflow monotonic trends and change points with a primary attribution of short-term or long-term precipitation for the 75-year period are located throughout the Northeast. Gages where trends and change points are attributed to urban effects are concentrated in New Jersey and areas near Washington, D.C. Most of the gages that have 75-year trends and change points attributed to large impoundments are located in western New York and northeastern Pennsylvania.

Conclusions

Design floods are estimates of peak streamflows that may cause damage or failure at bridges, culverts, and other structures. Traditional computations of design floods, such as the 100-year flood, incorporate the assumption that past peak flows are representative of future ones. For the Northeast region of the United States, this assumption is not valid for many basins containing large impoundments and those having substantial urban effects. Design-flood calculations for these basins using all historical peak flows may produce results that are not representative of future floods. Many basins in the Northeast have peak-flow trends and change points that were attributed to short-term (storm-event) and long-term precipitation changes. Higher amounts of long-term precipitation can lead to higher soil moisture and greater peak flows for a given amount of storm-event precipitation. It is important to consider whether future short-term and long-term precipitation will lead to peak flows that are similar to historical peak flows. More work is needed for the parts of the Northeast to determine the influence of snowmelt on peak flows, including its interaction with short-term and long-term precipitation.

References Cited

Alley, W.M., 1984, The Palmer Drought Severity Index—Limitations and assumptions: Journal of Climate and Applied Meteorology, v. 23, no. 7, p. 1100–1109.

Armstrong, W.H., Collins, M.J., and Snyder, N.P., 2014, Hydroclimatic flood trends in the northeastern United States and linkages with large-scale atmospheric circulation patterns: Hydrological Sciences Journal, v. 59, no. 9, p. 1636–1655, accessed August 2019, at https://www.tandfonline.com/doi/full/10.1080/02626667.2013.862339.

Berghuijs, W.R., Woods, R.A., Hutton, C.J., and Sivapalan, M., 2016, Dominant flood generating mechanisms across the United States: Geophysical Research Letters, v. 43, no. 9, p. 4382–4390, accessed August 10, 2021, at https://doi.org/10.1002/2016GL068070.

Chamberlain, S., 2019, rnoaa—'NOAA' weather data from R: R package version 0.8.4, accessed February 12, 2019, at https://CRAN.R-project.org/package=rnoaa.

Collins, M.J., 2009, Evidence for changing flood risk in New England since the late 20th century: Journal of the American Water Resources Association, v. 45, no. 2, p. 279–290.

Collins, M.J., Kirk, J.P., Pettit, J., DeGaetano, A.T., McCown, M.S., Peterson, T.C., Means, T.N., and Zhang, X., 2014, Annual floods in New England (USA) and Atlantic Canada—Synoptic climatology and generating mechanisms: Physical Geography, v. 35, no. 3, p. 195–219.

Dai, A., Trenberth, K.E., and Qian, T., 2004, A global dataset of Palmer Drought Severity Index for 1870–2002—Relationship with soil moisture and effects of surface warming: Journal of Hydrometeorology, v. 5, no. 6, p. 1117–1130.

Dudley, R.W., Archfield, S.A., Hodgkins, G.A., Renard, B., and Ryberg, K.R., 2018, Peak-streamflow trends and change-points and basin characteristics for 2,683 U.S. Geological Survey streamgages in the conterminous U.S. (ver. 3.0, April 2019): U.S. Geological Survey data release, accessed October 30, 2019, at https://doi.org/10.5066/P9AEGXY0.

Dupigny-Giroux, L.A., Mecray, E.L., Lemcke-Stampone, M.D., Hodgkins, G.A., Lentz, E.E., Mills, K.E., Lane, E.D., Miller, R., Hollinger, D.Y., Solecki, W.D., Wellenius, G.A., Sheffield, P.E., MacDonald, A.B., and Caldwell, C., 2018, Northeast, chap. 18 *of* Reidmiller, D.R., Avery, C.W., Easterling, D.R., Kunkel, K.E., Lewis, K.L.M., Maycock, T.K., and Stewart, B.C., eds., Impacts, risks, and adaptation in the United States—Fourth National Climate Assessment, Volume II: Washington, D.C., U.S. Global Change Research Program, p. 669–742, accessed August 10, 2021, at https://doi.org/10.7930/NCA4.2018.CH18.

Falcone, J.A., 2011, GAGES–II—Geospatial attributes of gages for evaluating streamflow, [version II]: U.S. Geological Survey dataset, accessed August 25, 2015, at http://water.usgs.gov/GIS/metadata/usgswrd/XML/gagesII_Sept2011.xml.

Falcone, J.A., 2015, U.S. conterminous wall-to-wall anthropogenic land use trends (NWALT), 1974–2012: U.S. Geological Survey Data Series 948, 33 p. plus appendixes 3–6 as separate files, accessed September 11, 2018, at http://dx.doi.org/10.3133/ds948.

Falcone, J.A., Carlisle, D.M., Wolock, D.M., and Meador, M.R., 2010, GAGES—A stream gage database for evaluating natural and altered flow conditions in the conterminous United States: Ecology, v. 91, no. 2, p. 621, abstract and link to dataset accessed August 25, 2015, at http://esapubs.org/Archive/ecol/E091/045/metadata.htm.

FitzHugh, T.W., and Vogel, R.M., 2011, The impact of dams on flood flows in the United States: River Research and Applications, v. 27, no. 10, p. 1192–1215.

Fry, J.A., Xian, G., Jin, S., Dewitz, J.A., Homer, C.G., Yang, L., Barnes, C.A., Herold, N.D., and Wickham, J.D., 2011, Completion of the 2006 National Land Cover Database for the Conterminous United States: Photogrammetric Engineering and Remote Sensing, v. 77, no. 9, p. 858–864.

Graf, W.L., 2006, Downstream hydrologic and geomorphic effects of large dams on American rivers: Geomorphology, v. 79, nos. 3–4, p. 336–360.

Helsel, D.R., and Hirsch, R.M., 1992, Statistical methods in water resources: New York, Elsevier, 522 p.

Hirsch, R.M., and Ryberg, K.R., 2012, Has the magnitude of floods across the USA changed with global CO_2 levels?: Hydrological Sciences Journal, v. 57, no. 1, p. 1–9.

Hodgkins, G.A., and Dudley, R.W., 2005, Changes in the magnitude of annual and monthly streamflows in New England, 1902–2002: U.S. Geological Survey Scientific Investigations Report 2005–5135, 37 p.

Hodgkins, G.A., Dudley, R.W., Archfield, S.A., and Renard, B., 2019, Effects of climate, regulation, and urbanization on historical flood trends in the United States: Journal of Hydrology, v. 573, p. 697–709.

Hollis, G.E., 1975, The effect of urbanization on floods of different recurrence interval: Water Resources Research, v. 11, no. 3, p. 431–435.

Ivancic, T.J., and Shaw, S.B., 2015, Examining why trends in very heavy precipitation should not be mistaken for trends in very high river discharge: Climatic Change, v. 133, no. 4, p. 681–693.

Kunkel, K.E., Stevens, L.E., Stevens, S.E., Sun, L., Janssen, E., Wuebbles, D., Rennells, J., DeGaetano, A., and Dobson, J.G., 2013, Part 1. Climate of the Northeast U.S., *of* Regional climate trends and scenarios for the U.S. National Climate Assessment: National Oceanic and Atmospheric Administration NOAA Technical Report NESDIS 142–1, 79 p.

Leopold, L.B., 1968, Hydrology for urban land planning—A guidebook on the hydrologic effects of urban land use: U.S. Geological Survey Circular 554, 18 p.

Lins, H.F., and Slack, J.R., 2005, Seasonal and regional characteristics of U.S. streamflow trends in the United States from 1940 to 1999: Physical Geography, v. 26, no. 6, p. 489–501.

Magilligan, F.J., and Nislow, K.H., 2005, Changes in hydrologic regime by dams: Geomorphology, v. 71, nos. 1–2, p. 61–78.

Mann, H.B., 1945, Nonparametric tests against trend: Econometrica, v. 13, no. 3, p. 245–259.

Menne, M.J., Durre, I., Vose, R.S., Gleason, B.E., and Houston, T.G., 2012, An overview of the Global Historical Climatology Network-Daily database: Journal of Atmospheric and Oceanic Technology, v. 29, no. 7, p. 897–910, accessed September 11, 2018, at https://doi.org/10.1175/JTECH-D-11-00103.1.

National Oceanic and Atmospheric Administration [NOAA], 2018, Palmer Drought Severity Index data: NOAA National Centers for Environmental Information, National Climate Indices, accessed September 7, 2018, at ftp://ftp.ncdc.noaa.gov/pub/data/cirs/climdiv/climdiv-pdsidv-v1.0.0-20180806.

Palmer, W.C., 1965, Meteorological drought: U.S. Weather Bureau Research Paper 45, 58 p.

Pettitt, A.N., 1979, A non-parametric approach to the change-point problem: Journal of the Royal Statistical Society, Series C (Applied Statistics), v. 28, no. 2, p. 126–135.

R Core Team, 2018, R—A language and environment for statistical computing, version 3.5.0: R Foundation for Statistical Computing software release, accessed June 4, 2018, at https://www.R-project.org/.

Rice, J.S., Emanuel, R.E., Vose, J.M., and Nelson, S.A., 2015, Continental US streamflow trends from 1940 to 2009 and their relationships with watershed spatial characteristics: Water Resources Research, v. 51, no. 8, p. 6262–6275.

Ryberg, K.R., Hodgkins, G.A., and Dudley, R.W., 2020, Change points in annual peak streamflows—Method comparisons and historical change points in the United States: Journal of Hydrology, v. 583, article 124307, accessed August 10, 2021, at https://doi.org/10.1016/j.jhydrol.2019.124307.

Sauer, V.B., Thomas, W.O., Jr., Stricker, V.A., and Wilson, K.V., 1983, Flood characteristics of urban watersheds in the United States: U.S. Geological Survey Water-Supply Paper 2207, 63 p.

Seaber, P.R., Kapinos, F.P., and Knapp, G.L., 1987, Hydrologic unit maps: U.S. Geological Survey Water-Supply Paper 2294, 63 p. [Also available at https://doi.org/10.3133/wsp2294.]

Sen, P.K., 1968, Estimates of the regression coefficient based on Kendall's tau: Journal of the American Statistical Association, v. 63, no. 324, p. 1379–1389.

Slater, L.J., and Villarini, G., 2016, Recent trends in U.S. flood risk: Geophysical Research Letters, v. 43, no. 24, p. 12428–12436.

Theil, H., 1950, A rank-invariant method of linear and polynomial analysis, Part III: Proceedings of the Koninklijke Nederlandse Akademie van Wettenschappen [Proceedings of the Royal Netherlands Academy of Sciences], Series A, Mathematical Sciences, v. 53, p. 1397–1412.

Thornton, P.E., Thornton, M.M., Mayer, B.W., Wilhelmi, N., Wei, Y., Devarakonda, R., and Cook, R.B., 2014, Daymet—Daily surface weather data on a 1-km grid for North America, version 2: Oak Ridge National Laboratory, Distributed Active Archive Center (ORNL DAAC) database, accessed March 19, 2019, at http://dx.doi.org/10.3334/ORNLDAAC/1219. [Data obtained by using the following search parameters: Time period: 1980-01-01 to 2017-12-31. Spatial range: N=48.1, S=36.5, E=-066.0, W=-081.0.]

U.S. Geological Survey, 2007, North America elevation 1-kilometer-resolution GRID [dataset]: U.S. Geological Survey ScienceBase Catalog website, accessed May 1, 2019, at https://www.sciencebase.gov/catalog/item/4fb5495ee4b04cb937751d6d.

Williams, G.P., and Wolman, M.G., 1984, Downstream effects of dams on alluvial rivers: U.S. Geological Survey Professional Paper 1286, 83 p.

York, B.C., Ryberg, K.R., Asquith, W.H., Chase, K.J., Dickinson, J.E., Dudley, R.W., Harden, T.M., Hodgkins, G.A., Holtschlag, D.J., Humberson, D.G., Konrad, C.P., Levin, S.B., Restivo, D.E., Sando, R., Sando, S.K., Swain, E.D., Tillery, A.C., and Totten, A.R., 2022, Attributions for nonstationary peak streamflow records across the conterminous United States, 1941–2015 and 1966–2015: U.S. Geological Survey data release, https://doi.org/10.5066/P9FOUVWG.

Attribution of Monotonic Trends and Change Points in Peak Streamflow in the Southwest Region of the United States, 1941–2015 and 1966–2015

By Tessa M. Harden and Jesse E. Dickinson

Chapter F of
Attribution of Monotonic Trends and Change Points in Peak Streamflow Across the Conterminous United States Using a Multiple Working Hypotheses Framework, 1941–2015 and 1966–2015
Karen R. Ryberg, editor

Prepared in cooperation with
U.S. Department of Transportation
Federal Highway Administration

Professional Paper 1869

U.S. Department of the Interior
U.S. Geological Survey

U.S. Geological Survey, Reston, Virginia: 2022

For more information on the USGS—the Federal source for science about the Earth, its natural and living resources, natural hazards, and the environment—visit https://www.usgs.gov or call 1–888–ASK–USGS.

For an overview of USGS information products, including maps, imagery, and publications, visit https://store.usgs.gov.

Suggested citation:
Harden, T.M., and Dickinson, J.E., 2022, Attribution of monotonic trends and change points in peak streamflow in the Southwest region of the United States, 1941–2015 and 1966–2015, chap. F *of* Ryberg, K.R., ed., Attribution of monotonic trends and change points in peak streamflow across the conterminous United States using a multiple working hypotheses framework, 1941–2015 and 1966–2015: U.S. Geological Survey Professional Paper 1869, p. F1–F23, https://doi.org/10.3133/pp1869.

Associated data for this publication:
Dudley, R.W., Archfield, S.A., Hodgkins, G.A., Renard, B., and Ryberg, K.R., 2018, Peak-streamflow trends and changepoints and basin characteristics for 2,683 U.S. Geological Survey streamgages in the conterminous U.S. (ver. 3.0, April 2019): U.S. Geological Survey data release, https://doi.org/10.5066/P9AEGXY0.

York, B.C., Ryberg, K.R., Asquith, W.H., Chase, K.J., Dickinson, J.E., Dudley, R.W., Harden, T.M., Hodgkins, G.A., Holtschlag, D.J., Humberson, D.G., Konrad, C.P., Levin, S.B., Restivo, D.E., Sando, R., Sando, S.K., Swain, E.D., Tillery, A.C., and Totten, A.R., 2022, Attributions for nonstationary peak streamflow records across the conterminous United States, 1941–2015 and 1966–2015: U.S. Geological Survey data release, https://doi.org/10.5066/P9FOUVWG.

ISSN 2330-7102 (online)

Acknowledgments

The work described in this professional paper was funded by the Federal Highway Administration of the U.S. Department of Transportation through Interagency Agreement DTFH6116X30020, “Flood Frequency Estimation for Hydraulic Design.”

The authors thank Adam Stonewall and Mike Kohn, U.S. Geological Survey, for providing thoughtful reviews.

Contents

Figures

Table

Conversion Factors

Multiply	By	To obtain
	Length	
foot (ft)	0.3048	meter (m)
meter (m)	3.281	foot (ft)
	Flow rate	
cubic foot per second (ft^3/s)	0.02832	cubic meter per second (m^3/s)

Datum

Horizontal coordinate information is referenced to the North American Datum of 1983 (NAD 83).

Vertical coordinate information is referenced to the North American Vertical Datum of 1988 (NAVD 88).

Altitude, as used in this chapter, refers to distance above the vertical datum.

Supplemental Information

A “water year” is the 12-month period from October 1 through September 30 of the following year that is designated by the calendar year in which it ends.

The 75-year and 50-year study periods described in this report span water years 1941–2015 and 1966–2015, respectively.

Abbreviations

>	greater than
≥	greater than or equal to
<	less than
≤	less than or equal to
GAGES-II	Geospatial Attributes of Gages for Evaluating Streamflow, Version II
HCDN-2009	Hydro-Climatic Data Network 2009
HUC2	two-digit hydrologic unit code
HUC4	four-digit hydrologic unit code
NAD 83	North American Datum of 1983
NAVD 88	North American Vertical Datum of 1988
NOAA	National Oceanic and Atmospheric Administration
NWIS	National Water Information System
p-value	attained significance level
USACE	U.S. Army Corps of Engineers
USGS	U.S. Geological Survey

Attribution of Monotonic Trends and Change Points in Peak Streamflow in the Southwest Region of the United States, 1941–2015 and 1966–2015

By Tessa M. Harden[1] and Jesse E. Dickinson[1]

Abstract

In the United States, the attribution of monotonic trends and change points in annual peak-streamflow data is important for water resource management and for flood-risk assessment in order to adjust for future changes in flood-frequency analyses. This chapter describes the attribution of monotonic trends and change points in annual peak-streamflow data in the Southwest region of the United States. The work described was part of a national study by the U.S. Geological Survey (USGS), in cooperation with the Federal Highway Administration of the U.S. Department of Transportation, to identify and make attributions for statistically significant monotonic trends and change points in annual peak streamflow across the conterminous United States.

Attributions were made for monotonic trends and change points in annual peak-streamflow records for water years 1941–2015 (a period of 75 years) and 1966–2015 (a period of 50 years) at selected USGS streamgages. Most monotonic trends and change points in both time periods are negative, except for those attributed to urban effects. Change points that are earlier in the streamgage record (before the mid-1980s) are mostly attributed to large artificial impoundments while those later in the streamgage record (after the mid-1980s) are mostly attributed to climate variables such as long-term precipitation, air temperature, and snowpack. Spatially, monotonic trends in annual peak streamflow in northern and central California and parts of Colorado and Utah are most commonly attributed to large artificial impoundments. The most common primary attribution in southern California is urban effects. Monotonic trends and change points at many streamgages in Arizona and in high-altitude areas of Colorado and Utah are attributed to changes in long-term precipitation and snowpack.

Introduction

The magnitudes of floods in the Southwest region of the United States (fig. F1) are changing over time. These changes are a concern for many reasons, including their potential effect on the management of water resources, the hydrologic design of transportation and flood-control infrastructure, the operation and storage capacity of reservoirs, and the meeting of hydropower and irrigation demands (Lins and Slack, 1999; McCabe and Wolock, 2002; Miller and Piechota, 2011). Of particular concern are the trends in annual peak streamflow, given their importance in flood-frequency analysis and flood-hazard assessments (England and others, 2018). Over the past century, the economic losses from floods have generally increased and may continue to increase in the future (Dettinger, 2011; Whitfield, 2012).

Past studies have linked trends in flooding to changes in climate variables (Lins and Slack, 1999; Jain and Lall, 2001; Villarini and others, 2009; Vogel and others, 2011; Hodgkins and others, 2017), land cover (Beighley and Moglen, 2002; Blöschl and others, 2007; Saghafian and others, 2008), and anthropogenic modifications of river systems (Tockner and Stanford, 2002; Kondolf and Batalla, 2005; Willis and others, 2011). The goal of such studies is often to link the observed trends in annual peak-streamflow data to potential drivers, or "attributions," for those trends. In the highly regulated drainage basins of the Southwest region, the combined effects of climate, land-cover change, and water management on trends in peak streamflow are often complex and difficult to differentiate. For example, in a highly regulated stream, a trend in peak streamflow due to artificial wastewater and water-supply discharges may obscure a trend related to climate, land cover, or other variables.

Purpose and Scope

This chapter describes attribution of statistically significant (p-value<0.10 unless otherwise specified, where the p-value is the attained significance level) monotonic trends and change points in the Southwest region. The work described was part of a larger national study by the U.S. Geological Survey (USGS), in cooperation with the Federal Highway Administration of the U.S. Department of Transportation, to identify and make attributions for monotonic trends and change points in annual peak streamflow across the conterminous United States using a multiple working hypotheses

[1]U.S. Geological Survey.

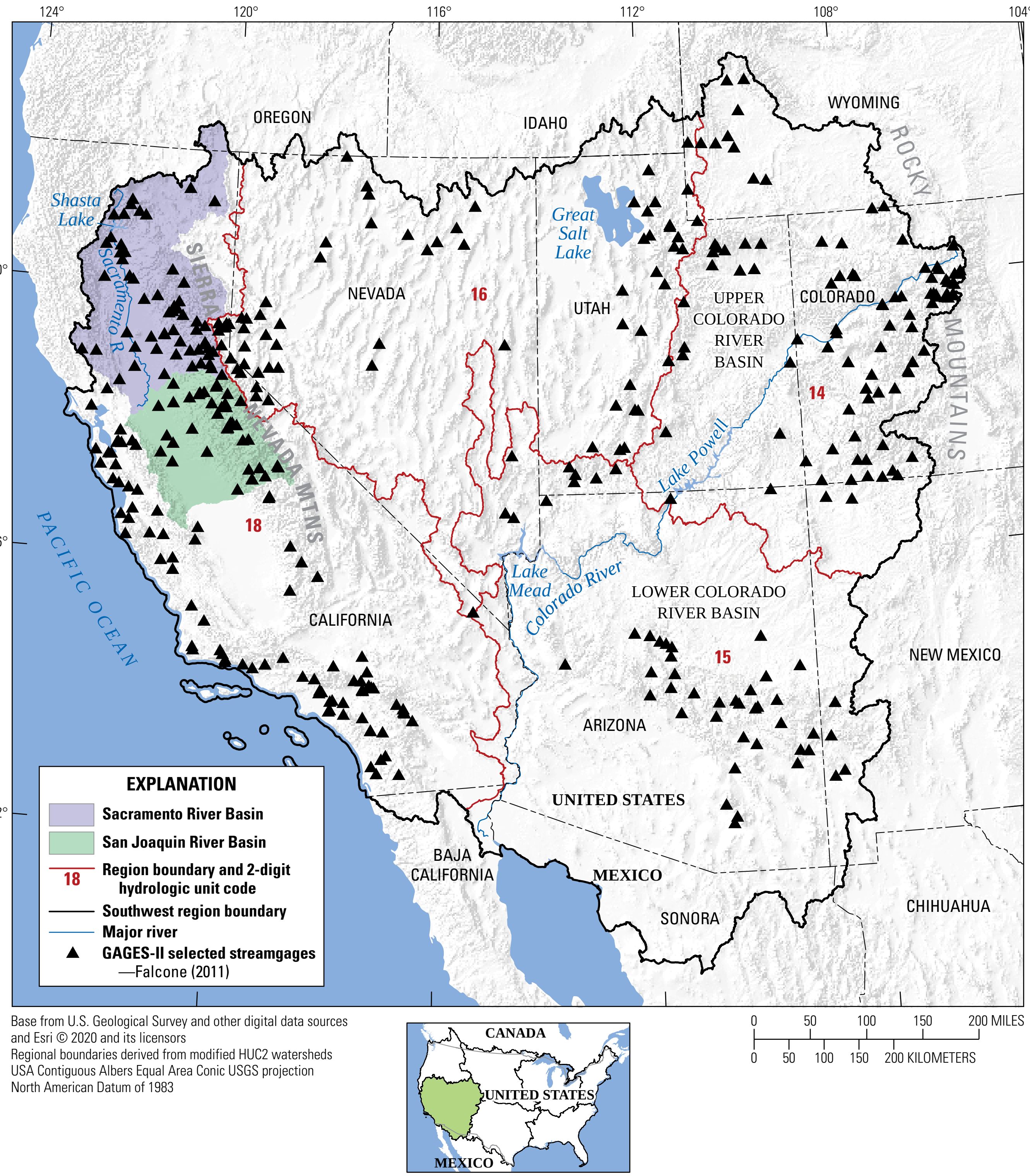

Figure F1. Map showing the streamgages where monotonic trends and change points were evaluated in the Southwest region of the United States. Although the southern part of the Southwest region extends into Mexico because of the topography of stream drainage basins, the watersheds considered for monotonic trend and change-point attributions are within the conterminous United States. For this study, the regions were based on watersheds identified by two-digit hydrologic unit codes (HUC2s) described by Seaber and others (1987) and were modified slightly by adding or subtracting subregions (HUC4s) to achieve geographic cohesiveness or hydrologic-setting similarity. This region is based on watersheds identified by two-digit hydrologic unit codes HUC 14, HUC 15, HUC 16, and HUC 18, excluding subregion 1801, from Seaber and others (1987). Term: GAGES-II, Geospatial Attributes of Gages for Evaluating Streamflow, Version II (Falcone, 2011).

framework (Hodgkins and others, 2019; Barth and others, this volume, chap. A).

Monotonic trends are gradual changes in which peak streamflow is generally increasing or generally decreasing, but the change is not necessarily linear. In this study, monotonic trends are indicated by statistically significant results of a Mann-Kendall trend test (Helsel and others, 2020). Change points (also called step trends) are abrupt changes in the distribution parameters of annual peak streamflow. In this study, change points represent a statistically significant sudden change in the median of the distribution as indicated by the Pettitt test (Pettitt, 1979). In this chapter, use of the single term “trend” refers to a change that can be either a monotonic trend or change point.

This chapter identifies primary and, in some cases, secondary attributions of monotonic trends and change points in annual peak-streamflow data at select USGS streamflow gaging stations (streamgages) in the Southwest region. Streamgage-site data, climate data, and statistical approaches were used to evaluate and make attributions for monotonic trends and change points in annual peak streamflows for two different time periods, 1941–2015 (a 75-year period) and 1966–2015 (a 50-year period), at USGS streamgages in regulated, urbanized, and minimally altered basins. Also provided are levels of evidence (Barth and others, this volume, chap. A) for each attribution at each streamgage based on available supporting evidence (York and others, 2022).

This study was designed to address the following questions: (1) Are there spatial patterns in the type of primary attribution (for example, large artificial impoundments, urban effects, and climate variables) of monotonic trends and change points in annual peak-streamflow data? (2) What primary attributions contribute to the largest percentage change in median annual peak streamflow? and (3) Are there differences in the primary attributions of change points that occur early in the peak streamflow record compared to those later in the record? Information on the attribution of peak streamflow monotonic trends and change points can help inform flood-frequency analyses, which may reduce uncertainty and inform assessments of future flood risk and water supply.

Study Area

The Southwest region study area covers hydrologic unit code (HUC) water resource regions (Seaber and others, 1987) 14, 15, 16, and most of 18; this area includes Arizona, most of California, Nevada, and Utah, and parts of Colorado, Idaho, New Mexico, Oregon, and Wyoming (fig. F1). The largest drainage basins in the region are the Upper and Lower Colorado River Basins (HUCs 14 and 15, respectively) which drain most of the study region except for the southeastern corner of California and the Great Basin region of Nevada. Although the southern part of the Southwest region extends into Mexico because of the topography of stream drainage basins, the watersheds considered for monotonic trend and change-point attributions are within the conterminous United States.

Streamflow in the Upper Colorado River Basin (includes parts of Colorado, New Mexico, Utah, and Wyoming) exists within a supply-driven environment (Miller and Piechota, 2008), which means that the water supply is sourced from seasonal snowpack and precipitation events. Wintertime precipitation is dominated by frontal storms with typical life cycles of 1–4 days that migrate into the central Rocky Mountains from the North Pacific region (Carson, 2007). Annual peak streamflow in this region is largely associated with snowmelt (Spahr and others, 2000; Solander and others, 2017). Colorado River streamflow in the Lower Colorado River Basin (includes parts of Arizona, California, and Nevada) is demand driven (Miller and Piechota, 2008). This means that water supply is largely driven by water releases from the Upper Colorado River Basin (HUC 14), which are dictated by consumptive use and regulated primarily by the Colorado River Compact of 1922 (https://babel.hathitrust.org/cgi/pt?id=uc2.ark:/13960/t5gb2180q&view=1up&seq=3&skin=2021) and the United States Code (43 U.S.C. 617, et seq.; https://www.govinfo.gov/app/details/USCODE-2014-title43/USCODE-2014-title43-chap12A-subchapI-sec617). The major basins in California (for example, the Sacramento and San Joaquin River Basins; fig. F1) included in this study area function similarly. Streamflow in the headwaters at high- and mid-altitude settings in the Sierra Nevada Mountains is supply driven and water supply is dominated by snowmelt and wintertime precipitation events from frontal systems and atmospheric rivers (Wilby and Dettinger, 2000). Streamflow in the downstream reaches of the California basins is highly regulated to meet the water needs of large population centers, irrigation, and water transfers and diversions.

Non-Climatic Drivers of Annual Peak-Streamflow Trends

The main non-climatic drivers of changes in streamflow trends in the Southwest region are water-management practices (dams, water diversions, and water transfers), changes in land cover, and changes in land use (Stogner, 2000). Dams and other water-control structures (such as diversions and pumping stations) have had a substantial influence on the spatial and temporal distribution of annual peak streamflows (Villarini and Slater, 2017) as well as the magnitude of annual peak streamflows across the United States (Graf, 2006).

The Southwest region is a semi-arid to arid landscape and has had one of the greatest population increases in the United States over the second half of the 20th century (Hobbs and Stoops, 2002). The increase in water demand has been met largely through streamflow storage in artificial impoundments behind dams, water diversions, and interbasin water transfers (Bureau of Reclamation, 2019). The first, second, and eighth largest reservoirs in the United States are along the Colorado River (Lake Powell and Lake Mead) and the Sacramento River (Shasta Lake) (fig. F1). These reservoirs store and provide water, generate hydroelectric power, act to control flooding, and facilitate irrigation for tens of millions of people in Arizona, California, Colorado, Nevada, New Mexico, Utah, and Wyoming.

Urbanization has been shown to have statistically significant effects on annual peak-streamflow magnitudes (Hollis, 1975; Ng and Marsalek, 1989; Changnon and Demissie, 1996; Rose and Peters, 2001). Urbanization tends to result in increases in impervious surfaces, in channelization of streams, and in stormwater infrastructure. The effects of urbanization include reduced infiltration and increased runoff (Zhu and others, 2007), both of which typically lead to higher annual peak streamflows.

Climatic Drivers of Annual Peak-Streamflow Trends

A natural driver of annual peak-streamflow trends is climate (mainly air temperature, precipitation, and snowpack). Changes in these climate variables can have a direct effect on annual peak streamflow (Stogner, 2000; Novotny and Stefan, 2007; Solander and others, 2017). The climate and hydrological cycle of the Southwest region has shifted over much of the 20th and early 21st century (Barnett and others, 2008). Much of the Southwest recently underwent one of the largest droughts in historical records (Piechota and others, 2004; Cook and others, 2010) and, based on projected temperature increases simulated in general circulation models, more severe droughts are expected. For example, one study by Woodhouse and others (2010) estimates that, by 2100, the severity of droughts might exceed anything seen in the paleoclimate records. During the last few decades, the surface-air temperature increase in the Southwest was much greater than the increase in the global mean (Chylek and others, 2014). Even a slight increase in temperature and decrease in precipitation could have a strong effect on the climate of the Southwest region in a matter of years to decades (Seager and others, 2007; MacDonald, 2010).

Since the beginning of instrumental records in 1895, air temperatures at the turn of the 21st century have been the highest in a multiyear period (Chylek and others, 2014; Woodhouse and others, 2016). At the same time, total precipitation has been decreasing since a record wet period that was centered around the early 1980s. However, 5-year moving-average precipitation was more than two standard deviations below the mean annual precipitation (from 1895 to 2012) only during the early 1900s and during a period of several years in the 1950s (Chylek and others, 2014). The precipitation decrease after the mid-1980s is not outside the range of natural variability and is similar to a decrease that occurred during the wet period between the early 1940s and 1955 (Chylek and others, 2014). After the turn of the 21st century, dry conditions prevailed, and the Southwest has experienced the most persistent droughts since records began in 1895 (U.S. Environmental Protection Agency, 2016; National Oceanic and Atmospheric Administration, 2018). Unlike the dust bowl era of the 1930s, the turn of the century drought is believed to have been caused by an increase in temperature more than a decrease in precipitation (Woodhouse and others, 2016). The third and fourth National Climate Assessments showed that heavy precipitation events (99th percentile of daily precipitation) have increased almost everywhere across the Nation in the last three to five decades, except for in the Southwest region (Walsh and others, 2014; Easterling and others, 2017). Chylek and others (2014) determined that the trend for overall mean annual precipitation for 1895–2012 is slightly positive, but not statistically significant. Thus, the Southwest has experienced a warmer climate but a nearly unchanged rate of precipitation for well over a hundred years.

Previous studies have documented decreasing trends in snow-water equivalent and snow-cover extent in high- and mid-altitude regions in the western United States, including Arizona, California, Colorado, Nevada, Utah, and Wyoming (Cayan and others, 2001; Mote and others, 2005; Clow, 2010; Miller and Piechota, 2011; Siler and others, 2019). These trends appear to be attributed to increasing springtime temperatures, despite winter precipitation increases in some areas (Stewart, 2009). Decreases in snowpack are coupled with shifts toward earlier runoff in recent decades (Knowles and others, 2006); these changes have been attributed to more precipitation falling as rain instead of snow (Dettinger and Cayan, 1995; Cayan and others, 2001). These shifts in the timing of snowmelt can affect streamflow magnitude. In some locations, such as the Uinta Mountains of northeastern Utah, streamflow magnitudes have been relatively high in recent decades (Carson, 2007). Solander and others (2017) documented increases in maximum streamflow (defined as the flood with annual exceedance probability of 0.01 [a 1 percent chance of occurring within a given year]) in March and April but decreases of up to 41 percent during June and July for streams above 2,300 meters (7,500 feet [ft]) above sea level north of 39° N. latitude in the Colorado River Basin. Changing snow accumulation and melting patterns are likely the primary causes of the changes in the timing and magnitude of these maximum streamflows (Solander and others, 2017).

Atmospheric warming due to the continued release of anthropogenic greenhouse gases is expected to result in an increase in the magnitude of floods (Trenberth, 1999; Intergovernmental Panel on Climate Change, 2008) by increasing the amount of moisture (and therefore precipitable water) in the atmosphere. However, Hirsch and Ryberg (2012) showed that, in the Southwest region, increasing greenhouse gas concentrations in the atmosphere will likely lead to a decrease in flood magnitudes. They suggest the potential decrease is likely the result of changing storm tracks or, more likely, a decrease in winter snowpack caused by greenhouse gas forcing in drainage basins where annual peak streamflow is largely the result of snowmelt. However, natural variability of precipitation and air temperature is known to be substantial in this region; this variability makes it difficult to clearly attribute the recent drying and warming to greenhouse gas forcing (Lehner and others, 2018). Lehner and others (2018) showed that, while the warming is largely due to greenhouse gas forcing, the drying is mostly due to internal climate variability.

Annual Peak-Streamflow Data

Hodgkins and others (2019) identified 393 USGS streamgages in the Southwest region (fig. F1) with sufficient length of record and continuity for use in the attributional analysis. The selected streamgages represent regulated, urbanized, and minimally altered drainage basins, as defined in Hodgkins and others (2019). For this chapter, regulated basins were defined as having substantial reservoir storage. Urbanized basins were defined as having high urban development with low reservoir storage. Minimally altered basins were defined as being relatively free from human disturbance or modification; streamgages in these basins are part of the Hydro-Climatic Data Network 2009 (HCDN-2009), a subset of USGS streamgages for which streamflow primarily reflects meteorological conditions (Lins, 2012). The regulated and urbanized basins were classified using normalized dam storage and the percentage of developed land from the Geospatial Attributes of Gages for Evaluating Streamflow, Version II (GAGES-II) database (Falcone and others, 2010; Falcone, 2011). Annual peak-streamflow data for this chapter were from water years 1941 to 2015 (a 75-year period) and 1966 to 2015 (a 50-year period) for the Southwest region and were obtained from the USGS National Water Information System (NWIS; U.S. Geological Survey, 2018a).

Precipitation and Air Temperature Data

Precipitation and air temperature data for water years 1941–2015 and 1966–2015 were obtained from the National Climate Data Center (National Oceanic and Atmospheric Administration, 2018). Monthly average temperature and precipitation data were compiled, as well as average monthly minimum and maximum temperature data for each climate division (National Oceanic and Atmospheric Administration, 2018) that coincide with the streamgages in this study. The climate divisions are intended to represent spatial variations in climate (Guttman and Quayle, 1996). Precipitation and temperature data were also collected for coinciding climate divisions to obtain representative climate data for each streamgage. A precipitation sum and temperature mean for annual and seasonal periods was calculated for the climate divisions. The annual periods represent water years. The seasons were defined as October–December, January–March, April–June, and July–September. We also defined two longer seasons, October–March and April–September, to represent accumulation and melt seasons for drainage basins where annual peak streamflow is largely the result of snowmelt.

Attributions for Trends in Annual Peak-Streamflow Data

A list of possible attributions associated with monotonic trends and change points in annual peak-streamflow data in the Southwest region was created for this study (see Barth and others, this volume, chap. A, table A1). The list included multiple climate variables such as long-term precipitation, short-term precipitation, snowpack, and air temperature. Also included were small artificial impoundments, large artificial impoundments, groundwater withdrawals, surface-water withdrawals, artificial wastewater and water-supply discharges, interbasin water transfers, and urban effects. In this chapter, the forest cover/land cover attribution was used instead of the deforestation and wildfire attribution that was described in chapter A. Table F1 contains the attributions for monotonic trends and change points in annual peak streamflow for the streamgages in the Southwest region, and a general description of each attribution. Secondary attributions were made based on similar criteria as the primary attributions, but they had less supporting evidence. Secondary attributions were not made at every streamgage. For this chapter, the results discussed are for primary attributions unless otherwise specified.

All primary attributions were assigned a level of evidence (“robust evidence,” “medium evidence,” “limited evidence,” or “additional information required”) based on the amount and consistency of supporting information, including analyses done in this study as well as previous analyses in published literature. For a full discussion of all levels of evidence, see chapter A (Barth and others, this volume, chap. A).

Without building water balance models for each drainage basin, making primary (and in some cases secondary) attributions for monotonic tends and change points in annual peak-streamflow data can be challenging. However, to do this for the Southwest region, we followed four main steps: (1) access USGS water-year summaries for each streamgage; (2) conduct a literature search and review directed by information contained in the water-year summary, which typically related to artificial impoundments, diversions, or other water-control structures; (3) examine the strength of correlation to a variety of annual and seasonal climate variables; and (4) examine the timing of annual peak streamflows to help identify the primary climate-related flood mechanism or mechanisms (spring snowmelt, summer monsoon, wintertime rainstorms) and identify any changes in this timing.

Table F1. List of attributions used in the multiple working hypotheses framework to assess potential causal mechanisms for statistically significant monotonic trends and change points in annual peak-streamflow records from the Southwest region of the conterminous United States.

[Attributions were made in this study on the basis of peak-streamflow records and ancillary datasets. Table modified from Barth and others (this volume, chap. A, table A1)]

Attribution	General description
	Climate variability
Short-term precipitation	Short-term precipitation (event-related heavy and extreme precipitation) or increases in heavy precipitation.
Long-term precipitation	Long-term precipitation (monthly to multiyear precipitation representative of month-long storm systems, antecedent wetness or dryness, climatic persistence, or multidecadal climate variability caused by oceanic or atmospheric patterns).
Snowpack	Snowpack and ice development and melt (caused by seasonal air temperature and precipitation) or solid precipitation.
Air temperature	Air temperature other than snowpack related.
	Impoundments and diversions
Large artificial impoundments	Large artificial impoundments that are big enough to influence peak streamflow.
Small artificial impoundments	Small artificial impoundments, such as run-of-the-river dams.
Surface-water withdrawals	Surface-water withdrawals, such as irrigation, municipal water supply, or other.
Groundwater withdrawals	Groundwater withdrawals, such as irrigation, municipal water supply, or other.
Artificial wastewater and water-supply discharges	Wastewater effluent or other water-supply discharge.
Interbasin water transfers	Water transfers between drainage basins.
	Land-use and land-cover changes
Forest cover/land cover	Significant changes in land cover vegetation, including those caused by wildfires.
Urban effects	Urban effects, such as how urban land covers affect precipitation patterns and storm runoff. Urban effects also include increases in impervious area and stormwater infrastructure, curbs and gutters, and loss of wetlands. Urban water use is not included.
	Unknown causes
Unknown causes	Unknown causes, including statistical analysis methods that may result in false positives for monotonic trends or change points; therefore, there may be no known mechanism for causing a trend or change point.

USGS Water-Year Summaries and Existing Literature

The USGS water-year summary from NWIS (U.S. Geological Survey, 2018a) was accessed for each streamgage record. Water-year summaries for each site include information on surface-water records such as the period of record, quality of records, streamgage type and datum, record of extremes, factors affecting the flow, diversions, and water transfers.

Any regulation from reservoirs that was noted in water-year summaries was investigated by reviewing documentation about the reservoirs—such as reservoir type (flood-control or run-of-the-river), storage capacity, and date of completion (or date of significant modification)—and then determining the effect on annual peak streamflows. Much of this information can be found through the National Inventory of Dams (maintained by the U.S. Army Corps of Engineers [U.S. Army Corps of Engineers, 2018]), the Bureau of Reclamation (Bureau of Reclamation, 2018), and the USGS California Water Science Center drainage basin schematics (U.S. Geological Survey, 2018b) for California and boundary States. Little information is available about the quantity of streamflow diversions unless the diversion is gaged.

A cursory literature search was performed for each site or drainage basin for which a primary attribution was still not made after examining the water-year summary. Where appropriate, primary attributions were made based on previous studies. For example, the U.S. Forest Service (1994) documented several sites in Utah—including near USGS streamgage 09378630 at Recapture Creek near Blanding—where focused restoration efforts and better management practices over a few decades have transformed hillsides from unvegetated and gullied to vegetated with contour terraces, which has significantly reduced runoff and erosion. At this streamgage, the primary attribution was forest cover/land cover.

Climate Data Correlations

The relations between changes in annual peak streamflows and climate variables were evaluated by using a Kendall's tau correlation (Kendall, 1975) between annual peak-streamflow data and precipitation and air temperature data. Kendall's tau is a distribution-free, nonparametric measure of the strength of correlation or dependence between two variables. Relations between annual peak streamflows and long-term changes in precipitation and air temperature were evaluated using summed precipitation data and averaged air temperature data (arithmetic mean) to obtain values for water years and for four seasons (October–December, January–March, April–June, and July–September) in each water year. Relations between changes in annual peak streamflows and snowpack were evaluated using the same data summed and averaged for the snow accumulation period (October–March) and the snowmelt period (April–September). Kendall's tau correlation coefficient values of ≥0.30 and ≤−0.30 were considered strongly positively and strongly negatively correlated, respectively. In general, we assumed that a strong correlation was necessary to make primary attributions related to climate. All of the strongly correlated variables were statistically significant, almost all at p-value<0.001.

Trends in the Timing of Annual Peak Streamflow, Precipitation, and Air Temperature

Significant trend signals in annual peak streamflow and the climate data (precipitation and air temperature) were determined using the Mann-Kendall trend test. Trend signals which happen in the same increasing or decreasing directions may provide evidence for an attribution. For example, a positive trend in both precipitation and peak streamflow provides evidence for an attribution, while a negative trend in precipitation and a positive trend in peak streamflow would not provide evidence. We also searched for trend signals in the timing of peak streamflow, which was calculated as a monotonic trend in the mean day of the year of the annual peak streamflow (hereby referred to as "day of peak streamflow"). Monotonic trends in the day of peak streamflow were calculated at streamgages where most of the annual peak streamflow occurred in the months of April–July. We assumed that monotonic trends in annual peak streamflow during April–July were driven by changes in snowmelt processes. At these streamgages, the peak streamflow in some years could occur in months other than April–July, and those dates were not included in the trend test.

We evaluated the significance of trend signals in the streamflow peaks and climate data by using the Mann-Kendall trend test (Mann, 1945; Kendall, 1975; Gilbert, 1987) as implemented by Hodgkins and others (2019); this implementation, which accounts for serial correlation, is available from Dudley and others (2018). The Mann-Kendall trend test is a distribution-free, nonparametric test used to identify a monotonic trend in a series. The modifications by Hodgkins and others (2019) account for different assumptions of independence, short-term persistence, and long-term persistence in the data (Cohn and Lins, 2005). The independence assumption is standard for the Mann-Kendall test. Under the short-term persistence assumption, the Mann-Kendall statistic was calculated with a variance that is scaled by a factor related to the lag-1 autocorrelation coefficient (Hamed and Rao, 1998). Assuming long-term persistence, the variance was scaled by factors related to the Hurst coefficient (Hamed, 2008). Trend significance (defined at p-value<0.05) was calculated for the water year, October–March, and April–September mean of precipitation and air temperature for each climate division that contained a streamgage.

Mean Julian Date of Annual Peak Streamflow

The day of peak streamflow during the water year can be related to flood-generating mechanisms that are most common at different seasons of the year (Villarini, 2016). The day of peak streamflow was used to help differentiate between possible climate-related attributions for each streamgage and to assess any temporal changes in those attributions. Villarini (2016) found that streamflow peaks related to mid-latitude cyclones occur in October–March over much of the western United States, and that snowmelt-generated flood events in higher elevations in Colorado and Utah generally occur in April–May. In this study, if the peak streamflow at minimally altered basins was strongly correlated to October–March precipitation and the peak streamflow occurred mostly in fall or winter (October–March), then these trends were attributed to long-term precipitation. Peaks that occurred in April–July were assumed to be caused by snowmelt and these trends were attributed to snowpack. For both of these attributions (long-term precipitation and snowpack), air temperature is assumed to play a role. Increasing air temperatures can exacerbate the effects of even relatively modest precipitation deficits (Woodhouse and others, 2016) and change the character of wintertime precipitation from snow to rain during the cold season. However, when the streamflow peaks were strongly correlated to air temperature only and the trends could not be explained any other way, these trends were attributed to air temperature.

The day of peak streamflow was represented by the mean Julian date, or day-of-year number, of the occurrence of each annual streamflow peak for each streamgage. The mean Julian date was computed by using circular statistics (Villarini, 2016) using the MATLAB script CircStat (Berens, 2009). In situations where the day of peak streamflow is highly variable from year to year, multiple flood-generating processes over several seasons may be important. The variability of the mean Julian date of the peak streamflow was determined as the resultant length (a measure of precision; Villarini, 2016). A greater resultant length (closer to one) indicates less variability, and a shorter resultant length (closer to zero) indicates greater variability. Villarini (2016) reported that the resultant lengths of peak streamflow in snowmelt-dominated regions of the western United States are often greater than 0.9, indicating strong seasonality and low variability in the day of peak streamflow. The exception is in snowmelt-dominated areas of the Sierra Nevada where the resultant length ranged from 0.4 to 0.9 because of the additional influence of atmospheric rivers (Villarini, 2016).

Increases in winter and spring air temperatures at streamgages with snowmelt-dominated peak streamflow typically result in increased winter runoff, reduced peak water equivalent stored as snow, and earlier peak streamflow (Gleick and Chalecki, 1999; Knowles and Cayan, 2002; Dettinger and others, 2004; Service, 2004). In this chapter, changes in snowmelt timing were evaluated by selecting the streamgages that had at least half of their streamflow peaks occur from April to July. It was assumed that these streamflow peaks were the result of warming spring air temperatures that initiate snowmelt. Mean air temperature in February–May has been found to be significantly correlated to the center of mass of streamflow in winter and spring in the conterminous United States, which suggests an important relation between air temperature and snowmelt in streams (Dudley and others, 2017). Trend significance in the day of the April–July streamflow peak was calculated using the modified Mann-Kendall trend test. Trend signals that passed at least one of the three assumptions for data independence, short-term persistence, and long-term persistence as implemented by Hodgkins and others (2019) were determined to be significant. From the set of streamgages with statistically significant changes in April–June day of peak streamflow (where p-value<0.05), we then identified a subset of those streamgages where the air temperature trend was positive. Air temperature was secondarily attributed to trends for this subset of streamgages.

Results and Discussion

Of the 393 streamgages used in this analysis of the Southwest region, 56 and 86 streamgages had 75- and 50-year monotonic trends in annual peak-streamflow data, respectively. For change points, 54 and 62 streamgages had 75- and 50-year change points in annual peak-streamflow data, respectively. Only 20 streamgages had monotonic trends in both time periods and only 18 streamgages had change points in both time periods. Figure F2 shows the spatial distribution of streamgages with 75-year (fig. F2*A*, *C*) and 50-year (fig. F2*B*, *D*) monotonic trends and change points in the Southwest region. In general, peak-streamflow data have negative trends across the Southwest during both time periods, except for urban streams in coastal southern California and a few high-altitude (>4,500 ft) streams in California, Colorado, and Utah (fig. F2).

Spatial Distribution of Attributions

Figure F3 shows the spatial distribution of attributions for both the 75-year and 50-year monotonic trends and change points. All urban effect attributions were clustered near coastal California for both time periods. Although the Southwest region has experienced substantial increases in population over the last several decades (Hobbs and Stoops, 2002), annual peak streamflow monotonic trends and change points were not attributed to urban effects outside of southern and central California. In general, monotonic trends and change points for annual peak-streamflow data for clusters of streamgages in central California, western Colorado, and northern Utah were attributed to large artificial impoundments. Despite large water infrastructure projects in Arizona such as the Central Arizona Project (CAP; Bureau of Reclamation, 2019) that delivers water from the Colorado River to central and southern Arizona, annual peak-streamflow trends seen in Arizona were generally not primarily attributed to small or large artificial impoundments. For the 1966–2015 period, long-term precipitation was the main attribution for monotonic trends and change points in Arizona. As expected, snowpack was the primary attribution for trends at high-altitude streamgages in California, Colorado, and Utah.

Monotonic Trends

Monotonic trends in annual peak-streamflow data in the Southwest region are generally negative in both the 50-year and 75-year time periods, with some exceptions (fig. F2*A*, *B*; York and others, 2022). In the 75-year period, 11 of 56 streamgages with significant monotonic trends in annual peak-streamflow data had positive trends, all of which are located in California (fig. F2*A*). Positive monotonic trends at streamgages located on the southern coast of California were attributed to urban effects (fig. F3*A*). Positive monotonic trends at the other streamgages located more inland in California were attributed to small and large artificial impoundments (fig. F3*A*).

In the 50-year period, 10 of 86 streamgages with significant monotonic trends in annual peak-streamflow data had positive trends (6 in California, 3 in Colorado, and 1 in Utah; fig. F2*B*). Positive monotonic trends at two streamgages in Colorado were attributed to snowpack and might reflect the local increase in snowpack that was seen in some drainage basins in the Upper Colorado River Basin (Miller and Piechota, 2011). The other positive monotonic trend in Colorado was attributed to a large artificial impoundment, as are the positive monotonic trends for two streamgages in California. One positive monotonic trend in California was attributed to long-term precipitation, but with limited supporting evidence. The three other positive monotonic trends for streamgages in California were attributed to urban effects and artificial waste-water discharges. One streamgage in Utah had a positive trend in annual peak-streamflow magnitude, but the cause is unknown.

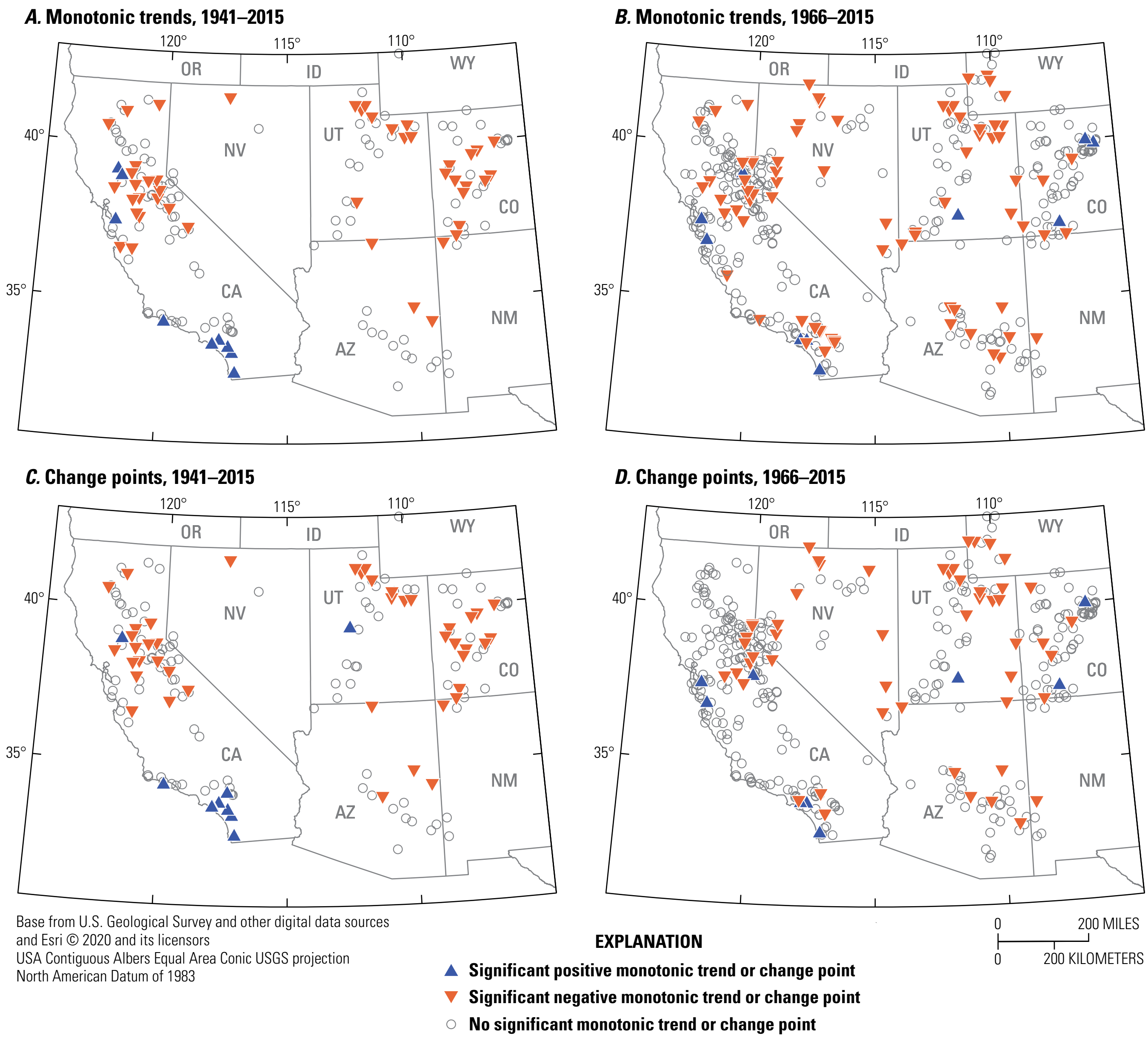

Figure F2. Maps of the Southwest region showing the spatial distribution and direction (positive or negative) of statistically significant (*A*, *B*) monotonic trends and (*C*, *D*) change points in annual peak-streamflow data for streamgages in this study for the time periods of 1941–2015 and 1966–2015. Monotonic trends and change points are statistically significant if the *p*-value<0.10. Because of the small scale of the maps in this chapter, some symbols overprint, and so the counts derived from a visual inspection of the figure may not match numbers given in other parts of this chapter.

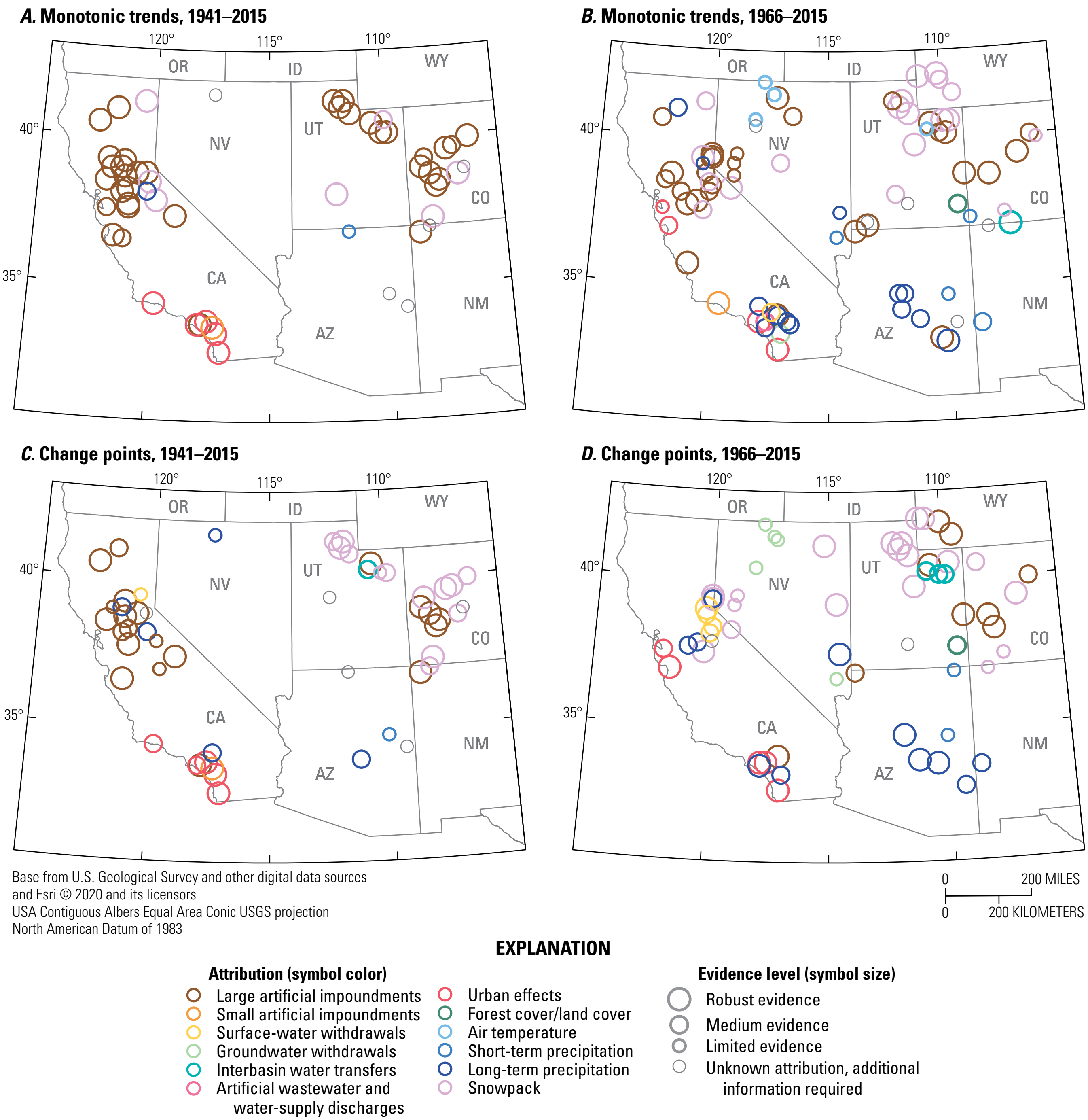

Figure F3. Maps of the Southwest region showing the spatial distribution and levels of evidence of attributions for statistically significant (*A*, *B*) monotonic trends and (*C*, *D*) change points in annual peak-streamflow data for streamgages in this study for the time periods of 1941–2015 and 1966–2015. Colors indicate different attributions and the sizes of the circles indicate levels of evidence for those attributions. Monotonic trends and change points are statistically significant if the *p*-value<0.10.

In the 75-year period, attributions for monotonic trends were mostly similar to attributions for change points (see the section "Timing and Magnitude of Change Points"). Most monotonic trends were attributed to small and large artificial impoundments (64 percent) with a lesser number being attributed to snowpack (12 percent), urban effects (11 percent), and unknown causes (9 percent) (fig. F4*A*).

Monotonic trends in the 50-year period were mostly attributed to large artificial impoundments (35 percent), snowpack (22 percent), and long- and short-term precipitation (a combined 21 percent) (fig. F4*B*). The primary attribution was unknown for 6 percent of the monotonic trends. The rest of the attributions in the 50-year period each account for less than 5 percent of the total streamgages with significant monotonic trends (fig. F4*B*). A few streamgages in Nevada and Utah have negative monotonic trends that were primarily attributed to air temperature; however, air temperature was the secondary attribution for many of the monotonic trends in the 50-year period (York and others, 2022). The 75-year monotonic trends are dominated by the influence of large artificial impoundments. During the 50-year period, the influence of the impoundments was less substantial compared to the 75-year period and climate-related attributions such a snowpack, precipitation, and air temperature played a larger role in monotonic trends in annual peak streamflow.

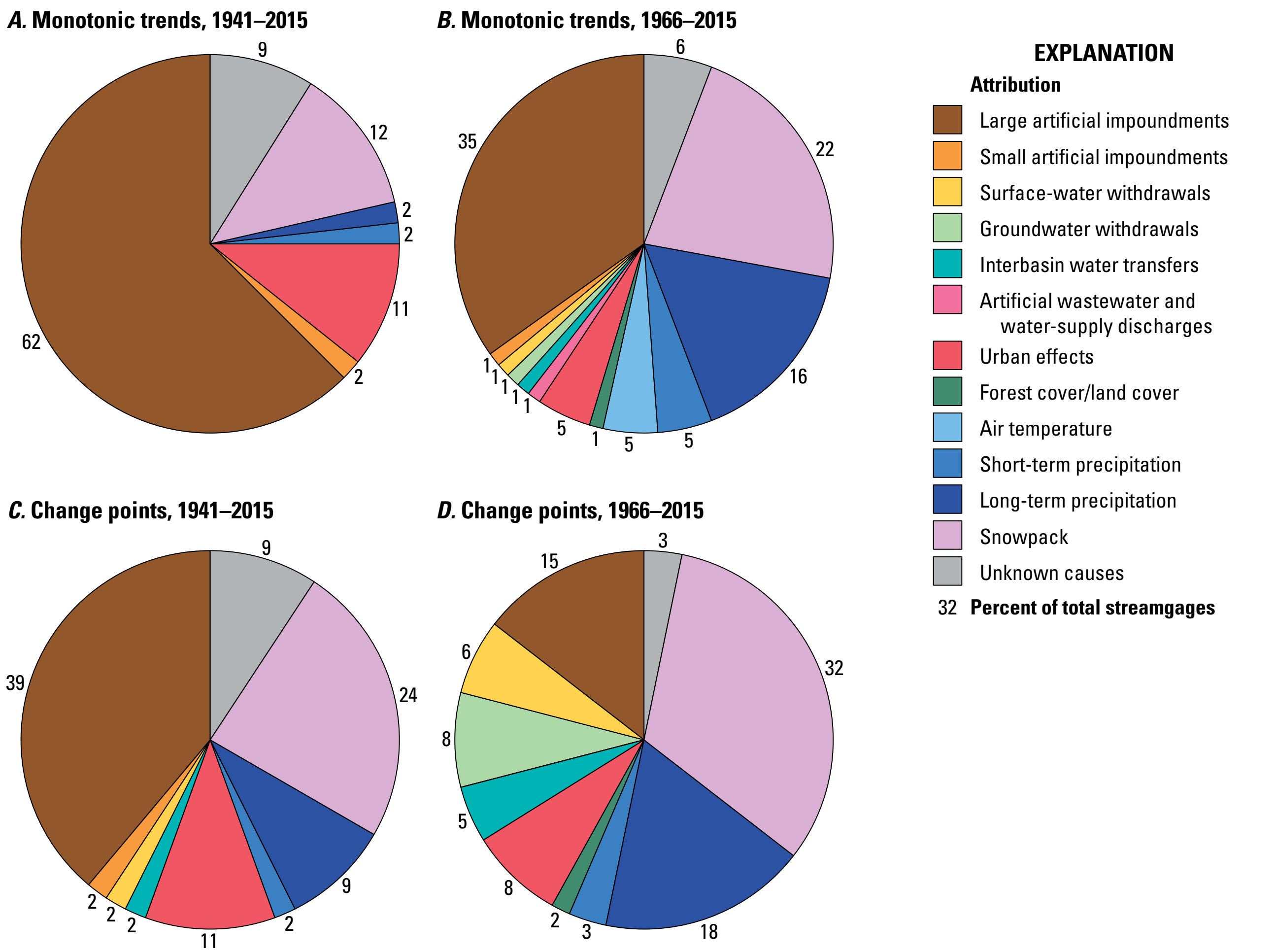

Figure F4. Pie charts showing the percentages of attributions for statistically significant (*A*, *B*) monotonic trends and (*C*, *D*) change points in annual peak-streamflow data for streamgages in the Southwest region for the time periods of 1941–2015 and 1966–2015. Attributions are shown in terms of the percentage of total streamgages with monotonic trends or change points. Monotonic trends and change points are statistically significant if the *p*-value<0.10.

Timing and Magnitude of Change Points

For the 75-year period from 1941 to 2015, 54 streamgages had positive or negative change points (fig. F2*C*; Ryberg and others, 2019; York and others, 2022). The years of the change points are shown in figure F5. Most change points were clustered into four distinct time periods: 1954–1967, 1970–1979, 1985–1987, and 1995. Change points in the two earlier periods can be mostly attributed to the construction of large artificial impoundments, which coincided with the peak of dam building (1940–1980) in the United States (Ho and others, 2017; U.S. Army Corps of Engineers, 2018). By about the mid-1970s, dam building in the Southwest region had slowed, although a few large dams and reservoirs were completed in the mid-1980s and later (for example, the Ridgeway Reservoir on the Uncompahgre River in Colorado in 1986 and the Upper Stillwater Reservoir on Rock Creek in Utah in 1987). As dam building slowed in the 1970s, urbanization increased to the point of having an influence on annual peak streamflow. Of the six streamgages with change points that were attributed to urban effects, five occurred from 1974 to 1979. All six of these change points were positive, and all occurred in coastal southern California (figs. F2*C*, F3*C*).

In a 3-year period from 1985 to 1987, data at 15 streamgages showed change points, all of which were negative. Change points at 11 of those streamgages were attributed to climate-related attributions (long-term precipitation, short-term precipitation, or snowpack). Of the remaining four change points, one was attributed to interbasin water transfers and three were attributed to large artificial impoundments. The two streamgages with change points in 1995 are climate related as well (long-term precipitation and snowpack; fig. F3*C*).

The streamgages where change points were attributed to large artificial impoundments had the greatest change in magnitude (in terms of the median annual peak streamflow before compared to after the change point). These streamgages are mainly located in central California, but a small number are in Colorado. Almost all of these impoundments are on relatively large river systems, so the change in magnitude of the median peak streamflow reflects the drainage basin size. Most negative change points have a decrease of 3–70 percent from pre- to post-change-point median peak streamflow; most positive change points have an increase of 2–8 times from pre- to post-change-point median peak streamflow. With few exceptions, changes in magnitude of median peak streamflow occur at the high-altitude streamgages in western Colorado and northern Utah and were attributed to both snowpack and large artificial impoundments; these changes were relatively small when compared to change points at other streamgages in the Southwest region.

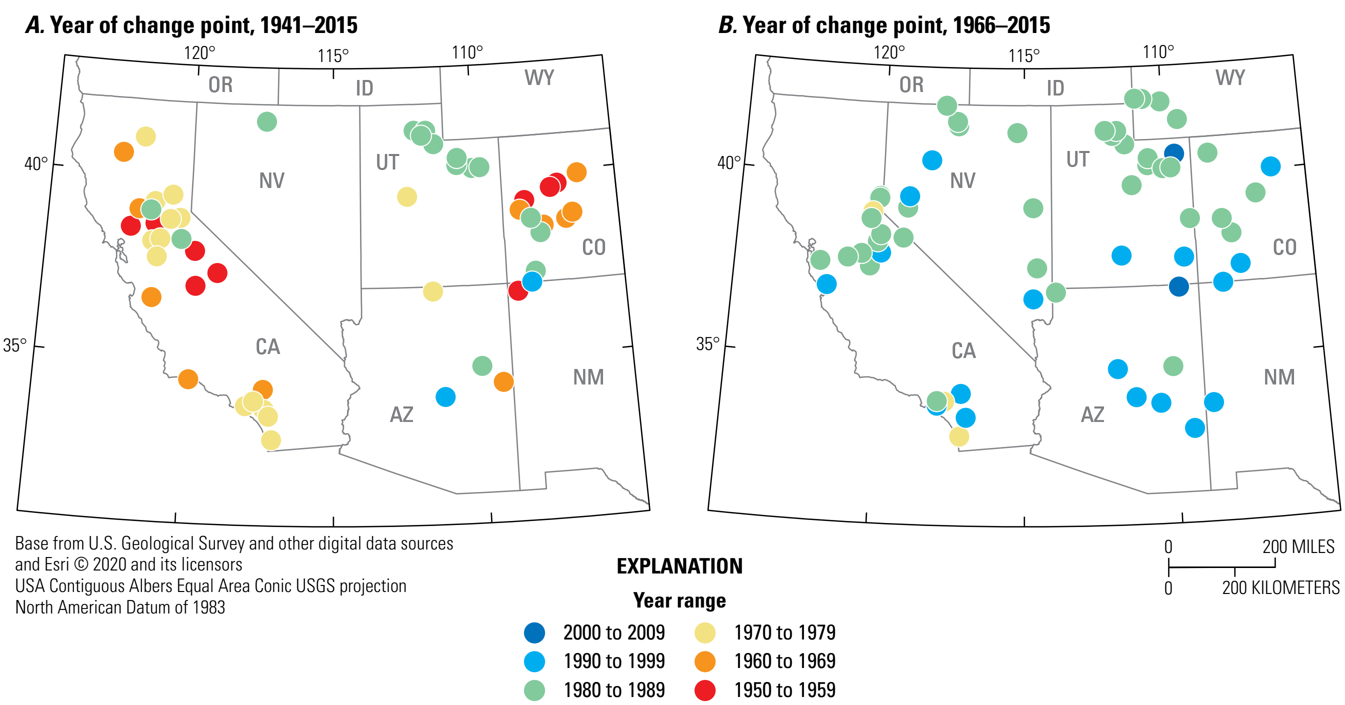

Figure F5. Maps of the Southwest region showing the year of the statistically significant change point of annual peak streamflow for the time periods of (*A*) 1941–2015 and (*B*) 1966–2015. Change points are statistically significant if the *p*-value<0.10.

In the 50-year period from 1966 to 2015, 62 streamgages had change points, most of which were negative (fig. F2*D*). Change points for 53 of the 62 streamgages occurred relatively later in the record (34 from 1985–1987 and 19 from 1993–1999) when compared to the 75-year change points (fig. F5). Most change points were attributed to snowpack (19), precipitation (11), and large artificial impoundments (8) (fig. F3*D*). However, contrary to expectations, five were attributed to groundwater withdrawals near small streams.

The relatively small number of change points attributed to large artificial impoundments in the 50-year period when compared to the 75-year period is likely due to the fact that most impoundments that affect annual peak streamflow in the Southwest region were already in place by the late 1960s. For this study, change points in peak streamflow were primarily attributed to small or large artificial impoundments only if the impoundment was completed within 5 years of the change point or if it underwent significant modification at or near the change point. Changes in reservoir operations due to climate, water demand, or ecological reasons were not considered.

The magnitudes of the changes in median annual peak streamflow for the 50-year period are lower when compared to the 75-year period (fig. F6*A, B*). The greatest changes in magnitude occurred in central Arizona and were primarily attributed to long-term precipitation and secondarily attributed to air temperature. While long-term precipitation was identified as the primary attribution for decreases in annual peak streamflow, air temperature certainly plays an important role (McCabe and others, 2017; Xiao and others, 2018). Change-point dates for peak streamflow at these streamgages were in the late 1990s. The percentage change of the median peak streamflow, either positive or negative, is just as high in the 50-year period as in the 75-year period; the few exceptions occurred mostly in Colorado (fig. F6*C, D*).

In the 75-year period from 1941 to 2015, most change points that occurred before the 1980s were attributed to large artificial impoundments in the form of dam building and reservoir filling. The overall effect of these impoundments was a 57 percent reduction in median annual peak streamflow for the affected rivers. Increased urban effects played a substantial role in the increase in median annual peak streamflow at streamgages with change points starting in the middle-to-late 1970s. In general, affected gages were in small drainage basins and only accounted for 11 percent of the total median peak streamflow for the streamgages with change points. However, urban effects are attributed to a 411 percent increase in median peak streamflow on affected streams. In the 75-year period, change points that were identified in the mid-1980s and mid-1990s were almost all attributed to either precipitation or snowpack. In contrast to the 75-year period, most change points in the 50-year period were attributed to climate-related variables (fig. F4*D*), either snowpack (32 percent of streamgages) or precipitation (21 percent of streamgages). These two attributions accounted for a 63 percent reduction in median peak streamflow for this period.

In the 75-year period, climate-related attributions (snowpack, long-term precipitation, and short-term precipitation) were made for 35 percent of change points (fig. F4*C*); these attributions accounted for a 49 percent net reduction in median annual peak streamflow for the affected streams. Anthropogenic attributions (small and large artificial impoundments, interbasin water transfers, surface-water withdrawals, and urban effects) were made for 56 percent of change points (fig. F4*C*); these attributions accounted for a 50 percent net reduction in median peak streamflow for the affected streams. The total overall reduction in median peak streamflow is 115,00 cubic feet per second (ft^3/s) and 47,400 ft^3/s for anthropogenic and climate-related attributions, respectively. The magnitude of this discrepancy in median peak streamflow between the anthropogenic and climate-related attributions reflects the greater number of total streamgages with artificial impoundments on their corresponding stream or river.

In the 50-year period, most change points occurred in the mid-1980s or late-1990s. Climate-related attributions (snowpack, long-term precipitation, and short-term precipitation) accounted for 53 percent of the total change points (fig. F4*D*). These climate-related attributions accounted for a reduction in median annual peak streamflow for affected streams by 63 percent, a total reduction of 19,800 ft^3/s in the Southwest region. Anthropogenic attributions (large artificial impoundments, interbasin water transfers, groundwater withdrawals, surface-water withdrawals, and urban effects) accounted for 42 percent of the change points. These anthropogenic attributions accounted for a reduction in median peak streamflow for affected streams by 33 percent, a total reduction of 62,227 ft^3/s. Despite the similarity in percentages of total primary attributions in the 50-year period, the total reduction in median peak streamflow from anthropogenic attributions was more than three times greater than that of the climatic attributions. This discrepancy is likely due to the size of the drainage basins; larger basins are more desirable for human modification of streamflow due to the perceived higher flood risk and greater water availability.

Seasonal Variability of Annual Peak Streamflow

Figure F7 shows the day of peak streamflow for each streamgage with a significant monotonic trend or change point. For all trends and all time periods, regardless of the primary attribution of the trend, the seasonal pattern is similar. Streamflow peaks for lower elevation streamgages in much of California mostly occur in fall and winter because of the intensity of winter storms from the Pacific Ocean. Streamflow peaks for higher elevation streamgages in California, Colorado, Utah, and Wyoming mostly occur in spring and early summer due to high volumes of snowmelt. Streamflow peaks for streamgages in much of Arizona and southern Nevada mostly occur in both summer and winter months, which is likely the result of summertime monsoon moisture and wintertime storms from the Pacific Ocean.

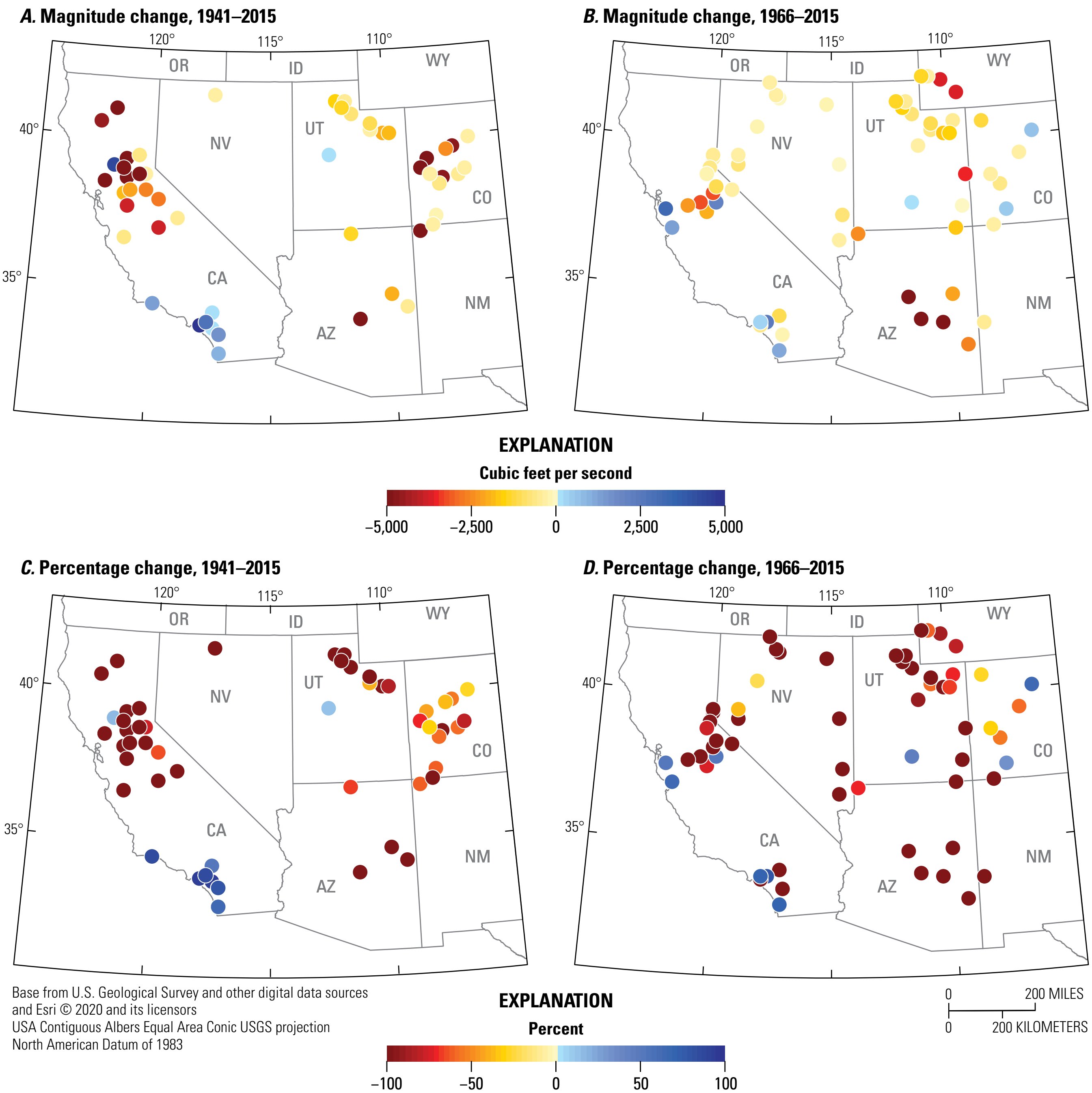

Figure F6. Maps of the Southwest region showing (*A*, *B*) the magnitude change and (*C*, *D*) the percentage change of median annual peak streamflow before and after the statistically significant change point for the time periods of 1941–2015 and 1966–2015. Change points are statistically significant if the *p*-value<0.10.

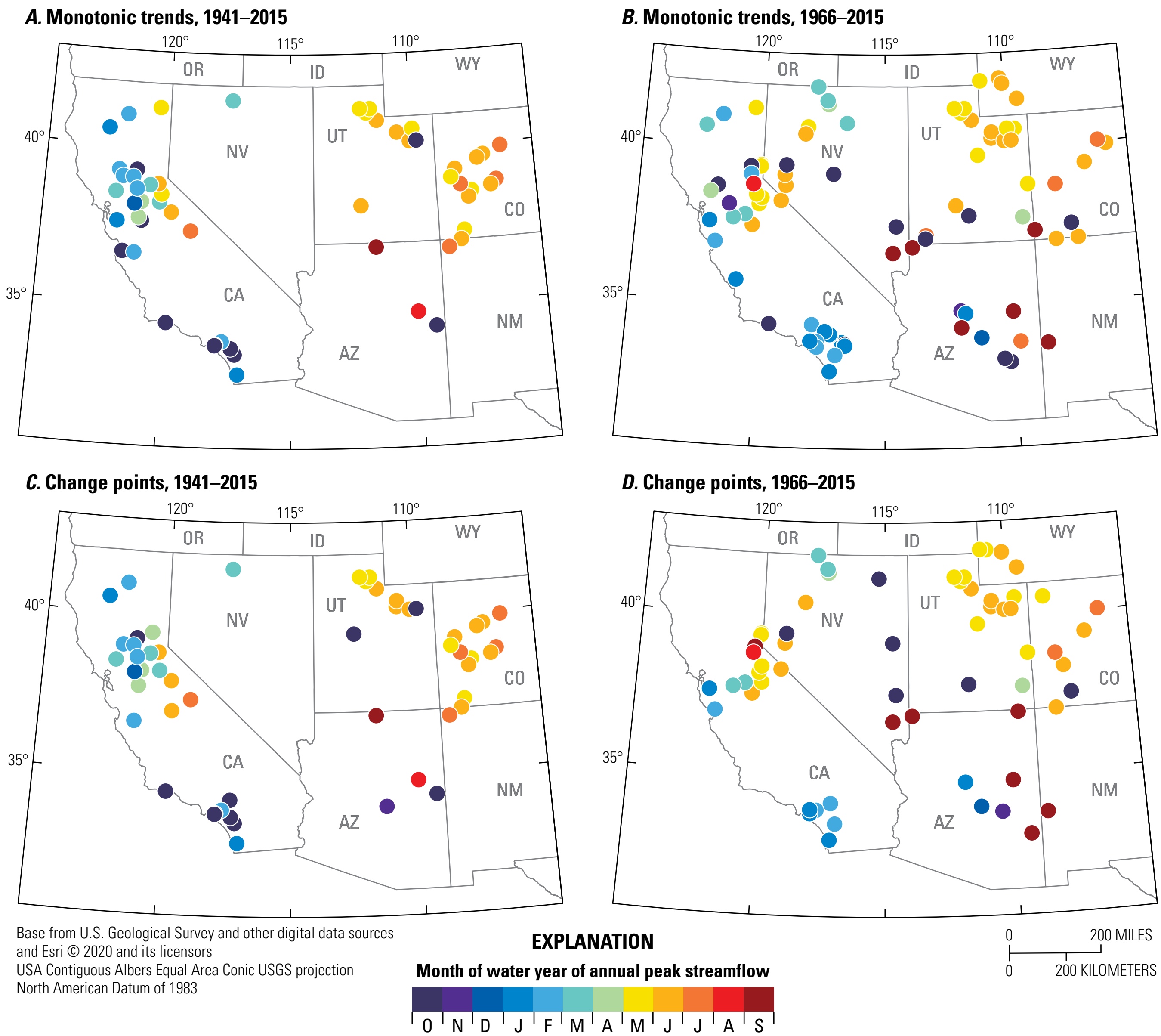

Figure F7. Maps of the Southwest region showing the mean day of the year of the annual peak streamflow (grouped into months) for streamgages that have statistically significant (*A*, *B*) monotonic trends and (*C*, *D*) change points for the time periods of 1941–2015 and 1966–2015. In the explanation, months are designated by the first letter of their names. Monotonic trends and change points are statistically significant if the *p*-value<0.10.

Figure F8 shows the variability in the day of peak streamflow as a resultant length. In the 75-year period, most of the streamgages in California with monotonic trends and change points experienced a high degree of variability in the day of peak streamflow, as indicated by the blue and green shades (fig. F8*A, C*). This variability likely reflects the influence of large artificial impoundments and urban effects on the timing and the magnitude of peak streamflows. For example, rain from winter storms from the Pacific Ocean would normally result in high streamflows; however, this water is now stored in artificial impoundments, which reduces the streamflow from such storms. Water stored in these impoundments is often released during times of increased water demand, which is typically during the drier seasons (often late spring and summer). If the winter is especially wet, the water stored in the large artificial impoundments may be released sooner to allow for storage space through the spring. If a winter is especially dry, water may be released later in the year and the day of peak streamflow might shift from winter to late spring or even summer as a result. High-altitude streamgages in Colorado and Utah show little variability in the seasonality of streamflow peaks (fig. F8*A, C*), even on streams with large artificial impoundments.

For the 50-year period, the least amount of variability in the day of peak streamflow occurs along the California coast, including the streamgages with trends attributed to urban effects. High-altitude streamgages in northern Utah and southwestern Wyoming also show little seasonal variability in the day of peak streamflow. The most variability is in Arizona (likely due to summer monsoons and Pacific Ocean storms in fall and winter), interior central California (likely due to large artificial impoundments), and eastern Nevada. Making attributions for peak streamflow trends in Nevada was challenging and most of the attributions had low levels of evidence, as indicated by the small circles in figure F3*B, D*.

Effects of Air Temperature and Snowpack on Annual Peak Streamflow

We examined the role of air temperature on annual peak streamflow in watersheds where peak streamflow is largely the result of snowmelt. For the 50-year and 75-year periods, we found very few streamgages that had statistically significant (p-value<0.05) trends in the timing of the April–July streamflow peaks (fig. F9). In the 75-year period, eight streamgages had a shift in the day of peak streamflow, four of which were earlier in the year (negative) and the other four of which were later in the year (positive) (fig. F9*A*, *C*). In the 50-year period, only four streamgages had trends in the day of peak streamflow, three of which were earlier in the year and one of which was later in the year (fig. F9*B*, *D*). All four streamgages with trends in day of peak streamflow in northern Utah had streamflow peaks that occurred later in the year. These streamgages are similar in altitude to the streamgages in Colorado (all between about 5,100 ft and 8,000 ft) but are at a higher altitude than the streamgages in California and Nevada (all between 1,075 ft and 4,470 ft). The streamgages in Utah with trends in the day of peak streamflow have some degree of regulation that could be affecting the timing of the peaks. For example, USGS streamgage 09279000 at Rock Creek near Mountain Home has a change-point date of 1987, a time when the Southwest region was experiencing a large-scale shift from wet to dry conditions. Coincidently, Upper Stillwater Reservoir, which affects streamflows in Rock Creek, was completed in 1987 (Bureau of Reclamation, 2022). Therefore, the shift in day of annual peak streamflow could reflect reservoir operations more than an increase in wintertime air temperatures. The other three streamgages in northern Utah with trends in the day of peak streamflow later in the year for the 75-year period are all regulated by large artificial impoundments and diversions. Like at the Rock Creek streamgage, these streamgages have change points of either 1986 or 1987, which were attributed to changes in snowpack. However, the shift towards peak streamflow occurring later could reflect reservoir operations and not wintertime air temperatures.

Two streamgages in California (fig. F9*A*, *C*), two in Nevada (fig. F9*B*, *D*), and three in the Rocky Mountains of Colorado (two in fig. F9*A*, *C*; one in fig. F9*B*, *D*) have trends towards earlier day of peak streamflow. This is consistent with the findings of Cayan and others (2001) and McCabe and Clark (2005) who attributed the earlier timing to naturally occurring variability in winter and spring air temperatures and in precipitation form or timing. This is also consistent with the findings of Stewart and others (2005) and Knowles and Cayan (2002) who attributed the timing shift to increasing air temperatures due to global warming. All streamgages with trends in the timing of the snowmelt runoff peaks had negative monotonic trends and change points in magnitude for both time periods regardless of the direction of the shift in the day of peak streamflow.

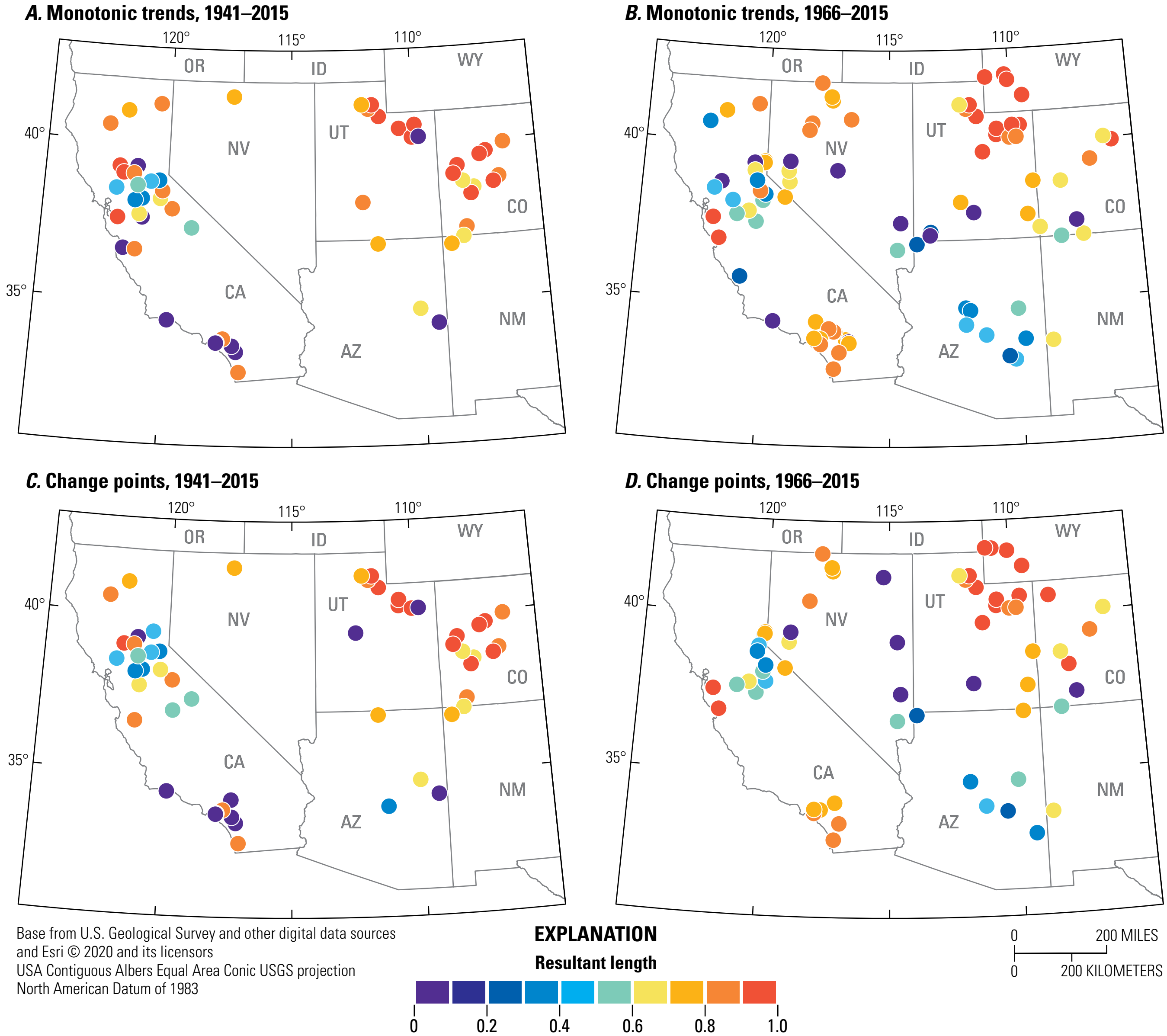

Figure F8. Maps of the Southwest region showing the variability of the mean day of the year of the annual peak streamflow as the resultant length for streamgages that have statistically significant (*A*, *B*) monotonic trends and (*C*, *D*) change points for the time periods of 1941–2015 and 1966–2015. A greater resultant length (closer to one) indicates less year-to-year variability in the day of peak streamflow and a shorter resultant length (closer to zero) indicates greater year-to-year variability. Monotonic trends and change points are statistically significant if the *p*-value<0.10.

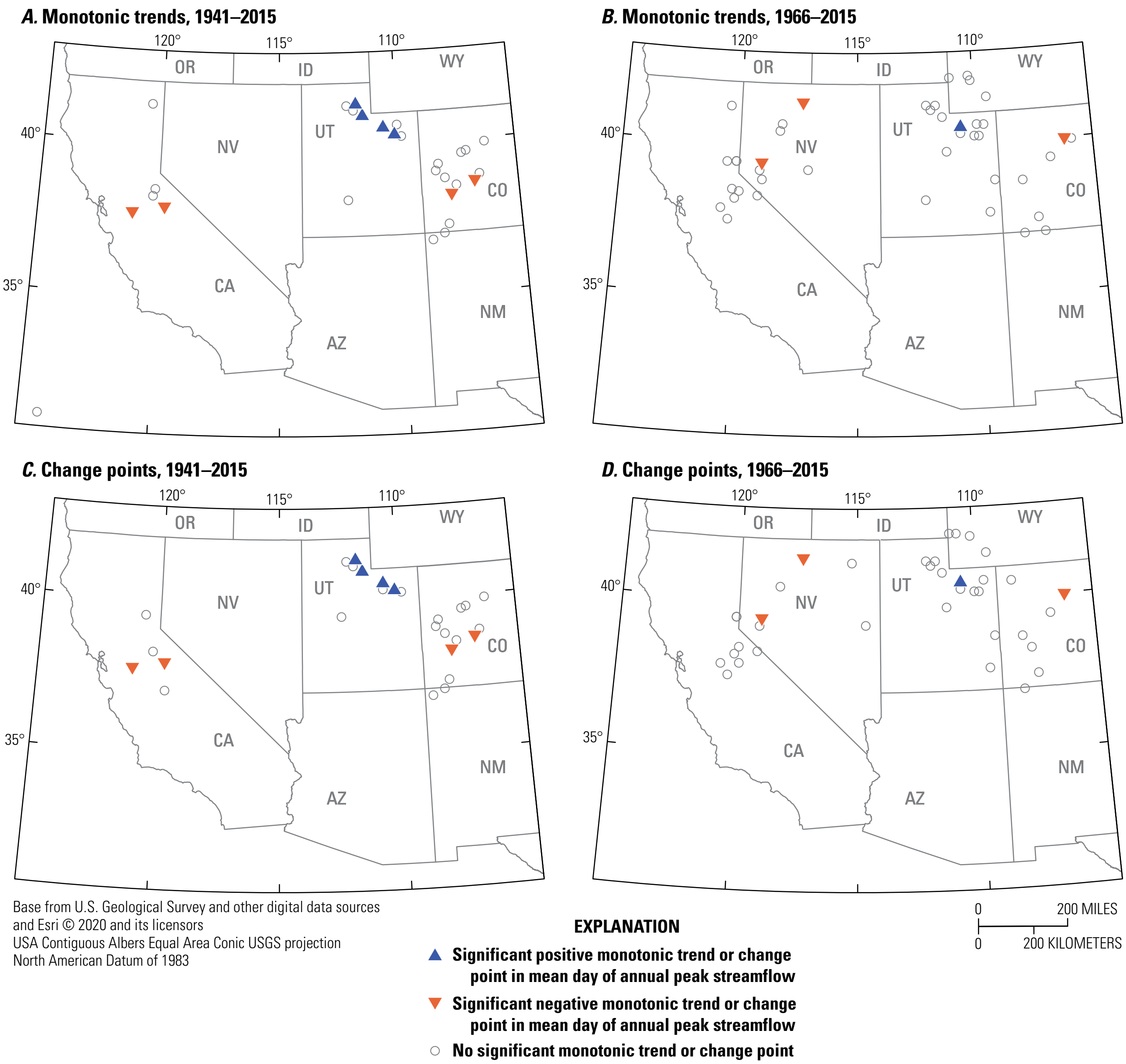

Figure F9. Maps of the Southwest region showing streamgages with statistically significant (*A*, *B*) monotonic trends and (*C*, *D*) change points in the mean day of the year of the annual peak streamflow for the time periods of 1941–2015 and 1966–2015 where at least half of streamflow peaks occurred from April to July and where snowmelt is assumed to be the dominant flood-generating process. Monotonic trends and change points are statistically significant if the *p*-value<0.05.

Summary

In this study, 393 streamgages in the Southwest region of the United States with complete records for the 75-year and 50-year periods defined in Dudley and others (2018) were tested for statistically significant monotonic trends and change points in annual peak streamflow. For the 75-year period from 1941 to 2015, 56 of the 393 streamgages in the Southwest region had monotonic trends, most of which were negative. Large artificial impoundments were the primary attributions for 62 percent of the monotonic trends in the 75-year period. Other primary attributions were snowpack (12 percent), urban effects (11 percent), and unknown causes (9 percent).

For the 50-year period from 1966 to 2015, 86 of the 393 streamgages had monotonic trends, most of which were negative. Climate-related attributions were more prominent in the 50-year period than in the 75-year period. The most common climate-related primary attributions for monotonic trends in this period were snowpack (22 percent), long-term precipitation (16 percent), short-term precipitation (5 percent), and air temperature (5 percent). The most common anthropogenic primary attributions were large artificial impoundments (35 percent) and urban effects (5 percent). Other anthropogenic factors such as groundwater withdrawals and surface-water withdrawals were primary attributions for monotonic trends at very few streamgages.

Of the 393 streamgages in this study, 54 and 62 had change points from 1941 to 2015 and 1966 to 2015, respectively. In the 75-year period, the most common primary attributions for change points in annual peak streamflow were large artificial impoundments (39 percent), snowpack (24 percent), urban effects (11 percent), and long-term precipitation (9 percent). With few exceptions, increases in peak streamflow in the 75-year period were attributed to urban effects; decreases in peak streamflow were attributed to all other attributions. Change points were clustered into four distinct time periods: 1954–1967, 1970–1979, 1985–1987, and 1995. The change points for the two earlier time periods were mostly attributed to large artificial impoundments and urban effects for drainage basins along the California coast. The change points for the two later time periods were mostly attributed to large-scale changes in climate (snowpack and long-term precipitation). For the most part, the greatest changes in magnitude (measured in total median annual peak streamflow) were attributed to large artificial impoundments (negative changes) and urban effects (positive changes).

In the 50-year period, change points were mostly negative and were mostly attributed to climate-related factors like snowpack (32 percent) and long-term precipitation (18 percent). Change points were also attributed to large artificial impoundments (15 percent), urban effects (8 percent), and surface-water withdrawals (6 percent). Most change points from 1966 to 2015 were clustered into two distinct periods (1985–1987 and 1993–1999) and were related to large-scale shifts in climate. The greatest change in median annual peak-streamflow magnitude before and after the change points occurred at three streamgages in central Arizona; this change was attributed to changes to long-term precipitation that began at the start of the 21st century.

We found few statistically significant shifts in the mean day of the year of the annual peak streamflow (day of peak streamflow) in the 75-year and 50-year periods. The 75-year period showed more variability in the day of peak streamflow (which was often attributed to urban effects) than the 50-year period. Overall, monotonic trends or change points in annual peak streamflow that were attributed to large artificial impoundments had the most variability in the day of peak streamflow when compared to basins where other attributions were made. The one exception to this is in Arizona where the day of peak streamflow showed a high degree of variability, which was mostly attributed to long-term precipitation.

Conclusions

Making attributions for monotonic trends and change points in annual peak-streamflow data is challenging due to the complex interaction among climate, land cover, and human management of water resources. This chapter reviews existing literature and climate data and uses statistical procedures to assign primary, and in some cases secondary, attributions and statements of confidence to trends in annual peak streamflow at various streamgages in the Southwest region of the United States. This information is intended to help inform flood-frequency analyses as well as to help reduce the uncertainty in assessments of flood risk and water supply in the future.

References Cited

Barnett, T.P., Pierce, D.W., Hidalgo, H.G., Bonfils, C., Santer, B.D., Das, T., Bala, G., Wood, A.W., Nozawa, T., Mirin, A.A., Cayan, D.R., and Dettinger, M.D., 2008, Human-induced changes in the hydrology of the western United States: Science, v. 319, no. 5866, p. 1080–1083.

Beighley, R.E., and Moglen, G.E., 2002, Trend assessment in rainfall-runoff behavior in urbanizing watersheds: Journal of Hydrologic Engineering, v. 7, no. 1, p. 27–34, accessed June 2019 at https://doi.org/10.1061/(ASCE)1084-0699(2002)7:1(27).

Berens, P., 2009, CircStat—A MATLAB toolbox for circular statistics: Journal of Statistical Software, v. 31, no. 10, 21 p., accessed February 2019 at http://www.jstatsoft.org/v31/i10.

Blöschl, G., Ardoin-Bardin, S., Bonell, M., Dorninger, M., Goodrich, D., Gutknecht, D., Matamoros, D., Merz, B., Shand, P., and Szolgay, J., 2007, At what scales do climate variability and land cover change impact on flooding and low flows?: Hydrological Processes, v. 21, no. 9, p. 1241–1247.

Bureau of Reclamation, 2018, Projects and facilities: Bureau of Reclamation database, accessed November 2018 at https://www.usbr.gov/projects/.

Bureau of Reclamation, [2019], Projects and facilities—Central Arizona Project: Bureau of Reclamation web page, accessed July 2019 at https://www.usbr.gov/projects/index.php?id=504.

Bureau of Reclamation, [2022], Projects and facilities—Upper Stillwater Dam: Bureau of Reclamation web page, accessed August 22, 2022, at https://www.usbr.gov/projects/index.php?id=257.

Carson, E.C., 2007, Temporal and seasonal trends in streamflow in the Uinta Mountains, northeastern Utah, and relation to climatic fluctuations: Arctic, Antarctic, and Alpine Research, v. 39, no. 4, p. 521–528.

Cayan, D.R., Kammerdiener, S.A., Dettinger, M.D., Caprio, J.M., and Peterson, D.H., 2001, Changes in the onset of spring in the western United States: Bulletin of the American Meteorological Society, v. 82, no. 3, p. 399–415.

Changnon, S.A., and Demissie, M., 1996, Detection of changes in streamflow and floods resulting from climate fluctuations and land use-drainage changes: Climate Change, v. 32, no. 4, p. 411–421.

Chylek, P., Dubey, M.K., Lesins, G., Li, J., and Hengartner, N., 2014, Imprint of the Atlantic multi-decadal oscillation and Pacific decadal oscillation on southwestern US climate—Past, present, and future: Climate Dynamics, v. 43, p. 119–129, accessed May 2019 at https://doi.org/10.1007/s00382-013-1933-3.

Clow, D.W., 2010, Changes in the timing of snowmelt and streamflow in Colorado—A response to recent warming: Journal of Climate, v. 23, no. 9, p. 2293–2306.

Cohn, T.A., and Lins, H.F., 2005, Nature's style—Naturally trendy: Geophysical Research Letters, v. 32, no. 23, article L23402, 5 p., accessed May 2019 at https://doi.org/10.1029/2005GL024476.

Cook, E.R., Seager, R., Heim, R.R., Jr., Vose, R.S., Herweijer, C., and Woodhouse, C., 2010, Megadroughts in North America—Placing IPCC projections of hydroclimatic change in a long-term paleoclimate context: Journal of Quaternary Science, v. 25, no. 1, p. 48–61.

Dettinger, M., 2011, Climate change, atmospheric rivers, and floods in California—A multimodel analysis of storm frequency and magnitude changes: JAWRA, Journal of the American Water Resources Association, v. 47, no. 3, p. 514–523.

Dettinger, M.D., and Cayan, D.R., 1995, Large-scale atmospheric forcing of recent trends toward early snowmelt in California: Journal of Climate, v. 8, no. 3, p. 606–623.

Dettinger, M.D., Cayan, D.R., Meyer, M.K., and Jeton, A.E., 2004, Simulated hydrologic responses to climate variations and change in the Merced, Carson, and American River basins, Sierra Nevada, California, 1900–2099: Climate Change, v. 62, nos. 1–3, p. 283–317.

Dudley, R.W., Archfield, S.A., Hodgkins, G.A., Renard, B., and Ryberg, K.R., 2018, Peak-streamflow trends and change-points and basin characteristics for 2,683 U.S. Geological Survey streamgages in the conterminous U.S. (ver. 3.0, April 2019): U.S. Geological Survey data release, accessed January 2019 at http://doi.org/10.5066/P9AEGXY0.

Dudley, R.W., Hodgkins, G.A., McHale, M.R., Kolian, M.J., and Renard, B., 2017, Trends in snowmelt-related streamflow timing in the conterminous United States: Journal of Hydrology, v. 547, p. 208–221.

Easterling, D.R., Kunkel, K.E., Arnold, J.R., Knutson, T., LeGrande, A.N., Leung, L.R., Vose, R.S., Waliser, D.E., and Wehner, M., 2017, Precipitation change in the United States, chap. 7 *of* Wuebbles, D.J., Fahey, D.W., Hibbard, K.A., Dokken, D.J., Stewart, B.C., and Maycock, T.K., eds., Climate science special report, v. 1 *of* Fourth national climate assessment: Washington, D.C., U.S. Global Change Research Program, p. 207–230, accessed June 2019 at http://doi.org/10.7930/J0H993CC.

England, J.F., Jr., Cohn, T.A., Faber, B.A., Stedinger, J.R., Thomas, W.O., Jr., Veilleux, A.G., Kiang, J.E., and Mason, R.R., Jr., 2018, Guidelines for determining flood flow frequency—Bulletin 17C (ver. 1.1, May 2019): U.S. Geological Survey Techniques and Methods, book 4, chap. B5, 148 p., accessed May 2019 at https://doi.org/10.3133/tm4B5.

Falcone, J.A., 2011, GAGES-II—Geospatial attributes of gages for evaluating streamflow: U.S. Geological Survey dataset, accessed January 2019 at http://pubs.er.usgs.gov/publication/70046617.

Falcone, J.A., Carlisle, D.M., Wolock, D.M., and Meador, M.R., 2010, GAGES—A stream gage database for evaluating natural and altered flow conditions in the conterminous United States: Ecology, v. 91, no. 2, p. 621.

Gilbert, R.O., 1987, Statistical methods for environmental pollution monitoring: New York, Van Nostrand Reinhold Company, 384 p.

Gleick, P.H., and Chalecki, E.L., 1999, The impacts of climatic changes for water resources of the Colorado and Sacramento-San Joaquin River Basins: JAWRA, Journal of the American Water Resources Association, v. 35, no. 6, p. 1429–1441.

Graf, W.L., 2006, Downstream hydrologic and geomorphic effects of large dams on American Rivers: Geomorphology, v. 79, nos. 3–4, p. 336–360.

Guttman, N.B., and Quayle, R.G., 1996, A historical perspective of U.S. climate divisions: Bulletin of the American Meteorological Society, v. 77, no. 2, p. 293–304.

Hamed, K.H., 2008, Trend detection in hydrologic data—The Mann–Kendall trend test under the scaling hypothesis: Journal of Hydrology, v. 349, nos. 3–4, p. 350–363.

Hamed, K.H., and Rao, A.R., 1998, A modified Mann-Kendall trend test for autocorrelated data: Journal of Hydrology, v. 204, nos. 1–4, p. 182–196.

Helsel, D.R., Hirsch, R.M., Ryberg, K.R., Archfield, S.A., and Gilroy, E.J., 2020, Statistical methods in water resources: U.S. Geological Survey Techniques and Methods, book 4, chap. A3, 458 p. [Supersedes USGS Techniques of Water-Resources Investigations, book 4, chap. A3, ver. 1.1. Also available at https://doi.org/10.3133/tm4A3.]

Hirsch, R.M., and Ryberg, K.R., 2012, Has the magnitude of floods across the USA changed with global CO_2 levels?: Hydrological Sciences Journal, v. 57, no. 1, p. 1–9, accessed May 2019 at https://doi.org/10.1080/02626667.2011.621895.

Ho, M., Lall, U., Allaire, M., Devineni, N., Kwon, H.H., Pal, I., Raff, D., and Wegner, D., 2017, The future role of dams in the United States of America: Water Resources Research, v. 53, no. 2, p. 982–998.

Hobbs, F., and Stoops, N., 2002, Demographic trends in the 20th century: U.S. Census Bureau, Census 2000 Special Reports, CENSR–4, [variously paged; 213 p.]. [Also available at https://www.census.gov/prod/2002pubs/censr-4.pdf.]

Hodgkins, G.A., Dudley, R.W., Archfield, S.A., and Renard, B., 2019, Effects of climate, regulation, and urbanization on historical flood trends in the United States: Journal of Hydrology, v. 573, p. 697–709.

Hodgkins, G.A., Whitfield, P.H., Burn, D.H., Hannaford, J., Renard, B., Stahl, K., Fleig, A.K., Madsen, H., Mediero, L., Korhonen, J., Murphy, C., and Wilson, D., 2017, Climate-driven variability in the occurrence of major floods across North America and Europe: Journal of Hydrology, v. 552, p. 704–717, accessed April 2019 at https://doi.org/10.1016/j.jhydrol.2017.07.027.

Hollis, G.E., 1975, The effect of urbanization on floods of different recurrence interval: Water Resources Research, v. 11, no. 3, p. 431–435.

Intergovernmental Panel on Climate Change, 2008, Climate change 2007—Synthesis report (edited by Core Writing Team, R.K. Pachauri, and A. Reisinger)—Contribution of Working Groups I, II and III to the Fourth Assessment Report of the Intergovernmental Panel on Climate Change: Geneva, Switzerland, Intergovernmental Panel on Climate Change, 103 p. [Also available at https://www.ipcc.ch/site/assets/uploads/2018/02/ar4_syr_full_report.pdf.]

Jain, S., and Lall, U., 2001, Floods in a changing climate—Does the past represent the future?: Water Resources Research, v. 37, no. 12, p. 3193–3205, accessed March 2019 at https://doi.org/10.1029/2001WR000495.

Kendall, M.G., 1975, Rank correlation methods (4th ed.): London, United Kingdom, Charles Griffin & Co., 202 p.

Knowles, N., and Cayan, D.R., 2002, Potential effects of global warming on the Sacramento/San Joaquin watershed and the San Francisco estuary: Geophysical Research Letters, v. 29, no. 18, p. 38-1 to 38-4, accessed April 2019 at https://doi.org/10.1029/2001GL014339.

Knowles, N., Dettinger, M.D., and Cayan, D.R., 2006, Trends in snowfall versus rainfall in the Western United States: Journal of Climate, v. 19, no. 18, p. 4545–4559.

Kondolf, G.M., and Batalla, R.J., 2005, Hydrological effects of dams and water diversions on rivers of Mediterranean-climate regions—Examples from California, chap. 11 *of* Garcia, C., and Batalla, R.J., eds., Catchment dynamics and river processes—Mediterranean and other climate regions: Developments in Earth Surface Processes, v. 7, p. 197–211.

Lehner, F., Deser, C., Simpson, I.R., and Terray, L., 2018, Attributing the U.S. Southwest's recent shift into drier conditions: Geophysical Research Letters, v. 45, no. 12, p. 6251–6261, accessed May 2019 at https://doi.org/10.1029/2018GL078312.

Lins, H.F., 2012, USGS Hydro-Climatic Data Network 2009 (HCDN–2009): U.S. Geological Survey Fact Sheet 2012–3047, 4 p., accessed March 2019 at https://pubs.usgs.gov/fs/2012/3047/.

Lins, H.F., and Slack, J.R., 1999, Streamflow trends in the United States: Geophysical Research Letters, v. 26, no. 2, p. 227–230.

MacDonald, G.M., 2010, Water, climate change, and sustainability in the southwest: Proceedings of the National Academy of Sciences of the United States of America, v. 107, no. 50, p. 21256–21262.

Mann, H.B., 1945, Nonparametric tests against trend: Econometrica, v. 13, no. 3, p. 245–259.

McCabe, G.J., and Clark, M.P., 2005, Trends and variability in snowmelt runoff in the western United States: Journal of Hydrometeorology, v. 6, no. 4, p. 476–482.

McCabe, G.J., and Wolock, D.M., 2002, A step increase in streamflow in the conterminous United States: Geophysical Research Letters, v. 29, no. 24, p. 38-1 to 38-4.

McCabe, G.J., Wolock, D.M., Pederson, G.T., Woodhouse, C.A., and McAfee, S., 2017, Evidence that recent warming is reducing Upper Colorado River flows: Earth Interactions, v. 21, no. 10, p. 1–14.

Miller, W.P., and Piechota, T.C., 2008, Regional analysis of trend and step changes observed in hydroclimatic variables around the Colorado River Basin: Journal of Hydrometeorology, v. 9, no. 5, p. 1020–1034.

Miller, W.P., and Piechota, T.C., 2011, Trends in western U.S. snowpack and related Upper Colorado River Basin streamflow: JAWRA, Journal of the American Water Resources Association, v. 47, no. 6, p. 1197–1210.

Mote, P.W., Hamlet, A.F., Clark, M.P., and Lettenmaier, D.P., 2005, Declining mountain snowpack in western North America: Bulletin of the American Meteorological Society, v. 86, no. 1, p. 39–50.

National Oceanic and Atmospheric Administration, 2018, National Centers for Environmental Information—Climate monitoring: National Oceanic and Atmospheric Administration, National Centers for Environmental Information data archive, accessed March 2018 at https://www.ncdc.noaa.gov/climate-monitoring/.

Ng, H.Y.F., and Marsalek, J., 1989, Simulation of the effects of urbanization on basin streamflow: JAWRA, Journal of the American Water Resources Association, v. 25, no. 1, p. 117–124.

Novotny, E.V., and Stefan, H.G., 2007, Stream flow in Minnesota—Indicator of climate change: Journal of Hydrology, v. 334, nos. 3–4, p. 319–333.

Pettitt, A.N., 1979, A non-parametric approach to the change-point problem: Journal of the Royal Statistical Society, Series C (Applied Statistics), v. 28, no. 2, p. 126–135.

Piechota, T., Timilsena, J., Tootle, G., and Hidalgo, H., 2004, The western U.S. drought—How bad is it?: Eos, Transactions, American Geophysical Union, v. 85, no. 32, p. 301–304, accessed March 2019 at https://doi.org/10.1029/2004EO320001.

Rose, S., and Peters, N.E., 2001, Effects of urbanization on streamflow in the Atlanta area (Georgia, USA)—A comparative hydrological approach: Hydrological Processes, v. 15, no. 8, p. 1441–1457.

Ryberg, K.R., Hodgkins, G.A., and Dudley, R.W., 2019, Change points in annual peak streamflows—Method comparisons and historical change points in the United States: Journal of Hydrology, v. 583, article 124307, 13 p., accessed August 2019 at https://doi.org/10.1016/j.jhydrol.2019.124307.

Saghafian, B., Farazjoo, H., Bozorgy, B., and Yazdandoost, F., 2008, Flood intensification due to changes in land use: Water Resources Management, v. 22, no. 8, p. 1051–1067.

Seaber, P.R., Kapinos, F.P., and Knapp, G.L., 1987, Hydrologic unit maps: U.S. Geological Survey Water-Supply Paper 2294, 63 p., 1 pl.

Seager, R., Ting, M., Held, I., Kushnir, Y., Lu, J., Vecchi, G.A., Huang, H.-P., Harnik, N., Leetmaa, A., Lau, N.-C., Li, C., Velez, J., and Naik, N., 2007, Model projections of an imminent transition to a more arid climate in southwestern North America: Science, v. 316, no. 5828, p. 1181–1184.

Service, R.F., 2004, As the West goes dry: Science, v. 303, no. 5661, p. 1124–1127.

Siler, N., Proistosescu, C., and Po-Chedley, S., 2019, Natural variability has slowed the decline in western U.S. snowpack since the 1980s: Geophysical Research Letters, v. 46, no. 1, p. 346–355.

Solander, K.C., Bennett, K.E., and Middleton, R.S., 2017, Shifts in historical streamflow extremes in the Colorado River Basin: Journal of Hydrology—Regional Studies, v. 12, p. 363–377.

Spahr, N.E., Apodaca, L.E., Deacon, J.R., Bails, J.B., Bauch, N.J., Smith, C.M., and Driver, N.E., 2000, Water quality in the Upper Colorado River Basin, Colorado, 1996–98: U.S. Geological Survey Circular 1214, 33 p., accessed June 2019 at https://pubs.water.usgs.gov/circ1214/.

Stewart, I.T., 2009, Changes in snowpack and snowmelt runoff for key mountain regions: Hydrologic Processes, v. 23, no. 1, p. 78–94.

Stewart, I.T., Cayan, D.R., and Dettinger, M.D., 2005, Changes towards earlier streamflow timing across western North America: Journal of Climate, v. 18, no. 8, p. 1136–1155.

Stogner, R.W., Sr., 2000, Trends in precipitation and streamflow and changes in stream morphology in the Fountain Creek watershed, Colorado, 1939–99: U.S. Geological Survey Water-Resources Investigations Report 2000–4130, 43 p.

Tockner, K., and Stanford, J.A., 2002, Riverine flood plains—Present state and future trends: Environmental Conservation, v. 29, no. 3, p. 308–330.

Trenberth, K.E., 1999, Conceptual framework for changes of extremes of the hydrological cycle with climate change: Climatic Change, v. 42, p. 327–339.

U.S. Army Corps of Engineers, 2018, National inventory of dams: U.S. Army Corps of Engineers database, accessed December 2018 at http://nid.usace.army.mil/.

U.S. Environmental Protection Agency, 2016, A closer look—Temperature and drought in the Southwest: U.S. Environmental Protection Agency web page, accessed June 2019 at https://www.epa.gov/climate-indicators/southwest#ref4.

U.S. Forest Service, [1994], Vegetation changes on the Manti-La Sal National Forest—A photographic study using comparative photographs from 1902–1992: Price, Utah, U.S. Department of Agriculture, Forest Service, Intermountain Region, Manti-La Sal National Forest, 128 p.

U.S. Geological Survey, 2018a, USGS water data for the Nation: U.S. Geological Survey National Water Information System database, accessed December 2018 at https://doi.org/10.5066/F7P55KJN.

U.S. Geological Survey, 2018b, Water data—Annual reports—Principal inflows, diversions, and storage schematics: U.S. Geological Survey, California Water Science Center web page, accessed March 2019 at https://ca.water.usgs.gov/data/waterdata/schematics2007.html.

Villarini, G., 2016, On the seasonality of flooding across the continental United States: Advances in Water Resources, v. 87, p. 80–91.

Villarini, G., Serinaldi, F., Smith, J.A., and Krajewski, W.F., 2009, On the stationarity of annual flood peaks in the continental United States during the 20th century: Water Resources Research, v. 45, no. 8, article W08417, 17 p., accessed January 2019 at https://doi.org/10.1029/2008WR007645.

Villarini, G., and Slater, L., 2017, Climatology of flooding in the United States, *in* Cutter, S.L., ed., Oxford research encyclopedia of natural hazard science: Oxford, England, Oxford University Press, accessed February 2019 at https://doi.org/10.1093/acrefore/9780199389407.013.123.

Vogel, R.M., Yaindl, C., and Walter, M., 2011, Nonstationarity—Flood magnification and recurrence reduction factors in the United States: JAWRA, Journal of the American Water Resources Association, v. 47, no. 3, p. 464–474.

Walsh, J., Wuebbles, D., Hayhoe, K., Kossin, J., Kunkel, K., Stephens, G., Thorne, P., Vose, R., Wehner, M., Willis, J., Anderson, D., Doney, S., Feely, R., Hennon, P., Kharin, V., Knutson, T., Landerer, F., Lenton, T., Kennedy, J., and Somerville, R., 2014, Our changing climate, chap. 2 *of* Melillo, J.M., Richmond, T.C., and Yohe, G.W., eds., Climate change impacts in the United States—The third national climate assessment: Washington, D.C., U.S. Global Change Research Program, p. 19–67.

Whitfield, P.H., 2012, Floods in future climates—A review: Journal of Flood Risk Management, v. 5, no. 4, p. 336–365, accessed July 2019 at https://doi.org/10.1111/j.1753-318X.2012.01150.x.

Wilby, R.L., and Dettinger, M.D., 2000, Streamflow changes in the Sierra Nevada, California, simulated using statistically downscaled general circulation model scenario of climate change, chap. 6 *of* McLaren, S.J., and Kniveton, D.R., eds., Linking climate change to land surface change: Norwell, Mass., Kluwer Academic Publishers, p. 99–121.

Willis, A.D., Lund, J.R., Townsley, E.S., and Faber, B.A., 2011, Climate change and flood operations in the Sacramento Basin, California: San Francisco Estuary and Watershed Science, v. 9, no. 2, 18 p.

Woodhouse, C.A., Meko, D.M., MacDonald, G.M., Stahle, D.W., and Cook, E.R., 2010, A 1,200-year perspective of 21st century drought in southwestern North America: Proceedings of the National Academy of Sciences, v. 107, no. 50, p. 21283–21288.

Woodhouse, C.A., Pederson, G.T., Morino, K., McAfee, S.A., and McCabe, G.J., 2016, Increasing influence of air temperature on upper Colorado River streamflow: Geophysical Research Letters, v. 43, no. 5, p. 2174–2181, accessed May 2019 at https://doi.org/10.1002/2015GL067613.

Xiao, M., Udall, B., and Lettenmaier, D.P., 2018, On the causes of declining Colorado River streamflows: Water Resources Research, v. 54, no. 9, p. 6739–6756.

York, B.C., Ryberg, K.R., Asquith, W.H., Chase, K.J., Dickinson, J.E., Dudley, R.W., Harden, T.M., Hodgkins, G.A., Holtschlag, D.J., Humberson, D.G., Konrad, C.P., Levin, S.B., Restivo, D.E., Sando, R., Sando, S.K., Swain, E.D., Tillery, A.C., and Totten, A.R., 2022, Attributions for nonstationary peak streamflow records across the conterminous United States, 1941–2015 and 1966–2015: U.S. Geological Survey data release, https://doi.org/10.5066/P9FOUVWG.

Zhu, T., Lund, J.R., Jenkins, M.W., Marques, G.F., and Ritzema, R.S., 2007, Climate change, urbanization, and optimal long-term floodplain protection: Water Resources Research, v. 43, no. 6, article W06421, 11 p., accessed March 2019 at https://doi.org/10.1029/2004WR003516.

Attribution of Monotonic Trends and Change Points in Peak Streamflow in the South-Central Region of the United States, 1941–2015 and 1966–2015

By Anne C. Tillery, William H. Asquith, and Delbert G. Humberson

Chapter G of
Attribution of Monotonic Trends and Change Points in Peak Streamflow Across the Conterminous United States Using a Multiple Working Hypotheses Framework, 1941–2015 and 1966–2015
Karen R. Ryberg, editor

Prepared in cooperation with
U.S. Department of Transportation
Federal Highway Administration

Professional Paper 1869

U.S. Department of the Interior
U.S. Geological Survey

U.S. Geological Survey, Reston, Virginia: 2022

For more information on the USGS—the Federal source for science about the Earth, its natural and living resources, natural hazards, and the environment—visit https://www.usgs.gov or call 1–888–ASK–USGS.

For an overview of USGS information products, including maps, imagery, and publications, visit https://store.usgs.gov.

Suggested citation:
Tillery, A.C., Asquith, W.H., and Humberson, D.G., 2022, Attribution of monotonic trends and change points in peak streamflow in the South-Central region of the United States, 1941–2015 and 1966–2015, chap. G *of* Ryberg, K.R., ed., Attribution of monotonic trends and change points in peak streamflow across the conterminous United States using a multiple working hypotheses framework, 1941–2015 and 1966–2015: U.S. Geological Survey Professional Paper 1869, p. G1–G34, https://doi.org/10.3133/pp1869.

Associated data for this publication:
Dudley, R.W., Archfield, S.A., Hodgkins, G.A., Renard, B., and Ryberg, K.R., 2018, Peak-streamflow trends and change-points and basin characteristics for 2,683 U.S. Geological Survey streamgages in the conterminous U.S. (ver. 3.0, April 2019): U.S. Geological Survey data release, https://doi.org/10.5066/P9AEGXY0.

York, B.C., Ryberg, K.R., Asquith, W.H., Chase, K.J., Dickinson, J.E., Dudley, R.W., Harden, T.M., Hodgkins, G.A., Holtschlag, D.J., Humberson, D.G., Konrad, C.P., Levin, S.B., Restivo, D.E., Sando, R., Sando, S.K., Swain, E.D., Tillery, A.C., and Totten, A.R., 2022, Attributions for nonstationary peak streamflow records across the conterminous United States, 1941–2015 and 1966–2015: U.S. Geological Survey data release, https://doi.org/10.5066/P9FOUVWG.

ISSN 2330-7102 (online)

Acknowledgments

The work described in this professional paper was funded by the Federal Highway Administration of the U.S. Department of Transportation through Interagency Agreement DTFH6116X30020, “Flood Frequency Estimation for Hydraulic Design.” The authors would like to thank Meghan Bell and Daniel Wagner, both of the U.S. Geological Survey, for thorough and insightful reviews.

Contents

Figures

Tables

Conversion Factors

U.S. customary units to International System of Units

Multiply	By	To obtain
	Length	
inch (in.)	2.54	centimeter (cm)
foot (ft)	0.3048	meter (m)
mile (mi)	1.609	kilometer (km)
	Area	
acre	0.004047	square kilometer (km^2)
square mile (mi^2)	2.590	square kilometer (km^2)
	Volume	
acre-foot (acre-ft)	1,233	cubic meter (m^3)
acre-foot (acre-ft)	0.001233	cubic hectometer (hm^3)
	Flow rate	
cubic foot per second (ft^3/s)	0.02832	cubic meter per second (m^3/s)

International System of Units to U.S. customary units

Multiply	By	To obtain
	Area	
square kilometer (km^2)	247.1	acre
square kilometer (km^2)	0.3861	square mile (mi^2)
	Volume per square unit of area	
megaliter per square kilometer (ML/km^2)	2.099	acre-foot per square mile ($acre\text{-}ft/mi^2$)

Temperature in degrees Fahrenheit (°F) may be converted to degrees Celsius (°C) as follows:

$$°C = (°F – 32) / 1.8.$$

Datum

Horizontal coordinate information is referenced to the North American Datum of 1983 (NAD 83).

Supplemental Information

A “water year” is the 12-month period from October 1 through September 30 of the following year that is designated by the calendar year in which it ends.

The 75- and 50-year study periods described in this report span water years 1941–2015 and 1966–2015, respectively. The period of record in figures G6–G9 extends through water year 2017 (2 years more than the core monotonic trend and change-point hypothesis testing that ended in water year 2015), and in figures G4–G5 and G10–G11 the period of record includes years before water year 1941 because such data were available at the time of assembly of ancillary figures specific to the South-Central region. The extra years of data in the figures, before water year 1941 and after water year 2015, were not used to establish monotonic trends and change points in the 75- and 50-year study periods.

Abbreviations

>	greater than
<	less than
CP	change point
GAGES-II	Geospatial Attributes of Gages for Evaluating Streamflow, Version II
GIS	geographic information system
MGBT	multiple Grubbs-Beck test
NAD 83	North American Datum of 1983
NID	National Inventory of Dams
NOAA	National Oceanic and Atmospheric Administration
NWALT	National Water-Quality Assessment Program (NAWQA) Wall-to-Wall Anthropogenic Land Use Trends (dataset for the conterminous United States)
PDSI	Palmer Drought Severity Index
p-value	attained significance level
USACE	U.S. Army Corps of Engineers
USGS	U.S. Geological Survey

Attribution of Monotonic Trends and Change Points in Peak Streamflow in the South-Central Region of the United States, 1941–2015 and 1966–2015

By Anne C. Tillery,[1] William H. Asquith,[1] and Delbert G. Humberson[2]

Abstract

The national U.S. Geological Survey (USGS) streamgaging network has monitored streamflow over many decades and in some cases exceeding a century. Annual peak-streamflow data for a wide variety of watersheds are available through the USGS National Water Information System. Retrospective analysis of the peak streamflows through the identification of monotonic trends and change points is useful to many water-resources stakeholders. The general history of changes in peak streamflow could be attributed to various possible causes including anthropogenic modification of the landscape, water-resources development, and climate cycles and change.

The magnitude of annual peak streamflows can change over time, potentially affecting water-resources and infrastructure decisions. This study used a multiple working hypotheses framework to attribute primary and secondary drivers to monotonic trends and change points in annual peak streamflows for a 50-year period (water years 1966–2015) and a 75-year period (water years 1941–2015) for 332 streamgages in the South-Central region of the United States. A total of 179 monotonic trends (100 in the 50-year period, 1966–2015, and 79 in the 75-year period, 1941–2015) and 149 change points (76 in the 50-year period, 1966–2015, and 73 in the 75-year period, 1941–2015) were detected at a significance level of p=0.10 (computed p-values for the hypothesis test that are less than 0.10 are declared as statistically significant) in the South-Central region, the vast majority of which indicated decreases in peak streamflows with time.

This study was restricted to consider 11 unique to semi-unique attributions for each detected monotonic trend or change point. These 11 possible attributions are based on data availability and applicability in the South-Central region and are classified under the following larger groups: climatological and meteorological, flood-water or erosion-control impoundments, water-resources development, land-use patterns, and unknown. Only 8 of the 11 attributions (within the larger groups) were considered applicable in the South-Central region including long-term precipitation, air temperature, large artificial impoundments, small artificial impoundments, groundwater withdrawals, surface-water withdrawals, urban effects, and unknown.

Attributions assigned in the South-Central region (other than “unknown”) were commonly anthropogenic. The majority of monotonic trends and change points identified in the South-Central region were negative, that is, a direction of smaller magnitudes of peak streamflow with time. For negative monotonic trends and negative change points in annual peak streamflow, attributions mainly included large artificial impoundments, small artificial impoundments, and groundwater and surface-water withdrawals. The few positive monotonic trends and positive change points observed were generally attributed to urbanization. Because of the clear attribution of monotonic trends and change points in annual peak streamflow to anthropogenic factors such as large and small artificial impoundments, urbanization, and groundwater and surface-water withdrawals, the rigorous assessment of climatic impacts in the South-Central region would require normalization for these anthropogenic factors prior to attributing climate as the cause of monotonic trends in annual peak streamflow.

Introduction

The U.S. Geological Survey (USGS) streamgaging network is a national asset designed for long-term, continuous monitoring of streamflow at hundreds of streamgage locations; the data from the network are used in the computation of annual streamflow statistics. At some sites, the period of record may exceed a century. Annual peak-streamflow data for a wide variety of watersheds are available through the USGS National Water Information System (NWIS) (U.S. Geological Survey, 2019). Detailed descriptions of peak-streamflow data and their uses were provided by Asquith and others (2017) and England and others (2018).

Retrospective analysis of peak streamflows and their characteristics through time is useful to many water-resources stakeholders. For example, drainage and transportation engineers engaged in design analysis of peak-streamflow

[1]U.S. Geological Survey.

[2]International Boundary and Water Commission.

frequency need to make decisions as to which USGS streamgage data are included in flood-frequency analyses, which generally cannot mathematically account for nonstationarity in peak streamflows. Identifying statistically significant monotonic trends (hereinafter referred to as monotonic trends or just trends) in peak streamflow, in conjunction with change-point analysis, is a useful first step in understanding the history of peak streamflow at a streamgage. When monotonic trends and (or) change points are detected (detection of one does not imply detection of the other), the identification or attribution of possible drivers of the monotonic trends and change points (including urbanization, water-resources development, and climate) enhances the general understanding of the history of peak streamflow in a given area.

As part of a national synopsis, Dudley and others (2018), published results of statistical tests involving trend and change-point analyses of peak streamflows for 2,683 streamgages in the conterminous United States. The statistical analyses included results of the Mann-Kendall test (Helsel and others, 2020) for monotonic trends of the annual peak-streamflow time-series data. The Mann-Kendall test produces the Kendall's tau statistic, which is a succinct measure of association (similar to a correlation coefficient).

The trend analysis of peak streamflow also included results of the Pettitt test (Ryberg and others, 2019) for change points in the median of annual peak-streamflow values. The Pettitt test (Pettitt, 1979) is an evaluation of whether two populations of peak streamflows exist in the sample, as distinguished by median annual peak-streamflow values. The test also identifies the year of any detected change. Dudley and others (2018) set statistical significance at a 0.10 two-tail level, and unless otherwise stated, the term "statistically significant" hereinafter refers to a *p*-value resulting from a given statistical hypothesis test of less than 0.10. Statistical significance means that a trend or change point has been detected. Finally, additional studies on the large-scale evaluation of trends in peak streamflow are available in Dickinson and others (2019) and Hodgkins and others (2019).

This chapter concerns attribution of detected monotonic trends and change points for a 332-streamgage subset of the 2,683 streamgages used by Dudley and others (2018) located in the South-Central region of the United States (fig. G1). Within the South-Central region, all 332 streamgages met the approximately 50-year criteria (water years 1966–2015, fig. G1) of Dudley and others (2018) and Hodgkins and others (2019). A water year represents the 12-month period between October 1 and September 30 of the following year that is designated by the calendar year in which it ends; for example, the water year ending September 30, 2015, is referred to as "water year 2015." Of the 332 streamgages, a subset of 165 streamgages also met the 75-year criteria (water years 1941–2015, fig. G1). These two periods hereinafter are referred to as the "50-year" and "75-year" periods, respectively. To fulfill the criteria, the streamgages were required to have peak-streamflow data for the 50- and (or) 75-year period and have data for at least 8 of 10 years (80 percent) for each applicable decade (Hodgkins and others, 2019). Listings of all 332 streamgages analyzed for this study, including whether any statistically significant monotonic trends or change points were detected, are available in Tillery and others (2022; files SC_site_manifest.csv, SC_50yr_ChangePT.csv, SC_50yr_Trend.csv, SC_75yr_ChangePT.csv, and SC_75yr_Trend.csv). Note that although the southwestern part of the South-Central region extends into Mexico because of the topography of stream drainage basins, the watersheds considered for monotonic trend and change-point attributions are within the conterminous United States. The South-Central region for this study is made up of three water-resources regions identified by two-digit hydrologic unit codes (HUC2s) described by Seaber and others (1987): water-resources regions 11 (Arkansas-White-Red), 12 (Texas-Gulf), and 13 (Rio Grande).

This chapter of the professional paper describes a study that was part of a larger USGS effort to identify and characterize changes in peak streamflows across the conterminous United States (Barth and others, this volume, chap. A). This larger USGS effort builds upon a previous study by the USGS and the Federal Highway Administration (FHWA) of the U.S. Department of Transportation to identify statistically significant monotonic trends and change points in annual peak streamflows across the conterminous United States (Dudley and others, 2018; Hodgkins and others, 2019; Ryberg and others, 2019). In an effort to develop a cohesive national approach for incorporating potential or observed changes into flood-frequency estimates when necessary, national and regional experts from the USGS and cooperators worked together to develop a multiple working hypotheses framework for attributions and a common vocabulary for making provisions of confidence.

Physical Setting and Peak Streamflows

Watersheds within the South-Central region are characterized by a large range of physiographic and climatologic settings (Carr, 1967; U.S. Geological Survey, 1984, 1985, 1986, 1988, 1990, 1991; O'Connor and Costa, 2003; Burnett, 2008; Bomar, 2017). The physiography encompasses humid coastal plains, humid upland forests, cropping and grazing agriculture, semi-arid continental steppe, mountainous desert, lush intra-mountain basins, and snow-capped mountain peaks. The general change from west to east in mean annual precipitation from the extreme southeast corner to the extreme southwest corner of the South-Central region is approximately 50 inches (Northwest Alliance for Computational Science and Engineering, 2019).

Peak streamflows in the South-Central region result from an immensely complicated suite of hydrometeorologic processes operating on substantial variations in time and space within watersheds. For example, for each water year, watersheds in the humid eastern part of the South-Central region might experience annual peak streamflows resulting from runoff from periods of intense regional precipitation. Watersheds in the semi-arid central part of the South-Central region may

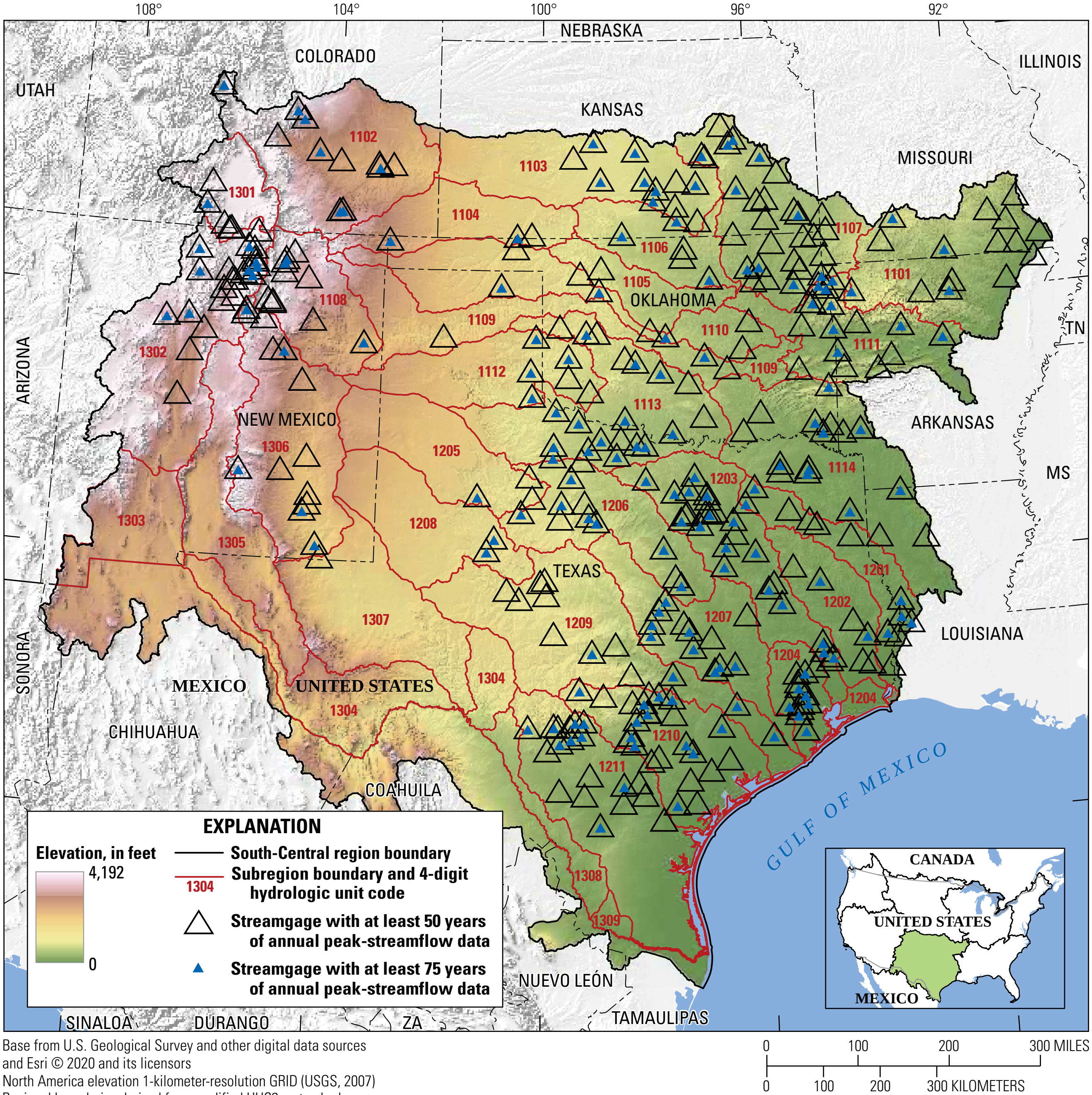

Base from U.S. Geological Survey and other digital data sources
and Esri © 2020 and its licensors
North America elevation 1-kilometer-resolution GRID (USGS, 2007)
Regional boundaries derived from modified HUC2 watersheds
USA Contiguous Albers Equal Area Conic USGS projection
North American Datum of 1983

Figure G1. Map showing the locations of 332 U.S. Geological Survey streamgages within the South-Central region (Tillery and others, 2022) with streamgages with at least 50 years of annual peak-streamflow data for water years 1966–2015 (open triangles) and streamgages with at least 75 years of annual peak-streamflow data for water years 1941–2015 (blue-filled triangles, subset of 165 streamgages). For this study, the regions were based on watersheds identified by two-digit hydrologic unit codes (HUC2s) described by Seaber and others (1987), and some regions were modified slightly by adding or subtracting subregions (HUC4s) to achieve geographic cohesiveness or hydrologic-setting similarity. Streamgage locations shown are from the Geospatial Attributes of Gages for Evaluating Streamflow, Version II (GAGES-II) from Falcone (2011). Note that although the southwestern part of the South-Central region extends into Mexico because of the topography of stream drainage basins, the watersheds considered for monotonic trend and change-point attributions are within the conterminous United States (U.S. Geological Survey, 2019).

experience peak streamflow resulting from short-duration runoff from localized storms, peak streamflows no greater in magnitude than baseflow, or watershed-scale precipitation. Watersheds in the arid western part of the South-Central region may experience no annual peak streamflows or persistent baseflow that could be recorded as the annual peak. During periods of unusually widespread, short-duration/high-intensity precipitation, and particularly when such precipitation is preceded by a period of abundant precipitation, large peak streamflows (floods) can occur in any watersheds in the South-Central region. For a given watershed in the South-Central region, the peak streamflows can range three or more orders of magnitude in a 50- or 75-year period of record.

Anthropogenic impacts to the landscape and hydrologic cycle are also considerable in the South-Central region at both local and regional scales. Land use in the South-Central region can range from major urban development with high population density in metropolitan areas to effectively unpopulated regions. Anthropogenic impacts include the development of water resources from the entirety of watersheds to small parts of watersheds. Water resources developments include the following: major flood impoundments and reservoirs; minor but spatially dense flood-water retention structures; reservoirs for municipal water supply and irrigation; substantial contour-farming practices for soil conservation; and groundwater withdrawals, for both large-scale production agriculture and municipal drinking-water supply.

Because peak streamflows are the end-result of several hydrologic components functioning on various time scales, any type of water resource development can affect the magnitudes of peak streamflows. From a water budget perspective, there are several possible inputs to streamflow, including precipitation, snowmelt runoff, spring flow, irrigation deliveries and returns, groundwater fluctuations, and wastewater return flows (effluent). In the arid and semi-arid parts of the South-Central region, such inputs can represent substantial fractions of the recorded annual peak streamflow during some years. There are also multiple possible streamflow outputs, including evapotranspiration, subsurface seepage, surface-water diversion, and groundwater extraction. Depending on the hydrologic setting of each watershed, water that reaches a streamgage could have been exposed to several, if not all, of these water-budget demands.

Previous Studies

Some prior studies on streamflow monotonic trends and change points have been made within the South-Central region (Rasmussen and Perry, 2001; Brauer and others, 2015; Thomas and others, 2019). The most common are studies restricted to relatively localized areas and very few streamgages. Studies using large numbers of streamgages are primarily cited herein. In Texas, Villarini and Smith (2013) studied the validity of the stationarity assumption (lack of trends in the moments of the probability distribution) and the impact of tropical cyclones on the upper tail of the flood-peak distribution, and they concluded that tropical cyclones play a diminished role in shaping the upper tail of the flood-peak distribution compared with areas of the eastern United States, which is subject to frequent tropical hurricanes.

Asquith and others (2007a, b) provided visualizations of trends in percentages of zero daily mean streamflow and annual mean, maximum (peak) streamflows, and minimum streamflows for 712 streamgages in Texas. Asquith and Heitmuller (2008) provided visualizations of trends in annual mean and annual-harmonic mean streamflow for 620 streamgages in Texas. Asquith and Barbie (2014) considered more than 500 continuous-record streamgages in the 2013 active streamgage network in Texas, and they analyzed streamflow records for monotonic trends in annual mean streamflow for 38 selected long-term streamgages that were active as of water year 2012 and with record lengths ranging from 49 to 97 cumulative years. These streamgages included watersheds believed to represent natural and unregulated conditions. The monotonic trend analysis detected two statistically significant positive trends (p-value<0.01, one-tail significance level), one statistically significant negative trend (p-value<0.01, one-tail significance level), and 35 instances without a statistically significant trend (p-value<0.02, two-tail significance level).

Since the early 1980s, magnitude and frequency of peak streamflows have been studied at approximately 10-year intervals in New Mexico (Thomas and Gold, 1982; Waltemeyer, 1986; Thomas and others, 1994; Waltemeyer, 1996; Waltemeyer, 2006a; Waltemeyer, 2008). Waltemeyer (2006b) described the collection of annual peak-streamflow data within a network of crest-stage and flood-hydrograph streamgages in New Mexico using small pressure transducers as later documented by Sauer and Turnipseed (2010). Two flood-frequency reports have been published for streams in Kansas, one by Irza (1966) and another more recently by Painter and others (2017). Magnitude and frequency of peak streamflows have been studied in Oklahoma since the early 1970s (Sauer, 1974; Thomas and Corley, 1977; Tortorelli and Bergman, 1985; Tortorelli and McCabe, 2001; Lewis, 2010; Smith and others, 2015; Lewis and others, 2019).

Since the mid-1990s, magnitude and frequency of peak streamflows have been studied in Texas (Asquith and Slade, 1997; Asquith and Thompson, 2008; Asquith and Roussel, 2009; Asquith and others, 2018). Harwell and Asquith (2011) described the collection of peak-streamflow data within a network of crest-stage and flood-hydrograph streamgages in Texas also using crest-stage streamgages equipped with small pressure transducers as described by Sauer and Turnipseed (2010).

Selection of Attributions for Analysis

The approach used for this national study is a modification of multiple working hypotheses as described by Harrigan and others (2014). Possible environmental contributors to detected trends and change points, termed “attributions,” were identified in Barth and others (this volume, chap. A). Not all attributions identified are applicable to every region included in the overall study. For example, a subset of attributions was selected for evaluation in the South-Central region based on applicability to the region and availability of data. Available data sources were semi-quantitatively and qualitatively studied to evaluate the possibility of each attribution to contribute to the detected monotonic trend or change point. After tabulation of streamgage-specific attributions and the completion of author-led annotations, the likeliest candidate(s) were chosen for primary and secondary attributions of the detected monotonic trend or change point.

By design, the study described in this chapter was restricted to consider 11 unique to semi-unique environmental contributors to which detected monotonic trends or change points could be attributed. The 11 attributions listed by classification are (1) long-term precipitation; (2) air temperature; (3) large artificial impoundments; (4) small artificial impoundments; (5) groundwater withdrawals; (6) surface-water withdrawals; (7) wastewater return flows; (8) agricultural crops; (9) grazing activity; (10) urban effects (land-use patterns); and (11) unknown. These 11 attributions can be categorized in the following larger groups: climatological and meteorological (includes attributions 1–2); flood-water or erosion-control impoundments (includes attributions 3–4); water-resources development (includes attributions 5–7); land-use patterns (includes attributions 8–10); and unknown (includes attribution 11). The level of evidence supporting assignment of a potential attribution was also evaluated in accordance with table G1. Both monotonic trends and change points detected in the 50-year and 75-year periods were investigated for the 332 streamgages in the South-Central region with the requisite period of record.

Table G1. Explanation for the different evidence levels assigned for each attribution.

Evidence level	Level explanation
Robust	One or more of the following: strong and consistent results, multiple sources (datasets, studies, analyses), well-documented data, and attribution is consistent with causal mechanisms.
Medium	Moderate consistency, emerging results, or weight of evidence points in the direction of attribution but there may be some divergent findings.
Limited	Limited sources or inconsistent findings.
Additional information required	Insufficient evidence to make an attribution.

Data Sources

There are three sources of external data acquired or consulted for this chapter: (1) the USGS published streamflows, land-use patterns, and regional groundwater-depletion information; (2) the National Oceanic and Atmospheric Administration (NOAA) monthly climatological data; and (3) the U.S. Army Corps of Engineers dam (reservoir) construction information for dams upstream from each streamgage. Various types of aerial and satellite imagery available online using Google Earth (https://www.google.com/earth; accessed November 16, 2021) were reviewed for the watersheds of select streamgages. The three sources of data are discussed below.

U.S. Geological Survey Streamflow, Land-Use, and Groundwater-Depletion Datasets

Various datasets within the NWIS (U.S. Geological Survey, 2019) were used including peak streamflows, associated qualification codes (Wagner and others, 2017), and daily mean streamflows. NWIS also provides the streamgage location and the drainage area including, if applicable, a separate contributing drainage area entry.

Additionally, streamgage station descriptions were reviewed. These descriptions, which usually include a streamgage history, are not publicly available in the NWIS database. The descriptions are available on a streamgage-by-streamgage basis upon request to the local USGS office that operates a given streamgage, provided the description is nonsensitive information. The streamgage station descriptions summarize periods of record and can include remarks about the streamgage history and information about historical peak streamflows. Notes may also mention the factors in the watershed (of the streamgage) that affect peak streamflow, such as diversions, reservoirs, seepage, withdrawals, and wastewater return.

The Geospatial Attributes of Gages for Evaluating Streamflow, Version II (GAGES-II) dataset (Falcone, 2011) and the National Water-Quality Assessment Program (NAWQA) Wall-to-Wall Anthropogenic Land Use Trends (NWALT) dataset (Falcone, 2015) were also used in this study (fig. G2*A*). A polygon representing the watershed of each streamgage was obtained from the GAGES-II dataset. Additionally, the GAGES-II dataset provided information regarding the number of dams within each watershed and the total reservoir storage capacity normalized by drainage area for the years grouped by decade. Individually, these decadal breaks are referred to as "pre1940," "pre1950," "pre1960," "pre1970," "pre1980," "pre1990," and "2009." Unfortunately, there is no reservoir storage capacity accumulation to the year 2000 provided in the GAGES-II dataset. Reservoir storage capacity is measured in volume per square unit of area (megaliters per square kilometer) and is reported as accumulation to one of the decadal breaks. For example, reservoir storage capacity through the year 1980 in the watershed of streamgage 08136000, located at the Concho River at San Angelo, Texas, is about 165 megaliters per square kilometer.

A

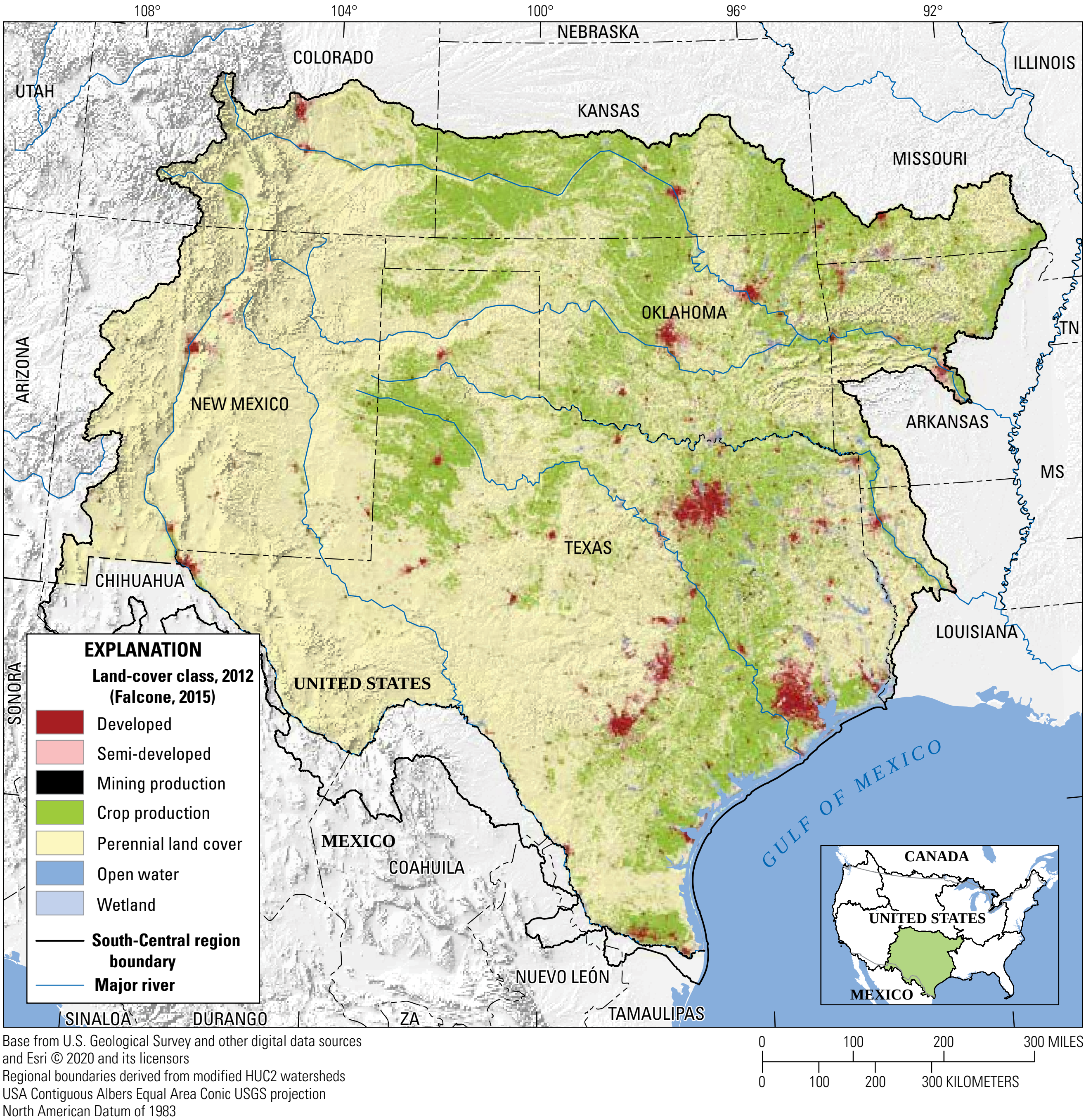

Figure G2. Maps showing the 2012 NWALT land-cover classes for the South-Central region and the extent of the High Plains (Ogallala) aquifer in relation to the South-Central region and the changes in the aquifer water levels from predevelopment through 2013. *A*, The 2012 NWALT land-cover classes; *B*, The extent of the High Plains (Ogallala) aquifer. The South-Central region boundary is based on watersheds identified by two-digit hydrologic unit codes (HUC2s) described by Seaber and others (1987). Land-cover classes for 2012 that are shown in part *A* are from Falcone (2015). The crop production land-cover class in part *A* includes "pasture/hay/grazing" as used in this chapter. Because of the map scale, the mining production and wetland classes in part *A* may be easier to see if the view is zoomed in. NWALT, National Water-Quality Assessment Program (NAWQA) Wall-to-Wall Anthropogenic Land Use Trends (dataset for the conterminous United States) (Falcone, 2015).

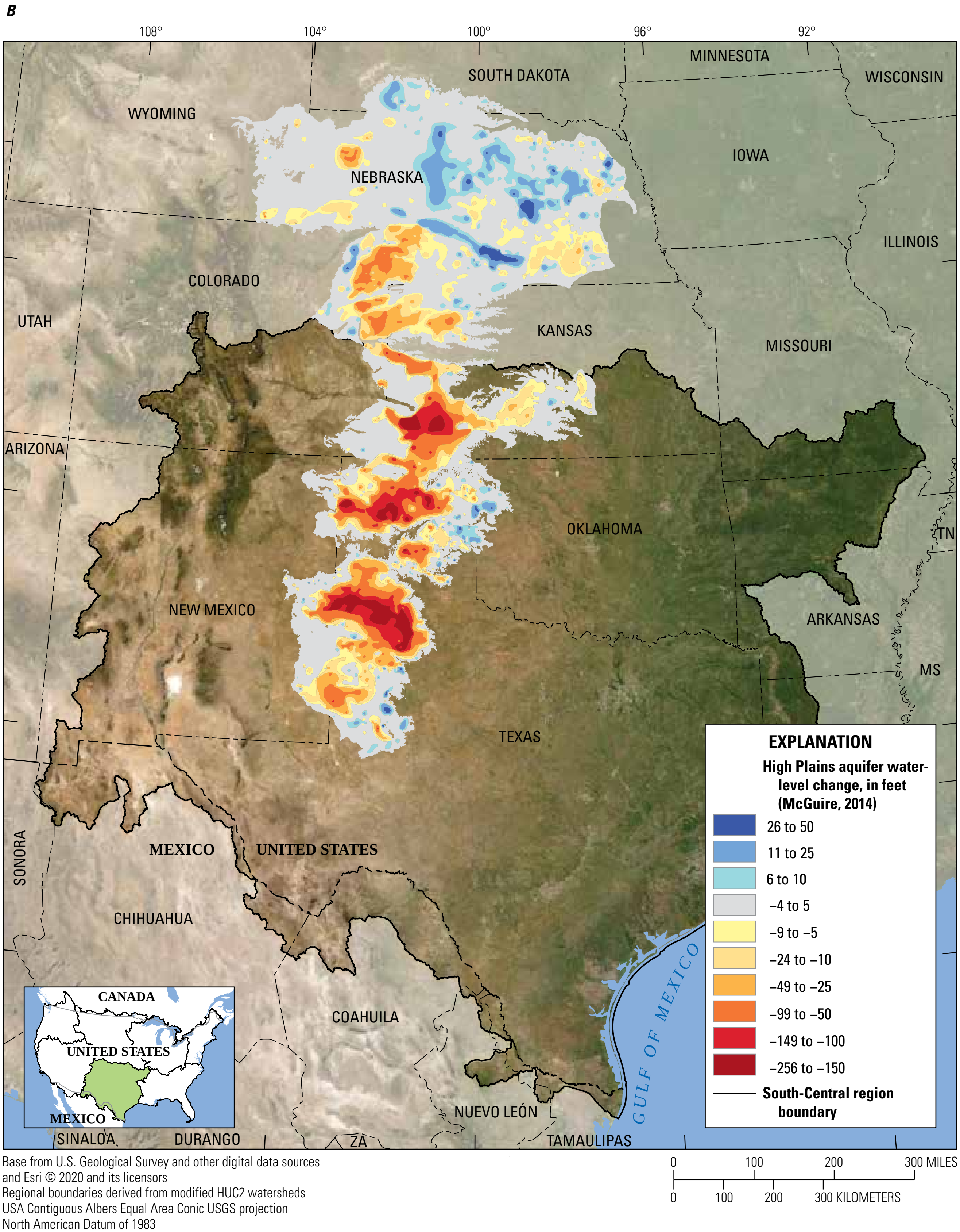

Figure G2. —Continued

The NWALT dataset provides gridded information on land-use change over time (decadal). For the South-Central region, the land-use categories were limited to open water and wetlands, low use (perennial land cover), mining production, general agricultural cropping (including groupings for production crops and pasture, hay, and grazing), and urban development (including developed and semi-developed). Finally, regional groundwater depletion data and other changes from predevelopment to modern times (predevelopment through 2013) for the High Plains part of the South-Central region were integrated with the streamgage data using a geographic information processing system. The High Plains part of the South-Central region is loosely defined by the extent of the High Plains (Ogallala) aquifer as shown by McGuire (2014) and also shown in figure G2*B*.

National Oceanic and Atmospheric Administration (NOAA) Climatological Datasets

Figure G3 shows climate divisions in the South-Central region that were identified by the National Oceanic and Atmospheric Administration (2019). Comprehensive monthly climate division data were acquired for the period January 1895 through December 2018, with some months missing in the National Oceanic and Atmospheric Administration (2018) dataset. Downloaded text files of climate-division arithmetic-mean meteorological data included monthly precipitation, the Palmer Drought Severity Index (PDSI; Palmer, 1965), and the monthly average temperature; the PDSI uses precipitation and temperature to estimate relative dryness and relies on a rudimentary water-budget model to determine moisture supply (Alley, 1984).

U.S. Army Corps of Engineers National Inventory of Dams

The U.S. Army Corps of Engineers (USACE) National Inventory of Dams (NID) database (U.S. Army Corps of Engineers, 2019) for each State was acquired, joined, and then clipped to the South-Central region boundary. The information available in the NID database about the dams and reservoirs that are upstream from the streamgages included the location, purpose, approximate construction date, and total reservoir storage capacity (the NID storage term is in acre-feet).

The NID database was then repetitively clipped within a geographic information system (GIS) using polygons that represent the watersheds of each of the streamgages. One clipping per streamgage was made to create a table of NID structures that are upstream from each associated streamgage. These data were used to construct detailed spreadsheets with author-led annotation to facilitate streamgage-specific scrutiny of the following two distinct attributions: (1) large artificial impoundments, and (2) small artificial impoundments.

Similar applications of the NID have been used by previous studies to better understand the long-term effect of regulation on streamflows. The NID database was used by Asquith (2001) to study the effects of regulation identified by graphical change-point analysis on summary statistics of annual peak streamflows in Texas. Asquith and others (2021) released software to overlay geospatial polygons on the NID, temporally accumulate reservoir storages within a polygon, and optionally bind annual peak-streamflow data on a year-by-year basis to cumulative reservoir storages. This year-by-year basis of reservoir storage assignment contrasts with the decadal-based accumulation used in this attribution study.

Watershed and Streamflow Record Characterization and Analysts' Confidence in Detected Monotonic Trends and Change Points

Preceding the attribution phase of this study, a qualitative evaluation of background data and hydrologic context was made. First, familiarity with the watersheds of individual streamgages and associated streamflow records was achieved through overview site characterization. Streamflow records included the peak streamflows as well as daily mean streamflows. Various diagnostic plots were created (Asquith and others, 2022a; Konrad and York, 2022) and the results were evaluated by analysts for overview characterization of the sites. The streamgage record review always included the entire period for which each streamgage was in operation, even if it was longer than the period of analysis for the current study because a wholistic view of the streamgage record is helpful in understanding the streamflow history and patterns at each streamgage. Diagnostic plots used for this purpose and shown in this section will therefore show the entire period of record for each streamgage regardless of the period of analysis.

For an initial overview of each investigated streamgage and its watershed, the information regarding the size of the drainage area, the streamgage-specific period of record, and any notes on factors affecting streamflow were obtained from the streamgage station descriptions. Streamgage station descriptions include information on the years that the streamgage was regulated, the years it was affected by diversions, groundwater or surface-water withdrawals, and years when streamflows were affected by the return flow from irrigated lands. To supplement this information, polygons representing contributing drainage areas, as defined by the GAGES-II dataset (Falcone, 2011) were loaded into Google Earth (https://www.google.com/earth) for an author-led, visual inspection of aerial imagery. Whereas, relatively small watersheds could be inspected in detail, a thorough study of imagery for relatively large watersheds was not feasible. The visual inspection of aerial imagery, therefore, focused on identifying the approximate location of headwaters for a streamgage to determine if there were any potential effects on streamflow such as major irrigation infrastructure, the dominance of

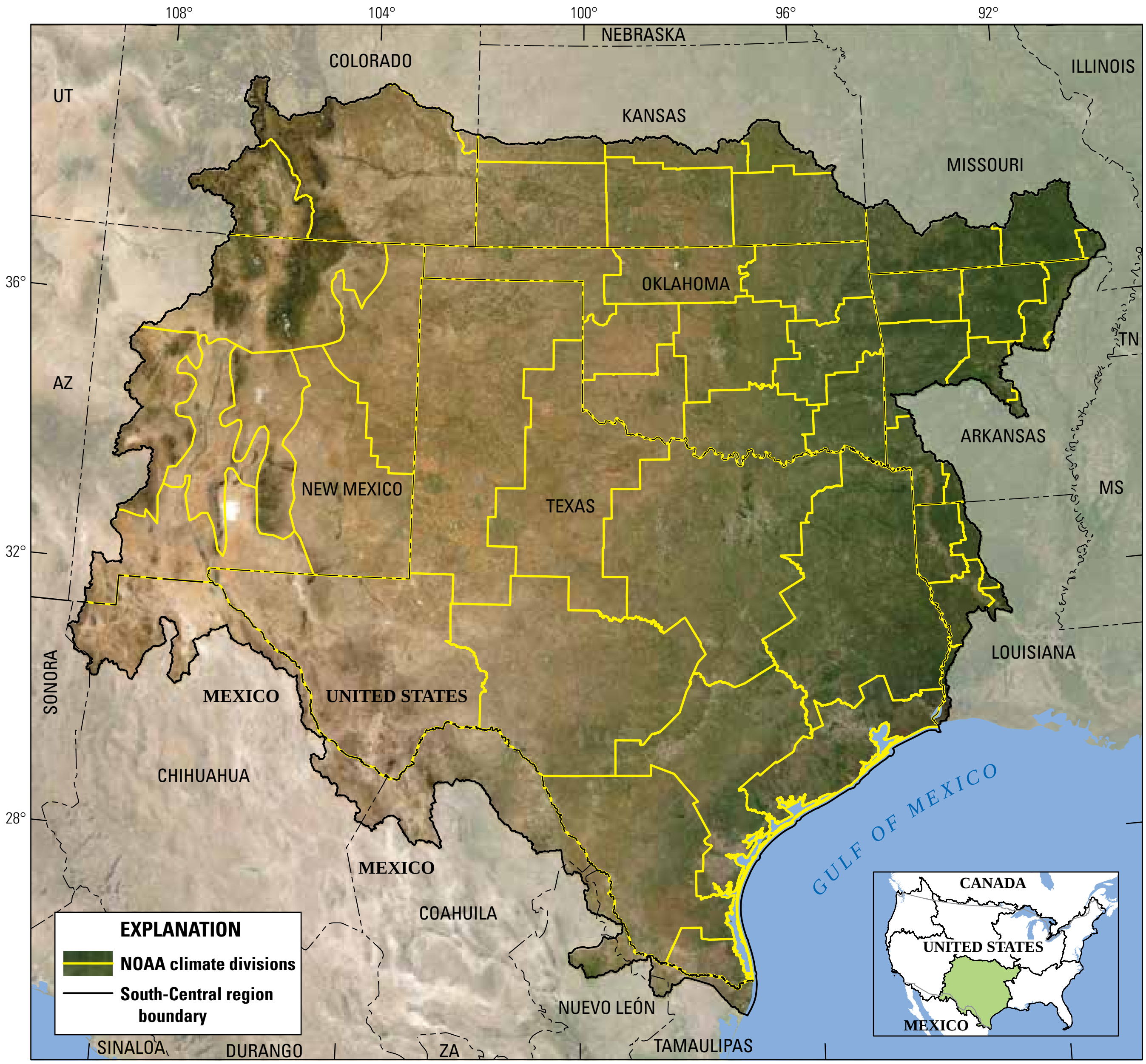

Base from U.S. Geological Survey and other digital data sources and Esri © 2020 and its licensors
Regional boundaries derived from modified HUC2 watersheds
USA Contiguous Albers Equal Area Conic USGS projection
North American Datum of 1983

Figure G3. Map showing the NOAA climate divisions in the South-Central region. Climate divisions are from NOAA (2019). The South-Central region boundary is based on watersheds identified by two-digit hydrologic unit codes (HUC2s) described by Seaber and others (1987). NOAA, National Oceanic and Atmospheric Administration. Yellow borders of NOAA climate divisions appear dashed where they coincide with political boundaries.

agricultural versus urban land cover, or other obvious effects on streamflow.

For example, streamgage 08136000, located at the Concho River at San Angelo, Texas, shows a positive trend in mean annual peak streamflow over the 50-year period and a negative trend in mean annual peak streamflow over the 75-year period. The streamgage station description also has remarks that indicate that greater than 10 percent of its contributing drainage area has been regulated since 1931. This statement of regulation is considered semi-quantitative. The streamgage station description also indicates that, at times, zero flow exists (the stream is dry) and there are diversions for irrigation, industrial, and municipal supply that are upstream from the streamgage.

After characterizing the watershed, the next step was to characterize the streamflow record. The detection of trends is sensitive to the selected starting and ending years and how the period of streamflow record relates to climate cycles. Spurious (false) detection of trends can occur. For example, if the start of the analyzed period occurred during a cluster of small peak streamflows, and the end of the analyzed period occurred during a cluster of relatively large peak streamflows, then a spurious detection of a positive trend may result. To help evaluate spurious trend detections, statistical graphics using the Mann-Kendall test (showing the calculated Kendall's tau value), were plotted for each streamgage for every combination of starting and ending years over the period in which the streamgage was in operation (fig. G4). For each combined starting and ending year, a color is plotted that indicates the colloquial "strength" of the Kendall's tau value.

Kendall's tau values close to zero indicate lack of a trend in peak streamflows with time. Kendall's tau values further away from zero indicate increasing confidence in a trend in peak streamflows with time for a given sample size. A Kendall's tau value between 0.05 and −0.05 has no color assigned to it and indicates a weak or no trend in peak streamflows. A Kendall's tau value greater than 0.10 indicates a positive trend in peak streamflows (light green to dark blue in fig. G4) with darker shades indicating increasing confidence in the trend. A Kendall's tau value less than −0.10 indicates a negative trend in peak streamflows (pale orange to dark red in fig. G4) with darker shades, again, indicating increasing confidence in the trend. This example (fig. G4) shows that for most combinations of starting and ending years, there was no trend (large area covered in white) or the detected trend was negative for this streamgage. The plot shows only a few small areas of light green to dark blue indicating possible positive trends, which is an indication that those would not be true trends but rather an artifact of a few unusual peak-streamflow values near the start or end of those specific periods. A robust trend analysis of peak streamflow for this streamgage should show no trend or no negative trend. Figure G4 provides evidence to conclude that a detected positive trend in peak streamflows during the 50-year period (water years 1966–2015) is likely to be spurious at this streamgage. It is apparent on the plot that the positive trend is not representative of the overall trend in the peak streamflows. However, the detected negative trend in peak streamflow during the 75-year period (water years 1941–2015) is shown for nearly all combinations of starting and ending years (where the starting year is 1960 or before), which indicates that it is less likely to be spurious. In addition to suggesting a spurious detection for the 50-year period, figure G4 also suggests that an event occurred near 1960 that caused peak streamflows to stabilize at a lower value than for the 75-year period.

The next step in characterizing the streamflow record involved observing a plot of peak streamflows with time that was derived from the peak-streamflow tables (fig. G5). The vertical dashed lines indicate water years for which data are missing, and the number 6 that is plotted as a data point beginning in the late 1930s indicates that the peak streamflow was affected by regulation or diversion for that year. Code 6 and other discharge qualification codes are described by Wagner and others (2017). In this example, it is shown that the peak-streamflow database is mostly consistent with the notes in the streamgage station description that states flow at the streamgage has been affected by regulation since 1931. The horizontal green lines show the median peak streamflow before and after a detected 75-year change point in 1962. The change-point detection for the early 1960s is self-evident on visual inspection of the time series in figure G5.

The final step in characterizing the watershed and peak-streamflow data was to visualize how the streamflow regime has or has not changed over time using quantile-Kendall plots. The streamflows that are depicted cover the full range of quantiles of the daily-mean streamflow distribution, from the lowest flow of the year, through the median flow, to the highest flow. The quantile-Kendall plot is a type of visualization in which the ranked, daily mean streamflows for each year are evaluated using the Mann-Kendall test. The plot is based on calculating the Mann-Kendall test for a sequence of annual streamflow statistics of each same-day statistic available in the record (N-day), where N=1 is defined as the annual daily minimum nonexceedance probability 1/(365+1), where N=365 is the annual daily maximum nonexceedance probability 365/(365+1), and the 366 days of leap years is ignored. For the quantile-Kendall plots, emphasis focuses on daily mean streamflows.

Quantile-Kendall plots for streamgage 08136000 show differences in trends and statistical significance for the 50- and 75-year periods (figs. G6 and G7). Although these plots do not indicate the quantity of change in daily streamflow, the plots do indicate whether or not parts of the daily streamflow regime have tendencies towards increasing or decreasing daily streamflow over time. From figure G6, it is apparent that almost the entire streamflow regime for the 50-year period has nonsignificant Kendall's tau values (fig. G6, p-value>0.05, blue circles), with most being positive (indicating nonsignificant positive trends). The uppermost Kendall's tau values (red circles) in figure G6, however, are considered statistically significant (p-value<0.05). For the 75-year period (fig. G7), it is apparent that the entire streamflow regime has negative

Kendall's tau values (indicating a negative trend), with approximately 40 percent of the streamflow regime considered statistically significant (fig. G7, p-value<0.05, red circles).

The lack of statistically significant monotonic trends for the 50-year period (fig. G6) suggests that most of the flow regime has been approximately stable since about 1966. The plot of the 75-year period (fig. G7) suggests that the watershed is producing less water overall at the streamgage; however, only the larger flows show statistically significant negative monotonic trends. What is not clear in the quantile-Kendall plots is the actual decrease in magnitude of the annual daily streamflows.

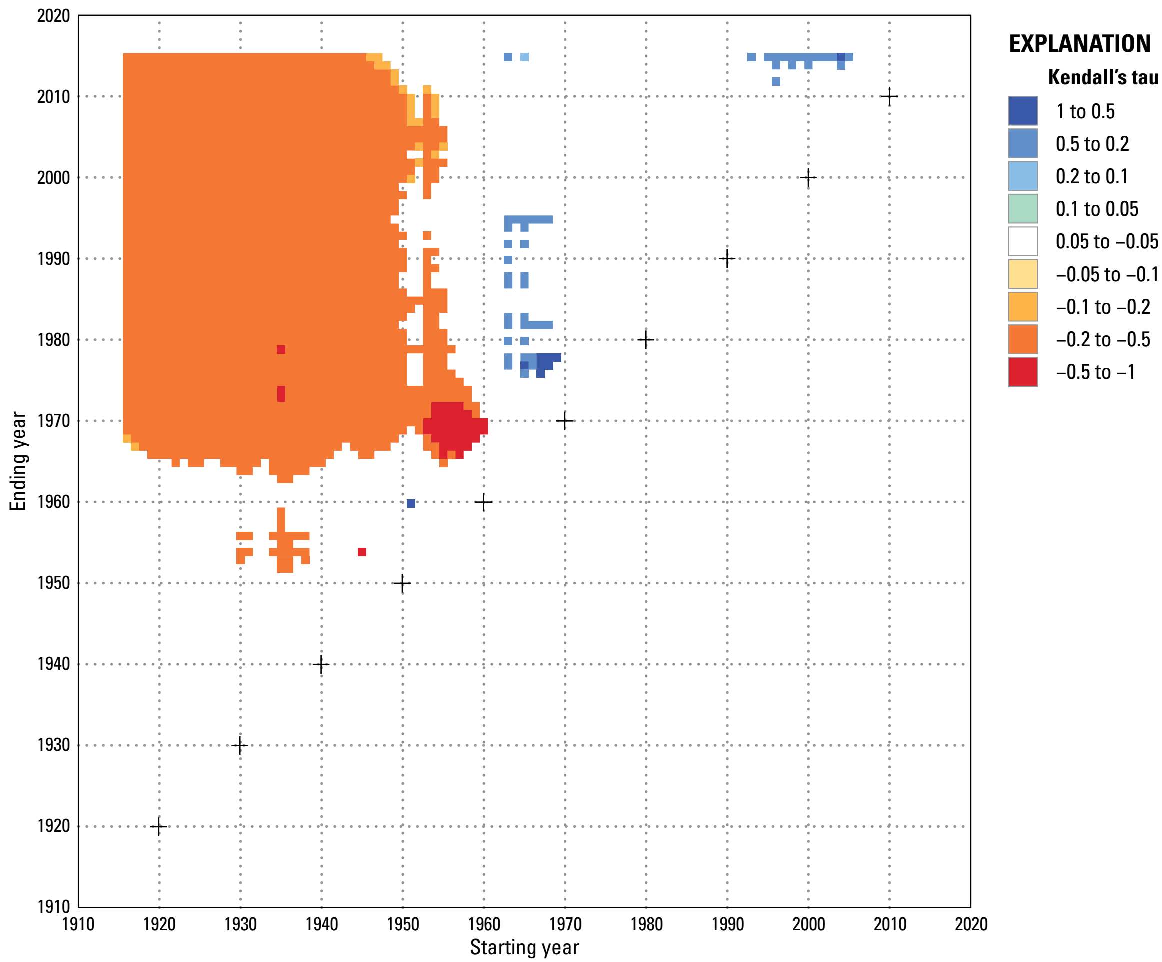

Figure G4. Flag plot from the Mann-Kendall test showing the resulting Kendall's tau values as measures of detected monotonic trends in annual peak streamflows with time at U.S. Geological Survey streamgage 08136000, located at Concho River at San Angelo, Texas. Positive Kendall's tau values indicate increasing peak streamflow with time; the higher the Kendall's tau value (darker shades of blue) the stronger the relation. Negative Kendall's tau values indicate decreasing peak streamflow with time; the lower the Kendall's tau value (bright orange to dark red) the stronger the relation. Each Kendall's tau value represents a unique starting to ending water year combination (n=10,000) for the 100-year period of record for each streamgage. Some data plotted in the figure are before water year 1941 (see "Supplemental Information" in the front matter for further details). Figure from Konrad and York (2022; file "FlagPlots_Trends.zip").

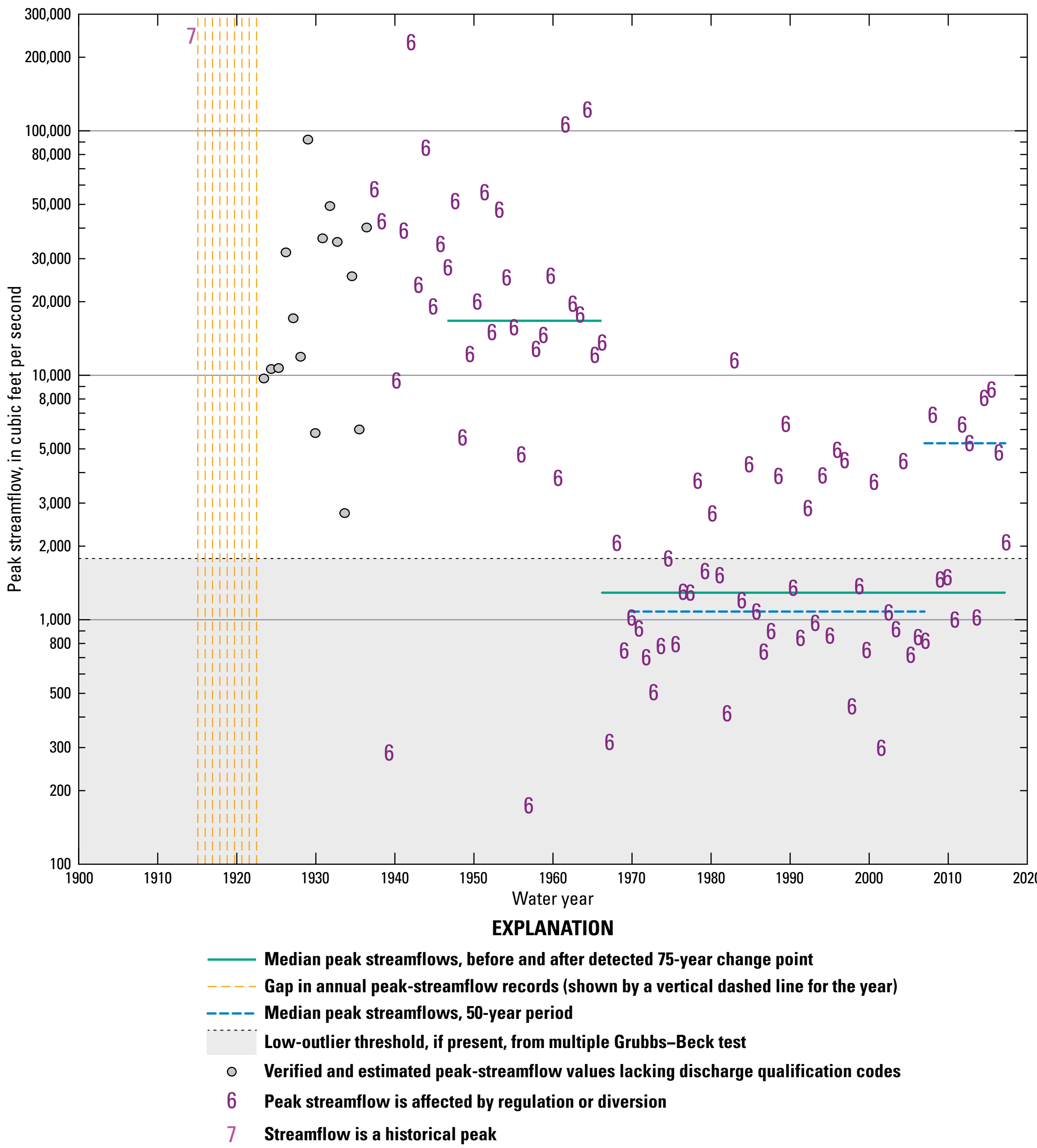

Figure G5. Diagram showing the relation between annual peak streamflow (peak discharge) and water year for U.S. Geological Survey streamgage 08136000, located at Concho River at San Angelo, Texas. The diagram helps visualize the changes in annual peak streamflow with time and helps compare the temporal patterns and groups of the peak streamflows with the results of the monotonic trend analysis. Note that the streamgage station history indicates regulation starting in 1931 but the data files show regulation started in the late 1930s. The visualization of record gaps and the placement of qualification codes (6 and 7) are from the “plotPeakCodes()” function from the MGBT package by Asquith and others (2019) in the R language (R Core Team, 2019). Some data plotted in the figure are before water year 1941 (see “Supplemental Information” in the front matter for further details). Figure modified from Asquith and others (2022a, file Vispk_code.zip); similar diagrams for other streamgages are also available in Asquith and others (2022a). MGBT, multiple Grubbs-Beck test.

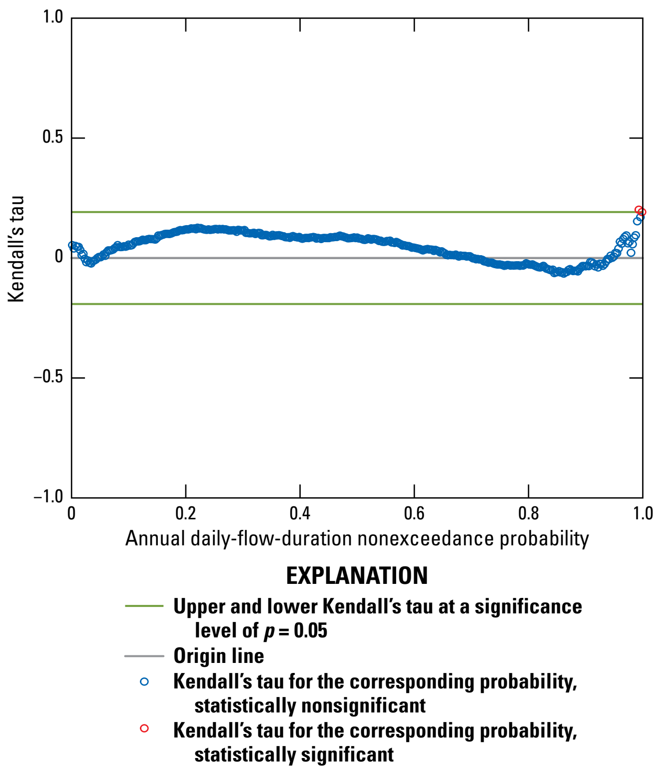

Figure G6. Quantile-Kendall plot for water years 1966–2017 (includes the 50-year period) at U.S. Geological Survey streamgage 08316000, located at Concho River at San Angelo, Texas. Almost the entire streamflow regime for the 50-year period has nonsignificant Kendall's tau values (*p*-value>0.05, blue circles), with most being positive (indicating nonsignificant positive trends). The uppermost Kendall's tau values (red circles), however, are considered statistically significant (*p*-value<0.05). The horizontal axis is the annual daily-flow-duration nonexceedance probability for daily-streamflow (with daily streamflow values increasing to the right) and the vertical axis is the corresponding Kendall's tau value for a given nonexceedance probability. The green horizontal lines (above and below the origin line) differentiate between significant and nonsignificant Kendall's tau values at a significance level *p*-value<0.05. Data plotted are for water years 1966–2017 (52 total years) with 2 years shown after water year 2015 (see "Supplemental Information" in the front matter for further details). Data from U.S. Geological Survey National Water Information System (U.S. Geological Survey, 2019).

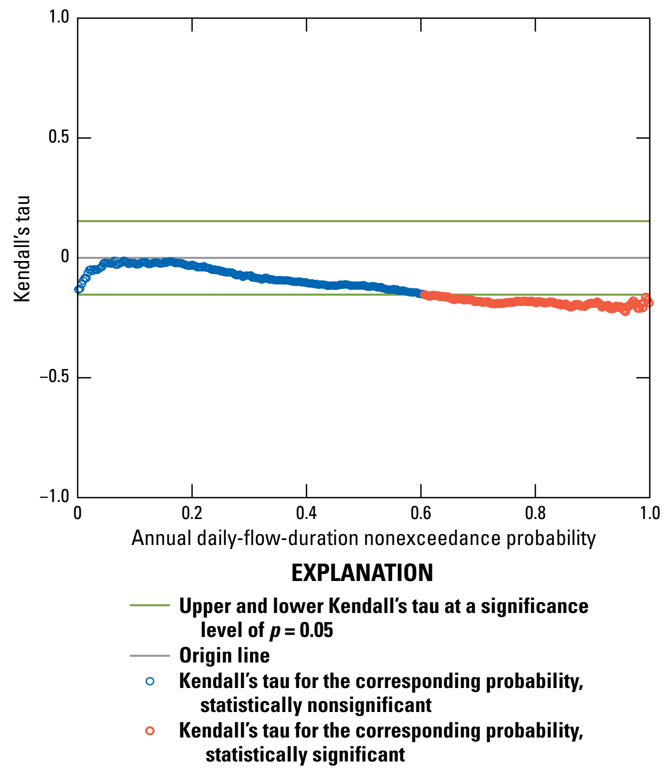

Figure G7. Quantile-Kendall plot for water years 1941–2017 (includes the 75-year period) at U.S. Geological Survey streamgage 08136000, located at Concho River at San Angelo, Texas. For this period, the entire streamflow regime has negative Kendall's tau values (indicating a negative monotonic trend), with approximately 40 percent of the streamflow regime considered statistically significant (*p*-value<0.05). The horizontal axis is the annual daily-flow-duration nonexceedance probability for daily-streamflow (with daily streamflow values increasing to the right) and the vertical axis is the corresponding Kendall's tau value for a given nonexceedance probability. The green horizontal lines (above and below the origin line) differentiate between significant and nonsignificant Kendall's tau values at a significance level *p*-value<0.05. Data plotted are for water years 1941–2017 (77 total years) with 2 years shown after water year 2015 (see "Supplemental Information" in the front matter for further details). Data from U.S. Geological Survey National Water Information System (U.S. Geological Survey, 2019).

Evaluation of Attributions

Climatological and Meteorological Attributions

Review of precipitation is beneficial because precipitation, in large part, generates peak streamflow, with the limitation that only monthly precipitation associated with the month of the peak streamflow is analyzed and not individual storm precipitation. Whereas the use of monthly data implicitly prevents investigating the effects of individual storm events on peak streamflow, it does facilitate a review of general climatological factors in relation to peak streamflow. As a result of using monthly precipitation data, there is no available measure of antecedent moisture in the watersheds in this study. Consultation of the Palmer Drought Severity Index (PDSI) complemented the review of precipitation because the PDSI is a measure of precipitation deficit or abundance and, therefore, includes antecedent moisture. Abundant antecedent moisture in the watershed that is monitored by a given streamgage is expected to result in greater peak streamflow for a given precipitation input than drier antecedent conditions. Finally, changes in temperature could influence the PDSI and may be in turn related to changes in precipitation patterns. Correlations between annual peak streamflow and air temperature changes were also evaluated for these reasons.

Determining climatological and meteorological attributions relied on a two-step process. The first step was to use the Mann-Kendall test to check for monotonic trends in each of the three climatological and meteorological datasets used in the study (monthly precipitation, PDSI, and monthly temperature) that matched the direction of trends detected in peak streamflow. If there was no trend detected, or if there was a trend but it was not in the same direction (positive or negative) as the detected trend or change point in peak streamflow, then the analysis ended. If a trend was detected and it was in the same direction (positive or negative) as the detected trend or change point in peak streamflow, the second step was to check that the climatological and (or) meteorological data were correlated with peak streamflow (as measured by the calculated Kendall's tau values using the Mann-Kendall test). If there was no correlation, even if the trend in climatological or meteorological data supported the detected monotonic trend or change point in peak streamflow, then neither long-term precipitation nor air temperature were assigned as attributions.

Long-Term Precipitation Attribution

The long-term precipitation attribution was evaluated using (1) the monthly precipitation data for each NOAA climate division in the South-Central region, and (2) the PDSI. The basic steps for the approach included: (1) assigning each streamgage to a NOAA climate division based on geographical coordinates for the streamgage, (2) identifying the month and year of peak streamflow at each streamgage, and (3) pairing each peak streamflow with the corresponding monthly precipitation and PDSI from its assigned climate division for the 50- and 75-year periods.

Time-series scatterplots were then created of the monthly precipitation and PDSI associated with each annual peak (one monthly precipitation and one PDSI value per annual peak) by year for each streamgage. Peak streamflows were also plotted by year. Finally, the Mann-Kendall test was used to calculate the Kendall's tau values for each scatterplot as a measure of relative association of the monthly precipitation, PDSI, and peak streamflow with time. These plots, for which limited examples are presented in this section, are available from Asquith and others (2022b). The figure explanations in these time-series scatterplots encompass the description for thousands of such plots available from Asquith and others (2022b).

A useful example of the processing related to long-term precipitation analysis is using streamgage 08136000, located at Concho River at San Angelo, Texas (fig. G8). For this streamgage, the concurrent years of annual peak streamflow, monthly precipitation, and PDSI were the 75-year period (water years 1941–2015). Figures G8*A* to G8*C* show monthly precipitation, PDSI, and annual peak streamflow by year, respectively; and figures G8*D* and G8*E* show the relation between annual peak streamflow and the associated monthly precipitation and PDSI, respectively. Figures G8*D* and G8*E* are auxiliary to the time-series scatterplots in figures G8*A* to G8*C* because the former two figures depict the coupling strength between the monthly precipitation (fig. G8*A*) or PDSI (fig. G8*B*) and annual peak streamflow.

Precipitation associated with the month of each annual peak streamflow has a negative monotonic trend (shown as squares, fig. G8*A*), but the trend is statistically nonsignificant (shown as black, fig. G8*A*). The red plus symbols superimposed on the black squares indicate that there is a statistically significant relation between precipitation and annual peak streamflow.

Palmer Drought Severity index (PDSI) has a negative monotonic trend (shown as squares, fig. G8*B*), but the trend is statistically nonsignificant (shown as black, fig. G8*B*). The black squares are shown filled to indicate there is a relation between monthly precipitation and annual peak streamflow (fig. G8*E*) or a relation between the PDSI and annual peak streamflow (fig. G8*E*). The Kendall's tau value is 0.129 for monthly precipitation and annual peak streamflow (fig. G8*D*) and 0.107 for PDSI and annual peak streamflow (fig. G8*E*).

Annual peak streamflow has a statistically significant (shown as red, p-value<0.10, fig. G8*C*) negative monotonic trend (shown as squares, fig. G8*C*). This trend indicates that annual peak streamflows have been decreasing with time, whereas neither precipitation nor the PDSI show statistically significant (p-value<0.10) negative monotonic trends. It is useful in this type of data review to consider whether the value of Kendall's tau is positive or negative (whether it is less than or greater than zero). For streamgage 08136000, both monthly precipitation (fig. G8*D*) and the PDSI (fig. G8*E*) are positively correlated (shown with circles) with annual peak streamflow, but only the positive correlation of monthly precipitation and annual peak streamflow is statistically significant (shown as red, *p*-value<0.10, fig. G8*D*).

In the example, because neither monthly precipitation nor the PDSI showed statistically significant trends over time, the interpretation is that neither monthly precipitation nor the PDSI are primary attributions of the observed trend in peak streamflow. Conversely, if monthly precipitation and (or) the PDSI showed statistically significant trends in the same direction (positive or negative) as the trend in peak streamflow and were also significantly correlated with peak streamflow, monthly precipitation would have been identified as the attribution. If only one of the two variables showed statistically significant correlation, but the correlation was better with monthly precipitation, then precipitation was assigned as an attribution, but the evidence level is considered “limited” (table G1). If both variables showed statistically significant correlation, then the evidence level is considered as “medium” (table G1). Long-term precipitation was never an attribution assigned an evidence level of “robust.”

Although a direct metric of snowpack was not evaluated, the possibility of trends in snowpack affecting peak streamflow was indirectly evaluated by looking at the seasonal timing of peak streamflow for streamgages that had at least 25 percent of their headwaters in mountainous regions, particularly streamgages in northern New Mexico. If roughly half of all peak streamflows occurred during months associated with runoff from snowmelt (March–May) then the streamgage was noted as having peak streamflows affected by snowpack.

Air Temperature Attribution

Air temperature attribution was evaluated using the same methodology as long-term precipitation, using monthly temperature data from NOAA (National Oceanic and Atmospheric Administration, 2018). For streamgage 08136000, temperature does not show a statistically significant trend (*p*-value<0.10) or correlation to peak streamflow for the 75-year period during water years 1941–2015 (fig. G9). In the example in figure G9, air temperature is not interpreted as the primary driver of the monotonic trend in peak streamflow. If air temperature had a statistically significant trend (*p*-value<0.10) or correlation with peak streamflow, then it was assigned as a possible attribution.

Flood-Water or Erosion-Control Impoundments Attributions

Large Artificial Impoundments Attribution

In addition to the streamgage station descriptions and peak streamflows available from NWIS (U.S. Geological Survey, 2019), information in the GAGES-II and NID datasets were examined to determine the potential for peak streamflows to be affected by impoundments (Falcone, 2011; U.S. Army Corps of Engineers, 2019). To begin, a GIS was used to identify all dams within the watershed of each study streamgage in the NID database. Information available from the NID database includes the purpose of each dam (for example, flood control, water supply, or wildlife pond), construction date, impounded drainage area, and maximum storage capacity. Information gathered from the GAGES-II dataset included the number of dams and reservoir storage capacity (in megaliters per square kilometer) for the following years: 1939, 1949, 1959, 1969, 1979, 1989, and 2009 (fig. G10). Unfortunately, there is no reservoir storage capacity for the year 1999 provided in the GAGES-II dataset, but the year 2009 is included. The GAGES-II authors used what they termed an enhanced version of the NID dataset dating from 2009 to complete that field in their release data. These values are represented by the blue bars in figure G10 for streamgage 08136000, where the upper part of the figure (fig. G10*A*) shows reservoir (dam) storage capacity, and the lower part of the figure (fig. G10*B*) indicates the total number of dams. The gray and black boxplots represent decadal groupings of peak streamflow; where available peak-streamflow data for water years 1930–1939 coincide with the 1939 bar and the available peak-streamflow data for water years 1940–1949 coincide with the 1949 bar, and so on for 1959, 1969, 1979, and 1989. The peak streamflows (in cubic feet per second [log scale]) and year of dam storage capacity are shown for the watershed in figure G10*A*. Peak streamflows and total number of dams for the year are shown for the watershed in figure G10*B*.

Unlike the NOAA climatological data, no statistical analyses were performed when examining the impoundment data from the NID and GAGES-II data. Instead, this attribution relied on qualitative interpretation of (1) plots like the two shown in figure G10, (2) data compiled from the NID database, (3) streamgage-station analysis notes, and (4) manual inspection of aerial imagery within the watershed. In the case of streamgage 08136000 (fig. G10), there was a large increase in reservoir storage capacity between 1960 and 1970 but only a small increase in the number of dams, and this large increase coincides with the largest percentage decrease in decadal peak streamflow. The NID data show that the largest reservoir in the watershed, Twin Buttes, has a maximum storage capacity of 1,087,530 acre-feet (U.S. Army Corps of Engineers, 2019) and is located approximately 10 miles upstream from the streamgage. The second largest reservoir (O.C. Fisher Lake) in the watershed, has a storage capacity of 766,000 acre-feet and is located approximately 4 miles upstream from the streamgage. These reservoirs were built in 1962 and 1952, respectively, with the largest reservoir, Twin Buttes, having been built for flood-control purposes. These construction years are consistent with the decreases in decadal peak streamflow and the detected negative change points (fig. G5). Given these multiple lines of supporting evidence, large artificial impoundments was chosen as a primary attribution of the monotonic trend in peak streamflow with a robust level of evidence.

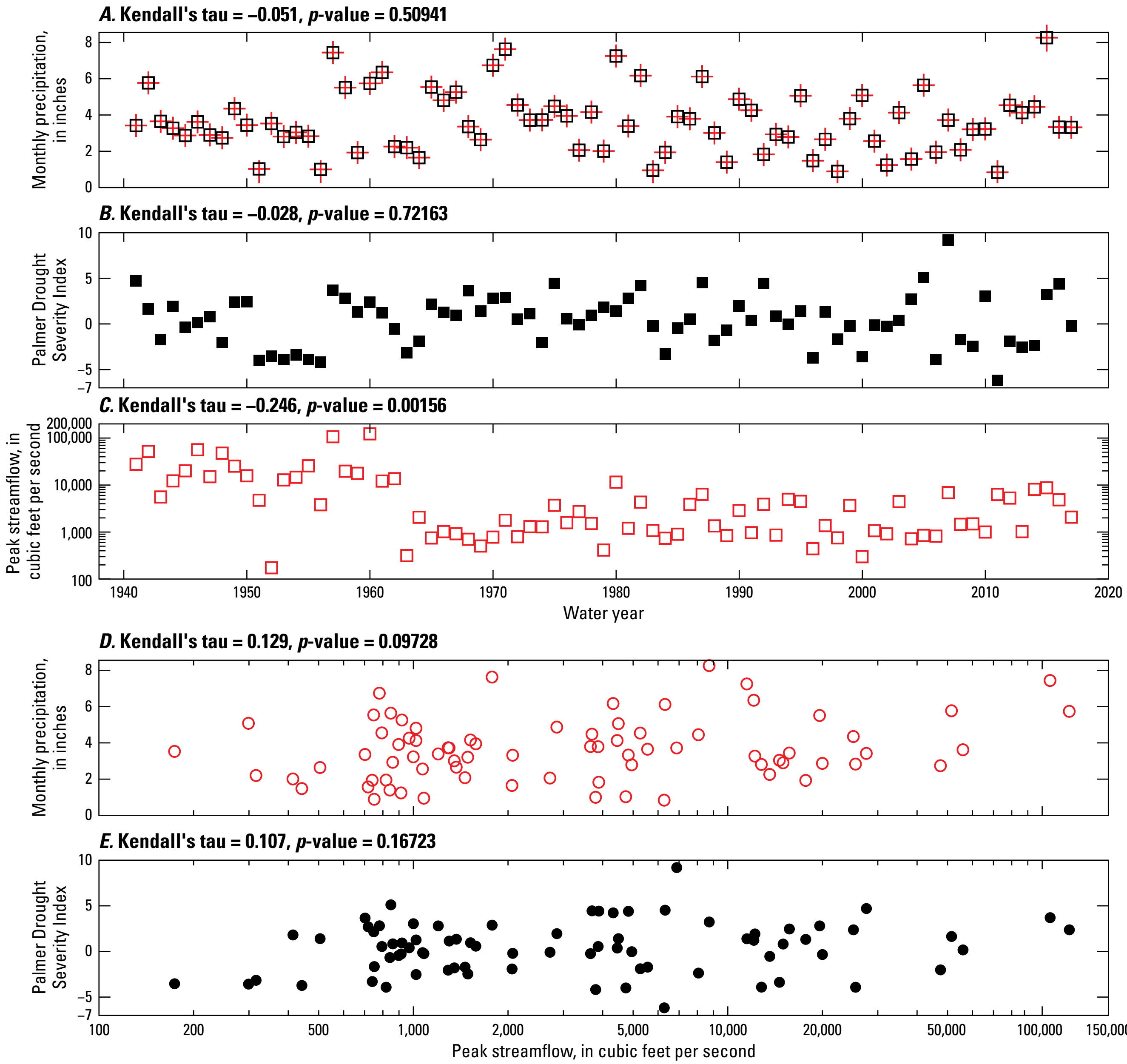

EXPLANATION

[Includes the complete color and symbol scheme from 6,640 similar visualizations in Asquith and others (2020b). Not all are present in fig. G8]

Color—Represents the statistical significance of applicable Kendall's tau

Red Statistically significant at the 0.10 level (*p*-value<0.10)

Black Statistically nonsignificant at the 0.10 level (*p*-value>0.10)

■ □ ■ □ **Monotonic trend negative (downward in magnitude; Kendall's tau<0)**

● ○ ● ○ **Monotonic trend positive (upward in magnitude; Kendall's tau>0)**

\+ **Kendall's tau *p*-value is <0.10 when the corresponding parameter of the vertical axis (precipitation or PDSI) is tested by Kendall's tau with annual peak streamflows**

Filled symbol—Implies that the corresponding parameter of the vertical axis, precipitation or PDSI, has the weaker coupling* to annual peak streamflow of the two parameters

Open symbol—Implies that the corresponding parameter of the vertical axis, precipitation or PDSI, has the stronger coupling* to annual peak streamflow of the two parameters

*Coupling is measured by Kendall's tau between the corresponding parameter of the vertical axis (precipitation or PDSI) and annual peak streamflow (horizontal axis). The parameter of lesser (closer to zero) Kendall's tau value is shown as filled symbols.

Small Artificial Impoundments Attribution

The construction of many small impoundments over a short period of time in a watershed can combine to effect changes in peak streamflow and was evaluated using similar boxplot analysis. Although, the total reservoir storage capacity in the watershed for streamgage 07141200 (fig. G11) is approximately an order of magnitude smaller than for streamgage 08136000 (fig. G10), located at Concho River at San Angelo, Texas, the number of dams in the watershed is approximately an order of magnitude greater. For the period available for analysis (pre-1940–2009), there is a decrease in decadal peak streamflow that coincides with a large increase in the number of dams installed from the 1960s to the 1980s, but reservoir storage capacity does not show the same increase. This decrease in peak streamflow is consistent with a statistically significant change point in water year 1974 that was detected in the peak-streamflow record using the Pettitt test. The NID data indicate that at least 58 of the dams within the contributing drainage area were constructed during this period, 30 of which with the purpose of flood control, and having a mean storage capacity of only 1,621 acre-feet. These data suggest small artificial impoundments as the attribution, however, the general central tendency of the peak streamflows and their interquartile range (pre-1940) is notably less than the period spanning the 1940s and 1950s and is in a period prior to an increase in dam infrastructure (fig. G11). Whether or not the depression in the peak streamflows during the 1930s is Dust Bowl related is a historical curiosity, but not germane to the purposes of this study. Small reservoirs was therefore noted as a possible attribution. The evidence level was assigned as “limited” because although the evidence supports a decrease in peak streamflow during the appropriate decade, there is nothing in the evidence that points particularly to water year 1974.

Water-Resources Development Attribution

The datasets used in the evaluation of water-resources development are qualitative only and used with limited confidence levels in identifying either groundwater or surface-water withdrawals as a primary driver of monotonic trends or change points. Conceptually, the gradual nature of withdrawals, in contrast to the known date of construction of a major flood-control reservoir, implies that withdrawals have more utility in attribution of a monotonic trend than for a change point.

However, the quantile-Kendall plots provide insight into changes with time in various flow regimes. If long-term withdrawals have removed enough groundwater and bank storage to affect peak streamflows, then it can be assumed that they would also affect other parts of the streamflow regime. Both groundwater and surface-water withdrawals were ruled out as factors if the streamgage had a positive monotonic trend or a positive change point in peak streamflow over time. However, if statistically significant (p-value<0.05) negative monotonic trends were evident in the low to middle ranges of the quantile-Kendall plots, then additional information was considered necessary to attribute monotonic trends to groundwater withdrawals. Statistical significance for the quantile-Kendall plots was based on a p-value<0.05 as opposed to the higher value used elsewhere in this chapter (statistical significance defined as p-value<0.10) because the serial correlation in the daily values in which the plots were based would suggest that stricter control (a higher value) should be used.

Figure G8 (facing page). Scatterplots showing the analysis results for U.S. Geological Survey streamgage 08136000, located at Concho River at San Angelo, Texas, for water years 1941–2017 (includes the 75-year period) using complex coloring and nomenclature schemes expressing data relations, Kendall’s tau values (negative or positive), and statistical significance. *A*, Relation between water year and monthly precipitation; same month and year as annual peak streamflow. *B*, Relation between water year and the Palmer Drought Severity Index (PDSI); same month and year as annual peak streamflow. *C*, Relation between water year and annual peak streamflow. *D*, Relation between annual peak streamflow and monthly precipitation for water years 1941–2017; same month and year as annual peak streamflow. *E*, relation between annual peak streamflow and the PDSI for water years 1941–2017; same month and year as annual peak streamflow. Monthly precipitation (*y*-axis in parts *A* and *D*) is the precipitation of the month in which annual peak streamflow occurred. The *x*-axis (water year) in part *C* is for parts *A*, *B*, and *C*; the *x*-axis in part *E* (peak streamflow) is for parts *D* and *E*. Data plotted are for water years 1941–2017 (77 total years) with 2 years shown after water year 2015 (see “Supplemental Information” in the front matter for further details). Monthly precipitation and PDSI data are from National Oceanic and Atmospheric Administration (2018), and annual peak-streamflow data are from USGS National Water Information System (U.S. Geological Survey, 2019).

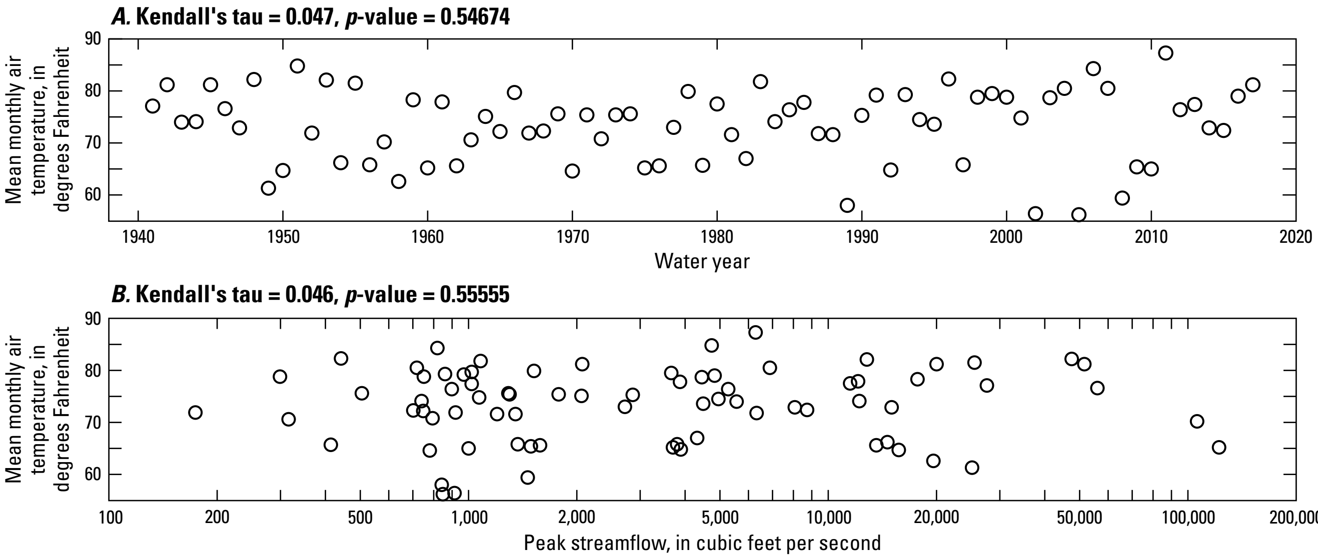

EXPLANATION

[Includes the complete color and symbol scheme from 2,256 similar visualizations in Asquith and others (2020b). Not all are present in fig. G9]

Color—Represents the statistical significance of applicable Kendall's tau

Red Statistically significant at the 0.10 level (*p*-value<0.10)

Black Statistically nonsignificant at the 0.10 level (*p*-value>0.10)

Monotonic trend negative (downward in magnitude; Kendall's tau<0)

Monotonic trend positive (upward in magnitude; Kendall's tau>0)

Kendall's tau *p*-value is <0.10 when the corresponding parameter of the vertical axis (precipitation or PDSI) is tested by Kendall's tau with annual peak streamflows

Figure G9. Scatterplots showing water year and annual peak streamflow versus mean monthly air temperature for U.S. Geological Survey streamgage 08136000, located at Concho River at San Angelo, Texas, for water years 1941–2017 (includes the 75-year period) using complex coloring and nomenclature schemes expressing data relations, Kendall's tau values (negative or positive), and statistical significance. *A*, Water year versus mean monthly air temperature; *B*, Peak streamflow versus mean monthly air temperature. Mean monthly air temperature is associated with the month of peak streamflow. Data plotted are for water years 1941–2017 (77 total years) with 2 years shown after water year 2015 (see "Supplemental Information" in the front matter for further details). The monthly air temperature data are from National Oceanic and Atmospheric Administration (2018). Annual peak-streamflow data are from USGS National Water Information System (U.S. Geological Survey, 2019).

Groundwater Withdrawals Attribution

The potential for groundwater withdrawals to affect peak streamflow in each watershed was evaluated using several methods. First, the streamgage station descriptions were examined for any mention of groundwater withdrawals in the watershed. Second, aerial imagery was examined for central pivot irrigation in the watershed. Third, watershed boundaries were investigated for correlation with mapped areas of groundwater decline in the High Plains aquifer (McGuire, 2014). Finally, if the lowest 20–30 percent of the quantile-Kendall plots did not show any statistically significant negative trends, then groundwater withdrawals were ruled out as an attribution. Despite limited evidence, groundwater withdrawals were occasionally attributed as the primary driver of decreasing peak streamflow if (1) the contributing drainage area of the streamgage was located in an area of persistent regional groundwater decline as determined by McGuire (2014), (2) the streamgage had a negative monotonic trend in the low flow regime, and (3) no other attributions were determined to be viable.

Surface-Water Withdrawals Attribution

Attributions of trends in peak streamflow of surface-water withdrawals were evaluated using both notes from the streamgage station descriptions and aerial imagery to determine the presence of canals and ditches that divert flow from streams. For example, surface-water withdrawals were attributed as a driver of trends in peak streamflow for streamgage 08144500, located at San Saba River at Menard, Texas, because a canal that diverts water around the streamgage (through the town of Menard) was clearly visible in aerial imagery. Additionally, if the midrange part of the streamflow regime (20–70 percent nonexceedance probability in the quantile-Kendall plots) did not show statistically significant negative trends, then surface-water withdrawals were ruled out as a possible attribution, because surface-water withdrawals would likely affect other parts of the flow regime in addition to peak streamflow.

Wastewater and Water-Supply Discharges Attribution

Because most of the detected trends in peak streamflow in the South-Central region were negative, wastewater return flows was often immediately ruled out as a possible primary driver of trends in peak streamflow. Otherwise, the quantile-Kendall plots, streamgage station descriptions, land-cover data, and aerial imagery that were examined were of limited use in determining if artificial flows into the system were driving a positive trend in peak streamflow. In cases where positive trends in peak streamflow were detected, and it was noted in the streamgage station descriptions that (1) streamflows were affected by wastewater return flows, or (2) urban land use increased upstream of the streamgage, then wastewater and water-supply discharges were attributed as potential drivers of trends in peak streamflow.

Land-Use Attributions—Agricultural Crops Attribution, Grazing Activity Attribution, and Urban Effects Attribution

Land use in watersheds visually resides in both discrete or distinct types of the landscape, but land use also has a gradual component wherein the landscape gradually changes

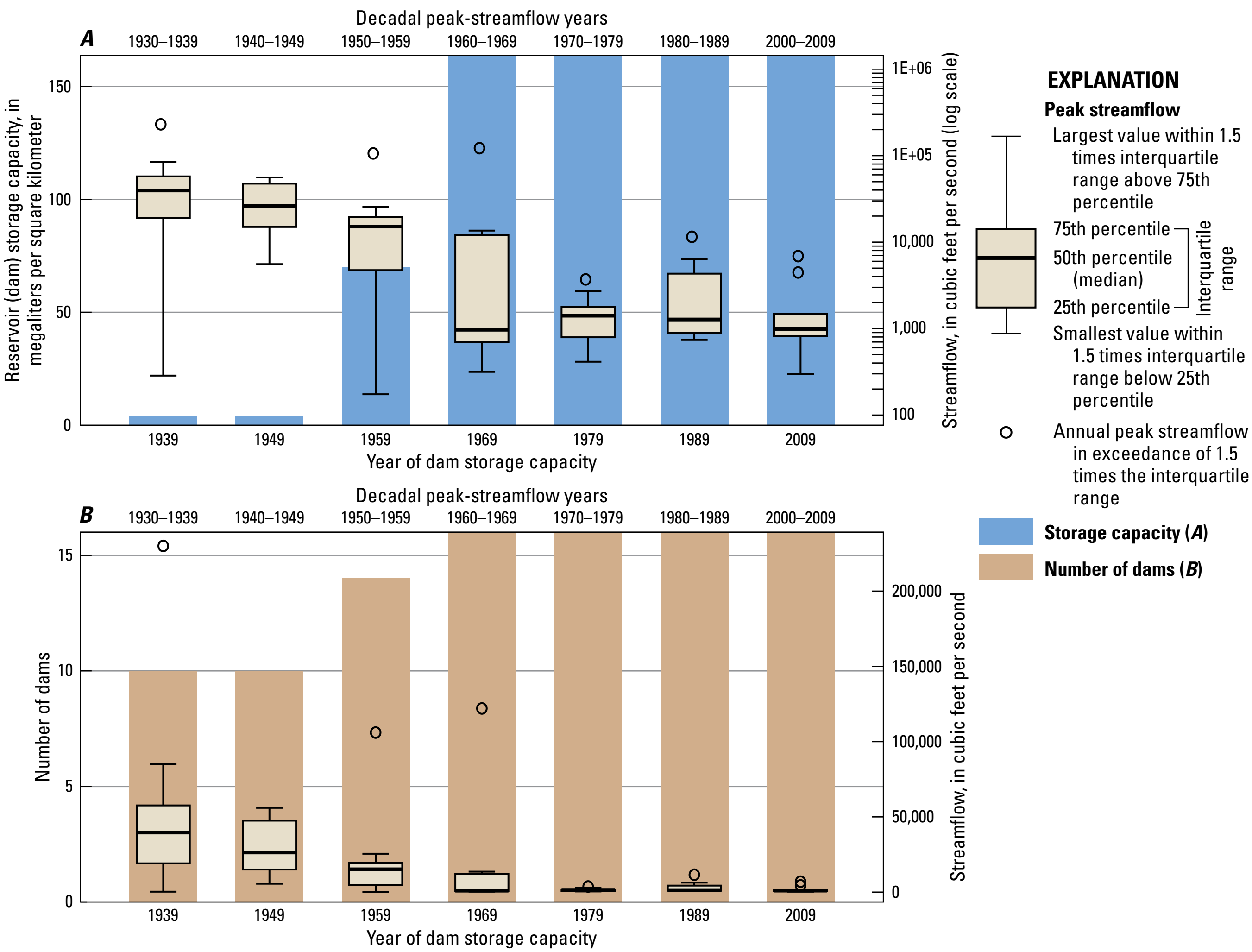

Figure G10. Boxplots of annual peak streamflow overlain with columns showing *A*, reservoir (dam) storage capacity (blue columns), and *B*, total number of dams (light-brown columns) in the watershed for U.S. Geological Survey streamgage 08136000, located at Concho River at San Angelo, Texas. The plots illustrate the large increase in reservoir storage capacity between 1960 and 1970, with only a small increase in the number of dams, and an increase in storage capacity coinciding with the largest percentage decrease in decadal peak streamflow. The boxplots represent decadal groupings of peak streamflow. Data included in the plots for water years 1930–1940 are before water year 1941 (see "Supplemental Information" in the front matter for further details). The dam storage capacity is from the NID database (U.S. Army Corps of Engineers, 2019). The number of dams is from the GAGES-II dataset (Falcone, 2011). No data are available for 1990–1999. GAGES-II, Geospatial Attributes of Gages for Evaluating Streamflow, Version II; NID, National Inventory of Dams.

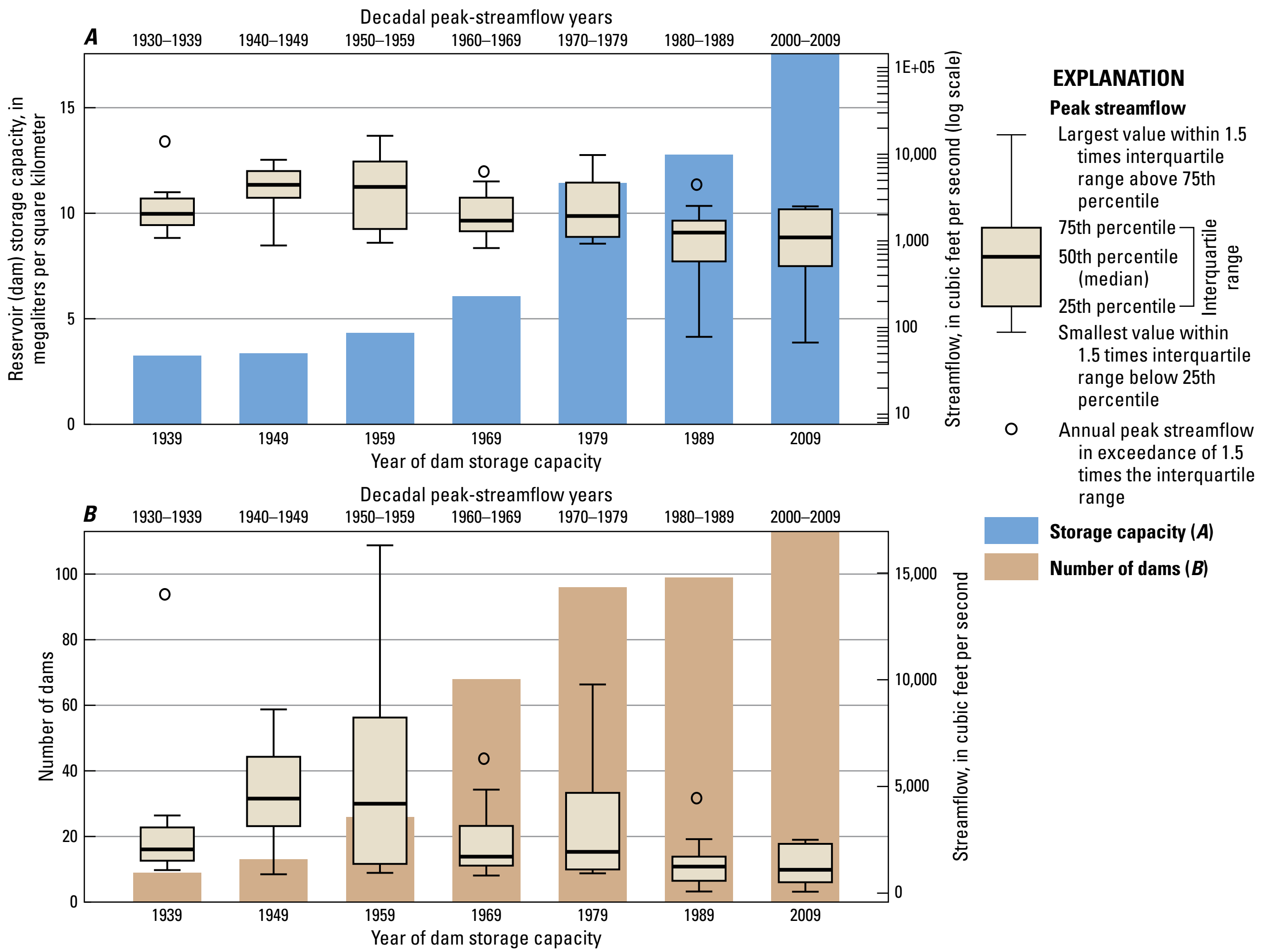

Figure G11. Boxplots of annual peak streamflow overlain with columns showing *A*, reservoir (dam) storage capacity (blue columns), and *B*, total number of dams (light-brown columns) in the watershed for U.S. Geological Survey streamgage 07141200, located at Pawnee River at Rozel, Kansas. The plots indicate that the decrease in decadal peak streamflow coincides with a large increase in the number of dams installed from the 1960s to the 1980s, but reservoir storage capacity does not show the same increase. This decrease in peak streamflow is consistent with a statistically significant change point in water year 1974 that was detected in the peak-streamflow record using the Pettitt test (Pettitt, 1979). The boxplots represent decadal groupings of peak streamflow. Data included in the plots for water years 1930–1940 are before water year 1941 (see “Supplemental Information” in the front matter for further details). The dam storage capacity is from the NID database (U.S. Army Corps of Engineers, 2019). The number of dams is from the GAGES-II dataset (Falcone, 2011). No data are available for 1990–1999. GAGES-II, Geospatial Attributes of Gages for Evaluating Streamflow, Version II; NID, National Inventory of Dams.

from one type to another. The terrain has an obvious role in the types of land-use patterns that are plausible. For this study, “land-use attributions” is a term encompassing several aggregated lumped classifications described in this section.

Similar to the impoundments, trends in land use were investigated through the use of peak streamflow shown as boxplots of the percentage of land use over time for each land-use category (fig. G12). Land-use data were obtained from the NWALT dataset, which provides geospatial raster data of land use for the years 1974, 1982, 1992, 2002, and 2012 (Falcone, 2015). The land-use “classes” from Falcone (2015) were grouped under three land-use categories for this chapter: (1) developed, (2) crops, and (3) pasture/hay/grazing (table G2). The “developed” category shows areas of urban development and is used for evaluating urban effects. The “crops” category is used in evaluating agricultural crops, and the “pasture/hay/grazing” category is used in evaluating grazing activity. The total percentage of the contributing drainage area of each streamgage in each category was determined for each year of the NWALT data. The percentages were then plotted with decadal peak streamflow (fig. G12).

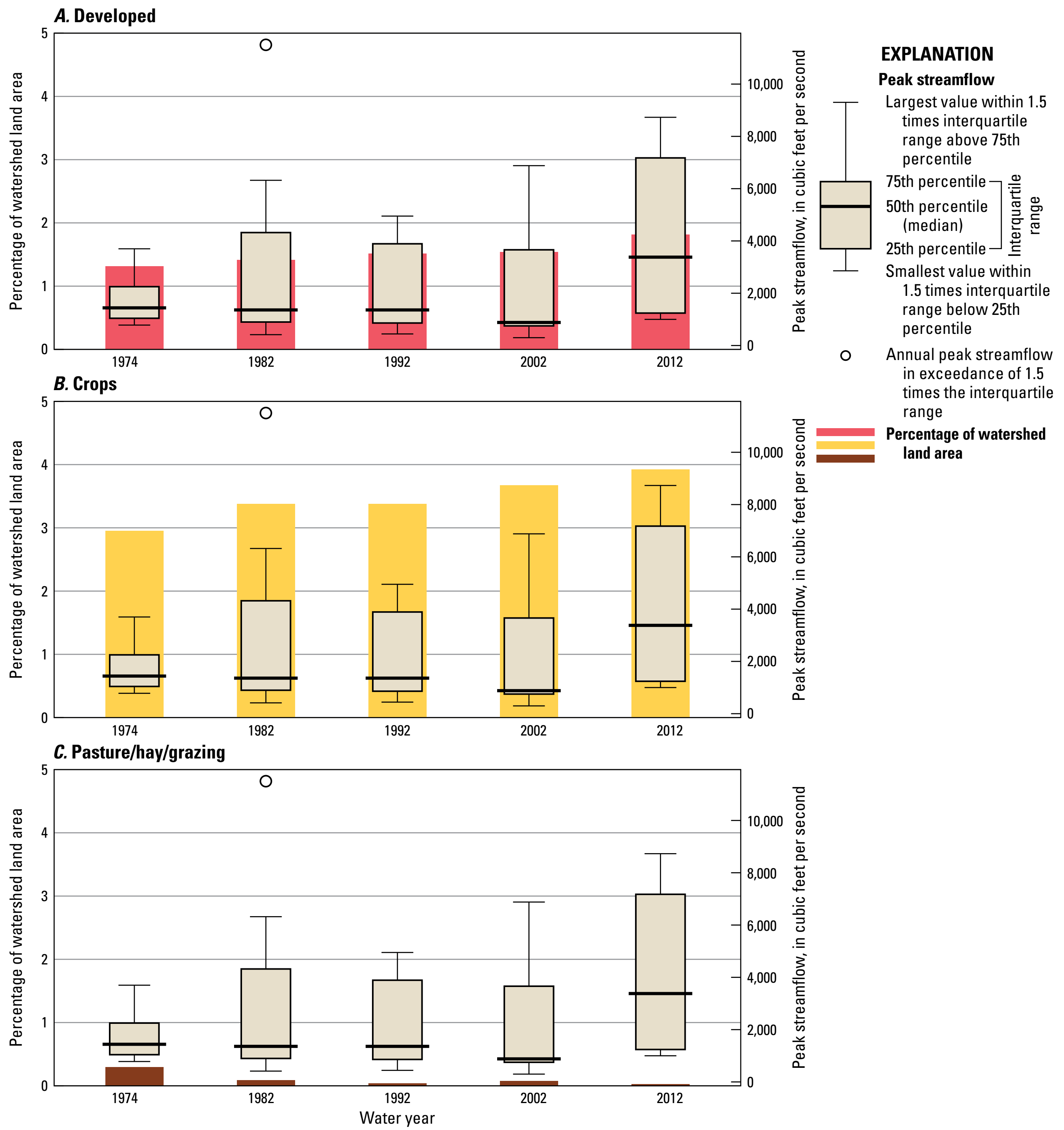

Figure G12. Boxplots of annual peak streamflow overlain with columns showing the percentage of watershed land area versus water year for land-use categories classified as *A*, developed; *B*, crops; and *C*, pasture/hay/grazing for U.S. Geological Survey streamgage 08136000, located at Concho River at San Angelo, Texas. The percentage of watershed land area is shown by the columns in parts *A*, *B*, and *C*. In this example, the three land-use categories (developed, crops, pasture/hay/grazing) do not show trends or correlations with changes in decadal peak streamflow. The land-cover data are from the NWALT dataset (Falcone, 2015), which is limited to years 1974, 1982, 1992, 2002, and 2012. NWALT, National Water-Quality Assessment Program (NAWQA) Wall-to-Wall Anthropogenic Land Use Trends (dataset for the conterminous United States).

Table G2. Attribution land-use categories and their component NWALT land-cover classes and subclasses.

[NWALT class numbers, class names, and subclasses are from Falcone (2015). NWALT, National Water-Quality Assessment Program (NAWQA) Wall-to-Wall Anthropogenic Land Use Trends (dataset for the conterminous United States)]

Land-use categories in this chapter	NWALT land-cover class number, class name, and subclass
Developed	21: Developed—Major Transportation 22: Developed—Commercial/Services 23: Developed—Industrial/Military 24: Developed—Recreation 25: Developed—Residential, High Density 26: Developed—Residential, Low-Medium Density 27: Developed—Developed, Other 31: Semi-Developed—Urban Interface High 32: Semi-Developed—Urban Interface Low Medium 33: Semi-Developed—Anthropogenic Other
Crops	43: Production—Crops
Pasture/hay/grazing	44: Production—Pasture/Hay 45: Production—Grazing Potential

In the example from streamgage 08136000, the three land-use categories (developed, crops, pasture/hay/grazing) do not show trends or correlations with changes in decadal peak streamflow for the limited years (1974, 1982, 1992, 2002, and 2012) available in the NWALT dataset (fig. G12). Minimal land-use change for developed, crops, and pasture/hay/grazing was common for streamgages in the South-Central region, but this could be a function of the streamgage selection criteria for the trend analysis and the limited years years of NWALT data that were available. In the South-Central region, no monotonic trends or change points were attributed to trends in cropland or grazing area. However, the trend in the percentage of the watershed in developed land use was occasionally correlated with a trend in peak streamflow in this study. In these cases, urban effects were determined to be a possible attribution. An example of a streamgage where urban effects were determined to be a primary driver is at streamgage 08074500, located at Whiteoak Bayou at Houston, Texas (fig. G13). In this example, nearly the entire contributing drainage area is urbanized, developed land.

Unknown Attribution

On a site-specific basis, if consideration of all possible attributions did not produce semiquantitative or qualitative evidence for any of the potential drivers that were evaluated, then “unknown” was assigned as the attribution. The confidence level for the “unknown” attribution was always “additional information required.”

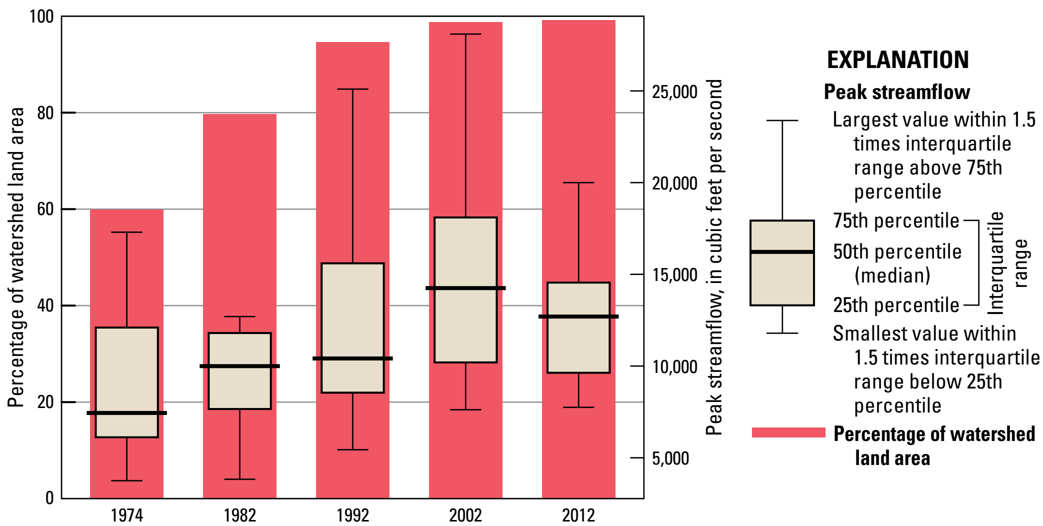

Figure G13. Boxplots of decadal peak streamflow overlain with columns showing the percentage of the watershed land area in the developed land-use category for U.S. Geological Survey streamgage 08074500, located at Whiteoak Bayou at Houston, Texas. This shows an example of a watershed with rapidly increasing development such that the increasing peak streamflows might be attributed to urbanization. The data are from the NWALT dataset (Falcone, 2015), which is limited to water years 1974, 1982, 1992, 2002, and 2012. NWALT, National Water-Quality Assessment Program (NAWQA) Wall-to-Wall Anthropogenic Land Use Trends (dataset for the conterminous United States).

Attribution of Monotonic Trends and Change Points in Peak Streamflow in the South-Central Region

The methods described in the previous sections were applied to each streamgage with a detected monotonic trend or change point. For each streamgage, observations from the various data sources were aggregated for final evaluation. After evaluation, a hydrologic judgment was used to determine the most likely candidate as the primary and (or) secondary driver of monotonic trends or change points in peak streamflow. If evidence suggested that two or more attributions could be affecting peak streamflow, the attribution with the strongest influence or correlation was chosen as the primary attribution and the remaining attribution was considered the secondary attribution. In many cases, it was not possible to determine a candidate and the attribution was left as “unknown” with the corresponding confidence level of “additional information required.”

Most of the attributions selected for this study showed gradual change with time, such as monthly precipitation, monthly temperature, and land-use categories. Certain water-resource development activities, such as groundwater withdrawals and surface-water diversions, do not cause instantaneous changes to peak streamflow, rather the changes develop over several years. For attribution of trends, it was sufficient to establish that a trend in an attribution was correlated with a trend in peak streamflow. However, a persistent trend in an attribution cannot explain an abrupt increase or decrease in peak streamflow as indicated by a change point. For attribution of drivers of change points, the confidence level of “robust” was only used when something dramatic occurred, such as a dam or dams being completed within a few years of a detected change point. In particular, for attributions assigned to change points, a confidence level of “limited evidence” was used when attributions showed trends consistent with the direction of a change point but there was no evidence indicating the year the change point occurred. The confidence level “medium evidence” was assigned if two or more lines of evidence explained the direction of the change but there was no evidence indicating the year the change point occurred.

Detected Monotonic Trends and Change Points

A generalized summary of the results of the monotonic trend and change-point analysis (Dudley and others, 2018; Hodgkins and others, 2019) for the South-Central region is listed in table G3. For both the 50- and 75-year periods, there were more monotonic trends detected than change points. No analysis was done as a part of this study to evaluate how often the monotonic trends and change points were correlated at each streamgage. Similarly, no analysis was done to evaluate how often the trends in the 50- and 75-year periods agreed in terms of direction (positive or negative) or how often the change points in the 50- and 75-year periods were in agreement at each streamgage. For both periods, there were far more negative monotonic trends and change points detected (indicative of floods becoming smaller [decreasing] in magnitude through time) than positive monotonic trends or positive change points (indicative of floods becoming larger [increasing] in magnitude through time). For each period, the range and the average percent change were calculated for streamgages with detected monotonic trends or change points, with an average percent change of −44 to −37 percent.

Negative monotonic trends or change points in streamflow are prevalent in the western and central parts of the South-Central region, from central New Mexico through central Texas, respectively (fig. G14). The majority of sites with no detected monotonic trends or change points are located in the eastern third of the South-Central region. Those sites in the eastern third of the South-Central region that did have detected streamflow monotonic trends or change points show a mix of positive and negative changes in peak streamflows with time.

Table G3. Summary of monotonic trends and change-point analyses for the South-Central region.

[The range of positive and negative change, in percent (%), is calculated only among those streamgages that have detected monotonic trends, and percent is expressed relative to the period of record analyzed and is calculated on the basis of the Sen slope (Sen, 1968); for additional information see Dudley and others (2018). Data from Dudley and others (2018). CP, change point; No., number]

Monotonic trend or change-point analysis	No. of streamgages analyzed	No. of streamgages with monotonic trend or CP	No. of streamgages with no monotonic trend or CP	No. of streamgages with positive monotonic trend or CP	Range of positive change, in %	No. of streamgages with negative monotonic trend or CP	Range of negative change, in %
Monotonic trend analysis							
50-year monotonic trends	332	100	232	14	33 to 716	86	−120 to −22.6
75-year monotonic trends	165	79	86	5	69.4 to 910	74	−119 to −21.8
Change-point analysis							
50-year change points	332	76	256	12	12.9 to 143	64	−99.88 to −17.39
75-year change points	165	73	92	6	39.6 to 358	67	−99.88 to −16.22

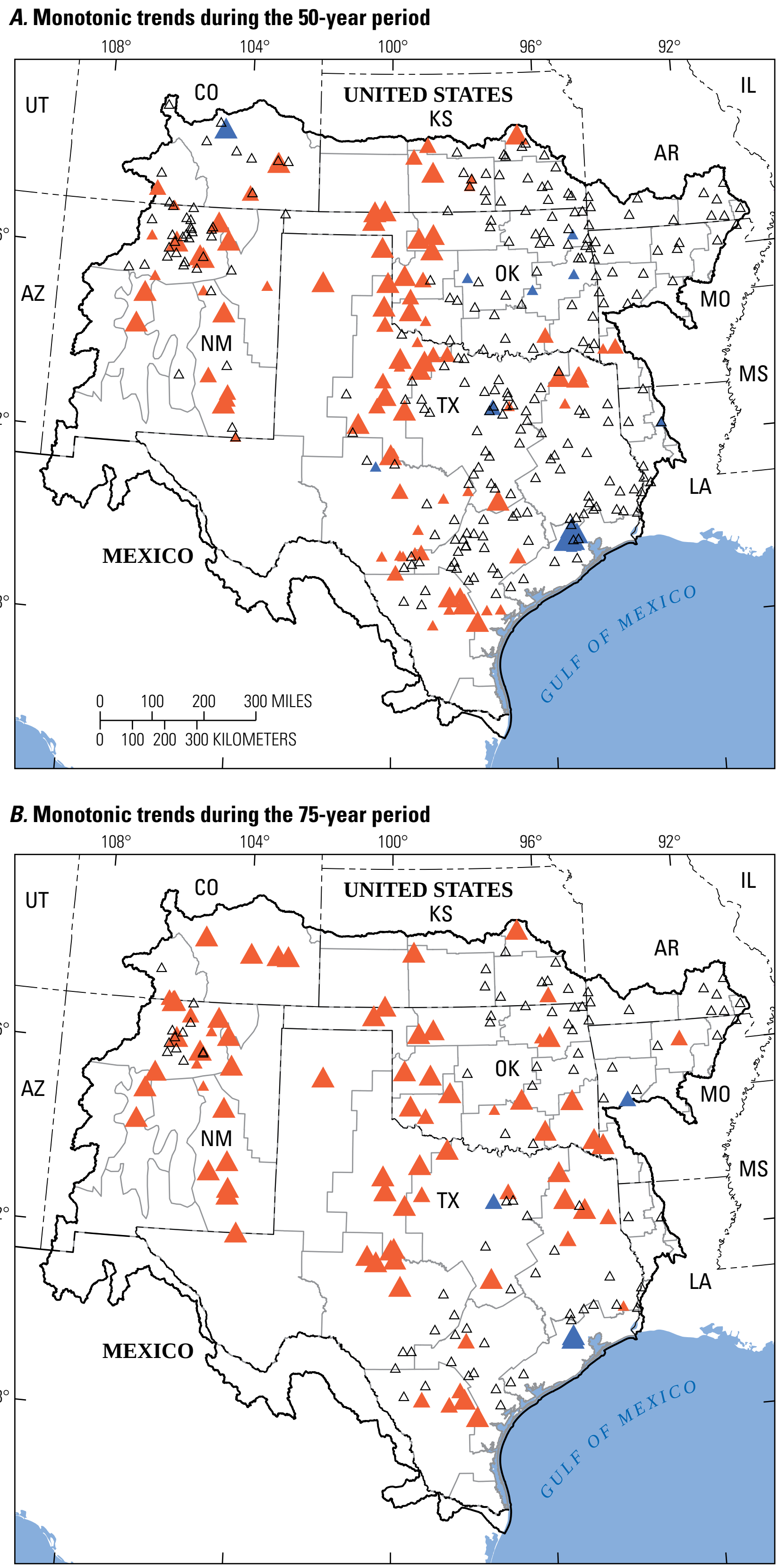

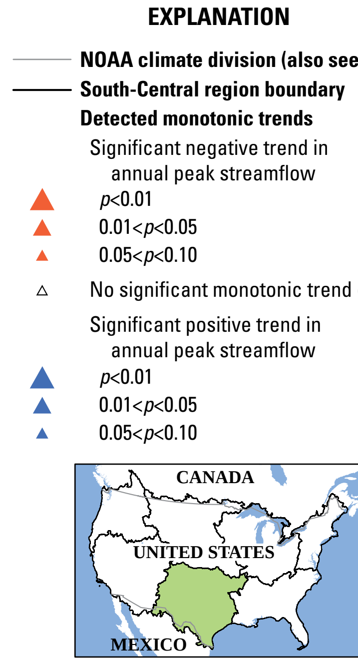

Base from U.S. Geological Survey and other digital data sources
and Esri © 2020 and its licensors
Regional boundaries derived from modified HUC2 watersheds
USA Contiguous Albers Equal Area Conic USGS projection
North American Datum of 1983

Figure G14. Maps showing streamgage locations in the South-Central region having *A*, statistically significant monotonic trends in annual peak streamflow during the 50-year period (water years 1966–2015); *B*, statistically significant monotonic trends in annual peak streamflow during the 75-year period (water years 1941–2015); *C*, statistically significant change points in annual peak streamflow during the 50-year period (water years 1966–2015); and *D*, statistically significant change points in annual peak streamflow during the 75-year period (water years 1941–2015). The orange triangles indicate statistically significant negative monotonic trends or change points; the blue triangles indicate statistically significant positive monotonic trends or change points; and the open triangles indicate no statistically significant monotonic trends or change points were detected. Size of the orange and blue triangles is reflective of the significance as determined by the *p*-value. The South-Central region boundary is based on watersheds identified by two-digit hydrologic unit codes (HUC2s) described by Seaber and others (1987). Streamgage locations shown are from the Geospatial Attributes of Gages for Evaluating Streamflow, Version II (GAGES-II) from Falcone (2011). The data are from NOAA (2019). NOAA, National Oceanic and Atmospheric Administration.

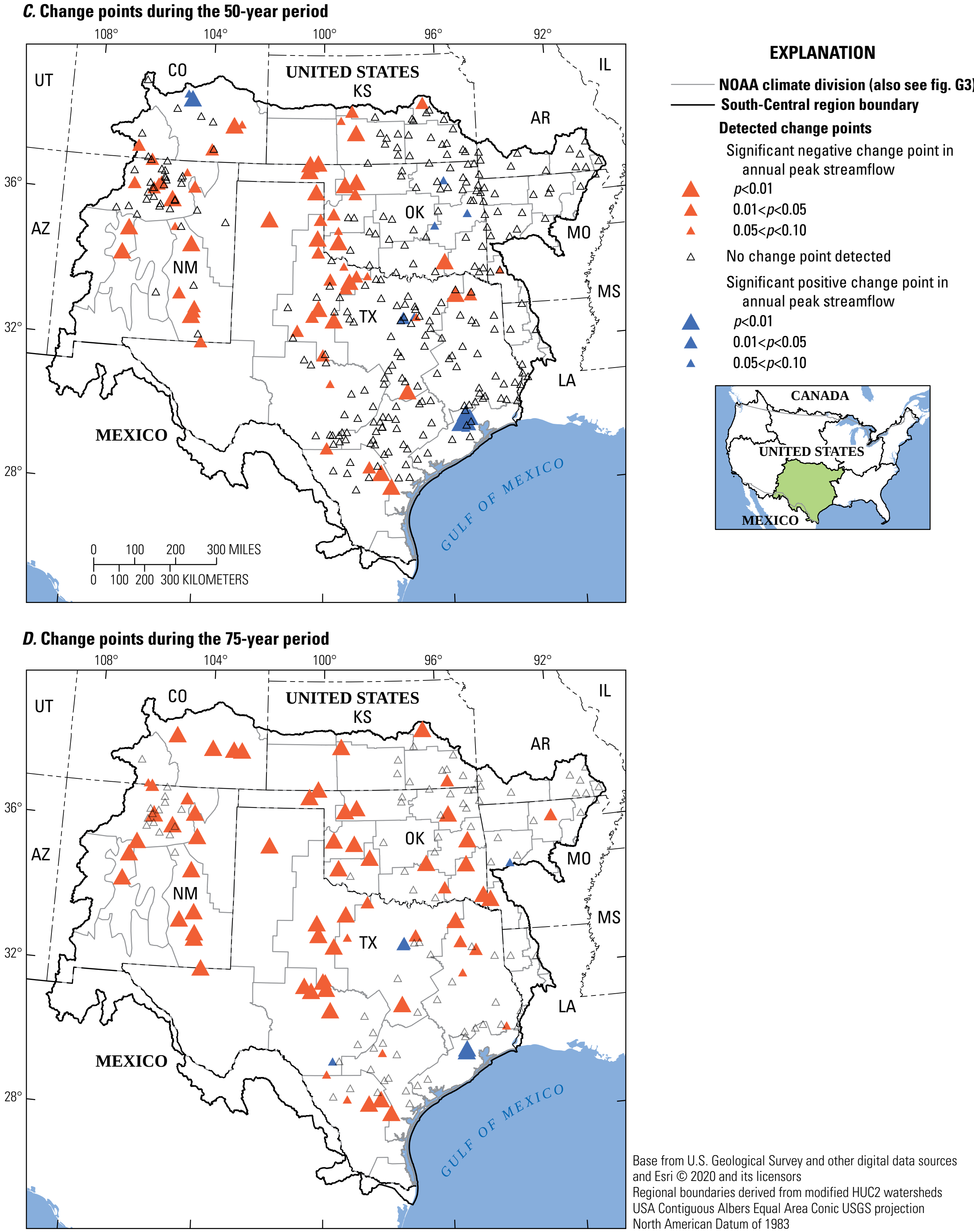

Figure G14. —Continued

Primary and Secondary Attribution Results

A summary of primary and secondary attributions for statistically significant monotonic trends or change points along with the confidence level and author-led annotations is provided by York and others (2022). Bar charts of the distribution of primary attributions of monotonic trends and change points corresponding to the 50-year and 75-year periods are shown in figure G15.

Despite the evaluation of 11 candidate attributions for monotonic trends and change points, only 8 were assigned to any of the streamgages (figs. G15, G16). Attributions assigned in the South-Central region included long-term precipitation, air temperature (secondary attribution only), large artificial impoundments, small artificial impoundments, groundwater withdrawals, surface-water withdrawals, urban effects, and unknown. Wastewater return flows, agricultural crops, and grazing activities were not assigned as either primary or secondary attributions to any monotonic trends or change points in the South-Central region.

Among the known attributions, large artificial impoundments was the primary attribution assigned most frequently throughout the region, particularly for negative monotonic trends and change points. Large artificial impoundments was the only attribution that was assigned with a robust evidence level for any of the detected monotonic trends or change points outside of a single instance where small artificial impoundments was assigned with a robust confidence level. For the few streamgages that had positive monotonic trends or change points (indicative of larger floods with time), the most frequently assigned attribution (other than unknown) was urban effects (a land-use attribution). Further, urban effects was never assigned as an attribution for a negative trend or change point.

For the 50-year period, 100 streamgages have statistically significant monotonic trends (14 positive and 86 negative). Large artificial impoundments was assigned as the primary attribution to 31 trends, with 16 at the robust confidence level, and as a secondary attribution to 2 trends. Outside of "unknown," other common attributions included: small artificial impoundments (12 trends as primary, 1 trend with robust evidence, and 2 trends as secondary), long-term precipitation (11 trends), and urban effects (8 trends). Groundwater withdrawals and surface-water withdrawals had 2 and 1 attributions, respectively, with surface-water withdrawals also assigned as a secondary attribution to 3 trends. The "unknown" attribution was assigned to 35 trends, 5 trends were interpreted as likely spurious (false) detections, and 13 trends were interpreted as possible spurious detections.

For the 75-year period, 79 streamgages have statistically significant monotonic trends, 5 positive and 74 negative. Similar to the 50-year period, large artificial impoundments was the most frequent attribution, assigned as a primary attribution to 39 trends (24 at the robust evidence level) and as a secondary attribution to 3 trends. Small artificial impoundments was assigned as the primary attribution to 7 monotonic trends and as a secondary attribution to 5 trends, with fewer attributions assigned to long-term precipitation (3 trends), urban effects (3 trends), and surface-water withdrawals (1 trend). "Unknown" was assigned as the attribution to 26 trends, and 2 trends were interpreted as possible spurious detections.

For the 50-year period, 76 streamgages had a statistically significant change point (12 positive and 64 negative). As with trends, the most frequently assigned known attribution was large artificial impoundments, which was chosen as a primary attribution for 21 change points (6 at the robust evidence level) and as a secondary attribution for 3 change points. Of the known attributions, long-term precipitation was the second most common primary attribution assigned for 12 change points (although never at the robust evidence level) and as a secondary attribution for 5 change points among known attributions. Less frequently assigned known attributions were urban effects (8 change points) and small artificial impoundments (7 primary and 4 secondary change points). Groundwater withdrawals and surface-water withdrawals were assigned as primary attributions to 4 and 2 change points, respectively, and as secondary attributions to 1 and 2 change points, respectively. The "unknown" attribution was assigned to 22 change points, and 4 change points were interpreted as being spurious detections.

For the 75-year period, 73 streamgages had a statistically significant change point (6 positive and 67 negative). Again, the most frequently assigned known attribution was large artificial impoundments, which was chosen as a primary attribution for 37 change points (22 at the robust evidence level) and as a secondary attribution for 1 change point. Small artificial impoundments was the second most common known primary attribution, assigned to 7 change points (although never at the robust evidence level) and assigned as a secondary attribution for 12 change points. Less common attributions included long-term precipitation (4 primary and 6 secondary change points) and urban effects (3 primary and 2 secondary change points). The "unknown" attribution was assigned to 22 change points, and 2 change points were interpreted as being spurious detections.

The detected change-point years (years when changes were identified) spanned the periods of analysis for both the 50- and 75-year periods (fig. G17), although a couple of years stand out. For the 50-year period, there were 11 change points detected in 1995. For the 75-year period, there were 7 change points detected in 1982. Five of the 11 change points for the 50-year period are in New Mexico and were attributed to long-term precipitation, although at the medium evidence level.

Discussion of Attribution Determinations

Although negative monotonic trends and negative change points in peak streamflows with time occurred more frequently than positive monotonic trends or positive change points in the South-Central region, the number of streamgages that showed no monotonic trends or change points outnumbered those

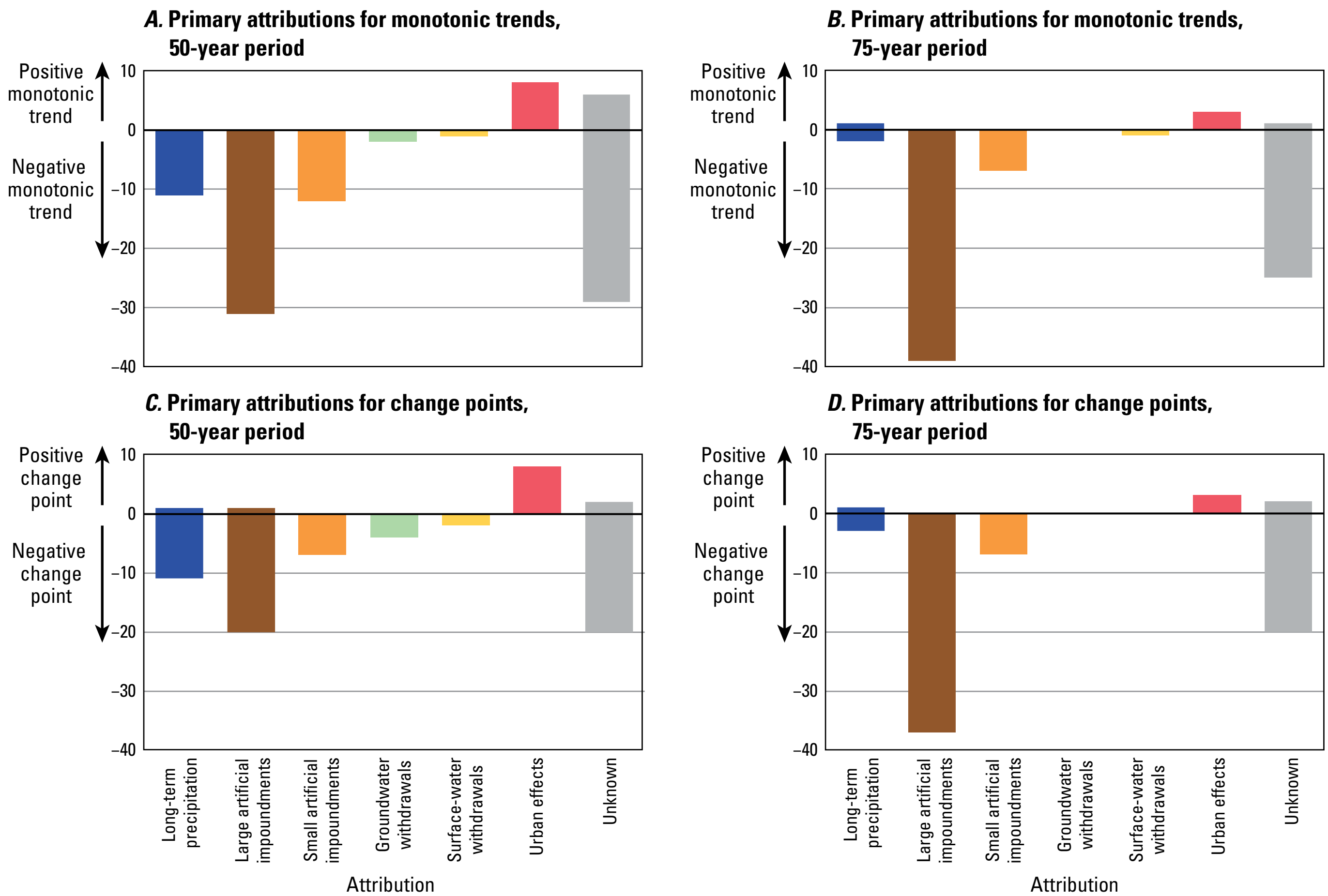

Figure G15. Bar graphs showing the distribution of primary attributions of monotonic trends and change points detected during the 50- and 75-year periods. *A*, Distribution of primary attributions of monotonic trends detected during the 50-year period (water years 1966–2015); *B*, Distribution of primary attributions of monotonic trends detected during the 75-year period (water years 1941–2015); *C*, Distribution of primary attributions of change points detected during the 50-year period (water years 1966–2015); and *D*, Distribution of primary attributions of change points detected during the 75-year period (water years 1941–2015). The lack of bars for some attributions in parts *B* and *D* means that those attributions were not assigned for the monotonic trends or change points indicated in those graphs. While air temperature was evaluated as an attribution for detected monotonic trends and change points, ultimately, it was not assigned as a primary attribution for any detected monotonic trends or change points. For this reason, air temperature is not present as a primary attribution in the figure. Data from York and others (2022).

having monotonic trends or change points. When attributions other than “unknown” were assigned in this region, most were associated with anthropogenic activity, such as large artificial impoundments, small artificial impoundments, and groundwater and surface-water withdrawals. The few positive monotonic trends and positive change points observed were generally attributed to urbanization. Although 11 attributions were considered for each monotonic trend or change point, only 7 (including unknown) were assigned as primary attributions.

It is generally logical that the construction of a large impoundment, particularly one designed for flood control, has a substantial effect on peak streamflow downstream of the impoundment. It is considerably more difficult to show a connection between peak streamflow and gradually changing characteristics of a watershed, such as long-term precipitation, air temperature, or groundwater withdrawals. It is not surprising, therefore, that a robust confidence level would be assigned when monotonic trends were attributed to large artificial impoundments, particularly in the case of change points when the construction and filling of a large artificial impoundment (upstream of the streamgage) can lead to a relatively abrupt change in peak streamflows.

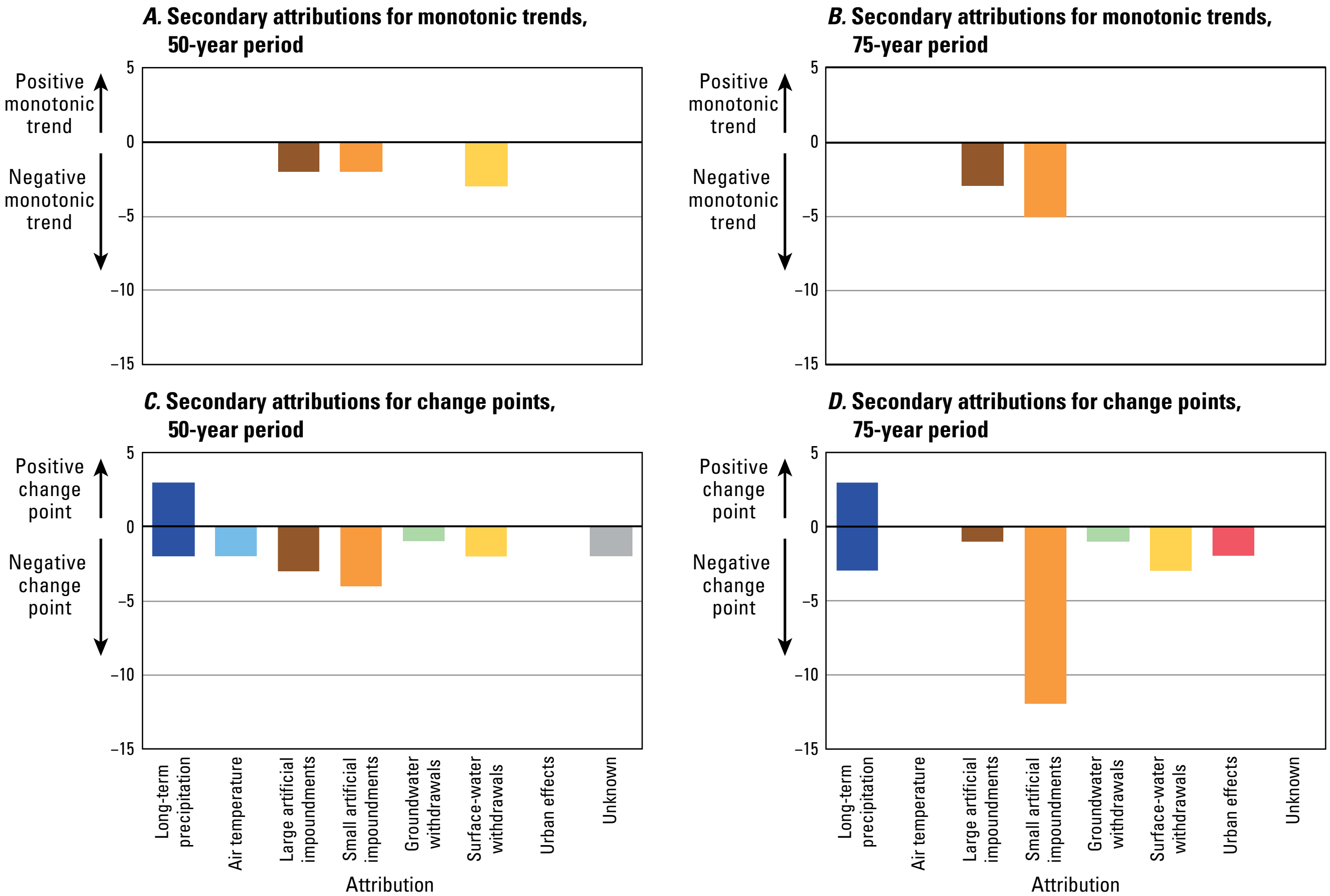

Figure G16. Bar graphs showing the distribution of secondary attributions of monotonic trends and change points detected during the 50- and 75-year periods. *A*, Distribution of secondary attributions of monotonic trends detected during the 50-year period (water years 1966–2015); *B*, Distribution of secondary attributions of monotonic trends detected during the 75-year period (water years 1941–2015); *C*, Distribution of secondary attributions of change points detected during the 50-year period (water years 1966–2015); and *D*, Distribution of secondary attributions of change points detected during the 75-year period (water years 1941–2015). The lack of bars for some attributions in parts *A*–*D* means that those attributions were not assigned for the monotonic trends or change points indicated in those graphs. Data from York and others (2022).

The hydrometeorological variability of the South-Central region makes it difficult to define a single primary driver of monotonic trends and change points in peak streamflow. It should be noted that the methodology presented here is an abstract approach to attributions of monotonic trends and change points in peak streamflow. Whereas, this level of analysis may be acceptable for large-scale regional analysis, attribution at the site-level scale warrants a more detailed review of the hydrometeorological setting.

The most frequently applied attribution, large artificial impoundments, is consistent with the number of negative monotonic trends in peak streamflow, negative change points, and large artificial impoundments in the South-Central region. This is also consistent with the lack of substantial relations between peak streamflow and monthly precipitation, which supports the hypothesis of large-scale decoupling of annual peak streamflow from climatic input. This decoupling seems counterintuitive at first, considering snowmelt and precipitation are generally the main surface-water inputs. However, the decoupling of peak streamflows from climatic input by large artificial impoundments was not specifically analyzed in this study.

When positive trends in peak streamflow were observed, they were usually in an urbanized watershed. This is expected because of the increased runoff in urban areas resulting from the substantial percentage of impervious surfaces and the rapid delivery of surface runoff to streams by drainage improvements, such as curbs and gutters.

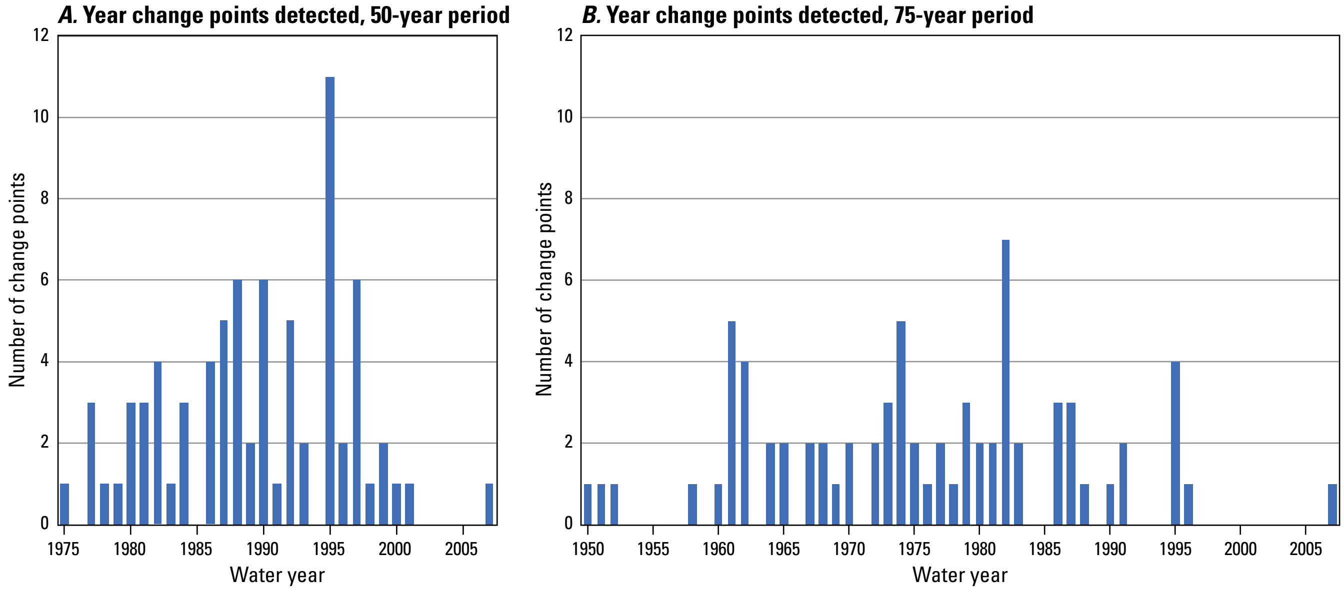

Figure G17. Histogram showing the years that change points were detected during the 50- and 75-year periods. *A*, Years that change points were detected during the 50-year period (water years 1966–2015). *B*, Years that change points were detected during the 75-year period (water years 1941–2015). The histograms include the years when change points were detected and do not show the entire 50- and 75-year periods (1941–2015). Data from Dudley and others (2018).

While the results of this study are realistic, they could also be biased by the types of data studied and the methods used to analyze them. For example, the methods used here did not test for the possibility that trends in peak streamflow were related to trends in snowpack, and several streamgages in the South-Central region have montane headwaters. Also, only monthly NOAA climate data for the climate region in which the streamgages reside were considered as drivers of trends in peak streamflow. However, many of the watersheds of the streamgages in the study span multiple climate regions. On the other hand, the monthly precipitation or temperature for an entire climate region might not be representative of that in a smaller watershed. Analyses including a metric of snowpack with precipitation and temperature data that is summarized by the watershed (rather than using averages calculated for a NOAA climate division) could provide enhanced assessments of the effects of climatic attributions on peak streamflow.

There are other limitations with the approach used in this chapter that could be improved upon. The low number of attributions related to groundwater and surface-water withdrawals could be a result of using quantile-Kendall plots to indirectly ascertain the impact of withdrawals. Although these plots allowed for a rapid assessment on a regional scale, these plots may not have provided conclusive evidence on their own, and their use would have been improved by using, where available, data on withdrawals obtained from water resource management agencies. Whereas the NWALT data provided convenient and useful geospatial layers for examining land-cover change over time, they only went as far back as 1974. This limited time frame constrained the usefulness of the NWALT data in ascertaining effects of land-cover change during the 75-year period. The station descriptions of streamgages stored as part of the NWIS dataset (U.S. Geological Survey, 2019) were useful in getting nuanced information about a streamgage history. The value that decades of record-keeping brings to a study like this is immense; however, the quality of the streamgage station descriptions varies considerably from streamgage to streamgage, with some streamgages having extensive notes concerning the history, whereas others have very few notes. Data quality was also variable in the NID dataset; some of the dams appeared to plot in the wrong location when comparing location coordinates with aerial imagery. In one case, the location of a reservoir was confirmed to be in the wrong watershed. Further, the maximum storage attribute in the NID dataset was often inconsistent with values in the GAGES-II dataset.

Finally, the methods used here heavily relied on a combination of statistical analysis, subjective interpretation of several datasets, and hydrologic judgement to determine the primary drivers of trends in peak streamflow. When the driver of a trend is a large reservoir regulating peak streamflow as measured at a streamgage, then it is a simple matter to have high confidence in attributing the observed trend to the reservoir. More nuanced relations between environmental factors, such as groundwater and surface-water withdrawals, and peak streamflow, were difficult to discern. In such cases, the relation was often unclear and therefore determined as having insufficient supporting evidence.

Summary

The U.S. Geological Survey (USGS) streamgaging network has monitored streamflow over many decades and in some cases exceeding a century. Annual peak-streamflow data for a wide variety of watersheds are available through the USGS National Water Information System (NWIS) (U.S. Geological Survey, 2019). Retrospective analysis of annual peak streamflows, through the identification of monotonic temporal trends in conjunction with change-point analysis, is useful to many water-resources stakeholders. The general history of changes in peak streamflow could be attributed to various possible causes, including anthropogenic modification of the landscape, water-resources development, and climate cycles and change.

Trends in peak streamflow potentially impact water-resources and infrastructure decisions. This study used a multiple working hypotheses framework to pursue a primary and secondary attribution for detected monotonic trends and change points in the annual peak streamflows of a population of streamgages. The periods of record that were analyzed were the 50-year period (water years 1966–2015) and the 75-year period (water years 1941–2015). In the South-Central region, there were 332 streamgages with 50 years or more of peak streamflows recorded, and 165 streamgages with 75 years or more of peak streamflows recorded. A statistical significance level of p=0.10 was used, and in this study, attribution of climatic or land-use factors to monotonic trends and change points is restricted to streamgages having p-values less than 0.10 for the respective statistical tests.

The monotonic trend test for the 50-year period resulted in 100 of 332 streamgages with statistically significant trends, leading to 100 primary attributions and 7 secondary attributions. When including “unknown” attributions, the largest number of primary attributions included unknown (35 primary attributions), large artificial impoundments (31 primary attributions), small artificial impoundments (12 primary attributions), and long-term precipitation (11 primary attributions). Eight positive trends were attributed to urban effects, which are contrary to the effects of regulation from reservoirs and impoundments.

For the 75-year period, the trend test resulted in 79 of 165 streamgages with statistically significant trends, leading to 79 primary attributions and 8 secondary attributions. The largest number of primary attributions included large artificial impoundments (39 primary attributions), unknown (26 primary attributions), small artificial impoundments (7 primary attributions), and long-term precipitation and urban effects (each included 3 primary attributions).

The change-point analysis for the 50-year period resulted in 76 streamgages with statistically significant change points, leading to 76 primary and 26 secondary attributions. Including “unknown” attributions, the largest number of primary attributions included unknown (22 primary attributions), large artificial impoundments (21 primary attributions), long-term precipitation (12 primary attributions), and urban effects (8 primary attributions).

The change-point analysis for the 75-year period resulted in 73 of 165 streamgages with statistically significant change points, leading to 73 primary and 25 secondary attributions. The distribution of primary attributions was similar to the 50-year period with large artificial impoundments (37 primary attributions), unknown (22 primary attributions), small artificial impoundments (7 primary attributions), and long-term precipitation (4 primary attributions) being the top four.

In the context of climate change, the analysis here is semi-quantitative. Statistical tests were used to quantify the monotonic trends and change points. Correlation of the limited climatic variables used with peak streamflows was quantitative. However, the climate variables considered were monthly precipitation and air temperature for the month a peak streamflow occurred, which may not exhibit effects of climate change. The Palmer Drought Severity Index represented an aggregate influence of precipitation and air temperature. For monotonic trends and change points, long-term precipitation was determined to be a primary attribution less often than large artificial impoundments, small artificial impoundments, and other unknown factors. Because of the seemingly clear attribution of monotonic trends and change points in peak streamflow to the physical impacts of anthropogenic factors such as large artificial impoundments, small artificial impoundments, and urban effects, the assessment of climatic impacts on peak streamflow would be difficult. Whether looking at systematic climate change or multidecadal climate variability, the effects of these anthropogenic factors would need to be removed prior to assessing climate as a cause of monotonic trends or change points in peak streamflow.

References Cited

Alley, W.M., 1984, The Palmer Drought Severity Index—Limitations and assumptions: Journal of Climate and Applied Meteorology, v. 23, no. 7, p. 1100–1109, accessed June 20, 2019, at https://doi.org/10.1175/1520-0450(1984)023<1100:TPDSIL>2.0.CO;2.

Asquith, W.H., 2001, Effects of regulation on L-moments of annual peak streamflow in Texas: U.S. Geological Survey Water-Resources Investigations Report 01–4243, 66 p., accessed June 24, 2021, at https://doi.org/10.3133/wri014243.

Asquith, W.H., and Barbie, D.L., 2014, Trend analysis and selected summary statistics of annual mean streamflow for 38 selected long-term U.S. Geological Survey streamgages in Texas, water years 1916–2012 (ver. 1.1, August 2014): U.S. Geological Survey Scientific Investigations Report 2013–5230, 16 p., accessed November 19, 2019, at https://doi.org/10.3133/sir20135230.

Asquith, W.H., Cleveland, T.G., Yesildirek, M.V., Zhang, J., Fang, Z.N., and Otto, L.D., 2021, scNIDaregis—Geospatial processing of dams in the United States from the National Inventory of Dams with a State-level aggregation scheme, demonstrated for selected dams in eight States in South-Central region of the United States, and post-processing features for basin-specific tabulation: U.S. Geological Survey software release, Reston, Va., accessed June 24, 2021, at https://doi.org/10.5066/P90NJVB9.

Asquith, W.H., England, J.F., and Herrmann, G.R., 2019, MGBT—Multiple Grubbs-Beck low-outlier test: U.S. Geological Survey software release, R package, ver. 1.0.2, accessed November 19, 2019, at https://doi.org/10.5066/P9CW9EF0.

Asquith, W.H., Harwell, G.R., and Winters, K.E., 2018, Annual and approximately quarterly series peak streamflow derived from interpretations of indirect measurements for a crest-stage gage network in Texas through water year 2015: U.S. Geological Survey Scientific Investigations Report 2018–5107, 24 p., accessed November 19, 2019, at https://doi.org/10.3133/sir20185107.

Asquith, W.H., and Heitmuller, F.T., 2008, Summary of annual mean and annual harmonic mean statistics of daily mean streamflow for 620 U.S. Geological Survey streamflow-gaging stations in Texas through water year 2007: U.S. Geological Survey Data Series 372, 1,259 p., accessed November 19, 2019, at https://doi.org/10.3133/ds372.

Asquith, W.H., Humberson, D.G., Tillery, A.C., and York, B.C., 2022b, Breed climate data, *in* York, B.C., Ryberg, K.R., Asquith, W.H., Chase, K.J., Dickinson, J.E., Dudley, R.W., Harden, T.M., Hodgkins, G.A., Holtschlag, D.J., Humberson, D.G., Konrad, C.P., Levin, S.B., Restivo, D.E., Sando, R., Sando, S.K., Swain, E.D., Tillery, A.C., and Totten, A.R., Attributions for nonstationary peak streamflow records across the conterminous United States, 1941–2015 and 1966–2015: U.S. Geological Survey data release, file breedClimate.zip, https://doi.org/10.5066/P9FOUVWG. [Data directly accessible at https://www.sciencebase.gov/catalog/item/5d8a4cfae4b0c4f70d0ae683.]

Asquith, W.H., Kiang, J.E., and Cohn, T.A., 2017, Application of at-site peak-streamflow frequency analyses for very low annual exceedance probabilities: U.S. Geological Survey Scientific Investigations Report 2017–5038, 93 p., accessed November 19, 2019, at https://doi.org/10.3133/sir20175038.

Asquith, W.H., and Roussel, M.C., 2009, Regression equations for estimation of annual peak-streamflow frequency for undeveloped watersheds in Texas using an L-moment-based, PRESS-minimized, residual-adjusted approach: U.S. Geological Survey Scientific Investigations Report 2009–5087, 48 p., accessed November 19, 2019, at https://doi.org/10.3133/sir20095087.

Asquith, W.H., and Slade, R.M., Jr., 1997, Regional equations for estimation of peak-streamflow frequency for natural basins in Texas: U.S. Geological Survey Water-Resources Investigations Report 96–4307, 68 p., 1 pl., accessed November 19, 2019, at https://doi.org/10.3133/wri964307.

Asquith, W.H., and Thompson, D.B., 2008, Alternative regression equations for estimation of annual peak-streamflow frequency for undeveloped watersheds in Texas using PRESS minimization: U.S. Geological Survey Scientific Investigations Report 2008–5084, 40 p., accessed November 19, 2019, at https://doi.org/10.3133/sir20085084.

Asquith, W.H., Tillery, A.C., and York, B.C., 2022a, Visual peak data, *in* York, B.C., Ryberg, K.R., Asquith, W.H., Chase, K.J., Dickinson, J.E., Dudley, R.W., Harden, T.M., Hodgkins, G.A., Holtschlag, D.J., Humberson, D.G., Konrad, C.P., Levin, S.B., Restivo, D.E., Sando, R., Sando, S.K., Swain, E.D., Tillery, A.C., and Totten, A.R., Attributions for nonstationary peak streamflow records across the conterminous United States, 1941–2015 and 1966–2015: U.S. Geological Survey data release, file VISpk.zip, https://doi.org/10.5066/P9FOUVWG. [Data directly accessible at https://www.sciencebase.gov/catalog/item/5d8a4ce9e4b0c4f70d0ae680.]

Asquith, W.H., Vrabel, J., and Roussel, M.C., 2007a, Summary of annual mean, maximum, minimum, and L-scale statistics of daily mean streamflow for 712 U.S. Geological Survey streamflow-gaging stations in Texas through 2003: U.S. Geological Survey Data Series 248, 721 p., accessed November 19, 2019, at https://doi.org/10.3133/ds248.

Asquith, W.H., Vrabel, J., and Roussel, M.C., 2007b, Summary of percentages of zero daily mean streamflow for 712 U.S. Geological Survey streamflow-gaging stations in Texas through 2003: U.S. Geological Survey Data Series 247, 721 p., accessed November 19, 2019, at https://doi.org/10.3133/ds247.

Bomar, G.W., 2017, Weather in Texas—The essential handbook (3d ed.): Austin, Tex., University of Texas Press, 290 p.

Brauer, D., Baumhardt, R.L., Gitz, D., Gowda, P., and Mahan, J., 2015, Characterization of trends in reservoir storage, streamflow, and precipitation in the Canadian River watershed in New Mexico and Texas: Lake and Reservoir Management, v. 31, no. 1, p. 64–79, accessed November 19, 2019, at https://doi.org/10.1080/10402381.2015.1006348.

Burnett, J., 2008, Flash floods in Texas: College Station, Tex., River Books, Texas A&M University Press, 330 p.

Carr, J.T., Jr., 1967, The climate and physiography of Texas: Texas Water Development Board Report 53, 27 p. [Also available at https://www.twdb.texas.gov/publications/reports/numbered_reports/doc/R53/R53.pdf.]

Dickinson, J.E., Harden, T.M., and McCabe, G.J., 2019, Seasonality of climatic drivers of flood variability in the conterminous United States: Scientific Reports, v. 9, article 15321, 10 p., accessed August 20, 2018, at https://doi.org/10.1038/s41598-019-51722-8.

Dudley, R.W., Archfield, S.A., Hodgkins, G.A., Renard, B., and Ryberg, K.R., 2018, Peak-streamflow trends and change-points and basin characteristics for 2,683 U.S. Geological Survey streamgages in the conterminous U.S. (ver. 3.0, April 2019): U.S. Geological Survey data release, accessed February 26, 2022, at https://doi.org/10.5066/P9AEGXY0.

England, J.F., Jr., Cohn, T.A., Faber, B.A., Stedinger, J.R., Thomas, W.O., Jr., Veilleux, A.G., Kiang, J.E., and Mason, R.R., Jr., 2018, Guidelines for determining flood flow frequency—Bulletin 17C (ver. 1.1, May 2019): U.S. Geological Survey Techniques and Methods, book 4, chap. B5, 148 p., accessed August 30, 2019, at https://doi.org/10.3133/tm4B5.

Falcone, J.A., 2011, GAGES-II—Geospatial attributes of gages for evaluating streamflow—Metadata: accessed August 30, 2018, at https://water.usgs.gov/lookup/getspatial?gagesII_Sept2011.

Falcone, J.A., 2015, U.S. conterminous wall-to-wall anthropogenic land use trends (NWALT), 1974–2012: U.S. Geological Survey Data Series 948, 33 p., plus appendixes 3–6 as separate files, accessed November 1, 2018, at https://doi.org/10.3133/ds948.

Harrigan, S., Murphy, C., Hall, J., Wilby, R.L., and Sweeney, J., 2014, Attribution of detected changes in streamflow using multiple working hypotheses: Hydrology and Earth System Sciences, v. 18, no. 5, p. 1935–1952, accessed November 1, 2018, at https://doi.org/10.5194/hess-18-1935-2014.

Harwell, G.R., and Asquith, W.H., 2011, Annual peak streamflow and ancillary data for small watersheds in central and western Texas: U.S. Geological Survey Fact Sheet 2011–3082, 4 p., accessed November 20, 2019, at https://doi.org/10.3133/fs20113082.

Helsel, D.R., Hirsch, R.M., Ryberg, K.R., Archfield, S.A., and Gilroy, E.J., 2020, Statistical methods in water resources: U.S. Geological Survey Techniques and Methods, book 4, chap. A3, 458 p., accessed July 13, 2022, at https://doi.org/10.3133/tm4a3. [Supersedes USGS Techniques of Water-Resources Investigations, book 4, chap. A3, version 1.1.]

Hodgkins, G.A., Dudley, R.W., Archfield, S.A., and Renhard, B., 2019, Effects of climate, regulation, and urbanization on historical flood trends in the United States: Journal of Hydrology, v. 573, p. 697–709, accessed May 1, 2019, at https://doi.org/10.1016/j.jhydrol.2019.03.102.

Irza, T.J., 1966, Preliminary flood-frequency relations for small streams in Kansas: Washington, D.C., U.S. Geological Survey Open-File Report, 19 p., accessed November 20, 2019, at https://doi.org/10.3133/ofr6667.

Konrad, C.P., and York, B.C., 2022, Flag plots of trends, *in* York, B.C., Ryberg, K.R., Asquith, W.H., Chase, K.J., Dickinson, J.E., Dudley, R.W., Harden, T.M., Hodgkins, G.A., Holtschlag, D.J., Humberson, D.G., Konrad, C.P., Levin, S.B., Restivo, D.E., Sando, R., Sando, S.K., Swain, E.D., Tillery, A.C., and Totten, A.R., Attributions for nonstationary peak streamflow records across the conterminous United States, 1941–2015 and 1966–2015: U.S. Geological Survey data release, file FlagPlots_Trends.zip, https://doi.org/10.5066/P9FOUVWG. [Data directly accessible at https://www.sciencebase.gov/catalog/item/5d94f431e4b0c4f70d1022da.]

Lewis, J.M., 2010, Methods for estimating the magnitude and frequency of peak streamflows for unregulated streams in Oklahoma: U.S. Geological Survey Scientific Investigations Report 2010–5137, 41 p., accessed November 20, 2019, at https://doi.org/10.3133/sir20105137.

Lewis, J.M., Hunter, S.L., and Labriola, L.G., 2019, Methods for estimating the magnitude and frequency of peak streamflows for unregulated streams in Oklahoma developed by using streamflow data through 2017: U.S. Geological Survey Scientific Investigations Report 2019–5143, 39 p., accessed November 20, 2019, at https://doi.org/10.3133/sir20195143.

McGuire, V.L., 2014, Water-level changes and change in water in storage in the High Plains aquifer, predevelopment to 2013 and 2011–13: U.S. Geological Survey Scientific Investigations Report 2014–5218, 14 p., accessed August 30, 2018, at https://doi.org/10.3133/sir20145218.

National Oceanic and Atmospheric Administration, 2018, U.S. climate division data files: accessed August 8, 2018, at ftp://ftp.ncdc.noaa.gov/pub/data/cirs/climdiv/.

National Oceanic and Atmospheric Administration, 2019, U.S. climate divisions: National Oceanic and Atmospheric Administration, National Centers for Environmental Information website, accessed March 26, 2019, at https://www.ncdc.noaa.gov/monitoring-references/maps/us-climate-divisions.php.

Northwest Alliance for Computational Science and Engineering, 2019, PRISM climate data, 30-year normals: Northwest Alliance for Computational Science and Engineering website, accessed November 21, 2019, at https://prism.oregonstate.edu/normals/.

O'Connor, J.E., and Costa, J.E., 2003, Large floods in the United States—Where they happen and why: U.S. Geological Survey Circular 1245, 13 p., accessed September 10, 2018, at https://doi.org/10.3133/cir1245.

Palmer, W.C., 1965, Meteorological drought: U.S. Weather Bureau Research Paper no. 45, 58 p.

Painter, C.C., Heimann, D.C., and Lanning-Rush, J.L., 2017, Methods for estimating annual exceedance-probability streamflows for streams in Kansas based on data through water year 2015 (ver. 1.1, September 2017): U.S. Geological Survey Scientific Investigations Report 2017–5063, 20 p., accessed November 20, 2019, at https://doi.org/10.3133/sir20175063.

Pettitt, A.N., 1979, A non-parametric approach to the change-point problem: Journal of the Royal Statistical Society, Series C [Applied Statistics], v. 28, no. 2, p. 126–135. [Also available at https://www.jstor.org/stable/2346729.]

Rasmussen, T.J., and Perry, C.A., 2001, Trends in peak flows of selected streams in Kansas: U.S. Geological Survey Water-Resources Investigations Report 01–4203, 14 p., 8 figs., and 12 tables as separate files, accessed November 20, 2019, at https://doi.org/10.3133/wri014203.

R Core Team, 2019, R—A language and environment for statistical computing, version 3.6.1: R Foundation for Statistical Computing software release, accessed November 22, 2019, at https://www.r-project.org.

Ryberg, K.R., Hodgkins, G.A., and Dudley, R.W., 2019, Change points in annual peak streamflows—Method comparisons and historical change points in the United States: Journal of Hydrology, v. 583, article 124307, 13 p., accessed October 13, 2021, at https://doi.org/10.1016/j.jhydrol.2019.124307.

Sauer, V.B., 1974, Flood characteristics of Oklahoma streams—Techniques for calculating magnitude and frequency of floods in Oklahoma, with compilations of flood data through 1971: U.S. Geological Survey Water Resources Investigations 52–73, 306 p., accessed November 20, 2019, at https://doi.org/10.3133/wri7352.

Sauer, V.B., and Turnipseed, D.P., 2010, Stage measurement at gaging stations: U.S. Geological Survey Techniques and Methods, book 3, chap. A7, 45 p., accessed September 10, 2019, at https://doi.org/10.3133/tm3A7.

Seaber, P.R., Kapinos, F.P., and Knapp, G.L., 1987, Hydrologic unit maps: U.S. Geological Survey Water-Supply Paper 2294, 63 p., 1 pl., accessed March 9, 2021, at https://pubs.usgs.gov/wsp/wsp2294/.

Sen, P.K., 1968, Estimates of the regression coefficient based on Kendall's tau: Journal of the American Statistical Association, v. 63, no. 324, p. 1379–1389. [Also available at https://doi.org/10.1080/01621459.1968.10480934.]

Smith, S.J., Lewis, J.M., and Graves, G.M., 2015, Methods for estimating the magnitude and frequency of peak streamflows at ungaged sites in and near the Oklahoma Panhandle: U.S. Geological Survey Scientific Investigations Report 2015–5134, 35 p., accessed November 20, 2019, at https://doi.org/10.3133/sir20155134.

Thomas, B.E., Hjalmarson, H.W., and Waltemeyer, S.D., 1994, Methods for estimating magnitude and frequency of floods in the southwestern United States: U.S. Geological Survey Open-File Report 93–419, 211 p., accessed November 20, 2019, at https://doi.org/10.3133/ofr93419.

Thomas, E.D., Venkataraman, K., Chraibi, V., and Kannan, N., 2019, Hydrologic trends in the upper Nueces River basin of Texas—Implications for water resource management and ecological health: Hydrology, v. 6, no. 1, 24 p., accessed November 20, 2019, at https://doi.org/10.3390/hydrology6010020.

Thomas, R.P., and Gold, R.L., 1982, Techniques for estimating flood discharges for unregulated streams in New Mexico: U.S. Geological Survey Water-Resources Investigations 82–24, 42 p., accessed November 20, 2019, at https://doi.org/10.3133/wri8224.

Thomas, W.O., and Corley, R.K., 1977, Techniques for estimating flood discharges for Oklahoma streams—Techniques for calculating magnitude and frequency of floods in Oklahoma from rural and urban areas under 2500 square miles, with compilations of flood data through 1975: U.S. Geological Survey Water-Resources Investigations Report 77–54, 170 p., accessed November 20, 2019, at https://doi.org/10.3133/wri7754.

Tillery, A.C., Humberson, D.G., Asquith, W.H., and York, B.C., 2022, Attributions for nonstationary peak streamflow records in the South Central region, 1941–2015 and 1966–2015, and supporting information, *in* York, B.C., Ryberg, K.R., Asquith, W.H., Chase, K.J., Dickinson, J.E., Dudley, R.W., Harden, T.M., Hodgkins, G.A., Holtschlag, D.J., Humberson, D.G., Konrad, C.P., Levin, S.B., Restivo, D.E., Sando, R., Sando, S.K., Swain, E.D., Tillery, A.C., and Totten, A.R., Attributions for nonstationary peak streamflow records across the conterminous United States, 1941–2015 and 1966–2015: U.S. Geological Survey data release, files SC_site_manifest.csv, SC_50yr_ChangePT.csv, SC_50yr_Trend.csv, SC_75yr_ChangePT.csv, and SC_75yr_Trend.csv, https://doi.org/10.5066/P9FOUVWG. [Data directly accessible at https://www.sciencebase.gov/catalog/item/5cd5be46e4b0e8a309e4622e.]

Tortorelli, R.L., and Bergman, D.L., 1985, Techniques for estimating flood peak discharges for unregulated streams and streams regulated by small floodwater retarding structures in Oklahoma: U.S. Geological Survey Water-Resources Investigations Report 84–4358, 85 p., accessed November 20, 2019, at https://doi.org/10.3133/wri844358.

Tortorelli, R.L., and McCabe, L.P., 2001, Flood frequency estimates and documented and potential extreme peak discharges in Oklahoma: U.S. Geological Survey Water-Resources Investigations Report 01–4152, 39 p., accessed November 20, 2019, at https://doi.org/10.3133/wri20014152.

U.S. Army Corps of Engineers, 2019, National inventory of dams: U.S. Army Corps of Engineers website, accessed November 21, 2019, at https://nid.sec.usace.army.mil/ords/f?p=105:19.

U.S. Geological Survey, 1984, National water summary 1983—Hydrologic events and issues: U.S. Geological Survey Water-Supply Paper 2250, 243 p., accessed August 3, 2018, at https://doi.org/10.3133/wsp2250.

U.S. Geological Survey, 1985, National water summary 1984—Hydrologic events, selected water-quality trends, and ground-water resources: U.S. Geological Survey Water-Supply Paper 2275, 467 p., accessed August 30, 2018, at https://doi.org/10.3133/wsp2275.

U.S. Geological Survey, 1986, National water summary 1985—Hydrologic events and surface-water resources: U.S. Geological Survey Water-Supply Paper 2300, 506 p., accessed August 30, 2018, at https://doi.org/10.3133/wsp2300.

U.S. Geological Survey, 1988, National water summary 1986—Hydrolsogic events and ground-water quality: U.S. Geological Survey Water-Supply Paper 2325, 560 p., accessed August 30, 2018, at https://doi.org/10.3133/wsp2325.

U.S. Geological Survey, 1990, National water summary 1987—Hydrologic events and water supply and use: U.S. Geological Survey Water-Supply Paper 2350, 553 p., accessed August 30, 2018, at https://doi.org/10.3133/wsp2350.

U.S. Geological Survey, 1991, National water summary 1988–89—Hydrologic events and floods and droughts: U.S. Geological Survey Water-Supply Paper 2375, 591 p., accessed August 30, 2018, at https://doi.org/10.3133/wsp2375.

U.S. Geological Survey, 2007, North America elevation 1-kilometer-resolution GRID [dataset]: U.S. Geological Survey ScienceBase Catalog website, accessed May 1, 2019, at https://www.sciencebase.gov/catalog/item/4fb5495ee4b04cb937751d6d.

U.S. Geological Survey, 2019, USGS water data for the Nation: U.S. Geological Survey National Water Information System database, accessed April 22, 2019, at https://doi.org/10.5066/F7P55KJN.

Villarini, G., and Smith, J.A., 2013, Flooding in Texas—Examination of temporal changes and impacts of tropical cyclones: Journal of the American Water Resources Association, v. 49, no. 4, p. 825–837, accessed November 20, 2019, at https://doi.org/10.1111/jawr.12042.

Wagner, D., Kiang, J.E., and Asquith, W.H., 2017, Appendix 1—U.S. Geological Survey streamgaging methods and annual peak streamflow, *in* Asquith, W.H., Kiang, J.E., and Cohn, T.A., Application of at-site peak-streamflow frequency analyses for very low annual exceedance probabilities: U.S. Geological Survey Scientific Investigations Report 2017–5038, p. 52–66, accessed August 30, 2018, at https://doi.org/10.3133/sir20175038.

Waltemeyer, S.D., 1986, Techniques for estimating flood-flow frequency for unregulated streams in New Mexico: U.S. Geological Survey Water-Resources Investigations Report 86–4104, 56 p., accessed November 20, 2019, at https://doi.org/10.3133/wri864104.

Waltemeyer, S.D., 1996, Analysis of the magnitude and frequency of peak discharge and maximum observed peak discharge in New Mexico: U.S. Geological Survey Water-Resources Investigations Report 96–4112, 79 p., accessed November 20, 2019, at https://doi.org/10.3133/wri964112.

Waltemeyer, S.D., 2006a, Analysis of the magnitude and frequency of peak discharges for the Navajo Nation in Arizona, Utah, Colorado, and New Mexico: U.S. Geological Survey Scientific Investigations Report 2006–5306, 42 p., accessed November 20, 2019, at https://doi.org/10.3133/sir20065306.

Waltemeyer, S.D., 2006b, Automated crest-stage gage application in ephemeral streams in New Mexico: U.S. Geological Survey Fact Sheet 2005–3136, 4 p., accessed November 20, 2019, at https://doi.org/10.3133/fs20053136.

Waltemeyer, S.D., 2008, Analysis of the magnitude and frequency of peak discharge and maximum observed peak discharge in New Mexico and surrounding areas: U.S. Geological Survey Scientific Investigations Report 2008–5119, 106 p., accessed November 20, 2019, at https://doi.org/10.3133/sir20085119.

York, B.C., Ryberg, K., Asquith, W.H., Chase, K.J., Dickinson, J.E., Dudley, R.W., Harden, M., Hodgkins, G.A., Holtschlag, D.J., Humberson, D.G., Konrad, C.P., Levin, S.B., Restivo, D.E., Sando, R., Sando, S.K., Swain, E.D., Tillery, A.C., and Totten, A.R., 2022, Attributions for nonstationary peak streamflow records across the conterminous United States, 1941–2015 and 1966–2015: U.S. Geological Survey data release, https://doi.org/10.5066/P9FOUVWG.

Attribution of Monotonic Trends and Change Points in Peak Streamflow in the Southeast Region of the United States, 1941–2015 and 1966–2015

By Eric D. Swain

Chapter H of

Attribution of Monotonic Trends and Change Points in Peak Streamflow Across the Conterminous United States Using a Multiple Working Hypotheses Framework, 1941–2015 and 1966–2015

Karen R. Ryberg, editor

Prepared in cooperation with
U.S. Department of Transportation
Federal Highway Administration

Professional Paper 1869

U.S. Department of the Interior
U.S. Geological Survey

U.S. Geological Survey, Reston, Virginia: 2022

For more information on the USGS—the Federal source for science about the Earth, its natural and living resources, natural hazards, and the environment—visit https://www.usgs.gov or call 1–888–ASK–USGS.

For an overview of USGS information products, including maps, imagery, and publications, visit https://store.usgs.gov.

Suggested citation:
Swain, E.D., 2022, Attribution of monotonic trends and change points in peak streamflow in the Southeast region of the United States, 1941–2015 and 1966–2015, chap. H *of* Ryberg, K.R., ed., Attribution of monotonic trends and change points in peak streamflow across the conterminous United States using a multiple working hypotheses framework, 1941–2015 and 1966–2015: U.S. Geological Survey Professional Paper 1869, p. H1–H52, https://doi.org/10.3133/pp1869.

Associated data for this publication:
Dudley, R.W., Archfield, S.A., Hodgkins, G.A., Renard, B., and Ryberg, K.R., 2018, Peak-streamflow trends and change-points and basin characteristics for 2,683 U.S. Geological Survey streamgages in the conterminous U.S. (ver. 3.0, April 2019): U.S. Geological Survey data release, https://doi.org/10.5066/P9AEGXY0.

York, B.C., Ryberg, K.R., Asquith, W.H., Chase, K.J., Dickinson, J.E., Dudley, R.W., Harden, T.M., Hodgkins, G.A., Holtschlag, D.J., Humberson, D.G., Konrad, C.P., Levin, S.B., Restivo, D.E., Sando, R., Sando, S.K., Swain, E.D., Tillery, A.C., and Totten, A.R., 2022, Attributions for nonstationary peak streamflow records across the conterminous United States, 1941–2015 and 1966–2015: U.S. Geological Survey data release, https://doi.org/10.5066/P9FOUVWG.

ISSN 2330-7102 (online)

Acknowledgments

The work described in this professional paper was funded by the Federal Highway Administration of the U.S. Department of Transportation through Interagency Agreement DTFH6116X30020, “Flood Frequency Estimation for Hydraulic Design.” We thank David Holtschlag of the U.S. Geological Survey (USGS) for the overall attribution framework that we used in this chapter, David Holtschlag and Alex Totten (USGS) for the antecedent precipitation analysis code, and Toby Feaster and Anthony Gotvald of the USGS for their thoughtful reviews of the manuscript.

Contents

Figures

Tables

[Tables H1–H9 follow the References Cited for chapter H]

Conversion Factors

U.S. customary units to International System of Units

Multiply	By	To obtain
	Length	
inch (in.)	2.54	centimeter (cm)
inch (in.)	25.4	millimeter (mm)
foot (ft)	0.3048	meter (m)
	Volume	
cubic foot (ft^3)	0.02832	cubic meter (m^3)

International System of Units to U.S. customary units

Multiply	By	To obtain
	Area	
square kilometer (km^2)	0.3861	square mile (mi^2)

Datum

Horizontal coordinate information is referenced to the North American Datum of 1983 (NAD 83).

Supplemental Information

A “water year” represents the 12-month period from October 1 through September 30 of the following year that is designated by the calendar year in which it ends.

The 75-year and 50-year study periods described in this report span water years 1941–2015 and 1966–2015, respectively.

The term “post-step peak streamflow” is the median annual peak streamflow after the change-point year, and the term “pre-step peak streamflow” is the median annual peak streamflow before the change-point year.

Abbreviations

>	greater than
<	less than
FHWA	Federal Highway Administration
ft^3/s	cubic feet per second
ft^3/s/yr	cubic feet per second per year
GAGES-II	Geospatial Attributes of Gages for Evaluating Streamflow, Version II
HUCs	hydrologic unit codes
in/yr	inches per year
km^2	square kilometers
LWRPF	largest watershed and reductions in peak flow
MWHs	multiple working hypotheses
NAD 83	North American Datum of 1983
NOAA	National Oceanic and Atmospheric Administration
NWIS	National Water Information System
p-value	attained significance level
USGS	U.S. Geological Survey

Attribution of Monotonic Trends and Change Points in Peak Streamflow in the Southeast Region of the United States, 1941–2015 and 1966–2015

By Eric D. Swain[1]

Abstract

This report builds upon a previous effort by the U.S. Geological Survey and the Federal Highway Administration of the U.S. Department of Transportation to identify statistically significant monotonic trends and change points in annual peak streamflow for streamgages in the conterminous United States. Methods were used to identify statistically significant monotonic trends and change points of annual peak streamflow for 357 streamgages in the Southeast region of the United States for the 50-year period (water years 1966–2015) and the 75-year period (water years 1941–2015). Statistics of annual peak streamflow and the correlation between precipitation and annual peak streamflow were included in the analyses of monotonic trends and change points. In addition to the statistical analyses, hydrologic settings that affect each site were characterized and incorporated into the process of determining the attributions of detected monotonic trends or change points. Comparison of the years identified in the median change point analysis with historical events helped attribute the causal factors. Also, precipitation statistics, documentation of water usage, and reservoir construction information were used to support the attributions.

The most common attributions for monotonic trends and change points in annual peak-streamflow data are the direct anthropogenic alteration to waterways, such as surface-water withdrawals, the construction of large artificial impoundments, surface-water withdrawal from large artificial impoundments, and interbasin water transfer. Urban effects and wastewater and industrial discharges also were likely attributions in locations with significant monotonic trend and change point statistics. The attributes of groundwater withdrawals, agricultural drainage activities, and short-term precipitation tend to be less significant. The study indicated that reservoirs and water supplies in the Atlanta area are associated with peak-streamflow changes in the watershed, as well as those same factors in other urban centers such as Augusta and Macon, Georgia, and Charlotte, North Carolina. Population growth in smaller municipalities also is indicated to substantially affect smaller river systems, likely through industrial and commercial water use, land-use-driven river diversions, and irrigation over the 50- and 75-year periods that were analyzed in this report.

Introduction

This chapter of the professional paper uses the statistics of annual peak streamflow, along with relevant hydrologic features, for 357 streamgages in the Southeast region of the United States, to identify the causal attributions of monotonic trends and change points in annual peak streamflow during the 50-year period (water years 1966–2015) and the 75-year period (water years 1941–2015). A monotonic trend indicates annual peak streamflow is generally increasing or generally decreasing, but the change is not necessarily linear. Change points are abrupt changes in the distribution parameters of annual peak streamflow. In addition to statistical analyses, hydrologic factors that may affect changes in annual peak streamflow at each streamgage were determined.

This chapter is also part of a larger U.S. Geological Survey (USGS) effort to identify and characterize changes in peak streamflows across the conterminous United States (Barth and others, this volume, chap. A). This larger USGS effort builds upon a previous study by the USGS and the Federal Highway Administration (FHWA) of the U.S. Department of Transportation to identify statistically significant monotonic trends and change points in annual peak streamflows across the conterminous United States (Dudley and others, 2018; Hodgkins and others, 2019; Ryberg and others, 2019). In an effort to develop a cohesive, national approach for incorporating potential or observed changes into flood-frequency estimates when necessary, national and regional experts from the USGS and cooperators worked together to develop a multiple working hypotheses (MWHs) framework for attributions and a common vocabulary for making provisions of confidence. The MWHs involve the development of several hypotheses that might explain the changes in annual peak streamflow (Chamberlin, 1965). The MWHs are not conclusive; they are developed based on hydrologic factors that are likely to affect peak streamflows in each watershed, and attributions of

[1]U.S. Geological Survey.

monotonic trends and change points were determined based on the statistics of the peak streamflow, a survey of the spatial and temporal proximity of geographic features that can affect peak streamflow, and statistical tests of precipitation/annual peak-streamflow relationships. The distribution of MWHs in the Southeast region is discussed in the report along with the significance of the changes in annual peak streamflow.

Further, subject matter experts from the USGS and cooperators have divided the conterminous United States into seven water resources regions, which are geographic areas that either contain the entire drainage area of a major river or combine drainage areas of geographically proximate rivers. These seven water resources regions are defined by hydrologic unit codes (HUCs) described in Seaber and others (1987). Water-resources regions and their associated hydrologic unit codes within the Southeast region are shown on figure H1 and include 03 (South Atlantic-Gulf), 06 (Tennessee), and 08 (Lower Mississippi).

Study Area and Background

The study area for this report is the Southeast region of the United States and includes all or parts of the States of Alabama, Arkansas, Florida, Georgia, Kentucky, Louisiana, Mississippi, Missouri, North Carolina, South Carolina, Tennessee, and Virginia. Environmental conditions and hydrology vary significantly across this region, from the mountainous Appalachians to the flat topography of southern Florida (fig. H1). To relate streamgage data to historical anthropogenic changes, the USGS developed the Geospatial Attributes of Gages for Evaluating Streamflow, Version II (GAGES-II) time series dataset (Falcone, 2011), which compiled data derived from consistent sources of land use at selected streamgages, including the Southeast region of the United States.

The average precipitation in the Southeast region averages around 50 inches per year (in/yr), including ice and snow in all States in the Southeast region except most of Florida and southern Georgia (North Carolina Climate Office, 2019). The average annual precipitation ranges from 43 in/yr in Virginia to 54 in/yr in Florida. The yearly distribution of precipitation varies across the Southeast region. Georgia and Alabama have their wet seasons from June through August, and North Carolina, South Carolina, Virginia, and Florida have wet seasons from June through September. Florida has the starkest contrast between seasonal rainfalls, with summer monthly precipitation totals that are 4 to 5 inches higher than the total precipitation during winter months, and Virginia has the lowest contrast between seasonal rainfalls with only about an inch of variation of precipitation between months (North Carolina Climate Office, 2019).

The hydrology in the Southeast region is affected by multiple factors that cause changes in annual peak streamflow. Factors include urban growth, regulation of reservoirs, and surface-water withdrawals. Urban development is a substantial and growing part of the land cover, but there are still large perennial land cover and crop production areas (fig. H2). The Southeast region's population has dramatically increased since 1940, which has changed land and water use over time. The rise in urban population is accompanied by an increase in urbanized areas. For example, population increases of between 25 and 35 percent from 1970 to 2000 were found in the Lower Ocmulgee, Lower Oconee, Ohoopee, and Altamaha watersheds (Anandhi and others, 2018). Substantial increases in groundwater and surface-water withdrawals are associated with (1) industrial use, (2) increased population demands, and (3) the alteration of the hydrologic cycle via water and wastewater infrastructure that can alter both recharge and subsurface drainage. Additional impacts of urbanization are the growing areas of impervious surfaces such as parking lots, asphalt, roofing, and concrete and gravel roads, which prevent rainwater infiltration into the soil and cause direct runoff to storm drainage systems (Anandhi and others, 2018).

Streamgage Selection and Data Compilation

For the Southeast region, the analysis of monotonic trends and change points used 357 selected streamgages from the GAGES-II dataset (Falcone, 2011) (fig. H3, table H1 [tables H1–H9 follow the References Cited]). Annual peak-streamflow data for these streamgages came from the USGS National Water Information System (NWIS) peak-flow files (Ryberg and others, 2019). The compiled data in the data release (Dudley and others, 2018) include streamgage identification number, name, drainage area, latitude, longitude, percent urban land use, dam storage, streamgage classification, record completeness status, lag-1 autocorrelation, trend slopes and significance, peaks-over-threshold counts, trends in the numbers of peaks-over-threshold, and change-point years and values for median and scale.

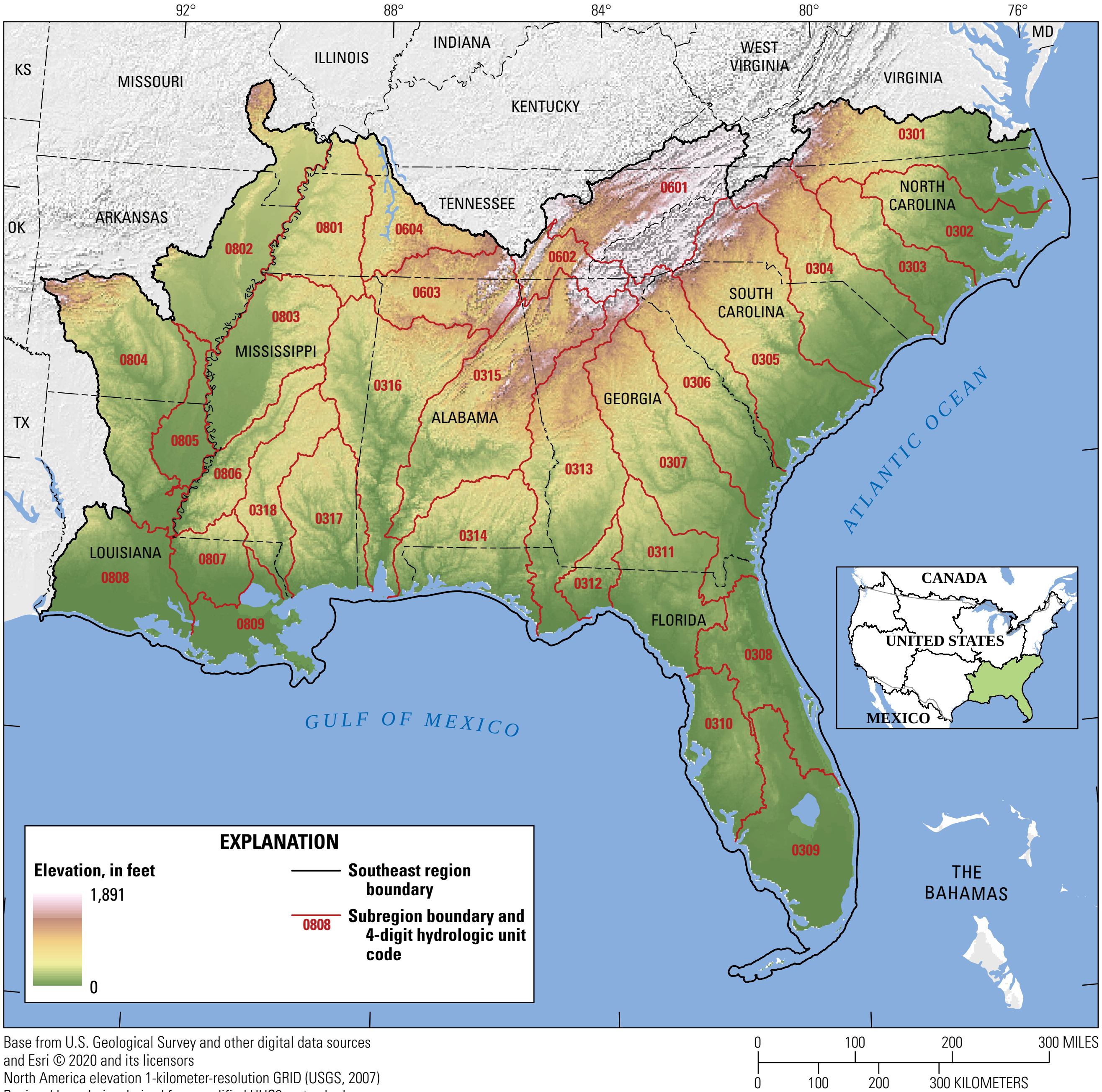

Base from U.S. Geological Survey and other digital data sources and Esri © 2020 and its licensors
North America elevation 1-kilometer-resolution GRID (USGS, 2007)
Regional boundaries derived from modified HUC2 watersheds
USA Contiguous Albers Equal Area Conic USGS projection
North American Datum of 1983

Figure H1. Map showing the Southeast region of the United States where attributions are assigned to monotonic trends and change points in annual peak streamflow. For this study, the regions were based on watersheds identified by two-digit hydrologic unit codes (HUC2s) described by Seaber and others (1987), and some regions were modified slightly by adding or subtracting subregions (HUC4s) to achieve geographic cohesiveness or hydrologic-setting similarity. The Southeast region consists of three water-resources regions: 03 (South Atlantic-Gulf), 06 (Tennessee), and 08 (Lower Mississippi).

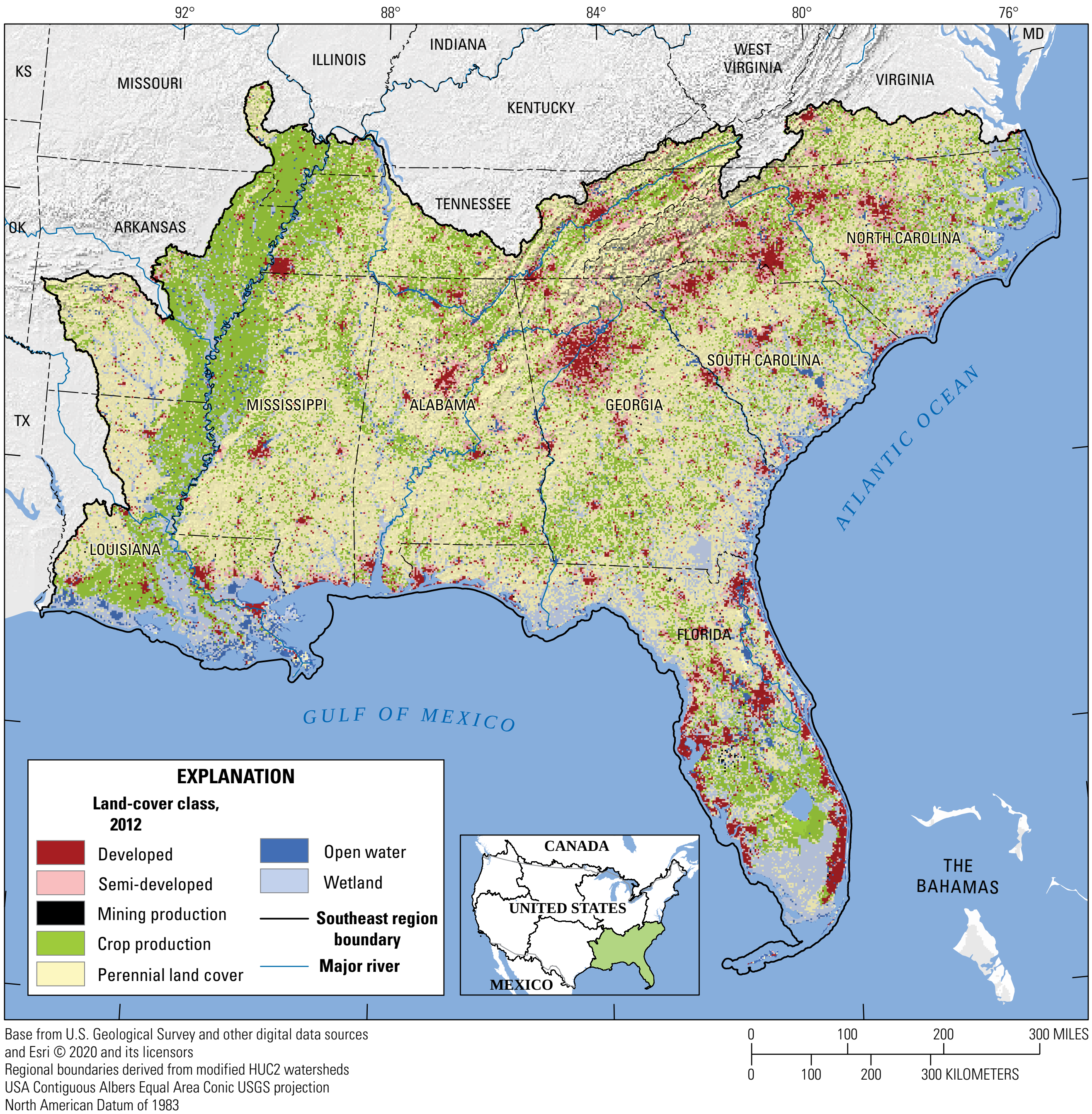

Figure H2. Map showing the anthropogenic land-cover classes within the Southeast region of the United States in 2012. Land-cover classes are from Falcone (2015).

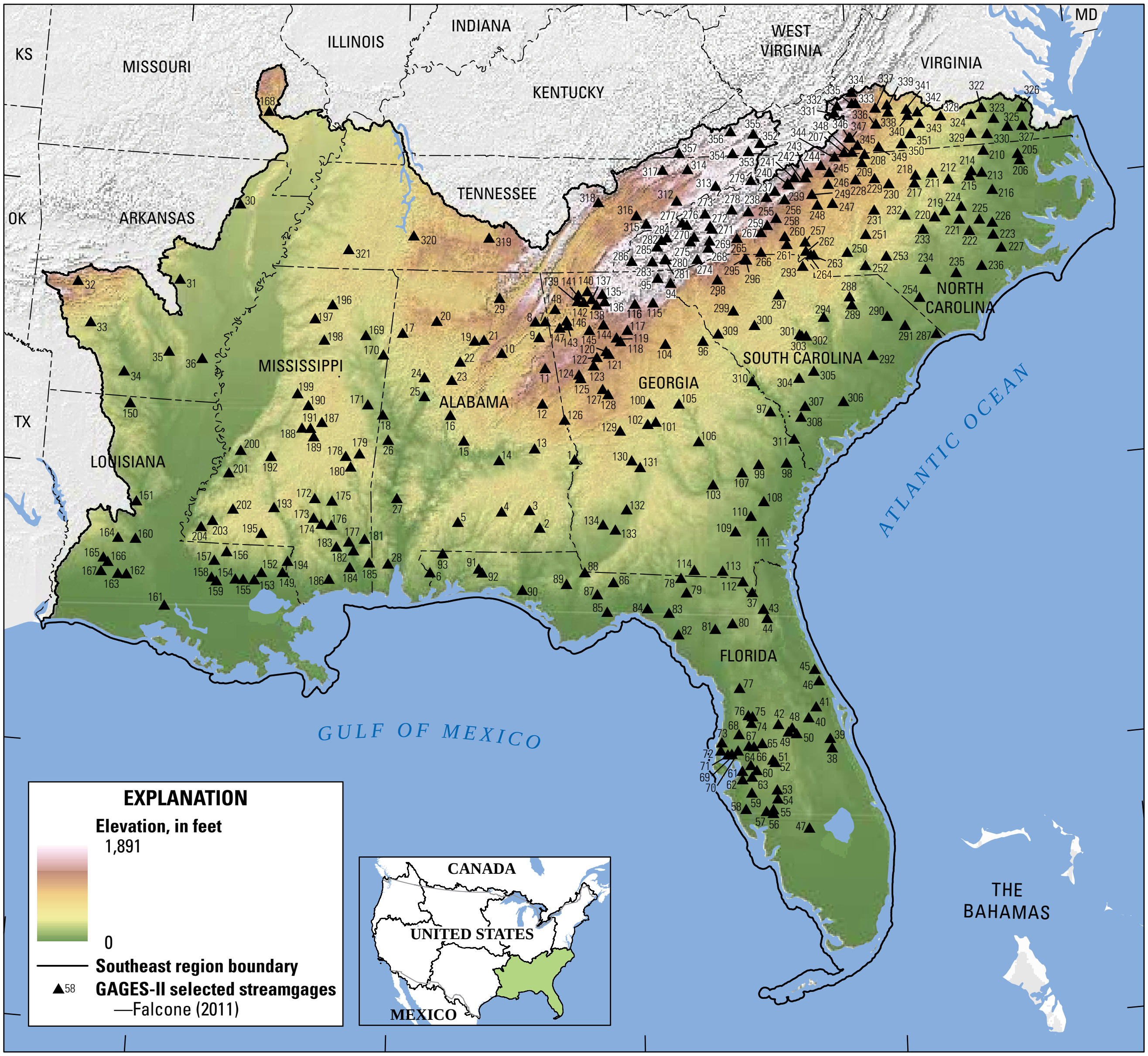

Base from U.S. Geological Survey and other digital data sources
and Esri © 2020 and its licensors
North America elevation 1-kilometer-resolution GRID (USGS, 2007)
Regional boundaries derived from modified HUC2 watersheds
USA Contiguous Albers Equal Area Conic USGS projection
North American Datum of 1983

0 100 200 300 MILES
0 100 200 300 KILOMETERS

Figure H3. Map showing the locations of 357 U.S. Geological Survey streamgages within the Southeast region selected for attribution of monotonic trends and change points. Numbers 1 to 357 correspond to streamgage descriptions in table H1. GAGES-II, Geospatial Attributes of Gages for Evaluating Streamflow, Version II.

Methods

The attribution of monotonic trends and change points in annual peak streamflow utilizes statistical methods and hydrologic principles to determine the most likely causes of observed monotonic trends in annual peak streamflow. Statistical analyses are used to detect monotonic trends in annual peak-streamflow magnitudes, monotonic trends in the scale of the annual peak-streamflow range, and the correlation of precipitation events to annual peak streamflow. An evaluation of proximal hydrologic features, natural and anthropogenic, is used to develop the potential attributions for monotonic trends and change points in annual peak streamflow in the study region and determine the most likely primary attributions. The general procedure that is followed in this report to attribute monotonic trends and change points in annual peak streamflow in the Southeast region consists of:

(1) determining the relevant MWHs;

(2) determining the significance of monotonic trends and change points in annual peak streamflow;

(3) describing the relationship between monotonic trends and change points in annual peak streamflow and watershed area;

(4) assessing the correlation of monotonic trends and change points in annual peak streamflow and the changes in watershed precipitation;

(5) developing primary and secondary attributions based on relevant MWHs and hydrologic occurrences that affect each streamgage; and

(6) examining and quantifying the types of attributions of monotonic trends and change points in peak streamflow.

Determining Attributions with Multiple Working Hypotheses

The likely attributions affecting annual peak streamflows are developed through MWHs as shown in table H2. Agricultural drainage activities, urban effects, large artificial impoundments, and surface-water and groundwater withdrawals are some of the attributions included in the MWHs in the Southeast region. The application of these potential attributions to locations with monotonic trends and change points in annual peak streamflow is made through precipitation correlation analyses, knowledge of local hydrology, research of structural changes to the hydrologic system and landscape, and hydrologic principles. The level of evidence indicates the confidence in the attributions and is determined based on the available supporting information.

Determining the Significance of Monotonic Trends and Change Points in Annual Peak Streamflow

Several statistical methods were applied to determine the significance of monotonic trends and change points in annual peak streamflow. For this study, the change point in the median of annual peak streamflows was determined using the Pettitt method (Pettitt, 1979). This method determines an effective year when the annual peak streamflows change, which is useful in determining the causal mechanisms of monotonic trends and change points. The probability that the median change point is significant is higher at smaller *p*-values of the Pettitt method, so to define the significance of the median statistics the streamgages with a *p*-value less than 0.10 were assigned attributions. The time period before the change-point year is referred to as “pre-step” and the time period after the change-point year is referred to as “post-step.” The pre-step and post-step median annual peak streamflows are directly computed from the series of annual peak-streamflow values and the change points. Monotonic trends in the instantaneous magnitude of annual peak streamflow are computed on the basis of the Sen slope (Sen, 1968), yielding a second measure to rank and identify potential attributions for the change in median annual peak streamflow at each site. Although it would be possible for the monotonic trend and change point analyses to indicate different trends in the change of the magnitude (higher or lower in peak streamflow) in all the streamgages analyzed in the Southeast region, both methods indicated the same trends in peak streamflow.

An additional statistic used to define the changes in annual peak streamflow is the scale of the interquartile range, a measure of the range of annual peak streamflows (Ross and others, 2011). The pre-step and post-step interquartile ranges, the difference between the 25th and 75th percentiles of the annual peak streamflows, are computed with the Mood test (Mood, 1954). Locations with a change in the interquartile range scale of greater than 50 percent of the initial value are assigned attributions of the change point in annual peak streamflow. This provides an additional set of scale statistics for determining attributions along with the median statistics.

Determining the Relationship Between Monotonic Trends in Annual Peak Streamflow and Drainage Area

To examine factors affecting the annual peak streamflow, the monotonic trend in the instantaneous magnitude of annual peak streamflow was determined by the median statistic method, calculated from the Sen slope (Sen, 1968), and was compared to the drainage area of the streamgage using data from the 75-year period (water years 1941–2016) and data from the 50-year period (water years 1966–2016).

This relationship helps determine the attributions of monotonic trends and change points in annual peak streamflow that may be related to drainage area.

Determining the Correlation Between Annual Peak Streamflow and Watershed Precipitation

For streamgages where temporally discrete structural changes to the hydrologic system are not apparent or where large-scale storms are a likely factor in annual peak streamflow, a statistical analysis of the correlation between precipitation and annual peak streamflow was performed. For a given streamgage, National Oceanic and Atmospheric Administration (NOAA) precipitation streamgages located within the watershed were identified and data from selected streamgages are compared statistically (National Oceanic and Atmospheric Administration, National Weather Service, 2019). The analysis included two Mann-Kendall trend tests, one on precipitation and the other on annual peak-streamflow (Hirsch and others, 1982). A partial Mann-Kendall trend test also was performed on the correlation of precipitation and the trends in annual peak streamflow (Hirsch and others, 1982). The *p*-values for statistical significance were calculated for each of these three tests (table H3) as well as a Pearson's rho correlation between median peak streamflow and watershed precipitation. Generally, it is considered that changes in annual peak streamflow can be attributed to changes in precipitation if all three of these *p*-value tests indicate significance. If the Kendall trends in annual peak streamflow and precipitation are both positive or both negative but the partial Mann-Kendall trend test does not show them as significantly correlated, precipitation may be a secondary attribution for monotonic trends and change points in annual peak streamflow, with another causal factor being the primary attribution.

Attributions of Monotonic Trends and Change Points in Annual Peak Streamflow

The statistics used in this study show different aspects of the magnitudes in annual peak streamflow. The median change-point statistics are useful in determining the timing of magnitude changes, the monotonic trend statistics are useful for showing the direction of the change in magnitude, and the scale statistic is useful in showing if the range in magnitude increased or decreased. An increase in the median annual peak streamflow likely indicates higher runoff from an increase in urbanized areas or the increase in agricultural runoff. A decrease in the median annual peak streamflow can be due to surface-water withdrawals, large or small artificial impoundments, reduction of water-levels due to groundwater withdrawals, or other hydrologic causal factors. An increase in the scale of the range in median annual peak streamflow may indicate urban effects (regulation), or impoundment usage, but a reduction in the scale of the range in median annual peak streamflow can also be the result of impoundments. By developing insights from these statistical analyses, the possible attributions of monotonic trends and change points in annual peak streamflow can be better identified.

For streamgages which are identified as having significant monotonic trends and change points in median annual peak streamflow, the process of determining attributions include the assessment of landscape and hydrologic features and the changes that affect each streamgage location. Upstream water usage and impoundments were identified, and the dates of the change points in the annual peak streamflows were compared to dates of construction and impoundment regulation changes. Substantial population increases corresponding to construction and land cover, construction of treatment plants withdrawing from the water body, and the building of impoundments were identified. While the attributions contributing to changes in annual peak streamflow may correspond exactly to the timing of the change points in annual peak streamflow, they should precede or occur near the time of the change point in annual peak streamflow. Other attributions from table H2 are considered in the report with the supporting evidence needed to make the attribution.

A secondary attribution may be defined when multiple factors may have importance. A large impoundment may have changes in withdrawals, leading to a primary attribution of large artificial impoundments and a secondary attribution of surface-water withdrawals. This helps differentiate between the construction of an impoundment, which only has a primary attribution of the impoundment, and changes in the operation of the impoundment, which then can have a secondary attribution of surface-water withdrawals. Also, if precipitation and annual peak streamflows are shown to be similar in trend, but the correlation is not certain, precipitation can be considered as a secondary attribution.

The "level of evidence" for attributions of monotonic trends and change points is based on the confidence in the supporting evidence for assigned attributions. Generally, if the change-point data correspond temporally to a specific event, such as the construction of a reservoir or the construction of a treatment plant upstream in the waterway, then this is considered robust evidence for an attribution. If the monotonic trend and change point data correspond generally to the growth in an upstream population center, agriculture, or some other land use, then this is considered medium evidence for an attribution. If poorly documented landscape changes (such as an assumed increase in impervious cover due to population increase) are identified as the cause of a monotonic trend or change point and only a rough estimate of the dates of occurrence of a landscape change can be determined, then this is considered limited evidence for an attribution.

Reference data for identifying attributions come from multiple sources and are linked in the "attribution notes and citations" for each streamgage in the spreadsheet files in Swain and York (2022). The data sources include the following: census data, State parks adjacent to reservoirs, municipal water-supply and water-treatment utilities, water-management districts, conservation service websites, consulting firms, U.S. Army Corps of Engineers regulations, environmental assessments, county government records, departments of natural regulations in the associated States, historical web pages, hydropower utilities, and other sources.

Results

The methods were applied to the 357 streamgages shown in figure H3. The significance of monotonic trends and change points in median annual peak streamflow, the relationship of the changes in annual peak streamflow and drainage area, and the correlation between the change points in annual peak streamflow and precipitation in the watershed are examined to determine which documented regional factors should be considered attributions of monotonic trends and change points in annual peak streamflow. Assigning attributions is a subjective process, and therefore an unknown measure of uncertainty could be introduced by omission of other relevant factors.

Relationship Between Monotonic Trends in Annual Peak Streamflow and Drainage Area

For each streamgage, the magnitude of the monotonic trend in annual peak streamflow is compared to the drainage area for data from the 50-year period (water years 1966–2016) and data from the 75-year period (water years 1941–2016; fig. H4). The relation between annual peak streamflow and drainage area is somewhat linear for lower streamflow values, but data from both the 50-year and 75-year periods show a greater, negative monotonic trend in annual peak streamflow (reduction in annual peak streamflows) for the largest drainage areas (figs. H4*A*, H4*B*). When comparing the change-point percentage change in median annual peak streamflow with the drainage area, the relationship is less obvious but still apparent with a nonlinear best-fit line (figs. H4*C*, H4*D*). For the purposes of defining locations with the largest values of both drainage areas and reductions in annual peak streamflows, the 25 streamgages within the box in figure H4*A* were selected and shown on the map in figure H5. These streamgages are referred to as the largest watershed and reductions in peak flow (LWRPF) in tables 4 to 9. The areal distribution of these streamgages, with a noted absence in Arkansas, Kentucky, Louisiana, Missouri, and Virginia, is through the middle of the Southeast region and generally corresponds to locations with larger river systems that are affected by population growth and management-driven structural changes.

Correlation Between Annual Peak Streamflow and Watershed Precipitation

Table 3 shows the results of the statistical analysis of the correlation between median annual peak streamflow and watershed precipitation to identify monotonic trends for streamgages where temporally discrete structural changes to the hydrologic system are not apparent or where large-scale storms are a likely factor. Of the 18 streamgage locations tested (table H3), only streamgage 0204950 (located along the Blackwater River near Franklin, Virginia) indicated a significant effect on median annual peak streamflow from changes in watershed precipitation and therefore a primary attribution. If a streamgage location is tested for the correlation between median annual peak streamflow and watershed precipitation it is identified in tables H4 to H7 in the “Notes” column.

Attributions of Change Points in Annual Peak Streamflow Relevant to MWHs and Hydrologic Occurrences

The likely attributions of change points in median annual peak streamflow during the 50-year period (water years 1966–2016), are shown in table H4. Data for the 50-year period from 74 of the 357 streamgages in the Southeast region indicate statistically significant change points in annual peak streamflow, including data for 14 of the 25 LWRPF streamgages. The majority of these streamgages indicate a decrease in median annual peak streamflow over the 50-year period. Primary attributions include surface-water and groundwater withdrawals, large artificial impoundments, small artificial impoundments, artificial wastewater and water-supply discharges, interbasin water transfers, urban effects, and short-term precipitation. Secondary attributions include surface-water withdrawals, interbasin water transfers, urban effects, short-term precipitation, and long-term precipitation.

Twenty-nine of the 74 streamgages in table H4 have a change point that occurred in 1998. Drought condition affected several States in the Southeast region during the period from 1998 to 2002 (Weaver, 2005). Figure H6 shows streamflow in cubic feet per second from 1941 to 2015 and the year the change point occurred for six of the streamgages in three States (Georgia, North Carolina, and South Carolina); all six streamgages have precipitation and streamflow data results shown in table H3. The three streamgages with a change point year of 1998 (streamgages 02337500, 02100500, and 02173500) do not have *p*-values that indicate a significant correlation of median annual peak streamflow and precipitation. And these three streamgages also have groundwater and surface-water withdrawals or large artificial impoundments upstream, which are affected by available water and droughts. Given the difficulty of separating precipitation effects from water-management operations that may correlate to precipitation, a secondary attribution of short-term precipitation is assigned to most of the streamgages with a change point year of 1998 (table 4). The exceptions to this assignment are streamgages 02223500 and 02100500, which have heavily regulated stream reaches located upstream, and 03455500, which was heavily impacted by hurricanes Frances and Ivan.

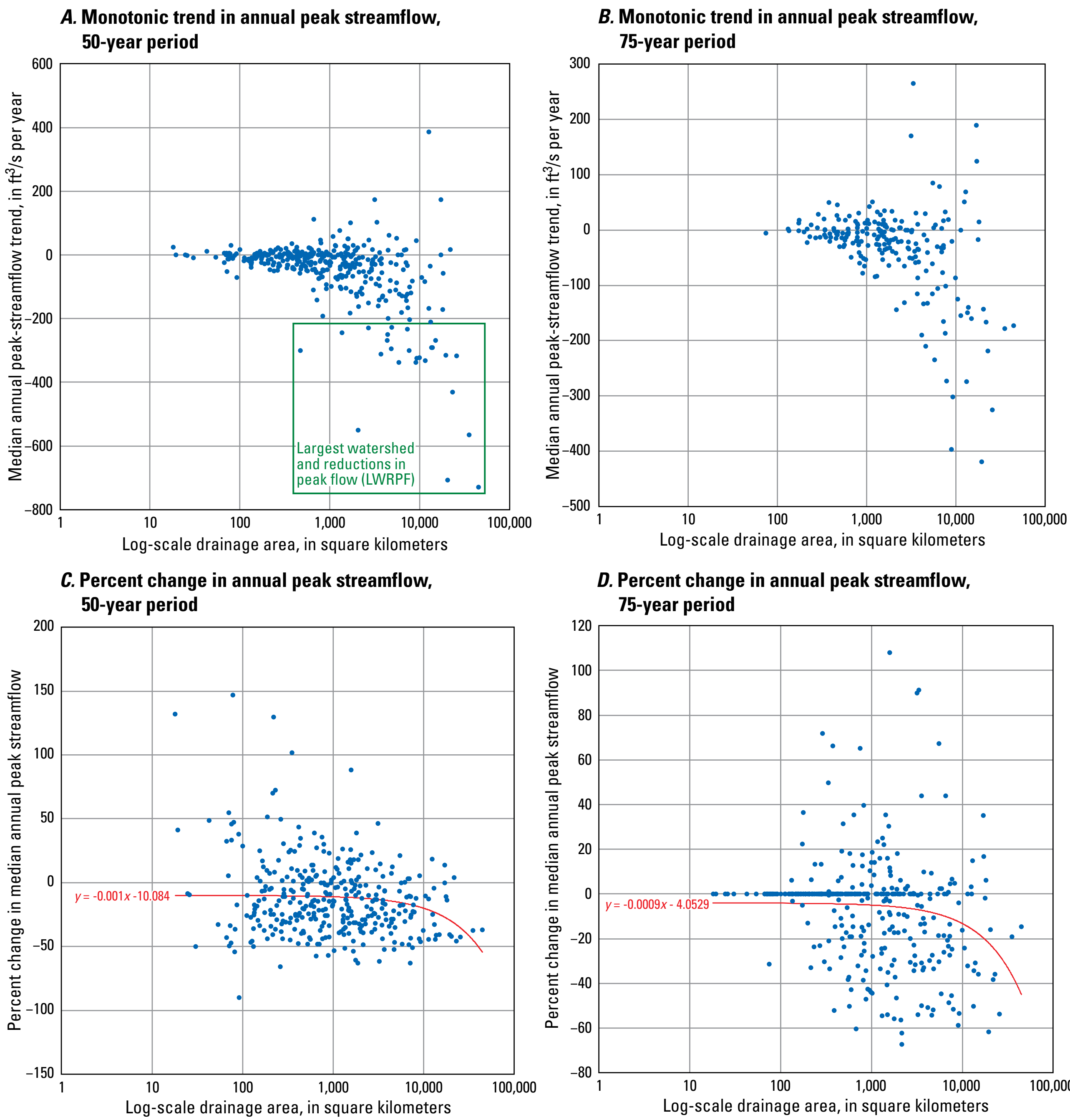

Figure H4. Scatterplots showing the magnitude of monotonic trends (*A* and *B*) and change-point percent changes (*C* and *D*) in median annual peak streamflow versus drainage area for the 50- and 75-year periods. *A*, Plot showing the monotonic trend in median annual peak streamflow and drainage area for the 50-year period (water years 1966–2015). *B*, Plot showing the monotonic trend in median annual peak streamflow and drainage area for the 75-year period (water years 1941–2015). *C*, Plot showing the percent change in median annual peak streamflow and drainage area for the 50-year period (water years 1966–2015). *D*, Plot showing the percent change in median annual peak streamflow and drainage area for the 75-year period (water years 1941–2015). The location of the 25 selected GAGES-II streamgages within the box area in figure H4*A*, defined as the largest watershed and reductions in peak flow (LWRPF), is shown on the map in figure H5. The nonlinear best-fit lines in *C* and *D* indicate greater-magnitude reductions in median annual peak streamflows at the watersheds with the largest areas. ft³/s, cubic feet per second. Data from Swain and York (2022), which is part of York and others (2022).

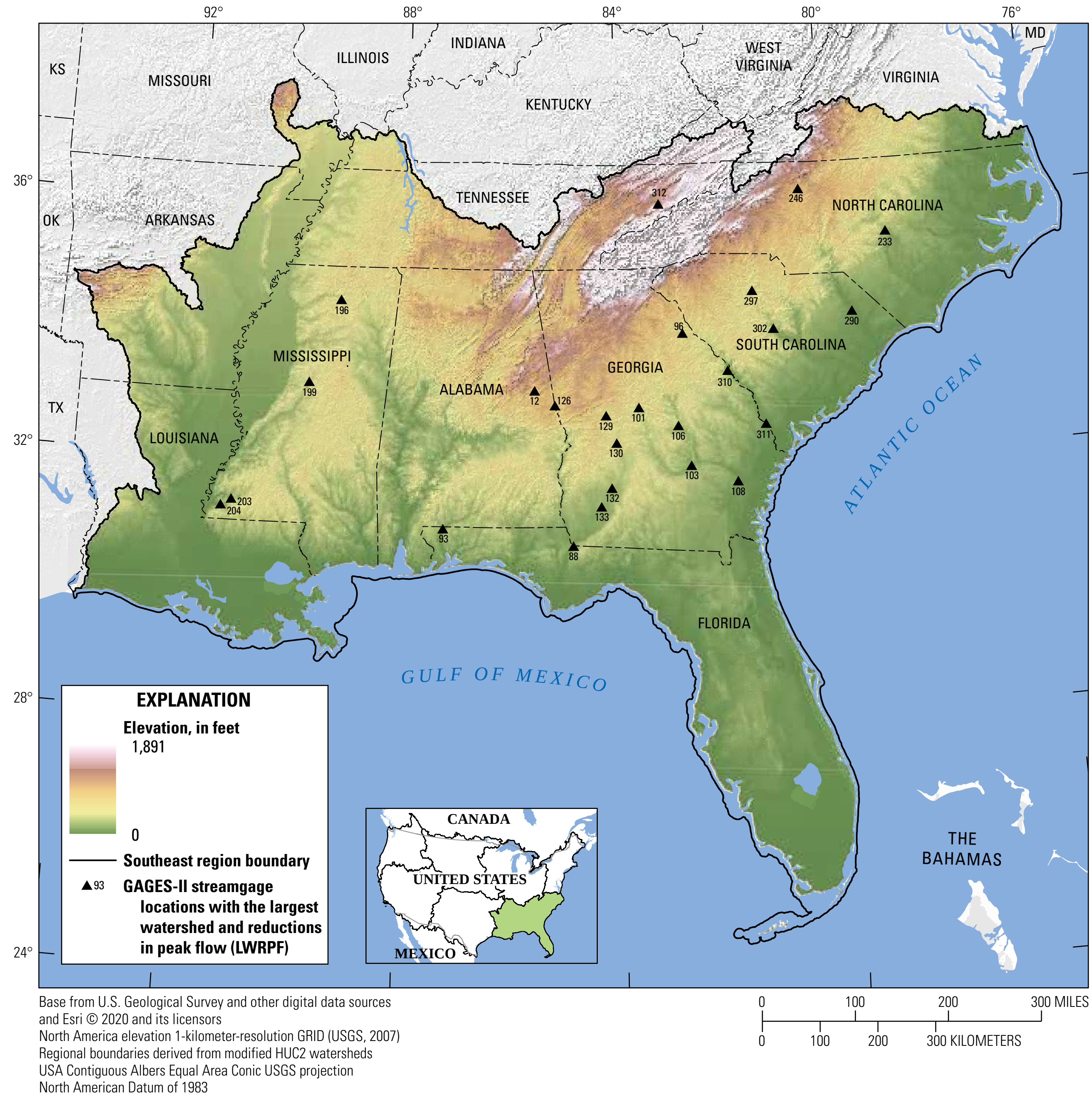

Figure H5. Map showing the 25 selected GAGES-II streamgage locations within the Southeast region with the largest watershed and reductions in peak flow (LWRPF). The 25 LWRPF streamgages are shown within the box in figure H4*A*. The number next to each streamgage location corresponds to the map location number in table H1. GAGES-II streamgages are from Falcone (2011). GAGES-II, Geospatial Attributes of Gages for Evaluating Streamflow, Version II.

Figure H7*A* shows the percentage of the 74 streamgages corresponding to each primary attribution for change points in median annual peak streamflow for the 50-year period (water years 1961–2015). Along with the primary attributions listed in table H2, there are two attributions modified by an asterisk (*). The attribution “large artificial impoundments*” modifies the primary attribution “large artificial impoundments” to indicate a secondary attribution (short-term precipitation, interbasin water transfer, surface water withdrawals, or urban effects) substantially affects the streamgage. This contrasts with “large artificial impoundments” without the asterisk, which refers to the construction of the large impoundment. The attribution “short-term precipitation*” modifies the primary attribution “short-term precipitation” to indicate a secondary attribution “long-term precipitation.” This combination of primary and secondary attributions indicates that hurricanes or tropical storms are a factor at the streamgage. A distribution of attributions by the number of streamgages shows that 31.1 percent of streamgages have change points from large artificial impoundments* and 16.2 percent have change points from both surface-water and groundwater withdrawals (fig. H7*A*). Change points from large artificial impoundments accounted for 10.8 percent of the streamgages (fig. H7*A*), indicating construction of the impoundment rather than operation of the impoundment. Other attributions of change points for streamgages for the 50-year period include interbasin water transfers (9.5 percent), urban effects (6.8 percent), artificial wastewater and water supply discharges (5.4 percent), small artificial impoundments (1.4 percent), short-term precipitation* (1.4 percent), and short-term precipitation (1.4 percent) (fig. H7*A*).

The change point statistics of the median annual peak streamflow for the 75-year period (water years 1941–2015) indicated the *p*-value is less than 0.1 for 63 streamgages, including 10 of the LWRPF streamgages (table H5). The smaller number of streamgages identified in the data from the 75-year period is primarily due to fewer streamgages with a continuous record from the 75-year period. The same four primary attributions in the 75-year analysis period (fig. H7*B*) are determined to be dominant, as were the four primary attributions in the 50-year analysis period (fig. H7*A*), but the distribution varies somewhat. Primary attributions of change points for the 75-year period included large artificial impoundments, which accounted for 23.8 percent of the streamgages; large artificial impoundments*, which accounted for 22.2 percent of the streamgages; surface-water withdrawals, which accounted for 15.9 percent of the streamgages; and groundwater withdrawals, which accounted for 12.7 percent of the streamgages. The higher percentage of large artificial impoundments in the 75-year period (23.8 percent) compared to the 50-year period (10.8 percent) is due to a greater number of impoundments being constructed over the 75-year period than the 50-year period.

Short-term precipitation, short-term precipitation* (short-term precipitation with a secondary attribution), and small artificial impoundments are possible attributions in the 50-year period but not in the 75-year period (fig. H7*B*). Flooding from Hurricane Floyd in 1999 and another large storm in 2006 (at streamgage 02049500, at Blackwater River near Franklin, Va.) resulted in a significant correlation between precipitation and the increase in median annual peak streamflow for the 50-year period, but not for the 75-year period. The two streamgages identified as having significant change points in annual peak streamflow due to small artificial impoundments for the 50-year period were (1) streamgage 03455500 at West Fork Pidgeon River above Lake Logan near Hazelwood, N.C., and (2) streamgage 02169500 at Congaree River at Columbia, S.C. These two streamgages were not considered to have a statistically significant change point in median annual peak streamflow over the 75-year period (tables H4, H5).

Totaling the attributions by the number of streamgages does not account for the relative magnitudes of change points in median annual peak streamflow between streamgages, so the fraction of streamgages for each attribution were also weighted by the post-step peak streamflow (table H5; fig. H8*A*). This yields the attribution of change points associated with the highest percentage of streamgages for the 50-year median analysis as large artificial impoundments* (44.6 percent of the streamgages), followed by surface-water withdrawals (23.0 percent of the streamgages), and large artificial impoundments (13.6 percent of the streamgages). Large artificial impoundments* is consistently the attribution of change points determined to be associated with the largest percentage of streamgages for the 50-year period whether weighted by the number of streamgages (fig. H7*A*) or by post-step median annual peak streamflow (fig. H8*A*). The dominance of large artificial impoundments for the highest percentage of streamgages is evident, but it must also be considered that the operation of large artificial impoundments is affected by a variety of factors, including water supply, power generation, precipitation, and population. These factors also affect the attribution surface-water withdrawals, which involves non-impoundment related water use.

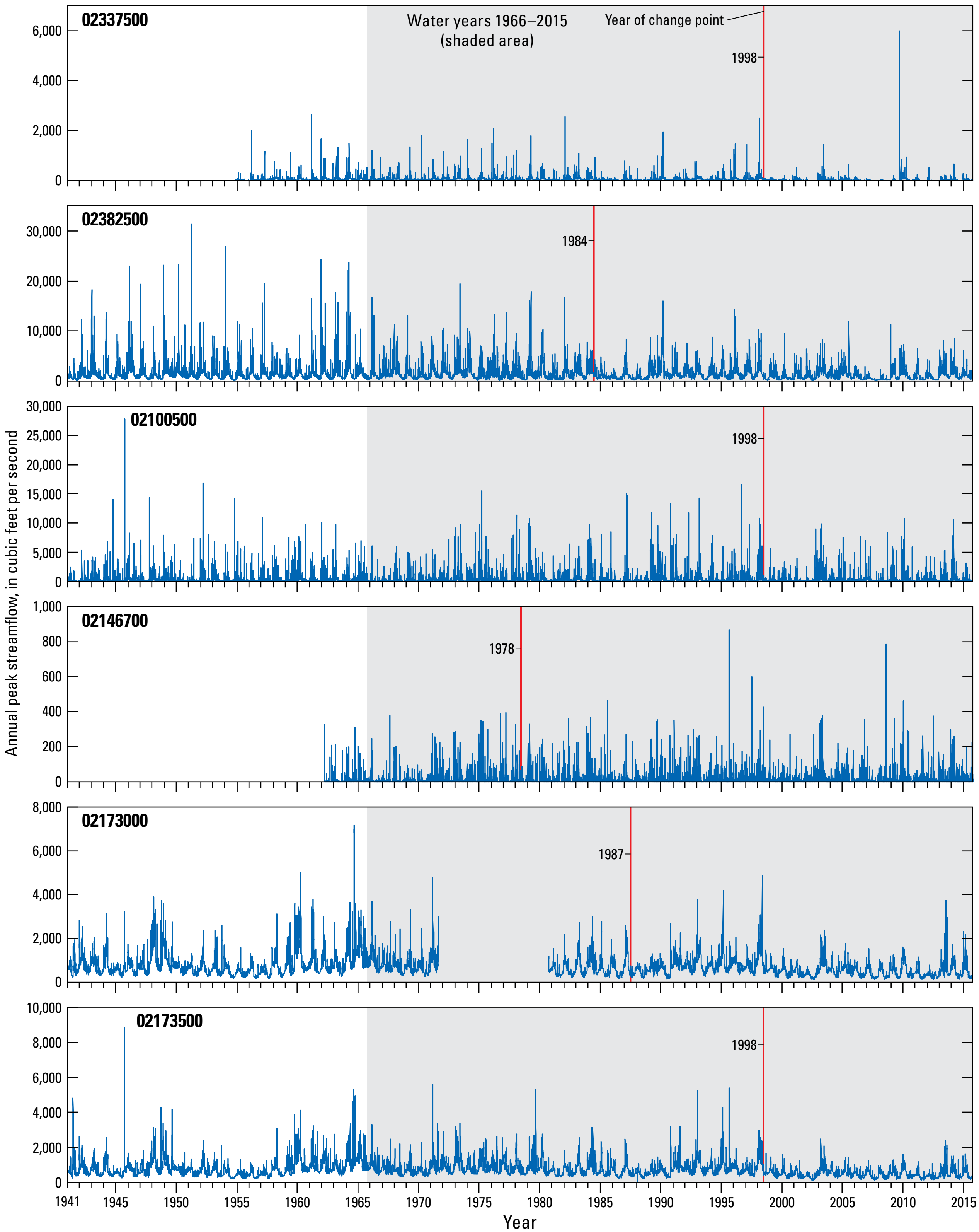

Figure H6. Graphs showing the daily streamflow from 6 selected streamgages from Georgia (02337500 and 02382500), North Carolina (02100500 and 02146700), and South Carolina (02173000 and 02173500) for the 50-year period (water years 1966–2015, shaded on the graphs). Associated streamgage locations shown in figure H3 are numbers 124 and 138 (02337500 and 02382500) in Georgia, 231 and 264 (02100500 and 02146700) in North Carolina, and 304 and 305 (02173000 and 02173500) in South Carolina. The red line in each of the six graphs indicates the year the change point in annual peak streamflow was identified from the change-point data and statistics in table H4. The gaps in data for three of the streamgages (02337500, 02146700, and 02173000) are years when no data were recorded due to streamgage failure or inactivation. Data from Swain and York (2022).

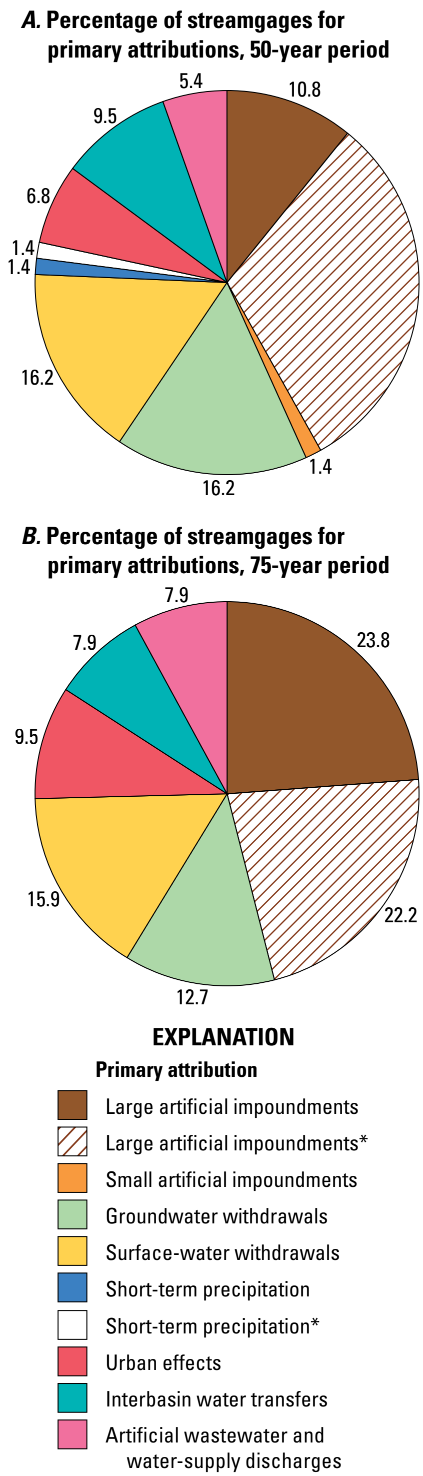

Figure H7. Pie charts showing the percentage of streamgages for primary attributions of change points in median annual peak streamflow for the 50- and 75-year periods. *A*, Percentage of streamgages for primary attributions for the 50-year period (water years 1966–2015). *B*, Percentage of streamgages for primary attributions for the 75-year period (water years 1941–2015). Each pie chart wedge in parts *A* and *B* represents the percentage of streamgages for the indicated primary attribution. “Large artificial impoundments*” has a primary attribution of large artificial impoundments with the asterisk (*) indicating a significant secondary attribution of short-term precipitation, interbasin water transfer, surface water withdrawals, or urban effects (see tables H4–H7); and “short-term precipitation*” has a primary attribution of short-term precipitation with the asterisk (*) indicating a secondary attribution of long-term precipitation (hurricanes and tropical storms) (see tables H4–H7). Data from Swain and York (2022).

The results of the 75-year median attribution analysis are also weighed by post-step median annual peak streamflows, which resulted in large artificial impoundments as the attribution of change points associated with the highest percentage of streamgages at 28.9 percent, slightly more than large artificial impoundment* at 26.1 percent (fig. H8*B*). These results that show large artificial impoundments associated with the highest percentage of streamgages and large artificial impoundments* associated with the second highest percentage of streamgages is the same as when the 75-year median attribution analysis is weighted by the number of streamgages (fig. H7*B*). Once again, the 75-year median attribution analysis indicates a higher percentage of change points due to large artificial impoundments than the 50-year median attribution analysis, because more impoundments were constructed over the 75-year period, and it indicates a smaller percentage of change points due to withdrawals from large artificial impoundments. However, these two attributions (large artificial impoundments and large artificial impoundments*) are merely differentiating between the creation of large impoundments and the operations of large impoundments, respectively, so the importance of impoundment reservoirs, their water-supply withdrawals and hydropower/flood-control regulation in the median annual peak streamflow in the Southeast region is emphasized by all of the median statistic results (figs. H7, H8). For the attributions of change points in median annual peak streamflow, short-term precipitation, short-term precipitation*, and small artificial impoundments are the only primary attributions for the 50-year period, but not for the 75-year period (figs. H7, H8).

The monotonic trend data for the 50-year period are tabulated and ranked by streamgage according to the monotonic trend in annual peak streamflow (table H6). Comparison of the rank of the pre-step and post-step median annual peak streamflows in table H4 (columns 5, 6) with the rank of monotonic trends in median annual peak streamflow in table H6 (column 4) shows that the same direction (positive or negative) is indicated in both the monotonic trend analysis in median annual peak streamflow and the change point analysis in median annual peak streamflow, and it also indicates a similar rank of the change point magnitudes of the streamgages (column 7 in tables H4–H5 and column 4 in tables H6–H7). The monotonic trend data for the 75-year period (table H7) also ranks the streamgages by the monotonic trend in median annual peak streamflow in a similar order as the rank of streamgages by the change points in pre-step and post-step median annual peak streamflows (table H5).

The pre-step and post-step interquartile ranges, the difference between the 75th and 25th percentiles of the median annual peak streamflow, are computed with the Mood test (Mood, 1954). The interquartile range statistics in median annual peak streamflow are assigned attributions for all streamgages where the percent change between the interquartile ranges in the 75- and 50-year periods before and after the change point (pre- and post-step median annual peak streamflow, respectively) is greater than 50 percent. For the 50-year period, this includes 31 streamgages (table H8). When distributed by the number of streamgages, large artificial impoundments with a significant secondary attribution (large artificial impoundments*) is the attribution with the highest percentage of streamgages at 35.5 percent, followed by interbasin water transfers at 22.6 percent, and large artificial impoundments at 12.9 percent (fig. H9*A*). The attribution interbasin water transfers was determined to be associated with only 9.5 percent of the streamgages in the 50-year change point analysis in median annual peak streamflow (fig. H7*A*). The Mood test that determines the interquartile range statistic detects changes in the range of the annual peak streamflow, whereas the median change point analysis (fig. H7*A*) detects change points in the magnitude of the median annual peak streamflow. Comparison of figures H7*A* and H9*A* indicates that streamgages with the attribution interbasin water transfers have less change in the magnitude of the annual peak streamflow relative to the interquartile range of the annual peak streamflow. The interbasin water transfers attribution covers most structural changes that do not involve impoundments, such as modifications of riverways and the redistribution of water through withdrawal and release. The large artificial impoundment attribution tends to affect the magnitudes of median annual peak streamflow more substantially, as the impoundments are a more dramatic modification to the riverflow system.

Distributing the 50-year interquartile range by the post-step median annual peak streamflows (post-step flows) indicates that large artificial impoundments* is by far the attribution with the highest percentage of streamgages at 61.7 percent, followed by large artificial impoundments with the second highest percentage of streamgages at 14.9 percent (fig. H10*A*). When weighting the attributions for the 50-year interquartile range (fig. H9*A*), the attribution interbasin water transfers is the second highest percentage of streamgages (22.6 percent), but it changes to the third highest percentage of streamgages (8.9 percent) when weighting by the post-step interquartile range (fig. H10*A*). Weighting the results by the magnitudes or the interquartile ranges of the annual peak streamflow consistently increases the percentage of streamgages associated with large artificial impoundments both with and without secondary attributions.

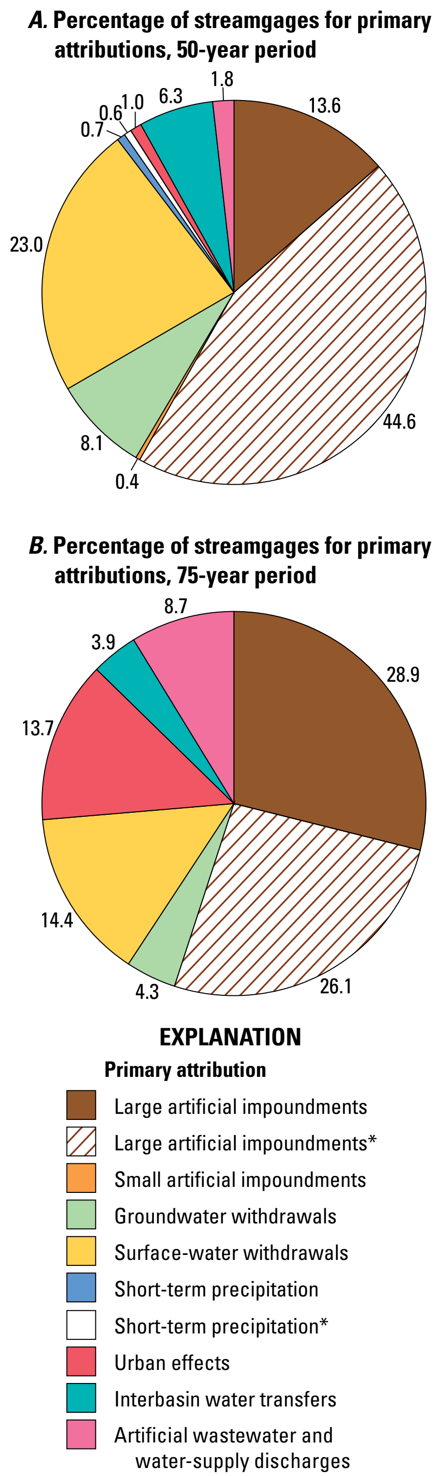

Figure H8. Pie charts showing the percentage of streamgages for primary attributions of change points weighted by the median annual peak streamflow after the change-point year (post-step flow) for the 50- and 75-year periods. *A*, Percentage of streamgages for primary attributions weighted by the median annual peak streamflow after the change-point year (post-step flow) for the 50-year period (water years 1966–2015). *B*, Percentage of streamgages for primary attributions weighted by the median annual peak streamflow after the change-point year (post-step flow) for the 75-year period (water years 1941–2015). Each pie chart wedge in parts *A* and *B* represents the percentage of streamgages for the indicated primary attribution. "Large artificial impoundments*" has a primary attribution of large artificial impoundments with the asterisk (*) indicating a significant secondary attribution of short-term precipitation, interbasin water transfer, surface water withdrawals, or urban effects (see tables H4–H7); and "short-term precipitation*" has a primary attribution of short-term precipitation with the asterisk (*) indicating a secondary attribution of long-term precipitation (hurricanes and tropical storms) (see tables H4–H7). Data from Swain and York (2022).

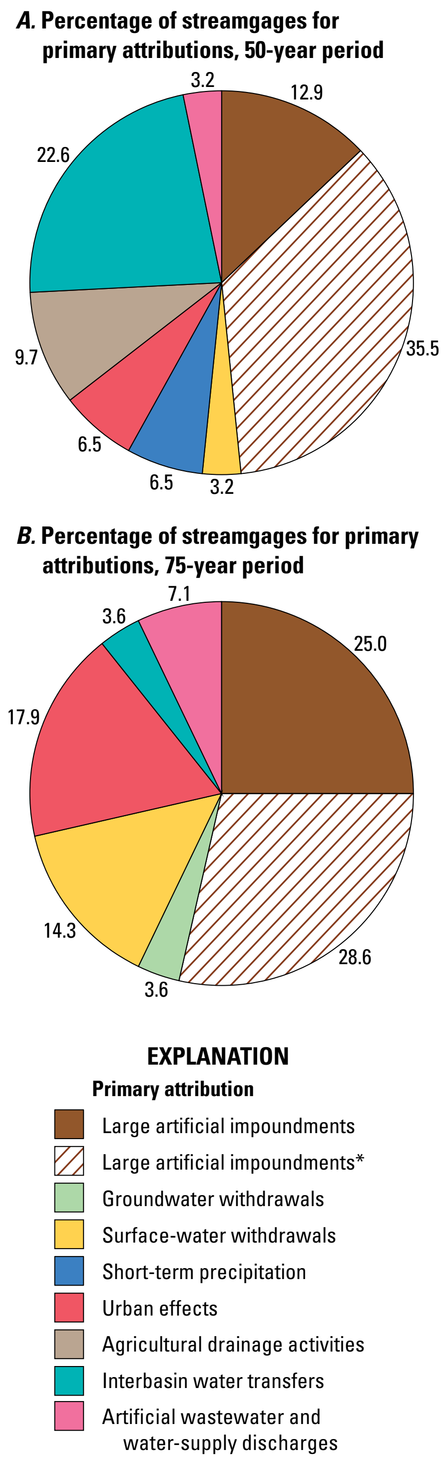

Figure H9. Pie charts showing the percentage of streamgages for primary attributions of change points in median annual peak streamflow using the interquartile range (Mood test) for the 50- and 75-year periods. *A*, Percentage of streamgages for primary attributions of change points for the 50-year period (water years 1966–2015). *B*, Percentage of streamgages for primary attributions of change points for the 75-year period (water years 1941–2015). Each pie chart wedge in parts *A* and *B* represents the percentage of streamgages for the indicated primary attribution. “Large artificial impoundments*” has a primary attribution of large artificial impoundments with the asterisk (*) indicating a significant secondary attribution of short-term precipitation, interbasin water transfer, surface water withdrawals, or urban effects (see tables H4–H7). Data from Swain and York (2022).

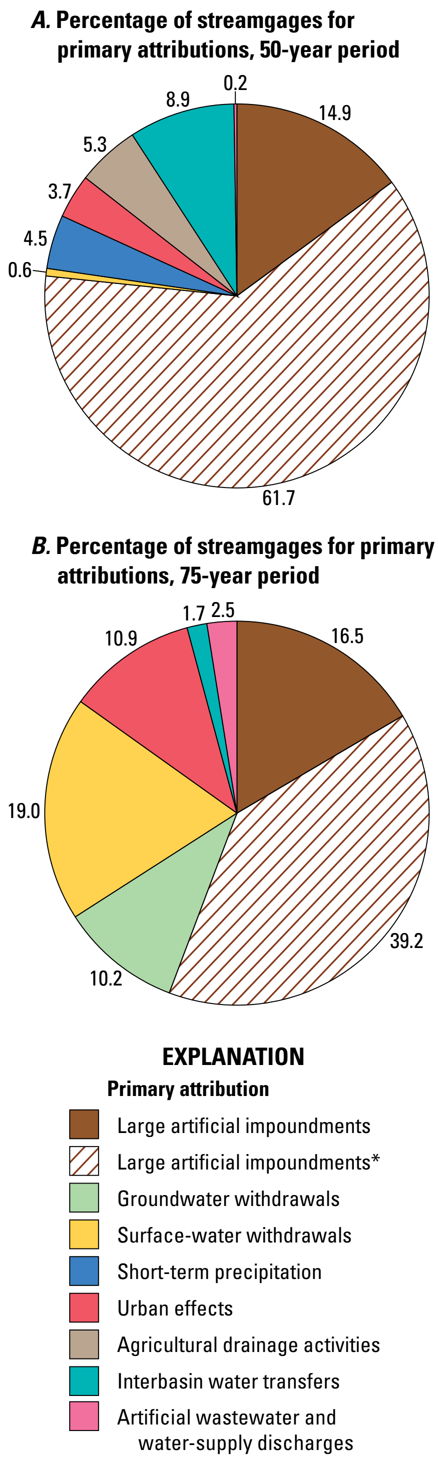

Figure H10. Pie charts showing the percentage of streamgages for primary attributions of change points in median annual peak streamflow weighted by the interquartile range (Mood test) after the change-point year (post-step flow) for the 50- and 75-year periods. *A*, Percentage of streamgages for the indicated primary attributions for the 50-year period (water years 1966–2015). *B*, Percentage of streamgages for the indicated primary attributions for the 75-year period (water years 1941–2015). Each pie chart wedge in parts *A* and *B* represents the percentage of streamgages for the indicated primary attribution. "Large artificial impoundments*" has a primary attribution of large artificial impoundments with the asterisk (*) indicating a significant secondary attribution of short-term precipitation, interbasin water transfer, surface water withdrawals, or urban effects (see tables H4–H7). "Post-step flow" is the median annual peak streamflow after the change-point year. Data from Swain and York (2022).

The interquartile range in annual peak streamflow for the 75-year period yielded 28 streamgages where the percent change between the pre-step and post-step interquartile ranges is greater than 50 percent (table H9). Large artificial impoundments* is the attribution with the highest percentage of streamgages at 28.6 percent, followed by large artificial impoundments at 25.0 percent of the streamgages (fig. H9*B*). The urban effects attribution was associated with the third highest percentage of streamgages at 17.9 percent, higher than the other analyses. This indicates that, over the 75-year period, the increases in impervious areas and the changes in runoff patterns affect the range of annual peak streamflow more than in the 50-year period, reflecting urban growth since the early 1940s. Distributing the 75-year interquartile range by the post-step annual peak streamflows (post-strep flows) yields large artificial impoundments* as the attribution with the highest percentage of streamgages at 39.2 percent, and surface-water withdrawals with the second highest percentage of streamgages at 19.0 percent (fig. H10*B*). Large artificial impoundments was associated with the third highest percentage of streamgages at 16.5 percent. For the interquartile range analysis, short-term precipitation and agricultural drainage activities are the only important attributions for the 50-year period that are not significant in the 75-year period. Groundwater withdrawals is the only important attribution for the 75-year period that is not significant in the 50-year period (figs. H9, H10).

Summary

The methods applied in this report use a variety of indicators and interpretations to determine the attributions of monotonic trends and change points in annual peak streamflow for the 50-year period (1966–2015) and 75-year period (1941–2015), and care must be taken when interpreting these results. The primary element bringing uncertainty into this analysis are the assumptions in the attributions of monotonic trends and change points. The criteria used to determine the attributions and hydrologic occurrences for significant monotonic trends and change points in the annual peak streamflow are chosen in an attempt to find the most likely cause for the monotonic trend or change point based on the available information for each streamgage site, but the correlation of the attribution and the monotonic trend or change point does not prove causality. The confidence in the attribution is indicated in the level of evidence in tables H4 to H9; either robust evidence, medium evidence, limited evidence, or additional information required. A minimum categorization of “limited evidence” was specified for the majority of the streamgages, which means that a reasonable explanation for the monotonic trend or change point in annual peak streamflow could be determined at most streamgage locations.

The attributions of monotonic trends or change points in annual peak streamflow that most consistently affect the greatest number of streamgages generally involve direct anthropogenic alterations to the waterways. Combining the 50- and 75-year change-point analyses, the following attributions are indicated in descending order of occurrence: large artificial impoundments* (the * indicates a secondary attribution substantially affects the streamgage), large artificial impoundments (with no secondary attribution), surface-water withdrawals, groundwater withdrawals, interbasin water transfer, urban effects, and with equal occurrences small artificial impoundments, short-term precipitation, and short-term precipitation* (the * indicates a secondary attribution of long-term precipitation; this combination of primary and secondary attributions indicates that hurricanes or tropical storms are a factor at the streamgage).

Geographically, attributions of monotonic trends and change points in annual peak streamflow are associated with large population centers such as Atlanta, Georgia, and to a lesser degree the cities of Augusta and Macon, Georgia, and Charlotte, North Carolina, likely because of impoundment and reservoir construction, water use. and effects of changing land cover that are associated with these locations. Smaller municipalities are also indicated to affect smaller river systems, because the percentage of population growth can be substantial over the periods of time that were analyzed.

The attributions developed in this report may be of interest in local studies and identifying hydrologic factors for water-management decision making. The integration of this analysis of the Southeast region with the other regions of the United States may help supply the Nation with important annual peak-streamflow information.

References Cited

Anandhi, A., Crandall, C., and Bentley, C., 2018, Hydrologic characteristics of streamflow in the Southeast Atlantic and Gulf Coast hydrologic region during 1939–2016 and conceptual map of potential impacts: Hydrology, v. 5, no. 3, 18 p., accessed September 25, 2020, at https://doi.org/10.3390/hydrology5030042.

Chamberlin, T.C., 1965, The method of multiple working hypotheses (reprint): Science, v. 148, no. 3671, p. 754–759, accessed September 25, 2020, at https://doi.org/10.1126/science.148.3671.754.

Dudley, R.W., Archfield, S.A., Hodgkins, G.A., Renard, B., and Ryberg, K.R., 2018, Peak-streamflow trends and change-points and basin characteristics for 2,683 U.S. Geological Survey streamgages in the conterminous U.S. (ver. 3.0, April 2019): U.S. Geological Survey data release, accessed April 15, 2021, at https://doi.org/10.5066/P9AEGXY0.

Falcone, J.A., 2011, GAGES-II—Geospatial attributes of gages for evaluating streamflow: U.S. Geological Survey dataset, accessed October 29, 2020, at https://water.usgs.gov/lookup/getspatial?gagesII_Sept2011.

Falcone, J.A., 2015, U.S. conterminous wall-to-wall anthropogenic land use trends (NWALT), 1974–2012: U.S. Geological Survey Data Series 948, 33 p., plus appendixes 3–6 as separate files, accessed October 29, 2020, https://doi.org/10.3133/ds948.

Hirsch, R.M., Slack, J.R., and Smith, R.A., 1982, Techniques of trend analysis for monthly water quality data: Water Resources Research, v. 18, no. 1, p. 107–121. [Also available at https://doi.org/10.1029/WR018i001p00107.]

Hodgkins, G.A., Dudley, R.W., Archfield, S.A., and Renard, B., 2019, Effects of climate, regulation, and urbanization on historical flood trends in the United States: Journal of Hydrology, v. 573, p. 697–709, accessed December 30, 2020, at https://doi.org/10.1016/j.jhydrol.2019.03.102.

Mood, A.M., 1954, On the asymptotic efficiency of certain nonparametric two-sample tests: Annals of Mathematical Statistics, v. 25, no. 3, p. 514–522. [Also available at https://www.jstor.org/stable/2236833.]

National Oceanic and Atmospheric Administration, National Weather Service, 2019, Precipitation frequency—Data server: National Oceanic and Atmospheric Administration, National Weather Service web page, accessed May 8, 2019, at https://hdsc.nws.noaa.gov/hdsc/pfds/pfds_series.html.

North Carolina Climate Office, 2019, Southeast precipitation: North Carolina Climate Office web page, accessed May 8, 2019, at https://climate.ncsu.edu/edu/SEPrecip.

Pettitt, A.N., 1979, A non-parametric approach to the change-point problem: Journal of the Royal Statistical Society, Series C [Applied Statistics], v. 28, no. 2, p. 126–135. [Also available at https://www.jstor.org/stable/2346729.]

Powell, E.J., and Keim, B.D., 2015, Trends in daily temperature and precipitation extremes for the southeastern United States—1948–2012: Journal of Climate, v. 28, no. 4, p. 1592–1612, accessed May 19, 2021, at https://doi.org/10.1175/JCLI-D-14-00410.1.

Ross, G.J., Tasoulis, D.K., and Adams, N.M., 2011, Nonparametric monitoring of data streams for changes in location and scale: Technometrics, v. 53, no. 4, p. 379–389, accessed October 15, 2020, at https://doi.org/10.1198/TECH.2011.10069.

Ryberg, K.R., Hodgkins, G.A., and Dudley, R.W., 2019, Change points in annul peak streamflows—Method comparisons and historical change points in the United States: Journal of Hydrology, v. 583, article 124307, 13 p., accessed October 15, 2020, at https://doi.org/10.1016/j.jhydrol.2019.124307.

Seaber, P.R., Kapinos, F.P., and Knapp, G.L., 1987, Hydrologic unit maps: U.S. Geological Survey Water-Supply Paper 2294, 63 p., 1 pl. in pocket, accessed February 18, 2022, at https://doi.org/10.3133/wsp2294.

Sen, P.K., 1968, Estimates of the regression coefficient based on Kendall's tau: Journal of the American Statistical Association, v. 63, no. 324, p. 1379–1389. [Also available at https://doi.org/10.1080/01621459.1968.10480934.]

Singh, S.P, and Singh, V., 2016, Addressing rural decline by valuing agricultural ecosystem services and treating food production as a social contribution: Tropical Ecology, v. 57, no. 3, p. 381–392. [Also available at https://radicalecologicaldemocracy.org/wp-content/uploads/2016/04/Singh-and-Singh-paper.pdf.]

Swain, E.D., and York, B.C., 2022, Attributions for nonstationary peak streamflow records in the Southeast region, 1941–2015 and 1966–2015, and supporting information, *in* York, B.C., Ryberg, K.R., Asquith, W.H., Chase, K.J., Dickinson, J.E., Dudley, R.W., Harden, T.M., Hodgkins, G.A., Holtschlag, D.J., Humberson, D.G., Konrad, C.P., Levin, S.B., Restivo, D.E., Sando, R., Sando, S.K., Swain, E.D., Tillery, A.C., and Totten, A.R., Attributions for nonstationary peak streamflow records across the conterminous United States, 1941–2015 and 1966–2015: U.S. Geological Survey data release, https://doi.org/10.5066/P9FOUVWG. [Data directly accessible at https://www.sciencebase.gov/catalog/item/5cd5be1be4b0e8a309e46227.]

Tollan, A., 2002, Land-use change and floods—What do we need most, research or management?: Water Science and Technology, v. 45, no. 8, p. 183–190, accessed May 19, 2021, at https://doi.org/10.2166/wst.2002.0176.

Traylor, J.P., and Zlotnik, V.A., 2016, Analytical modeling of irrigation and land use effects on streamflow in semi-arid conditions: Journal of Hydrology, v. 533, p. 591–602, accessed May 19, 2021, at https://doi.org/10.1016/j.jhydrol.2015.12.006.

U.S. Geological Survey, 2007, North America elevation 1-kilometer-resolution GRID [dataset]: U.S. Geological Survey ScienceBase Catalog website, accessed May 1, 2019, at https://www.sciencebase.gov/catalog/item/4fb5495ee4b04cb937751d6d.

Weaver, J.C., 2005, The drought of 1998–2002 in North Carolina—Precipitation and hydrologic conditions: U.S. Geological Survey Scientific Investigations Report 2005–5053, 88 p. [Also available at https://doi.org/10.3133/sir20055053.]

York, B.C., Ryberg, K.R., Asquith, W.H., Chase, K.J., Dickinson, J.E., Dudley, R.W., Harden, T.M., Hodgkins, G.A., Holtschlag, D.J., Humberson, D.G., Konrad, C.P., Levin, S.B., Restivo, D.E., Sando, R., Sando, S.K., Swain, E.D., Tillery, A.C., and Totten, A.R., 2022, Attributions for nonstationary peak streamflow records across the conterminous United States, 1941–2015 and 1966–2015: U.S. Geological Survey data release, https://doi.org/10.5066/P9FOUVWG.

Tables H1–H9

Table H1. Streamgages used in this report to determine attributions of monotonic trends and change points in annual peak streamflow in the Southeast region of the United States.

[The map locations (1–357) of streamgages are shown in figure H3. Data from Dudley and others (2018); streamgage names are quoted from the National Water Information System. For additional notes on streamgages, see Swain and York (2022). ABV, above; AL, Alabama; AL., Alabama; AR, Arkansas; CR, Creek; FL, Florida; FLA, Florida; FLA., Florida; FT., Fort; GA, Georgia; LA, Louisiana; L&D, lock and dam; MO, Missouri; MS, Mississippi; MT., Mount; n.a., not available; NC, North Carolina; N F, North Fork; nr, near; NR, near; NR., near; R, River; R., River; RD, Road; SC, South Carolina; S F, South Fork; St., Saint; TN, Tennessee; US, United States; VA, Virginia; WILM, William; km², square kilometers]

Streamgage number	State	Streamgage name/location	Drainage area, in km²	Map location (fig. H3)
02342500	AL	UCHEE CREEK NEAR FORT MITCHELL, AL.	834.0	1
02361000	AL	CHOCTAWHATCHEE RIVER NEAR NEWTON, AL.	1,776.7	2
02363000	AL	PEA RIVER NEAR ARITON AL	1,289.8	3
02371500	AL	CONECUH RIVER AT BRANTLEY AL	1,295.0	4
02374500	AL	MURDER CREEK NEAR EVERGREEN AL	455.8	5
02376500	AL	PERDIDO RIVER AT BARRINEAU PARK, FL	1,020.5	6
02398300	AL	CHATTOOGA RIVER ABOVE GAYLESVILLE AL	947.9	7
02399200	AL	LITTLE RIVER NEAR BLUE POND AL	515.4	8
02400100	AL	TERRAPIN CREEK AT ELLISVILLE AL	652.7	9
02401390	AL	BIG CANOE CREEK AT ASHVILLE AL	365.2	10
02412000	AL	TALLAPOOSA RIVER NEAR HEFLIN, AL.	1,160.3	11
02414500	AL	TALLAPOOSA RIVER AT WADLEY AL	4,338.2	12
02419000	AL	UPHAPEE CREEK NEAR TUSKEGEE AL	862.5	13
02421000	AL	CATOMA CREEK NEAR MONTGOMERY AL	751.1	14
02422500	AL	MULBERRY CREEK AT JONES AL	525.8	15
02424000	AL	CAHABA RIVER AT CENTREVILLE AL	2,659.9	16
02438000	AL	BUTTAHATCHEE RIVER BELOW HAMILTON AL	717.4	17
02448500	AL	NOXUBEE RIVER NR GEIGER, AL	2,841.2	18
02450000	AL	MULBERRY FORK NEAR GARDEN CITY, AL.	927.2	19
02450250	AL	SIPSEY FORK NEAR GRAYSON AL	238.5	20
02455000	AL	LOCUST FORK NEAR CLEVELAND, AL.	784.8	21
02456500	AL	LOCUST FORK AT SAYRE, AL.	2,292.1	22
02462000	AL	VALLEY CREEK NEAR OAK GROVE AL	383.3	23
02464000	AL	NORTH RIVER NEAR SAMANTHA AL	577.6	24
02465000	AL	BLACK WARRIOR RIVER AT NORTHPORT AL	12,483.7	25
02467500	AL	SUCARNOOCHEE RIVER AT LIVINGSTON AL	1,572.1	26
02469800	AL	SATILPA CREEK NEAR COFFEEVILLE AL	424.8	27
02471001	AL	CHICKASAW CREEK NEAR KUSHLA AL	323.7	28
03574500	AL	PAINT ROCK RIVER NEAR WOODVILLE AL	828.8	29
07077380	AR	Cache River at Egypt, AR	1,815.6	30
07264000	AR	Bayou Meto near Lonoke, AR	536.1	31
07356000	AR	Ouachita River near Mount Ida, AR	1,072.3	32
07361500	AR	Antoine River at Antoine, AR	461.0	33
07362100	AR	Smackover Creek near Smackover, AR	997.1	34
07363500	AR	Saline River near Rye, AR	5,439.0	35
07364150	AR	Bayou Bartholomew near McGehee, AR	1,491.8	36
02231000	FL	ST. MARYS RIVER NEAR MACCLENNY, FL	1,813.0	37
02231600	FL	JANE GREEN CREEK NEAR DEER PARK, FL	642.3	38
02232200	FL	WOLF CREEK NEAR DEER PARK, FL	66.6	39

Table H1. Streamgages used in this report to determine attributions of monotonic trends and change points in annual peak streamflow in the Southeast region of the United States.—Continued

[The map locations (1–357) of streamgages are shown in figure H3. Data from Dudley and others (2018); streamgage names are quoted from the National Water Information System. For additional notes on streamgages, see Swain and York (2022). ABV, above; AL, Alabama; AL., Alabama; AR, Arkansas; CR, Creek; FL, Florida; FLA, Florida; FLA., Florida; FT., Fort; GA, Georgia; LA, Louisiana; L&D, lock and dam; MO, Missouri; MS, Mississippi; MT., Mount; n.a., not available; NC, North Carolina; N F, North Fork; nr, near; NR, near; NR., near; R, River; R., River; RD, Road; SC, South Carolina; S F, South Fork; St., Saint; TN, Tennessee; US, United States; VA, Virginia; WILM, William; km^2, square kilometers]

Streamgage number	State	Streamgage name/location	Drainage area, in km^2	Map location (fig. H3)
02233200	FL	LITTLE ECONLOCKHATCHEE RIVER NEAR UNION PARK, FL	70.2	40
02233500	FL	ECONLOCKHATCHEE RIVER NEAR CHULUOTA, FL	624.2	41
02236500	FL	BIG CREEK NEAR CLERMONT, FL	176.1	42
02245500	FL	SOUTH FORK BLACK CREEK NEAR PENNEY FARMS, FL	347.1	43
02246000	FL	NORTH FORK BLACK CREEK NEAR MIDDLEBURG, FL	458.4	44
02247510	FL	TOMOKA RIVER NEAR HOLLY HILL, FL	198.9	45
02248000	FL	SPRUCE CREEK NEAR SAMSULA, FL	86.5	46
02256500	FL	FISHEATING CREEK AT PALMDALE, FL	805.5	47
02263800	FL	SHINGLE CREEK AT AIRPORT NEAR KISSIMMEE, FL	231.0	48
02264000	FL	CYPRESS CREEK AT VINELAND, FL	75.9	49
02266300	FL	REEDY CREEK NEAR VINELAND, FL	219.1	50
02294491	FL	SADDLE CREEK AT the P–11 Water Conservation Structure NEAR BARTOW FL	349.6	51
02294650	FL	PEACE RIVER AT BARTOW FL	1,010.1	52
02295637	FL	PEACE RIVER AT ZOLFO SPRINGS FL	2,139.3	53
02296500	FL	CHARLIE CREEK NEAR GARDNER FL	854.7	54
02296750	FL	PEACE RIVER AT ARCADIA FL	3,540.5	55
02297100	FL	JOSHUA CREEK AT NOCATEE FL	341.9	56
02297310	FL	HORSE CREEK NEAR ARCADIA FL	564.6	57
02298830	FL	MYAKKA RIVER NEAR SARASOTA FL	593.1	58
02299950	FL	MANATEE RIVER NEAR MYAKKA HEAD FL	169.1	59
02300100	FL	LITTLE MANATEE RIVER NEAR FT. LONESOME FL	81.3	60
02300500	FL	LITTLE MANATEE RIVER NEAR WIMAUMA FL	385.9	61
02300700	FL	BULLFROG CREEK NEAR WIMAUMA FL	75.4	62
02301300	FL	SOUTH PRONG ALAFIA RIVER NEAR LITHIA FL	277.1	63
02301500	FL	ALAFIA RIVER AT LITHIA FL	867.6	64
02301900	FL	FOX BRANCH NEAR SOCRUM, FL	24.6	65
02302500	FL	BLACKWATER CREEK NEAR KNIGHTS FL	284.9	66
02303000	FL	HILLSBOROUGH RIVER NEAR ZEPHYRHILLS FL	569.8	67
02303400	FL	CYPRESS CREEK NEAR SAN ANTONIO FL	145.0	68
02303800	FL	CYPRESS CREEK NEAR SULPHUR SPRINGS FL	414.4	69
02306500	FL	SWEETWATER CREEK NEAR SULPHUR SPRINGS FL	19.2	70
02307000	FL	ROCKY CREEK NEAR SULPHUR SPRINGS FL	90.6	71
02307359	FL	BROOKER CREEK NEAR TARPON SPRINGS FL	77.7	72
02310000	FL	ANCLOTE RIVER NEAR ELFERS FL	187.8	73
02312000	FL	WITHLACOOCHEE RIVER AT TRILBY, FL	1,476.3	74
02312200	FL	LITTLE WITHLACOOCHEE RIVER AT RERDELL, FL	375.5	75
02312500	FL	WITHLACOOCHEE RIVER AT CROOM, FL	2,097.9	76
02313000	FL	WITHLACOOCHEE RIVER NEAR HOLDER, FL	4,726.7	77
02319000	FL	WITHLACOOCHEE RIVER NEAR PINETTA, FLA.	5,490.8	78

Table H1. Streamgages used in this report to determine attributions of monotonic trends and change points in annual peak streamflow in the Southeast region of the United States.—Continued

[The map locations (1–357) of streamgages are shown in figure H3. Data from Dudley and others (2018); streamgage names are quoted from the National Water Information System. For additional notes on streamgages, see Swain and York (2022). ABV, above; AL, Alabama; AL., Alabama; AR, Arkansas; CR, Creek; FL, Florida; FLA, Florida; FLA., Florida; FT., Fort; GA, Georgia; LA, Louisiana; L&D, lock and dam; MO, Missouri; MS, Mississippi; MT., Mount; n.a., not available; NC, North Carolina; N F, North Fork; nr, near; NR, near; NR., near; R, River; R., River; RD, Road; SC, South Carolina; S F, South Fork; St., Saint; TN, Tennessee; US, United States; VA, Virginia; WILM, William; km², square kilometers]

Streamgage number	State	Streamgage name/location	Drainage area, in km²	Map location (fig. H3)
02319500	FL	SUWANNEE RIVER AT ELLAVILLE, FLA	18,052.2	79
02321500	FL	SANTA FE RIVER AT WORTHINGTON SPRINGS, FLA.	1,489.2	80
02322500	FL	SANTA FE RIVER NEAR FORT WHITE, FLA.	2,634.0	81
02324000	FL	STEINHATCHEE RIVER NEAR CROSS CITY, FLA.	906.5	82
02324400	FL	FENHOLLOWAY RIVER NEAR FOLEY, FLA.	155.4	83
02326000	FL	ECONFINA RIVER NEAR PERRY, FLA.	512.8	84
02327100	FL	SOPCHOPPY RIVER NR SOPCHOPPY, FLA.	264.2	85
02329000	FL	OCHLOCKONEE RIVER NR HAVANA, FLA.	2,952.6	86
02330000	FL	OCHLOCKONEE RIVER NR BLOXHAM, FLA.	4,403.0	87
02358000	FL	APALACHICOLA RIVER AT CHATTAHOOCHEE FLA	44,547.8	88
02359000	FL	CHIPOLA RIVER NR ALTHA, FLA.	2,022.8	89
02366500	FL	CHOCTAWHATCHEE RIVER NR BRUCE, FLA.	11,354.5	90
02368000	FL	YELLOW RIVER AT MILLIGAN, FLA.	1,616.2	91
02369000	FL	SHOAL RIVER NR CRESTVIEW, FLA.	1,227.7	92
02375500	FL	ESCAMBIA RIVER NEAR CENTURY, FL	9,886.0	93
02177000	GA	CHATTOOGA RIVER NEAR CLAYTON, GA	536.1	94
02178400	GA	TALLULAH RIVER NEAR CLAYTON, GA	151.3	95
02192000	GA	BROAD RIVER NEAR BELL, GA	3,677.8	96
02198000	GA	BRIER CREEK AT MILLHAVEN, GA	1,673.1	97
02202500	GA	OGEECHEE RIVER NEAR EDEN, GA	6,863.5	98
02203000	GA	CANOOCHEE RIVER NEAR CLAXTON, GA	1,437.4	99
02212600	GA	FALLING CREEK NEAR JULIETTE, GA	187.0	100
02213000	GA	OCMULGEE RIVER AT MACON, GA	5,801.6	101
02213500	GA	TOBESOFKEE CREEK NEAR MACON, GA	471.4	102
02215500	GA	OCMULGEE RIVER AT LUMBER CITY, GA	13,416.1	103
02217500	GA	MIDDLE OCONEE RIVER NEAR ATHENS, GA	1,030.8	104
02223000	GA	OCONEE RIVER AT MILLEDGEVILLE, GA	7,640.5	105
02223500	GA	OCONEE RIVER AT DUBLIN, GA	11,395.9	106
02225500	GA	OHOOPEE RIVER NEAR REIDSVILLE, GA	2,874.9	107
02226000	GA	ALTAMAHA RIVER AT DOCTORTOWN, GA	35,223.8	108
02226500	GA	SATILLA RIVER NEAR WAYCROSS, GA	3,211.6	109
02227500	GA	LITTLE SATILLA RIVER NEAR OFFERMAN, GA	1,706.8	110
02228000	GA	SATILLA RIVER AT ATKINSON, GA	7,226.1	111
02228500	GA	NORTH PRONG ST. MARYS RIVER AT MONIAC, GA	414.4	112
02314500	GA	SUWANNEE RIVER AT US 441, AT FARGO, GA	2,926.7	113
02317500	GA	ALAPAHA RIVER AT STATENVILLE, GA	3,548.3	114
02331600	GA	CHATTAHOOCHEE RIVER NEAR CORNELIA, GA	815.8	115
02333500	GA	CHESTATEE RIVER NEAR DAHLONEGA, GA	396.3	116
02334430	GA	CHATTAHOOCHEE RIVER AT BUFORD DAM, NEAR BUFORD, GA	2,693.6	117

Table H1. Streamgages used in this report to determine attributions of monotonic trends and change points in annual peak streamflow in the Southeast region of the United States.—Continued

[The map locations (1–357) of streamgages are shown in figure H3. Data from Dudley and others (2018); streamgage names are quoted from the National Water Information System. For additional notes on streamgages, see Swain and York (2022). ABV, above; AL, Alabama; AL., Alabama; AR, Arkansas; CR, Creek; FL, Florida; FLA, Florida; FLA., Florida; FT., Fort; GA, Georgia; LA, Louisiana; L&D, lock and dam; MO, Missouri; MS, Mississippi; MT., Mount; n.a., not available; NC, North Carolina; N F, North Fork; nr, near; NR, near; NR., near; R, River; R., River; RD, Road; SC, South Carolina; S F, South Fork; St., Saint; TN, Tennessee; US, United States; VA, Virginia; WILM, William; km^2, square kilometers]

Streamgage number	State	Streamgage name/location	Drainage area, in km^2	Map location (fig. H3)
02335000	GA	CHATTAHOOCHEE RIVER NEAR NORCROSS, GA	3,030.3	118
02335700	GA	BIG CREEK NEAR ALPHARETTA, GA	186.5	119
02336000	GA	CHATTAHOOCHEE RIVER AT ATLANTA, GA	3,755.5	120
02336300	GA	PEACHTREE CREEK AT ATLANTA, GA	224.8	121
02337000	GA	SWEETWATER CREEK NEAR AUSTELL, GA	616.4	122
02337170	GA	CHATTAHOOCHEE RIVER NEAR FAIRBURN, GA	5,335.4	123
02337500	GA	SNAKE CREEK NEAR WHITESBURG, GA	91.9	124
02338000	GA	CHATTAHOOCHEE RIVER NEAR WHITESBURG, GA	6,293.7	125
02339500	GA	CHATTAHOOCHEE RIVER AT WEST POINT, GA	9,194.5	126
02344500	GA	FLINT RIVER NEAR GRIFFIN, GA	704.5	127
02344700	GA	LINE CREEK NEAR SENOIA, GA	261.6	128
02347500	GA	FLINT RIVER AT US 19, NEAR CARSONVILLE, GA	4,791.5	129
02349605	GA	FLINT RIVER AT GA 26, NEAR MONTEZUMA, GA	7,562.8	130
02349900	GA	TURKEY CREEK AT BYROMVILLE, GA	123.0	131
02352500	GA	FLINT RIVER AT ALBANY, GA	13,752.8	132
02353000	GA	FLINT RIVER AT NEWTON, GA	14,866.5	133
02353500	GA	ICHAWAYNOCHAWAY CREEK AT MILFORD, GA	1,605.8	134
02380500	GA	COOSAWATTEE RIVER NEAR ELLIJAY, GA	611.2	135
02381600	GA	FAUSETT CREEK NEAR TALKING ROCK, GA	25.9	136
02382200	GA	TALKING ROCK CREEK NEAR HINTON, GA	308.2	137
02382500	GA	COOSAWATTEE RIVER AT CARTERS, GA	1,349.4	138
02383500	GA	COOSAWATTEE RIVER NEAR PINE CHAPEL, GA	2,152.3	139
02385800	GA	HOLLY CREEK NEAR CHATSWORTH, GA	165.8	140
02387000	GA	CONASAUGA RIVER AT TILTON, GA	1,779.3	141
02387500	GA	OOSTANAULA RIVER AT RESACA, GA	4,149.2	142
02388500	GA	OOSTANAULA RIVER NEAR ROME, GA	5,477.8	143
02392000	GA	ETOWAH RIVER AT CANTON, GA	1,587.7	144
02394000	GA	ETOWAH RIVER AT ALLATOONA DAM, ABV CARTERSVILLE, GA	2,906.0	145
02395980	GA	ETOWAH RIVER AT GA 1 LOOP, NEAR ROME, GA	4,664.6	146
02397000	GA	COOSA RIVER (MAYO'S BAR) NEAR ROME, GA	10,463.6	147
02398000	GA	CHATTOOGA RIVER AT SUMMERVILLE, GA	497.3	148
02492000	LA	Bogue Chitto River near Bush, LA	3,141.7	149
07366200	LA	Little Corney Bayou near Lillie, LA	538.7	150
07373000	LA	Big Creek at Pollock, LA	132.1	151
07375000	LA	Tchefuncte River near Folsom, LA	266.8	152
07375500	LA	Tangipahoa River at Robert, LA	1,673.1	153
07376000	LA	Tickfaw River at Holden, LA	639.7	154
07376500	LA	Natalbany River at Baptist, LA	205.9	155
07377000	LA	Amite River near Darlington, LA	1,502.2	156

Table H1. Streamgages used in this report to determine attributions of monotonic trends and change points in annual peak streamflow in the Southeast region of the United States.—Continued

[The map locations (1–357) of streamgages are shown in figure H3. Data from Dudley and others (2018); streamgage names are quoted from the National Water Information System. For additional notes on streamgages, see Swain and York (2022). ABV, above; AL, Alabama; AL., Alabama; AR, Arkansas; CR, Creek; FL, Florida; FLA, Florida; FLA., Florida; FT., Fort; GA, Georgia; LA, Louisiana; L&D, lock and dam; MO, Missouri; MS, Mississippi; MT., Mount; n.a., not available; NC, North Carolina; N F, North Fork; nr, near; NR, near; NR., near; R, River; R., River; RD, Road; SC, South Carolina; S F, South Fork; St., Saint; TN, Tennessee; US, United States; VA, Virginia; WILM, William; km², square kilometers]

Streamgage number	State	Streamgage name/location	Drainage area, in km²	Map location (fig. H3)
07377500	LA	Comite River near Olive Branch, LA	375.5	157
07378000	LA	Comite River near Comite, LA	735.6	158
07378500	LA	Amite River near Denham Springs, LA	3,315.2	159
07382000	LA	Bayou Cocodrie near Clearwater, LA	621.6	160
07385700	LA	Bayou Teche at Keystone L&D nr St. Martinville, LA	n.a.	161
08010000	LA	Bayou Des Cannes near Eunice, LA	339.3	162
08012000	LA	Bayou Nezpique near Basile, LA	1,364.9	163
08013000	LA	Calcasieu River nr Glenmora, LA	1,292.4	164
08013500	LA	Calcasieu River near Oberlin, LA	1,950.3	165
08014500	LA	Ouiska Chitto Creek Near Oberlin, LA	1,320.9	166
08015500	LA	Calcasieu River near Kinder, LA	4,403.0	167
07037500	MO	St. Francis River near Patterson, MO	2,476.0	168
02436500	MS	TOWN CREEK NR NETTLETON, MS	1,605.8	169
02439400	MS	BUTTAHATCHEE RIVER NR ABERDEEN, MS	2,066.8	170
02448000	MS	NOXUBEE RIVER AT MACON, MS	1,989.1	171
02472000	MS	LEAF RIVER NR COLLINS, MS	1,924.4	172
02472500	MS	BOUIE CREEK NR HATTIESBURG, MS	787.4	173
02473000	MS	LEAF RIVER AT HATTIESBURG, MS	4,527.3	174
02473500	MS	TALLAHALA CREEK AT LAUREL, MS	616.4	175
02474500	MS	TALLAHALA CREEK NR RUNNELSTOWN, MS	1,585.1	176
02475000	MS	LEAF RIVER NR MCLAIN, MS	9,052.0	177
02475500	MS	CHUNKY RIVER NR CHUNKY, MS	955.7	178
02476500	MS	SOWASHEE CREEK AT MERIDIAN, MS	134.9	179
02477000	MS	CHICKASAWHAY RIVER AT ENTERPRISE, MS	2,377.6	180
02478500	MS	CHICKASAWHAY RIVER AT LEAKESVILLE, MS	6,967.1	181
02479000	MS	PASCAGOULA RIVER AT MERRILL, MS	17,068.0	182
02479155	MS	CYPRESS CREEK NR JANICE, MS	136.2	183
02479300	MS	RED CREEK AT VESTRY, MS	1,142.2	184
02479560	MS	ESCATAWPA RIVER NEAR AGRICOLA MS	1,455.6	185
02481000	MS	BILOXI RIVER AT WORTHAM, MS	249.2	186
02482000	MS	PEARL RIVER AT EDINBURG, MS	2,341.3	187
02482550	MS	PEARL RIVER NR CARTHAGE, MS	3,486.1	188
02483000	MS	TUSCOLAMETA CREEK AT WALNUT GROVE, MS	1,064.5	189
02484000	MS	YOCKANOOKANY RIVER NR KOSCIUSKO, MS	784.8	190
02484500	MS	YOCKANOOKANY RIVER NR OFAHOMA, MS	1,214.7	191
02486000	MS	PEARL RIVER AT JACKSON, MS	8,212.9	192
02488500	MS	PEARL RIVER NR MONTICELLO, MS	12,931.8	193
02489500	MS	Pearl River near Bogalusa, LA	17,024.0	194
02490500	MS	BOGUE CHITTO NR TYLERTOWN, MS	1,274.3	195

Table H1. Streamgages used in this report to determine attributions of monotonic trends and change points in annual peak streamflow in the Southeast region of the United States.—Continued

[The map locations (1–357) of streamgages are shown in figure H3. Data from Dudley and others (2018); streamgage names are quoted from the National Water Information System. For additional notes on streamgages, see Swain and York (2022). ABV, above; AL, Alabama; AL., Alabama; AR, Arkansas; CR, Creek; FL, Florida; FLA, Florida; FLA., Florida; FT., Fort; GA, Georgia; LA, Louisiana; L&D, lock and dam; MO, Missouri; MS, Mississippi; MT., Mount; n.a., not available; NC, North Carolina; N F, North Fork; nr, near; NR, near; NR., near; R, River; R., River; RD, Road; SC, South Carolina; S F, South Fork; St., Saint; TN, Tennessee; US, United States; VA, Virginia; WILM, William; km^2, square kilometers]

Streamgage number	State	Streamgage name/location	Drainage area, in km^2	Map location (fig. H3)
07268000	MS	LITTLE TALLAHATCHIE RIVER AT ETTA, MS	1,362.3	196
07274000	MS	YOCONA RIVER NR OXFORD, MS	678.6	197
07283000	MS	SKUNA RIVER AT BRUCE, MS	657.9	198
07289350	MS	BIG BLACK RIVER AT WEST, MS	2,659.9	199
07290000	MS	BIG BLACK RIVER NR BOVINA, MS	7,283.0	200
07290650	MS	BAYOU PIERRE NR WILLOWS, MS	1,693.9	201
07291000	MS	HOMOCHITTO RIVER AT EDDICETON, MS	468.8	202
07292500	MS	HOMOCHITTO RIVER AT ROSETTA, MS	2,038.3	203
07295000	MS	BUFFALO RIVER NR WOODVILLE, MS	466.2	204
02053200	NC	POTECASI CREEK NEAR UNION, NC	582.7	205
02053500	NC	AHOSKIE CREEK AT AHOSKIE, NC	163.9	206
02068500	NC	DAN RIVER NEAR FRANCISCO, NC	334.1	207
02071000	NC	DAN RIVER NEAR WENTWORTH, NC	2,727.3	208
02074000	NC	SMITH RIVER AT EDEN, NC	1,393.4	209
02080500	NC	ROANOKE RIVER AT ROANOKE RAPIDS, NC	21,714.5	210
02081500	NC	TAR RIVER NEAR TAR RIVER, NC	432.5	211
02081747	NC	TAR R AT US 401 AT LOUISBURG, NC	1,105.9	212
02082770	NC	SWIFT CREEK AT HILLIARDSTON, NC	429.9	213
02082950	NC	LITTLE FISHING CREEK NEAR WHITE OAK, NC	458.4	214
02083000	NC	FISHING CREEK NEAR ENFIELD, NC	1,362.3	215
02083500	NC	TAR RIVER AT TARBORO, NC	5,653.9	216
02085070	NC	ENO RIVER NEAR DURHAM, NC	365.2	217
02085500	NC	FLAT RIVER AT BAHAMA, NC	385.9	218
02087500	NC	NEUSE RIVER NEAR CLAYTON, NC	2,978.5	219
02088000	NC	MIDDLE CREEK NEAR CLAYTON, NC	216.3	220
02088500	NC	LITTLE RIVER NEAR PRINCETON, NC	600.9	221
02089000	NC	NEUSE RIVER NEAR GOLDSBORO, NC	6,213.4	222
02089500	NC	NEUSE RIVER AT KINSTON, NC	6,972.2	223
02090380	NC	CONTENTNEA CREEK NEAR LUCAMA, NC	417.0	224
02091000	NC	NAHUNTA SWAMP NEAR SHINE, NC	208.2	225
02091500	NC	CONTENTNEA CREEK AT HOOKERTON, NC	1,898.5	226
02092500	NC	TRENT RIVER NEAR TRENTON, NC	435.1	227
02093800	NC	REEDY FORK NEAR OAK RIDGE, NC	53.4	228
02094500	NC	REEDY FORK NEAR GIBSONVILLE, NC	339.3	229
02096500	NC	HAW RIVER AT HAW RIVER, NC	1,569.5	230
02100500	NC	DEEP RIVER AT RAMSEUR, NC	903.9	231
02102000	NC	DEEP RIVER AT MONCURE, NC	3,714.0	232
02102500	NC	CAPE FEAR RIVER AT LILLINGTON, NC	8,971.7	233
02105500	NC	CAPE FEAR R AT WILM O HUSKE LOCK NR TARHEEL, NC	12,566.6	234

Table H1. Streamgages used in this report to determine attributions of monotonic trends and change points in annual peak streamflow in the Southeast region of the United States.—Continued

[The map locations (1–357) of streamgages are shown in figure H3. Data from Dudley and others (2018); streamgage names are quoted from the National Water Information System. For additional notes on streamgages, see Swain and York (2022). ABV, above; AL, Alabama; AL., Alabama; AR, Arkansas; CR, Creek; FL, Florida; FLA, Florida; FLA., Florida; FT., Fort; GA, Georgia; LA, Louisiana; L&D, lock and dam; MO, Missouri; MS, Mississippi; MT., Mount; n.a., not available; NC, North Carolina; N F, North Fork; nr, near; NR, near; NR., near; R, River; R., River; RD, Road; SC, South Carolina; S F, South Fork; St., Saint; TN, Tennessee; US, United States; VA, Virginia; WILM, William; km^2, square kilometers]

Streamgage number	State	Streamgage name/location	Drainage area, in km^2	Map location (fig. H3)
02106500	NC	BLACK RIVER NEAR TOMAHAWK, NC	1,750.8	235
02108000	NC	NORTHEAST CAPE FEAR RIVER NEAR CHINQUAPIN, NC	1,551.4	236
02111000	NC	YADKIN RIVER AT PATTERSON, NC	74.6	237
02111180	NC	ELK CREEK AT ELKVILLE, NC	131.8	238
02111500	NC	REDDIES RIVER AT NORTH WILKESBORO, NC	231.0	239
02112000	NC	YADKIN RIVER AT WILKESBORO, NC	1,305.4	240
02112120	NC	ROARING RIVER NEAR ROARING RIVER, NC	331.5	241
02112250	NC	YADKIN RIVER AT ELKIN, NC	2,242.9	242
02112360	NC	MITCHELL RIVER NEAR STATE ROAD, NC	204.1	243
02113850	NC	ARARAT RIVER AT ARARAT, NC	598.3	244
02114450	NC	LITTLE YADKIN RIVER AT DALTON, NC	110.9	245
02115360	NC	YADKIN RIVER AT ENON, NC	4,387.4	246
02116500	NC	YADKIN RIVER AT YADKIN COLLEGE, NC	5,905.2	247
02118000	NC	SOUTH YADKIN RIVER NEAR MOCKSVILLE, NC	792.5	248
02118500	NC	HUNTING CREEK NEAR HARMONY, NC	401.4	249
02126000	NC	ROCKY RIVER NEAR NORWOOD, NC	3,553.5	250
02128000	NC	LITTLE RIVER NEAR STAR, NC	274.5	251
02129000	NC	PEE DEE R NR ROCKINGHAM, NC	17,775.1	252
02133500	NC	DROWNING CREEK NEAR HOFFMAN, NC	474.0	253
02134500	NC	LUMBER RIVER AT BOARDMAN, NC	3,180.5	254
02138500	NC	LINVILLE RIVER NEAR NEBO, NC	172.8	255
02142000	NC	LOWER LITTLE RIVER NR ALL HEALING SPRINGS, NC	73.0	256
02142900	NC	LONG CREEK NEAR PAW CREEK, NC	42.5	257
02143000	NC	HENRY FORK NEAR HENRY RIVER, NC	215.5	258
02143040	NC	JACOB FORK AT RAMSEY, NC	66.6	259
02143500	NC	INDIAN CREEK NEAR LABORATORY, NC	179.2	260
02144000	NC	LONG CREEK NEAR BESSEMER CITY, NC	82.4	261
02146300	NC	IRWIN CREEK NEAR CHARLOTTE, NC	79.5	262
02146600	NC	MCALPINE CR AT SARDIS ROAD NEAR CHARLOTTE, NC	100.0	263
02146700	NC	MCMULLEN CR AT SHARON VIEW RD NEAR CHARLOTTE, NC	18.0	264
02149000	NC	COVE CREEK NEAR LAKE LURE, NC	204.6	265
02151500	NC	BROAD RIVER NEAR BOILING SPRINGS, NC	2,266.2	266
02152100	NC	FIRST BROAD RIVER NEAR CASAR, NC	156.7	267
03439000	NC	FRENCH BROAD RIVER AT ROSMAN, NC	175.9	268
03443000	NC	FRENCH BROAD RIVER AT BLANTYRE, NC	766.6	269
03446000	NC	MILLS RIVER NEAR MILLS RIVER, NC	172.8	270
03451000	NC	SWANNANOA RIVER AT BILTMORE, NC	336.7	271
03451500	NC	FRENCH BROAD RIVER AT ASHEVILLE, NC	2,447.5	272
03453500	NC	FRENCH BROAD RIVER AT MARSHALL, NC	3,449.9	273

Table H1. Streamgages used in this report to determine attributions of monotonic trends and change points in annual peak streamflow in the Southeast region of the United States.—Continued

[The map locations (1–357) of streamgages are shown in figure H3. Data from Dudley and others (2018); streamgage names are quoted from the National Water Information System. For additional notes on streamgages, see Swain and York (2022). ABV, above; AL, Alabama; AL., Alabama; AR, Arkansas; CR, Creek; FL, Florida; FLA, Florida; FLA., Florida; FT., Fort; GA, Georgia; LA, Louisiana; L&D, lock and dam; MO, Missouri; MS, Mississippi; MT., Mount; n.a., not available; NC, North Carolina; N F, North Fork; nr, near; NR, near; NR., near; R, River; R., River; RD, Road; SC, South Carolina; S F, South Fork; St., Saint; TN, Tennessee; US, United States; VA, Virginia; WILM, William; km², square kilometers]

Streamgage number	State	Streamgage name/location	Drainage area, in km²	Map location (fig. H3)
03455500	NC	W F PIGEON R ABOVE LAKE LOGAN NR HAZELWOOD, NC	71.5	274
03456500	NC	EAST FORK PIGEON RIVER NEAR CANTON, NC	133.4	275
03459500	NC	PIGEON RIVER NEAR HEPCO, NC	906.5	276
03460000	NC	CATALOOCHEE CREEK NEAR CATALOOCHEE, NC	127.4	277
03463300	NC	SOUTH TOE RIVER NEAR CELO, NC	112.1	278
03479000	NC	WATAUGA RIVER NEAR SUGAR GROVE, NC	238.5	279
03500000	NC	LITTLE TENNESSEE RIVER NEAR PRENTISS, NC	362.6	280
03500240	NC	CARTOOGECHAYE CREEK NEAR FRANKLIN, NC	147.9	281
03503000	NC	LITTLE TENNESSEE RIVER AT NEEDMORE, NC	1,129.2	282
03504000	NC	NANTAHALA RIVER NEAR RAINBOW SPRINGS, NC	134.4	283
03512000	NC	OCONALUFTEE RIVER AT BIRDTOWN, NC	476.6	284
03513000	NC	TUCKASEGEE RIVER AT BRYSON CITY, NC	1,696.4	285
03550000	NC	VALLEY RIVER AT TOMOTLA, NC	269.4	286
02110500	SC	WACCAMAW RIVER NEAR LONGS, SC	2,874.9	287
02130900	SC	BLACK CREEK NEAR MCBEE, SC	279.7	288
02130910	SC	BLACK CREEK NEAR HARTSVILLE, SC	448.1	289
02131000	SC	PEE DEE RIVER AT PEEDEE, SC	22,869.6	290
02135000	SC	LITTLE PEE DEE R. AT GALIVANTS FERRY, SC	7,226.1	291
02136000	SC	BLACK RIVER AT KINGSTREE, SC	3,242.7	292
02146000	SC	CATAWBA RIVER NEAR ROCK HILL, SC	7,899.5	293
02148000	SC	WATEREE RIVER NR. CAMDEN, SC	13,131.2	294
02154500	SC	NORTH PACOLET RIVER AT FINGERVILLE, SC	300.4	295
02155500	SC	PACOLET RIVER NEAR FINGERVILLE, SC	549.1	296
02156500	SC	BROAD RIVER NEAR CARLISLE, SC	7,226.1	297
02162500	SC	SALUDA RIVER NEAR GREENVILLE, SC	771.8	298
02163500	SC	SALUDA RIVER NEAR WARE SHOALS, SC	1,502.2	299
02167000	SC	SALUDA RIVER AT CHAPPELLS, SC	3,522.4	300
02169000	SC	SALUDA RIVER NEAR COLUMBIA, SC	6,526.8	301
02169500	SC	CONGAREE RIVER AT COLUMBIA, SC	20,331.4	302
02169570	SC	GILLS CREEK AT COLUMBIA, SC	154.4	303
02173000	SC	SOUTH FORK EDISTO RIVER NEAR DENMARK, SC	1,864.8	304
02173500	SC	NORTH FORK EDISTO RIVER AT ORANGEBURG, SC	1,769.0	305
02175000	SC	EDISTO RIVER NR GIVHANS, SC	7,070.7	306
02175500	SC	SALKEHATCHIE RIVER NEAR MILEY, SC	883.2	307
02176500	SC	COOSAWHATCHIE RIVER NEAR HAMPTON, SC	525.8	308
02192500	SC	LITTLE RIVER NEAR MT. CARMEL, SC	562.0	309
02197000	SC	SAVANNAH RIVER AT AUGUSTA, GA	19,450.8	310
02198500	SC	SAVANNAH RIVER NEAR CLYO, GA	25,511.4	311
03455000	TN	FRENCH BROAD RIVER NEAR NEWPORT, TN	4,812.2	312

Table H1. Streamgages used in this report to determine attributions of monotonic trends and change points in annual peak streamflow in the Southeast region of the United States.—Continued

[The map locations (1–357) of streamgages are shown in figure H3. Data from Dudley and others (2018); streamgage names are quoted from the National Water Information System. For additional notes on streamgages, see Swain and York (2022). ABV, above; AL, Alabama; AL., Alabama; AR, Arkansas; CR, Creek; FL, Florida; FLA, Florida; FLA., Florida; FT., Fort; GA, Georgia; LA, Louisiana; L&D, lock and dam; MO, Missouri; MS, Mississippi; MT., Mount; n.a., not available; NC, North Carolina; N F, North Fork; nr, near; NR, near; NR., near; R, River; R., River; RD, Road; SC, South Carolina; S F, South Fork; St., Saint; TN, Tennessee; US, United States; VA, Virginia; WILM, William; km², square kilometers]

Streamgage number	State	Streamgage name/location	Drainage area, in km²	Map location (fig. H3)
03465500	TN	NOLICHUCKY RIVER AT EMBREEVILLE, TN	2,084.9	313
03491000	TN	BIG CREEK NEAR ROGERSVILLE, TN	122.5	314
03497300	TN	LITTLE RIVER ABOVE TOWNSEND, TN	274.5	315
03498500	TN	LITTLE RIVER NEAR MARYVILLE, TN	696.7	316
03528000	TN	CLINCH RIVER ABOVE TAZEWELL, TN	3,817.6	317
03540500	TN	EMORY RIVER AT OAKDALE, TN	1,978.8	318
03598000	TN	DUCK RIVER NEAR SHELBYVILLE, TN	1,245.8	319
03604000	TN	BUFFALO RIVER NEAR FLAT WOODS, TN	1,157.7	320
07029500	TN	HATCHIE RIVER AT BOLIVAR, TN	3,833.2	321
02044500	VA	NOTTOWAY RIVER NEAR RAWLINGS, VA	821.0	322
02045500	VA	NOTTOWAY RIVER NEAR STONY CREEK, VA	1,494.4	323
02046000	VA	STONY CREEK NEAR DINWIDDIE, VA	292.7	324
02047000	VA	NOTTOWAY RIVER NEAR SEBRELL, VA	3,732.2	325
02047500	VA	BLACKWATER RIVER NEAR DENDRON, VA	751.1	326
02049500	VA	BLACKWATER RIVER NEAR FRANKLIN, VA	1,587.7	327
02051000	VA	NORTH MEHERRIN RIVER NEAR LUNENBURG, VA	145.0	328
02051500	VA	MEHERRIN RIVER NEAR LAWRENCEVILLE, VA	1,429.7	329
02052000	VA	MEHERRIN RIVER AT EMPORIA, VA	1,927.0	330
02053800	VA	S F ROANOKE RIVER NEAR SHAWSVILLE, VA	282.3	331
02054500	VA	ROANOKE RIVER AT LAFAYETTE, VA	657.9	332
02055000	VA	ROANOKE RIVER AT ROANOKE, VA	994.6	333
02055100	VA	TINKER CREEK NEAR DALEVILLE, VA	30.3	334
02056000	VA	ROANOKE RIVER AT NIAGARA, VA	1,318.3	335
02058400	VA	PIGG RIVER NEAR SANDY LEVEL, VA	909.1	336
02059500	VA	GOOSE CREEK NEAR HUDDLESTON, VA	486.9	337
02060500	VA	ROANOKE RIVER AT ALTAVISTA, VA	4,615.4	338
02061500	VA	BIG OTTER RIVER NEAR EVINGTON, VA	815.8	339
02062500	VA	ROANOKE (STAUNTON) RIVER AT BROOKNEAL, VA	6,226.3	340
02064000	VA	FALLING RIVER NEAR NARUNA, VA	427.3	341
02065500	VA	CUB CREEK AT PHENIX, VA	252.8	342
02066000	VA	ROANOKE (STAUNTON) RIVER AT RANDOLPH, VA	7,681.9	343
02069700	VA	SOUTH MAYO RIVER NEAR NETTLERIDGE, VA	221.4	344
02070000	VA	NORTH MAYO RIVER NEAR SPENCER, VA	279.7	345
02072000	VA	SMITH RIVER NEAR PHILPOTT, VA	556.8	346
02072500	VA	SMITH RIVER AT BASSETT, VA	670.8	347
02073000	VA	SMITH RIVER AT MARTINSVILLE, VA	981.6	348
02074500	VA	SANDY RIVER NEAR DANVILLE, VA	287.5	349
02075500	VA	DAN RIVER AT PACES, VA	6,700.3	350
02077000	VA	BANISTER RIVER AT HALIFAX, VA	1,416.7	351

Table H1. Streamgages used in this report to determine attributions of monotonic trends and change points in annual peak streamflow in the Southeast region of the United States.—Continued

[The map locations (1–357) of streamgages are shown in figure H3. Data from Dudley and others (2018); streamgage names are quoted from the National Water Information System. For additional notes on streamgages, see Swain and York (2022). ABV, above; AL, Alabama; AL., Alabama; AR, Arkansas; CR, Creek; FL, Florida; FLA, Florida; FLA., Florida; FT., Fort; GA, Georgia; LA, Louisiana; L&D, lock and dam; MO, Missouri; MS, Mississippi; MT., Mount; n.a., not available; NC, North Carolina; N F, North Fork; nr, near; NR, near; NR., near; R, River; R., River; RD, Road; SC, South Carolina; S F, South Fork; St., Saint; TN, Tennessee; US, United States; VA, Virginia; WILM, William; km^2, square kilometers]

Streamgage number	State	Streamgage name/location	Drainage area, in km^2	Map location (fig. H3)
03471500	VA	S F HOLSTON RIVER AT RIVERSIDE, NEAR CHILHOWIE, VA	198.4	352
03473000	VA	S F HOLSTON RIVER NEAR DAMASCUS, VA	784.8	353
03478400	VA	BEAVER CREEK AT BRISTOL, VA	69.7	354
03488000	VA	N F HOLSTON RIVER NEAR SALTVILLE, VA	572.4	355
03524000	VA	CLINCH RIVER AT CLEVELAND, VA	1,380.5	356
03531500	VA	POWELL RIVER NEAR JONESVILLE, VA	826.2	357

Table H2. List of attributions used in the multiple working hypotheses framework to assess potential causal factors for monotonic trends and change points in median annual peak streamflow in the Southeast region.

Attributions	General description	Potential influence	Comments and additional information	Data source
Short- and long-term precipitation	Long-term precipitation shows climate variability, and short-term precipitation has more uncertainty. A primary attribution of short-term precipitation combined with a secondary attribution of long-term precipitation is indicated in figures with an asterisk (*) as "short-term precipitation*." This combination of primary and secondary attributions includes hurricanes or tropical storms.	An increase or decrease in precipitation may increase or decrease flooding or flood frequency. Short-term events are related to peak streamflows.	Precipitation trends in the Southeast region from 1948 to 2012 show an overall increase, except for more easterly locations, particularly in South Carolina. Fall has become significantly wetter, while spring and summer have become drier on average (Powell and Keim, 2015).	Available at http://www.prism.oregonstate.edu/ or the U.S. Historical Climatology Network at https://www.ncei.noaa.gov/products/land-based-station/us-historical-climatology-network.
Large and small artificial impoundments	Regulation and dams. A primary attribution of large artificial impoundments combined with a secondary attribution (short-term precipitation, interbasin water transfer, surface water withdrawals, or urban effects) is indicated in figures with an asterisk (*) as "large artificial impoundments*."	Regulation has shown to be associated with increases and decreases of streamflow.	Large artificial impoundments are major dam works on primary rivers, while small artificial impoundments can be private or alterations to small streams. The peak years for building of dams in the United States were from 1950 to 1970.	Lists of dams are available at https://www.usbr.gov/projects/facilities.php?type=Dam.
Surface-water withdrawals	Regulation and withdrawals	Water supply reduces the available surface water and is correlated to population size.	Surface water may be used to supply urban or agricultural usage.	Information is localized for municipalities.
Groundwater withdrawals	Groundwater pumping	Water supply reduces the available groundwater and is correlated to population size.	Groundwater is a common source for municipal supply and agricultural usage.	Information is localized for municipalities.
Artificial wastewater and water-supply discharges	Urbanization and population water needs	The disposal of wastewater and other water-supply discharge may influence any receiving water bodies.	Correlated with population size as well as water withdrawals and usage.	Available at https://www.census.gov/topics/population.html.
Agricultural drainage activities	Irrigation practices	Irrigation has been shown to be associated with a reduction in streamflow (Singh and Singh, 2016; Traylor and Zlotnik, 2016).	Correlated with urban development.	Available at https://pubs.er.usgs.gov/publication/cir1441.
Interbasin water transfers	Regulation and water use	Water withdrawals in one municipality move water from another municipality and affect major waterways upstream and downstream.	Instead of a defined withdrawal or discharge, interbasin transfers redistribute streamflows and affect peak streamflows.	Information is localized for municipalities.
Urban effects	Impervious surface, storm drainage systems, catch basins, and detention ponds	An increased impervious surface may contribute to greater urban runoff through reduced infiltration capacity (Tollan, 2002). The need for storm drainage is also higher.	Correlated with the percentage of land use that is considered developed and populated. Would be important for an urban-scale model with different areas of the urban setting having different percentages of impervious surface.	Available at https://www.ers.usda.gov/data-products/major-land-uses/. Data available from 1945 to 2012.

Table H3. Results of the statistical analysis of the correlation between median annual peak streamflow and watershed precipitation to identify monotonic trends in the Southeast region.

[Streamgages are chosen that do not have distinct local attributions of peak-streamflow changes. The *p*-values represent the statistical significance or the probability of obtaining a result. A *p*-value less than 0.10 indicates the value is statistically significant; a *p*-value greater than 0.10 indicates the value is nonsignificant. The Pearson's rho value (-1.0 to +1.0) measures the strength of the linear correlation between two variables (median peak streamflow and watershed precipitation). The Kendall's tau value (-1.0 to +1.0) measures the strength and the direction of the monotonic trend for each variable (median peak streamflow and watershed precipitation). Data from Dudley and others (2018). For additional notes on streamgages, see Swain and York (2022). AL, Alabama; FL, Florida; GA, Georgia; MS, Mississippi; NC, North Carolina; SC, South Carolina; VA, Virginia]

Streamgage number	State	Streamgage number in fig. H3	*p*-value, peak streamflow and pre-cipitation monotonic trend	*p*-value, peak-streamflow monotonic trend	*p*-value, pre-cipitation monotonic trend	Pearson's rho correlation between peak streamflow and precipitation to identify monotonic trends	Kendall's tau, monotonic trend in peak streamflow	Kendall's tau, monotonic trend in precipitation	Streamgage name/location
02400100	AL	9	0.0024	0.0020	0.3533	0.4996	-0.2934	-0.0885	TERRAPIN CREEK AT ELLISVILLE AL
02266300	FL	50	0.0216	0.0152	0.4184	0.3773	0.2549	0.0857	REEDY CREEK NEAR VINELAND, FL
02198000	GA	97	0.0261	0.0262	0.8028	-0.0062	-0.1709	0.0202	BRIER CREEK AT MILLHAVEN, GA
02337500	GA	124	0.0211	0.0214	0.5635	0.4729	-0.2359	-0.0599	SNAKE CREEK NEAR WHITESBURG, GA
02382500	GA	138	0.2231	0.0432	0.0151	0.3767	-0.3704	-0.441	COOSAWATTEE RIVER NEAR PINE CHAPEL, GA
02439400	MS	170	0.7920	0.2035	0.0849	0.8252	-0.1251	-0.169	BUTTAHATCHEE RIVER NR ABERDEEN, MS
02484500	MS	191	0.7794	0.9602	0.2928	0.2084	0.0041	-0.0808	Yackanookany River near Ofahoma MS
02100500	NC	231	0.0488	0.0234	0.2605	0.4709	-0.1583	-0.0786	DEEP RIVER AT RAMSEUR, NC
02111000	NC	237	0.0782	0.0660	0.5705	0.4007	-0.1433	-0.0444	YADKIN RIVER AT PATTERSON, NC
02111500	NC	239	0.1679	0.1564	0.7298	0.2800	-0.1113	-0.0274	REDDIES RIVER AT NORTH WILKESBORO, NC
02146700	NC	264	0.0045	0.0048	0.7351	-0.0151	0.4372	-0.0563	MCMULLEN CR AT SHARON VIEW RD NEAR CHARLOTTE, NC
02136000	SC	292	0.2874	0.2121	0.4092	0.2791	-0.0897	-0.0607	BLACK RIVER AT KINGSTREE, SC
02173000	SC	304	0.0018	0.0023	0.7688	0.3284	-0.2266	-0.0223	SOUTH FORK EDISTO RIVER NEAR DENMARK, SC
02173500	SC	305	0.0041	0.0072	0.5980	0.5493	-0.2203	-0.0435	NORTH FORK EDISTO RIVER AT ORANGE-BURG, SC
02175000	SC	306	0.0196	0.0177	0.4538	-0.0588	-0.1824	-0.0588	EDISTO RIVER NEAR GIVHANS, SC
02175500	SC	307	0.7565	0.7426	0.2435	0.5123	-0.0284	-0.0995	SALKEHATCHIE RIVER NEAR MILEY, SC
02049500	VA	327	0.0082	0.0002	0.0009	0.3797	0.2901	0.263	BLACKWATER RIVER NEAR FRANKLIN, VA
02072500	VA	347	0.7189	0.3037	0.3037	0.8056	-0.2424	-0.242	SMITH RIVER AT BASSETT, VA

Table H4. Statistics and attributions of change points in median annual peak streamflow for 74 streamgages in the Southeast region for the 50-year period (water years 1966–2015).

[A *p*-value less than 0.10 indicates the value is statistically significant; a *p*-value greater than 0.10 indicates the value is nonsignificant. “Pre-step” peak streamflow refers to before the year of the change point, and “post-step” peak streamflow refers to after the year of the change point. The “rank” of streamgages (1 to 74) is the ratio of post-step streamflow to pre-step streamflow, with a rank of 1 being the highest ratio and a rank of 74 being the lowest ratio. The “level of evidence” is the confidence in the primary and secondary attributions. In the “Notes” column, “Tested” means the streamgage was tested for the correlation between precipitation and median annual peak streamflow. Change point data are from Dudley and others (2018). AL, Alabama; FL, Florida; GA, Georgia; MS, Mississippi; NC, North Carolina; SC, South Carolina; VA, Virginia; ft^3/s, cubic feet per second; LWRPF, largest watershed and reductions in peak flow; -, no secondary attribution; ~, for additional notes on streamgages see Swain and York (2022)]

Streamgage number	State	*p*-value	Year of change point in median annual peak streamflow	Pre-step median annual peak streamflow, in ft^3/s	Post-step median annual peak streamflow, in ft^3/s	Rank (1–74) of post-step/pre-step median annual peak streamflow	Primary attribution	Secondary attribution	Level of evidence	Notes
02400100	AL	0.0032	1982	9,070	5,720	39	Surface-water withdrawals	Short-term precipitation	Limited	Tested
02412000	AL	0.0157	1984	9,470	6,630	38	Large artificial impoundments	-	Robust	~
02414500	AL	0.0054	1984	34,700	21,600	65	Large artificial impoundments	-	Robust	LWRPF streamgage
02438000	AL	0.0796	2005	16,200	9,750	51	Groundwater withdrawals	-	Additional information required	Tested
02462000	AL	0.0217	1984	8,730	6,480	33	Artificial wastewater and water-supply discharges	-	Medium	~
03574500	AL	0.0258	2005	19,900	9,800	58	Interbasin water transfers	-	Additional information required	~
02233500	FL	0.0985	1981	1,520	2,930	1	Urban effects	-	Robust	~
02263800	FL	0.0925	1985	487	762	6	Urban effects	-	Robust	~
02266300	FL	0.0023	1985	282	539	7	Urban effects	Short-term precipitation	Medium	Tested
02294491	FL	0.0125	1978	273	438	8	Artificial wastewater and water-supply discharges	-	Robust	~
02297310	FL	0.0872	2005	1,940	915	17	Interbasin water transfers	Urban effects	Robust	~
02300100	FL	0.0124	2004	794	315	11	Groundwater withdrawals	-	Medium	~
02303800	FL	0.0251	1988	617	365	10	Groundwater withdrawals	-	Limited	~

Table H4. Statistics and attributions of change points in median annual peak streamflow for 74 streamgages in the Southeast region for the 50-year period (water years 1966–2015).—Continued

[A *p*-value less than 0.10 indicates the value is statistically significant; a *p*-value greater than 0.10 indicates the value is nonsignificant. "Pre-step" peak streamflow refers to before the year of the change point, and "post-step" peak streamflow refers to after the year of the change point. The "rank" of streamgages (1 to 74) is the ratio of post-step streamflow to pre-step streamflow, with a rank of 1 being the highest ratio and a rank of 74 being the lowest ratio. The "level of evidence" is the confidence in the primary and secondary attributions. In the "Notes" column, "Tested" means the streamgage was tested for the correlation between precipitation and median annual peak streamflow. Change point data are from Dudley and others (2018). AL, Alabama; FL, Florida; GA, Georgia; MS, Mississippi; NC, North Carolina; SC, South Carolina; VA, Virginia; ft^3/s, cubic feet per second; LWRPF, largest watershed and reductions in peak flow; -, no secondary attribution; ~, for additional notes on streamgages see Swain and York (2022)]

Streamgage number	State	*p*-value	Year of change point in median annual peak streamflow	Pre-step median annual peak streamflow, in ft^3/s	Post-step median annual peak streamflow, in ft^3/s	Rank (1–74) of post-step/pre-step median annual peak streamflow	Primary attribution	Secondary attribution	Level of evidence	Notes
02307359	FL	0.0569	2002	156	460	5	Urban effects	-	Robust	~
02313000	FL	0.0475	1989	2,150	1,170	16	Interbasin water transfers	-	Medium	~
02192000	GA	0.0046	1998	26,400	14,700	63	Interbasin water transfers	Short-term precipitation	Limited	LWRPF streamgage
02198000	GA	0.0217	1998	3,620	1,910	26	Artificial wastewater and water-supply discharges	Short-term precipitation	Limited	Tested
02202500	GA	0.0681	1998	12,000	6,170	49	Groundwater withdrawals	Short-term precipitation	Additional information required	~
02213000	GA	0.0115	1998	29,300	18,600	61	Large artificial impoundments	Short-term precipitation	Medium	LWRPF streamgage
02213500	GA	0.0306	1996	5,100	3,370	27	Large artificial impoundments	Interbasin water transfers	Additional information required	~
02215500	GA	0.0938	1998	25,900	18,500	53	Surface-water withdrawals	Short-term precipitation	Robust	LWRPF streamgage
02217500	GA	0.0188	1998	8,080	4,070	43	Surface-water withdrawals	Short-term precipitation	Robust	~
02223500	GA	0.0555	1998	31,000	17,200	68	Large artificial impoundments	-	Limited	LWRPF streamgage
02226000	GA	0.0851	1998	63,600	41,200	73	Surface-water withdrawals	Short-term precipitation	Robust	LWRPF streamgage
02334430	GA	0.0001	1986	9,670	11,000	2	Large artificial impoundments	Interbasin water transfers	Robust	~
02337170	GA	0.0324	1983	23,100	16,000	52	Large artificial impoundments	Interbasin water transfers	Medium	~

Table H4. Statistics and attributions of change points in median annual peak streamflow for 74 streamgages in the Southeast region for the 50-year period (water years 1966–2015).—Continued

[A *p*-value less than 0.10 indicates the value is statistically significant; a *p*-value greater than 0.10 indicates the value is nonsignificant. “Pre-step” peak streamflow refers to before the year of the change point, and “post-step” peak streamflow refers to after the year of the change point. The “rank” of streamgages (1 to 74) is the ratio of post-step streamflow to pre-step streamflow, with a rank of 1 being the highest ratio and a rank of 74 being the lowest ratio. The “level of evidence” is the confidence in the primary and secondary attributions. In the “Notes” column, “Tested” means the streamgage was tested for the correlation between precipitation and median annual peak streamflow. Change point data are from Dudley and others (2018). AL, Alabama; FL, Florida; GA, Georgia; MS, Mississippi; NC, North Carolina; SC, South Carolina; VA, Virginia; ft^3/s, cubic feet per second; LWRPF, largest watershed and reductions in peak flow; -, no secondary attribution; ~, for additional notes on streamgages see Swain and York (2022)]

Streamgage number	State	*p*-value	Year of change point in median annual peak streamflow	Pre-step median annual peak streamflow, in ft^3/s	Post-step median annual peak streamflow, in ft^3/s	Rank (1–74) of post-step/pre-step median annual peak streamflow	Primary attribution	Secondary attribution	Level of evidence	Notes
02337500	GA	0.0004	1998	3,250	466	35	Surface-water withdrawals	Short-term precipitation	Medium	Tested
02339500	GA	0.0372	1979	39,200	22,100	70	Large artificial impoundments	-	Robust	LWRPF streamgage
02344500	GA	0.0698	1998	5,320	2,490	37	Large artificial impoundments	Short-term precipitation	Robust	~
02344700	GA	0.0074	1998	3,200	1,260	29	Large artificial impoundments	Short-term precipitation	Medium	~
02349605	GA	0.0298	1998	25,500	13,500	64	Large artificial impoundments	Short-term precipitation	Robust	Tested
02352500	GA	0.0915	1998	31,300	21,400	56	Large artificial impoundments	Short-term precipitation	Robust	~
02353000	GA	0.1031	1998	28,900	18,700	59	Large artificial impoundments	Short-term precipitation	Robust	LWRPF streamgage
02382500	GA	0.0023	1984	5,780	4,360	22	Large artificial impoundments	-	Robust	~
02383500	GA	0.0069	1982	11,500	8,060	40	Large artificial impoundments	-	Robust	~
02394000	GA	0.0324	1993	9,050	8,320	13	Large artificial impoundments	Surface-water withdrawals	Limited	~
02439400	MS	0.0598	2005	24,000	13,400	60	Groundwater withdrawals	Short-term precipitation	Additional information required	Tested
02448000	MS	0.0251	1984	17,200	12,500	45	Interbasin water transfers	-	Robust	~
02484500	MS	0.0315	1984	10,200	5,910	44	Groundwater withdrawals	Short-term precipitation	Limited	Tested

Table H4. Statistics and attributions of change points in median annual peak streamflow for 74 streamgages in the Southeast region for the 50-year period (water years 1966–2015).—Continued

[A *p*-value less than 0.10 indicates the value is statistically significant; a *p*-value greater than 0.10 indicates the value is nonsignificant. "Pre-step" peak streamflow refers to before the year of the change point, and "post-step" peak streamflow refers to after the year of the change point. The "rank" of streamgages (1 to 74) is the ratio of post-step streamflow to pre-step streamflow, with a rank of 1 being the highest ratio and a rank of 74 being the lowest ratio. The "level of evidence" is the confidence in the primary and secondary attributions. In the "Notes" column, "Tested" means the streamgage was tested for the correlation between precipitation and median annual peak streamflow. Change point data are from Dudley and others (2018). AL, Alabama; FL, Florida; GA, Georgia; MS, Mississippi; NC, North Carolina; SC, South Carolina; VA, Virginia; ft^3/s, cubic feet per second; LWRPF, largest watershed and reductions in peak flow; -, no secondary attribution; ~, for additional notes on streamgages see Swain and York (2022)]

Streamgage number	State	*p*-value	Year of change point in median annual peak streamflow	Pre-step median annual peak streamflow, in ft^3/s	Post-step median annual peak streamflow, in ft^3/s	Rank (1–74) of post-step/pre-step median annual peak streamflow	Primary attribution	Secondary attribution	Level of evidence	Notes
02100500	NC	0.0019	1998	12,100	7,050	46	Large artificial impoundments	-	Limited	~
02102500	NC	0.0274	1999	30,600	20,600	57	Large artificial impoundments	Surface-water withdrawals	Robust	LWRPF streamgage
02111000	NC	0.0664	1998	1,300	774	12	Surface-water withdrawals	Short-term precipitation	Robust	Tested
02111180	NC	0.0415	1996	4,310	2,160	32	Surface-water withdrawals	-	Limited	~
02111500	NC	0.0937	1995	4,280	2,760	24	Surface-water withdrawals	Short-term precipitation	Robust	Tested
02112000	NC	0.0266	1998	7,890	5,080	36	Surface-water withdrawals	Short-term precipitation	Limited	~
02115360	NC	0.0894	1996	40,000	31,200	55	Surface-water withdrawals	-	Limited	~
02143040	NC	0.0984	1995	2,540	1,500	18	Interbasin water transfers	-	Additional information required	Tested
02146700	NC	0.0055	1978	925	1,690	4	Urban effects	-	Medium	Tested
03443000	NC	0.0372	1980	8,590	5,150	41	Large artificial impoundments	Surface-water withdrawals	Robust	~
03446000	NC	0.0315	1980	3,550	2,290	20	Large artificial impoundments	-	Medium	~
03451000	NC	0.0244	1998	3,230	1,730	23	Large artificial impoundments	Short-term precipitation	Limited	~
03455500	NC	0.0600	1998	4,080	2,390	25	Small impoundments	Short-term precipitation	Robust	~

Table H4. Statistics and attributions of change points in median annual peak streamflow for 74 streamgages in the Southeast region for the 50-year period (water years 1966–2015).—Continued

[A *p*-value less than 0.10 indicates the value is statistically significant; a *p*-value greater than 0.10 indicates the value is nonsignificant. “Pre-step” peak streamflow refers to before the year of the change point, and “post-step” peak streamflow refers to after the year of the change point. The “rank” of streamgages (1 to 74) is the ratio of post-step streamflow to pre-step streamflow, with a rank of 1 being the highest ratio and a rank of 74 being the lowest ratio. The “level of evidence” is the confidence in the primary and secondary attributions. In the “Notes” column, “Tested” means the streamgage was tested for the correlation between precipitation and median annual peak streamflow. Change point data are from Dudley and others (2018). AL, Alabama; FL, Florida; GA, Georgia; MS, Mississippi; NC, North Carolina; SC, South Carolina; VA, Virginia; ft^3/s, cubic feet per second; LWRPF, largest watershed and reductions in peak flow; -, no secondary attribution; ~, for additional notes on streamgages see Swain and York (2022)]

Streamgage number	State	*p*-value	Year of change point in median annual peak streamflow	Pre-step median annual peak streamflow, in ft^3/s	Post-step median annual peak streamflow, in ft^3/s	Rank (1–74) of post-step/pre-step median annual peak streamflow	Primary attribution	Secondary attribution	Level of evidence	Notes
03550000	NC	0.0527	1997	4,720	2,900	28	Artificial wastewater and water-supply discharges	-	Limited	~
02110500	SC	0.0772	2000	6,100	4,050	31	Short-term precipitation	Long-term precipitation	Robust	~
02130910	SC	0.0664	2000	770	542	9	Large artificial impoundments	Interbasin water transfers	Robust	~
02131000	SC	0.0217	1995	40,000	25,400	69	Large artificial impoundments	Surface-water withdrawals	Medium	LWRPF streamgage
02135000	SC	0.0342	2000	13,000	6,810	50	Groundwater withdrawals	-	Medium	~
02136000	SC	0.0074	2000	5,920	2,250	42	Groundwater withdrawals	Short-term precipitation	Limited	Tested
02148000	SC	0.1007	1998	30,500	17,000	66	Large artificial impoundments	Short-term precipitation	Limited	LWRPF streamgage
02167000	SC	0.0552	1998	14,000	6,170	54	Large artificial impoundments	Short-term precipitation	Limited	~
02169500	SC	0.0681	1998	74,900	43,800	74	Large artificial impoundments	Short-term precipitation	Limited	LWRPF streamgage
02173000	SC	0.0018	1987	2,850	1,540	21	Groundwater withdrawals	Short-term precipitation	Robust	Tested
02173500	SC	0.0003	1998	2,530	1,280	19	Groundwater withdrawals	Short-term precipitation	Robust	Tested
02175000	SC	0.0182	1998	9,980	4,780	47	Groundwater withdrawals	Short-term precipitation	Robust	~
02175500	SC	0.0166	2000	1,740	790	15	Interbasin water transfers	Short-term precipitation	Medium	Tested

Table H4. Statistics and attributions of change points in median annual peak streamflow for 74 streamgages in the Southeast region for the 50-year period (water years 1966–2015).—Continued

[A *p*-value less than 0.10 indicates the value is statistically significant; a *p*-value greater than 0.10 indicates the value is nonsignificant. "Pre-step" peak streamflow refers to before the year of the change point, and "post-step" peak streamflow refers to after the year of the change point. The "rank" of streamgages (1 to 74) is the ratio of post-step streamflow to pre-step streamflow, with a rank of 1 being the highest ratio and a rank of 74 being the lowest ratio. The "level of evidence" is the confidence in the primary and secondary attributions. In the "Notes" column, "Tested" means the streamgage was tested for the correlation between precipitation and median annual peak streamflow. Change point data are from Dudley and others (2018). AL, Alabama; FL, Florida; GA, Georgia; MS, Mississippi; NC, North Carolina; SC, South Carolina; VA, Virginia; ft^3/s, cubic feet per second; LWRPF, largest watershed and reductions in peak flow; -, no secondary attribution; ~, for additional notes on streamgages see Swain and York (2022)]

Streamgage number	State	*p*-value	Year of change point in median annual peak streamflow	Pre-step median annual peak streamflow, in ft^3/s	Post-step median annual peak streamflow, in ft^3/s	Rank (1–74) of post-step/pre-step median annual peak streamflow	Primary attribution	Secondary attribution	Level of evidence	Notes
02176500	SC	0.0753	1998	1,620	740	14	Groundwater withdrawals	Short-term precipitation	Limited	Tested
02197000	SC	0.0115	1998	34,200	22,700	62	Surface-water withdrawals	Short-term precipitation	Robust	LWRPF streamgage
02198500	SC	0.0426	1998	36,400	16,700	72	Surface-water withdrawals	Short-term precipitation	Robust	LWRPF streamgage
02049500	VA	0.0681	1991	3,280	4,600	3	Short-term precipitation	-	Robust	~
02060500	VA	0.0182	1996	19,300	13,800	48	Large artificial impoundments	Interbasin water transfers	Robust	~
02062500	VA	0.0251	1998	36,200	17,600	71	Large artificial impoundments	Short-term precipitation	Robust	~
02066000	VA	0.0462	1998	33,200	19,500	67	Large artificial impoundments	Short-term precipitation	Limited	~
02072500	VA	0.0066	1996	4,390	2,360	30	Large artificial impoundments	Interbasin water transfers	Medium	Tested
02073000	VA	0.0894	1996	7,550	5,090	34	Large artificial impoundments	Interbasin water transfers	Robust	~

Table H5. Statistics and attributions of change points in median annual peak streamflow for 74 streamgages in the Southeast region for the 75-year period (water years 1941–2015).

[A *p*-value less than 0.10 indicates the value is statistically significant; a *p*-value greater than 0.10 indicates the value is nonsignificant. “Pre-step” peak streamflow refers to before the year of the change point, and “post-step” peak streamflow refers to after the year of the change point. The “rank” of streamgages (1 to 74) is the ratio of post-step streamflow to pre-step streamflow, with a rank of 1 being the highest ratio and a rank of 74 being the lowest ratio. The “level of evidence” is the confidence in the primary and secondary attributions. In the “Notes” column, “Tested” means the streamgage was tested for the correlation between precipitation and median annual peak streamflow. Change point data are from Dudley and others (2018). AL, Alabama; FL, Florida; GA, Georgia; LA, Louisiana; MS, Mississippi; NC, North Carolina; SC, South Carolina; TN, Tennessee; VA, Virginia; ft^3/s, cubic feet per second; LWRPF, largest watershed and reductions in peak flow; -, no secondary attribution; ~, for additional notes on streamgages see Swain and York (2022)]

Streamgage number	State	*p*-value	Year of change point in median annual peak streamflow	Pre-step median annual peak streamflow, in ft^3/s	Post-step median annual peak streamflow, in ft^3/s	Rank (1–74) of post-step/pre-step median annual peak streamflow	Primary attribution	Secondary attribution	Level of evidence	Notes
02398300	AL	0.0270	1983	10,600	7,140	37	Large artificial impoundments	Surface-water withdrawals	Robust	~
02414500	AL	0.0241	1984	34,200	21,600	57	Large artificial impoundments	-	Robust	LWRPF streamgage
03574500	AL	0.0854	2005	19,800	9,800	53	Groundwater withdrawals	-	Medium	~
02294650	FL	0.0412	1960	1,340	808	14	Artificial wastewater and water-supply discharges	-	Robust	~
02295637	FL	0.0023	1974	4,170	2,800	24	Artificial wastewater and water-supply discharges	-	Robust	~
02296750	FL	0.0101	1960	8,070	4,910	34	Artificial wastewater and water-supply discharges	-	Robust	~
02301500	FL	0.0688	1968	2,860	2,090	16	Groundwater withdrawals	-	Robust	~
02303000	FL	0.0371	1970	2,360	1,550	17	Interbasin water transfers	-	Robust	~
02312500	FL	0.0108	1970	1,950	1,080	18	Interbasin water transfers	Urban effects	Robust	~
02313000	FL	0.0160	1989	2,160	1,170	19	Urban effects	-	Robust	~
02319000	FL	0.0957	1957	6,700	14,100	5	Urban effects	-	Robust	~
02192000	GA	0.0216	1998	23,000	14,700	48	Interbasin water transfers	Short-term precipitation	Limited	LWRPF streamgage
02198000	GA	0.0607	1998	3,660	1,910	26	Artificial wastewater and water-supply discharges	Short-term precipitation	Limited	Tested
02213000	GA	0.0394	1998	29,700	18,600	55	Large artificial impoundments	Short-term precipitation	Medium	LWRPF streamgage
02217500	GA	0.0616	1998	7,610	4,070	38	Surface-water withdrawals	Short-term precipitation	Robust	~
02223500	GA	0.0717	1983	33,500	24,400	51	Large artificial impoundments	-	Limited	LWRPF streamgage
02335000	GA	0.0008	1955	17,300	9,360	47	Large artificial impoundments	-	Robust	~

Table H5. Statistics and attributions of change points in median annual peak streamflow for 74 streamgages in the Southeast region for the 75-year period (water years 1941–2015).—Continued

[A *p*-value less than 0.10 indicates the value is statistically significant; a *p*-value greater than 0.10 indicates the value is nonsignificant. "Pre-step" peak streamflow refers to before the year of the change point, and "post-step" peak streamflow refers to after the year of the change point. The "rank" of streamgages (1 to 74) is the ratio of post-step streamflow to pre-step streamflow, with a rank of 1 being the highest ratio and a rank of 74 being the lowest ratio. The "level of evidence" is the confidence in the primary and secondary attributions. In the "Notes" column, "Tested" means the streamgage was tested for the correlation between precipitation and median annual peak streamflow. Change point data are from Dudley and others (2018). AL, Alabama; FL, Florida; GA, Georgia; LA, Louisiana; MS, Mississippi; NC, North Carolina; SC, South Carolina; TN, Tennessee; VA, Virginia; ft^3/s, cubic feet per second; LWRPF, largest watershed and reductions in peak flow; -, no secondary attribution; ~, for additional notes on streamgages see Swain and York (2022)]

Streamgage number	State	*p*-value	Year of change point in median annual peak streamflow	Pre-step median annual peak streamflow, in ft^3/s	Post-step median annual peak streamflow, in ft^3/s	Rank (1–74) of post-step/pre-step median annual peak streamflow	Primary attribution	Secondary attribution	Level of evidence	Notes
02339500	GA	0.0012	1976	40,900	23,900	60	Large artificial impoundments	-	Robust	LWRPF streamgage
02349605	GA	0.0456	1998	26,000	13,500	56	Large artificial impoundments	Short-term precipitation	Robust	Tested
02383500	GA	4.8 E-06	1980	13,600	8,060	43	Large artificial impoundments	-	Robust	~
02387500	GA	0.0004	1980	25,100	16,200	49	Large artificial impoundments	-	Robust	~
02388500	GA	0.0710	1966	27,800	23,100	41	Surface-water withdrawals	-	Robust	~
02394000	GA	0.0049	1986	9,260	8,640	15	Large artificial impoundments	Surface-water withdrawals	Limited	~
02492000	LA	0.0475	1971	15,300	26,400	3	Urban effects	-	Limited	~
07378500	LA	0.0216	1971	23,000	38,400	1	Urban effects	-	Medium	~
02489500	MS	0.0348	1972	41,200	54,300	2	Artificial wastewater and water-supply discharges	-	Robust	~
02068500	NC	0.0703	1971	3,150	4,480	10	Surface-water withdrawals	-	Limited	~
02080500	NC	4.9E-05	1958	53,200	21,500	63	Large artificial impoundments	-	Robust	~
02087500	NC	0.0269	1967	9,120	7,260	29	Large artificial impoundments	-	Limited	~
02100500	NC	0.0017	1998	12,100	7,050	42	Large artificial impoundments	-	Limited	~
02102500	NC	2.0E-07	1973	42,300	35,200	45	Large artificial impoundments	-	Robust	LWRPF streamgage
02111000	NC	0.0761	1998	1,260	774	13	Surface-water withdrawals	Short-term precipitation	Robust	Tested
02112000	NC	5.0E-05	1979	9,380	6,160	36	Surface-water withdrawals	-	Limited	~
03439000	NC	0.0355	1963	3,530	4,700	11	Large artificial impoundments	-	Medium	~
03443000	NC	0.1000	1980	7,920	5,150	33	Surface-water withdrawals	-	Robust	~
03451000	NC	0.0607	1998	3,000	1,730	23	Large artificial impoundments	Short-term precipitation	Limited	~
03550000	NC	0.0624	1997	4,420	2,900	25	Interbasin water transfers	-	Limited	~
02131000	SC	0.0184	1993	45,400	27,500	62	Large artificial impoundments	Surface-water withdrawals	Medium	LWRPF streamgage

Table H5. Statistics and attributions of change points in median annual peak streamflow for 74 streamgages in the Southeast region for the 75-year period (water years 1941–2015).—Continued

[A *p*-value less than 0.10 indicates the value is statistically significant; a *p*-value greater than 0.10 indicates the value is nonsignificant. "Pre-step" peak streamflow refers to before the year of the change point, and "post-step" peak streamflow refers to after the year of the change point. The "rank" of streamgages (1 to 74) is the ratio of post-step streamflow to pre-step streamflow, with a rank of 1 being the highest ratio and a rank of 74 being the lowest ratio. The "level of evidence" is the confidence in the primary and secondary attributions. In the "Notes" column, "Tested" means the streamgage was tested for the correlation between precipitation and median annual peak streamflow. Change point data are from Dudley and others (2018). AL, Alabama; FL, Florida; GA, Georgia; LA, Louisiana; MS, Mississippi; NC, North Carolina; SC, South Carolina; TN, Tennessee; VA, Virginia; ft^3/s, cubic feet per second; LWRPF, largest watershed and reductions in peak flow; -, no secondary attribution; ~, for additional notes on streamgages see Swain and York (2022)]

Streamgage number	State	*p*-value	Year of change point in median annual peak streamflow	Pre-step median annual peak streamflow, in ft^3/s	Post-step median annual peak streamflow, in ft^3/s	Rank (1–74) of post-step/pre-step median annual peak streamflow	Primary attribution	Secondary attribution	Level of evidence	Notes
02136000	SC	0.0112	1995	6,230	3,030	35	Groundwater withdrawals	Short-term precipitation	Limited	Tested
02146000	SC	0.0270	1979	36,800	21,100	59	Large artificial impoundments	Interbasin water transfers	Robust	~
02148000	SC	0.0245	1980	36,100	30,500	44	Large artificial impoundments	Surface-water withdrawals	Limited	LWRPF streamgage
02155500	SC	0.0373	1980	5,360	3,540	27	Large artificial impoundments	-	Robust	~
02163500	SC	0.0139	1978	10,400	9,150	21	Surface-water withdrawals	-	Limited	~
02167000	SC	0.0959	1998	13,300	6,170	46	Large artificial impoundments	Short-term precipitation	Limited	~
02169000	SC	0.0002	1963	10,700	18,300	4	Urban effects	-	Robust	~
02173000	SC	0.0012	1985	2,820	1,570	22	Groundwater withdrawals	Short-term precipitation	Robust	Tested
02173500	SC	0.0004	1987	2,600	1,460	20	Groundwater withdrawals	Short-term precipitation	Robust	Tested
02175000	SC	0.0164	1984	10,600	6,150	40	Groundwater withdrawals	-	Robust	~
02192500	SC	0.0985	1998	4,900	3,050	28	Groundwater withdrawals	Short-term precipitation	Limited	~
02197000	SC	0.0004	1980	38,300	29,200	52	Surface-water withdrawals	-	Robust	LWRPF streamgage
02198500	SC	0.0097	1980	36,600	19,500	61	Surface-water withdrawals	-	Robust	LWRPF streamgage
03598000	TN	0.0477	1977	17,700	13,400	39	Large artificial impoundments	-	Robust	~
02047500	VA	0.0772	1974	2,090	2,650	12	Urban effects	-	Robust	~
02049500	VA	0.0152	1974	2,970	4,320	9	Groundwater withdrawals	-	Robust	~
02051500	VA	0.0329	1971	5,560	8,690	6	Large artificial impoundments	-	Limited	~
02060500	VA	0.0035	1996	22,700	13,800	50	Large artificial impoundments	Interbasin water transfers	Robust	~
02061500	VA	0.1026	1971	6,010	9,000	7	Large artificial impoundments	-	Robust	~
02062500	VA	0.0379	1998	30,500	17,600	58	Large artificial impoundments	Short-term precipitation	Robust	~
02066000	VA	0.0498	1998	29,500	19,500	54	Large artificial impoundments	Short-term precipitation	Limited	~
02072500	VA	0.0033	1996	4,820	2,360	31	Large artificial impoundments	Interbasin water transfers	Medium	Tested

Table H5. Statistics and attributions of change points in median annual peak streamflow for 74 streamgages in the Southeast region for the 75-year period (water years 1941–2015).—Continued

[A *p*-value less than 0.10 indicates the value is statistically significant; a *p*-value greater than 0.10 indicates the value is nonsignificant. "Pre-step" peak streamflow refers to before the year of the change point, and "post-step" peak streamflow refers to after the year of the change point. The "rank" of streamgages (1 to 74) is the ratio of post-step streamflow to pre-step streamflow, with a rank of 1 being the highest ratio and a rank of 74 being the lowest ratio. The "level of evidence" is the confidence in the primary and secondary attributions. In the "Notes" column, "Tested" means the streamgage was tested for the correlation between precipitation and median annual peak streamflow. Change point data are from Dudley and others (2018). AL, Alabama; FL, Florida; GA, Georgia; LA, Louisiana; MS, Mississippi; NC, North Carolina; SC, South Carolina; TN, Tennessee; VA, Virginia; ft^3/s, cubic feet per second; LWRPF, largest watershed and reductions in peak flow; -, no secondary attribution; ~, for additional notes on streamgages see Swain and York (2022)]

Streamgage number	State	*p*-value	Year of change point in median annual peak streamflow	Pre-step median annual peak streamflow, in ft^3/s	Post-step median annual peak streamflow, in ft^3/s	Rank (1–74) of post-step/ pre-step median annual peak streamflow	Primary attribution	Secondary attribution	Level of evidence	Notes
02073000	VA	0.0366	1996	7,730	5,090	32	Large artificial impoundments	Interbasin water transfers	Robust	~
02074500	VA	0.0124	1971	2,780	4,930	8	Surface-water withdrawals	-	Medium	~
03531500	VA	0.0238	1979	11,400	8,960	30	Interbasin water transfers	-	Medium	~

Table H6. Statistics and attributions of monotonic trends in median annual peak streamflow for 74 streamgages in the Southeast region for the 50-year period (water years 1966–2015).

[The rank of streamgages (1 to 74) is based on the monotonic trend in median annual peak streamflow. The “level of evidence” is the confidence in the primary and secondary attributions. In the “Notes” column, “Tested” means the streamgage was tested for the correlation between precipitation and median annual peak streamflow. Monotonic trend data are from Dudley and others (2018). AL, Alabama; FL, Florida; GA, Georgia; MS, Mississippi; NC, North Carolina; SC, South Carolina; VA, Virginia; ft³/s/yr, cubic feet per second per year; LWRPF, largest watershed and reductions in peak flow; -, no secondary attribution; ~, for additional notes on streamgages see Swain and York (2022)]

Streamgage number	State	Monotonic trend in median annual peak streamflow, in ft³/s/yr	Rank (1–74) of monotonic trend in median annual peak streamflow	Primary attribution	Secondary attribution	Level of evidence	Notes
02400100	AL	-111	45	Surface-water withdrawals	Short-term precipitation	Limited	Tested
02412000	AL	-71.4	38	Large artificial impoundments	-	Robust	~
02414500	AL	-269	61	Large artificial impoundments	-	Robust	LWRPF streamgage
02438000	AL	-141	52	Groundwater withdrawals	-	Additional information required	Tested
02462000	AL	-42.3	27	Artificial wastewater and water-supply discharges	-	Medium	~
03574500	AL	-192	57	Interbasin water transfers	-	Additional information required	~
02233500	FL	17.0	4	Urban effects	-	Robust	~
02263800	FL	6.91	5	Urban effects	-	Robust	~
02266300	FL	6.64	6	Urban effects	Short-term precipitation	Medium	Tested
02294491	FL	5.29	7	Artificial wastewater and water-supply discharges	-	Robust	~
02297310	FL	-10.2	12	Interbasin water transfers	Urban effects	Robust	~
02300100	FL	-9.15	11	Groundwater withdrawals	-	Medium	~
02303800	FL	-6.0	9	Groundwater withdrawals	-	Limited	~
02307359	FL	3.58	8	Urban effects	-	Robust	~
02313000	FL	-24.7	18	Interbasin water transfers	-	Medium	~
02192000	GA	-312	65	Interbasin water transfers	-	Limited	LWRPF streamgage
02198000	GA	-45.2	30	Artificial wastewater and water-supply discharges	-	Limited	Tested
02202500	GA	-131	50	Groundwater withdrawals	-	Additional information required	~
02213000	GA	-337	70	Large artificial impoundments	Surface-water withdrawals	Medium	LWRPF streamgage
02213500	GA	-44.4	29	Large artificial impoundments	Interbasin water transfers	Additional information required	~
02215500	GA	-291	62	Surface-water withdrawals	-	Robust	LWRPF streamgage
02217500	GA	-98.9	42	Surface-water withdrawals	-	Robust	~
02223500	GA	-332	69	Large artificial impoundments	-	Limited	LWRPF streamgage

Table H6. Statistics and attributions of monotonic trends in median annual peak streamflow for 74 streamgages in the Southeast region for the 50-year period (water years 1966–2015).—Continued

[The rank of streamgages (1 to 74) is based on the monotonic trend in median annual peak streamflow. The "level of evidence" is the confidence in the primary and secondary attributions. In the "Notes" column, "Tested" means the streamgage was tested for the correlation between precipitation and median annual peak streamflow. Monotonic trend data are from Dudley and others (2018). AL, Alabama; FL, Florida; GA, Georgia; MS, Mississippi; NC, North Carolina; SC, South Carolina; VA, Virginia; $ft^3/s/yr$, cubic feet per second per year; LWRPF, largest watershed and reductions in peak flow; -, no secondary attribution; ~, for additional notes on streamgages see Swain and York (2022)]

Streamgage number	State	Monotonic trend in median annual peak streamflow, in $ft^3/s/yr$	Rank (1–74) of monotonic trend in median annual peak streamflow	Primary attribution	Secondary attribution	Level of evidence	Notes
02226000	GA	-565	73	Surface-water withdrawals	-	Robust	LWRPF streamgage
02334430	GA	45.8	2	Large artificial impoundments	Interbasin water transfers	Robust	~
02337170	GA	-111	46	Large artificial impoundments	Interbasin water transfers	Medium	~
02337500	GA	-71.3	37	Surface-water withdrawals	Short-term precipitation	Medium	Tested
02339500	GA	-325	68	Large artificial impoundments	-	Robust	LWRPF streamgage
02344500	GA	-55.9	34	Large artificial impoundments	Surface-water withdrawals	Robust	~
02344700	GA	-48.3	32	Large artificial impoundments	Surface-water withdrawals	Medium	~
02349605	GA	-300	64	Large artificial impoundments	Surface-water withdrawals	Robust	Tested
02352500	GA	-291	63	Large artificial impoundments	Surface-water withdrawals	Robust	~
02353000	GA	-268	60	Large artificial impoundments	Surface-water withdrawals	Robust	LWRPF streamgage
02382500	GA	-70.9	36	Large artificial impoundments	-	Robust	~
02383500	GA	-115	48	Large artificial impoundments	-	Robust	~
02394000	GA	-25.0	19	Large artificial impoundments	Surface-water withdrawals	Limited	~
02439400	MS	-163	55	Groundwater withdrawals	Short-term precipitation	Additional information required	Tested
02448000	MS	-131	51	Interbasin water transfers	-	Robust	~
02484500	MS	-76.8	40	Groundwater withdrawals	Short-term precipitation	Limited	Tested
02100500	NC	-107	44	Large artificial impoundments	-	Limited	~
02102500	NC	-338	71	Large artificial impoundments	Surface-water withdrawals	Robust	LWRPF streamgage
02111000	NC	-13.5	13	Surface-water withdrawals	Short-term precipitation	Robust	Tested
02111180	NC	-30.7	22	Surface-water withdrawals	-	Limited	~
02111500	NC	-32.3	24	Surface-water withdrawals	Short-term precipitation	Robust	Tested
02112000	NC	-62.6	35	Surface-water withdrawals	-	Limited	~
02115360	NC	-250	59	Surface-water withdrawals	-	Limited	~
02143040	NC	-23.5	16	Interbasin water transfers	-	Additional information required	Tested
02146700	NC	25.0	3	Urban effects	-	Medium	Tested
03443000	NC	-73.3	39	Large artificial impoundments	Surface-Water withdrawals	Robust	~

Table H6. Statistics and attributions of monotonic trends in median annual peak streamflow for 74 streamgages in the Southeast region for the 50-year period (water years 1966–2015).—Continued

[The rank of streamgages (1 to 74) is based on the monotonic trend in median annual peak streamflow. The "level of evidence" is the confidence in the primary and secondary attributions. In the "Notes" column, "Tested" means the streamgage was tested for the correlation between precipitation and median annual peak streamflow. Monotonic trend data are from Dudley and others (2018). AL, Alabama; FL, Florida; GA, Georgia; MS, Mississippi; NC, North Carolina; SC, South Carolina; VA, Virginia; ft^3/s/yr, cubic feet per second per year; LWRPF, largest watershed and reductions in peak flow; -, no secondary attribution; ~, for additional notes on streamgages see Swain and York (2022)]

Streamgage number	State	Monotonic trend in median annual peak streamflow, in ft^3/s/yr	Rank (1–74) of monotonic trend in median annual peak streamflow	Primary attribution	Secondary attribution	Level of evidence	Notes
03446000	NC	-23.6	17	Large artificial impoundments	-	Medium	~
03451000	NC	-31.1	23	Large artificial impoundments	Interbasin water transfers	Limited	~
03455500	NC	-52.9	33	Small impoundments	Short-term precipitation	Robust	~
03550000	NC	-28.0	21	Artificial wastewater and water-supply discharges	-	Limited	~
02110500	SC	-48.1	31	Short-term precipitation	Long-term precipitation	Robust	~
02130910	SC	-6.88	10	Large artificial impoundments	Interbasin water transfers	Robust	~
02131000	SC	-431	72	Large artificial impoundments	Surface-water withdrawals	Medium	LWRPF streamgage
02135000	SC	-123	49	Groundwater withdrawals	-	Medium	~
02136000	SC	-91.7	41	Groundwater withdrawals	Short-term precipitation	Limited	Tested
02148000	SC	-210	58	Large artificial impoundments	Surface-water withdrawals	Limited	LWRPF streamgage
02167000	SC	-142	53	Large artificial impoundments	Interbasin water transfers	Limited	~
02169500	SC	-708	74	Large artificial impoundments	Interbasin water transfers	Limited	LWRPF streamgage
02173000	SC	-38.9	26	Groundwater withdrawals	Short-term precipitation	Robust	Tested
02173500	SC	-34.7	25	Groundwater withdrawals	Short-term precipitation	Robust	Tested
02175000	SC	-144	54	Groundwater withdrawals	-	Robust	~
02175500	SC	-21.2	15	Interbasin water transfers	Short-term precipitation	Medium	Tested
02176500	SC	-17.8	14	Groundwater withdrawals	-	Limited	Tested
02197000	SC	-315	66	Surface-water withdrawals	-	Robust	LWRPF streamgage
02198500	SC	-318	67	Surface-water withdrawals	-	Robust	LWRPF streamgage
02049500	VA	50.0	1	Short-term precipitation	-	Robust	~
02060500	VA	-113	47	Large artificial impoundments	Interbasin water transfers	Robust	~
02062500	VA	-181	56	Large artificial impoundments	Interbasin water transfers	Robust	~
02066000	VA	-100	43	Large artificial impoundments	Surface-water withdrawals	Limited	~
02072500	VA	-44.2	28	Large artificial impoundments	Interbasin water transfers	Medium	Tested
02073000	VA	-27.7	20	Large artificial impoundments	Interbasin water transfers	Robust	~

Table H7. Statistics and attributions of monotonic trends in median annual peak streamflow for 74 streamgages in the Southeast region for the 75-year period (water years 1941–2015).

[The rank of streamgages (1 to 74) is based on the monotonic trend in median annual peak streamflow. The "level of evidence" is the confidence in the primary and secondary attributions. In the "Notes" column, "Tested" means the streamgage was tested for the correlation between precipitation and median annual peak streamflow. Monotonic trend data are from Dudley and others (2018). AL, Alabama; FL, Florida; GA, Georgia; LA, Louisiana; MS, Mississippi; NC, North Carolina; SC, South Carolina; TN, Tennessee; VA, Virginia; $ft^3/s/yr$, cubic feet per second per year; LWRPF, largest watershed and reductions in peak flow; -, no secondary attribution; ~, for additional notes on streamgages see Swain and York (2022)]

Streamgage number	State	Monotonic trend in median annual peak streamflow, in $ft^3/s/yr$	Rank (1–74) of monotonic trend in median annual peak streamflow	Primary attribution	Secondary attribution	Level of evidence	Notes
02398300	AL	-65.2	40	Large artificial impoundments	Surface-water withdrawals	Robust	~
02414500	AL	-134.0	49	Large artificial impoundments	-	Robust	LWRPF streamgage
03574500	AL	-60.0	39	Groundwater withdrawals	-	Medium	~
02294650	FL	-7.1	14	Artificial wastewater and water-supply discharges	-	Robust	~
02295637	FL	-42.2	31	Artificial wastewater and water-supply discharges	-	Robust	~
02296750	FL	-48.1	32	Artificial wastewater and water-supply discharges	-	Robust	~
02301500	FL	-20.0	23	Groundwater withdrawals	-	Robust	~
02303000	FL	-16.2	18	Interbasin water transfers	-	Robust	~
02312500	FL	-15.7	17	Interbasin water transfers	Urban effects	Robust	~
02313000	FL	-18.9	21	Urban effects	-	Robust	~
02319000	FL	84.8	4	Urban effects	-	Robust	~
02192000	GA	-115.0	47	Interbasin water transfers	-	Limited	LWRPF streamgage
02198000	GA	-17.6	19	Artificial wastewater and water-supply discharges	-	Limited	Tested
02213000	GA	-235.0	57	Large artificial impoundments	Surface-water withdrawals	Medium	LWRPF streamgage
02217500	GA	-28.5	26	Surface-water withdrawals	-	Robust	~
02223500	GA	-155.0	51	Large artificial impoundments	-	Limited	LWRPF streamgage
02335000	GA	-50.7	34	Large artificial impoundments	-	Robust	~
02339500	GA	-302.0	60	Large artificial impoundments	-	Robust	LWRPF streamgage
02349605	GA	-187.0	53	Large artificial impoundments	Surface-water withdrawals	Robust	Tested
02383500	GA	-144.0	50	Large artificial impoundments	-	Robust	~
02387500	GA	-190.0	54	Large artificial impoundments	-	Robust	~
02388500	GA	-115.0	48	Surface-water withdrawals	-	Robust	~
02394000	GA	-31.8	28	Large artificial impoundments	Surface-water withdrawals	Limited	~
02492000	LA	170.0	3	Urban effects	-	Limited	~
07378500	LA	265.0	1	Urban effects	-	Medium	~
02489500	MS	190.0	2	Artificial wastewater and water-supply discharges	-	Robust	~

Table H7. Statistics and attributions of monotonic trends in median annual peak streamflow for 74 streamgages in the Southeast region for the 75-year period (water years 1941–2015).—Continued

[The rank of streamgages (1 to 74) is based on the monotonic trend in median annual peak streamflow. The "level of evidence" is the confidence in the primary and secondary attributions. In the "Notes" column, "Tested" means the streamgage was tested for the correlation between precipitation and median annual peak streamflow. Monotonic trend data are from Dudley and others (2018). AL, Alabama; FL, Florida; GA, Georgia; LA, Louisiana; MS, Mississippi; NC, North Carolina; SC, South Carolina; TN, Tennessee; VA, Virginia; $ft^3/s/yr$, cubic feet per second per year; LWRPF, largest watershed and reductions in peak flow; -, no secondary attribution; ~, for additional notes on streamgages see Swain and York (2022)]

Streamgage number	State	Monotonic trend in median annual peak streamflow, in $ft^3/s/yr$	Rank (1–74) of monotonic trend in median annual peak streamflow	Primary attribution	Secondary attribution	Level of evidence	Notes
02068500	NC	20.4	10	Surface-water withdrawals	-	Limited	~
02080500	NC	-167.0	52	Large artificial impoundments	-	Robust	~
02087500	NC	-34.1	29	Large artificial impoundments	-	Limited	~
02100500	NC	-77.6	42	Large artificial impoundments	-	Limited	~
02102500	NC	-397.0	62	Large artificial impoundments	-	Robust	LWRPF streamgage
02111000	NC	-5.8	13	Surface-water withdrawals	Short-term precipitation	Robust	Tested
02112000	NC	-83.2	43	Surface-water withdrawals	-	Limited	~
03439000	NC	17.8	11	Large artificial impoundments	-	Medium	~
03443000	NC	-19.2	22	Surface-water withdrawals	-	Robust	~
03451000	NC	-8.3	15	Large artificial impoundments	Interbasin water transfers	Limited	~
03550000	NC	-13.6	16	Interbasin water transfers	-	Limited	~
02131000	SC	-219.0	56	Large artificial impoundments	Surface-water withdrawals	Medium	LWRPF streamgage
02136000	SC	-51.5	35	Groundwater withdrawals	Short-term precipitation	Limited	Tested
02146000	SC	-273.0	58	Large artificial impoundments	Interbasin water transfers	Robust	~
02148000	SC	-274.0	59	Large artificial impoundments	Surface-water withdrawals	Limited	LWRPF streamgage
02155500	SC	-30.4	27	Large artificial impoundments	-	Robust	~
02163500	SC	-53.1	36	Surface-water withdrawals	-	Limited	~
02167000	SC	-58.6	38	Large artificial impoundments	Interbasin water transfers	Limited	~
02169000	SC	78.6	5	Urban effects	-	Robust	~
02173000	SC	-18.7	20	Groundwater withdrawals	Short-term precipitation	Robust	Tested
02173500	SC	-22.4	24	Groundwater withdrawals	Short-term precipitation	Robust	Tested
02175000	SC	-77.5	41	Groundwater withdrawals	-	Robust	~
02192500	SC	-27.2	25	Groundwater withdrawals	-	Limited	~
02197000	SC	-419.0	63	Surface-water withdrawals	-	Robust	LWRPF streamgage
02198500	SC	-325.0	61	Surface-water withdrawals	-	Robust	LWRPF streamgage
03598000	TN	-84.3	44	Large artificial impoundments	-	Robust	~

Table H7. Statistics and attributions of monotonic trends in median annual peak streamflow for 74 streamgages in the Southeast region for the 75-year period (water years 1941–2015).—Continued

[The rank of streamgages (1 to 74) is based on the monotonic trend in median annual peak streamflow. The "level of evidence" is the confidence in the primary and secondary attributions. In the "Notes" column, "Tested" means the streamgage was tested for the correlation between precipitation and median annual peak streamflow. Monotonic trend data are from Dudley and others (2018). AL, Alabama; FL, Florida; GA, Georgia; LA, Louisiana; MS, Mississippi; NC, North Carolina; SC, South Carolina; TN, Tennessee; VA, Virginia; $ft^3/s/yr$, cubic feet per second per year; LWRPF, largest watershed and reductions in peak flow; -, no secondary attribution; ~, for additional notes on streamgages see Swain and York (2022)]

Streamgage number	State	Monotonic trend in median annual peak streamflow, in $ft^3/s/yr$	Rank (1–74) of monotonic trend in median annual peak streamflow	Primary attribution	Secondary attribution	Level of evidence	Notes
02047500	VA	16.0	12	Urban effects	-	Robust	~
02049500	VA	34.5	6	Groundwater withdrawals	-	Robust	~
02051500	VA	27.5	9	Large artificial impoundments	-	Limited	~
02060500	VA	-210.0	55	Large artificial impoundments	Interbasin water transfers	Robust	~
02061500	VA	30.2	7	Large artificial impoundments	-	Robust	~
02062500	VA	-106.0	46	Large artificial impoundments	Interbasin water transfers	Robust	~
02066000	VA	-102.0	45	Large artificial impoundments	Surface-water withdrawals	Limited	~
02072500	VA	-48.8	33	Large artificial impoundments	Interbasin water transfers	Medium	Tested
02073000	VA	-54.0	37	Large artificial impoundments	Interbasin water transfers	Robust	~
02074500	VA	28.3	8	Surface-water withdrawals	-	Medium	~
03531500	VA	-41.1	30	Interbasin water transfers	-	Medium	~

Table H8. Statistics of the interquartile-range analysis (Mood test), and the attributions of change points in median annual peak streamflow in the Southeast region for the 50-year period (water years 1966–2015).

[The "level of evidence" is the confidence in the primary and secondary attributions. In the "Notes" column, "Tested" means the streamgage was tested for the correlation between precipitation and median annual peak streamflow. Interquartile data are from Dudley and others (2018). AR, Arkansas; FL, Florida; GA, Georgia; LA, Louisiana; NC, North Carolina; SC, South Carolina; VA, Virginia; ft^3/s, cubic feet per second; LWRPF, largest watershed and reductions in peak flow; -, no secondary attribution; ~, for additional notes on streamgages see Swain and York (2022)]

Streamgage number	State	Change point year in median annual peak streamflow	Interquartile range of pre-step median annual peak streamflow, in ft^3/s	Interquartile range of post-step median annual peak streamflow, in ft^3/s	Primary attribution	Secondary attribution	Level of evidence	Notes
07077380	AR	1980	3,370	1,460	Interbasin water transfers	-	Medium	~
02236500	FL	1997	86.2	146	Interbasin water transfers	-	Medium	~
02294491	FL	2001	201	381	Artificial wastewater and water-supply discharges	-	Robust	~
02299950	FL	1979	743	2,220	Urban effects	-	Limited	~
02301900	FL	1987	222	571	Interbasin water transfers	-	Medium	~
02302500	FL	1996	584	1,050	Interbasin water transfers	-	Limited	~
02303000	FL	1996	1,250	2,620	Interbasin water transfers	-	Limited	~
02335000	GA	1998	1,460	3,120	Large artificial impoundments	Interbasin water transfers	Medium	~
02337500	GA	2005	2,280	987	Surface-water withdrawals	Short-term precipitation	Medium	Tested
02344500	GA	1983	3,070	4,800	Large artificial impoundments	Surface-water withdrawals	Robust	~
02344700	GA	1985	2,240	3,380	Large artificial impoundments	Surface-water withdrawals	Medium	~
02347500	GA	1987	11,700	26,300	Large artificial impoundments	Surface-water withdrawals	Robust	LWRPF streamgage
02349605	GA	1987	11,200	20,000	Large artificial impoundments	Surface-water withdrawals	Robust	Tested
02382500	GA	1972	4,950	1,600	Large artificial impoundments	-	Robust	~
02385800	GA	2003	2,380	3,780	Large artificial impoundments	-	Additional information required	~
02394000	GA	1989	362	1,140	Large artificial impoundments	Surface-water withdrawals	Limited	~
02398000	GA	2005	5,590	8,570	Large artificial impoundments	Surface-water withdrawals	Medium	~
08010000	LA	1972	4,450	1,890	Agricultural drainage activities	-	Medium	~
02053500	NC	1997	294	987	Agricultural drainage activities	-	Limited	~
02080500	NC	1974	1,270	6,670	Large artificial impoundments	Interbasin water transfers	Limited	~
02106500	NC	1982	2,460	5,290	Agricultural drainage activities	-	Medium	~
02151500	NC	1998	8,430	19,800	Large artificial impoundments	Urban effects	Medium	~
02130900	SC	2000	461	723	Large artificial impoundments	Interbasin water transfers	Limited	~
02155500	SC	1998	3,070	4,680	Large artificial impoundments	-	Robust	~

Table H8. Statistics of the interquartile-range analysis (Mood test), and the attributions of change points in median annual peak streamflow in the Southeast region for the 50-year period (water years 1966–2015).—Continued

[The “level of evidence” is the confidence in the primary and secondary attributions. In the “Notes” column, “Tested” means the streamgage was tested for the correlation between precipitation and median annual peak streamflow. Interquartile data are from Dudley and others (2018). AR, Arkansas; FL, Florida; GA, Georgia; LA, Louisiana; NC, North Carolina; SC, South Carolina; VA, Virginia; ft^3/s, cubic feet per second; LWRPF, largest watershed and reductions in peak flow; -, no secondary attribution; ~, for additional notes on streamgages see Swain and York (2022)]

Streamgage number	State	Change point year in median annual peak streamflow	Interquartile range of pre-step median annual peak streamflow, in ft^3/s	Interquartile range of post-step median annual peak streamflow, in ft^3/s	Primary attribution	Secondary attribution	Level of evidence	Notes
02169000	SC	1970	14,800	3,530	Urban effects	-	Robust	~
02175500	SC	1978	577	1,670	Interbasin water transfers	Short-term precipitation	Medium	Tested
02047500	VA	1998	1,920	3,170	Short-term precipitation	-	Robust	~
02049500	VA	1997	2,340	3,840	Short-term precipitation	-	Robust	~
02061500	VA	1985	6,950	13,000	Large artificial impoundments	-	Robust	~
02072000	VA	1993	2,290	974	Large artificial impoundments	Interbasin water transfers	Medium	Tested
03488000	VA	1998	4,100	6,270	Interbasin water transfers	-	Limited	~

Table H9. Statistics of the interquartile-range analysis (Mood test), and the attributions of change points in median annual peak streamflow in the Southeast region for the 75-year period (water years 1941–2015).

[The "level of evidence" is the confidence in the primary and secondary attributions. In the "Notes" column, "Tested" means the streamgage was tested for the correlation between precipitation and median annual peak streamflow. Interquartile data are from Dudley and others (2018). AL, Alabama; FL, Florida; GA, Georgia; MS, Mississippi; NC, North Carolina; SC, South Carolina; VA, Virginia; ft³/s, cubic feet per second; LWRPF, largest watershed and reductions in peak flow; -, no secondary attribution; ~, for additional notes on streamgages see Swain and York (2022)]

Streamgage number	State	Change point year in median annual peak streamflow	Interquartile range of pre-step median annual peak streamflow, in ft³/s	Interquartile range of post-step median annual peak streamflow, in ft³/s	Primary attribution	Secondary attribution	Level of evidence	Notes
02450000	AL	2005	17,500	36,600	Surface-water withdrawals	-	Limited	~
02246000	FL	2006	4,250	7,540	Urban effects	-	Medium	~
02177000	GA	1964	1,820	6,000	Artificial wastewater and water-supply discharges	-	Limited	~
02213000	GA	1956	36,200	16,800	Surface-water withdrawals	-	Medium	LWRPF streamgage
02335000	GA	1960	16,900	1,500	Large artificial impoundments	Interbasin water transfers	Medium	~
02339500	GA	1951	44,400	19,200	Large artificial impoundments	-	Robust	LWRPF streamgage
02344500	GA	1955	5,120	2,160	Large artificial impoundments	Surface-water withdrawals	Robust	~
02388500	GA	2005	9,190	14,500	Surface-water withdrawals	-	Robust	~
02394000	GA	1964	8,950	357	Large artificial impoundments	-	Robust	~
02478500	MS	1960	17,200	38,300	Groundwater withdrawals	-	Limited	~
07268000	MS	1980	18,200	67,600	Large artificial impoundments	Interbasin water transfers	Robust	LWRPF streamgage
02080500	NC	1950	22,700	7,130	Large artificial impoundments	-	Robust	~
02085500	NC	1973	3,950	6,560	Urban effects	-	Robust	~
02151500	NC	1998	7,430	19,800	Large artificial impoundments	Urban effects	Medium	~
03443000	NC	1945	9,630	4,410	Large artificial impoundments	Surface-water withdrawals	Robust	~
03451000	NC	1993	1,930	3,370	Surface-water withdrawals	-	Limited	~
02155500	SC	1998	3,050	4,680	Large artificial impoundments	-	Robust	~
02169000	SC	1965	6,630	14,800	Large artificial impoundments	Surface-water withdrawals	Robust	~
02197000	SC	1959	66,200	15,000	Large artificial impoundments	Surface-water withdrawals	Robust	LWRPF
02198500	SC	1957	53,800	22,100	Large artificial impoundments	Surface-water withdrawals	Robust	LWRPF streamgage
02047500	VA	1998	1,810	3,170	Urban effects	-	Robust	~
02055000	VA	2000	6,570	12,200	Large artificial impoundments	-	Robust	~
02056000	VA	1967	6,100	1,400	Urban effects	-	Medium	~
02059500	VA	1986	6,900	11,500	Urban effects	-	Limited	~
02061500	VA	1985	5,180	13,000	Large artificial impoundments	-	Robust	~
02070000	VA	1978	1,470	3,440	Artificial wastewater and water-supply discharges	-	Limited	~
02077000	VA	1967	2,790	5,620	Large artificial impoundments	-	Medium	~
03488000	VA	1998	4,040	6,270	Interbasin water transfers	-	Limited	~

For more information about this publication, contact
Chief, Analysis and Prediction Branch
Integrated Modeling and Prediction Division
Water Mission Area
U.S. Geological Survey
12201 Sunrise Valley Drive, Mail Stop 415
Reston, VA 20192

For additional information, visit
https://www.usgs.gov/mission-areas/water-resources

Publishing support provided by the
USGS Science Publishing Network,
Reston, Tacoma, and Lafayette
Publishing Service Centers

Editing by Elizabeth Good, David Shields,
and Zachary Younger

Graphics by Jacqueline Olson

Layout by Gloria Smith

Web support by Molly Newbrough

USGS

Ryberg, ed.—**Attribution of Monotonic Trends and Change Points in Peak Streamflow, Conterminous USA**—PP 1869

ISSN 2330-7102 (online)
https://doi.org/10.3133/pp1869